Recovery of Rare Earth Elements from Coal and Coal Byproducts via a Closed Loop Leaching Process:

Final Report

National Energy Technology Laboratory

3610 Collins Ferry Road

Morgantown, WV 26507-0880

7 June 2017

BATTELLE

DE-FE0027012
DUNS: 007901598

Recovery of Rare Earth Elements from Coal and Coal Byproducts via a Closed Loop Leaching Process:

Final Report

Prepared by:

Battelle
505 King Avenue
Columbus, Ohio 43201

Principal Investigator: Rick Peterson, P.E.

Submitted to:

U.S. Department of Energy
National Energy Technology Laboratory
3610 Collins Ferry Road
Morgantown, WV 26507-0880

7 June 2017

BATTELLE

Table of Contents

List of Figures

List of Tables

Executive Summary

The U.S. Department of Energy funded projects to identify a coal based source of rare earth elements (REE) that exceeds 300 ppm total REE content, and to extract them economically and in an environmentally benign process to a concentration approaching 2% by weight. Battelle met these objectives by implementing its Acid Digestion Process (ADP). The process can be economically applied to US coal sources, operate with high REE recoveries, produce a REE product of greater than 7% purity, and a zeolite byproduct that can help to subsidize the REE processing costs. Additionally, the design has been scaled to a 12.5 pound per hour integrated test unit for operation in the potential next phase.

At a high level, Battelle's ADP consists of the steps of pretreatment, acid leaching, acid recovery, product roasting, and solvent extraction pre-purification. In pretreatment, the ash is milled and treated with sodium hydroxide solution to remove some of the alumina and silica, which can then be turned into a zeolite byproduct. The remaining ash is then leached in acid to extract the REE, and dried to produce a high quality pozzolan material. The acid containing REE is roasted to convert base metals such as iron to oxides, allowing REE to be leached away from them with a water wash. The water containing REE is then upgraded in a solvent extraction step to prepare REE solutions for final separation into saleable products.

Based on the laboratory testing, ball milling and caustic pretreatment of the ash allows for high recovery of REE, with leaching efficiencies for scandium as high as 86% and near complete recovery of total REE as a weighted average. Milling of the ash to approximately 4-5 µm allows these recoveries to be realized with only a 60 minute contact with 10% sodium hydroxide solution at 90 °C, and leaching in 34% nitric acid for 30 minutes at 90 °C. Traditional aluminosilicate recovery from fly ash requires a caustic leach of 6 hours or more (Hollman, Steenbruggen, & Janssen-Jurkovicova, 1999), so this method represents a significant decrease in reaction time. The acid leaching reaction is slightly exothermic, at approximately 102 calories per gram of ash leached, which will reduce energy costs to heat the leach reactor. Acid leached fly ash, after roasting to recover acid, was shown at a preliminary level to have similar pozzolanic activity as unleached ash, preserving its value in construction/filler type applications.

Additionally, the caustic pretreatment leach should allow for production of a zeolite byproduct that can be used as an adsorbent or catalyst support material. A zeolite material was made in the lab from the silica and alumina leached from the ash, but additional work would be done in Phase 2 to make a higher value zeolite with the use of seed material or zeolite scaffolds. The higher value will ensure the zeolite can be placed in the market and improve the REE recovery economics.

Thermal roasting for recovery of the loaded acid oxidizes the iron and aluminum between 100 °C and 200 °C, generating an insoluble oxide material. In testing with actual leach solutions, 90% of the REE could be recovered from the roasted solids with a water leach, while omitting over 90% of the iron and aluminum, and over 60% of the uranium and thorium. The water leach had a concentration of 1.2% REE, effectively leading to over a 20x increase in purity of the REE over the fly ash feed.

Solvent extraction testing suggested that extraction for REE is satisfactory at pH of 3.4, where 61% of REEs are extracted at over 7% purity (over 120x concentration over the feed fly ash). The primary contaminants were sodium (due to a high starting concentration), aluminum, silica, calcium, and iron, but sodium, potassium, magnesium, and calcium were largely excluded from the extract. At pH 5, near quantitative REE can be achieved (over 99%), including less valuable

lanthanum and cerium, but purity drops to about 1.0% in the extract. In selective stripping tests, the REE were stripped in hydrochloric acid at around one molar. The scandium is expected to be recoverable by precipitating in sodium carbonate solution. These REE solutions could then be separated with commercial operations such as further solvent extraction or ion exchange, or an emerging technology could be used such as electrowinning or electrophoresis.

The results of the laboratory testing were used in the updated technoeconomic assessment model to predict the economics of the process, and they were used in the design of a continuous bench scale unit that integrates all of the operations. The key parameters that were used are a one-hour leach in 10% sodium hydroxide at 90 °C, with fly ash milled to ~4.5 µm, then acid leaching in 34% nitric acid at 90 °C. The loaded acid will be roasted at 150 °C to calcine iron and aluminum, separating them from REE in a water wash. This loaded water will be extracted at pH 3.5-4.0, scrubbed around pH 3.5 to remove base metals, stripped with 1 molar hydrochloric acid to recover REE, scrubbed with 2 M HCl to remove iron, then scandium recovered by precipitation with 10% sodium carbonate solution. Additional work to improve the stripping process will be done in pending Phase 2 testing.

The technoeconomic assessment suggested that at the 30 tonne per hour scale, the processing cost per tonne of fly ash feed is approximately $140 for a mature, commercial plant. This cost would allow it to be economically applied to 42% of US coal sources if ashed.

Using laboratory results and the generated CHEMCAD model, the process design was scaled up to 12.5 lbs/hr of coal ash feed. Process flow diagrams, piping and instrumentation diagrams, stream tables, mass and energy balances, utility requirements, vendor quotes, equipment lists, and a preliminary space claim diagram were generated for the integrated test unit.

The integrated continuous testing in the prospective Phase 2 work will investigate the impact of recycle streams on the process, which will introduce concentration cycles of contaminants and reduced acid and caustic strengths. Finally, the next phase will include optimization of zeolite production to generate a saleable, high value zeolite product. Successful validation of the integrated unit will progress the technology to a technology readiness level of 5, which is ready for scaling to an industrial scale pilot. This industrial scale demonstration would likely happen in the 2019-2020 timeframe.

When commercial, this process will reduce the environmental impact and cost of handling coal fly ash by converting it from an environmental liability that requires storage and monitoring into saleable REE and zeolite products. This will in turn elevate the demand for coal in power generation applications.

1.0 Introduction

As directed by Congress, the United States (U.S.) Department of Energy (DOE) is investigating the economic feasibility of recovery of rare earth elements (REEs) from domestic U.S. coal and coal byproducts. DOE's National Energy Technology Laboratory (NETL) has characterized a number of REE-bearing samples of coal and coal-related materials. Rare earth elements have been found in varying concentrations ranging up to 1,000 parts per million (ppm) by weight in the following materials in the United States: coal mine roof and floor materials, run-of-mine coal, prepared coal, partings, pit cleanings, coal preparation refuse, and tailings. REEs can be found in coal byproducts, including ash, coal-related sludge, and mine drainage. Certain coals can contain a higher ratio of heavy (generally more valuable) REEs than found in other sources of REEs such as natural ores, and DOE is particularly interested in sources that have higher than 300 ppm REE. Since most coal materials start at REE concentrations well below 1,000 ppm, the yield of REEs from any separation process is likely to be low, and minimizing costs is a key challenge. DOE therefore funded groups with novel processes able to recover REE from coal sources while minimizing the processing costs.

The rare earth elements are the 14 naturally occurring elements between lanthanum and lutetium on the periodic table, along with yttrium and scandium which have similar chemical properties. Their symbols and atomic numbers are listed in Table 1 for reference. They have become critical in renewable energy and defense applications, where they are used to make magnets for motors and generators, metal alloys, and in various sensor components. Occasionally, yttrium and scandium are considered separately, and so the group of rare earth elements is sometimes referred to as REE+Y+Sc for clarity in this report. Element 61, promethium, is not naturally occurring and not included in the analyses for this report.

Table 1: List of rare earth elements, their symbols, and their atomic numbers.

Rare Earth Elements, Symbols, and Atomic Numbers											
Sc	Scandium	21	**Pr**	Praseodymium	59	**Gd**	Gadolinium	64	**Er**	Erbium	68
Y	Yttrium	39	**Nd**	Neodymium	60	**Tb**	Terbium	65	**Tm**	Thulium	69
La	Lanthanum	57	**Sm**	Samarium	62	**Dy**	Dysprosium	66	**Yb**	Ytterbium	70
Ce	Cerium	58	**Eu**	Europium	63	**Ho**	Holmium	67	**Lu**	Lutetium	71

Battelle is validating the economic viability of recovering REEs from coal ash using its patented (US6011193) closed-loop Acid Digestion Process (ADP). Based on results from the sampling and characterization work, a Pulverized Coal Combustion (PCC) plant fly ash was selected as the target feedstock for the process. This plant is operating in Ohio on primarily Appalachian Basin coals, and had a high total REE+Y+Sc concentration at 545 ppm +/- 13 ppm. A preliminary technoeconomic analysis (TEA) done on Battelle's ADP process suggested that it could be economically applied to between 5% and 47% of U.S. coal sources, and based on this finding, additional lab testing and design work was started.

This report documents and summarizes sampling and characterization work that led to selection of a coal based REE source, lab testing that demonstrated feasibility of the ADP,

technoeconomic analyses that suggest the process can economically recover REE, and design of a continuous bench scale (12.5 pounds of fly ash per hour) testing unit that would be built in the second phase of the project.

2.0 Sampling and Characterization

To select a suitable process feedstock, Battelle sampled and characterized coal ash from three sources: from operating PCC power plants, an operating fluidized bed combustor (FBC) power plant, and residual material from Battelle's bio-based direct coal liquefaction process. Power plant samples were obtained with the support of commercial partners to find facilities that were representative of coal power stations. The FBC ash was obtained by contacting an operator of a known FBC power plant. Coal liquefaction ash was generated at Battelle using Middle Kittanning coal from Ohio due to its availability and known REE concentration above 300 ppm. A detailed sampling and characterization report can be found in Appendix A.

Samples that contained a significant amount of organic material such as liquefaction residual or raw coal were ashed prior to analysis, and the analytical results in this section are given on an ash basis. Solid samples were digested by either a sodium peroxide or lithium metaborate/ tetraborate fusion, dissolved in nitric acid, then analyzed for elements by Inductively Coupled Plasma Mass Spectrometry (ICP-MS). A sodium peroxide sinter was chosen for the digestion because the US Geological Survey (USGS) CoalQual data was largely analyzed with a sodium peroxide sinter digestion. This approach provided consistency when comparing Battelle's results with publicly available data. The borate fusion was also used with replicates on the reference material (NIST SRM 1633C) to aid in determining which method would be the most accurate and economical for trace element analyses going forward. Scandium and Lutetium were analyzed by Instrumental Neutron Activation Analysis (INAA) for most samples, as the current peroxide method is not calibrated for those two elements.

To verify the accuracy of the methods used, a standard reference material blank (NIST SRM 1633C) was also sent for analysis with each batch of samples, and was analyzed at least three times for each method. A comparison of the analytical methods results to the stated reference material values is included in Table 2, which provides the width of the confidence interval and t-test p-value for common analytes between the two digestion methods and the corresponding NIST standard. Underlined values indicate that the confidence interval was narrower and the t-test suggested greater similarity to the NIST value. In other words, these values were closer to NIST than the other method, and had less variability. There are many cases in Table 2 where the t-test covered the NIST value with 95% confidence, but it was due to high variability in the sample analyses rather than greater accuracy in the method.

Another indicator of the suitability of a method to a particular analyte is distance from the known mean (or NIST value). The mean distance of analysis results from the NIST value were compared between the borate fusion and sodium peroxide digestions, and summarized in Figure 1. Both methods skewed low of the NIST standard, suggesting that the digestions are not 100% efficient. The sum of all mean distances from the NIST value for sodium peroxide digestions was -111.35, versus -332.54 for borate digestions.

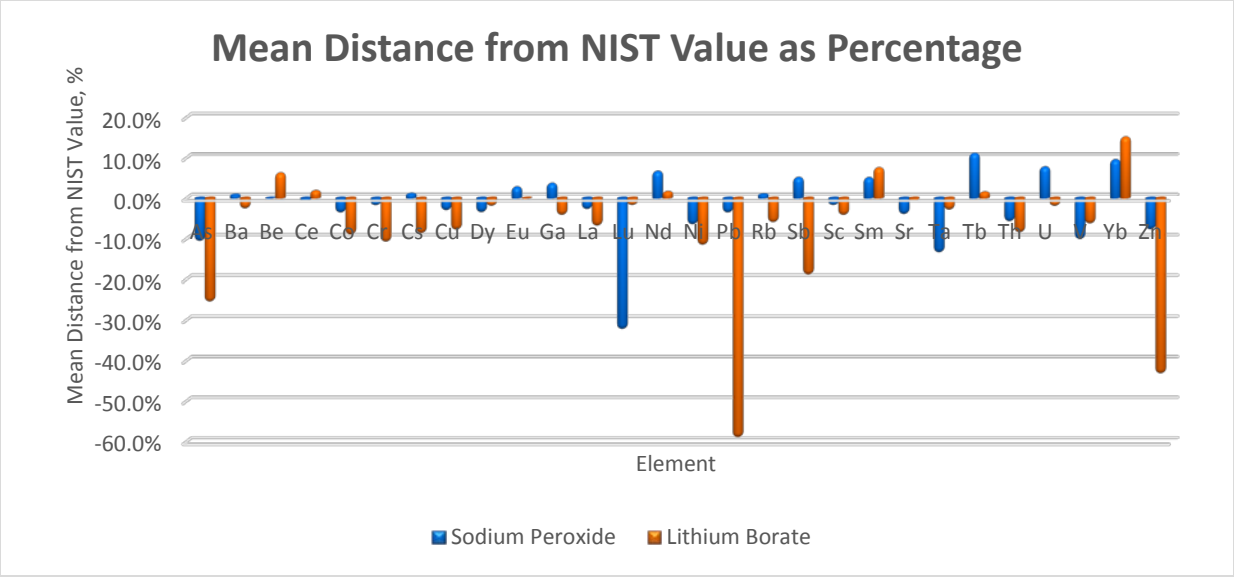

Figure 1: Mean distance of analytes from the NIST value for sodium peroxide and lithium borate digestion methods.

Table 2: Comparison of the Sodium Peroxide and Lithium Borate digestions to the NIST 1633C standard for common analytes. Underlined values indicate cases where the confidence interval was narrower AND the t-test indicated greater similarity to the standard material.

	Sodium peroxide		Lithium Borate	
Element	95% Confidence +/-	t-test p-value	95% Confidence +/-	t-test p-value
As	***26.09***	***0.082***	46.63	0.048
Ba	87.24	0.651	11.47	0.008
Be	2.48	1.000	N/A	N/A
Ce	29.11	0.862	5.17	0.109
Co	0.38	0.003	2.48	0.021
Cr	94.05	0.851	24.84	0.040
Cs	1.94	0.830	0.52	0.021
Cu	31.94	0.545	24.84	0.141
Dy	2.01	0.289	2.02	0.517
Eu	0.25	0.153	***0.14***	***1.000***
Ga	1.03	0.014	1.43	0.020
La	5.13	0.178	4.96	0.035
Lu	1.17	0.257	0.05	0.192
Nd	11.19	0.155	***3.71***	***0.246***
Ni	37.95	0.429	14.34	0.044
Pb	***10.70***	***0.298***	22.08	0.008
Rb	***6.25***	***0.481***	11.20	0.113
Sb	N/A	N/A	1.83	0.062
Sc	0.38	0.017	N/A	N/A
Sm	***1.12***	***0.065***	1.17	0.034
Sr	29.64	0.034	***17.97***	***0.380***
Ta	0.94	0.432	***0.29***	***0.556***
Tb	0.14	0.009	***0.14***	***0.297***
Th	***1.90***	***0.094***	2.68	0.087
U	1.37	0.153	1.46	0.642
V	21.66	0.028	N/A	N/A
Yb	***0.52***	***0.026***	0.63	0.015
Zn	***14.34***	***0.208***	103.42	0.052

Table 3: Elements analyzed for, along with the associated method. Note that generally a sample was analyzed by a single method, and so the analytes are not always the same between samples, but all were analyzed for REE+Y+Sc.

Element	Method	Element	Method	Element	Method
Al	Peroxide, Borate	Ho	Peroxide, Borate	Sc	Borate, INAA
Ag	Borate	Hf	Peroxide, Borate	Se	Borate
As	Peroxide, Borate	In	Peroxide, Borate	Si	Peroxide, Borate
B	Peroxide, Borate	K	Peroxide, Borate	Sm	Peroxide, Borate
Ba	Peroxide, Borate	La	Peroxide, Borate	Sn	Peroxide, Borate
Be	Peroxide, Borate	Li	Borate	Sr	Peroxide, Borate
Bi	Peroxide, Borate	Lu	Borate, INAA	Ta	Peroxide, Borate
Ca	Peroxide, Borate	Mg	Peroxide, Borate	Tb	Peroxide, Borate
Cd	Borate	Mn	Peroxide, Borate	Te	Borate
Ce	Peroxide, Borate	Mo	Peroxide, Borate	Th	Peroxide, Borate
Co	Peroxide, Borate	Na	Borate	Ti	Peroxide, Borate
Cr	Peroxide, Borate	Nb	Peroxide, Borate	Tl	Peroxide, Borate
Cs	Peroxide, Borate	Nd	Peroxide, Borate	Tm	Peroxide, Borate
Cu	Peroxide, Borate	Ni	Peroxide, Borate	U	Peroxide, Borate
Dy	Peroxide, Borate	P	Borate	V	Peroxide, Borate
Er	Peroxide, Borate	Pb	Peroxide, Borate	W	Peroxide, Borate
Eu	Peroxide, Borate	Pr	Peroxide, Borate	Y	Peroxide, Borate
Fe	Peroxide, Borate	Rb	Peroxide, Borate	Yb	Peroxide, Borate
Ga	Peroxide, Borate	S	Borate	Zn	Peroxide, Borate
Gd	Peroxide, Borate	Sb	Peroxide, Borate	Zr	Borate
Ge	Peroxide, Borate				

Analysis of the ash samples for morphology and crystallography was done by Scanning Electron Spectroscopy (SEM), Energy Dispersive Spectroscopy (EDS), and X-Ray Diffraction (XRD). X-Ray Diffraction was performed on all samples to understand which crystalline phases are present in the samples. Key samples were mounted in epoxy and polished so that a cross section could be examined. Grains were inspected to attempt to identify rare earth element phases as well as phases that contained valuable metals such as cobalt or zirconium. General morphological differences between high temperature (such as pulverized coal combustion), low temperature (such as fluidized bed combustion), and liquefaction ash were also noted.

2.1 Pulverized Coal Combustion Plant Samples

Pulverized coal combustion (PCC) ash was obtained from four operating power plants with the assistance of American Electric Power (AEP). Both bottom ash and fly ash samples were collected, and in one case feed coal samples were also obtained. A summary of the REE content for all of the PCC plant samples is shown in Table 4. PCC Plant A was unique in that it had two separate feed coal piles feeding different units. Feed Coal A was generally washed and had lower ash content than Feed Coal B and also had higher REE content. However, the feed coal samples did not originate from the same mine(s), and so no conclusions can be drawn about the effect of washing on coal ash REE concentration. The fly ash collected from PCC Plant A was associated with Feed Coal A, and since it had the highest REE+Y+Sc

concentrations, as well as attractive heavy rare earth to light rare earth (HREE/LREE) ratios, it was selected for replicate analyses to understand variability in the solids elemental analysis as well as build confidence in the starting concentration REE for later leaching tests. Two samples of this fly ash were taken. Sample 1 came from a single truckload of ash, while Sample 2 was collected from four separate truckloads.

Table 4: Summary of the REE content of PCC plant samples

	Total REE	Total REE+Y+Sc	HREE+Y	LREE+Sc	HREE/LREE
	ppm	ppm	ppm	ppm	Ratio
PCC Plant A Bottom Ash from Pile	287.46	373.06	89.26	283.8	0.31
PCC Plant A Fly Ash from Pile, Sample 1	410.3	556	151.9	404.1	0.37
PCC Plant A Fly Ash from Pile, Sample 2	429.45	574.05	153.65	420.4	0.36
PCC Plant A Feed Coal A	416.73	566.63	156.03	410.6	0.38
PCC Plant A Feed Coal B	269.44	342.54	73.74	268.8	0.27
PCC Plant A Fly Ash from Pile, Sample 1	409.26	548.26	146.95	401.31	0.36
PCC Plant A Fly Ash from Pile, Sample 1	399.69	537.69	145.59	392.1	0.37
PCC Plant A Fly Ash from Pile, Sample 1	400.54	539.54	147.87	391.67	0.37
PCC Plant B Fly Ash from Pile	278.29	367.49	86.09	281.4	0.30
PCC Plant B Bottom Ash from Pile	265.69	352.89	84.59	268.3	0.31
PCC Plant C Fly Ash from Pile	261.56	349.16	85.36	263.8	0.32
PCC Plant C Bottom Ash from Pile	259.89	341.89	81.19	260.7	0.31
PCC Plant D Fly Ash from Pile	307.07	391.07	80.8	310.27	0.26
PCC Plant D Bottom Ash from Pile	291.32	369.32	77.48	291.84	0.26

Although it appears that bottom ash has slightly lower concentration of total REE+Y+Sc than fly ash, the effect is small. PCC Plant A was omitted from this analysis since it is possible that the bottom ash analyzed originated from the lower starting concentration feed coal, and may not have been associated with the same feed as the fly ash. Feed Coal A and Samples 1 and 2 of the fly ash do not exhibit meaningful differences in total rare earth concentration, also supporting the expectation that bottom ash REE concentrations are close to fly ash.

2.2 Fluidized Bed Combustor Plant Samples

Fluidized bed combustor (FBC) ash samples were obtained from a plant in West Virginia. These samples are of particular interest due to their lower combustion temperature, which may help to avoid vitrification of the ash particles. Vitrification is expected to reduce the leaching efficiency of REE since the glassy phases are largely resistant to acid attack. A summary of the REE content in the FBC ash is provided in Table 5. Rare earth element concentrations were generally lower than observed in the PCC plant samples, but this is partially due to dilution from the addition of lime to the combustor. Calcium concentrations were roughly 10 times higher in FBC ash than the PCC ash, increasing from around 2% by mass to roughly 20% by mass, due to the lime. Sulfur concentrations are also higher in the FBC ash, as expected, since the lime is added to scrub sulfate from the process. Although the leaching recovery of REE from FBC ash is likely to be high, the quantity of ash available from FBC plants is small compared to that for PCC plants. As of 2013, over 90% of the global coal power generation capacity was from PCC plants (IEA Clean Coal Centre, 2013).

Table 5: Summary of the REE Concentration of FBC Plant Samples

	Total REE	Total REE+Y+Sc	HREE+Y	LREE+Sc	HREE/LREE
	ppm	ppm	ppm	ppm	Ratio
Fluidized Bed Combustor Fly Ash	147.5	188.1	38.6	149.5	0.258
Fluidized Bed Combustor Bottom Ash	121.4	153.2	30.5	122.7	0.249

2.3 Coal Liquefaction Residual Material Samples

Ash from Battelle's bio-based coal liquefaction process was taken from pilot scale tests. The process dissolves coal in a proprietary biosolvent, which prevents the ash from experiencing high temperature oxidizing environments. After digestion of the coal, the resulting oil is centrifuged to remove ash and heavy carbon deposits, and this residual material is what was analyzed at Battelle. It was separated into two density cuts as well as four particle size cuts to determine whether a simple mechanical separation could cause meaningful concentration of the sample. Figure 3 shows the concentration of REE through the processing of the coal liquefaction ash, and Figure 2 indicates how the ratio of heavy to light REE changed through the process.

It appears that the coal liquefaction process enriches REE over the feed coal. It is notable that the ash content of the coal liquefaction process samples used in this analysis was low; in the range of 7% ash, where it is normally expected to be 30% ash or higher based on prior lab testing with the process. Pilot plant operations indicate that this observed difference could be due to higher coking of the coal conversion process, but could also be due to preferential collection of larger particle size ashes in the centrifuge. Beyond these cases, the REE enrichment could be caused by lesser dissolution of coal components that bear REE elements, causing differential enrichment.

The coal liquefaction process also appears to enrich the ash with the more valuable heavy rare earth components, as indicated in Figure 2. Although the liquefaction process does seem to enrich REE, simple density and particle size separations of the residual material did not have a significant effect on REE enrichment. It is likely that the particle sizes of the residual material are large compared to a typical grain of rare earth, which is on the order of µm. Much finer milling would likely be required to liberate the REE components for separation by flotation, and a non-standard particle size sorting process would be required to significantly enrich the REE by particle size cuts.

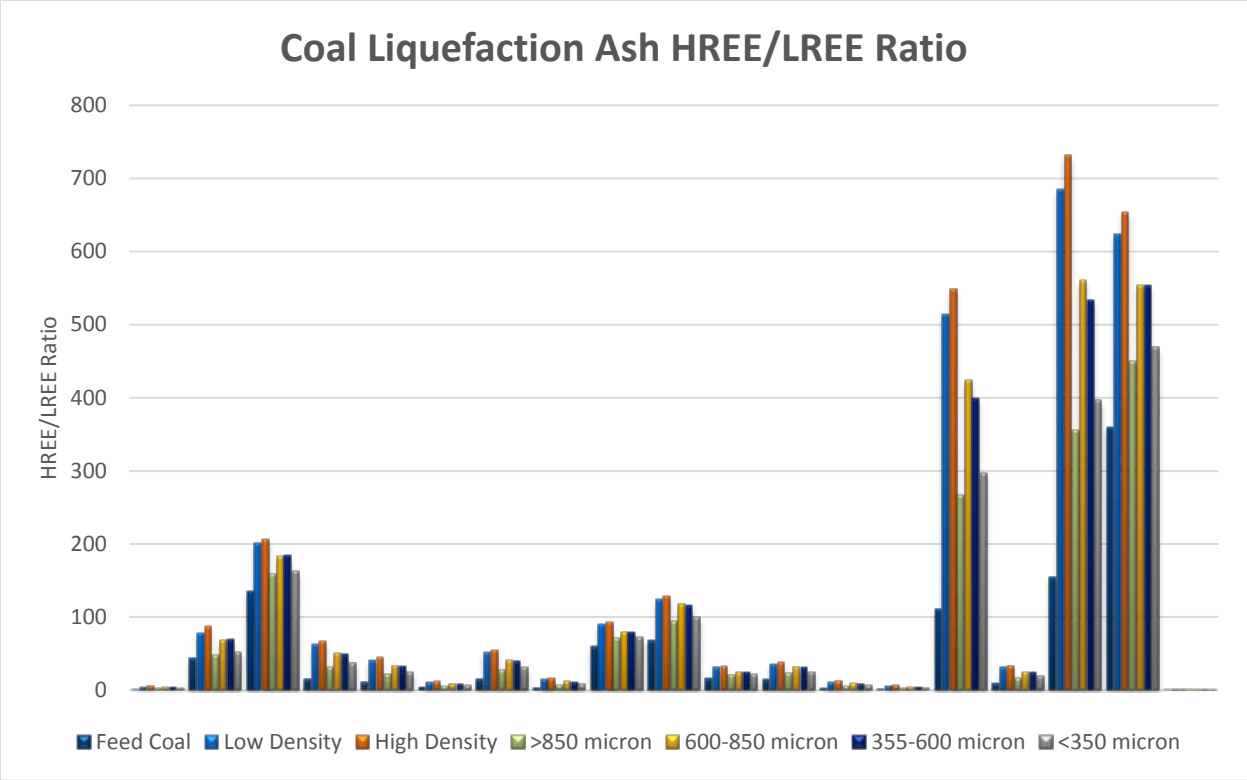

Figure 2: Ratio of heavy to light REE in the coal liquefaction ash treatments.

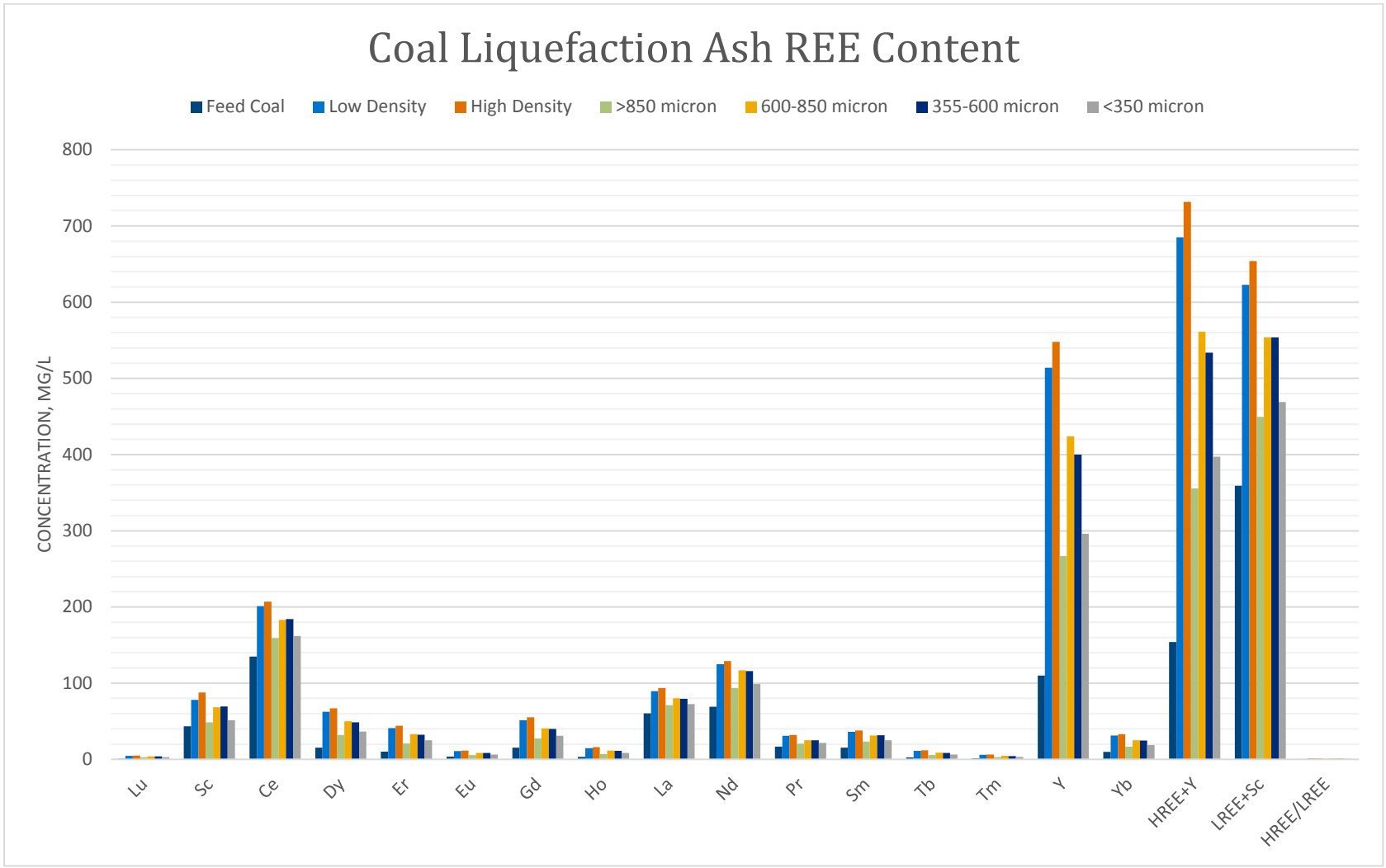

Figure 3: Chart of REE concentrations in the feed coal, density cuts and particle size cuts for coal liquefaction ash.

2.4 Key Findings from Different Coal Sources

Pulverized coal combustion, fluidized bed combustion, and liquefaction ashes experience progressively lower temperatures in their processing. To understand how these temperatures affect the phases present in the ashes, coal was ashed in a lab furnace at 1,200 °C and 800 °C to conceptually represent PCC ash and FBC ash in a controlled environment. The key differences in the different coal processing steps analyzed and considered are oxidative environments, where the higher temperature ashes have experienced a more aggressive oxidation, and the liquefaction ash is largely un-oxidized as evidenced by the presence of iron sulfide grains. The furnace ash samples are morphologically different from operating plant fly ashes (jagged opposed to spherical), likely since the furnace ash can sinter and is influenced physically by neighboring particles, whereas the fly ash cools while suspended in air. There did not appear to be a change in the form of rare earth compounds between 800 °C and 1,200 °C ash. In the samples analyzed, Yttrium appeared more prevalent in the 800 °C. However, the sampling was not statistically rigorous, so we cannot positively comment on a change of Yttrium form in the 1,200 °C sample.

X-ray diffraction was performed on the samples to understand how crystallography changed between different ash treatments, with the expectation that crystallography changes may provide insight into leachability. Starting from the same Middle Kittanning Ohio Coal source, samples were liquefied, heated at 800 °C and at 1,200 °C in a furnace, to generate a controlled comparison between treatments that generate the ash which will be fed to Battelle's process. The crystallography results are summarized in Figure 4. Notable changes include the apparent conversion of pyrite to pyrrhotite and an amorphous iron phase in the coal liquefaction process. Also, overall crystallinity of the ash increased between 800 °C and 1,200 °C, where the expectation was for an increase in the vitrified, amorphous phases at higher temperatures. It appears that instead, the aluminum and silica changed to a mullite phase, which is a refractory phase that would also resist acid leaching.

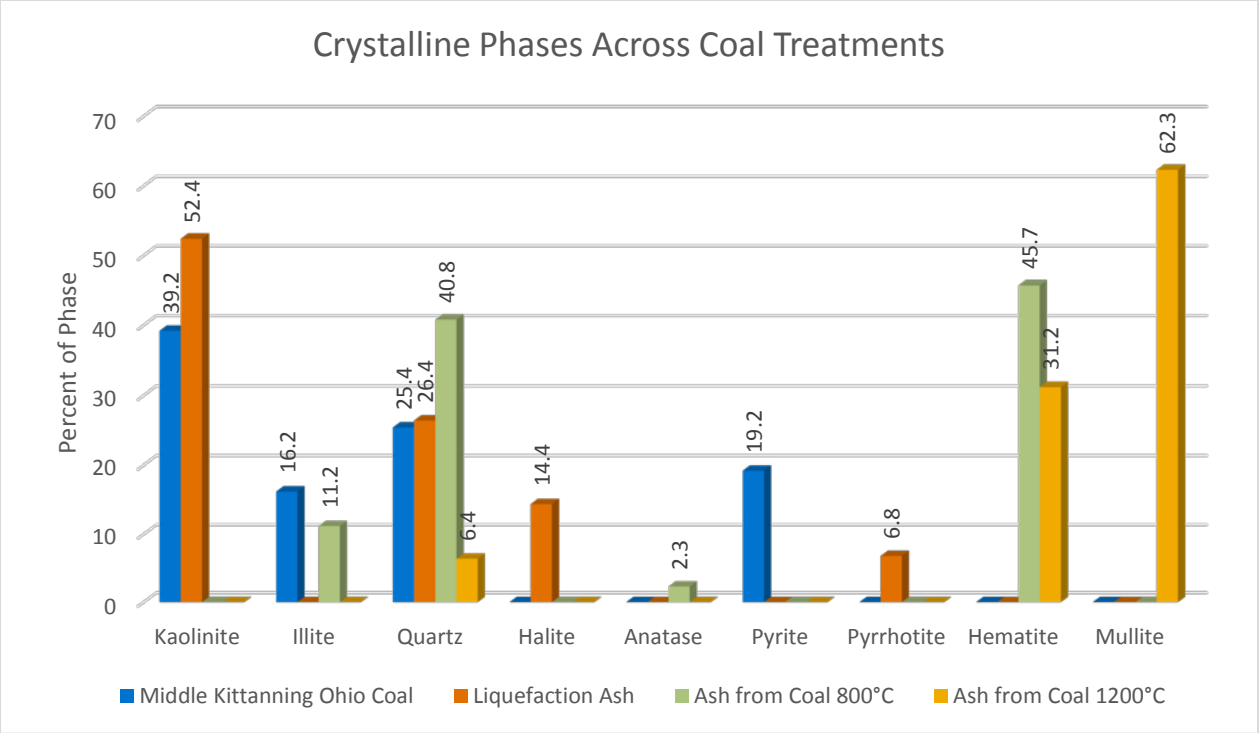

Sample	% Crystalline	Kaolinite	Illite	Quartz	Halite	Anatase	Pyrite	Pyrrhotite	Hematite	Mullite
Middle Kittanning Ohio Coal	5.0	39.2	16.2	25.4	0.0	0.0	19.2	0.0	0.0	0.0
Liquefaction Ash	7.1	52.4	0.0	26.4	14.4	0.0	0.0	6.8	0.0	0.0
Ash from Coal 800 °C	34.6	0.0	11.2	40.8	0.0	2.3	0.0	0.0	45.7	0.0
Ash from Coal 1200 °C	41.6	0.0	0.0	6.4	0.0	0.0	0.0	0.0	31.2	62.3

Figure 4: Identified crystalline phases across coal ashing treatments, beginning with Ohio Middle Kittanning Coal.

2.5 Material Values

To decide which feedstock to pursue with Battelle's ADP, prices (see Table 6) were assigned to key REE compounds as well as a few other elements that showed potentially high values. These prices are for pure, metallic elements, unless otherwise indicated, and although they do not necessarily reflect the latest market values, are helpful in comparing feedstocks. Using the elemental analyses for 26 tested samples (excluding NIST standard runs), the value of these materials in a ton of ash was calculated, adjusting the price to a pure form by molecular weights when prices were reported for an oxide or carbonate.

Table 6: Representative prices for pure metal forms (unless noted otherwise) of elements of interest. Data from http://mineralprices.com/ (Accessed 14 April 2016)

Element	Price	Unit
La	7	$/kg
Ce	7	$/kg
Pr	85	$/kg
Nd	60	$/kg
Sm	7	$/kg
Eu	150	$/kg
Gd	55	$/kg
Tb	550	$/kg
Dy	350	$/kg
Er	95	$/kg
Y	35	$/kg
Sc	15,000	$/kg
Sb	9.92	$/kg
Bi	27.34	$/kg
Cd	1.94	$/kg
Co	22.99	$/kg
Mg	1.99	$/kg
Mn	1.63	$/kg
Mo	13.23	$/kg
Se	57.32	$/kg
W (WO3)	4.99	$/kg
U (U3O8)	80.47	$/kg
V (V2O5)	48.72	$/kg
Cu	7.80	$/kg
Sn	14.66	$/kg
Ni	8.61	$/kg
Ag	553.10	$/kg
Li_2CO_3	5	$/kg*

*http://fortune.com/2016/06/06/lithium-price-tesla-metal-future/

As illustrated in Figure 5, Scandium dominates the material values, representing roughly 91% of the value of materials within the ash. Vanadium accounts for 3.4% of the value, which is greater than any of the rare earths other than Scandium, and Lithium contributes nearly as much value as Neodymium. Scandium, Vanadium, Yttrium, and Lithium are expected to be leachable at least in part by nitric acid and are candidates going forward as byproducts to subsidize rare earth element recovery from coal ash. Scandium should be considered as a primary product in the process due to its value. It is primarily used as an alloying compound with aluminum to make high performance, lightweight alloys and increased production may serve to increase the

potential applications and, consequently, the currently small market. Vanadium is also used largely as an alloying compound to strengthen steel but is also useful as a catalyst. Lithium is currently in high demand for the manufacture of lithium ion batteries, which are enabling for many green technologies as well as consumer electronics. Cobalt is also used in battery electrodes as a catalyst and in many high performance alloys and magnets. Vanadium, Lithium, and Cobalt recovery will be evaluated for feasibility in subsequent tasks as the process is developed.

The average and median concentrations for these compounds in the 26 samples analyzed are compared to over 3,000 samples from the USGS CoalQual database in Table 7, and indicate that the values observed in Battelle's testing are representative, supporting the conclusion that these byproducts are likely to be available in other ash streams. The CoalQual samples are from Ohio, Pennsylvania, West Virginia, and Kentucky and were converted to an ash basis for this comparison.

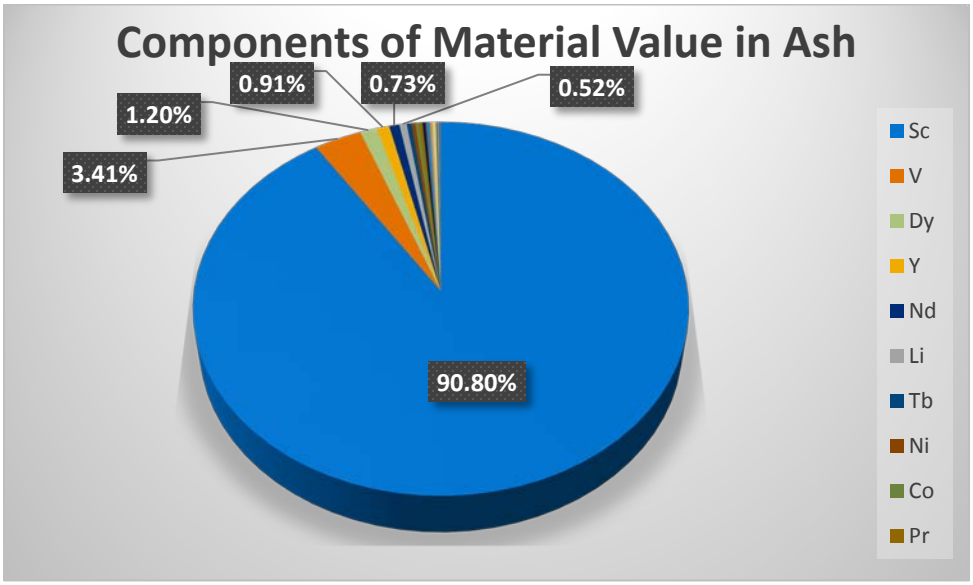

Figure 5: Components of the average material value in the measured ash samples. Scandium and Vanadium values both represented more than the rare earth elements, and are candidates for byproducts to subsidize the REE recovery.

Table 7: Comparison of Battelle's sample analyses to USGS CoalQual database values for byproducts of interest in coal ash.

		Co	Li	Ni	Sc	V	Y
CoalQual	Average	79.61	149.52	187.31	39.08	201.26	83.56
	Median	50.40	130.13	130.27	34.22	179.82	70.07
Battelle Tests	Average	74.03	126.62	204.62	39.11	253.04	168.10
	Median	43.00	123.00	110.00	35.80	265.50	106.50

Within the rare earth elements in coal, Dysprosium represents the highest value, as shown in Figure 6. Combined with Neodymium, Terbium, and Praseodymium, these four elements

account for over 75% of the rare earth element value in the ash. Accordingly, Battelle's Acid Digestion Process has and will be tailored to focus on these rare earth components.

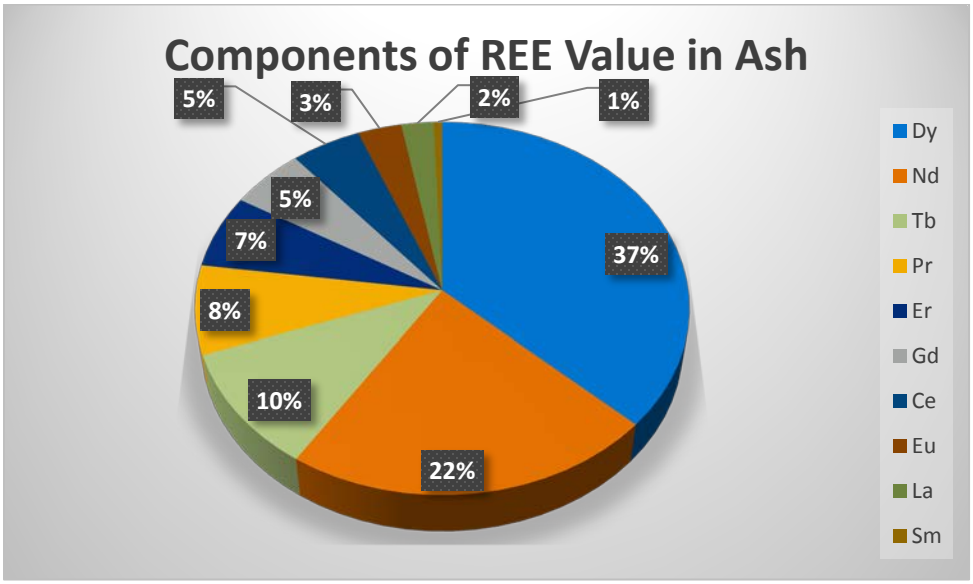

Figure 6: REE value components in the coal ash samples analyzed by Battelle.

2.6 Conclusions

Based on the analytical results, the feasibility study focused on PCC Plant A fly ash as a feedstock for Battelle's ADP. The PCC Plant A fly ash has:

- a higher Total REE+Y+Sc concentration than all other operating plant ashes sampled, at 545 ppm +/- 13.4 ppm
- a high HREE/LREE ratio at 0.37 +/- 0.008
- significant amounts of Scandium (36 ppm +/- 1.4 ppm), Vanadium (279 ppm +/- 12 ppm), Yttrium (104 ppm +/- 5.3 ppm), Cobalt (44 ppm +/- 2.5 ppm), and Lithium (~166 ppm), which can be valuable process byproducts with robust market outlets.

Although the coal liquefaction ash had a greater concentration of heavy rare earths, there is some risk for implementation since the liquefaction process is not yet commercial.

3.0 Laboratory Testing

3.1 Introduction

Laboratory testing of the ADP was performed before and after the project's GO/NO GO decision point. Testing done before the project's GO/NO GO decision with the funding groups is described in this report as the feasibility testing, and was done to support the original feasibility study. More details on this testing and the feasibility study are provided in Appendix B.

Prior to the commencement of testing after the GO/NO GO, a plan was developed to ensure that key results for leaching parameters, calorimetry, and product recovery would be statistically valid and defensible. This test plan is available as Appendix C. Beyond this test plan, some preliminary tests were performed to investigate options to improve process performance. In particular, options were tested to improve the REE leaching efficiency, generate a catalyst and adsorbent support product from the caustic pretreatment step, and enhance product quality with solvent extraction. The detailed laboratory testing report is provided in Appendix D.

The leaching efficiency tests included grinding, ball milling, thermal shock to the ash, and pre-treatment with caustic solution. The solvent extraction tests investigated selectivity for metals extraction with pH, and selectivity for metals stripping with pH, acid concentration, and acid type. The catalyst support product testing investigated how a zeolite type product may be generated from the ash pretreatment solution.

3.2 Feasibility Testing

3.2.1 Preliminary Leaching Studies

3.2.1.1 Pulverized Coal Combustion Ash

Tests on PCC ash were performed at multiple nitric acid concentrations: 17%, 34%, 51%, and 68%. It has been Battelle's experience that nitric acid concentrations above 34% can cause passivation of iron materials, reducing leaching efficiency, and this reduction was also observed using PCC sources. Table 8 describes the leaching efficiency for each rare earth element according to starting acid concentration. The table demonstrates the reduced leaching efficiency at higher acid concentrations, which is likely due to passivation of the bulk aluminum and iron phases preventing further leaching. Aluminum and iron leach efficiency averaged 11.5% and 6.1%, respectively, in the 17% and 34% acid concentrations, compared to 3.4% and 2.4% and 51% and 68% acid concentrations, respectively, supporting this hypothesis. The last column in the table indicates the best leaching efficiencies achieved in the preliminary testing, which was after milling of the ash to break up vitrified sections, and which were used in the technoeconomic assessment. Milling was performed in a ball mill, and caused reduction of particle sizes from 10-100 µm to 1-40 µm as indicated in Figure 7. These particles sizes provide an indication of the level of milling that would be required in the full scale plant.

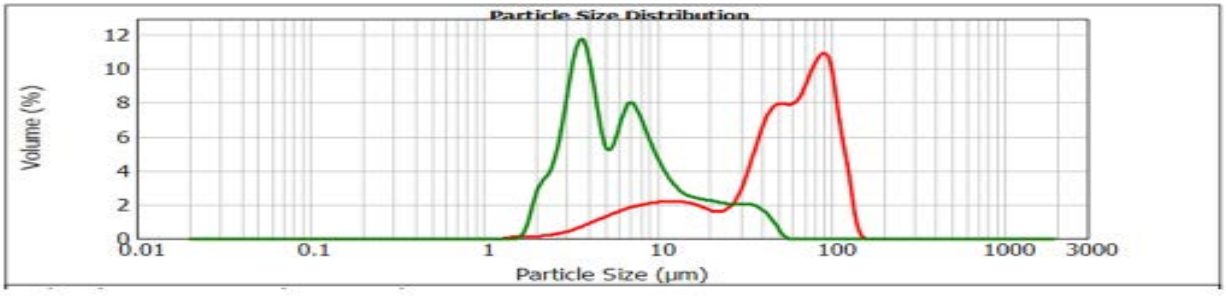

Figure 7: Particle size distributions for PCC ash before (red line) and after (green line) wet ball milling

Table 8: Leaching efficiencies for rare earth elements and starting acid concentrations for the leach.

Element	Starting Nitric Acid Concentration in PCC Fly Ash Leaches						
	17%	17%	17%	34%	51%	68%	34% (milled)
Sc	19.2%	20.8%	21.5%	21.5%	N/A	N/A	55.3%
Y	24.6%	26.7%	28.0%	28.0%	14.9%	13.0%	46.9%
La	19.0%	19.3%	20.0%	19.0%	9.9%	8.2%	35.4%
Ce	21.0%	21.5%	21.7%	27.0%	11.9%	9.9%	34.0%
Pr	20.3%	21.7%	22.4%	22.9%	11.6%	10.0%	36.3%
Nd	20.8%	22.6%	23.4%	23.9%	12.3%	10.5%	39.5%
Sm	22.5%	24.0%	25.0%	25.4%	13.7%	11.8%	40.5%
Eu	22.7%	24.5%	25.4%	26.4%	14.8%	12.7%	42.4%
Gd	25.0%	27.2%	28.5%	28.8%	15.7%	13.7%	45.2%
Tb	23.3%	25.5%	26.9%	28.1%	15.4%	13.4%	44.3%
Dy	24.1%	26.2%	27.6%	28.6%	15.5%	13.0%	41.9%
Ho	24.6%	26.8%	28.0%	28.6%	15.2%	13.3%	41.8%
Er	23.8%	26.2%	27.5%	27.8%	14.8%	12.6%	43.8%
Tm	23.0%	25.2%	26.4%	26.9%	14.4%	12.0%	42.2%
Yb	21.2%	23.1%	24.7%	24.8%	12.9%	10.6%	36.3%
Lu	21.2%	22.6%	23.9%	24.3%	13.0%	10.2%	34.6%

Besides leaching efficiency, selectivity for REE will also affect overall product economics. The percent of REE leached compared to all measured elements (59 elements were analyzed for in the leach solutions) were compared for each test, and results are shown in Table 9. These results suggest that high concentration leaches are more selective, but beyond 34%, seemed to have reduced REE leaching efficiency. There are several strategies for enhancing the purity of the mixed REE concentrate, many of which will be discussed in later sections. It is expected that this number can be improved by selective roasting of the solution, removing bulk iron and aluminum phases, and pre-washing of the material, removing a lot of the calcium and other water soluble salts that would otherwise consume acid in the process.

Table 9: Percent of REE in all 59 measured elements by leach concentration, indicating selectivity of the leaches.

Test Concentration	REE+Y+Sc out of all measured solutes
17%	0.24%
17%	0.24%
17%	0.22%
34%	0.33%
51%	0.31%
68%	0.34%
34% (milled)	0.27%

Leached and roasted fly ash was also tested preliminarily for pozzolanic activity. The leached ash is heated to convert nitrate salts to oxides and evaporate nitric acid, leaving it dry, acid free, and compatible as a pozzolan material. Figure 8 shows coupons prepared with leached and unleached fly ash from the ADP process, which were tested and suggested that leaching did not affect pozzolanic activity. Coupon A was made with leached fly ash, B with unleached fly ash, and C without any fly ash addition. The compressive strength tests, following ASTM method C39/C39M for A, B, and C were 3,420 psi, 3,420 psi, and 3,250 psi, respectively, suggesting that leaching fly ash does not affect pozzolanic activity.

Figure 8: Coupons prepared for preliminary testing of pozzolanic activity in leached ash.

3.2.1.2 Fluidized Bed Combustor Ash

The fluidized bed combustor ash was run multiple times with 17% nitric acid, and exhibited higher leach efficiencies for REE than PCC ash, as indicated in Table 10. However, the selectivity was significantly lower, as shown in Table 11. The improved efficiency is likely due to the lower furnace temperatures in a fluidized bed combustor, which leads to less vitrification of the ash, providing better access to the REE for the acid leach solution. The reduced selectivity is also likely impacted by reduced vitrification, but also the high calcium concentration in the ash, which is typically acid soluble and 'dilutes' the rare earth elements in calcium. Fluidized bed combustor ash was not pursued further in testing due to its much lower availability than PCC ash (PCC plants represent 90% of coal power capacity (IEA Clean Coal Centre, 2013)) and complications with calcium concentrations.

Table 10: Leaching efficiencies by element in the FBC leaching tests, note that cells marked N/A were below detection limits in the analysis.

Element	Starting Nitric Acid Concentration in FBC Leach Tests		
	17%	17%	17%
Sc	N/A	N/A	N/A
Y	37.4%	38.6%	37.9%
La	68.0%	71.7%	70.6%
Ce	62.5%	65.9%	63.7%
Pr	69.2%	73.7%	71.2%
Nd	62.5%	64.6%	62.2%
Sm	65.9%	70.7%	67.9%
Eu	62.8%	66.4%	62.6%
Gd	63.1%	66.2%	63.6%
Tb	56.0%	58.2%	64.4%
Dy	55.2%	59.5%	57.9%
Ho	46.2%	49.8%	46.4%
Er	47.8%	48.9%	46.0%
Tm	38.3%	40.7%	39.5%
Yb	42.3%	42.2%	41.2%
Lu	N/A	N/A	N/A

Table 11: Percent of REE in all 59 measured elements in FBC leach tests, indicating selectivity of the leaches.

Concentration	REE+Y+Sc out of all measured solutes
17%	0.051%
17%	0.051%
17%	0.051%

3.2.1.3 Coal Liquefaction Residual Material

Residual material from the 1 ton per day (tpd)direct coal liquefaction pilot plant was leached with nitric acid to determine whether the acid digestion process could be applied to this material. Results for two trials at 17% nitric acid concentration are presented in Table 12. Leaching efficiency was significantly less than either the PCC or FBC ash, and there are a couple possible reasons. The liquefaction residual material contains a large amount of carbon, which is likely blocking access of the leach solution to the mineral portion containing rare earth elements. Additionally, the carbon-laden material was less dense than the leach solution, which created difficulties in obtaining good mixing within the round bottom flask used for leaching. To establish whether the carbon residual was impacting the leaching results, a sample was ashed at 500 °C to remove carbon, and leached with nitric acid. This sample realized an overall REE+Y+Sc

leaching efficiency of 66%, which suggests that the carbon must be removed from the liquefaction residual to treat it effectively with the acid digestion process.

Table 12: Leaching efficiencies by element in the liquefaction residual material leaching tests, note that cells marked N/A were below detection limits in the analysis.

Concentration	Starting Nitric Acid Concentration in Liquefaction Residual Leach Tests	
	17%	17%
Sc	N/A	N/A
Y	3.4%	3.0%
La	13.9%	13.5%
Ce	13.2%	10.5%
Pr	10.2%	7.9%
Nd	8.5%	7.7%
Sm	11.0%	8.7%
Eu	N/A	N/A
Gd	8.9%	6.5%
Tb	N/A	N/A
Dy	3.1%	1.9%
Ho	N/A	N/A
Er	3.3%	N/A
Tm	N/A	N/A
Yb	5.0%	3.7%
Lu	N/A	N/A

3.2.2 Preliminary Purification Studies

It is projected that with only thermal processing and water washes to remove iron, aluminum, calcium, magnesium, sodium, and potassium, the purity of the REE solution can be upgraded to 3-5%. However, an additional upgrading of the solution is required even before feeding to a final purification/separation step such as solvent extraction. Preliminary tests were performed to understand what options for pre-purification would be viable for the product and are described in this section.

Initial tests were done for selective extraction of REE using a commercial extractant, CYANEX 572, which is specifically designed for application to rare earth elements. Leach solution was adjusted to between pH 1 and 1.5 with sodium carbonate solution prior to the extraction, which was done with an extractant of 15wt% CYANEX 572 and balance SOLVENT 467 aliphatic diluent. The extractant was combined with leach solution at an extractant to aqueous ratio of 1:4, and shaken for 20 minutes to remove REE. Extraction of heavy REE was better than light REE, however recovery of light REE was low, indicating that pH should be elevated for better extraction. Table 13 shows the extraction percent by REE. It is expected that this extraction will omit most mono- and divalent metals, and results suggest it omitted aluminum as well. However, the mass balance calculations were inconclusive, with many base metals showing an increase in the extracted solution after contact; additional replicates are needed to make a final conclusion. If negative mass balance calculations are assumed to be non-extraction, as expected, then the primary contaminants were iron (91% extracted) and titanium (99.8% extracted).

Table 13: Percent extraction by 15% CYANEX 572 at a starting pH of 1.0-1.5. *Scandium was below detection limits in the analysis, so removal is at least 47%.

Element	Percent Extracted
Sc	47.16%*
Y	85.35%
La	None Observed
Ce	None Observed
Pr	None Observed
Nd	None Observed
Sm	None Observed
Eu	None Observed
Gd	None Observed
Tb	25.60%
Dy	55.30%
Ho	74.86%
Er	88.63%
Tm	97.47%
Yb	98.79%
Lu	98.59%

Selective precipitation tests were conducted by pH change, and indicated that titanium could be precipitated with minimal effort. A pH change from 1.5 to 2.5 reduced titanium concentrations from 12,900 µg/L to 1,790 µg/L (86% reduction). With removal of titanium by pH adjustment, recovery of all REE with the higher pH extraction, and prior iron removal by the roasting step, the purity of the extracted REE would be roughly 50%, and indicates these combined steps are a promising approach for pre-purification of the REE solution.

3.3 Leaching Efficiency Improvement Testing

The following preliminary tests were run to investigate which method was the most efficient for REE leaching. Pulverized coal combustion (PCC) plant fly ash was used for all the tests:

1. High Temperature Leaching: testing of temperature effects on total leach efficiency of PCC fly ash at different concentrations of nitric acid
2. Comminution: grinding and ball milling of PCC fly ash, along with combined milling and leaching
3. Thermal Shock: leaching of PCC fly ash after thermal shock at different conditions
4. Caustic Pretreatment: leaching of PCC fly ash after pretreatment with different concentrations of sodium hydroxide solution

Caustic pretreatment proved to be the most effective means to improve leaching efficiency, and so is reported in detail, while the others are omitted for brevity. Details those not discussed in this report can be found in the Phase 1 Lab Testing Report, included as Appendix D.

The caustic pretreatment will leach silica and alumina from ash particles giving better access to the rare earth elements in the acid leaching step. Six tests were performed. The caustic solution used was sodium hydroxide, and three different concentrations were tested (10%, 5%, and 1% sodium hydroxide) at two different temperatures (20 °C and 90 °C). Every pretreatment was done with a residence time of one hour, and unmilled PCC Fly Ash as starting material. After pretreatment, leaching with 34% nitric acid was performed at 90 °C with a residence time of 30 minutes. After leaching, a sample was taken for analysis of scandium via Inductively Coupled Plasma Optical Emission Spectrometry (ICP-OES) through a Battelle method. After the first round of testing, an extra test was done using milled PCC Fly Ash as starting material with 10% sodium hydroxide solution at 90 °C for one hour. See Table 14 for conditions and results for each test. Based on the results of these tests (% of scandium leached), a decision was made to proceed with 10% sodium hydroxide solution at 90 °C for one hour on milled fly ash as the pretreatment method.

Table 14 - Test conditions and results for caustic pretreatment follow by acid leaching

Test	Concentration of sodium hydroxide (w/w)	Caustic Temperature/Reaction time	Concentration of nitric acid	Acid Leach Temperature/Reaction time	Scandium % leached
1	10%	20 °C / 1 hour	34%	90 °C / 30 min	23.17%
2	10%	90 °C / 1 hour	34%	90 °C / 30 min	54.27%
3	5%	20 °C / 1 hour	34%	90 °C / 30 min	23.05%
4	5%	90 °C / 1 hour	34%	90 °C / 30 min	38.08%
5	1%	20 °C / 1 hour	34%	90 °C / 30 min	23.40%
6	1%	90 °C / 1 hour	34%	90 °C / 30 min	21.77%
Extra	10% (milled ash)	90 °C / 1 hour	34%	90 °C / 30 min	88.21%

3.4 Product Roasting Investigation

After pretreatment of fly ash, the REE was extracted with nitric acid solution. The acid digestion leads to formation of nitrate salts with the general molecule formula $M(NO_3)_x$, where $M(Al^{3+}$, Si^{2+}, Sc^{3+}, Eu^{3+}…) is the cation extracted from fly ash and X is the valence: +1 (for Na, K,..), +2 (Ca, Mg, Sr,..) and +3 (Ce, La, Cu, Fe, Al, Si,..). The thermal decomposition of nitrate salts $M(NO_3)_x$ will lead to metal oxides, which can be insoluble in water.

Based on the ICP analysis of fly ash, we selected representative nitrate elements to briefly study their decomposition at different temperatures. Each selected element was dissolved in deionized (DI) water, dried at temperature below 90 °C (to remove the water) then calcined in a box furnace. The calcined material is leached in DI water and inspected visually for solubility. Presence of residual solids indicated the decomposition of the selected element at the designated temperature. Table 15 reports the decomposition temperature range of each compound.

Table 15: Approximate thermal decomposition temperatures for selected nitrates

Compound	Approximate decomposition temperature range (°C)
$Fe(NO_3)_3$	100-150
$Al(NO_3)_3$	100-150
$Ce(NO_3)_3$	200-300
$Dy(NO_3)_3$	200-300
$Sc(NO_3)_3$	200-300
$Nd(NO_3)_3$	200-300
$La(NO_3)_3$	200-300
$Ca(NO_3)_2$	>450
$NaNO_3$	>450

Thermal decomposition was then performed on blended nitrate streams. Table 16 reports the selected precursors, the amount of each precursor, calculated amount of each element and the concentration of each element. The resulting mixture was dissolved in DI water under strong stirring to promote dissolution, then a heating lamp was used to evaporate water gently (During drying the temperature at solution surface was between 70 °C and 90 °C). After this step, the solid material was subject to cyclical treatments that consist of:

- dissolution in water,
- filtration,
- dry under heating lamp, and,
- heat treatment in a box furnace at different temperatures.

Table 16: Model blended nitrate solution composition

Compound	Salt (g)	Metal (g)	Element (wt%)
$NaNO_3$	5.76	1.558	20
$Al(NO_3)_3 \cdot 9H_2O$	16.24	1.169	15
$Ca(NO_3)_2 \cdot 4H_2O$	11.50	1.948	25
$Fe(NO_3)_3 \cdot 9H_2O$	11.27	1.558	20
$La(NO_3)_3 \cdot 6H_2O$	1.21	0.390	5
$Nd(NO_3)_3 \cdot 6H_2O$	1.18	0.390	5
$Dy(NO_3)_3 \cdot xH_2O$	0.84	0.390	5
$Sc(NO_3)_3 \cdot xH_2O$	2.00	0.390	5
Total	50.00	7.791	100

Table 17 reports the Energy Dispersive Spectroscopy (EDS) analysis of the sample produced from the roasting process. Iron and aluminum nitrates can decompose at temperature between 100 °C to 200 °C, REE nitrates decomposed at temperature between 300 °C and 400 °C and sodium and calcium nitrates require temperature above 400 °C to decompose. This result suggests that separation between iron, aluminum, and REE can be achieved by controlling the temperature of calcination of the dried nitrate solution.

Table 17: Energy Dispersive Spectroscopy analytical results for residues of blended nitrates after calcining at selected temperatures. Results are in molar percent, and highlighted cells indicate key components of each fraction.

Element	100°C (no filtration)	100°C - 200°C	300°C	400°C (insoluble)	400°C (soluble)
Dy	1.5%	0.0%	10.1%	9.9%	0.1%
Al	7.0%	20.2%	24.2%	4.7%	0.1%
Sc	2.3%	4.6%	10.2%	0.2%	1.0%
La	2.1%	0.0%	2.0%	16.7%	1.1%
Nd	2.4%	0.0%	6.9%	39.7%	0.0%
Fe	10.6%	39.7%	8.1%	2.9%	0.0%
O	46.1%	32.5%	35.5%	21.0%	50.5%
N	11.2%	2.5%	1.9%	2.5%	15.9%
Na	7.4%	0.4%	0.6%	1.1%	3.6%
Ca	9.2%	0.0%	0.6%	1.3%	27.7%
Si	0.0%	0.1%	0.0%	0.0%	0.0%

Based on testing results from the model compounds, tests were performed on leachate from fly ash. One hundred (100) grams of fly ash was leached in nitric acid for 24 hours, then the slurry was filtered via 0.22-micron filter. The fraction of dissolved material was 11.5% without any pretreatment of ash. This residual material was subject to several cycles of dissolution in DI water, filtration, drying and heat treatment at different temperatures. The goal is to collect the material that decomposed to an insoluble oxide following each heat treatment; however, the amount of material recovered on the filter was difficult to evaluate. Ultimately, the dissolved material obtained from acid leaching was treated at a single temperature of 200 °C.

Due to low resolution of EDS for trace elements, the solids and water leach solutions were also analyzed by ICP-MS after treatment at 200 °C. Figure 9 and Figure 10 report the % distribution of each element in the two fractions. The distribution of element “E” is calculated as follow:

- % (E) in residual material = $\frac{mass(E) in\ residual}{mass\ (E)\ in\ reisual + mass\ of\ (E)\ in\ solution} * 100$
- % (E) in solution = 100-%(E) in residual

Figure 9 suggests that most of the REE nitrates produced by leaching of fly ash in nitric acid solution are not decomposed to oxides after 200 °C heat treatment. However, most of the aluminum and iron decomposed to oxides, therefore, they can be separated from the REE. This result is in good correlation with charge density theory. Around 70% of scandium is converted to oxide at 200 °C, and it is anticipated that additional scandium can be recovered at a lower roasting temperature.

Figure 10 shows the % distribution for the other elements between the water leach and residual solids. It illustrates that most of the titanium, vanadium, chromium, niobium, molybdenum, indium, tin, tungsten, and antimony nitrates decompose to insoluble oxide and therefore can be separated from REE. Other elements such as manganese, gallium, and lead decomposed partially to insoluble oxides. These preliminary results show that roasting can be used to separate REE from many other elements. More work is required to optimize the process temperature and recover additional scandium.

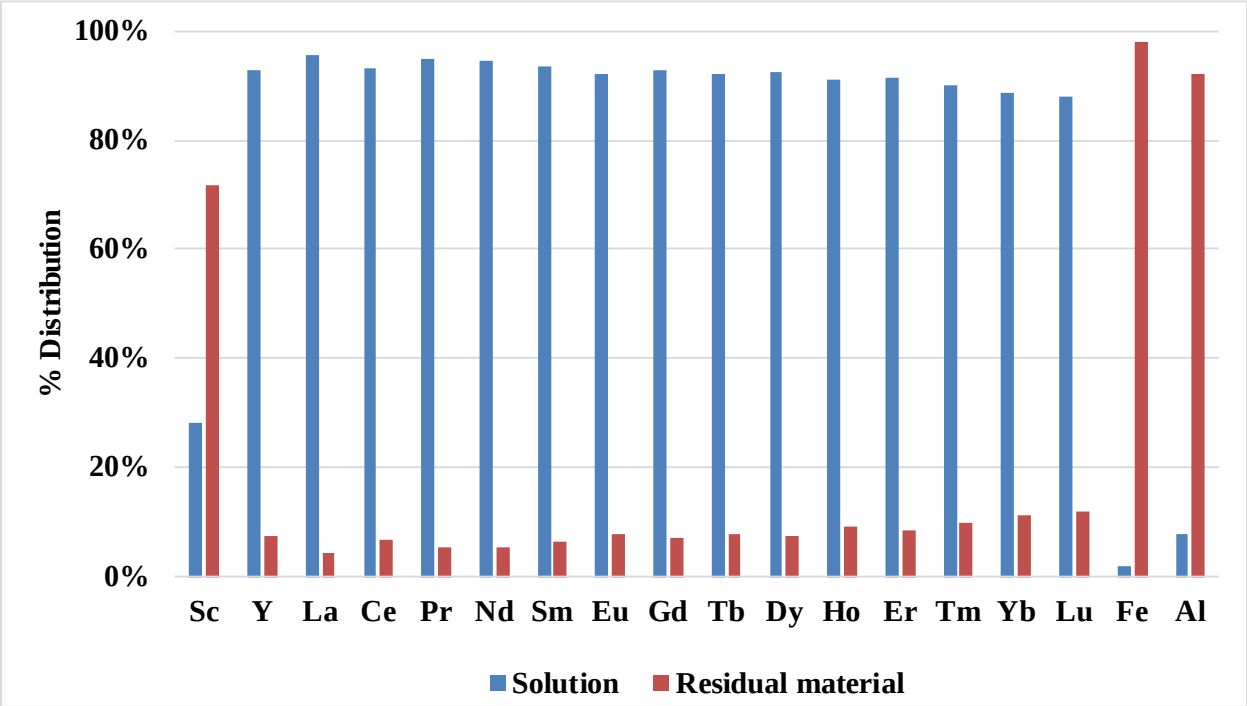

Figure 9: Distribution of REE+Y+Sc in solution and in residual material after treatment at 200 °C and then leaching with DI water. Recovery of REE+Y was high in the water wash, while iron, aluminum, and scandium were preferentially found in the solid residual material.

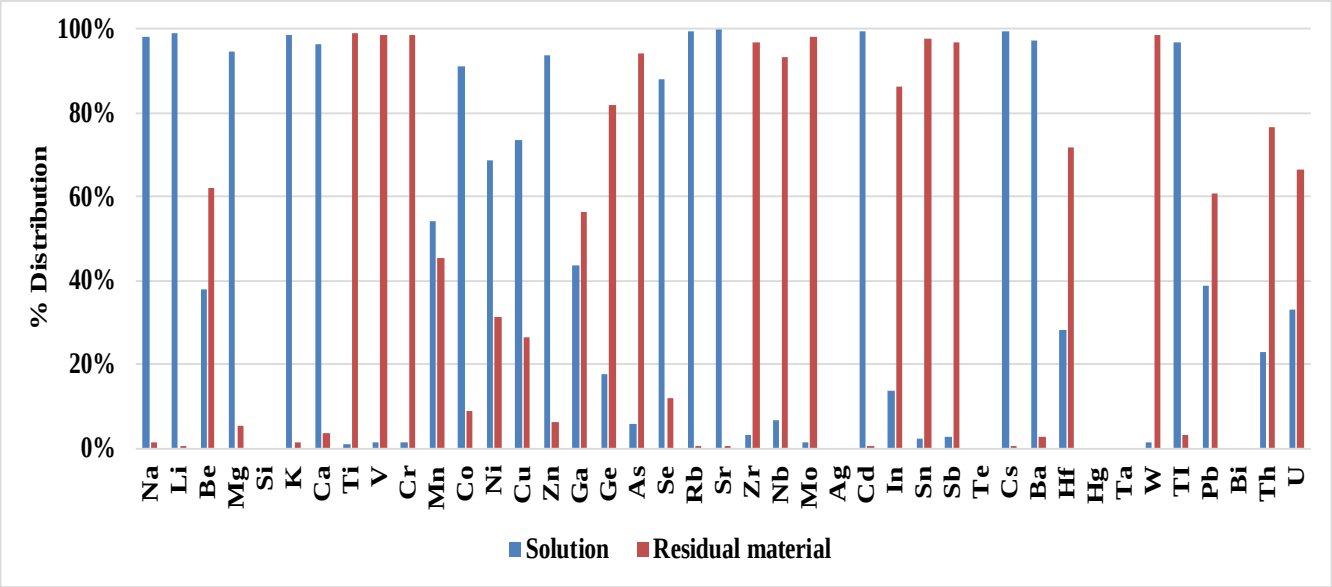

Figure 10: Distribution of other elements in solution and in residual material after treatment at 200°C and then leaching with DI water.

Table 18 summarizes the total REE distribution in the solution and the residual solid material. Total REE represents 1.2 wt% of the elements detected by ICP-MS in the aqueous solution, suggesting nearly a 1.2 wt% purity on a solid basis. This is over a 20x increase in REE purity over the fly ash starting material with a concentration of approximately 545 ppm REE. Recovery of total REE was 90% across the roasting process.

Table 18: Weight percent total REE in solution and remaining in the residual solids, indicating good separation by thermal roasting of the leach solution.

	Solution	Residual material
Total REE + Sc + Y	90.0%	10.0%
REE+Y+Sc out of total measured	1.20%	0.10%

3.5 Solvent Extraction Upgrading Tests

In order to upgrade the rare earth element concentration after leaching, solvent extraction will be used for removal of monovalent and divalent cations along with select transition metals. The preliminary laboratory tests were run to investigate the concentration of rare earth that can be achieved. Additional details can be found in the laboratory testing report (Appendix D). Two sets of tests were run:

1. Extraction of rare earth elements from rare earth loaded leach solution at different pHs.
2. Stripping of rare earth elements using different acids and concentrations for the stripping solution.

CYANEX 572 was used for solvent extraction experiments. CYANEX 572 is a phosphorus based chelating extractant formulated for the extraction and purification of rare earth elements. It has an extraction strength profile which allows efficient extraction of the heavy rare earth

elements while allowing the back extraction / stripping operation to utilize lower strip acid concentrations (Cytec, 2017). The concentration used for the extraction testing was 15% CYANEX 572 in SOLVENT 467 diluent.

Extraction tests used leach solution from fly ash, which was dried using a heating lap (about 150 °C). Then, dry material was leached in DI water (250 ml). Table 19 shows the percent recovery after DI water leaching. Residual material is the solid material that didn't dissolve after DI water leaching. Loaded solution is the solution used for extraction testing. From these results, it can be concluded that the residual material is rich in iron as was predicted and observed in the roasting experiments.

Table 19 – Percent recoveries of rare earths, iron, alumina, and silica after DI water leaching of dry material at 150 °C. Also, purity or selectivity of rare earth calculations as stated.

Species	% Recovery	
	Loaded Solution	Residual material
Sc	43.4%	56.63%
Y	86.7%	13.32%
La	84.7%	15.31%
Ce	77.8%	22.17%
Pr	87.2%	12.78%
Nd	88.3%	11.69%
Sm	87.4%	12.62%
Eu	87.9%	12.11%
Gd	88.0%	11.99%
Tb	86.2%	13.79%
Dy	86.7%	13.28%
Ho	87.2%	12.78%
Er	87.5%	12.50%
Tm	85.6%	14.40%
Yb	83.9%	16.08%
Lu	82.0%	18.02%
Fe	1.9%	98.09%
Al	28.4%	71.61%
Si	25.3%	74.69%
REE+Y+Sc out of total REE+Y+Sc Available	80.5%	19.46%
REE+Y+Sc out of total measured species (purity or selectivity)	0.49%	0.08%

For extraction testing, the loaded solution was adjusted to different pHs (See Table 20). Some key points should be explained regarding the analysis of these results. For the calculation of percent recovery in the extractant (organic phase), a mass balance was performed using the results from ICP-MS analysis done on the aqueous phase after extraction and the solution

loaded from leaching and roasting runs. Also, a negative mass in extractant was calculated for some species due to analytical error, so any negative mass calculated was assumed to be zero. Furthermore, some results obtained from ICP-MS analysis were below detection limits. Consequently, calculations were performed using the given detection limits. Table 20 shows the percent recoveries of rare earth elements and other species in the extractant after extraction of the solution at different pH. Also, this table shows the purity or selectivity at different pH.

Table 20 - Percent recoveries of rare earths, iron, alumina, and silica after extraction at different pH. Also, purity or selectivity of rare earth calculations as stated.

Species		% Recovery						
		pH 1.03	pH 2.04	pH 2.51	pH 3.34	pH 4.01	pH 4.48	pH 4.99
Rare Earth Elements	Sc	60.0%	90.00%	90.00%	50.00%	98.00%	60.00%	98.00%
	Y	68.4%	99.79%	99.78%	99.78%	99.88%	99.98%	100.00%
	La	0.0%	0.00%	0.00%	0.00%	72.02%	86.86%	98.28%
	Ce	0.0%	11.75%	7.43%	23.74%	95.23%	98.62%	99.90%
	Pr	0.0%	2.39%	5.41%	44.90%	97.20%	99.25%	99.95%
	Nd	0.0%	14.09%	18.21%	61.51%	98.12%	99.47%	99.97%
	Sm	0.0%	79.28%	82.87%	95.43%	99.70%	99.89%	100.00%
	Eu	0.0%	91.43%	92.91%	98.15%	99.81%	99.80%	99.99%
	Gd	0.0%	92.40%	94.07%	97.68%	99.77%	99.93%	100.00%
	Tb	0.0%	98.09%	98.27%	99.08%	99.83%	99.69%	99.98%
	Dy	31.2%	99.49%	99.57%	99.67%	99.89%	99.95%	100.00%
	Ho	51.4%	99.73%	99.74%	99.70%	99.90%	99.76%	99.99%
	Er	74.4%	99.58%	99.60%	99.67%	99.90%	99.91%	100.00%
	Tm	91.5%	99.83%	99.83%	99.15%	99.90%	99.32%	99.97%
	Yb	97.2%	99.95%	99.95%	99.85%	99.91%	99.88%	99.99%
	Lu	97.4%	99.77%	99.77%	98.84%	99.88%	99.07%	99.95%
Base Metals	Fe	89.6%	97.39%	97.39%	86.95%	99.48%	89.56%	99.48%
	Al	7.1%	0.00%	0.00%	0.80%	98.80%	99.47%	99.97%
	Si	60.0%	90.00%	90.00%	50.00%	98.00%	60.00%	98.00%
REE+Y+Sc out of total REE+Y+Sc Available		24.4%	50.88%	50.90%	60.98%	95.14%	95.93%	99.66%
REE+Y+Sc out of total measured species (purity or selectivity)[1]		1.37%	4.18%	4.19%	7.15%	0.88%	1.04%	1.04%
REE+Y+Sc out of total measured species excluding Silica (purity or selectivity)		2.11%	18.45%	18.76%	18.51%	0.97%	1.12%	1.17%

The highest selectivity, of rare earth elements was achieved when extraction was performed at a pH of 3.34. Purity at this pH was 7.15%, and recovery was 60.98% as shown in Table 20. The recovery was lower compared to the recovery at higher pH (4.01, 4.48, and 4.99). Even though at higher pH the recovery was better, selectivity was lower because at higher pH, other species would extract stronger as well. Also, a selectivity calculation excluding silica was done since

detection limits for silica were very high (between 4,000 and 200,000 µg/L), and solubility of silica in the nitric acid leach solution is expected to be very low.

The percent of each element stripped from the loaded extractant was calculated by mass balance for each of the conditions tested. In the first batch of tests where the extractant was loaded at pH 2.5, stripping was done with hydrochloric acid adjusted to pH levels measured by pH strips. The results are shown in Table 20. Results for scandium were below detection limits and could not be accurately calculated. The results suggest that most of the REE can be stripped at pH 1.0, and at high recoveries at pH 0.5. However, at pH 0.5 there will likely be contamination from iron and aluminum that are not removed in the roasting step. Thorium and Uranium can be excluded from the REE strip solution at pH 0.5. Strippability appears to decrease as the atomic number of the REE increases, with exception of yttrium, which behaves more similarly to the heavier rare earth elements.

Table 21 contains results for stripping done in various high strength acid mixtures. These tests were intended to remove challenging elements such as iron, scandium, uranium, and thorium. Scandium analytical results were generally below detection limits, and the mass balance could not be completed accurately. Sodium metabisulfite addition did not appear to help in stripping. Stripping for many metals appears to decrease from two to three molar hydrochloric acid solution, suggesting a change in the form of the ions. Uranium was not strongly stripped in any of the solutions, but thorium was in the hydrochloric/oxalic acid solution. Stripping in a basic solution of 10% sodium hydroxide or sodium carbonate removed 57% and 50% of the uranium, respectively, and may be used to scrub uranium from the extractant.

Table 21: Percent stripped results of key elements in hydrochloric acid solutions at different starting pH.

Percent Stripped for Key Elements at Different pH Levels						
Species	**pH 3.0**	**pH 2.5**	**pH 2.0**	**pH 1.6**	**pH 1.0**	**pH 0.5**
Sc	N/A	N/A	N/A	N/A	N/A	N/A
Y	0.0%	0.3%	0.1%	0.9%	23.0%	81.6%
La	19.4%	52.9%	81.0%	41.3%	38.0%	39.7%
Ce	5.0%	38.5%	83.9%	79.9%	82.1%	85.0%
Pr	2.8%	25.5%	80.0%	83.0%	86.8%	88.9%
Nd	1.7%	18.3%	72.6%	84.4%	89.0%	91.5%
Sm	0.1%	1.0%	18.7%	68.7%	93.0%	95.6%
Eu	0.2%	0.4%	8.7%	52.7%	88.7%	97.9%
Gd	0.1%	0.4%	6.5%	42.9%	89.2%	97.1%
Tb	0.2%	0.2%	1.3%	11.8%	72.0%	96.4%
Dy	0.0%	0.2%	0.4%	4.5%	50.6%	94.8%
Ho	0.2%	0.3%	0.2%	2.1%	35.8%	92.8%
Er	0.1%	0.4%	0.2%	0.6%	18.5%	88.9%
Tm	0.5%	0.6%	0.5%	0.5%	6.8%	77.0%
Yb	0.1%	0.7%	0.1%	0.2%	2.5%	58.5%
Lu	0.6%	0.7%	0.6%	0.6%	1.8%	41.3%
Fe	0.8%	2.5%	0.8%	0.8%	0.9%	71.4%
Al	0.4%	5.9%	17.6%	4.1%	6.8%	10.5%
Th	1.2%	1.6%	0.4%	0.7%	0.0%	0.0%
U	0.1%	0.1%	0.1%	0.1%	0.0%	0.0%

Table 22: Percent stripped results of key elements in various high strength acid solutions.

Percent Stripped for Key Elements in Different Stripping Solutions							
Species	**1 M HCl**	**1 M HCl + Sodium metabisulfite**	**2 M HCl**	**3 M HCl**	**5%:5% HCl:Oxalic acid**	**5%:5% HNO_3:H_3PO_4**	**10% H_2SO_4**
Sc	N/A	N/A	N/A	N/A	N/A	N/A	N/A
Y	84.7%	77.0%	88.2%	84.4%	88.9%	88.8%	85.2%
La **Ce** **Pr** **Nd** **Sm**	Were not Extracted into the Organic Phase						
Eu	100.0%	100.0%	100.0%	100.0%	100.0%	100.0%	100.0%
Gd	100.0%	100.0%	100.0%	100.0%	100.0%	100.0%	100.0%
Tb	100.0%	93.3%	100.0%	100.0%	100.0%	100.0%	100.0%
Dy	98.7%	88.9%	100.0%	97.4%	100.0%	100.0%	99.9%
Ho	93.6%	83.7%	97.8%	92.4%	100.0%	99.1%	93.6%
Er	91.3%	81.2%	94.8%	92.0%	96.8%	95.6%	89.5%
Tm	91.0%	81.4%	96.2%	93.9%	95.6%	93.3%	88.1%
Yb	89.2%	78.3%	97.0%	94.4%	98.8%	87.5%	90.1%
Lu	83.1%	71.7%	93.1%	90.3%	93.6%	76.5%	85.4%
Fe	69.6%	59.4%	93.6%	93.9%	90.7%	93.2%	84.4%
Al	81.5%	74.7%	85.0%	47.3%	100.0%	100.0%	100.0%
Th	0.2%	0.2%	0.7%	5.1%	84.3%	17.8%	47.7%
U	0.5%	0.4%	1.8%	4.6%	2.9%	3.8%	4.2%

3.6 Zeolite Production Testing

Based on extractability testing, the process for REE extraction from fly ash will include milling, caustic leaching, then acid leaching. To offset the cost of caustic pretreatment, we investigated the possibility of generating an aluminosilicate byproduct from the loaded caustic leach solution. In this testing, we demonstrated that it is possible to recover silicon and aluminum from caustic solution. Initial precipitates from the solution were amorphous, but it appears from XRD spectra that zeolite can be formed on the fly ash with incubation. Figure 11 shows the XRD profile of the product produced by treatment of fly ash in 2 M NaOH solution for 24 hours at temperature of 110 ^{o}C. It shows the loss of the broad hump between 16° and 36° 2θ (observed in raw fly ash XRD profile), suggesting conversion of amorphous phases during the hydrothermal treatment. The zeolitic phase produced has the formulation (Na3.6Al3.6Si12. 4O32:14H2O).

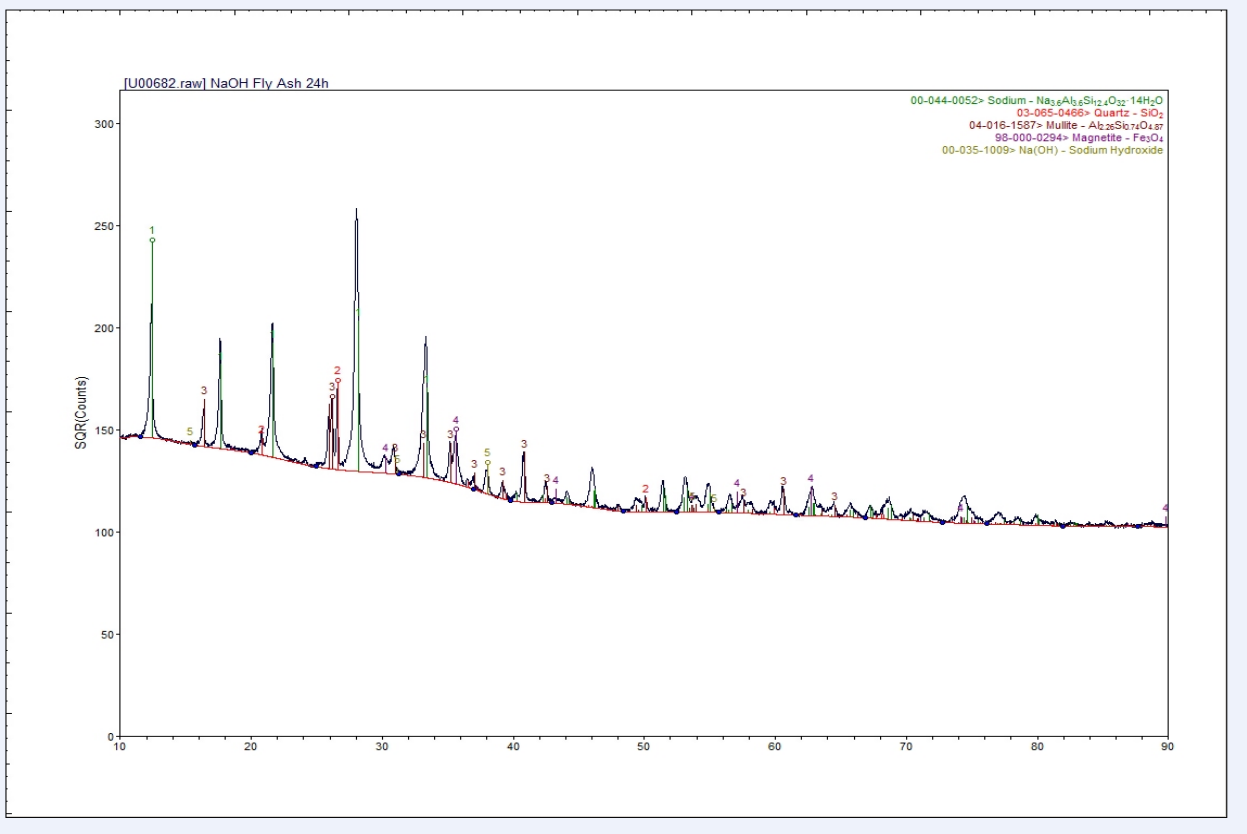

Figure 11: XRD results of product synthesis from treatment of fly ash with sodium hydroxide solution.

A two-step process was also investigated to generate a zeolite of higher value since the fly ash impurities would be excluded, allowing it to be usable in more applications and sold at a higher price. This type of process is supported by Hollman, et. al (Hollman, Steenbruggen, & Janssen-Jurkovicova, 1999). The conditions were selected to more closely mirror the pretreatments used in Battelle's process. One hundred (100) grams of fly ash were leached in 500 ml of 2.5 M NaOH solution at 90 ^{o}C for 1 hour. After filtration, trace amounts of HZSM5 powder (<0.1 mg) were dropped in 20 ml of the filtrate and placed in a 25 ml Teflon coated autoclave at 110 $^{\circ}$C for 48 hours. After cooling the reactor, the solution was filtered and residual material (around 10 mg) was analyzed by XRD and SEM. Table 21 reports the silica and alumina ratios in fly ash and the dissolved amount in caustic solution. The SiO_2/Al_2O_3 ratio is around 6.5. The XRD profile indicates that the deposited material is composed of vishnevite zeolite;

$KNa_{6.8}Al_6(SiO_2)6(SO_4)$ $(H_2O)_2$ with a mole ratio of Si/Al = 6.0. The XRD/SEM data (Figure 12 and Figure 13) show the needed crystal structure of the fly ash derived zeolite.

Table 23: Silica and alumina ratios present in the fly ash and in the caustic leachate solution as measured during zeolite experimentation.

Material	Element	wt%	Molar Ratio Si/Al	Molar Ratio SiO_2/Al_2O_3
Fly Ash	Al	13	2.1	3.3
	Si	22		
Caustic Leach Solution	Al	3.1	3.3	6.5
	Si	10.6		

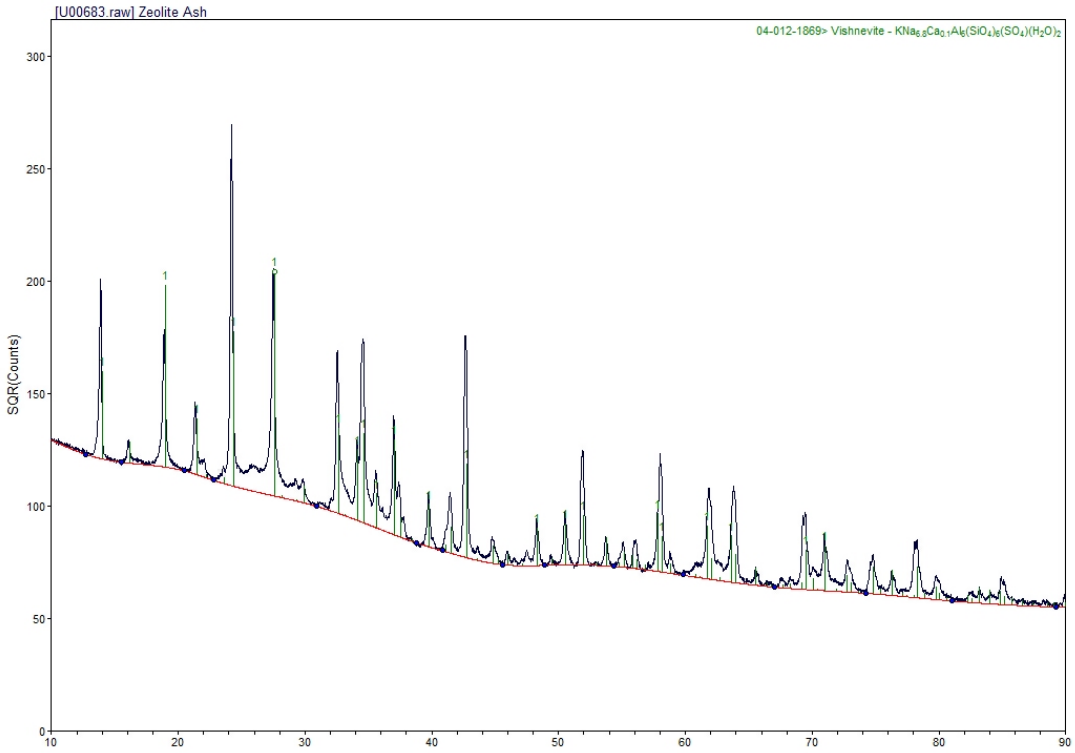

Figure 12: XRD of fly ash zeolite produced from hydrothermal treatment of filtered caustic solution that was contacted with fly ash for one hours at 90 °C.

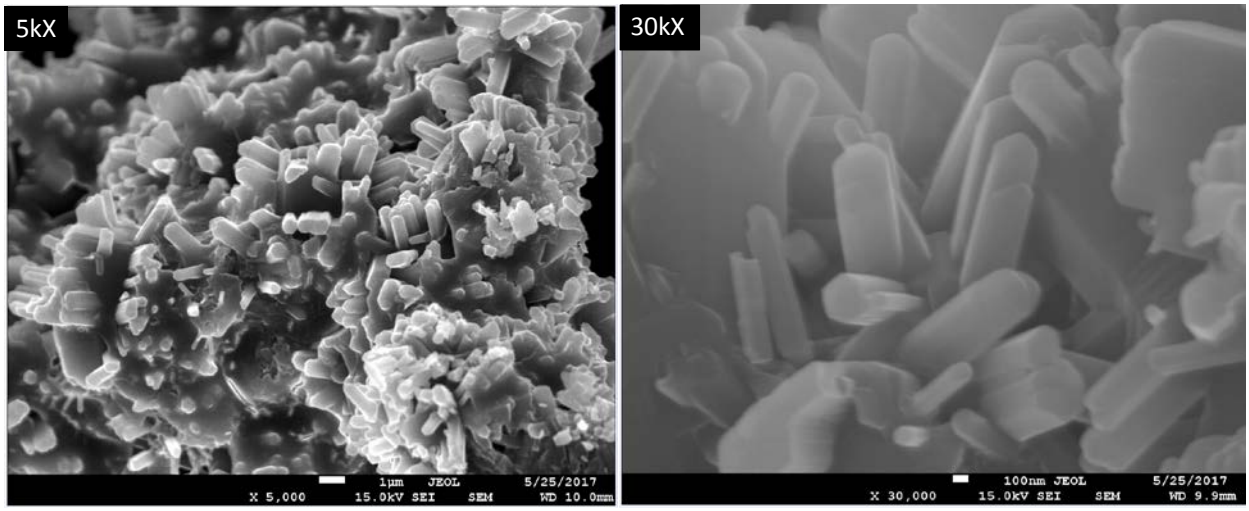

Figure 13: SEM of fly ash zeolite produced from hydrothermal treatment of filtered caustic solution that was contacted with fly ash for one hours at 90 °C.

This preliminary investigation shows that it is possible to prepare zeolite from caustic solution while residual material can be used for extraction of REE. However, more work is required to optimize the zeolite synthesis process such that the zeolite has strong market applications.

3.7 Calorimetry Testing

Calorimetry was run on milled ash and milled and caustic pretreated ash to understand how much heat the acid leaching reaction will generate. The milled and caustic leached samples were run in triplicate, with results shown in Table 22. The average heat of reaction was 101.85 calories per gram of ash feed, with a standard of deviation of 0.69 calories per gram.

Table 24: Calorimetry results for milled and caustic leached fly ash in nitric acid.

Sample ID	Δ T	T	Q (cal)	ΔH (cal/g)
Caustic Ash #1	0.4333	24.456	50.57	101.14
Caustic Ash #2	0.4365	19.567	50.95	101.89
Caustic Ash #3	0.4392	19.755	51.26	102.52

3.8 Parametric Leaching Tests

Results of Battelle's previous leaching tests and analysis of similar leaching processes indicate that for a given ash particle size and porosity, the efficiency of REE recovery is likely to be affected by four factors: (1) leaching time, (2) leaching temperature, (3) nitric acid concentration, and (4) acid freshness (function of number of times acid was used and concentration of dissolved reaction products). The influence of these factors was evaluated using a design of experiments approach, specifically the Box-Behnken surface response method (Box & Behnken, 1960). The design of experiment was used to maximize two types of process outcomes: (1) leaching efficiency, and (2) value of the extracted REE material. The leaching efficiency was defined as the fraction of REE element(s) that was extracted from the feed ash. The value of extracted REE material was defined as a total value of REE metal oxides extracted per unit mass of ash. Both quantities are appropriate measures of the REE recovery process and its economics.

Table 23 lists the leaching results obtained from the 27 tests in the design of experiment. All used ash that was milled to 4.5-micron average particle size, then leached in 10% sodium hydroxide solution for 1 hour at 90 °C. The leaching efficiency was determined using concentrations of specific elements (Sc, Y, REE) detected in the acid solutions after leaching, compared to the total amounts of these elements in the ash. The concentration of Sc was determined by two methods: (1) the ICP-MS method carried out by Activation Laboratories, and (2) an ICP-OES method at Battelle. Concentration of all other elements was determined by the ICP-MS method. The average REE+Y+Sc leaching efficiencies were calculated as a weighted average; weighted by the elemental concentrations of REE+Y+Sc in the feed ash. Some of the leaching efficiencies, reported in Table 23, are larger than the theoretical efficiency limit of 100%. This effect is caused by errors in measurements of both the leached element concentrations and the amounts of elements available in ash. The efficiencies exceeding 100 % were detected using the ICP-MS method, suggesting that this method carries an inherent error. The efficiency measurements based on the ICP-OES method were all below 100%. The total value of oxides extracted was calculated using the concentrations of leached elements and market prices of their oxides from mineralprices.com, accessed in December of 2016.

Table 25: Results obtained during the 27 leaching experiments. Note that the experiments were carried out in random order which was different from the order presented here.

Test number	Experimental Results			
	Sc leaching efficiency ICP-MS (%)	Sc leaching efficiency ICP-OES (%)	REE+Y+Sc average weighted leaching efficiency (%)	Total value of oxides extracted ($/metric ton)
1	68.00	46.62	58.13	187.15
2	89.27	65.27	81.08	245.30
3	117.25	71.01	91.05	321.34
4	152.35	83.35	111.26	416.02
5	110.62	77.93	91.25	303.37
6	117.40	82.09	103.21	323.52
7	88.64	72.82	77.49	244.38
8	87.22	76.44	77.18	240.89
9	72.86	59.52	68.10	201.45
10	104.45	68.78	92.04	287.84
11	134.02	77.01	105.40	366.65
12	90.09	79.84	86.84	249.96
13	81.54	78.50	73.15	225.26
14	116.15	65.29	88.76	317.76
15	135.44	86.58	112.56	372.18
16	99.70	79.56	82.46	274.32
17	78.71	74.24	79.04	219.04
18	67.93	56.96	59.75	187.60
19	108.49	81.47	99.45	299.86
20	71.90	74.60	72.19	198.51
21	104.6	68.94	89.41	287.72
22	94.88	68.43	85.63	261.99
23	107.43	76.23	88.02	294.55
24	139.55	78.07	109.09	382.26
25	98.63	75.98	100.45	271.80
26	79.70	70.80	77.48	221.05
27	87.36	69.24	79.46	241.52

Since scandium represents the highest value element within coal ash, it can be used as a simple proxy for REE leaching and economic recovery. Based on analysis from the design of experiment results, optimal leaching parameters for scandium were found, and suggest that 94% of scandium can be leached with a leaching time of 25 minutes in 34% nitric acid at 90 °C.

4.0 Process Design

4.1 Summary

Section 4.0 summarizes the design of a 12.5 pound per hour integrated bench scale pilot system for recovery of REE from coal fly ash. It includes the design basis, equipment list, mass and energy balances, and drawings for an integrated process testing system that will validate the process operation in the pending Phase 2 of work.

4.2 Process Description

4.2.1 Pretreatment and Aluminosilicate Byproduct Generation

The pretreatment begins with a milling step, which breaks down the ash particulates from a median particle size of 55 µm to 4.5 µm. This size reduction is intended to provide better access to the particle for leaching, and should be doable in a jet mill or stirred media mill. For the bench scale pilot unit, a jet mill has been preliminarily selected for the comminution operation.

Once the ash has been milled, it is treated with a sodium hydroxide solution to remove some of the silica and alumina present in the ash. This provides better access to REE in the acid leaching step. Lab testing suggested that one hour of leaching in 10% sodium hydroxide solution at 90 °C is sufficient to liberate REE in the acid step, and these parameters will be refined in the next phase of testing. The ash is filtered out of the caustic solution, and rinsed with water to remove entrained caustic before proceeding to the acid leaching section.

The caustic solution is loaded with silicate and aluminate, which can be precipitated into zeolite material. The exact conditions for zeolite precipitation are still being developed, but after the leach solution has been recycled several times, it will be taken for zeolite recovery. For this recovery step, it is assumed that neutralization of the solution will be required. Neutralization is done with nitric acid, which will produce a neutral pH sodium nitrate solution that could be used in agriculture for fertilizer. There are other means of zeolite production which may require temperature and aging of the solution, or use of a zeolite scaffold to generate the most useful form. The water rinse solution may also be used for precipitation of aluminosilicates.

4.2.2 Acid Leaching

After the pretreatment and zeolite production step, the ash is fed to the Acid Digestion Process and mixed with a dilute nitric acid stream (approximately 34 wt.%) before being pumped through a heater to an elevated, sub-boiling temperature, and into the leaching reactor. The leaching temperature is expected to be 90 °C. Within the reactor, mixing causes intimate contact of the ash with the nitric acid, allowing the REEs to be dissolved into the nitric acid solution. Selectivity for the rare earth elements is higher than that for iron, aluminum, and silicon in the ash, causing enrichment of the REE in the leach solution over the ash. The leach reactor is expected to be a continuously stirred tank reactor, with an average residence time of 25-30 minutes.

4.2.3 Acid Recovery and Product Generation

After the leach reaction, the ash is filtered out in a vacuum drum filter and transferred to an ash drying operation. The ash dryer is important for economic recovery of REE since the high temperatures will boil off and convert any entrained nitrates, allowing them to be recovered in the system. Additionally, this drying step prevents the discharge of nitrates from the ash

wherever it is used or stored. The ash dryer is planned to be a rotary-type drum dryer, heated to a temperature of 155 °C, and is indirectly heated to minimize costs associated with off-gas treatment. It is expected that the leaching operation will increase the surface area of the ash while removing some surface contaminants, which will improve the pozzolanic activity of the ash and make it ideal for use in cements. The leachate, containing unreacted nitric acid, is recycled to the reactor to ensure complete utilization of the acid fed to the process.

Off gases from the process, made up of nitric acid with NOx components, are swept with an air stream, and fed along with the REE-loaded leachate into a roasting operation. The roaster will operate in two steps, the first to concentrate the slurry, and the second to crystallize the rare-earth salts. The concentration step will use a conventional evaporation unit heated to 120 °C, while the crystallization step will be done in a spray dryer, reaching temperatures high enough (approximately 155 °C) to convert metal nitrates to oxides. By roasting the metal nitrate salts to dryness and then to a temperature around 155 °C, many non-rare earth metal salts are converted to metal oxides, releasing NOx gases, which are swept along with other process off-gases to the absorption column. Rare earth nitrates, however, are not converted to oxides at temperatures less than approximately 400 °C, and will therefore remain in their nitrate salt form (Stern, 1972). This step provides a water soluble rare earth concentrate, enriched in rare earth materials, suitable for feed to a hydrometallurgical process to separate and purify the rare earth elements.

As discussed, all off-gases of the process, consisting of nitric acid vapor and NOx gases, will flow to an absorption column system for recovery, swept to the column using excess air. Optionally, these vapors may be compressed and fed through a heat exchanger to preheat the acid feed to the roaster, then to a condenser to recover nitric acid for recycle, prior to being fed to the column. Any NO gas generated in the roaster, leaching, and ash drying processes needs to be oxidized to NO_2 prior to being absorbed back into the acid stream. This oxidation rate is improved at higher temperatures, and can occur in the drying and roasting processes with the presence of air. As the gas passes through the condenser, it is then cooled, which is preferable for the absorption of the NO_2 back into the liquid phase. Gas will flow through the absorption column in a single pass, where it is contacted with recycled nitric acid as an absorbent. The liquid recirculated in the column consists of acid recovered from the roaster. For the bench scale unit, the gases from the NOx absorption column will flow through a caustic scrubber tower to ensure no release of NOx gases. This tower will use sodium hydroxide solution to neutralize acidic gases prior to discharge. A small blowdown stream from this column is expected and will become a waste stream. The full-scale process may use other NOx control technologies than a caustic scrubber.

Nitric acid recovered in the column will be recycled back to the leach reactor to complete the acid recycle process. A small fraction of this stream will be sent to a distillation column, which will distill and separate the water-nitric acid mixture. The concentrated nitric acid recovered in the column will be recycled to the acid leaching process, while the water recovered in the distillate will be treated to a neutral pH and purged from the system. This purge ensures that a buildup of water does not occur in the process. Testing and simulation to date indicates that greater than 95% of acid (calculated as the fraction of makeup acid required verses the total acid feed requirement of the reactor) is able to be recovered through the acid roasting process and the absorption column used to recover the gas-phase nitrates. The process includes a small makeup acid stream, which feeds nitric acid to the process to maintain a constant concentration of nitric acid within the leach reactor.

4.2.4 Solvent Extraction Upgrading

In order to upgrade the REE concentrate, solvent extraction will be used for removal of monovalent and divalent cations along with select transition metals. The target is to provide a mixture of REE in solution that is of sufficient purity to enter a final separation process; it is Battelle's estimate that this purity level needs to be 90% as cations in solution. Schematically, this separation will be done in six sections after the dried REE concentrate is re-leached to liberate the nitrate salts:

1. **Extraction of the rare earth elements:** The re-leached solution of rare earth nitrates will be contacted with organic extractant to recover the rare earth elements. This step may also include a reducing agent, such as sodium metabisulfite, to reduce ferric iron to ferrous iron, which will then exclude iron from extraction. The pH of this section is carefully controlled to affect which elements are extracted and achieve good selectivity, and monovalent and divalent ions should be nearly completely excluded. However, there will be undesirable multivalent ions extracted. The aqueous phase from this section will be depleted in rare earth elements, and a waste stream.
2. **Metal pre-strip:** The organic phase from extraction will be exposed to a low concentration acid stream to remove metals that strip before the rare earth elements. This strip will include most divalent metals that may have been extracted in the first section. It will also likely remove some of the lighter, less valuable REE such as lanthanum and cerium. The aqueous from this section will also be a waste stream.
3. **REE strip**: The organic phase will then be exposed to moderately high concentration acid (near pH 0) in order to strip the REE from the extractant. This step will produce a relatively pure REE stream. This section may include a number of cross-flow stages to ensure a high purity REE concentrate for further processing.
4. **Scrub:** The organic phase will be contacted with high molarity acid solution, around 3.5 M, to remove high valent metals from the extractant. This extraction includes metals such as iron, thorium, titanium, and uranium. This aqueous stream will be a waste stream, but could also be used to recover potentially valuable materials.
5. **Scandium strip:** A slip stream of the organic effluent from the scrub section will be sent to scandium stripping. Scandium is expected to remain in the extractant after the scrub section, so it will be removed with a high pH precipitative strip. This step will cause precipitation of scandium hydroxide or potentially scandium carbonate. This precipitate will be recovered by filtration from the aqueous phase, and the aqueous phase will be recycled within the section.
6. **Water wash:** The organic phase after the scandium strip will be washed with a low ionic strength aqueous stream to remove any entrained base solution. The organic stream will then be mixed with the scrub organic effluent and recycled to the beginning of the process. The aqueous phase from this section will be a waste stream, and can be used to neutralize acidic waste streams from elsewhere in the process.

4.3 Design Drawings

4.3.1 Process Flow Diagram

Based on the conceptual process design, Battelle developed a Process Flow Diagram (PFD) of the proposed REE recovery process. Figure 14 shows the proposed PFD with pertinent stream

flows, temperatures, and pressures. The PFD will be updated to reflect any design changes made to the process during the finalization of process design task at the start of the Phase II effort. The overall process mass balance for the 12.5 lb/hr bench-scale demonstration system is shown in Table 24, while Table 25 and Table 26 show the overall energy balance (heating and cooling requirements) for the proposed system design. Detailed Piping and Instrumentation Diagrams (P&IDs) and stream tables (containing temperature, pressure, flow, and enthalpy information) can be found in Appendix H.

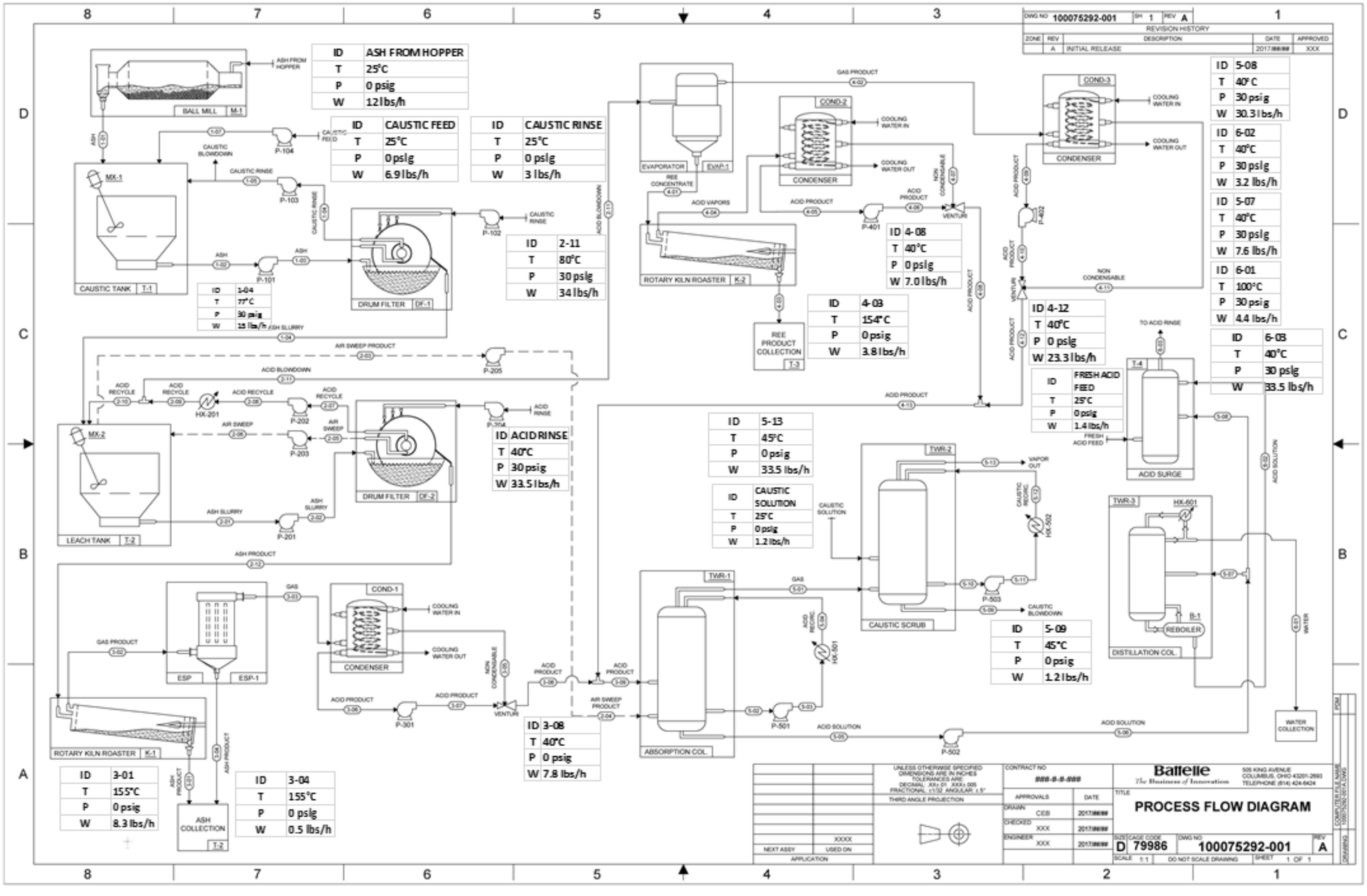

Figure 14: Preliminary PFD with pertinent stream composition.

Table 26: Mass balance for 12.5 lb/hr bench-scale process.

Feed/Product Stream	Flow Rate (lbs/hr)
Coal Fly Ash Feed (Feed)	12.09
Caustic Feed (Feed)	6.88
Caustic Rinse (Feed)	2.99
Air Sweep (Feed)	0.34
Caustic Scrubber Make-Up Solution (Feed)	1.17
Nitric Acid Feed (Feed)	2.65
"Water Blowdown" (Product)	7.03
Leached Ash from Roaster (Product)	8.90
Leached Ash from ESP (Product)	0.47
REE Product Stream (Product)	3.83
Caustic Scrubber Vapor Purge (Product)	0.37
Caustic Scrubber Blowdown (Product)	1.17
Distillation Column Water Purge (Product)	4.35

Table 27: Preliminary heat duty required for 12.5 lb/hr bench-scale process.

Unit Operation	Heat Duty (kW)
Leach Reactor Preheater	0.63
Rotary Drum Ash Dryer	2.18
Roasting Process Evaporator	6.66
Roasting Process Roaster	0.51

Table 28: Preliminary cooling duty required for 12.5 lb/hr bench-scale process.

Unit Operation	Cooling Duty (kW)
ESP Condenser	1.94
Evaporator Condenser	1.94
Roasting Process Condenser	6.63
Distillation Column Water Product HTXR	1.28
Distillation Column Acid Product HTXR	0.50

4.3.3 Space Claims/General Arrangement Drawings

Battelle obtained dimensional estimates for each major piece of equipment selected for the bench-scale system. Equipment was arranged in 3-D space to determine the optimal arrangement of equipment components not only in relation to one another on the floor space, but also in relation of the heights of the components relative to one another. Figure 15 shows the proposed general arrangement of the equipment specified to date for the bench-scale process. For clarity, component support structures and mounting hardware, process piping, and instrumentation have been eliminated from the drawing.

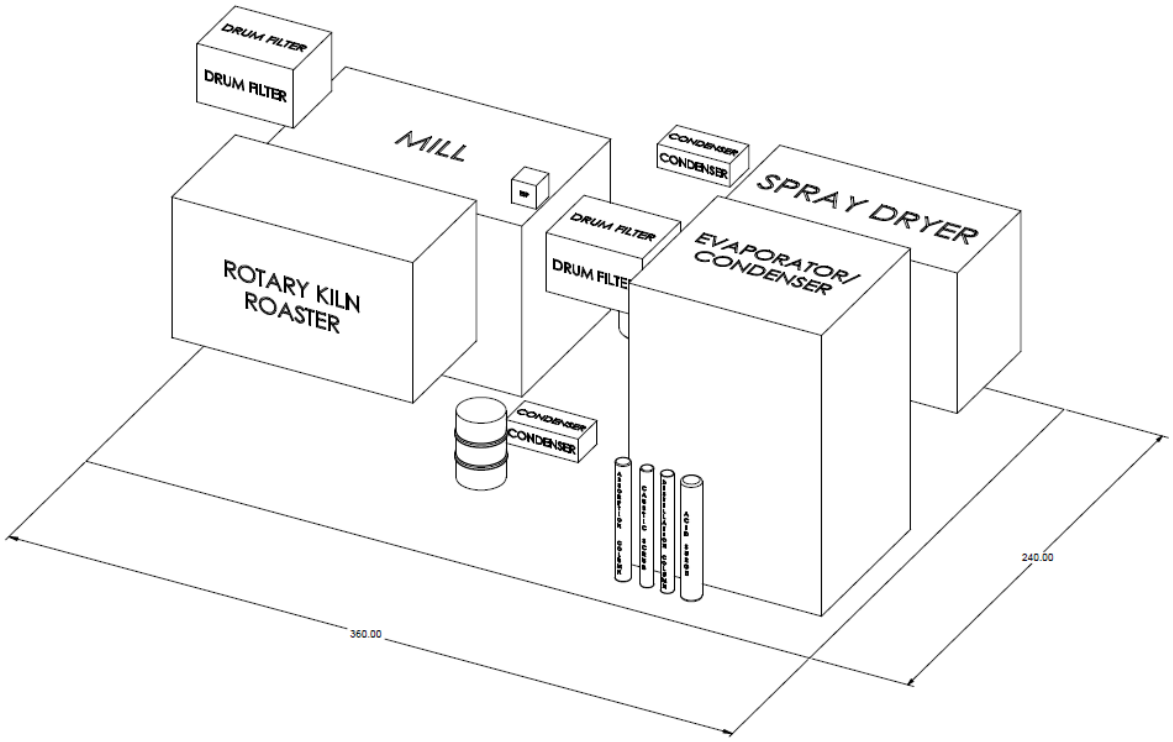

Figure 15: General arrangement drawing showing general space claim estimates for each major piece of equipment (units are in inches).

4.4 Equipment List

Battelle compiled a list of required equipment for the bench-scale demonstration unit based on the PFD and PIDs. For each piece of process equipment, the team reached out to vendors to obtain cost estimates for system components which met the requirements of the bench scale system. Table 27 shows a summary of required process equipment and instrumentation for the proposed bench-scale demonstration system. Equipment indicated with an asterisk (*) is process equipment which Battelle already has on hand, capable of being utilized for the demonstration project. Incorporating readily available equipment into the demonstration system will accelerate the procurement timeline and reduce system costs. A detailed discussion pertaining to the sizing of each major piece of process equipment can be found in Appendix H.

Table 29: Summary of required process equipment and associated purchase cost.

Equipment/Instrumentation	Quantity	Unit Price	Total Price
Mixing tank	1	$25,000	$25,000
Rotary drum filter	2	$64,485	$128,970
Electrostatic precipitator (ESP)*	1	N/A	N/A
Rotary kiln	1	$94,300	$94,300
Fluidized bed mill	1	$300,000	$300,000
Acid recovery system	1	$162,900	$162,900
Spray dryer	1	$190,000	$190,000
Condenser	2	$5,401	$10,802
Absorption column*	1	N/A	N/A
Distillation column*	1	N/A	N/A
Acid surge*	1	N/A	N/A
Caustic scrubber*	1	N/A	N/A
Thermocouples	12	$46	$560
Pressure Sensors (low temp.)	8	$161	$1,288
Pressure Sensors (high temp.)	6	$1,945	$11,670
Differential pressure sensors	4	$745	$2,981
Flowmeters (low temp.)	6	$985	$5,910
Flowmeters (high temp.)	12	$5,498	$65,974
Level Indicator/Controller	4	$540	$2,160
Pumps	14	$3,904	$54,656
Heat Exchanger - Nitric acid	1	$1,280	$1,280
Heat Exchanger - Caustic	1	$1,210	$1,210
Double gate valve - ash feed	1	$701	$701
Control valves	11	$3,302	$36,321
Eductors	3	$276	$827
Solenoid valves	2	$98	$196
Piping and Fittings	N/A	N/A	$4,500
		Total	**$1,102,206**

4.5 Environmental, Utility, and Site Requirements

Battelle evaluated the environmental, utility, and other site requirements for the proposed 12.5 lb/hour process. Due to the closed-loop nature of this bench-scale process, the environmental impacts are expected to be minimal. More than 95% of the nitric acid used in the process is recycled, which minimizes the amount which is produced as waste by the process. The primary process waste, which is a mixture of nitric acid and water, as well as spent caustic reagent from the pretreatment process is easily treated to a neutral pH and discharged as a process waste stream per Battelle site discharge permits. Similarly, for a larger pilot- or full-scale process, this stream would be treated via an on-site industrial water treatment plant. In certain scenarios, caustic reagent can be neutralized with nitric acid, creating a fertilizer which can be used in agriculture.

Gases produced within the process, primarily NOx gases, are captured in the process absorption column. This process not only allows for the bench-scale design to comply with any air pollutant permitting requirements, but also captures and converts nitrate-based gases to nitric acid capable of being recycled in the process. No other air pollutants defined in the National Ambient Air Quality Standards (NAAQS) are anticipated to be produced as part of this

project. A caustic scrubbing system will be used as a backup to the NOx regeneration system specified in the process design.

Leached ash, depleted in metal content, will be the primary solid effluent stream for the process. In a full-scale process, this leached ash may be used as a pozzolan, and it may be more desirable to place ash from the ADP versus standard power plant ash due to the expected increase in pozzolanic activity of the ash after the leach process. In regions where placement as a pozzolan is not possible, the leached ash from the ADP is expected to be less prone to leaching than traditional power plant ash due to reduced metal content. The leached ash is expected to be neutral in pH after being processed by the process ash dryer, as any remaining nitric acid will have been boiled off and recovered within the plant. For the proposed bench-scale system, the leached ash will be disposed of via a certified waste hauler, due to the relatively small (less than 7 tonnes) of ash expected to be used during testing.

Utility requirements for the proposed bench-scale process are of standard practice for bench- and pilot-scale systems. Due to the bench-scale nature, the majority of utility needs will ultimately be provided by local electrical service. Pumps, immersion heaters, heat trace, mixers, blowers, valves, and other instrumentation will be powered by standard 120 VAC, 240 VAC, or 480 VAC sources. Process cooling will be supplied through existing laboratory cooling water systems at a total rate of 3 gallons per minute (gpm) for the bench-scale process.

Additional site requirements include sufficient floor space and ceiling height for the process equipment specified for the bench-scale system. Battelle's existing facilities and laboratory spaces available will be sufficient for the purposes. Finally, fly ash storage and handling capabilities will be required to support this bench-scale demonstration. As mentioned previously, approximately 7 tonnes of ash is expected to be required throughout the demonstration. Battelle will maintain a storage facility, such that a single batch of fly ash can be obtained and used throughout the bench-scale demonstration.

5.0 Technoeconomic Assessment

5.1 Summary

The technoeconomic assessment conducted as part of the Task 3.0 feasibility study (see the report in Appendix B) was updated based on additional laboratory results and process updates, and followed the same methodology as in the feasibility study report. The CHEMCAD model originally constructed to support the TEA developed in Task 3.0 was updated to include pretreatment steps such as caustic leaching and zeolite production, and a caustic scrubber to prevent NO_x emissions. Solvent extraction and final separation/purification costs were also added in. The levelized cost of Battelle's recovery, from coal ash to salable product, is estimated to be $140 per tonne of ash fed. At this value, approximately 42% of US coal sources, if ashed, could be economically used as a feedstock to the Battelle process.

5.2 CHEMCAD Model Updates

Based upon the laboratory testing results, the CHEMCAD process model was updated to reflect changes. Notably, the pretreatment step was added, a caustic scrubber operation was incorporated, and leaching efficiencies were updated.

The pretreatment involves addition of sodium hydroxide solution to a recycle solution stream, mixing with milled ash, and heating to 90 °C. A stoichiometric reactor converts silica and alumina to sodium silicates and aluminates, according to a user inputted conversion factor (10%

in this case). The ash and caustic, aluminate, and silicate solution are separated in a filter, with most of the solution recycled. A small blowdown stream maintains mass in the recycle, and fresh caustic is fed to keep 10% sodium hydroxide solution in the system. The ash is washed in three stages on the filter, and the caustic blowdown solution and wash water are combined for aluminosilicate recovery. The ash continues to the leaching reactor. The model assumes, conservatively, that nitric acid will be needed to neutralize the aluminate/silicate solution to generate zeolite products. In this case, the neutralized solution will primarily contain sodium nitrate, which could be used as a nitrogen source at local farmlands. The aluminosilicate precipitate is a zeolite byproduct.

The caustic scrubber is included after the absorption column to neutralize trace amounts of NO_x vapors that may be remaining. It uses a 2% sodium hydroxide solution, which is recycled with a blowdown stream to maintain mass in the recycle loop, and a recirculation pump with a heat exchanger to remove the heat of neutralization in the column.

The final modification to the model was the adjustment of the leaching efficiencies based upon the lab testing results with ash pretreatment. This adjustment affects product yield as well as acid consumption. The updated leach efficiencies used in the model are shown in Table 28.

Table 30: Elemental leach efficiencies, based on laboratory testing, that were used in the updated CHEMCAD model of the process.

Element	Average %	Element	Average %	Element	Average %	Element	Average %
Na	99.00%	Ni	66.81%	In	93.39%	Ho	90.67%
Li	48.84%	Cu	99.00%	Sn	0.00%	Er	96.13%
Be	83.11%	Zn	99.00%	Sb	0.00%	Tm	87.34%
Mg	99.00%	Ga	99.00%	Te	0.00%	Yb	83.32%
Al	52.22%	Ge	0.00%	Cs	72.54%	Lu	74.55%
Si	0.00%	As	99.00%	Ba	99.21%	Hf	1.23%
K	66.33%	Se	99.00%	La	95.24%	Hg	0.00%
Ca	99.00%	Rb	56.46%	Ce	95.07%	Ta	0.00%
Sc	86.58%	Sr	99.00%	Pr	96.47%	W	0.00%
Ti	79.19%	Y	99.00%	Nd	98.41%	Tl	52.59%
V	41.72%	Zr	4.24%	Sm	97.68%	Pb	69.53%
Cr	49.21%	Nb	0.00%	Eu	97.35%	Bi	0.00%
Mn	80.36%	Mo	0.00%	Gd	99.74%	Th	99.99%
Fe	29.21%	Ag	0.00%	Tb	99.99%	U	62.48%
Co	80.45%	Cd	55.12%	Dy	94.59%		

5.3 Technoeconomic Assessment Assumptions

This section describes the key economic assumptions used to estimate the capital and operating costs of Battelle's ADP. These assumptions are important for understanding the context for the reported costs.

The baseline plant configurations, performance, and financial assumptions used for Battelle's ADP throughout this report are based on a widely-used set of "baseline" process characteristics specified by the U.S. Department of Energy as shown in Table 29.

Table 31: Key REE process performance and cost assumptions

REE Process Specification	Value
Performance Specifications	
Coal Ash Throughput	30 tonnes/hr
Coal Ash Source	PCC Plant A
Capacity Factor	75%
Financial Assumptions	
Cost Year and Type	2015 Constant Dollars
Annual Inflation Rate	0%
Real Escalation Rate	0%
Fixed Charge Factor	0.113
Years of Construction	3 years
Plant Book Life	30 years
Federal Tax Rate	36%
State Tax Rate	50%
Property Tax rate	0%
Project Contingency	10%
Process Contingency	10%

Process costs describe a mature, Nth-of-a-kind (NOAK) estimate of capital and operating costs. This assumption was selected as the basis for cost estimation in this work since it is more common than the alternative first-of-a-kind (FOAK) estimate used to denote the current state of an emerging technology. A more thorough understanding of the process is expected to reduce capital and operating costs, thereby reducing the overall capital and operating costs of the system.

The fixed charge factor is calculated based on year-by-year carrying charges and a present worth factor according to Equation 1:

$$FCF = \frac{CC_i * (1+i)^{-1} + CC_2 * (1+i)^{-2} + \cdots + CC_n * (1+i)^{-n}}{a_n}$$

where n is the book life of the plant, i is the interest rate, CC is the year by year carrying charges of the plant, and a_n is the present value worth factor for a uniform series. The year-by-year carrying charges are the sum of: (the return on debt, the return on equity, the payable income taxes, book depreciation, property taxes, and insurance)/the total plant cost (TPC). The value of a_n is calculated according to Equation 2:

$$a_n = \frac{(1+i)^n - 1}{i * (1+i)^n}$$

Changes in the assumptions in Table 29 can significantly change the overall results. Due to the large impact that assumptions can have on the final costs, the cost of production shown in this report is most usefully compared to other processes with comparable assumptions and are not to be compared directly with costs presented in other studies that use alternative assumptions.

Additional assumptions regarding specific capital and operating cost parameters, such as direct and indirect cost elements, reagent costs, and labor requirements are specified in the earlier Feasibility Study Report included in Appendix B.

5.3.1 Pretreatment and Byproduct Generation

Pretreatment assumed that zeolite precipitation would require nitric acid addition, which is conservative with regards to operating cost as many zeolite operations use thermal means that are expected to be less expensive, to generate zeolite rather than chemical addition. The price for the zeolite was back-calculated to cover the cost of the pretreatment operation, which amounts to $45 per tonne.

5.3.2 Purification and Separation

Purification and separation consists of solvent extraction to generate a mixed REE solution, followed by separation and production of salable REE products (99%+ purity oxides) via an emerging separation technology.

Solvent extraction circuit sizing and expected reagent usage calculations were developed in an EXCEL spreadsheet based on Battelle's past solvent extraction experience. Costs were scaled from a quote for a 300 gpm, 12 stage solvent extraction system obtained by a vendor who built the 100 gpm pilot system for treatment of acid mine drainage water. Figure 16 shows a schematic of the solvent extraction process.

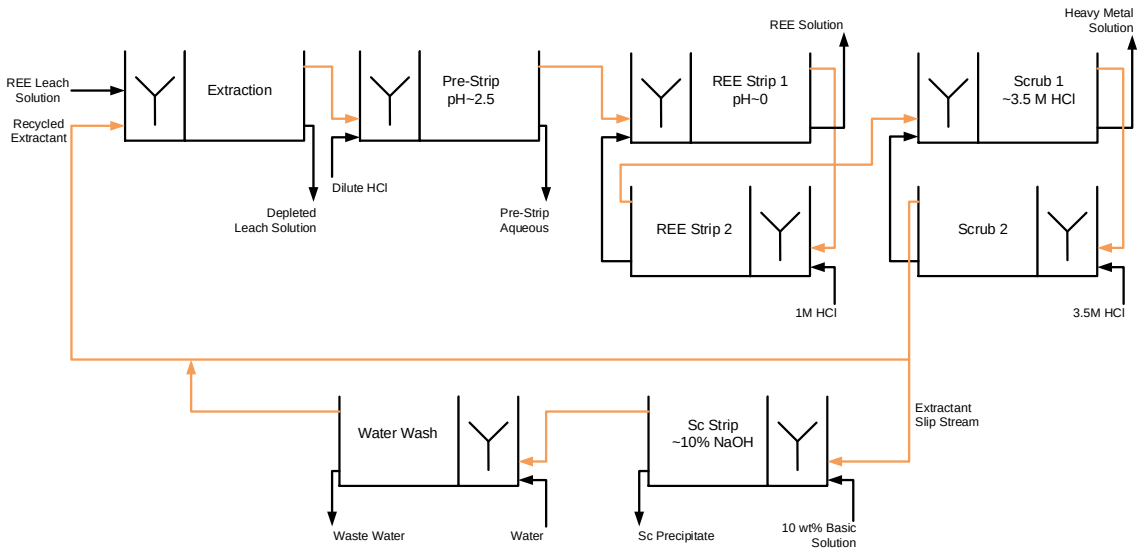

Figure 16: Flow schematic for the solvent extraction circuit to upgrade REE concentrate for feed to the final purification/separation step.

The solvent extraction balance assumed that the feed solution composition is the same as the leach solution, but with 50% of the iron removed by roasting. Organic losses in the aqueous phases were assumed to be 50 ppm, and mixing times and settling times were 5 minutes and 10 minutes, respectively. The extraction stage organic to aqueous ratio was about 1:2, but the stripping stage organic ratios were assumed to be maintained at 1:4 through internal recycles. Concentration factors were assumed to be 50x in each stripping section, but 100x in the scrubbing section. To be conservative, the extraction was assumed to require two stages, pre-strip two stages, REE stripping four stages, scrubbing four stages, scandium recovery two stages, and one stage for the water wash. Due to the generally low concentration of scandium, only 5% of the extractant is diverted to scandium recovery in each pass of the extractant.

The chemical consumption was calculated for each stage based on stoichiometric consumption of acid (or base) to the respective stripped compound(s), plus the amount of chemical required to achieve the pH or concentration listed for the stage in Figure 16. Feed rates were calculated from the concentration factors.

5.4 Technoeconomic Assessment Results

The procedure used in the technoeconomic assessment follows the Electric Power Research Institute's (EPRI) Technical Assessment Guide (TAG™) guidelines for cost estimation of emerging technologies. The total capital requirement (TCR) of a full scale rare earth separation and purification system includes the direct costs of purchasing and installing all processing equipment (denoted as the Process Facilities Capital, PFC), plus a number of indirect costs such as the general facilities cost, engineering and home office fees, contingency costs, and several categories of owner's costs. These costs are used to determine the overall cost of

extracting and purifying rare earth elements from coal ash. Figure 17 outlines the TAG method developed by EPRI.

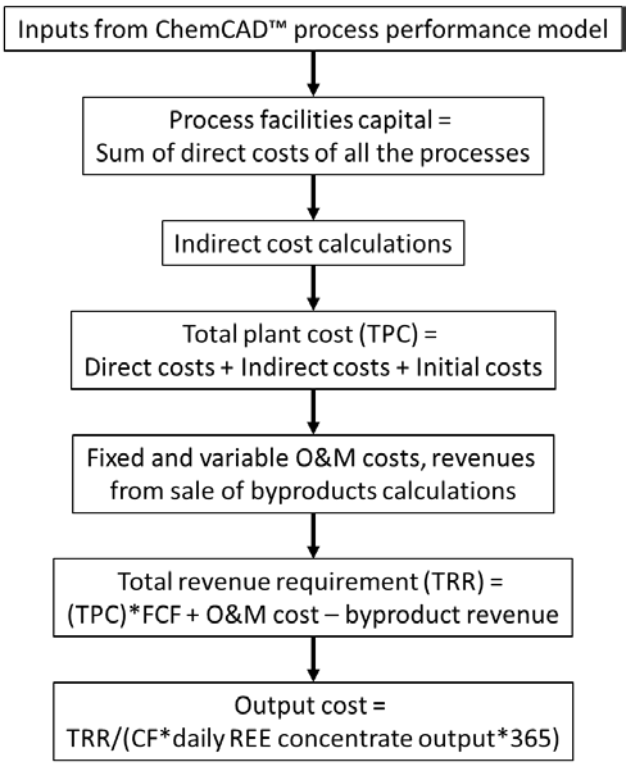

Figure 17: Method of cost assessment

5.4.1 Capital Cost

The process facilities capital (PFC) of a component refers to the capital required to purchase and install a major process at the facility. Ideally, these costs are known and come from prices quoted from an equipment manufacturer. When manufacturer data is not available, installed cost data is derived from references describing costs for installing similar processes. Equipment costs are then scaled using well-documented cost correlations. Table 30 lists the nominal cost values for a NOAK rare earth separation and purification system.

The total direct capital cost of Battelle's ADP is approximately $42 million. The most capital intensive process area is the evaporator-condenser associated with the acid recovery system which accounts for approximately half of the total direct capital costs of the system. The evaporator-condenser is used to recover nitric acid from the leachate stream. Despite the high capital cost, the process is necessary to reduce annual operating expenses associated with reagent cost.

Table 32: Installed costs for major process areas of the rare earth separation and purification facility.

Direct Costs for All Major Process Areas ($1000, 2015)			
Coal Ash Handling	$361	Evaporator Feed Pump	$7
Pre-treatment water wash	$224	Acid Recycle Pump	$7
Leach Reactor	$271	Acid Makeup Pump	$7
Knockout Vessel	$179	Sweep Blower	$3
Filter	$4,040	Column Blower	$9
Rotary Dryer	$2,277	Distillation Column	$333
Crystallizer/Custom Rotary Dryer	$3,350	Oxide and Nitrate separation	$64
Column	$217	REO SX and Purification	$15,770
ESP	$1,328		
Reactor Heat Exchanger	$199		
Column Heat exchanger	$218		
Evap Condenser	$12,698		
Roaster Condenser	$786		
Reactor Feed pump	$24		
Reactor Recirculation Pump	$19		
Column Sump Pump	$16		
Filter Pump	$24		
Process Facilities Capital*			**$42,400**
***Total Process Facility Capital (PFC) may not equal the sum of the components due to rounding error**			

The Process Facilities Capital costs, also known as the direct capital costs, are used to calculate the indirect capital costs associated with the Battelle's ADP. The total of the direct and indirect capital costs make up the elements of the total plant costs. The indirect costs include engineering and home office fees, general facilities capital, project and process contingencies, and royalty charges.

The sum of these costs, called the total plant cost (TPC), is developed on the basis of overnight construction. Overnight cost is the cost of a construction project if no interest was incurred during construction, as if the project was completed "overnight." These costs are summarized in Table 31.

Table 33: Summary of estimated direct and indirect capital costs for a NOAK rare earth separation and purification process. These costs are the basis for estimating the total plant cost-- a major component of the total capital requirement of the plant.

Capital Cost Elements	Nominal Value	Component Cost ($Million, 2015)
Process Facilities Capital (PFC)		$42.4
Engineering and Home Office Fees	7% PFC	$2.9
General Facilities	10% PFC	$4.2
Project Contingency	10% PFC	$4.2
Process Contingency	10% PFC	$4.2
Total Plant Cost (TPC) = Sum of the above		$58.1

The total capital requirement (TCR) includes all the capital necessary to complete the entire project. These items include the total plant cost (TPC), allowance for funds used during construction (AFUDC), prepaid royalties, inventory capital, and pre-production costs.

Table 32 summarizes the steps required to calculate the total capital requirement. The TCR for Battelle's ADP is approximately $61 million. This cost includes all direct and indirect capital costs associated with the project.

Table 34: Indirect capital costs for a NOAK rare earth separation and purification facility.

Capital Cost Elements	Nominal Value	Component Cost ($1000, 2015)
Total Plant Cost (TPC)		**$58,100**
AFUDC (interest during construction)	0.5% TPC	$291
Royalty Fees	0.5% PFC	$212
Pre-Production (fixed)	1 month fixed O&M	$415
Pre-Production Costs (Variable)	1 month variable O&M	$1,494
Inventory Capital	0.5% TPC	$291
Total Capital Requirement (TCR)		**$60,803**

5.4.2 Operating Costs

The operating and maintenance (O&M) costs are usually estimated for one year of operation. These can be divided into fixed O&M and variable O&M costs. These costs are discussed in this section. Note that all reference costs are adjusted to 2015 dollars from the source year using the SDRI Chemical Engineer Handbook Price Index.

The fixed O&M (FOM) costs include the costs of plant maintenance (materials and labor) and labor (operating, administrative, and support labor). Operating labor costs are estimated based on correlations between labor hour requirements and the plant's daily capacity.

Table 35: Fixed operating and maintenance cost parameters and their nominal values.

Fixed O&M Costs	Units	Nominal Value
Major Processing Steps	#	12
Cor'l'n for Op. Labor	Hrs./day-step	14
Operating Labor Rate	$/hr	$46.43
Total Maintenance Cost	%TPC	2.5%
Maint. Cost Allocated to Labor	% FOM Maint.	40%
Admin. & Support Labor Cost	% Total Labor	30%

The variable O&M (VOM) costs include the cost of materials consumed (make-up acid, process water, etc.), utilities, and services used (waste transport and disposal). These quantities are determined in the CHEMCAD performance model. The unit cost of each item (e.g. dollars per tonne of coal ash or dollars per tonne of transported REE concentrate) is a parameter specified as a cost input to the model. The total annual cost of each item is then calculated by multiplying the unit cost by the total annual quantity used or consumed. Total annual quantities are dependent upon the facility's annual operating capacity factor. The individual components of variable O&M costs are explained in more detail below. Note that the unit costs for all of the consumables are based on publicly available sources where available.

Table 36: Variable operating and maintenance cost components and their nominal values. Note that prices in parenthesis indicate a negative cost (or revenue) for marketable by-products. Note that the cost of zeolites was calculated to roughly offset the cost of the pre-treatment process equipment.

Variable O&M Costs	Units	Nominal Value
Coal Ash	$/tonne	$-
Makeup Nitric Acid	$/tonne	$600
Dilution Water	$/tonne	$0.30
Leached Ash Disposal	$/tonne	$10.3
Natural Gas	$/GJ	$1.26
Electricity	$/MWh	$6.73
SMBS inlet rate	$/tonne	$280
Hydrochloric acid	$/tonne	$115
Sodium Hydroxide	$/tonne	$320
Solvent (Extractant)	$/kg	$8.30
Wastewater	$/kliter	$0.30
Hazardous wastewater	$/kliter	$18.79
REO Purification Cost	$/kg	$2.00
Price for Fertilizer	$/tonne	$-
Price for Zeolites	$/tonne	$(45.03)
Price for Salable Ash Byproduct	$/tonne	$(30.00)

The nominal (default) values of all major operating and maintenance (O&M) costs in the Battelle's ADP cost model are summarized in Table 35.

Table 37: Variable and fixed operating cost component results for Battelle's ADP.

Variable Cost Component	Variable O&M Cost ($1000/yr, 2015)	Fixed Cost Component	Fixed O&M Cost ($1000/yr. 2015)
Coal Ash	$-	Operating Labor	$2,847
Makeup Nitric Acid	$14,029	Maintenance Material	$1,453
Makeup Water	$339	Maintenance Labor	$581
Solid and hazardous waste disposal	$788	Admin. & Support Labor	$1,029
Natural Gas	$53	**Total Fixed Costs**	**$5,910**
Electricity	$771		
Organic Solvent	$328	**Salable By-Products**	
Caustic	$392	Upgraded Coal Ash	$(2,290)
Hydrochloric Acid	$127	Zeolite	$(948)
Extractant	$407	Fertilizer	$-
Hazardous Disposal Costs	$462	**Total By-product Credits (Salable Products)**	**$(3,237)**
REO Purification O&M	$233		
Total Variable Costs	**$17,929**		

A robust way to evaluate the cost of resource intensive processes such as REE processing systems is to normalize the cost of production on the basis of incoming coal ash ($/tonne feedstock) and outgoing rare earth element product ($/kg rare earth oxide). The normalized cost, also known as the levelized cost of production (LCOP), represents the income that the processing facility would need to receive from the sale of products to fully recovery all capital and operating costs while earning a specified rate of return over the plant life. The LCOP is calculated first by quantifying the annual revenue requirement as shown in Equation 3.

$$Total\ Annual\ Revenue\ Requirement\ \left(\frac{\$}{yr}\right) = TCR * FCF + Fixed\ O\&M + Variable\ O\&M + ByProduct\ Credits$$

Financial parameters such as the annual rate of return, plant life, and other plant assumptions are embedded in the fixed charge factor (FCF) in order to annualize the total capital costs. Thus, the reported value represents the "levelized" annual revenue stream that a processing facility must realize from the sale of REE oxides to produce the same net present value as a stream of variable year-to-year costs over the life of the plant.

A summary of the levelized production costs reported based on the ash feedstock and mixed REE oxide products is shown in Table 36. Note that these results represent the cost if a plant were constructed using a mature (NOAK) iteration of the Battelle ADP.

Table 38: Cost model results using Nth-of-a-kind (NOAK) plant assumptions. These costs represent the cost of producing rare earth oxides from coal ash given a mature iteration of the separation and purification process.

Cost Component	$Million per year (2015)	$/Tonne Coal Ash Processed	$/kg REE Oxides
Annual Fixed Cost	$5.9	30	50.6
Annual Variable Cost	$17.9	91	153.6
Annualized Capital Cost	$6.9	135	59.0
By-Product Credits	(3.2)	(16)	(27.8)
Total Annual Revenue Requirement	27.5	140	235.4

For context to the levelized cost per tonne of coal ash fed, a histogram of recoverable REE value in US coal sources was generated. This histogram uses USGS CoalQual data (U.S. Geological Survey, 2015) to obtain REE concentrations in coal sources by state. These data were converted to a value in coal, on an ash basis, using the ash measurement from the database and the REE prices listed in Table 37.

Table 39: REE prices used in evaluation of coal source values, from mineralprices.com, accessed December 2016.

Element	Oxide Basis Value, $/kg
Sc	$4,200.00
Ce	$2.00
Dy	$230.00
Er	$34.00
Gd	$32.00
La	$2.00
Nd	$42.00
Pr	$52.00
Tb	$400.00
Y	$6.00

To make the histograms representative of US sources, the sample counts from each state were weighted based on the respective state's coal production from the EIA Coal Data Browser (Energy Information Administration, 2015). This histogram is shown in Figure 18, and indicates the distribution of recoverable REE values in US coals on a tonne of ash basis. The levelized process cost per tonne of coal ash for Battelle's recovery process is $140 from Table 36. At this process cost, approximately 42% of US coal sources, if ashed, could be pursued with Battelle's process.

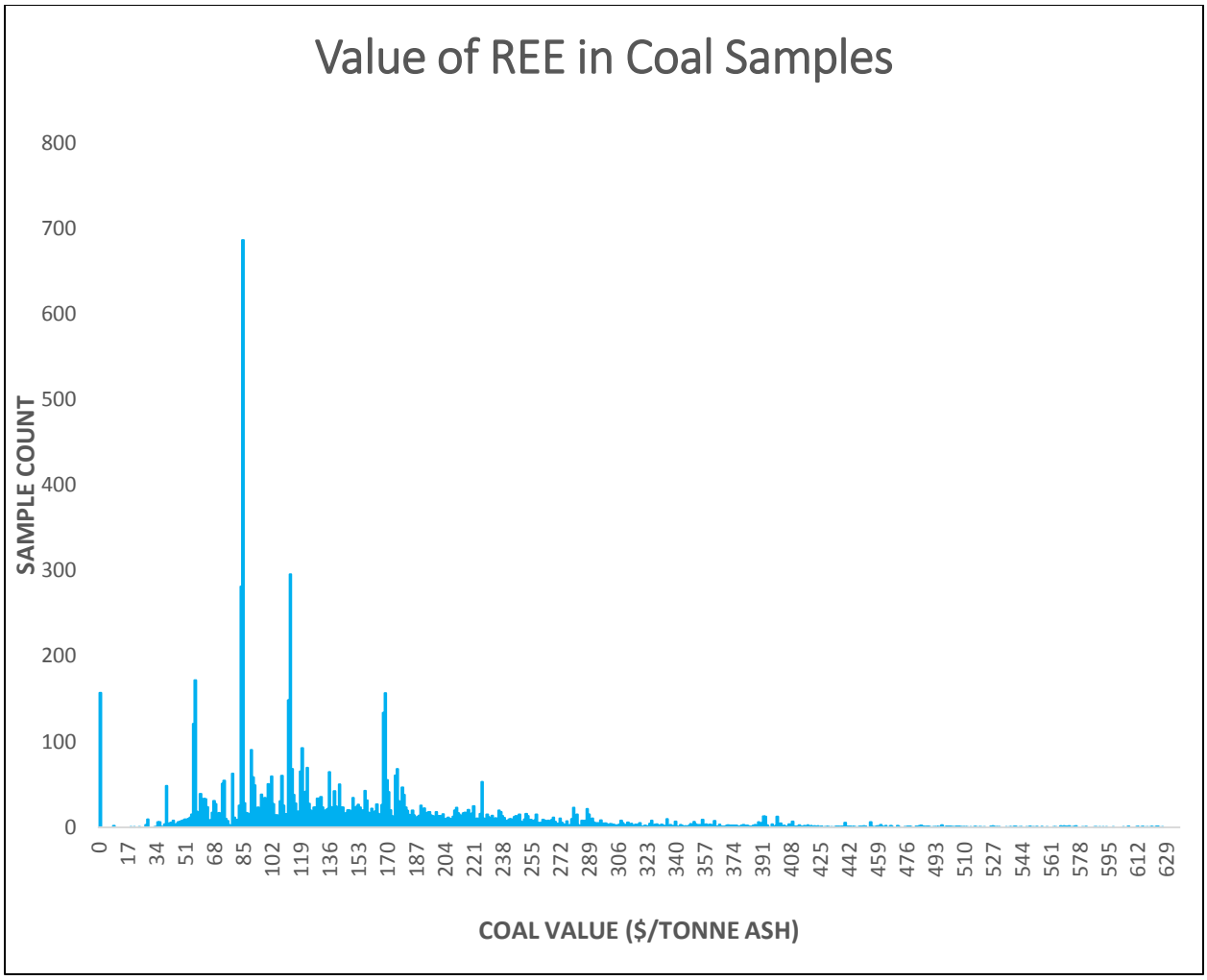

Figure 18: Histogram of REE values in US coal on an ash basis.

6.0 Marketing/Commercialization Discussion

6.1 Rare Earth Uses and Production

Rare earth elements are widely used in catalysts, glass manufacture, sensors, and magnets. The magnetic rare earth elements are particularly valuable as their high magnetism reduces the size of motors and generators used in electric vehicles and wind turbines. They additionally find use in defense applications for armoring alloys, weapons guidance systems, night vision goggles, and communication systems (King, 2016). As shown in Figure 19, lanthanum and cerium find the most use by volume, as they are the most common rare earth elements and commonly used in petroleum upgrading catalyst and glass manufacture. By value, however, the magnetic rare earths, such as neodymium, praseodymium, and dysprosium far outweigh most others.

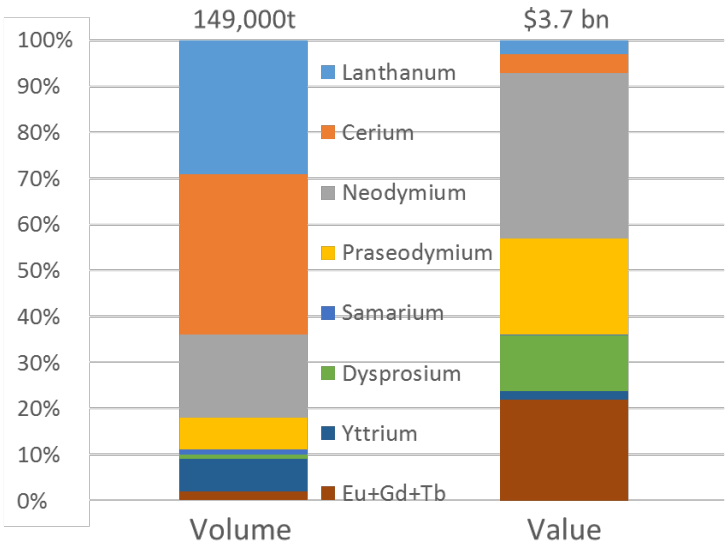

Figure 19: Global rare earth consumption by volume and value in 2015 (Argus, 2016).

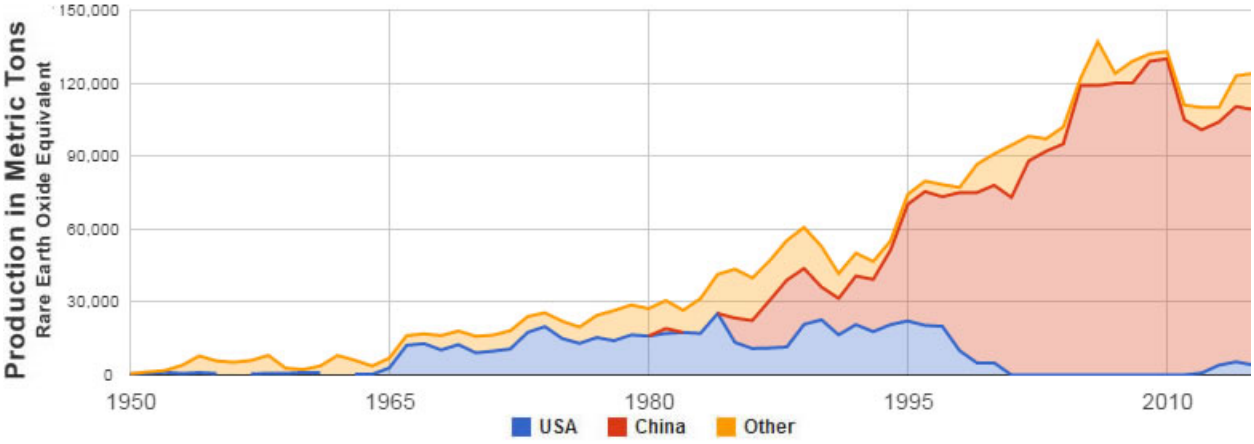

Figure 20: History of rare earth production, in metric tons of rare earth oxide equivalent, between 1950 and 2015. The United States' market share increased in the mid-1960s when color television increased demand. When China began selling REEs at very low prices in the late-1980s and early-1990s, mines in the United States were forced to close because they could no longer make a profit. When China cut exports in 2010, rare earth prices skyrocketed. That motivated new production in many areas (King, 2016).

Application of rare earth elements began in earnest with the advent of color television, which relied heavily on europium. The US controlled most of the REE supply for a few decades before China began to dominate production in the 1990s, as illustrated in Figure 20. US production came back online from the Mountain Pass mine in California briefly around 2013 after Chinese export restrictions caused a spike in REE prices. China has since relaxed these restrictions, lowering prices and causing the shutdown of the Mountain Pass mine.

China has enjoyed decades as the low-cost supplier of REE, due to a combination of subsidies to state-owned businesses and competitive deposits in the Bayan Obo region, Sichuan region, and South China adsorption clays. There is also production of REE from an Australian deposit, and there are known deposits around the world that have not yet or are not currently being exploited due to economic constraints, including the idled Mountain Pass mine in California. Figure 21 provides a flow chart of the typical REE value chain, with typical concentration ranges at each step. Mining of the ore is typically followed by physical beneficiation, which consists of milling and usually flotation or occasionally magnetic separation steps. The upgraded mineral concentrate is then ‘cracked’ to leach the rare earths into an acidic solution, which may be cleaned by selective precipitation and then fed to a solvent extraction circuit. Solvent extraction separates and purifies the individual REEs, and due to the chemical similarity between sequential REEs, this process can take hundreds of mixer settler stages. It is common for the concentrated strip solutions from solvent extraction to be precipitated with oxalate addition, then calcined to oxides for sale in the market.

The South China Clays are notable as a deposit since they are similar in both concentration of REE and distribution of heavy REE to many coal deposits. However, they are ion exchangeable deposits, which are simpler to exploit than phosphate minerals more common to coal deposits, which require chemical cracking. The South China clays are leached with ammonium sulfate solution, precipitated with oxalic acid, then calcined and sent for separation and purification with little need for mineral beneficiation and none for chemical cracking.

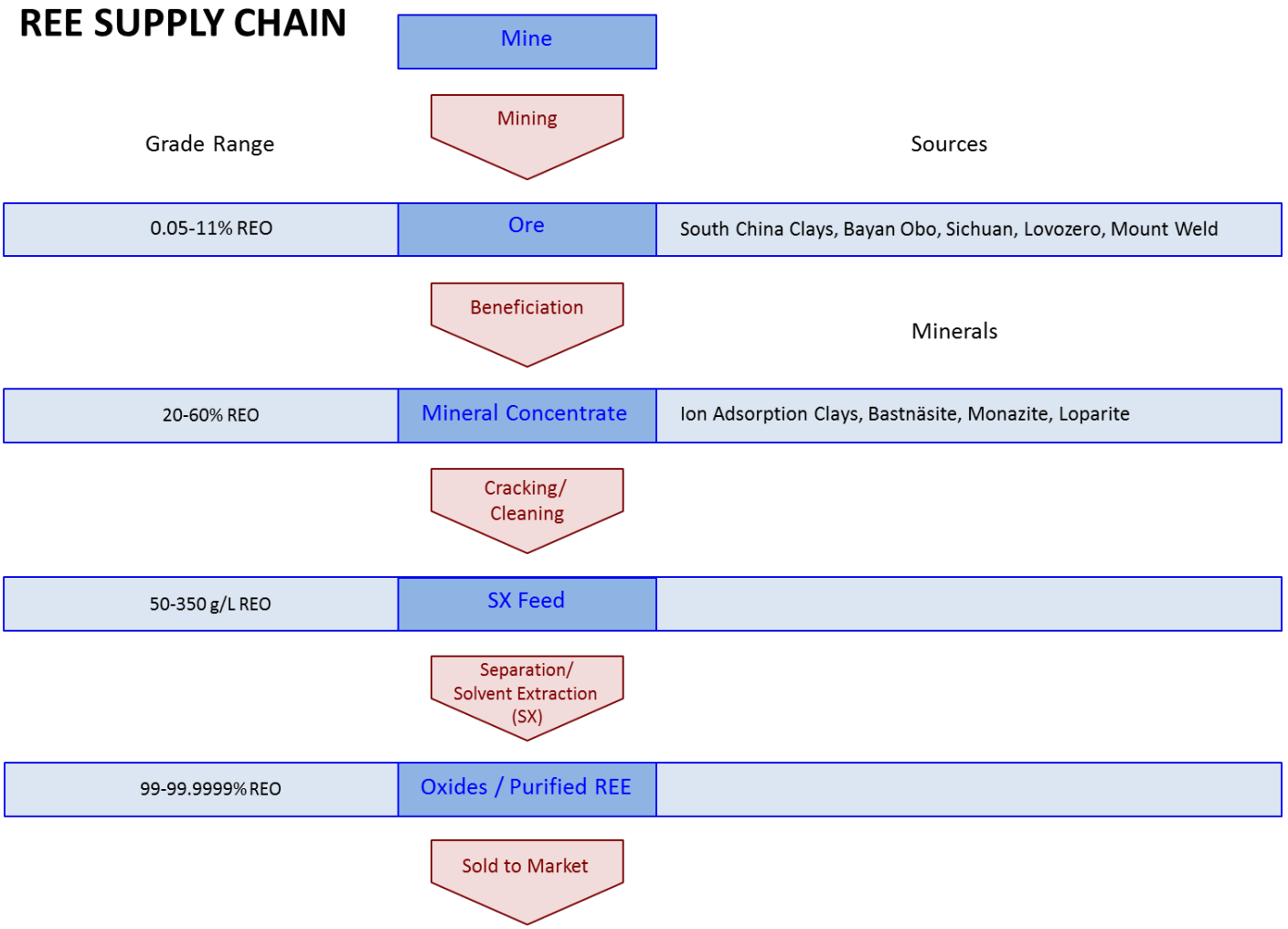

Figure 21: A flow chart of the REE supply chain, as provided by REE market consultants.

6.2 Rare Earth Price History

Recent REE price history has been dominated by Chinese trade policies, notably around 2010 when China installed export restrictions on rare earths, causing a spike in prices. The elevated prices led to the opening of new deposits, including the Mountain Pass mine. Since the relaxing of Chinese export restrictions, prices have dropped, pushing some producers out, although Australia continues to produce. From USGS's Mineral Commodity 2016 Summary (U.S. Geological Survey, 2016):

Through October 2015, China had exported 26,800 tons of rare-earth materials, a 20% increase compared with exports for the same period in 2014. Production of rare-earth oxide equivalent in Malaysia, derived from Australian mine production, was 7,750 tons through September 2015, a 55% increase compared with the same period in 2014. U.S. domestic consumption of rare-earth compounds and metals was estimated to be nearly unchanged compared with that of 2014. In October, the Mountain Pass mining and separation operations were idled indefinitely. Price declines were cited as a key factor in the suspension of operations. The suspension resulted in a decline in mine production and exports of rare-earth compounds.

Prices for REE have varied considerably based on natural market influence such as product demand, but have also been strongly influenced by geo-political policies, notably Chinese export restrictions as discussed earlier. Table 38 provides indicative global rare earth prices as available for consumption outside of China's domestic market. The highest prices are generally from the 2011 crisis, while current prices are near to an economical bottom. Battelle contracted with an external REE market consultant to obtain more specific current prices and peak prices for the economic analysis; the data is proprietary and included in a proprietary appendix.

Table 40: Indicative current and peak prices for rare earth oxides.

Element	Indicative Current Price	Indicative Peak Price
Sc	$4,200	N/A
Ce	$2	$60
Dy	$230	$2,032
Er	$34	N/A
Eu	$150	$3,800
Gd	$32	N/A
La	$2	$67
Nd	$42	$244
Pr	$52	N/A
Tb	$400	$2,974
Y	$6	$56

Current prices from mineralprices.com. Retrieved 12/12/2016. http://mineralprices.com/

Indicative peak prices from Humphries, M. (2013). Rare Earth Elements: The Global Supply Chain. Washington, D.C.: Congressional Research Service

Previous work performed by TetraTech under DOE contract DE-FE- 0004002 summarized published information concerning geology, geochemistry, and resource estimates of select coal basins in the Unites States, with emphasis on discerning distributions of rare earth elements. The U.S. Geological Survey (USGS) Coal Quality (CoalQual) Database is a collection of coal samples taken across the country to better understand the inherent heterogeneity of coal, and

was used extensively in this evaluation. Figure 22 shows the locations of samples from the lower 48 States included in the CoalQual Database.

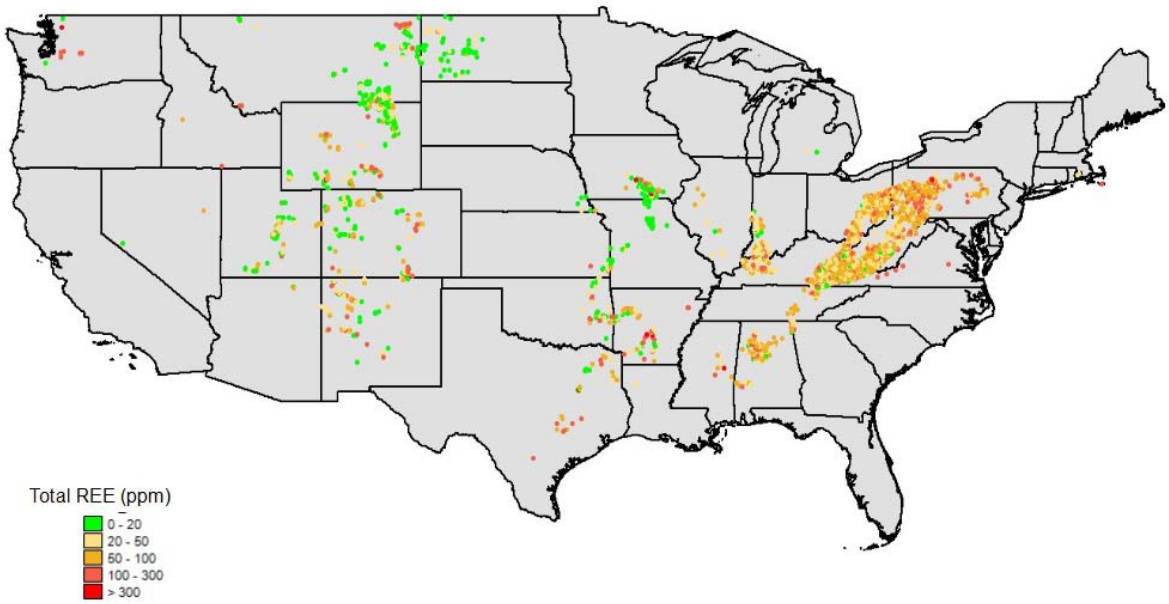

Figure 22: Sample distribution of Analyzed coals in USGS CoalQual Database (Richers & Andersen, 2015).

To expand our understanding of REE concentration to a nationally relevant level, Battelle used a weighting system when analyzing the REE content of the CoalQual samples. The U.S. Energy Information Administration (EIA) collects and reports coal disposition by state. Using the 2015 data collected by EIA, the percent of total US coal produced by each state was related to the number of samples USGS collected from that state. Dividing the percent of total coal the state produced by the percent of USGS samples from that state a weighted value was calculated. This weighting was used to generate a histogram with weighted counts such that it more closely represented the population of coal deposits in the US. We used current market prices of each REE to establish a baseline price. Next, we took the values in Table 38 and multiplied them by the concentration of each REE in the samples. This new value was divided by the percent ash of the sample finally producing a value per tonne of ash for each sample in the database. Using this information, we determined the economic viability of REE extraction from coal on a national level to target potential sources capable of supporting an economically viable extraction plant. Following this calculation, we complied our data into a histogram (see Section 5) to analyze the bulk number of samples that are financially prudent to pursue for our process of REE extraction.

6.3 Other Byproducts Discussion

Besides REE, the process will generate leached fly ash that exhibits high pozzolanic activity, as well as a zeolite material. In 2015, over 50% of the fly ash generated in the US was used in other applications, such as filler material for concrete (American Coal Ash Association, 2015). At a preliminary level, the unmilled leached ash was shown to have similar pozzolanic activity as unleached ash, and so this value should be preserved. It is expected that with milling and caustic leaching the pozzolanic activity of the leached ash will be increased due to increased surface areas, and this byproduct should still be salable as a filler material.

Zeolites are primarily used in industry for three applications: catalysis, gas separation, and ion exchange. These are described in more detail below:

- **Catalysis**

  Zeolites are extremely useful as catalysts for several important reactions involving organic molecules. The most important are cracking, isomerization and hydrocarbon synthesis. Zeolites can promote a diverse range of catalytic reactions including acid-base and metal induced reactions. The reactions can take place within the pores of the zeolite, which allows product control and selectivity (Bartholomew & Farrauto, 2006), (Lynas Corporation, 2017). Figure 23 shows regional usage of zeolites for catalysis worldwide.

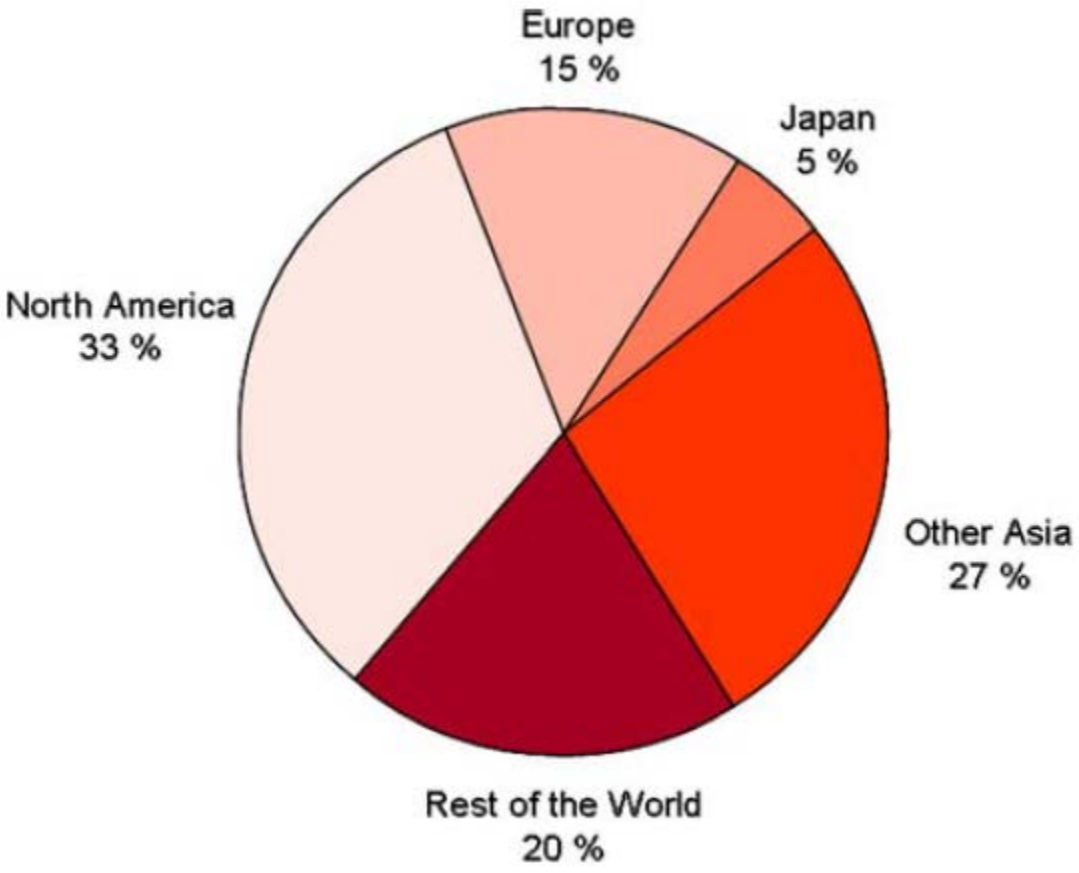

Figure 23: Annual zeolite catalyst consumption by region (Yilmaz & Muller, 2009).

- **Gas Separation**

  A widely-used property of zeolites is that of gas separation. The porous structure of zeolites can be used to "sieve" molecules having certain dimensions and allow them to enter the pores. This property can be fine-tuned by varying the structure by changing the size and number of cations around the pores. Other applications that can take place within the pore include polymerization of semiconducting materials and conducting

polymers to produce materials having unusual physical and electrical attributes (Gavalas, 2006) (Wang, Ho, Figueroa, & Dutta, 2015).

- **Ion Exchange**

  Hydrated cations within the zeolite pores are bound loosely to the zeolite framework, and can readily exchange with other cations when in aqueous media. Applications of this ion exchange behavior include water softening devices, and the use of zeolites in detergents and soaps. It is even possible to remove radioactive ions from contaminated water, as was demonstrated at nuclear accidents at Chernobyl and at Three-Mile Island (Townsend, 1986).

Prices for zeolite depend greatly upon the form, purity, and use, with naturally occurring (mined) zeolites generally commanding lower prices than synthetics. Natural zeolite prices range from $110 to $220 per short ton ($120-$240 per metric tonne) and are often used in agriculture, water purification, and odor control (USGS, 2017). Synthetic zeolites are synthesized from alumina and silica sources to have specific attributes, and are used for catalysis, detergents, and adsorbents. Catalyst zeolites command prices from $1/lb ($2,200/metric tonne) and up, adsorbents from $1-$2/lb ($2,200 - $4,400/metric tonne), and detergents around $0.30/lb ($660/metric tonne) (Bekkum, Flanigen, Jacobs, & Jansen, 2001).

Battelle's process will generate a synthetic zeolite of high purity due to its separation from the fly ash precursor. Although the final form and application have not yet been determined, it was assumed in the economics that it will be salable at a price of $600 per metric tonne. The Phase 2 effort will include research to investigate synthesis of valuable zeolite material and its applications.

6.4 Commercialization Plans

The ultimate goal for this technology is advancement to commercial practice (Technology Readiness Level (TRL) 9 by the Department of Energy's scale. At its current state, the technology for REE recovery from coal fly ash is at the low end of TRL 4, where the process has been validated in the lab in a batch setting with low fidelity integration between each successive process step. This integration was accomplished by feeding each step with outputs from the previous step, and data was acquired to allow design scale up to a continuous system. At the end of the proposed Phase 2 project, the technology will be at TRL 5, having been validated in a relevant environment on a continuous, integrated unit. Table 39 illustrates projected timelines for each successive TRL level along with potential funding sources, and key testing parameters at each stage.

Table 41: Expected technology maturation plan.

TRL Level	Timeline	Scale	Funding Sources	Key Test Parameters
4	May 2017	Beaker Scale	DOE, OCDO	Recoveries and Efficiencies
5	Q1 2019	12.5 lb/hr ash feed	DOE, OCDO	Recoveries and Efficiencies
6	Q1 2021	~0.5 ton/hr (~80x scale up)	Government, Industrial Partner	Stream Time, Operability, Consistency, Product Quality
7	Q1 2024	~15 ton/hr (~30x scale up)	Industrial Partner, Equity	Stream Time, Product Quality/Salability
8	Q1 2026	~15-30 ton/hr (commercial scale)	Equity/Debt	Stream Time, Product Quality
9	2026+	15-30 ton/hr	Equity/Debt	

Given the promising results of this phase, Battelle has applied for Phase 2 funding from government sources to bring the technology to a TRL 5. With the integrated continuous system operating in Phase 2, potential end users of the technology, including power plant operators, will be invited to tour the bench-scale plant. The economics will be updated based on results from the continuous plant, and used for business plans and marketing materials. Beyond the second phase of this project, it is expected that an industrial partner will contribute funding to development and demonstrations of the technology.

7.0 Conclusions and Next Steps

The U.S. Department of Energy funded projects to identify a coal based source of rare earth elements (REE) that exceeds 300 ppm total REE content, and to extract them economically and in an environmentally benign process to a concentration approaching 2% by weight. Battelle met these objectives by implementing its Acid Digestion Process (ADP). The process can be economically applied to US coal sources, operate with high REE recoveries, produce a REE product of greater than 7% purity, and a zeolite byproduct that can help to subsidize the REE processing costs. Additionally, the design has been scaled to a 12.5 pound per hour integrated test unit for operation in the potential next phase.

Based on the analytical results, PCC Plant A fly ash was selected as a feedstock for Battelle's ADP. The PCC Plant A fly ash has:

- a higher Total REE+Y+Sc concentration than all other operating plant ashes sampled, at 545 ppm +/- 13.4 ppm
- a high HREE/LREE ratio at 0.37 +/- 0.008
- significant amounts of Scandium (36 ppm +/- 1.4 ppm), Vanadium (279 ppm +/- 12 ppm), Yttrium (104 ppm +/- 5.3 ppm), Cobalt (44 ppm +/- 2.5 ppm), and Lithium (~166 ppm), which can be valuable process byproducts with robust market outlets.

Based on the laboratory testing, ball milling and caustic pretreatment of the ash allows for high recovery of REE, with leaching efficiencies for scandium as high as 86% and near complete recovery of total REE as a weighted average. Milling of the ash to approximately 4-5 µm allows these recoveries to be realized with only a 60 minute contact with 10% sodium hydroxide solution at 90 °C, and leaching in 34% nitric acid for 30 minutes at 90 °C. Traditional aluminosilicate recovery from fly ash requires a caustic leach of 6 hours or more (Hollman, Steenbruggen, & Janssen-Jurkovicova, 1999), so this method represents a significant decrease in reaction time. The acid leaching reaction is slightly exothermic, at approximately 102 calories per gram of ash leached, which will reduce energy costs to heat the leach reactor.

Additionally, the caustic pretreatment leach should allow for production of a zeolite byproduct that can be used as an adsorbent or catalyst support material. A zeolite material was made in the lab with the milled fly ash, but additional work can be done in Phase 2 to make a higher value zeolite with the use of seed material or zeolite scaffolds.

The first rare earth element recovery step by thermal roasting of the loaded acid can oxidize the iron and aluminum between 100 °C and 200 °C, generating an insoluble oxide material. In testing with actual leach solutions, 90% of the REE could be recovered from the roasted solids with a water leach, while omitting over 90% of the iron and aluminum, and over 60% of the uranium and thorium. The water leach had a concentration of 1.2% REE, effectively leading to over a 20x increase in purity of the REE over the fly ash feed.

Solvent extraction testing suggested that extraction for REE is satisfactory at pH of 3.4, where 61% of REEs are extracted at over 7% purity (over 120x concentration over the feed fly ash). The primary contaminants were sodium (due to a high starting concentration), aluminum, silica, calcium, and iron, but sodium, potassium, magnesium, and calcium were largely excluded from the extract. At pH 5, near quantitative REE can be achieved (over 99%), including less valuable lanthanum and cerium, but purity drops to about 1.0% in the extract. In selective stripping tests, the REE were stripped in hydrochloric acid at around one molar. The scandium is expected to be recoverable by precipitating in sodium carbonate solution. These REE solutions could then

be separated with commercial operations such as further solvent extraction or ion exchange, or an emerging technology could be used such as electrowinning or electrophoresis.

The results of the laboratory testing were used in the updated technoeconomic assessment model to predict the economics of the process, and they were used in the design of a continuous bench scale unit that integrates all of the operations. The key parameters that were used are a one-hour leach in 10% sodium hydroxide at 90 °C, with fly ash milled to ~4.5 µm, then acid leaching in 34% nitric acid at 90 °C. The loaded acid will be roasted at 150 °C to calcine iron and aluminum, separating them from REE in a water wash. This loaded water will be extracted at pH 3.5-4.0, scrubbed around pH 3.5 to remove base metals, stripped with 1 molar hydrochloric acid to recover REE, scrubbed with 2 M HCl to remove iron, then scandium recovered by precipitation with 10% sodium carbonate solution. Additional work to improve the stripping process will be done in pending Phase 2 testing.

The technoeconomic assessment suggested that at the 30 tonne per hour scale, the processing cost per tonne of fly ash feed is approximately $140 for a mature, commercial plant. This would allow it to be economically applied to 42% of US coal sources if ashed.

Using laboratory results and the generated CHEMCAD model, the process design was scaled up to 12.5 lbs/hr of coal ash feed. Process flow diagrams, piping and instrumentation diagrams, stream tables, mass and energy balances, utility requirements, vendor quotes, equipment lists, and a preliminary space claim diagram were generated for the integrated test unit.

The integrated continuous testing will investigate the impact of recycle streams on the process, which will introduce concentration cycles of contaminants and reduced acid and caustic strengths. Finally, the next phase will include optimization of zeolite production to generate a saleable, high value zeolite product.

8.0 References

American Coal Ash Association. (2015). *Fly Ash Production*. Retrieved from Production and Use Reports: https://www.acaa-usa.org/Portals/9/Files/PDFs/2015-Survey_Results_Charts.pdf

Argus. (2016). Argus Americas Rare Earths Summit. Denver: Argus.

Bartholomew, C. H., & Farrauto, R. J. (2006). *Fundamentals of Industrial Catalytic Processes, Second Edition.* Hoboken: John Wiley and Sons.

Battelle. (2017). *Recovery of Rare Earth Elements from Coal and Coal Byproducts via a Closed Loop Leaching Process: System Design Report.*

Bekkum, H. v., Flanigen, E., Jacobs, P., & Jansen, J. (2001). *Introduction to Zeolite Science and Practice, Second Edition.* Amsterdam: Elsevier.

Box, G., & Behnken, D. (1960). Some New Three Level Designs for the Study of Quantitative Variables. *Technometrics*, 455-475.

Cytec. (2017, April 15). *CYANEX 572 Solvent Extraction Reagent.* Retrieved from Cytec: https://www.cytec.com/sites/default/files/files/CYTEC_CYANEX_572_FINAL.pdf

Energy Information Administration. (2015, August). *Coal Data Browser*. Retrieved from www.eia.gov: http://www.eia.gov/beta/coal/data/browser/#/topic/20?agg=0,1&geo=vvvvvvvvvvvo&sec=vs&freq=A&start=2001&end=2013&ctype=map&ltype=pin&rtype=s&maptype=0&rse=0&pin=

Gavalas, G. R. (2006). Chapter 12: Zeolite Membranes for Gas and Liquid Separations. In Y. Yampolski, I. Pinnau, & B. Freeman, *Materials Science of Membranes for Gas and Vapor Separation.* Chichester: John Wiley and Sons.

Hollman, G. G., Steenbruggen, G., & Janssen-Jurkovicova, M. (1999). A Two-Step Process for the Synthesis of Zeolites from Coal Fly Ash. *Fuel*, 1225-1230.

Hollman, G., Steenbruggen, G., & Janssen-Jurkovicova, M. (1999). A Two-Step Process for the Synthesis of Zeolites from Coal Ash. *Fuel*, 1225-1230.

IEA Clean Coal Centre. (2013, November). *Profiles: Technoeconomic Analysis of PC versus CFB Combustion Technology.* Retrieved May 22, 2017, from http://www.iea-coal.org.uk/documents/83231/8837/Techno-economic-analysis-of-PC-versus-CFB-combustion-technology,-CCC/226

King, H. (2016). *Rare Earth Elements and Their Uses*. Retrieved from geology.com: http://geology.com/articles/rare-earth-elements/

Lynas Corporation. (2017, May 30). *Catalytic Cracking.* Retrieved from www.lynascorp.com: https://www.lynascorp.com/Technical%20Resources/Catalytic%20Cracking.pdf

Richers, B. R., & Andersen, H. (2015). *Assessment of Rare Earth Elemental Contents in Select United States Coal Basins.* Tetra Tech.

Stern, K. H. (1972). High Temperature Properties and Decomposition of Inorganic Salts, Part 3: Nitrates and Nitrites. *Journal of Physical and Chemical Reference Data, 1*(3).

Townsend, R. P. (1986). Ion Exchange in Zeolites: Some Recent Developments in Theory and Practice. *Pure and Applied Chemistry*.

U.S. Geological Survey. (2015). Coal Quality Database Version 3.0. Reston: USGS.

U.S. Geological Survey. (2016). *Mineral Commodities Summaries, Rare Earth Elements.* U.S. Geological Survey.

USGS. (2017, January). *minerals.usgs.gov.* Retrieved from Zeolites (Natural) Commodity Summary 2017: https://minerals.usgs.gov/minerals/pubs/commodity/zeolites/mcs-2017-zeoli.pdf

Wang, B., Ho, W. S., Figueroa, J. D., & Dutta, P. K. (2015). Bendable Zeolite Membranes: Synthesis and Improved Gas Separation Performance. *Langmuir*, 6894-6901.

Yilmaz, B., & Muller, U. (2009). Catalytic Applications of Zeolites in Chemical Industry. *Topics in Catalysis*, 888-895.

Appendices

Appendix A: Budget Period 1 Sampling and Characterization Report

Recovery of Rare Earth Elements from Coal and Coal Byproducts via a Closed Loop Leaching Process:

Sampling and Characterization Report

National Energy Technology Laboratory

3610 Collins Ferry Road

Morgantown, WV 26507-0880

18 August 2016

Recovery of Rare Earth Elements from Coal and Coal Byproducts via a Closed Loop Leaching Process: Sampling and Characterization Report

Prepared by:

Battelle
505 King Avenue
Columbus, Ohio 43201

Submitted to:

National Energy Technology Laboratory
3610 Collins Ferry Road
Morgantown, WV 26507-0880

18 August 2016

Contents

List of Tables

List of Figures

Executive Summary

Battelle aims to validate the economic viability of recovering rare earth elements (REEs) from coal ash using its patented closed-loop Acid Digestion Process (ADP). This will be accomplished by selecting a source of coal ash that consistently provides concentrations of rare earth elements above 300 parts per million by weight and in a form suitable for leaching. Ash from a power generation station, low temperature combustion coal ash, and ash from Battelle's coal liquefaction process were assessed, as the latter two forms may have mineralogy and other characteristics that simplify the leaching and separation. The regional availability of REE laden coal ash, the regional market for rare earth concentrates and coal combustion byproducts, and the system cost for rare earth recovery will be accounted for in a Techno-Economic Analysis (TEA). The assumptions and economic sensitivities in the process that are used in the TEA, and certain required design parameters will direct a small lab testing portion to inform the TEA assumptions and allow design of a bench scale system to demonstrate the process on a continuous basis.

This report covers the sampling and characterization portion of the project, where coal byproducts were analyzed to allow selection of a suitable feedstock for Battelle's process, as well as selection of key target materials for recovery to drive the process economics.

Within the rare earth elements in coal, Dysprosium (Dy) represents the highest value, and combined with Neodymium (Nd), Terbium (Tb), and Praseodymium (Pr), these 4 elements account for over 75% of the rare earth value in the ash. Accordingly, Battelle's process will be tailored to focus on these rare earth components. Scandium (Sc) represents the highest overall value within the ash, and will be a primary byproduct. Vanadium (V), Yttrium (Y), Lithium (Li), and Cobalt (Co) also represent a significant value, and will be evaluated as potential byproducts going forward.

Based on the analytical results, the feasibility study will focus on Pulverized Coal Combustion (PCC) Plant A fly ash as a feedstock for Battelle's Recycling Acid Leach Process. The PCC Plant A fly ash had a higher Total REE+Y+Sc concentration than all other operating plant ashes sampled, at 545 ppm +/- 13 ppm, as well as a higher heavy rare earth to light rare earth (HREE/LREE) ratio at 0.37 +/- 0.008. Additionally, it contains significant amounts of Scandium (36 ppm +/- 1.4 ppm), Vanadium (279 ppm +/- 12 ppm), Yttrium (104 ppm +/- 5 ppm), Cobalt (44 ppm +/- 2.5 ppm), and Lithium (~166 ppm), which can be valuable process byproducts with robust market outlets. Although the coal liquefaction ash had a greater concentration of total rare earths, there is some risk for implementation since the liquefaction process is not yet commercial. The low temperature ash may prove to be more leachable since it did not exhibit as high a level of refractory mullite concentration, but it would also likely demonstrate lower selectivity due to the high calcium content. Furthermore, the overall capacity of fluidized bed combustors is much lower than pulverized coal combustors, so there would be more risk in feedstock sourcing.

Going forward, Battelle will evaluate feasibility of its recycling acid leach process on PCC Plant A fly ash. Feasibility testing will compare leaching efficiency and selectivity of this ash with samples of liquefaction ash and FBC ash to validate assumptions regarding leaching kinetics, acid loading limits, and product purities. This information will be used to refine a process model built in CHEMCAD modeling software and feed into overall process economics and unit sizing to be used in the techno economic assessment as part of the Feasibility Study in the next project task.

1.0 Background

As directed by Congress, the United States (U.S.) Department of Energy (DOE) is investigating the economic feasibility of recovery of REEs from domestic U.S. coal and coal byproducts. DOE's National Energy Technology Laboratory (NETL) has characterized a number of REE-bearing samples of coal and coal-related materials. REEs have been generally found in varying concentrations ranging up to 1,000 parts per million by weight in the following materials in the United States: coal mine roof and floor materials, run-of-mine coal, prepared coal, partings, pit cleanings, coal preparation refuse, and tailings. REEs can be found in coal byproducts, including ash, coal-related sludge, and mine drainage. Certain coals can contain a higher ratio of heavy (generally more valuable) REEs than found in other sources of REEs such as natural ores. Given the potentially low REE concentrations in the feed materials, and subsequent potentially low yield of REEs from any separation process, minimizing costs is a key challenge. Physical and chemical separations may be useful in recovering REEs from coal and coal by-products. The forms in which REEs are present in these materials could drive the design of separation processes.

Battelle aims to validate the economic viability of recovering REEs from coal ash using its patented (US6011193) closed-loop Acid Digestion Process (ADP). This will be accomplished by selecting a source of coal ash that consistently provides concentrations of rare earth elements above 300 parts per million by weight and in a form suitable for leaching. Ash from a power generation station, low temperature combustion coal ash, and ash from Battelle's coal liquefaction process are being assessed, as the latter two forms may have mineralogy and other characteristics that simplify the leaching and separation. The regional availability of REE laden coal ash, the regional market for rare earth concentrates and coal combustion byproducts, and the system cost for rare earth recovery will be accounted for in a Techno-Economic Analysis (TEA). The assumptions and economic sensitivities in the process that are used in the TEA, and certain required design parameters will direct a small lab testing portion to validate the TEA and allow design of a bench scale system to prove the process on a continuous basis

This report covers the sampling and characterization portion of the project, where coal byproducts were analyzed to allow selection of a suitable feedstock for Battelle's process and subsequent project tasks. The sampling and characterization results also help to inform the process economics and future process design by assisting in the selection of key materials to target for recovery.

2.0 Approach

Battelle's approach includes characterization of ash from three sources, as illustrated in Figure 1. High temperature ash is typical of pulverized coal combustion power plants, where it is heated to upwards of 1,200°C in the furnace. This high temperature creates a vitrified, glassy ash particulate that may entrap rare earth elements in regions that are not amenable to acid leaching. Fluidized bed combustion facilities operate at lower furnace temperatures near 800°C, and should produce ash with less vitrification that is more easily leached. The coal liquefaction ash was not exposed to high temperature oxidation, and the rare earths should be near the mineral form in which they are found in the raw coal. The coal liquefaction ash was further processed to divide it into sections by density and by particle size to determine if there is a simple mechanical process that can be used to enrich the rare earth concentrations.

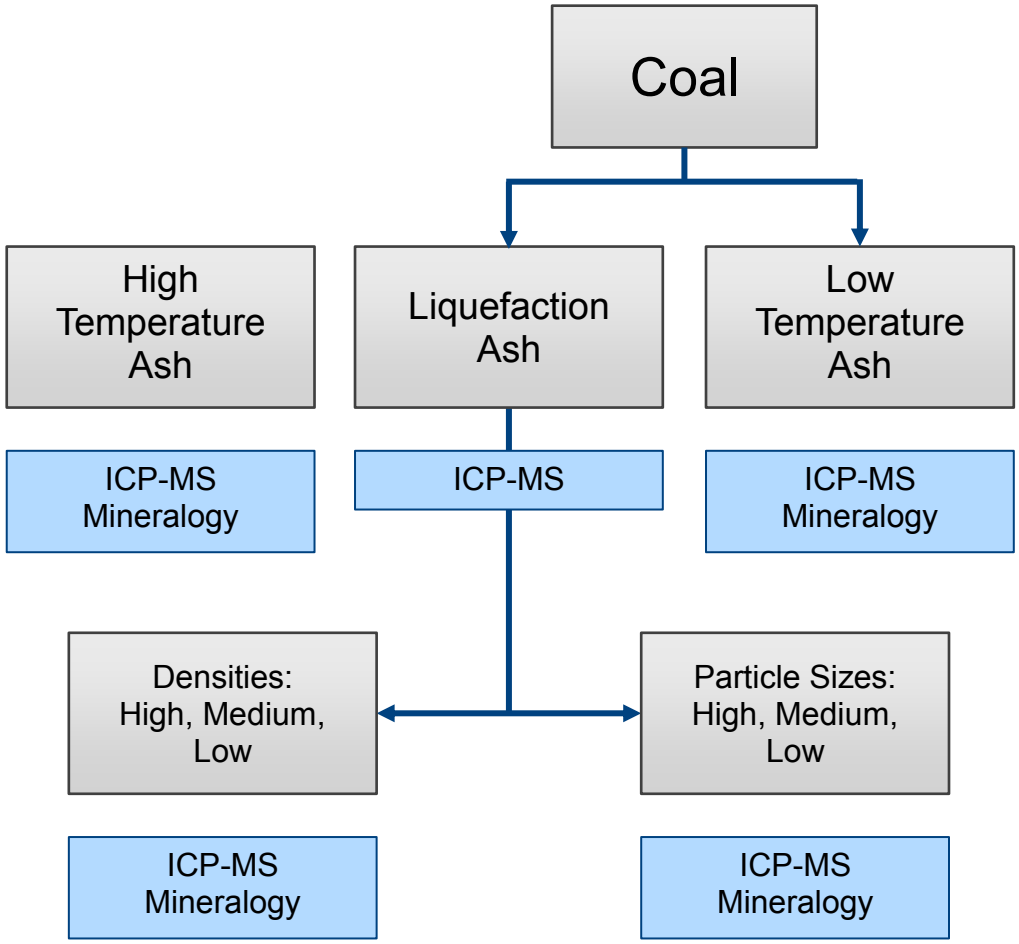

Figure 1: Schematic describing coal ash samples of interest in this study.

High temperature ash and low temperature ash were obtained from coal combustion power plants in the Appalachian Basin; the samples collected comprise feed coal, bottom ash and fly ash. The plant operations were noted to the extent possible, including any urea injections or other emissions control that would affect the state of the coal ash. There is not a direct association between the feed coal and the ash samples that were collected, since in many cases the plant operations included significant ash and coal storage, but the samples were taken as near to the production point as feasible. It was not feasible to obtain fly ash at different

points in the flue gas treatment train since this handling is largely automated, and safe access to the ash could not be provided until after the fly ash sources were combined. High temperature ash samples were obtained from pulverized coal plants, and low temperature ash samples were obtained from a fluidized bed coal combustor.

Beyond operating plant samples, low and high temperature ash tests were performed at Battelle. Middle Kittanning coal from Ohio was ashed in a furnace at both 1,200°C and 800°C to determine how temperature affects the morphology and crystallography of the ash for a known coal source. The weight percent of ash in the 1,200°C and 800°C samples was 6.34% and 7.55%, respectively. A picture of these two samples is provided in Figure 2. The low temperature ash had a red hue and was free flowing, while the high temperature ash had sintered into larger particles that were not free-flowing, and the color had turned much darker. These samples were analyzed by Scanning Electron Microscopy (SEM) and Energy Dispersive Spectroscopy (EDX) to understand the morphological differences between the two.

Selection of an ash source for pursuit in the subsequent feasibility study was made based on concentration of total REE + Y + Sc, as well as ash availability, and anticipated impacts of morphology and crystallography on the leaching and recovery process.

Figure 2: Samples of Middle Kittanning Coal from Ohio that were ashed at 1,200°C (left) and 800°C (right), indicating visual differences from combustion temperature.

2.1 Sample Locations

Data from the US Geological Survey (USGS) was used in conjunction with databases from the West Virginia Geological and Economic Survey (WVGES) and Pennsylvania Geological Survey

(PAGS) to identify coal samples locations that may have high REE concentrations. A map of sample concentrations in the area of study is shown in Figure 3. WVGES also provided access to its extensive coal sample inventory; two promising coal samples were obtained based upon prior USGS and WVGES analyses. These were samples 11250 and 13423 in the WVGES database. A standard table[1] for pure rare earth metal prices was used to assign approximate ash 'worth' throughout this report. Sample 11250 originates from the Fireclay coal seam and was calculated to contain roughly $30.22 of rare earth value per tonne of ash. Sample 13423 was collected from the Powellton coal seam and was estimated to contain $32.95 of rare earth value per tonne of ash.

In the initial examination of the USGS database, Kentucky coal was found to have generally higher rare earth concentrations on an ash basis than neighboring states. The Kentucky Geologic Survey (KGS) provided information about these high concentrations and identified the Fireclay coal seam as a target formation for this study. The Middle Pennsylvanian Fireclay coal seam has a unique layer of tonstein, a layer of ash deposited in a coal forming swamp. This volcanic ash overburden increases the concentration of REE's in the coal through multiple leaching and transport methods.

Power plant samples were obtained with the support of commercial partners to find facilities that were representative of coal power stations. The low temperature sample was obtained by contacting an operator of a known fluidized bed combustion power plant. Coal liquefaction ash was generated at Battelle and used Middle Kittanning coal from Ohio due to its availability and known REE concentration above 300 ppm.

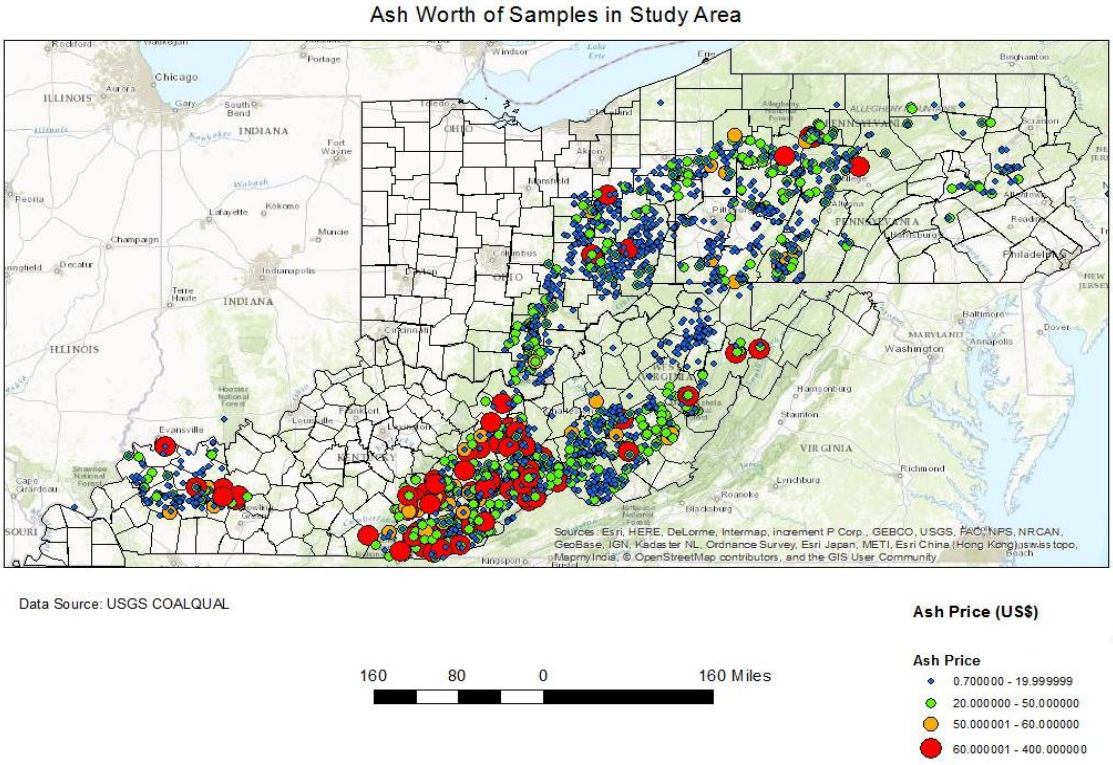

[1] http://mineralprices.com/ (Accessed 14 April 2016)

2.2 Analytical Methods

Coal Liquefaction Sample Preparation

The residual material (ash) from coal liquefaction has not previously been studied, and so was treated separately from low and high temperature ashes. Battelle's proprietary coal liquefaction process consists of blending coal with biomass derivative and bio-solvent at temperatures between 300°C and 500°C and pressure between 200 psi and 1000 psi. This process can convert 85% of coal to a liquid that can be upgraded to jet fuel or chemical products. The 15% residual material contains a considerable amount of ash. For purposes of comparison, coal samples contained around 7% ash, while the total residual material from the coal liquefaction process contained around 30% ash.

After the coal liquefaction process, the residual material is washed with tetrahydrofuran to remove any soluble hydrocarbons followed by filtration and drying under vacuum at 70°C. The washed, dry residual from the coal liquefaction was then separated based on the size and the density to determine if good concentration could be accomplished by relatively simple physical means.

The washed, dried coal liquefaction residual was sieved (or screened) to four fractions: above 800 µm; between 600 µm and 800 µm; between 355 µm and 600 µm; and below 355 µm. Approximately 10 grams of each fraction was calcined in a box furnace at a temperature of 800°C for 2 hours to determine the ash content. The weight percent of each fraction and of the

Figure 3: Map of Kentucky, Ohio, Pennsylvania, and West Virginia with the worth of coal ash labeled based on USGS COALQUAL data and standardized pure rare earth metal prices.

corresponding ash are reported in Table 1, and shown in the corresponding photos in Figure 2. The particle size does not appear to affect the ash content. It is possible that this correlation is affected by the mechanism of grinding in the initial coal liquefaction process and by the shape of the particles.

Table 1: Normalization of washed, dried coal liquefaction residual by particle size

Particle Size (µm)	wt% of each fraction	wt% ash in each fraction
>850	11	33.3
850-600	12.1	21.5
600-355	22.7	18.9
<355	54.2	26.3

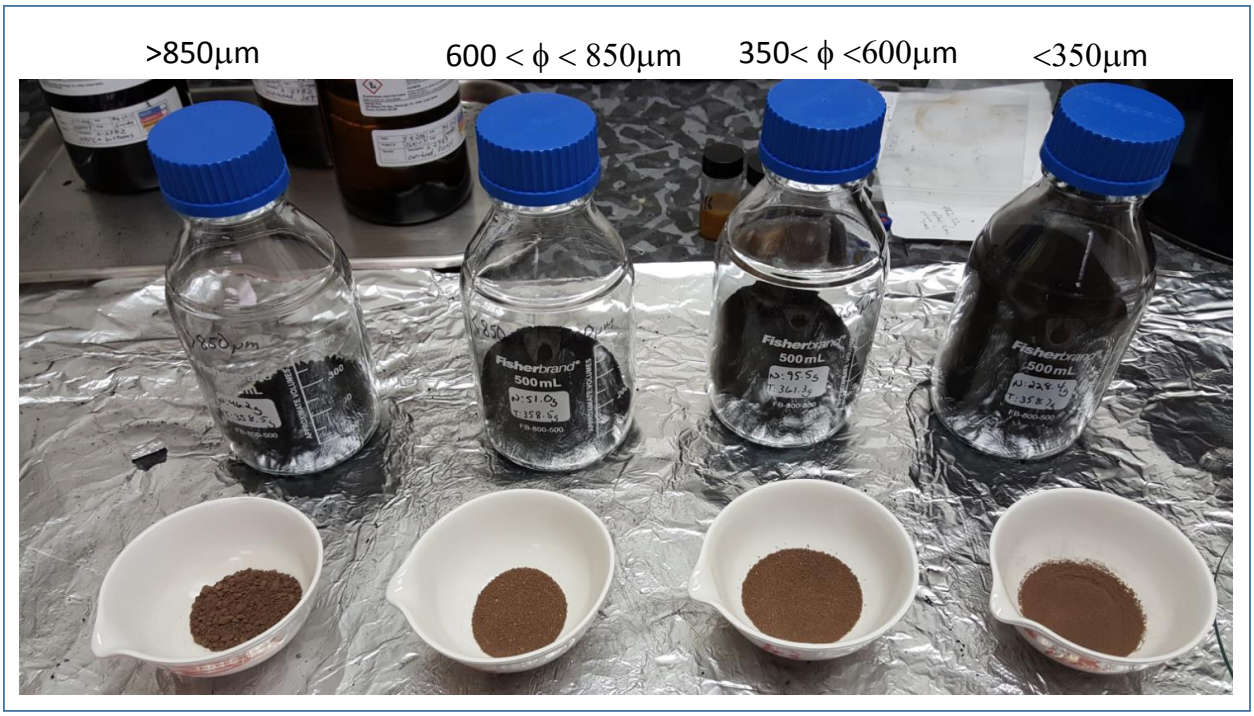

Figure 4: Photo of the four fractions and the corresponding ash

The coal liquefaction residual material is composed of heteroatoms and carbon material. The composition of heteroatoms depends on the coal source, but in general it is composed of alumina (density=3.95 g/cm^3), silicon (density=2.65 g/cm^3), and trace amounts of heavy metal (density>7g/cm^3) and of rare earth elements (density>5g/cm^3). The carbon material is composed of carbon, hydrogen and minor amounts of oxygen and sulfur, with density below 1 g/cm^3. Therefore, any liquid that has a density between 1 g/cm^3 and 2 g/cm^3 can be used to separate REE earth and heavy metal grains from carbon. Water was chosen as the media for gravity separation. Fifty grams of liquefaction residual was blended with 150 ml of DI water under strong stirring, then left to settle for 10 hours. Fifty percent of the liquefaction residual had a density below 1 g/cm^3.

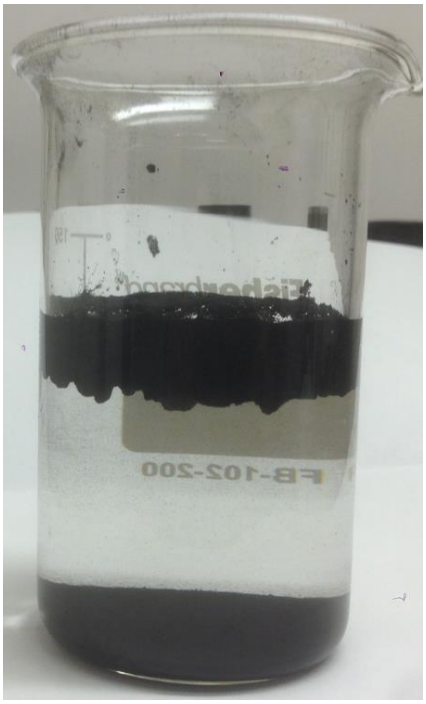

Figure 5: Photo of coal liquefaction residual separation based on the density using DI water

Standard Reference Material

Standard Reference Material (SRM) 1633C, trace elements in fly ash, was procured from the National Institute of Standards and Technology (NIST). Analytes of interest that have certified values, reference values, and information values are listed in Table 22, Table 33, and Table 44, respectively, along with the associated values.

Table 2: Certified values of elements of interest in SRM 1633C

Element of Interest	Certified Value in NIST SRM 1633C, mg/kg
Cobalt	42.9 +/- 3.5
Copper	173.7 +/- 6.4
Manganese	240.2 +/- 3.4

Table 3: Reference values of elements of interest in SRM 1633C

Element of Interest	Reference Value in NIST SRM 1633C, mg/kg
Chromium	258 +/- 6
Dysprosium	18.7 +/- 0.3
Europium	4.67 +/- 0.07
Lanthanum	87 +/- 2.6
Lutetium	1.32 +/- 0.03
Scandium	37.6 +/- 0.6
Terbium	3.12 +/- 0.06
Uranium	9.25 +/- 0.45

Table 4: Information values of elements of interest in SRM 1633C

Element of Interest	Information Value in NIST SRM 1633C, mg/kg
Cerium	180
Neodymium	87
Samarium	19
Ytterbium	7.7

This reference material was included as a blind sample when analysis was performed by external vendors. Additionally, it was analyzed for morphology and crystallography in house.

Elemental Analysis

Analysis was done externally for the elements listed in Table 6. Note that the analytical method dictated which elements were analyzed for, but all samples were analyzed for REE+Y+Sc. Samples that still contained a significant amount of organic material such as feed coal and liquefaction ash were ashed prior to analysis, and all analyses in this report are presented on an ash basis. All samples were digested by either a sodium peroxide or lithium metaborate/ tetraborate fusion, dissolved in nitric acid, then analyzed for elements by Inductively Coupled Plasma Mass Spectrometry (ICP-MS). A sodium peroxide sinter was chosen for the digestion because the USGS data was largely analyzed with a sodium peroxide sinter digestion. This provided consistency when comparing our results with what was already publicly available. The borate fusion was also used with replicates on the reference material to aid in determining which method would be most accurate and economical going forward. Scandium and Lutetium were analyzed by Instrumental Neutron Activation Analysis (INAA) for most samples, as the current peroxide method is not calibrated for those two elements.

In order to verify the accuracy of the methods used, a standard reference material blank (NIST SRM 1633C) was also sent for analysis with each batch of samples, and was analyzed at least 3 times for each method. A comparison of the analytical methods to the reference material values is included in

Table 5, which provides the width of the confidence interval and t-test p-value for common analytes between the two digestion methods and the corresponding NIST standard. Underlined values indicate that the confidence interval was narrower and the t-test suggested greater similarity to the NIST value. In other words, these values were closer to NIST than the other method, and had less variability. There are many cases in

Table 5 where the t-test covered the NIST value with 95% confidence, but this was due to high variability in the sample analyses rather than greater accuracy in the method.

Table 5: Comparison of the Sodium Peroxide and Lithium Borate digestions to the NIST 1633C standard for common analytes. Underlined values indicate cases where the confidence interval was narrower AND the t-test indicated greater similarity to the standard material.

	Sodium peroxide		Lithium Borate	
Element	95% Confidence +/-	t-test p-value	95% Confidence +/-	t-test p-value
As	***26.09***	***0.082***	46.63	0.048
Ba	87.24	0.651	11.47	0.008
Be	2.48	1.000	N/A	N/A
Ce	29.11	0.862	5.17	0.109
Co	0.38	0.003	2.48	0.021
Cr	94.05	0.851	24.84	0.040
Cs	1.94	0.830	0.52	0.021
Cu	31.94	0.545	24.84	0.141
Dy	2.01	0.289	2.02	0.517
Eu	0.25	0.153	***0.14***	***1.000***
Ga	1.03	0.014	1.43	0.020
La	5.13	0.178	4.96	0.035
Lu	1.17	0.257	0.05	0.192
Nd	11.19	0.155	***3.71***	***0.246***
Ni	37.95	0.429	14.34	0.044
Pb	***10.70***	***0.298***	22.08	0.008
Rb	***6.25***	***0.481***	11.20	0.113
Sb	N/A	N/A	1.83	0.062
Sc	0.38	0.017	N/A	N/A
Sm	***1.12***	***0.065***	1.17	0.034
Sr	29.64	0.034	***17.97***	***0.380***
Ta	0.94	0.432	***0.29***	***0.556***
Tb	0.14	0.009	***0.14***	***0.297***
Th	***1.90***	***0.094***	2.68	0.087
U	1.37	0.153	1.46	0.642
V	21.66	0.028	N/A	N/A
Yb	***0.52***	***0.026***	0.63	0.015
Zn	***14.34***	***0.208***	103.42	0.052

Another indicator of the suitability of a method to a particular analyte is distance from the known mean (or NIST value). To understand this, the mean distance of analysis results from the NIST value were compared between the borate fusion and sodium peroxide digestions. This is summarized in Figure 6. Both methods skewed low of the NIST standard, suggesting that the digestions are not 100% efficient. The sum of all mean distances from the NIST value for sodium peroxide digestions was -111.35, versus -332.54 for borate digestions.

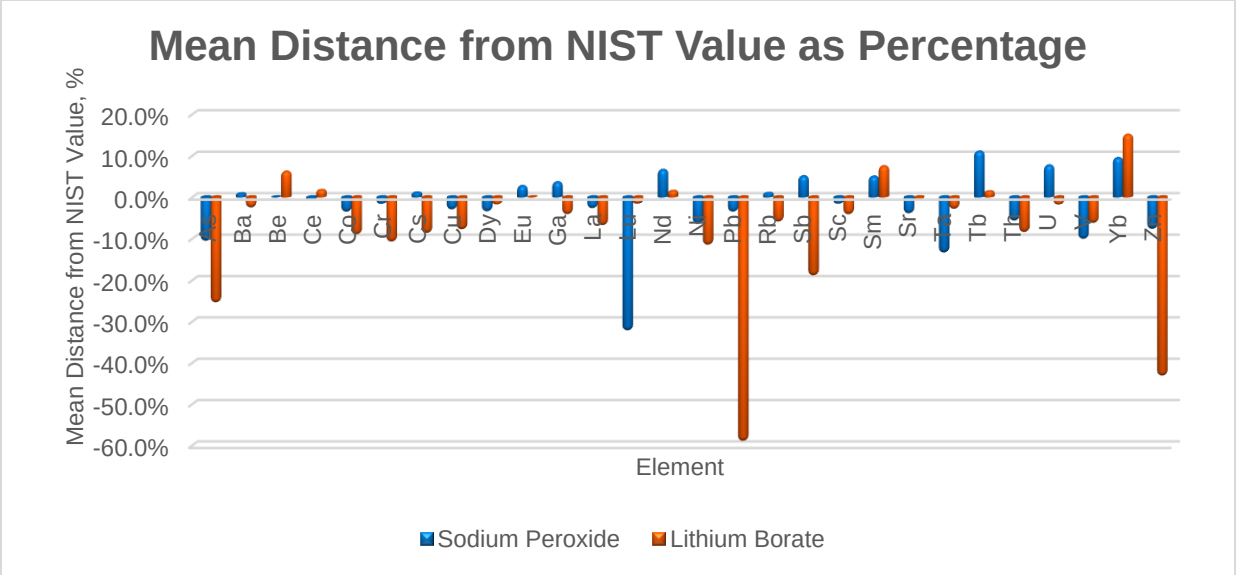

Figure 6: Mean distance of analytes from the NIST value for sodium peroxide and lithium borate digestion methods.

Table 6: Elements analyzed for, along with the associated method. Note that generally a sample was analyzed by a single method, and so the analytes are not always the same between samples, but all were analyzed for REE+Y+Sc.

Element	Method	Element	Method	Element	Method
Al	Peroxide, Borate	Ho	Peroxide, Borate	Sc	Borate, INAA
Ag	Borate	Hf	Peroxide, Borate	Se	Borate
As	Peroxide, Borate	In	Peroxide, Borate	Si	Peroxide, Borate
B	Peroxide, Borate	K	Peroxide, Borate	Sm	Peroxide, Borate
Ba	Peroxide, Borate	La	Peroxide, Borate	Sn	Peroxide, Borate
Be	Peroxide, Borate	Li	Borate	Sr	Peroxide, Borate
Bi	Peroxide, Borate	Lu	Borate, INAA	Ta	Peroxide, Borate
Ca	Peroxide, Borate	Mg	Peroxide, Borate	Tb	Peroxide, Borate
Cd	Borate	Mn	Peroxide, Borate	Te	Borate
Ce	Peroxide, Borate	Mo	Peroxide, Borate	Th	Peroxide, Borate
Co	Peroxide, Borate	Na	Borate	Ti	Peroxide, Borate
Cr	Peroxide, Borate	Nb	Peroxide, Borate	Tl	Peroxide, Borate
Cs	Peroxide, Borate	Nd	Peroxide, Borate	Tm	Peroxide, Borate
Cu	Peroxide, Borate	Ni	Peroxide, Borate	U	Peroxide, Borate
Dy	Peroxide, Borate	P	Borate	V	Peroxide, Borate
Er	Peroxide, Borate	Pb	Peroxide, Borate	W	Peroxide, Borate
Eu	Peroxide, Borate	Pr	Peroxide, Borate	Y	Peroxide, Borate
Fe	Peroxide, Borate	Rb	Peroxide, Borate	Yb	Peroxide, Borate
Ga	Peroxide, Borate	S	Borate	Zn	Peroxide, Borate
Gd	Peroxide, Borate	Sb	Peroxide, Borate	Zr	Borate
Ge	Peroxide, Borate				

Morphology and Crystallography

Analysis of the ash samples for morphology and crystallography was done by Scanning Electron Spectroscopy (SEM), Energy Dispersive Spectroscopy (EDX), and X-Ray Diffraction (XRD). XRD was performed on all samples to understand which crystalline phases are present in the samples. Key samples were mounted in epoxy and polished so that a cross section could be examined. Grains were inspected to attempt to identify rare earth phases as well as phases that contained valuable metals such as cobalt or zirconium. General morphological differences between high temperature, low temperature, and liquefaction ash were also noted.

Each polished mount was photographed as polished, first using an Olympus SZX12 stereo microscope and then an Olympus BX51 research microscope both with an Olympus DP-71 camera. The software used to collect the images was PAX-it! (version 8.0). The images were in a 24 bit format and the image size was 2040 by 1536 pixels. The images were collected in reflected light with various degrees of polarization and at several magnifications.

Each polished mount was lightly coated with carbon (for electrical conduction) and then imaged in a JEOL (JSM-7600F) SEM. A variety of detectors can be used to image the polished mounts. Both secondary and backscattered electron images were collected. Backscattered electron images are ideal for these types of samples because the images show brightness in the image as a function of atomic number. Heavier phases are brighter in the images and clearly allow for phase identification and distribution. The accelerating voltage employed during all analyses was 20kV. The image magnifications vary from mount to mount in an attempt to visualize the feature of interest.

All standard operating practices (SOP) or protocols for the calibration of the magnification and scale bars on images were followed. Magnification is checked every six months and was last checked on June 27, 2016 and both the X and Y directions on the image were in specification (less than one micron out in 100 micron measurements).

An EDAX Apollo X silicon drift detector attached to the JEOL 7600F SEM was used for x-ray collection (energy dispersive spectroscopy - EDS) for the chemistry determinations of various mineral phases seen in the polished mounts. The EDS data was collected using an accelerating voltage of 20kV and 10 to 50 second live time acquisitions typically in a spot mode approach. The raw data collected is supplied and was primarily used to identify phases thought present in each polished mount.

Standard operating practices (SOP) and protocols for the calibration of the energy dispersive spectrometer were followed and the EDS system was in specification prior to data collection.

Samples run by x-ray diffraction were prepared in the same manner. A portion of each sample was ground in an agate mortar with agate pestle. The fine powder for each was packed into a standard glass x-ray sample holder. Each slide was then x-rayed on a Rigaku Ultima IV wide angle powder diffractometer (XRD). Each sample was scanned from 10 to 90 degrees two-theta, using a 0.02 step size and a speed of 0.1 degree/minute. The x-ray radiation source used was a copper long fine focus x-ray tube operated at 40kV and 44 mA. All subsequent processing was done using Materials Data, Inc. (MDI) software (JADE 9.6+) and the Powder Diffraction File-4+ 2015 RDB.

All QA protocols followed are covered in the Standard Operating Procedure (SOP) for Ultima IV X-ray diffraction with Materials Data, Inc. JADE+ software. This includes mechanical alignment of the goniometer. The goniometer check using NBS 640b Silicon showed little change from the expected alignment values.

The collected x-ray patterns were processed by first modeling and then removing the background inherent in the x-ray trace as well as the Ka2 line contributions. Each derived pattern was then run through the extensive Search/Match programming module with accessibility to approximately 366,000 crystalline (inorganic and organic) indexed substances (Powder Diffraction File-4+ 2015 RDB). All sub-files, without employing a chemistry filter, were evaluated to attempt to match the crystal structure of the unknown material to any pattern(s) in the database. Computer identification was then followed up with manual processing and identification to obtain the list of phases thought to be present in each sample. REE-bearing phases were specifically examined to see if any patterns fit the small number of unindexed peaks. No REE phases were deemed present in XRD.

Two additional x-ray analyses were conducted; quantitative phase determination (whole pattern fitting (WPF)) and how much of the collected pattern was crystalline.

The MDI JADE software contains an option for whole pattern fitting of the collected data and Rietveld refinement of present crystal structures. Measured patterns are fitted to a diffraction model by non-linear least squares optimization in which certain parameters are varied to improve the fit of the model to the observed data. Modeling parameters include background, profile parameters, and lattice constants. Typically, the crystal structures of the phases of interest must be known along with atomic coordinates, occupancies and thermal parameters. In cases where the crystal structure is not known, then a reference pattern derived from the known d-spacings, line intensities, and corresponding crystallographic information including Miller indices and a value for the Reference Intensity Ratio (I/Ic) may be substituted.

A twelve-phase WPF control file was created and run to perform a least squares iteration of various refinable parameters to minimize the differences between the observed and the simulated pattern. After an initial refinement, each individual phase is checked against the refinement and adjusted (parameters to make it fit the observed pattern better) or removed if it does not fit the pattern. A second and sometimes a third refinement are then performed. A successful refinement is defined mathematically by the convergence of refinable parameters to meaningful values. The refined pattern can be checked against the observed data and the weight fractions of the individual phases are displayed. The total weight fractions must sum to 100%. Therefore, any phases not included in the refinement will cause uncertainties in the absolute values of the refined phases. The data uncertainties are believed to be ±3% to 5% depending on the abundance and complexity of the pattern.

X-ray diffraction will produce very distinct patterns for crystalline and amorphous materials. Crystalline materials give rise to sharp well-defined peaks, while poorly crystallized or materials with very small crystallites will generate more diffuse diffraction signals. Amorphous materials generate extremely broad humps or peaks that can also display the occasional harmonic.

A rigorous method of calculating percentage crystallinity involves measuring the total amorphous and the total crystalline diffraction intensities. A full XRD pattern is used. The true

background is determined first by employing the background fitting function. Next, the amorphous regions are added using peak profiling tools. Finally, the crystalline peaks are added for refinement using the peak profile tools. An iterative refinement program is run to fit these two components. The fitted profile should match the general pattern shape and the percentage crystallinity is then given by the ratio between these two intensities IC /(IC + IA).

3.0 Results

3.1 Elemental Analysis

High Temperature (Pulverized Coal Combustion) Samples

Pulverized coal combustion (PCC) ash was obtained from four operating power plants with the assistance of American Electric Power (AEP). Both bottom ash and fly ash samples were collected, and in one case feed coal samples were also obtained. A summary of the rare earth content for all of the PCC plant samples is shown in Table 7, while detailed analytical results are included as Appendix A. PCC Plant A was unique in that it had two separate feed coal piles feeding different units. Feed Coal A was generally washed and of higher quality than Feed Coal B and also had higher REE content. However, the feed coal samples did not originate from the same mine(s), and so no conclusions can be drawn about the effect of washing on coal ash REE concentration. The fly ash collected from PCC Plant A was associated with Feed Coal A, and since it had the highest REE+Y+Sc concentrations, as well as attractive HREE/LREE ratios, it was selected for replicate analyses to understand variability in the analytical methods as well as build confidence in the starting concentration REE for later leaching tests. Two samples of this fly ash were taken. Sample 1 came from a single truckload of ash, while Sample 2 was collected from four separate truckloads.

Table 7: Summary of the REE content of PCC plant samples

	Total REE	Total REE+Y+Sc	HREE+Y	LREE+Sc	HREE/LREE
	ppm	ppm	ppm	ppm	Ratio
PCC Plant A Bottom Ash from Pile	287.46	373.06	89.26	283.8	0.31
PCC Plant A Fly Ash from Pile, Sample 1	410.3	556	151.9	404.1	0.37
PCC Plant A Fly Ash from Pile, Sample 2	429.45	574.05	153.65	420.4	0.36
PCC Plant A Feed Coal A	416.73	566.63	156.03	410.6	0.38
PCC Plant A Feed Coal B	269.44	342.54	73.74	268.8	0.27
PCC Plant A Fly Ash from Pile, Sample 1	409.26	548.26	146.95	401.31	0.36
PCC Plant A Fly Ash from Pile, Sample 1	399.69	537.69	145.59	392.1	0.37
PCC Plant A Fly Ash from Pile, Sample 1	400.54	539.54	147.87	391.67	0.37
PCC Plant B Fly Ash from Pile	278.29	367.49	86.09	281.4	0.30
PCC Plant B Bottom Ash from Pile	265.69	352.89	84.59	268.3	0.31
PCC Plant C Fly Ash from Pile	261.56	349.16	85.36	263.8	0.32
PCC Plant C Bottom Ash from Pile	259.89	341.89	81.19	260.7	0.31
PCC Plant D Fly Ash from Pile	307.07	391.07	80.8	310.27	0.26
PCC Plant D Bottom Ash from Pile	291.32	369.32	77.48	291.84	0.26

Although it appears that bottom ash has slightly lower concentration of total REE+Y+Sc than fly ash, the effect is small and not statistically significant. PCC Plant A was omitted from this analysis since it is possible that the bottom ash analyzed originated from the lower starting concentration feed coal, and may not have been associated with the same feed as the fly ash. Feed Coal A and Samples 1 and 2 of the fly ash do not exhibit meaningful differences in total rare earth concentration, also supporting the expectation that bottom ash REE concentrations are close to fly ash.

Low Temperature (Fluidized Bed Combustion) Samples

Fluidized bed combustor (FBC) ash samples were obtained from a plant in West Virginia. These samples are of particular interest due to their lower combustion temperature, which may help to avoid vitrification of the ash particles. Vitrification is expected to reduce the leaching efficiency of REE since the glassy phases are largely resistant to acid attack. A summary of the REE content in the FBC ash is provided in Table 8. Rare earth concentrations were generally lower than observed in the PCC plant samples, but this is likely due to dilution from the addition of lime to the combustor. Calcium concentrations were roughly 10 times higher in FBC ash than the PCC ash, increasing from around 2% by mass to roughly 20% by mass. Sulfur concentrations are also higher, as expected, since the lime is added to scrub sulfate from the process. Although calcium would typically be expected to contaminate the leach solution, calcium sulfate generally has low acid solubility, and its impact would likely be minimal. Although the leaching recovery of REE from FBC ash is likely to be high, the quantity of ash available from FBC plants is small compared to that for PCC plants.

Table 8: Summary of the REE Concentration of FBC Plant Samples

	Total REE	Total REE+Y+Sc	HREE+Y	LREE+Sc	HREE/LREE
	ppm	ppm	ppm	ppm	Ratio
Fluidized Bed Combustor Fly Ash	147.5	188.1	38.6	149.5	0.258194
Fluidized Bed Combustor Bottom Ash	121.4	153.2	30.5	122.7	0.248574

Coal Liquefaction Samples

Ash from Battelle's bio-based coal liquefaction process was taken from pilot scale tests. The process dissolves coal in a proprietary biosolvent, which prevents the ash from experiencing high temperature oxidizing environments. After digestion of the coal, the resulting oil is centrifuged to remove ash and heavy carbon deposits, and this residual material is what was analyzed at Battelle. It was separated into two density cuts as well as four particle size cuts to determine whether a simple mechanical separation could cause meaningful concentration of the sample. Figure 8 shows the concentration of REE through the processing of the coal liquefaction ash, and Figure 7 indicates how the ratio of heavy to light REE changed through the process.

It appears that the coal liquefaction process enriches REE over the feed coal. It is notable that the ash content of the coal liquefaction process samples used in this analysis was low; in the range of 7% ash, where it is normally expected to be 30% ash or higher. Pilot plant operations indicate that this could be due to higher coking of the coal conversion process, but could also be due to preferential collection of larger particle size ashes in the centrifuge. Beyond these cases,

the REE enrichment could be caused by lesser dissolution of coal components that bear REE elements, causing differential enrichment.

The coal liquefaction process also appears to enrich the ash with the more valuable heavy rare earth components, as indicated in Figure 7. Although the liquefaction process does seem to enrich REE, simple density and particle size separations of the residual material did not have a significant effect on REE enrichment. It is likely that the particle sizes of the residual material are large compared to a typical grain of rare earth, which is on the order of microns. Much finer milling would likely be required to liberate the rare earth components for separation by flotation, and a non-standard particle size sorting process would be required to significantly enrich the REE by particle size cuts.

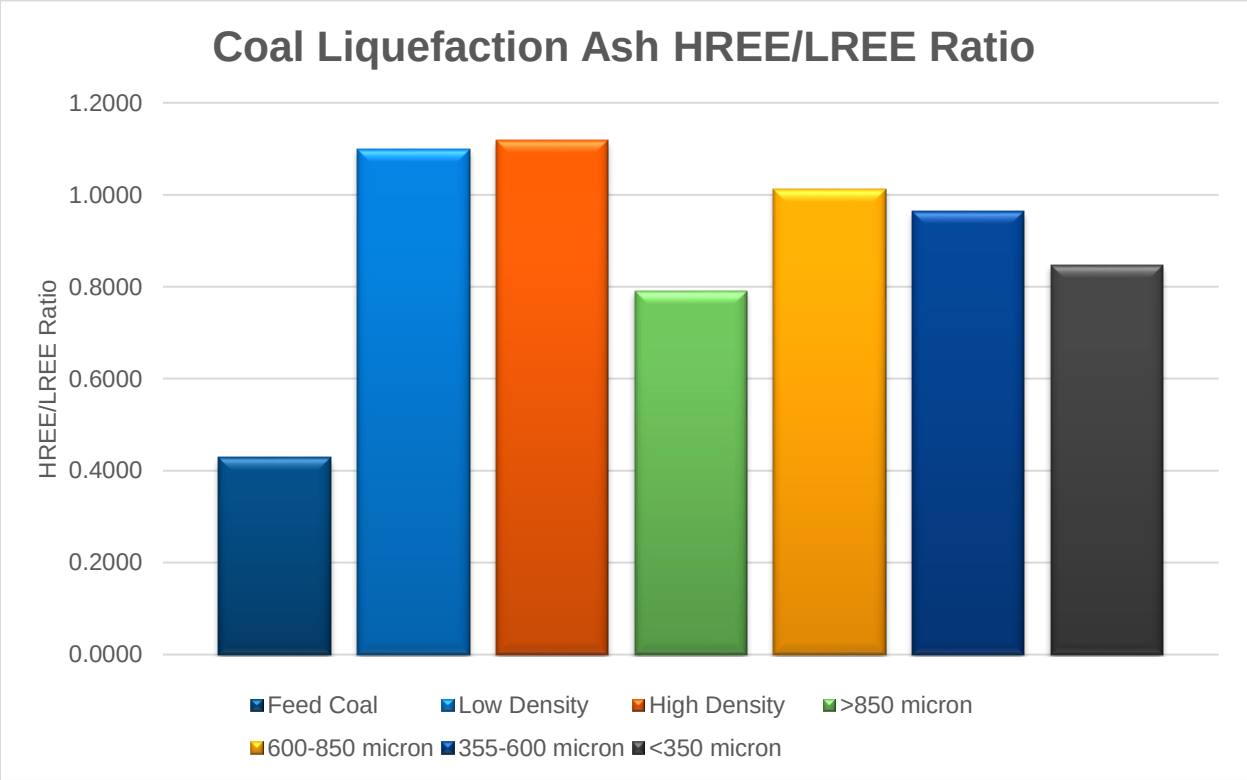

Figure 7: Ratio of heavy to light REE in the coal liquefaction ash treatments.

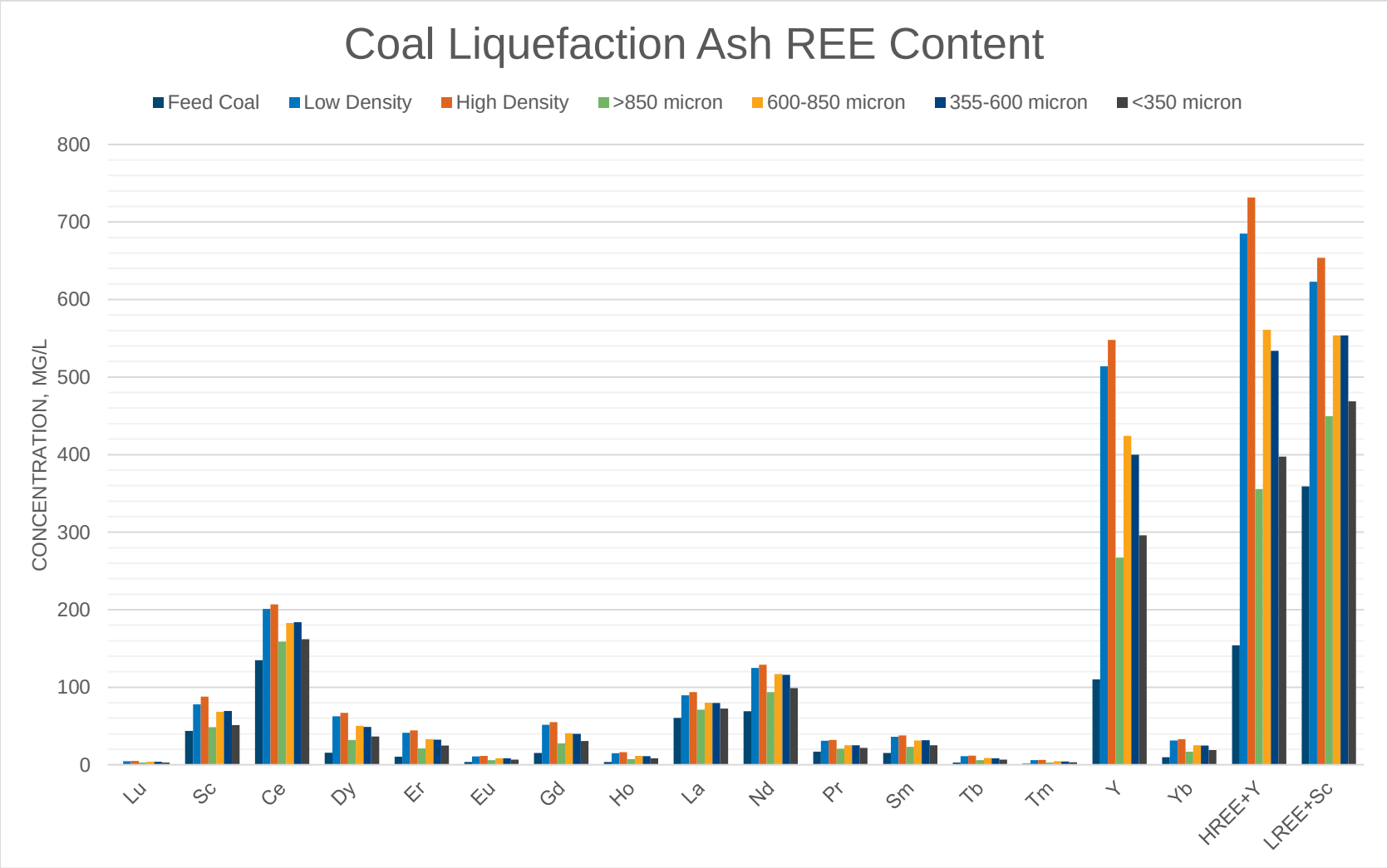

Figure 8: Chart of REE concentrations in the feed coal, density cuts and particle size cuts for coal liquefaction ash.

Coal Samples

Feed coal and raw coal samples were taken to understand the REE concentration as well as concentrations of other potentially valuable components. Two feed coal samples from PCC Plant A were sampled, the coal liquefaction feed coal was sampled, and raw coal samples provided by WVGES were also sampled. A summary of the REE content for these coals, along with other bulk phases, is provided in Table 9. One notable result from these analyses is the high total REE content of the Powellton seam coal, and in particular its high heavy rare earth content.

Table 9: Elemental Analysis Results for Feed and Raw Coal Samples

	% Ash	Al	Ca	Fe	K	Mg	S
	%	%	%	%	%	%	%
Fireclay Seam Coal	19.5	16.3	0.37	6.16	0.9	0.26	0.46
Powellton Seam Coal	3.99	15.7	1.01	7.98	1.7	0.42	1.06
Pulverized Coal Plant A Feed Coal A	7.56	14.3	0.95	12	1.7	0.41	0.82
Pulverized Coal Plant A Feed Coal B	12.1	10.7	1.52	15.4	1.5	0.5	1.17
Coal Liquefaction Feed Coal, Middle Kittanning, Ohio	14.7	12.8	1.59	2.43	0.5	0.47	0.86

	Si	Ti	Total REE	Total REE+Y+Sc	HREE+Y	LREE+Sc	HREE/LREE
	%	%	ppm	ppm	ppm	ppm	Ratio
Fireclay Seam Coal	25.1	0.9	871.23	1094.73	274.83	819.9	0.335199
Powellton Seam Coal	22.1	0.97	600.67	1000.67	457.77	542.9	0.843194
Pulverized Coal Plant A Feed Coal A	20.3	0.74	416.73	566.63	156.03	410.6	0.38
Pulverized Coal Plant A Feed Coal B	20.9	0.54	269.44	342.54	73.74	268.8	0.27
Coal Liquefaction Feed Coal, Middle Kittanning, Ohio	28.4	0.95	359.28	512.88	153.88	359	0.43

Material Values

In order to assist in decision making regarding which feedstock to pursue with Battelle's leaching process, values were assigned to key REE compounds as well as a few other elements that showed potentially high values. These values are for pure, metallic elements, unless otherwise indicated, and although they do not necessarily reflect the latest market values, are helpful in comparing feedstocks. The values used are listed in Table 10. Using the elemental analyses for 26 tested samples (excluding NIST standard runs), the value of these materials in a ton of ash was calculated, adjusting the price to a pure form by molecular weight when prices were reported for an oxide or carbonate. For the 26 samples tested, the average value per ton of ash was $645, with a median of $589 and range from $171 to $1,449.

Table 10: Representative prices for pure metal forms (unless noted otherwise) of elements of interest. Data from http://mineralprices.com/ (Accessed 14 April 2016)

Element	Price	Unit
La	7	$/kg
Ce	7	$/kg
Pr	85	$/kg
Nd	60	$/kg
Sm	7	$/kg
Eu	150	$/kg
Gd	55	$/kg
Tb	550	$/kg
Dy	350	$/kg
Er	95	$/kg
Y	35	$/kg
Sc	15,000	$/kg
Sb	9.92	$/kg
Bi	27.34	$/kg
Cd	1.94	$/kg
Co	22.99	$/kg
Mg	1.99	$/kg
Mn	1.63	$/kg
Mo	13.23	$/kg
Se	57.32	$/kg
W (WO3)	4.99	$/kg
U (U3O8)	80.47	$/kg
V (V2O5)	48.72	$/kg
Cu	7.80	$/kg
Sn	14.66	$/kg
Ni	8.61	$/kg
Ag	553.10	$/kg
Li_2CO_3	5	$/kg*
*http://fortune.com/2016/06/06/lithium-price-tesla-metal-future/		

As illustrated in Figure 9, Scandium dominates the material values, representing roughly 91% of the value of materials within the ash. Vanadium accounts for 3.4% of the value, which is greater than any of the rare earths other than Scandium, and Lithium contributes nearly as much value as Neodymium. Scandium, Vanadium, Yttrium, and Lithium are expected to be leachable at least in part by nitric acid and are candidates going forward as byproducts to subsidize rare earth recovery from coal ash. The average and median concentrations for these compounds in the 26 samples analyzed are compared to over 3,000 samples from the USGS CoalQual database in Table 11, and indicate that the values observed in Battelle's testing are

representative, supporting the conclusion that these byproducts are likely to be available in other ash streams. The CoalQual samples are from Ohio, Pennsylvania, West Virginia, and Kentucky and were converted to an ash basis for this comparison.

Scandium should be considered as a primary byproduct in the process due to its value. It is primarily used as an alloying compound with aluminum to make high performance, lightweight alloys and increased production may serve to increase the potential applications and, consequently, the currently small market. Vanadium is also used largely as an alloying compound to strengthen steel but is also useful as a catalyst. Lithium is currently in high demand for the manufacture of lithium ion batteries, which are enabling for many green technologies as well as consumer electronics. Cobalt is also used in battery electrodes as a catalyst and in many high performance alloys and magnets. Vanadium, Lithium, and Cobalt recovery will be evaluated for feasibility in subsequent project tasks as the process is developed.

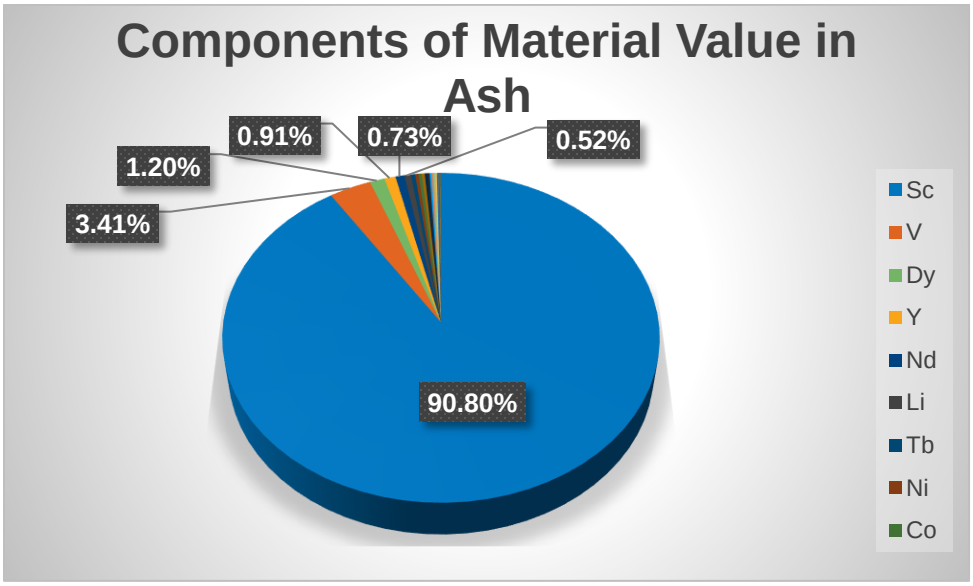

Figure 9: Components of the average material value in the measured ash samples. Scandium and Vanadium values both represented more than the rare earth elements, and are candidates for byproducts to subsidize the REE recovery.

Table 11: Comparison of Battelle's sample analyses to USGS CoalQual database values for byproducts of interest in coal ash.

		Co	Li	Ni	Sc	V	Y
CoalQual	Average	79.61	149.52	187.31	39.08	201.26	83.56
	Median	50.40	130.13	130.27	34.22	179.82	70.07
Battelle Tests	Average	74.03	126.62	204.62	39.11	253.04	168.10
	Median	43.00	123.00	110.00	35.80	265.50	106.50

Within the rare earth elements in coal, Dysprosium represents the highest value, as shown in Figure 10. Combined with Neodymium, Terbium, and Praseodymium, these 4 elements account for over 75% of the rare earth value in the ash. Accordingly, Battelle's process will be tailored to focus on these rare earth components.

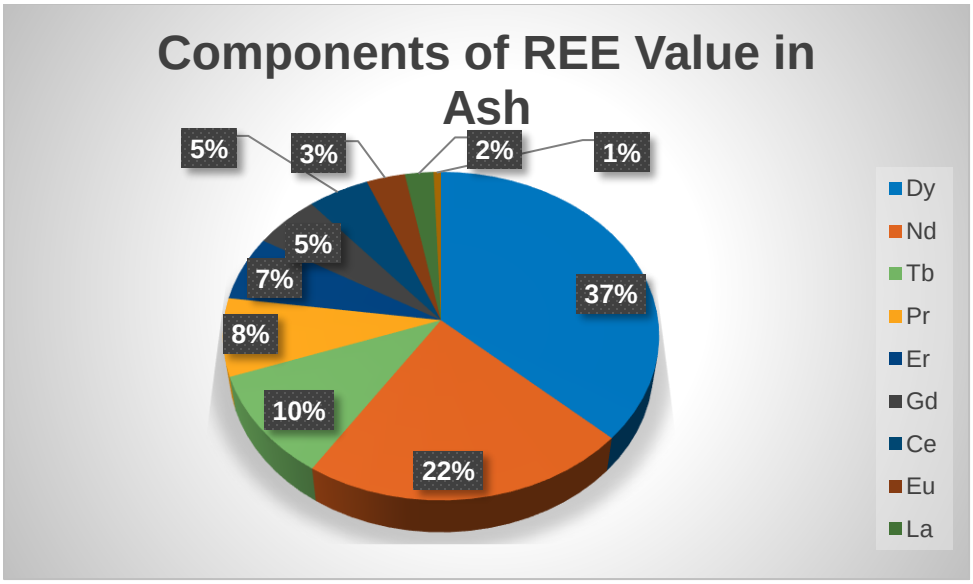

Figure 10: REE value components in the coal ash samples analyzed by Battelle.

3.2 Morphology and Crystallography

High Temperature (Pulverized Coal Combustion) Samples

High temperature ash from PCC Plant A and crushed Ohio Middle Kittanning Coal ashed in a furnace at 1,200°C furnace at 1,200°C were analyzed by SEM and EDX after mounting in epoxy, cutting, and polishing the cross section polishing the cross section to understand the form of REE within the ash as well as morphological differences. morphological differences.

Figure 11 provides a side by side comparison of the fly ash and furnace ash under optical

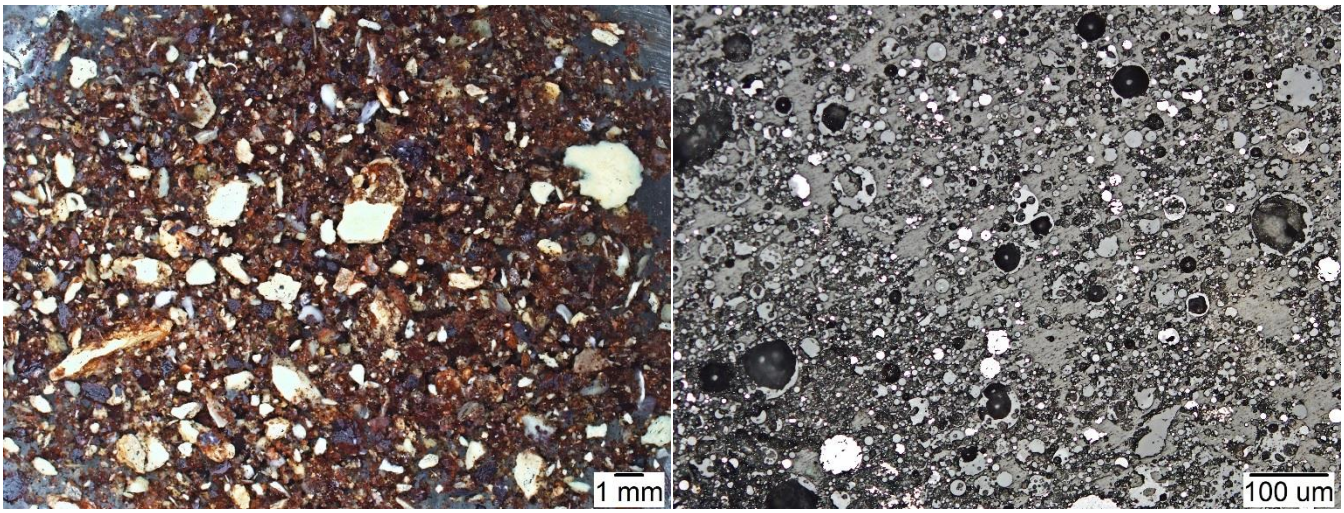

magnification.

Figure 11: Optical images of ash generated in a 1,200°C furnace (left) and PCC plant fly ash (right)

Low angle backscattering (LABE) in the SEM was used to highlight grains of higher molecular weight material in the 1,200°C sample, and these grains were interrogated by EDX to identify those which contained REE or materials of interest. In general, the host phase was

aluminosilicate, and the grains were large and jagged as it appeared the ash material had fused together in the furnace. Grains of Zircon and Hafnium were identified, as well as rare earth phosphate grains. These grains were generally small, on the order a few microns across, as shown in Figure 12. Grains were also found where thorium was associated with the rare earth phosphates, which is significant since thorium will likely become a radioactive waste stream in the rare earth processing. More detailed SEM and EDX data for the 1,200°C ash are provided in Appendix B.

The fly ash, as expected, had much smaller particle sizes, and appeared much more uniformly spherical, as shown in spherical, as shown in

Figure 11. This is likely attributable to solidification of the ash particulates while suspended in the vapor phase, as opposed to within a crucible.

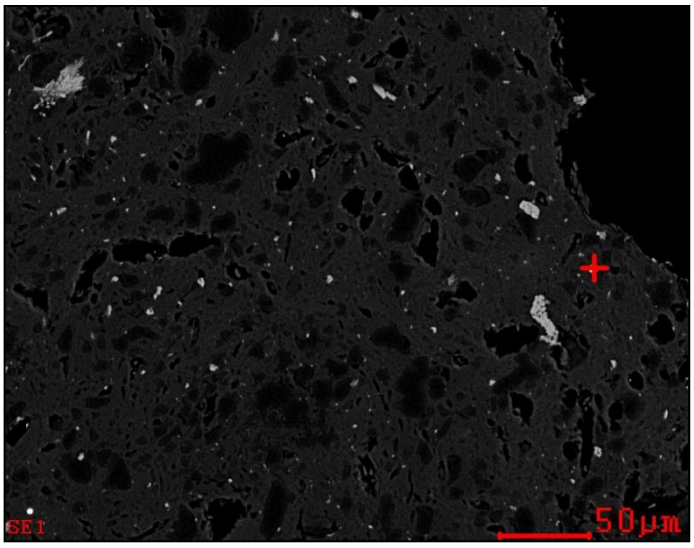

Element	Wt%	At%
CK	07.9	20.53
OK	21.3	41.39
MgK	00.2	00.22
AlK	01.6	01.79
SiK	17.4	19.32
ZrL	42.7	14.59
KK	00.3	00.27
TiK	00.1	00.05
FeK	00.9	00.49
HfL	07.7	01.34
Matrix	Correction	ZAF

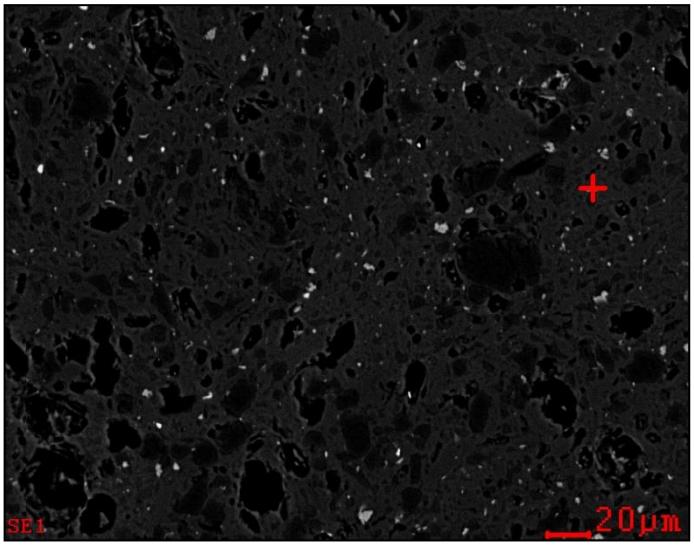

Element	Wt%	At%
CK	07.2	17.35
OK	20.8	37.59
MgK	00.6	00.70
AlK	13.9	14.91
SiK	13.7	14.08
PK	06.9	06.41
KK	01.3	00.96
CaK	00.5	00.39
TiK	00.3	00.16
LaL	07.8	01.63
CeL	16.6	03.42
PrL	01.9	00.38
NdL	07.4	01.48
FeK	01.0	00.53
Matrix	Correction	ZAF

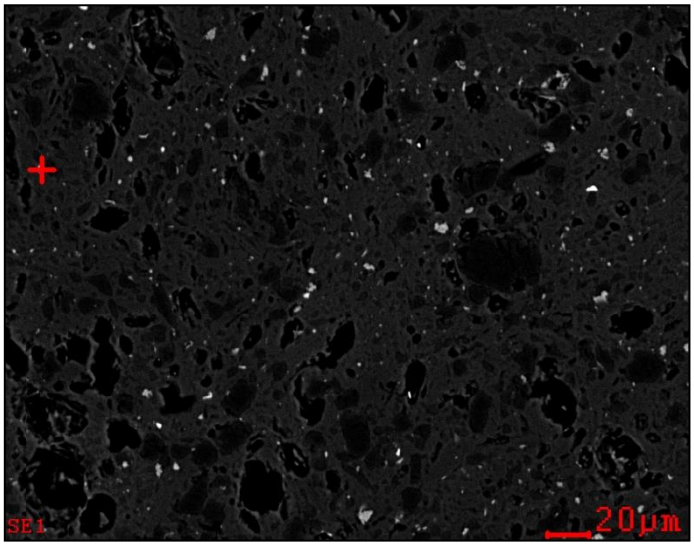

Element	Wt%	At%
CK	05.3	14.29
OK	21.6	43.43
MgK	00.5	00.60
AlK	07.7	09.22
SiK	10.5	12.03
PK	08.6	08.99
ThM	02.5	00.34
KK	01.1	00.88
TiK	00.2	00.16
LaL	08.6	01.99
CeL	17.7	04.06
PrL	02.7	00.61
NdL	09.6	02.15
SmL	02.1	00.46
FeK	01.4	00.79
Matrix	Correction	ZAF

Figure 12: Micrographs and EDX indicating zircon/hafnium phases, top, rare earth phosphates, middle, and rare earth phosphates with associated thorium, bottom, in ash generated at Battelle in a 1,200°C furnace.

Low Temperature (Fluidized Bed Combustion) Samples

Fluidized bed fly ash from PCC Plant A and crushed Ohio Middle Kittanning Coal ashed in a furnace at 800°C were analyzed by SEM and EDX after mounting in epoxy, cutting, and polishing the cross section to understand the form of REE within the ash as well as morphological differences. Figure 13 provides a side by side comparison of the fly ash and furnace ash under optical magnification.

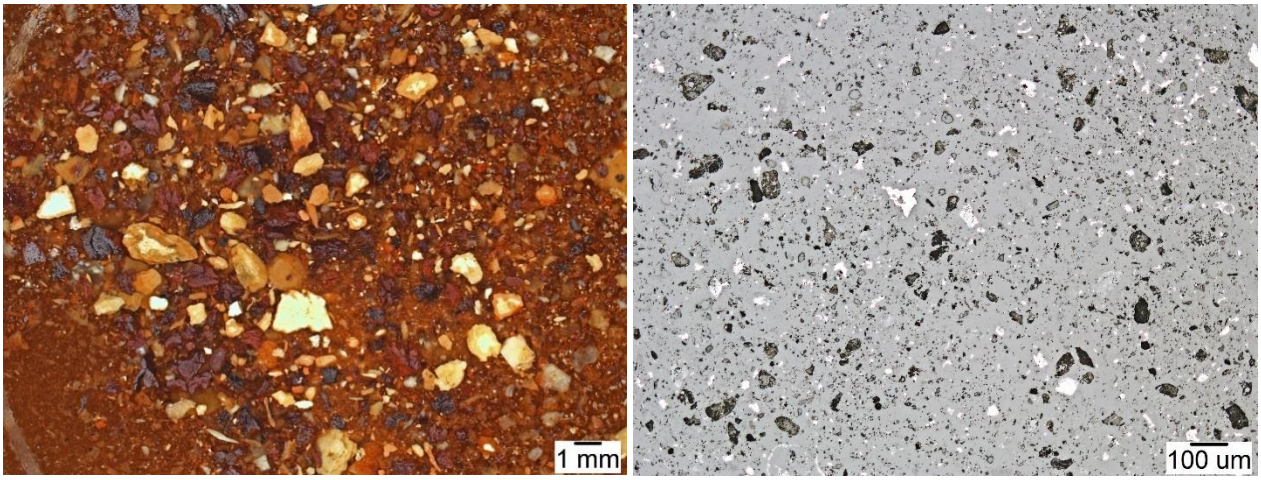

Figure 13: Optical images of ash generated in a 800°C furnace (left) and FBC plant fly ash (right)

The 800°C ash under SEM/EDX analysis was very similar to the 1,200°C ash, however there were grains of what appear to be Yttrium phosphate, as shown in Figure 14. Additionally, there were cases of rare earth phosphates scattered throughout a larger alumina/silica grain. More detailed SEM and EDX data for the 800°C ash are provided in Appendix C.

The fly ash from a low temperature fluidized bed combustion plant had generally smaller particle sizes than the furnace ash, as was observed in the high temperature cases. However, the particles are much less uniformly spherical than in the higher temperature PCC fly ash, which would seem to indicate much less vitrification from the high temperatures.

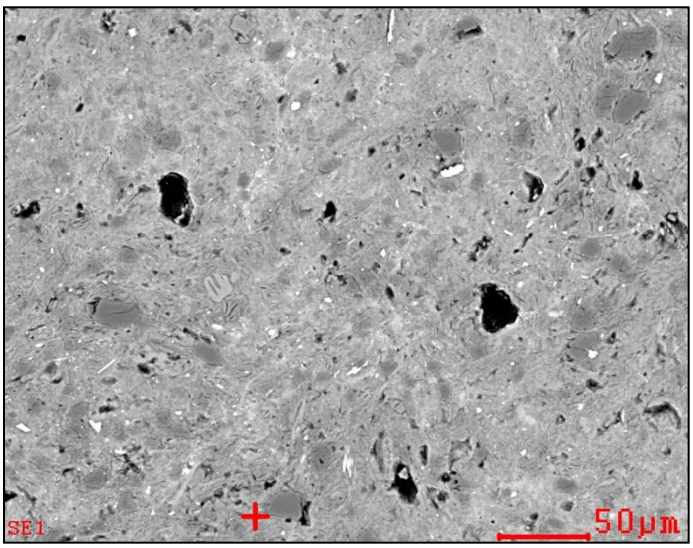

Element	Wt%	At%
OK	34.3	52.91
NaK	00.0	00.04
MgK	00.7	00.71
AlK	18.4	16.82
SiK	18.8	16.55
YL	14.8	04.12
PK	07.0	05.59
SK	00.0	00.00
ClK	00.0	00.03
KK	02.8	01.74
CaK	00.3	00.18
TiK	00.5	00.25
MnK	00.0	00.00
FeK	02.4	01.07
Matrix	Correction	ZAF

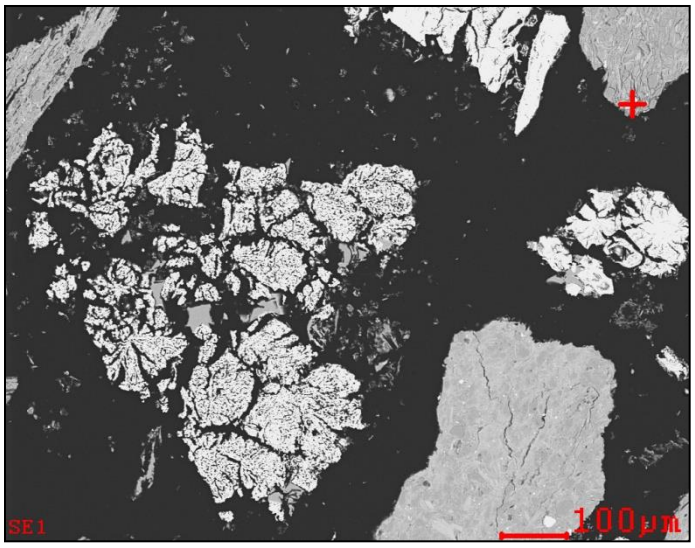

Element	Wt%	At%
OK	23.4	52.47
NaK	00.0	00.00
MgK	00.3	00.38
AlK	01.6	02.07
SiK	12.9	16.57
YL	08.3	03.37
PK	03.5	04.05
ZrL	45.2	17.82
SK	00.1	00.06
ClK	00.0	00.00
KK	00.3	00.26
CaK	00.6	00.57
TiK	00.1	00.06
LaL	00.0	00.00
CeL	00.2	00.06
PrL	00.0	00.00
NdL	00.1	00.04
MnK	00.0	00.00
FeK	03.5	02.22
Matrix	Correction	ZAF

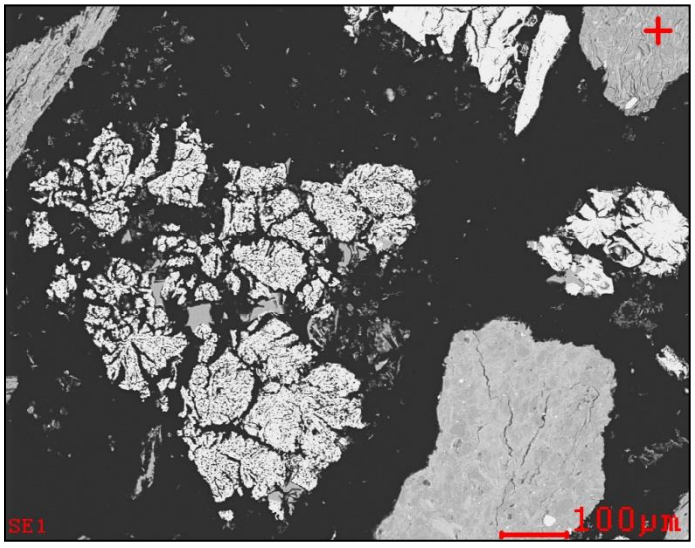

Element	Wt%	At%
OK	33.4	47.78
NaK	00.3	00.29
MgK	00.7	00.66
AlK	19.8	16.80
SiK	37.2	30.30
PK	00.0	00.00
SK	00.0	00.00
ClK	00.2	00.12
KK	04.4	02.57
CaK	00.1	00.07
TiK	00.6	00.28
LaL	00.3	00.04
CeL	00.3	00.04
PrL	00.2	00.03
NdL	00.1	00.02
MnK	00.0	00.01
FeK	02.4	00.99
Matrix	Correction	ZAF

Figure 14: 800°C furnace ash showing Yttrium Phosphate phases, as well as scattered rare earth content in a larger alumina/silica grain.

Coal Liquefaction Samples

Ash from Battelle's coal liquefaction process was collected from the pilot plant, and as shown in Figure 15, appeared to be composed of smaller grains than the furnace ashes that were loosely aggregated into larger grains. No REE phases could be identified in the SEM/EDX analysis, and

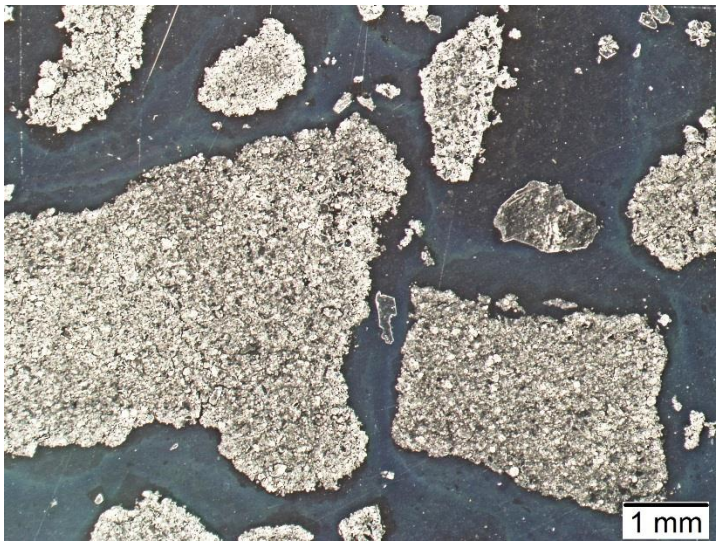

Figure 15: Optical image of the coal liquefaction ash analyzed, showing grains that appear to be aggregates of much smaller pieces.

the grains were largely carbon. Iron sulfide was readily identified, indicating minimal oxidation of the carbon. There were also grains in the SEM that appeared to show leaching of carbon from the ash material. Notable features are shown in Figure 16, while more detailed results are provided in Appendix D.

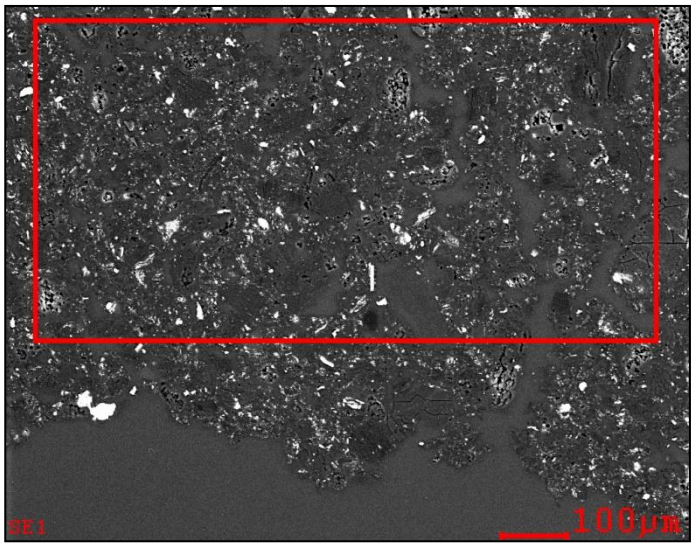

Element	Wt%	At%
CK	83.7	88.94
OK	11.4	09.05
NaK	00.2	00.13
MgK	00.1	00.03
AlK	00.9	00.45
SiK	01.1	00.50
PK	00.1	00.02
SK	00.9	00.38
ClK	00.9	00.32
KK	00.1	00.02
CaK	00.2	00.06
TiK	00.1	00.01
MnK	00.1	00.01
FeK	00.4	00.09
Matrix	Correction	ZAF

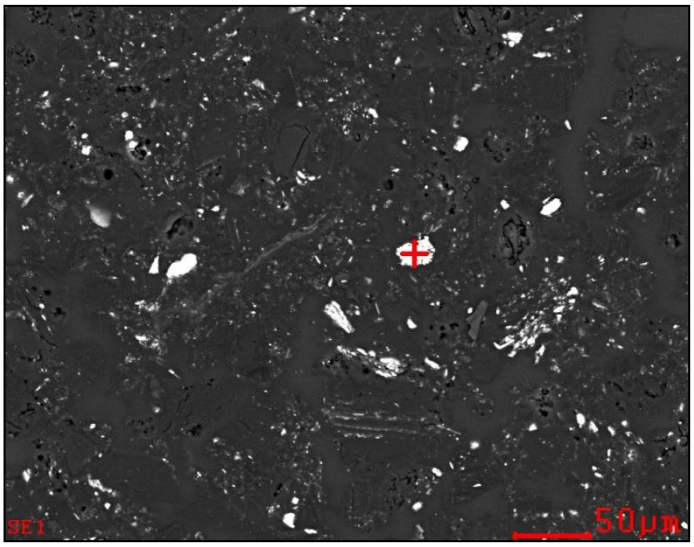

Element	Wt%	At%
OK	02.8	07.12
NaK	00.2	00.27
MgK	00.2	00.26
AlK	00.2	00.34
SiK	00.2	00.23
PK	00.2	00.20
SK	37.4	47.99
ClK	00.2	00.21
KK	00.0	00.00
CaK	00.0	00.03
TiK	00.1	00.08
MnK	00.1	00.10
FeK	58.6	43.16
Matrix	Correction	ZAF

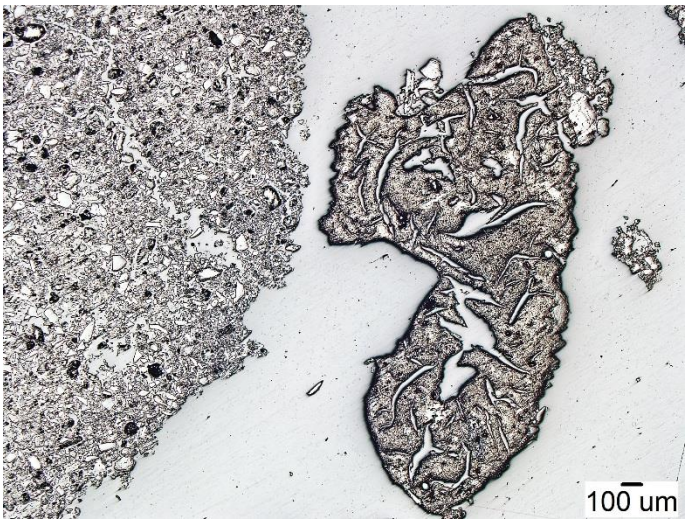

Figure 16: SEM/EDX of liquefaction ash, showing average elemental composition of a grain (top), embedded iron sulfide grains (middle), and apparent leaching of grains from the liquefaction process (bottom)

Key Findings from Different Processing Steps

The key differences in the different processing steps analyzed and considered are oxidative environments, where the higher temperature ashes have experienced a more aggressive oxidation, and the liquefaction ash is largely un-oxidized as evidenced by the presence of iron sulfide grains. The furnace ash samples are morphologically different from operating plant fly ashes, likely since the furnace ash can sinter and is influenced physically by neighboring particles, whereas the fly ash cools while suspended in air. There did not appear to be a change in the form of rare earth compounds between 800°C and 1,200°C ash. In the samples analyzed, Yttrium appeared more prevalent in the 800°C. However the sampling was not statistically rigorous, so we cannot positively comment on a change of Yttrium form in the 1,200°C sample.

XRD was done on the samples to understand how crystallography changed between the different ash treatments. This is summarized in Figure 17. Notable changes include the apparent conversion of pyrite to pyrrhotite and an amorphous iron phase in the coal liquefaction process. Also, overall crystallinity of the ash increased between 800°C and 1,200°C, where the expectation was for an increase in the vitrified, amorphous phases at higher temperatures. It appears that instead, the aluminum and silica changed to a mullite phase, which is a refractory phase that would also resist acid leaching.

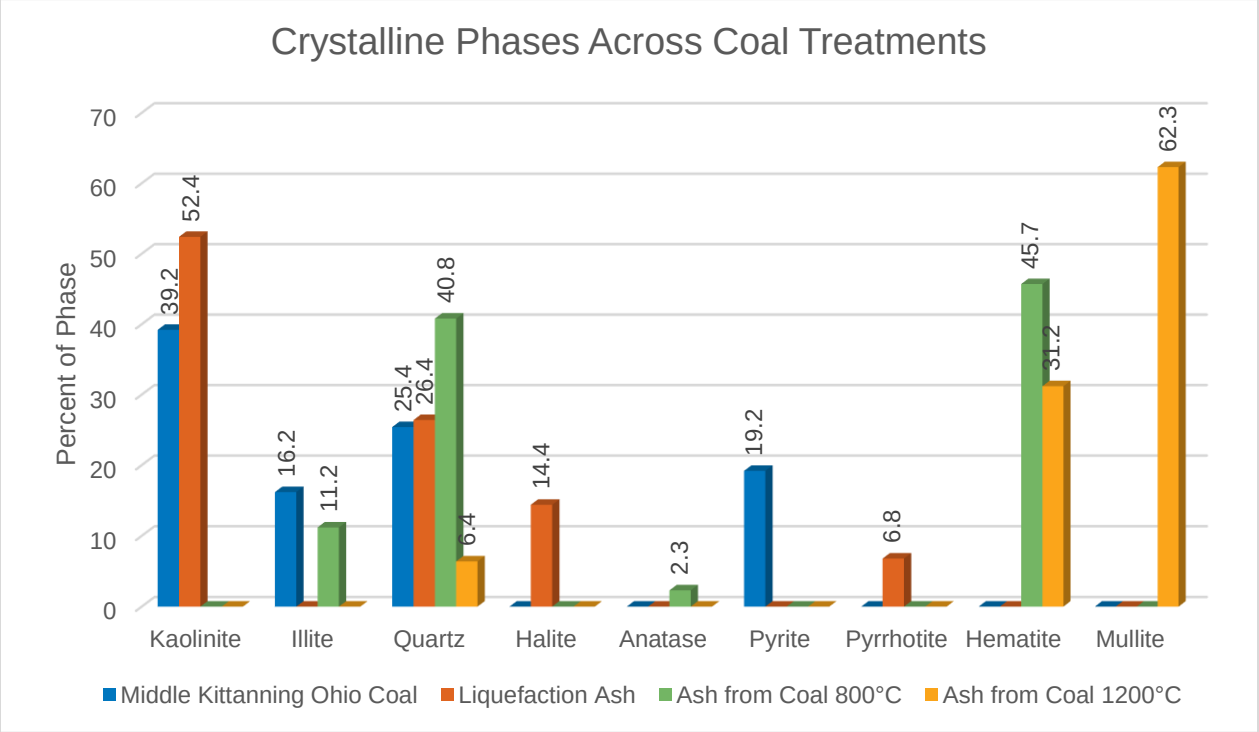

Sample	% Crystalline	Kaolinite	Illite	Quartz	Halite	Anatase	Pyrite	Pyrrhotite	Hematite	Mullite
Middle Kittanning Ohio Coal	5.0	39.2	16.2	25.4	0.0	0.0	19.2	0.0	0.0	0.0
Liquefaction Ash	7.1	52.4	0.0	26.4	14.4	0.0	0.0	6.8	0.0	0.0
Ash from Coal 800°C	34.6	0.0	11.2	40.8	0.0	2.3	0.0	0.0	45.7	0.0
Ash from Coal 1200°C	41.6	0.0	0.0	6.4	0.0	0.0	0.0	0.0	31.2	62.3

Figure 17: Identified crystalline phases across coal ashing treatments, beginning with Ohio Middle Kittanning Coal.

XRD was also performed on the fluidized bed combustor fly ash to understand how it differs from the other ash sources. The results are shown in Table 12, and indicate a much different structure than other ashes, primarily due to the addition of lime to the furnace in fluidized bed combustors.

Table 12: Summary of fluidized bed combustor ash crystallography.

	% Crystalline	Quartz	Anhydrite	Gehlenite	Hematite	Lime
FBC Fly Ash	35.7	36.3	21.9	17.5	13.6	10.6

It is also interesting to note the difference in color between the 800°C ash in Figure 13 and the 1,200°C ash in 1,200°C ash in

Figure 11, where the lower temperature ash appears much more red, which has darkened to gray in the high temperature ash. These two samples were derived from the same batch of Middle Kittanning coal from Ohio. Although both contain appreciable amounts of hematite, it is possible that the hematite has changed between lattice structures, changing the color, or that the mullite transition obscured the hematite color.

4.0 Conclusions and Next Steps

Within the rare earth elements in coal, Dysprosium represents the highest value, and combined with Neodymium, Terbium, and Praseodymium, these 4 elements account for over 75% of the rare earth value in the ash. Accordingly, Battelle's process will be tailored to focus on these rare earth components. Scandium represents the highest overall value within the ash, and will be a primary byproduct. Vanadium, Yttrium, Lithium, and Cobalt also represent a significant value, and will be evaluated as potential byproducts going forward.

Based on the analytical results, the feasibility study will focus on PCC Plant A fly ash as a feedstock for Battelle's Recycling Acid Leach Process. The PCC Plant A fly ash had a higher Total REE+Y+Sc concentration than all other operating plant ashes sampled, at 545 ppm +/- 13.4 ppm, as well as a higher HREE/LREE ratio at 0.37 +/- 0.008. Additionally, it contains significant amounts of Scandium (36 ppm +/- 1.4 ppm), Vanadium (279 ppm +/- 12 ppm), Yttrium (104 ppm +/- 5.3 ppm), Cobalt (44 ppm +/- 2.5 ppm), and Lithium (~166 ppm), which can be valuable process byproducts with robust market outlets. Although the coal liquefaction ash had a greater concentration of heavy rare earths, there is some risk for implementation since the liquefaction process is not yet commercial. The low temperature ash may prove to be more leachable since it did not exhibit as high a level of refractory mullite concentration, but it would also likely demonstrate lower selectivity due to the high calcium content. Furthermore, the overall capacity of fluidized bed combustors is much lower than pulverized coal combustors, so there would be more risk in feedstock sourcing.

Going forward, Battelle will evaluate feasibility of its recycling acid leach process on PCC Plant A fly ash. Feasibility testing will compare leaching efficiency and selectivity of this ash with samples of liquefaction ash and FBC ash to validate assumptions regarding leaching kinetics, acid loading limits, and product purities. This information will be used to refine a process model built in CHEMCAD modeling software and feed into overall process economics and unit sizing used in the techno economic assessment to be performed in the next project task.

Appendix A: Detailed Elemental Analysis Results

Sodium Peroxide Fusion/INAA Results

Analyte Symbol	Mass	Lu	Sc	Unashed Weight	Ashed Weight	% Ash	Al	As	B	Ba
Unit Symbol	g	ppm	ppm	g	g	%	%	ppm	ppm	ppm
Detection Limit		0.05	0.1				0.01	5	10	3
Analysis Method	INAA	INAA	INAA	none	none	none	FUS-Na2O2	FUS-MS-Na2O2	FUS-MS-Na2O2	FUS-MS-Na2O2
NIST trace elements in coal fly ash 1633C	1.71	0.55	36.8				13.2	177	60	1140
WVGES #11250 Fireclay Seam Coal	1.393	0.83	25.5	26.1	5.1	19.5	16.3	337	50	840
WVGES #13423 Powellton Seam Coal	0.863	1.17	51	32.6	1.3	3.99	15.7	151	110	9010
NIST trace elements in coal fly ash 1633C	1.396	0.7	36.9				13	156	90	1170
PCC Plant A Bottom Ash from Pile	1.715	0.36	22.3				10.1	< 5	230	339
PCC Plant A Fly Ash from Pile	1.593	0.7	36.7				13.5	144	590	426
PCC Plant A Fly Ash from Pile	1.623	0.65	35.6				13.6	141	550	486
PCC Plant A Feed Coal A	1.21	0.63	37.9	64.8	4.9	7.56	14.3	192	1390	388
PCC Plant A Feed Coal B	1.304	0.34	21.7	60.3	7.3	12.1	10.7	251	580	477
Ohio Coal from Coal Liquefaction Project	1.401	0.78	43.6	64.8	9.5	14.7	12.8	< 5	80	759
Centrifuge Tails; Coal Liquefaction Process	0.613	0.65	47.4	10.9	0.9	8.26	14.5	160	160	490
NIST trace elements in coal fly ash 1633C	1.212	1.43	37.1				12.6	166	70	1100
PCC Plant B Fly Ash	1.37	0.89	27.9				10.5	68	360	676
PCC Plant B Bottom Ash	1.639	0.79	26.4				9.93	< 5	180	599
PCC Plant C Fly Ash	1.229	0.86	26				9.85	126	320	351
PCC Plant C Bottom Ash	1.46	0.89	24.1				9.75	7	180	378
Coal Liquid Residual Light Phase	0.45	4.6	78	22.5	0.9	4	12.9	448	3880	471
Coal Liquid Residual Heavy Phase	0.355	5.06	87.9	19.1	0.6	3.14	12.9	458	4210	457
Coal Liquid Residual >= 850 micron size	0.356	2.78	48.5	22.5	1.8	8	12.9	277	3000	565
Coal Liquid Residual 850-600 micron size	0.317	3.89	68.4	24.6	1.2	4.88	13	313	4470	506
Coal Liquid Residual 600-355 micron size	0.328	3.93	69.5	23.7	1.2	5.06	12.9	333	5150	507
Coal Liquid Residual =< 355 micron size	0.372	2.89	51.3	22.8	1.5	6.58	12.6	327	3640	576
FBC Plant Fly Ash	1.098	< 0.05	12.9				6.88	24	100	472
FBC Plant Bottom Ash	1.257	< 0.05	10.3				5.32	10	30	412

Analyte Symbol	Be	Bi	Ca	Cd	Ce	Co	Cr	Cs	Cu	Dy
Unit Symbol	ppm	ppm	%	ppm	ppm	ppm	ppm	ppm	ppm	ppm
Detection Limit	3	2	0.01	2	0.8	0.2	30	0.1	2	0.3
Analysis Method	FUS-MS-Na2O2	FUS-MS-Na2O2	FUS-Na2O2	FUS-MS-Na2O2	FUS-MS-Na2O2	FUS-MS-Na2O2	FUS-MS-Na2O2	FUS-MS-Na2O2	FUS-MS-Na2O2	FUS-MS-Na2O2
NIST trace elements in coal fly ash 1633C	16	< 2	1.28	< 2	170	41.2	280	9.9	159	18.5
WVGES #11250 Fireclay Seam Coal	20	< 2	0.37	< 2	346	33.2	160	7	99	29.4
WVGES #13423 Powellton Seam Coal	256	4	1.01	2	197	313	210	6	428	39.4
NIST trace elements in coal fly ash 1633C	17	< 2	1.32	< 2	192	41.3	210	10	183	18.5
PCC Plant A Bottom Ash from Pile	14	< 2	1.21	< 2	116	32.2	110	6.7	99	9.8
PCC Plant A Fly Ash from Pile	30	< 2	1.27	< 2	162	46.2	160	10.1	127	16.4
PCC Plant A Fly Ash from Pile	27	< 2	1.32	39	168	45.1	160	10.1	123	17.1
PCC Plant A Feed Coal A	36	< 2	0.95	2	164	45.9	190	10.1	102	16.3
PCC Plant A Feed Coal B	9	7	1.52	< 2	110	145	110	9.7	54	8.6
Ohio Coal from Coal Liquefaction Project	10	< 2	1.59	3	135	30	90	2.6	159	15.4
Centrifuge Tails; Coal Liquefaction Process	16	15	1.92	12	188	32.1	430	4.3	132	16.8
NIST trace elements in coal fly ash 1633C	15	< 2	1.38	< 2	174	41.5	270	8.6	163	17.1
PCC Plant B Fly Ash	9	< 2	2.22	4	108	34.8	160	7.1	64	8.8
PCC Plant B Bottom Ash	8	< 2	2.2	< 2	103	37.7	250	5.1	48	8.5
PCC Plant C Fly Ash	11	2	1.71	2	101	36.9	180	6.5	72	8.6
PCC Plant C Bottom Ash	9	< 2	1.74	< 2	101	37.7	140	5.5	47	8.4
Coal Liquid Residual Light Phase	189	2	1.36	15	201	159	430	5.7	252	62.5
Coal Liquid Residual Heavy Phase	201	2	1.48	2	207	169	420	4.7	271	66.9
Coal Liquid Residual >= 850 micron size	83	3	0.93	2	159	105	590	6	190	31.9
Coal Liquid Residual 850-600 micron size	139	3	1.15	4	183	140	500	5.4	222	50.1
Coal Liquid Residual 600-355 micron size	143	11	1.25	2	184	144	490	6.1	230	48.7
Coal Liquid Residual =< 355 micron size	98	3	1.01	2	162	112	520	6.5	208	36.5
FBC Plant Fly Ash	< 3	< 2	18.1	< 2	58.9	15.5	100	6.4	39	4
FBC Plant Bottom Ash	< 3	< 2	23.7	< 2	48.2	11.6	90	3.8	16	3.3

Analyte Symbol	Er	Eu	Fe	Ga	Gd	Ge	Ho	Hf	In	K
Unit Symbol	ppm	ppm	%	ppm	ppm	ppm	ppm	ppm	ppm	%
Detection Limit	0.1	0.1	0.05	0.2	0.1	0.7	0.2	10	0.2	0.1
Analysis Method	FUS-MS-Na2O2	FUS-MS-Na2O2	FUS-Na2O2	FUS-MS-Na2O2	FUS-MS-Na2O2	FUS-MS-Na2O2	FUS-MS-Na2O2	FUS-MS-Na2O2	FUS-MS-Na2O2	FUS-Na2O2
NIST trace elements in coal fly ash 1633C	10	4.9	10.7	56.9	20.2	42.7	4.1	< 10	< 0.2	1.7
WVGES #11250 Fireclay Seam Coal	16.8	3.5	6.16	62.3	30.8	11.9	6.8	20	< 0.2	0.9
WVGES #13423 Powellton Seam Coal	26.1	7.3	7.98	178	32.5	140	9.9	< 10	< 0.2	1.7
NIST trace elements in coal fly ash 1633C	10.3	4.8	10.6	56.7	21.4	39.1	3.7	< 10	< 0.2	1.7
PCC Plant A Bottom Ash from Pile	6.1	2.6	20.5	17.9	11.1	19.3	2	< 10	< 0.2	1.2
PCC Plant A Fly Ash from Pile	9.8	3.8	13.2	62	17.2	92.3	3.4	< 10	< 0.2	1.6
PCC Plant A Fly Ash from Pile	10.4	4.2	13.3	61.2	18.2	86.2	3.5	< 10	2.1	1.7
PCC Plant A Feed Coal A	10.2	3.9	12	62	16.6	96.6	3.5	< 10	0.2	1.7
PCC Plant A Feed Coal B	5	2.3	15.4	32.9	9.8	22.7	1.8	< 10	< 0.2	1.5
Ohio Coal from Coal Liquefaction Project	10.3	3.7	2.43	47.9	15.3	11.5	3.4	20	0.2	0.5
Centrifuge Tails; Coal Liquefaction Process	10.3	4.2	4.53	68	17.5	48.8	3.5	10	1.3	1
NIST trace elements in coal fly ash 1633C	10.4	4.7	10.7	57.5	19.4	37.2	3.6	< 10	< 0.2	1.6
PCC Plant B Fly Ash	5.7	2.5	17.3	43.1	10.3	33.3	1.9	< 10	< 0.2	1.3
PCC Plant B Bottom Ash	5.4	2.4	24.8	22.6	10	14.5	1.9	< 10	< 0.2	1
PCC Plant C Fly Ash	5.4	2.3	18.5	35.1	10	29.8	1.8	< 10	0.6	1.3
PCC Plant C Bottom Ash	5.3	2.3	22.9	18.9	9.9	12.2	1.7	< 10	< 0.2	1.1
Coal Liquid Residual Light Phase	41.1	10.7	9.99	157	51.5	384	14.7	< 10	1	1.3
Coal Liquid Residual Heavy Phase	44.2	11.4	9.35	170	55.1	423	16.1	< 10	0.2	1.3
Coal Liquid Residual >= 850 micron size	21	5.8	10.4	83.4	27.6	172	7.2	10	0.3	1.7
Coal Liquid Residual 850-600 micron size	33.1	8.5	10	119	40.6	260	11.4	< 10	0.5	1.5
Coal Liquid Residual 600-355 micron size	32.3	8.4	9.94	127	39.8	286	11.1	10	0.3	1.4
Coal Liquid Residual =< 355 micron size	24.9	6.5	11	94.5	30.8	211	8.3	10	0.3	1.5
FBC Plant Fly Ash	2.5	1.1	6.17	19.1	4.8	2.2	0.9	< 10	< 0.2	1.5
FBC Plant Bottom Ash	2.2	1	3.54	13.2	4.1	< 0.7	0.7	< 10	< 0.2	0.9

Analyte Symbol	La	Li	Mg	Mn	Mo	Nb	Nd	Ni	Pb	Pr
Unit Symbol	ppm	ppm	%	ppm	ppm	ppm	ppm	ppm	ppm	ppm
Detection Limit	0.4	3	0.01	3	1	2.4	0.4	10	0.8	0.1
Analysis Method	FUS-MS-Na2O2	FUS-MS-Na2O2	FUS-Na2O2	FUS-MS-Na2O2	FUS-MS-Na2O2	FUS-MS-Na2O2	FUS-MS-Na2O2	FUS-MS-Na2O2	FUS-MS-Na2O2	FUS-MS-Na2O2
NIST trace elements in coal fly ash 1633C	82.2	195	0.47	266	29	29.3	88.4	120	89	21.9
WVGES #11250 Fireclay Seam Coal	170	166	0.26	75	15	44	168	70	112	43.5
WVGES #13423 Powellton Seam Coal	95.1	180	0.42	227	17	38.7	108	440	170	25.8
NIST trace elements in coal fly ash 1633C	85.5	170	0.47	258	27	24	92.6	140	96.7	23.6
PCC Plant A Bottom Ash from Pile	53.7	121	0.39	258	6	16.6	53.5	90	12.9	13.7
PCC Plant A Fly Ash from Pile	74	166	0.46	215	21	26.3	75.5	120	81.1	19.2
PCC Plant A Fly Ash from Pile	77.5	174	0.47	219	22	25.8	79.7	110	96.7	20
PCC Plant A Feed Coal A	75.7	188	0.41	175	12	27.4	77.1	130	86.2	19.8
PCC Plant A Feed Coal B	49.9	163	0.5	329	12	19.3	51.4	130	39.1	13.2
Ohio Coal from Coal Liquefaction Project	60.4	49	0.47	128	15	22.4	69	60	36.7	16.8
Centrifuge Tails; Coal Liquefaction Process	86.7	93	0.49	165	69	32.1	85.1	200	285	22.1
NIST trace elements in coal fly ash 1633C	86	187	0.45	243	25	24.9	97.4	110	89.5	22.1
PCC Plant B Fly Ash	52.7	99	0.46	239	11	21.8	55.9	80	61.5	13.3
PCC Plant B Bottom Ash	50	87	0.43	298	6	19.9	53.5	80	16.7	12.8
PCC Plant C Fly Ash	48.9	108	0.37	248	15	19.2	53	80	55.1	12.6
PCC Plant C Bottom Ash	48.4	96	0.37	271	3	18	52.3	80	13.8	12.6
Coal Liquid Residual Light Phase	89.5	122	0.42	135	49	25.1	125	570	190	31.1
Coal Liquid Residual Heavy Phase	93.6	123	0.42	142	50	30.7	129	610	174	32
Coal Liquid Residual >= 850 micron size	71.1	170	0.44	164	65	21.9	93.7	510	294	20.6
Coal Liquid Residual 850-600 micron size	80	156	0.43	158	60	22.8	117	460	249	25
Coal Liquid Residual 600-355 micron size	79.6	158	0.44	146	62	23	116	480	244	25
Coal Liquid Residual =< 355 micron size	72.4	166	0.42	153	75	22.3	99	440	277	21.6
FBC Plant Fly Ash	30	52	0.89	661	6	14.1	29.4	40	27.2	7.2
FBC Plant Bottom Ash	23.9	22	1.05	2370	2	10.3	24.8	30	15.6	5.9

Analyte Symbol	Rb	S	Sb	Se	Si	Sm	Sn	Sr	Ta	Tb
Unit Symbol	ppm	%	ppm	ppm	%	ppm	ppm	ppm	ppm	ppm
Detection Limit	0.4	0.01	2	0.8	0.01	0.1	0.5	3	0.2	0.1
Analysis Method	FUS-MS-Na2O2	FUS-Na2O2	FUS-MS-Na2O2	FUS-MS-Na2O2	FUS-Na2O2	FUS-MS-Na2O2	FUS-MS-Na2O2	FUS-MS-Na2O2	FUS-MS-Na2O2	FUS-MS-Na2O2
NIST trace elements in coal fly ash 1633C	121	0.18	9	5.8	21.6	19.5	4	861	1.2	3.5
WVGES #11250 Fireclay Seam Coal	76.8	0.46	6	1.8	25.1	32.6	16.6	650	2.6	5.6
WVGES #13423 Powellton Seam Coal	101	1.06	55	3.1	22.1	26.2	24.6	1270	1.3	7.1
NIST trace elements in coal fly ash 1633C	116	0.25	9	10.6	20.9	20.4	5.5	878	1.8	3.5
PCC Plant A Bottom Ash from Pile	78.2	0.83	8	1.9	17.6	10.9	1.8	514	1.3	1.8
PCC Plant A Fly Ash from Pile	118	0.44	12	10.8	20.7	15.7	6.9	786	2.1	2.9
PCC Plant A Fly Ash from Pile	118	0.49	10	7.2	21	17.2	10.9	879	2.2	3.1
PCC Plant A Feed Coal A	127	0.82	12	3.2	20.3	15.6	6.8	741	2.2	2.9
PCC Plant A Feed Coal B	103	1.17	4	2.1	20.9	10.5	5.4	383	1.5	1.6
Ohio Coal from Coal Liquefaction Project	26	0.86	4	3.3	28.4	15.2	6.1	503	1.5	2.7
Centrifuge Tails; Coal Liquefaction Process	55	4.23	11	1.3	21.7	17.4	16.9	1010	2.4	3
NIST trace elements in coal fly ash 1633C	119	0.18	9	13.8	22	20	3.8	855	1.1	3.4
PCC Plant B Fly Ash	93	0.86	9	8.5	20.3	10.8	5.8	869	1	1.7
PCC Plant B Bottom Ash	76.4	0.08	< 2	< 0.8	19	10.2	2.2	789	0.9	1.7
PCC Plant C Fly Ash	89.4	0.9	3	4.1	18.9	10	11.4	477	1	1.7
PCC Plant C Bottom Ash	77.5	0.21	< 2	1.1	19.2	10.1	2.2	533	0.9	1.7
Coal Liquid Residual Light Phase	87	1.23	63	< 0.8	21.3	36.1	17.8	507	< 0.2	11.1
Coal Liquid Residual Heavy Phase	85.7	1.34	68	0.8	20.7	37.8	18.2	544	< 0.2	11.8
Coal Liquid Residual >= 850 micron size	115	0.77	30	2.2	23.5	23.2	10.4	318	0.3	5.8
Coal Liquid Residual 850-600 micron size	102	0.93	45	1.4	22.7	31.4	9.5	440	< 0.2	8.8
Coal Liquid Residual 600-355 micron size	99.9	1.02	48	3.3	22.2	31.5	9.7	434	< 0.2	8.5
Coal Liquid Residual =< 355 micron size	107	0.88	36	3	22.6	25.2	11.2	348	0.3	6.5
FBC Plant Fly Ash	95.9	3.23	< 2	5.5	16.4	5.2	2.8	540	0.8	0.8
FBC Plant Bottom Ash	61.3	5.38	< 2	2.5	15.6	4.5	2.2	526	0.9	0.7

Analyte Symbol	Te	Th	Ti	Tl	Tm	U	V	W	Y	Yb	Zn
Unit Symbol	ppm	ppm	%	ppm	ppm	ppm	ppm	ppm	ppm	ppm	ppm
Detection Limit	6	0.1	0.01	0.1	0.1	0.1	5	0.7	0.1	0.1	30
Analysis Method	FUS-MS-Na2O2	FUS-MS-Na2O2	FUS-Na2O2	FUS-MS-Na2O2	FUS-MS-Na2O2	FUS-MS-Na2O2	FUS-MS-Na2O2	FUS-MS-Na2O2	FUS-MS-Na2O2	FUS-MS-Na2O2	FUS-MS-Na2O2
NIST trace elements in coal fly ash 1633C	< 6	21	0.69	6.2	1.5	9.6	263	8.1	121	8.2	220
WVGES #11250 Fireclay Seam Coal	< 6	77.1	0.9	6.9	2.7	22.6	158	9.2	198	14.7	80
WVGES #13423 Powellton Seam Coal	< 6	39	0.97	14.8	3.9	20.1	270	20.8	349	21.2	130
NIST trace elements in coal fly ash 1633C	< 6	22.5	0.67	6.3	1.4	9.7	247	7	116	8.6	220
PCC Plant A Bottom Ash from Pile	< 6	15.2	0.49	1.5	0.8	6.7	147	3.8	63.3	5.1	50
PCC Plant A Fly Ash from Pile	< 6	22.5	0.71	13.4	1.3	10.3	269	7.3	109	8.4	170
PCC Plant A Fly Ash from Pile	< 6	23	0.7	13.6	1.3	10.3	254	7.6	109	8.6	430
PCC Plant A Feed Coal A	< 6	23.6	0.74	10.6	1.4	10.2	304	8	112	9.1	160
PCC Plant A Feed Coal B	< 6	16.1	0.54	8.6	0.7	11.2	146	8.5	51.4	4.3	100
Ohio Coal from Coal Liquefaction Project	< 6	25.1	0.95	1.5	1.5	9.2	299	4.9	110	9.8	100
Centrifuge Tails; Coal Liquefaction Process	< 6	25.3	0.95	35.8	1.5	9.8	348	10.4	115	9	340
NIST trace elements in coal fly ash 1633C	< 6	21.5	0.7	6	1.4	10.6	261	4.9	119	8.5	210
PCC Plant B Fly Ash	< 6	16.1	0.57	6.2	0.8	8.8	229	2.9	61.3	5	140
PCC Plant B Bottom Ash	< 6	14.9	0.52	0.2	0.8	7.1	194	4	60.8	4.7	60
PCC Plant C Fly Ash	< 6	15.6	0.53	7.7	0.8	7.1	188	7.8	61.6	4.6	140
PCC Plant C Bottom Ash	< 6	14.9	0.5	0.4	0.8	6.1	174	2.6	57.9	4.5	50
Coal Liquid Residual Light Phase	< 6	31	0.71	20.8	5.9	20.3	434	24	514	31.2	430
Coal Liquid Residual Heavy Phase	< 6	31.8	0.71	20.6	6.4	21.5	467	26.3	548	33.1	380
Coal Liquid Residual >= 850 micron size	< 6	22.6	0.62	26.6	3	11.3	262	12.8	267	16.8	240
Coal Liquid Residual 850-600 micron size	< 6	27.9	0.79	23.1	4.5	14.9	341	16.6	424	25.2	270
Coal Liquid Residual 600-355 micron size	< 6	27.8	0.74	23.1	4.4	16.5	358	21.1	400	24.8	250
Coal Liquid Residual =< 355 micron size	< 6	24.3	0.64	27.4	3.3	13.2	299	15.8	296	18.9	250
FBC Plant Fly Ash	< 6	9.6	0.38	1.4	0.4	5.2	96	1.1	27.7	2.3	80
FBC Plant Bottom Ash	< 6	7.4	0.3	< 0.1	0.3	3.4	70	< 0.7	21.5	1.8	50

Lithium Borate Fusion Results

Analyte Symbol	SiO2	Al2O3	Fe2O3(T)	MnO	MgO	CaO	Na2O	K2O	TiO2	P2O5
Unit Symbol	**%**	**%**	**%**	**%**	**%**	**%**	**%**	**%**	**%**	**%**
Detection Limit	**0.01**	**0.01**	**0.01**	**0.001**	**0.01**	**0.01**	**0.01**	**0.01**	**0.001**	**0.01**
Analysis Method	**FUS-ICP**	**FUS-ICP**	**FUS-ICP**	**FUS-ICP**	**FUS-ICP**	**FUS-ICP**	**FUS-ICP**	**FUS-ICP**	**FUS-ICP**	**FUS-ICP**
NIST trace elements in coal fly ash 1633C	45.03	24.16	15.58	0.036	0.76	1.9	0.28	2.03	1.144	0.41
PCC Plant A Fly Ash from Pile	45.28	25.53	19.52	0.026	0.75	1.82	0.7	1.93	1.205	0.38
NIST trace elements in coal fly ash 1633C	45.35	24.08	15.58	0.035	0.75	1.86	0.27	1.98	1.128	0.41
PCC Plant A Fly Ash from Pile	45.5	25.28	19.15	0.026	0.74	1.83	0.71	1.94	1.186	0.38
NIST trace elements in coal fly ash 1633C	45.49	24.22	15.42	0.035	0.75	1.85	0.27	2.01	1.132	0.43
PCC Plant D Fly Ash	42.56	19.32	25.14	0.03	0.75	5.2	1.16	1.53	0.909	0.27
PCC Plant D Bottom Ash	41.84	19.76	30.19	0.036	0.68	3.67	0.5	1.41	0.891	0.16
PCC Plant A Fly Ash from Pile	45.83	25.39	18.98	0.027	0.73	1.86	0.73	1.98	1.253	0.43

Analyte Symbol	LOI	Total	Sc	Be	V	Cr	Co	Ni	Cu	Zn
Unit Symbol	%	%	ppm	ppm	ppm	ppm	ppm	ppm	ppm	ppm
Detection Limit		0.01	1	1	5	20	1	20	10	30
Analysis Method	FUS-ICP	FUS-ICP	FUS-ICP	FUS-ICP	FUS-ICP	FUS-MS	FUS-MS	FUS-MS	FUS-MS	FUS-MS
NIST trace elements in coal fly ash 1633C	7.71	99.02	36	17	268	230	40	110	150	180
PCC Plant A Fly Ash from Pile	2.28	99.43	37	29	279	170	45	110	100	180
NIST trace elements in coal fly ash 1633C	7.7	99.13	36	17	268	240	39	120	170	120
PCC Plant A Fly Ash from Pile	2.36	99.1	36	29	285	170	43	110	100	170
NIST trace elements in coal fly ash 1633C	7.69	99.32	36	17	268	220	38	120	160	100
PCC Plant D Fly Ash	2.21	99.09	30	11	235	160	34	90	60	110
PCC Plant D Bottom Ash	1.22	100.3	26	9	188	140	34	90	50	50
PCC Plant A Fly Ash from Pile	2.4	99.62	35	29	285	180	43	110	100	170

Analyte Symbol	Ga	Ge	As	Rb	Sr	Y	Zr	Nb	Mo	Ag
Unit Symbol	**ppm**	**ppm**	**ppm**	**ppm**	**ppm**	**ppm**	**ppm**	**ppm**	**ppm**	**ppm**
Detection Limit	**1**	**1**	**5**	**2**	**2**	**1**	**2**	**1**	**2**	**0.5**
Analysis Method	**FUS-MS**	**FUS-MS**	**FUS-MS**	**FUS-MS**	**FUS-ICP**	**FUS-ICP**	**FUS-ICP**	**FUS-MS**	**FUS-MS**	**FUS-MS**
NIST trace elements in coal fly ash 1633C	53	37	117	106	901	106	177	21	26	0.6
PCC Plant A Fly Ash from Pile	61	111	176	120	815	102	230	25	21	0.7
NIST trace elements in coal fly ash 1633C	53	41	149	115	888	105	164	22	27	0.5
PCC Plant A Fly Ash from Pile	59	99	153	116	796	102	233	24	20	0.7
NIST trace elements in coal fly ash 1633C	52	41	150	110	900	106	170	21	27	< 0.5
PCC Plant D Fly Ash	37	28	59	90	852	54	224	20	10	0.6
PCC Plant D Bottom Ash	20	9	8	79	761	52	226	18	4	< 0.5
PCC Plant A Fly Ash from Pile	60	93	135	117	817	104	238	24	22	0.6

Analyte Symbol	In	Sn	Sb	Cs	Ba	La	Ce	Pr	Nd	Sm
Unit Symbol	**ppm**	**ppm**	**ppm**	**ppm**	**ppm**	**ppm**	**ppm**	**ppm**	**ppm**	**ppm**
Detection Limit	**0.2**	**1**	**0.5**	**0.5**	**2**	**0.1**	**0.1**	**0.05**	**0.1**	**0.1**
Analysis Method	**FUS-MS**	**FUS-MS**	**FUS-MS**	**FUS-MS**	**FUS-ICP**	**FUS-MS**	**FUS-MS**	**FUS-MS**	**FUS-MS**	**FUS-MS**
NIST trace elements in coal fly ash 1633C	< 0.2	5	6.1	8.4	1099	78.7	181	20.9	86.7	19.9
PCC Plant A Fly Ash from Pile	0.2	6	11.3	9.7	413	74.7	161	18.2	73.1	16.6
NIST trace elements in coal fly ash 1633C	< 0.2	5	7.2	8.8	1091	82.3	185	21.9	89	20.6
PCC Plant A Fly Ash from Pile	< 0.2	6	10.2	9.3	417	72.9	157	17.8	71.8	16.2
NIST trace elements in coal fly ash 1633C	< 0.2	5	7.5	8.5	1099	82	184	21.5	89.5	20.8
PCC Plant D Fly Ash	< 0.2	5	3.1	7.3	552	60.4	125	14.3	55.5	11.7
PCC Plant D Bottom Ash	< 0.2	3	1.6	5.9	503	57.4	118	13.5	53.2	11.1
PCC Plant A Fly Ash from Pile	0.2	6	9.7	9.5	425	73.8	156	18	71.6	16.6

Analyte Symbol	Eu	Gd	Tb	Dy	Ho	Er	Tm	Yb	Lu	Hf
Unit Symbol	**ppm**	**ppm**	**ppm**	**ppm**	**ppm**	**ppm**	**ppm**	**ppm**	**ppm**	**ppm**
Detection Limit	**0.05**	**0.1**	**0.1**	**0.1**	**0.1**	**0.1**	**0.05**	**0.1**	**0.01**	**0.2**
Analysis Method	**FUS-MS**	**FUS-MS**	**FUS-MS**	**FUS-MS**	**FUS-MS**	**FUS-MS**	**FUS-MS**	**FUS-MS**	**FUS-MS**	**FUS-MS**
NIST trace elements in coal fly ash 1633C	4.62	20.5	3.1	17.4	3.3	9.2	1.39	8.6	1.28	4.7
PCC Plant A Fly Ash from Pile	3.81	16.9	2.7	17.1	3.4	9.8	1.39	9.2	1.36	6.2
NIST trace elements in coal fly ash 1633C	4.66	20.4	3.2	18.7	3.6	10.1	1.38	9.1	1.32	5
PCC Plant A Fly Ash from Pile	3.9	16.5	2.7	16.5	3.3	9.5	1.32	9	1.27	5.9
NIST trace elements in coal fly ash 1633C	4.73	20.6	3.2	18.9	3.6	10.1	1.46	8.9	1.29	4.7
PCC Plant D Fly Ash	2.57	10.8	1.7	10.2	2	5.8	0.86	5.4	0.84	5.4
PCC Plant D Bottom Ash	2.44	10.2	1.6	9.7	1.8	5.5	0.81	5.3	0.77	5.2
PCC Plant A Fly Ash from Pile	3.97	16.7	2.8	16.7	3.4	9.5	1.34	8.8	1.33	6.1

Analyte Symbol	Ta	W	Tl	Pb	Bi	Th	U
Unit Symbol	**ppm**	**ppm**	**ppm**	**ppm**	**ppm**	**ppm**	**ppm**
Detection Limit	**0.1**	**1**	**0.1**	**5**	**0.4**	**0.1**	**0.1**
Analysis Method	**FUS-MS**	**FUS-MS**	**FUS-MS**	**FUS-MS**	**FUS-MS**	**FUS-MS**	**FUS-MS**
NIST trace elements in coal fly ash 1633C	1.4	8	4.9	46	< 0.4	19.8	8.4
PCC Plant A Fly Ash from Pile	1.8	9	13.2	87	0.9	23	10.8
NIST trace elements in coal fly ash 1633C	1.6	8	4.6	42	< 0.4	21.8	9.5
PCC Plant A Fly Ash from Pile	1.7	9	12.6	78	0.7	22.3	10.5
NIST trace elements in coal fly ash 1633C	1.6	8	4.1	29	< 0.4	21.5	9.3
PCC Plant D Fly Ash	1.4	6	4.2	37	0.8	16.6	7
PCC Plant D Bottom Ash	1.3	4	0.6	14	< 0.4	15.7	5.9
PCC Plant A Fly Ash from Pile	1.7	8	12.4	72	0.6	22.7	10.7

Appendix B: High Temperature Ash SEM/EDX Results

AREA---AL-SI-OX

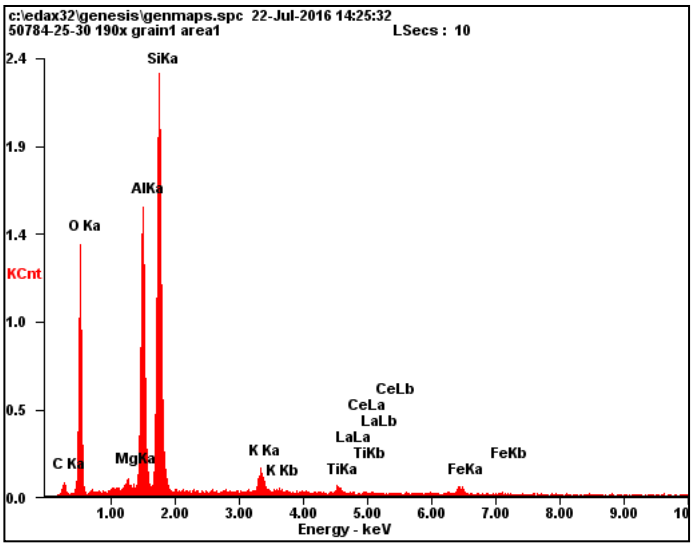

Element	Wt%	At%
CK	06.8	12.00
OK	34.0	44.92
MgK	00.8	00.68
AlK	18.0	14.09
SiK	33.4	25.15
KK	02.8	01.52
TiK	01.3	00.55
FeK	02.9	01.09
Matrix	Correction	ZAF

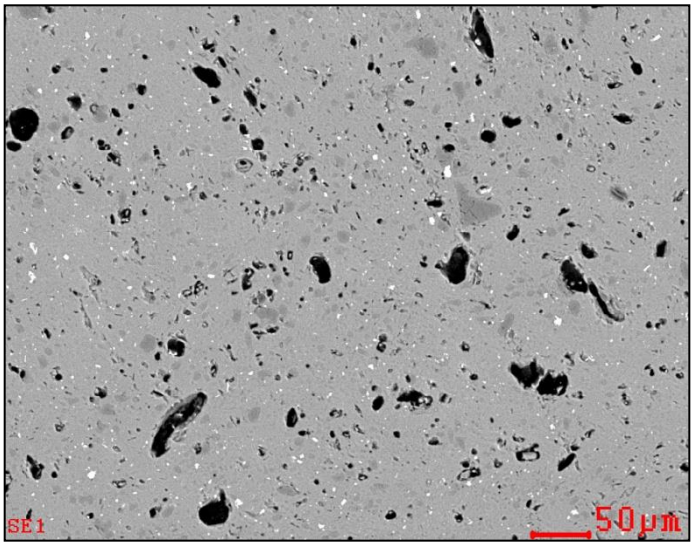

SI-OX

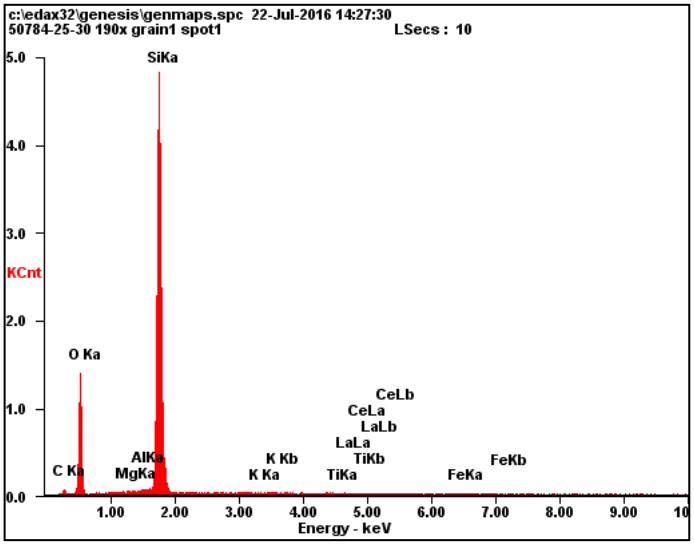

Element	Wt%	At%
CK	05.9	10.15
OK	36.7	47.64
MgK	00.1	00.05
AlK	00.4	00.30
SiK	56.3	41.57
KK	00.2	00.10
TiK	00.2	00.09
FeK	00.3	00.11
Matrix	Correction	ZAF

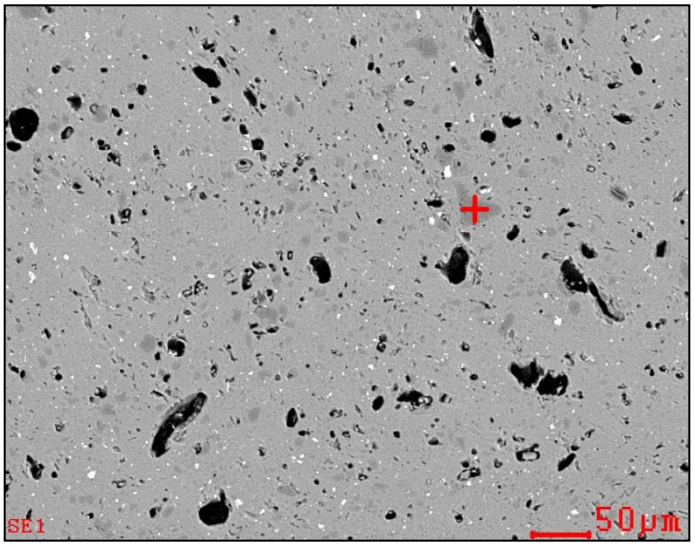

TI-OX

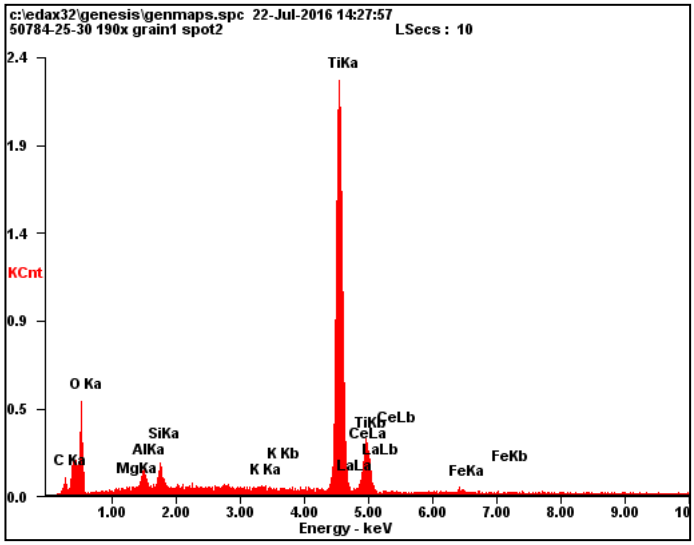

Element	Wt%	At%
CK	02.9	07.06
OK	26.4	48.17
MgK	00.4	00.51
AlK	01.7	01.80
SiK	01.8	01.84
KK	00.3	00.21
TiK	65.1	39.64
FeK	01.5	00.77
Matrix	Correction	ZAF

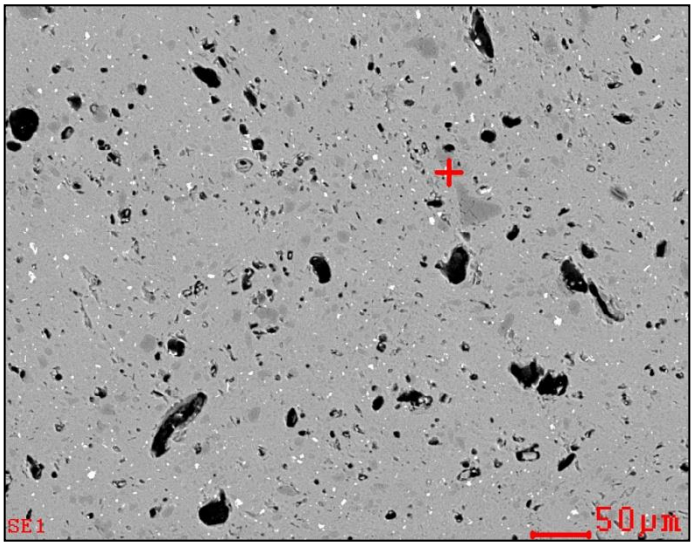

HOST PHASE- AL-SI-OX

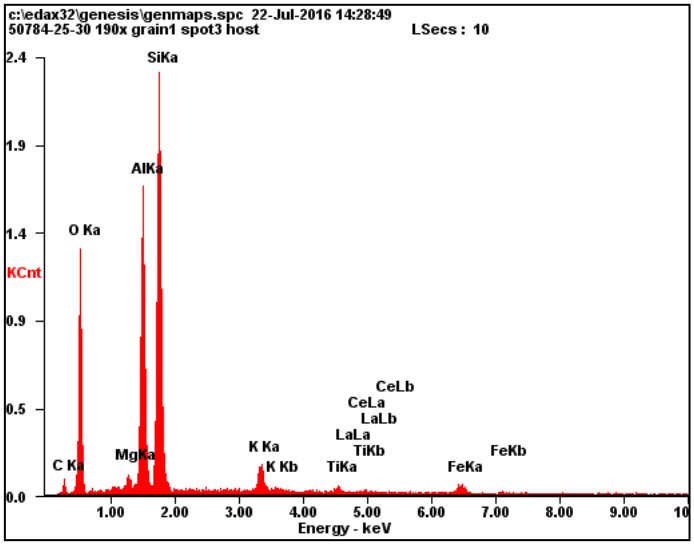

Element	Wt%	At%
CK	06.1	10.88
OK	34.1	45.42
MgK	01.0	00.84
AlK	18.7	14.75
SiK	32.5	24.60
KK	03.3	01.80
TiK	01.1	00.49
FeK	03.2	01.22
Matrix	Correction	ZAF

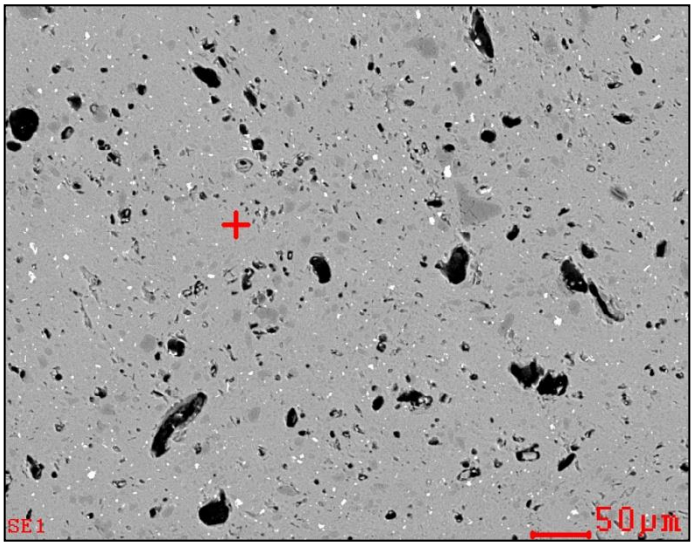

AREA---AL-SI-OX

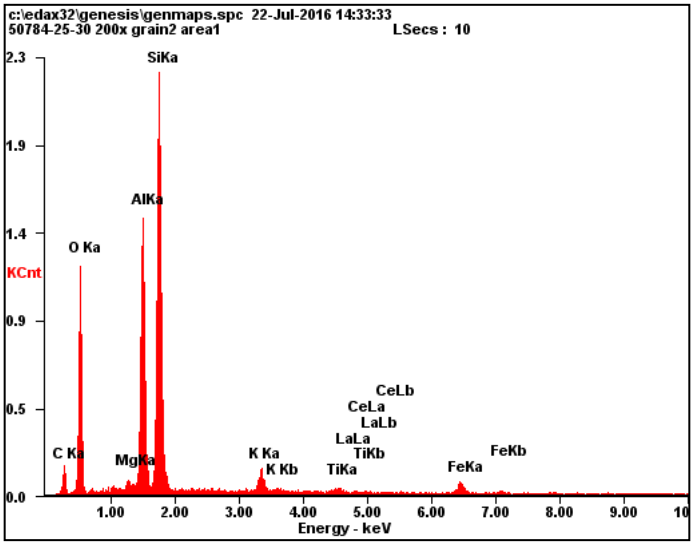

Element	Wt%	At%
CK	11.8	19.87
OK	32.6	41.42
MgK	00.6	00.53
AlK	16.7	12.59
SiK	31.4	22.68
KK	02.3	01.21
TiK	00.8	00.35
FeK	03.7	01.34
Matrix	Correction	ZAF

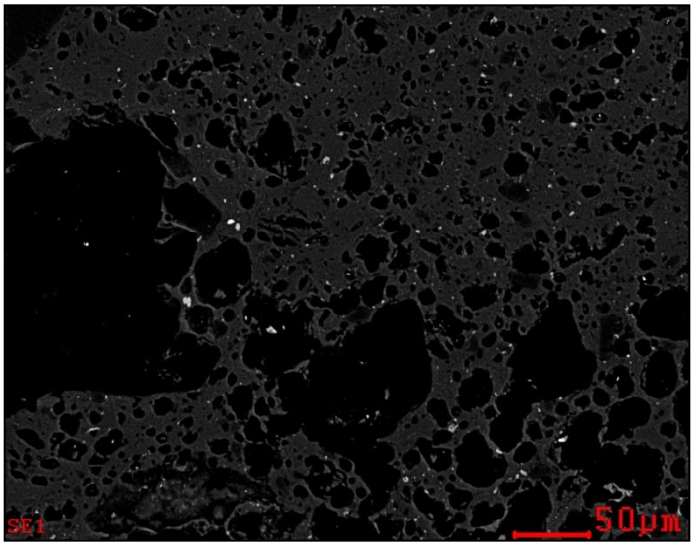

ZR-SI-OX

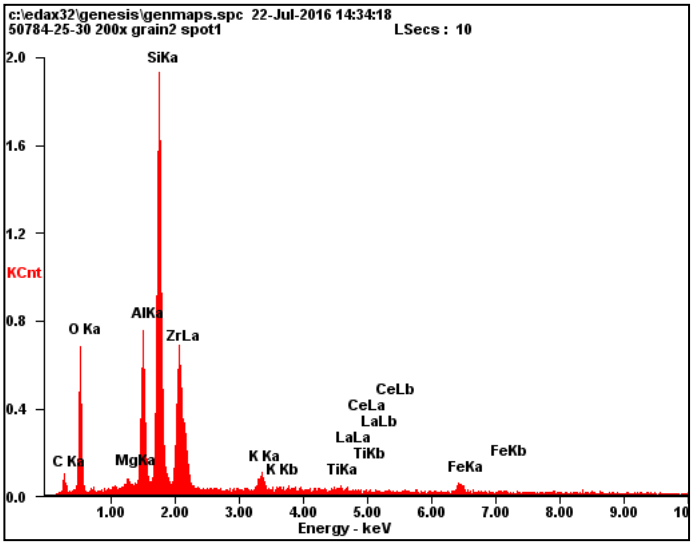

Element	Wt%	At%
CK	08.1	17.34
OK	24.9	39.79
MgK	00.6	00.61
AlK	08.5	08.09
SiK	25.7	23.47
ZrL	25.5	07.16
KK	02.1	01.35
TiK	01.1	00.58
FeK	03.5	01.60
Matrix	Correction	ZAF

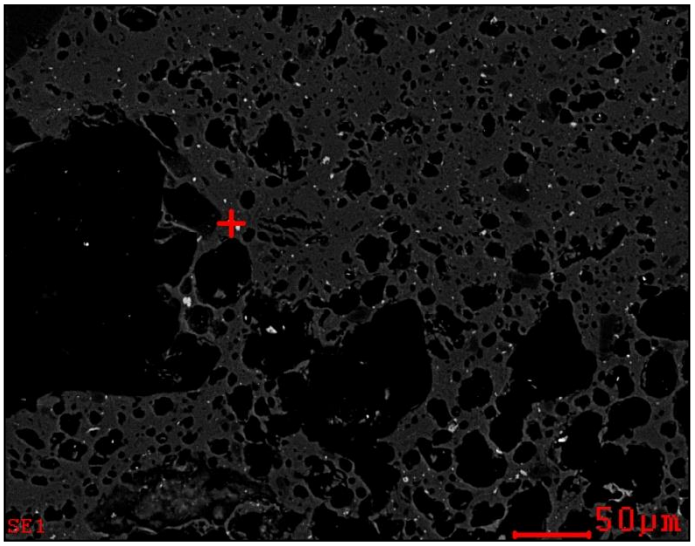

FE-TI-SI-OX

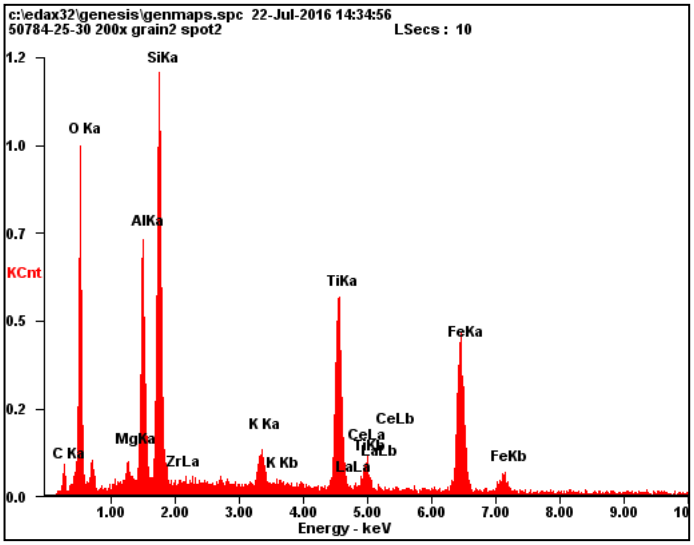

Element	Wt%	At%
CK	04.7	10.17
OK	26.3	43.11
MgK	01.1	01.22
AlK	09.1	08.82
SiK	16.2	15.16
ZrL	00.3	00.08
KK	01.9	01.26
TiK	15.7	08.59
FeK	24.7	11.59
Matrix	Correction	ZAF

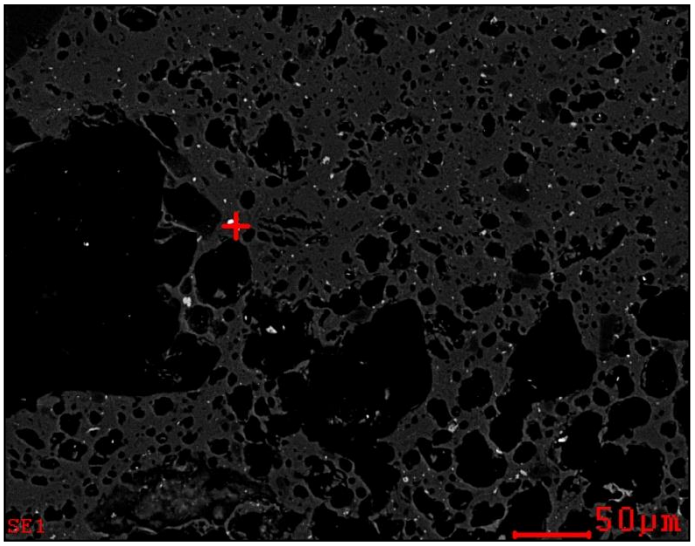

ZR-SI-OX-HF

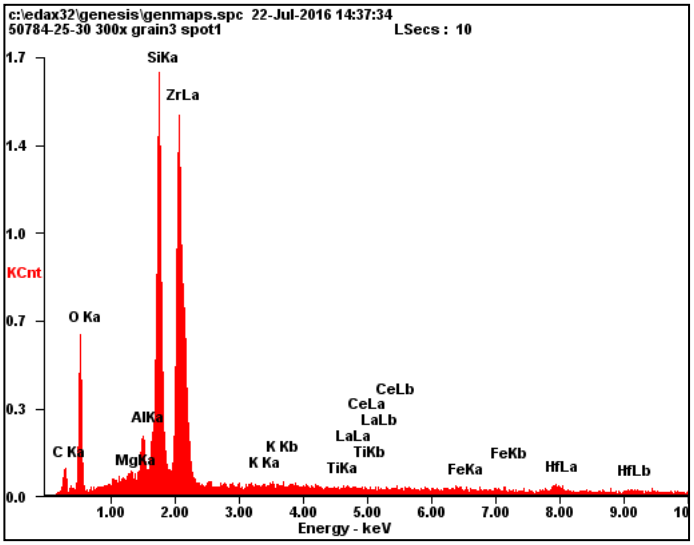

Element	Wt%	At%
CK	07.9	20.53
OK	21.3	41.39
MgK	00.2	00.22
AlK	01.6	01.79
SiK	17.4	19.32
ZrL	42.7	14.59
KK	00.3	00.27
TiK	00.1	00.05
FeK	00.9	00.49
HfL	07.7	01.34
Matrix	Correction	ZAF

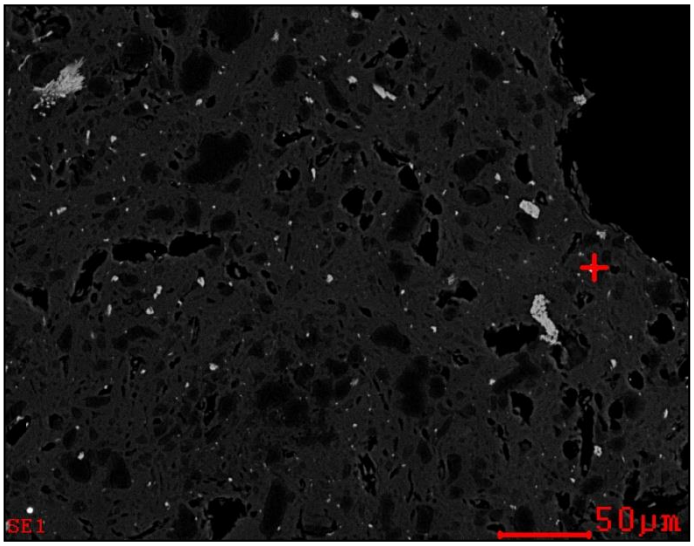

TI-SI-OX-HF

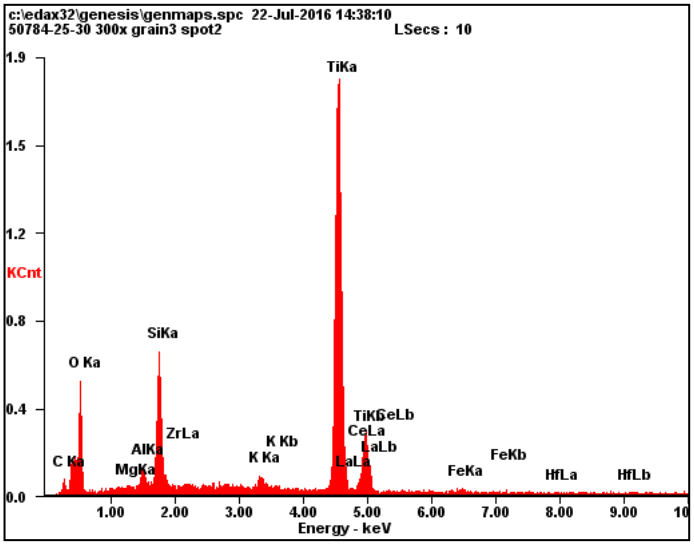

Element	Wt%	At%
CK	02.9	06.95
OK	26.9	47.93
MgK	00.4	00.48
AlK	01.4	01.49
SiK	08.2	08.30
ZrL	00.4	00.13
KK	00.9	00.63
TiK	55.6	33.10
FeK	01.3	00.67
HfL	02.0	00.32
Matrix	Correction	ZAF

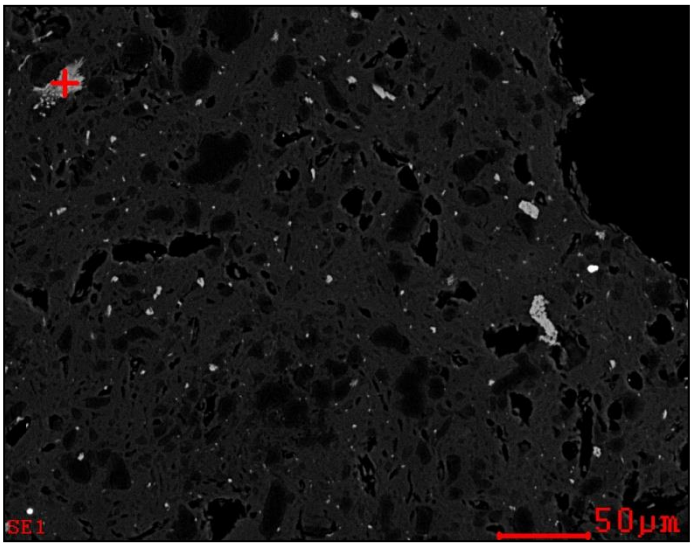

LREE-P-OX

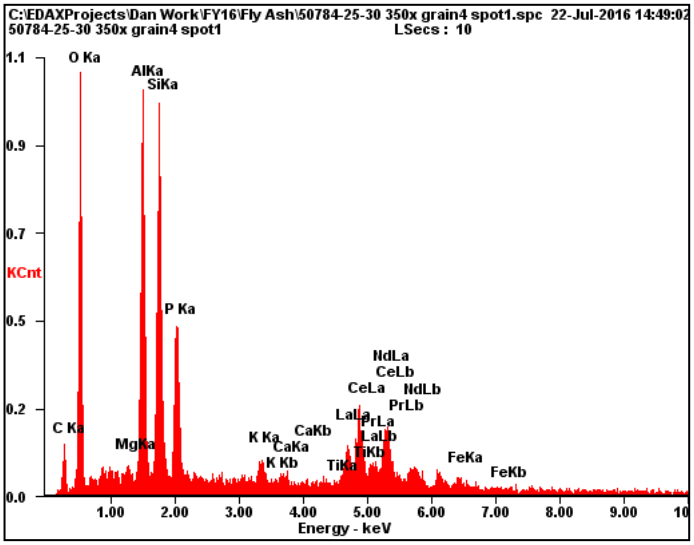

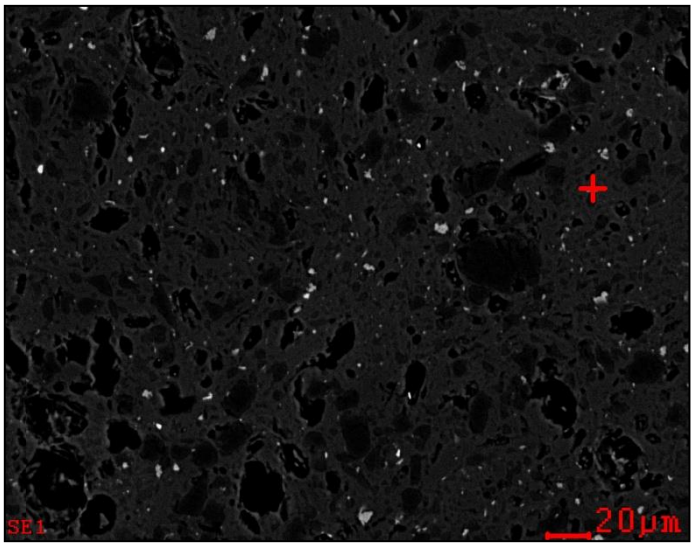

Element	*Wt%*	*At%*
CK	07.2	17.35
OK	20.8	37.59
MgK	00.6	00.70
AlK	13.9	14.91
SiK	13.7	14.08
PK	06.9	06.41
KK	01.3	00.96
CaK	00.5	00.39
TiK	00.3	00.16
LaL	07.8	01.63
CeL	16.6	03.42
PrL	01.9	00.38
NdL	07.4	01.48
FeK	01.0	00.53
Matrix	Correction	ZAF

LREE-P-OX -TH

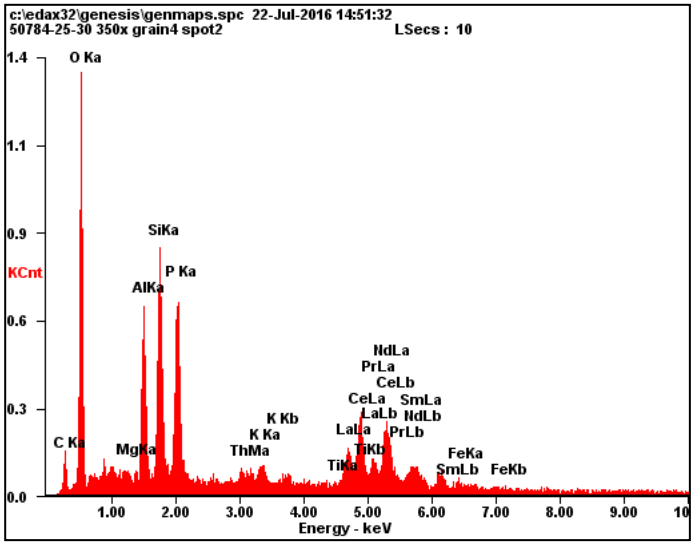

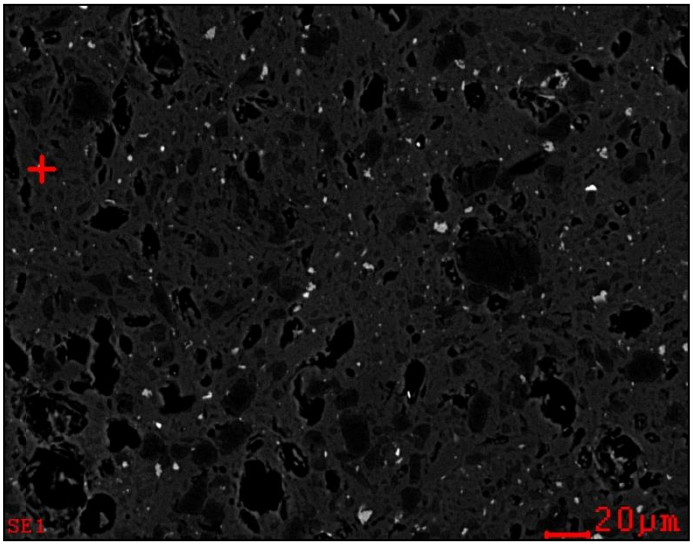

Element	Wt%	At%
CK	05.3	14.29
OK	21.6	43.43
MgK	00.5	00.60
AlK	07.7	09.22
SiK	10.5	12.03
PK	08.6	08.99
ThM	02.5	00.34
KK	01.1	00.88
TiK	00.2	00.16
LaL	08.6	01.99
CeL	17.7	04.06
PrL	02.7	00.61
NdL	09.6	02.15
SmL	02.1	00.46
FeK	01.4	00.79
Matrix	Correction	ZAF

AREA AL-SI-OX

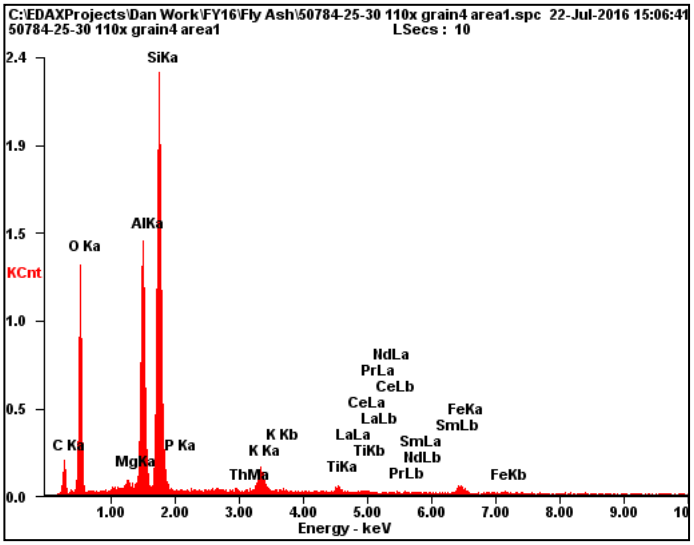

Element	Wt%	At%
CK	14.3	23.56
OK	32.6	40.30
MgK	00.6	00.51
AlK	15.3	11.23
SiK	30.8	21.66
KK	02.7	01.39
TiK	01.0	00.40
FeK	02.7	00.94
Matrix	Correction	ZAF

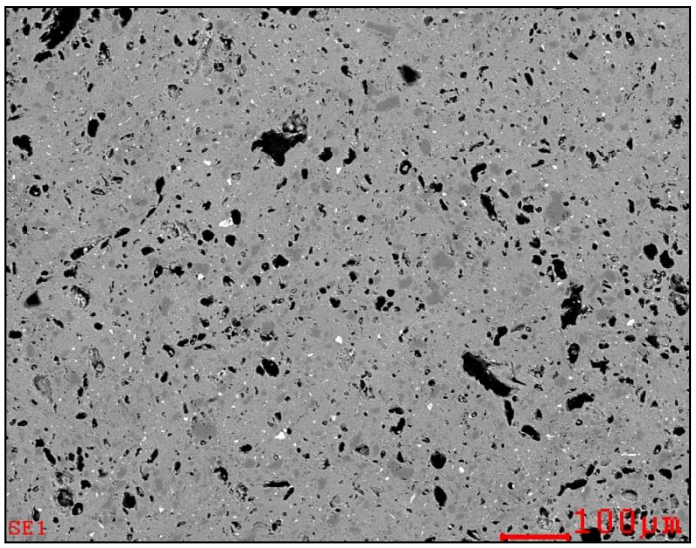

METAL-FE-CR-NI-MN STEEL

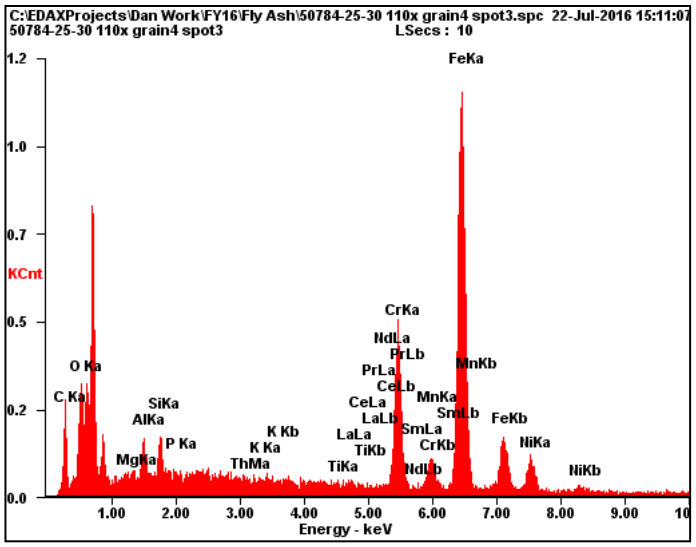

Element	Wt%	At%
MgK	00.2	00.34
AlK	01.9	03.75
SiK	02.0	03.71
KK	00.3	00.38
TiK	00.4	00.39
CrK	16.8	17.11
MnK	02.0	01.95
FeK	67.5	64.13
NiK	09.1	08.24
Matrix	Correction	ZAF

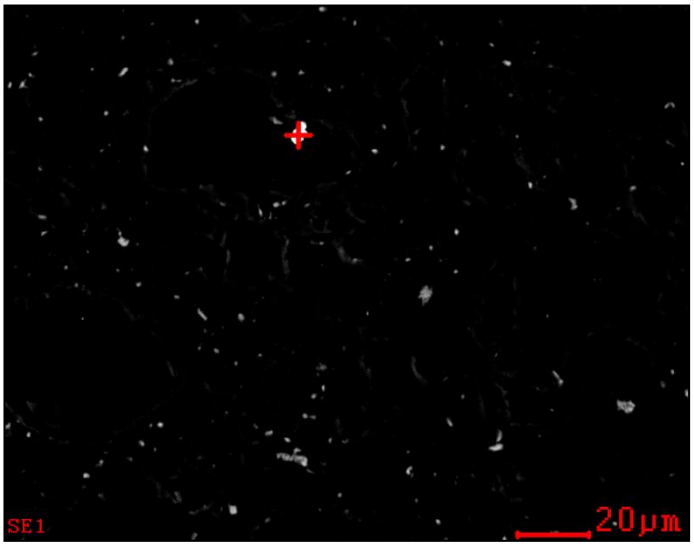

LREE-P-OX

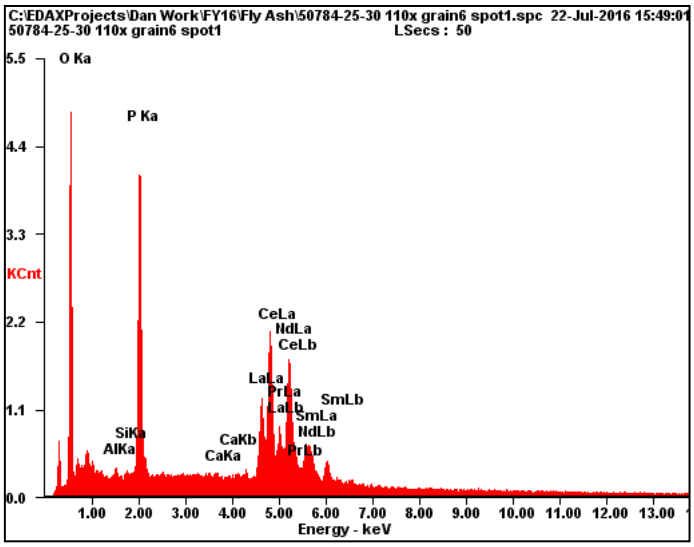

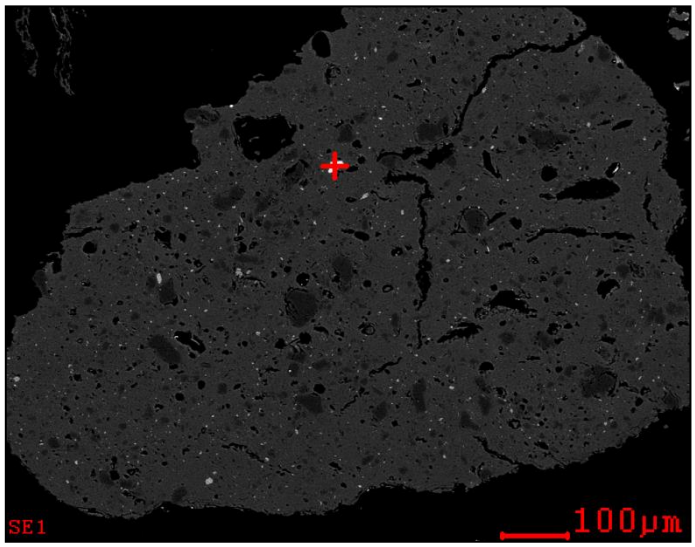

Element	Wt%	At%
OK	17.8	53.76
AlK	00.5	00.80
SiK	00.2	00.33
PK	14.0	21.84
CaK	00.2	00.24
LaL	16.0	05.54
CeL	32.7	11.25
PrL	03.0	01.03
NdL	14.1	04.72
SmL	01.5	00.48
Matrix	Correction	ZAF

ZR-SI-OX

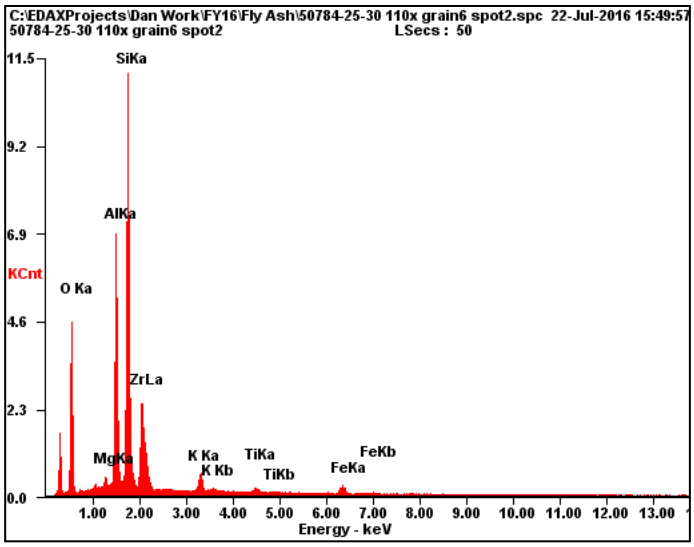

Element	Wt%	At%
OK	29.3	47.97
MgK	00.8	00.80
AlK	15.2	14.76
SiK	29.7	27.68
ZrL	19.2	05.52
KK	02.3	01.56
TiK	00.9	00.47
FeK	02.6	01.23
Matrix	Correction	ZAF

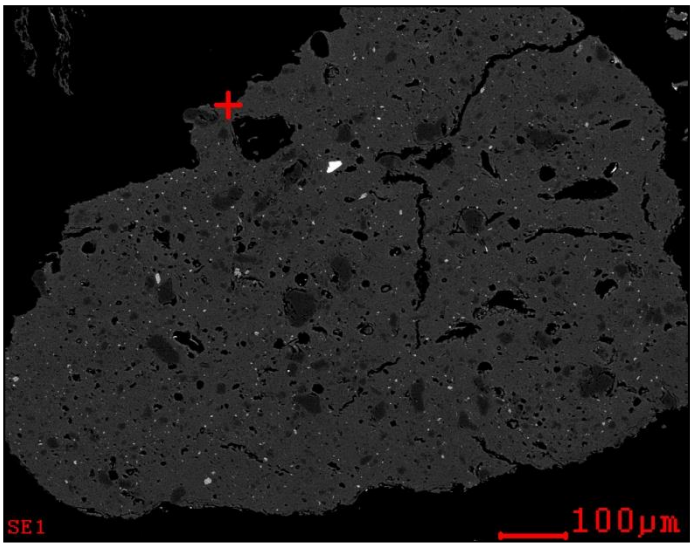

Appendix C: Low Temperature Ash SEM/EDX Results

AVERAGE OF GRAIN

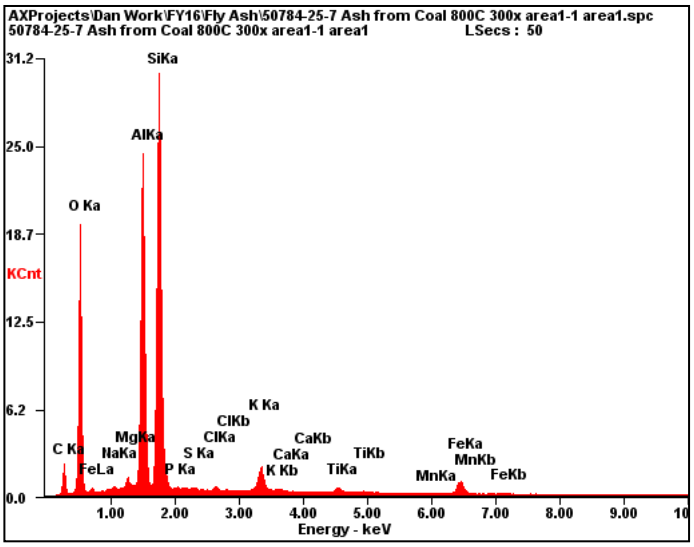

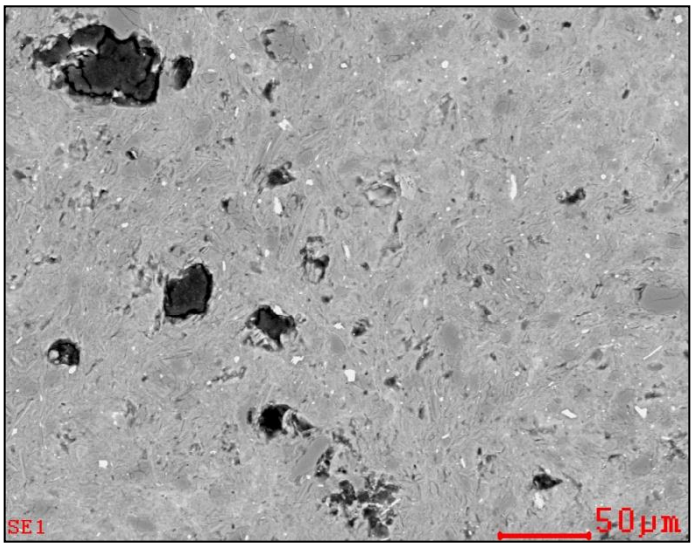

Element	Wt%	At%
CK	12.2	20.49
OK	33.2	41.73
NaK	00.2	00.17
MgK	00.7	00.55
AlK	18.2	13.56
SiK	28.6	20.54
PK	00.1	00.05
SK	00.1	00.03
ClK	00.2	00.10
KK	02.3	01.17
CaK	00.0	00.00
TiK	00.6	00.27
MnK	00.0	00.00
FeK	03.8	01.35
Matrix	Correction	ZAF

TI-OX

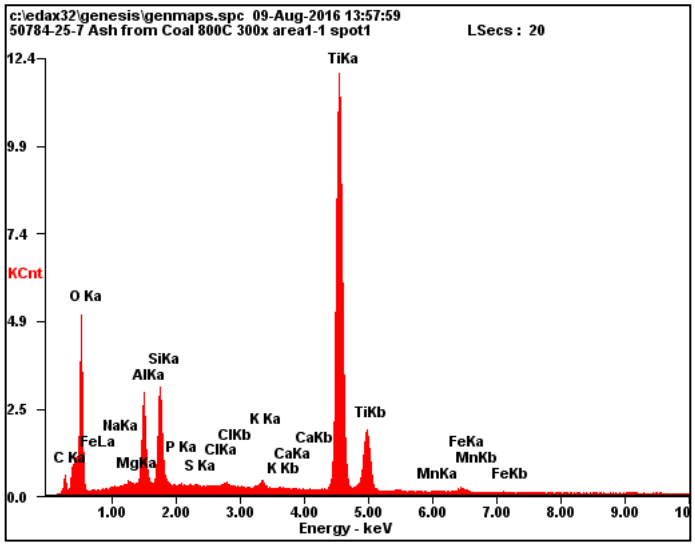

Element	Wt%	At%
OK	35.6	58.77
NaK	00.7	00.75
MgK	00.9	00.93
AlK	05.4	05.31
SiK	06.0	05.61
PK	00.3	00.29
SK	00.3	00.21
ClK	00.2	00.15
KK	00.5	00.36
CaK	00.1	00.04
TiK	49.0	27.03
MnK	00.0	00.02
FeK	01.1	00.52
Matrix	Correction	ZAF

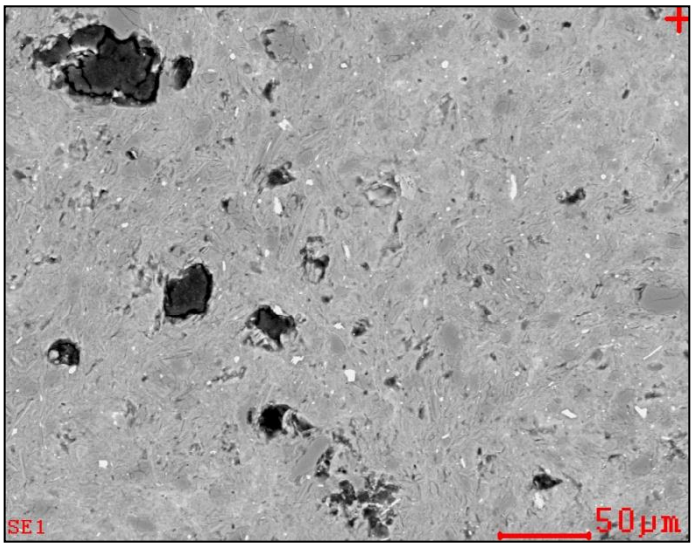

TI-OX

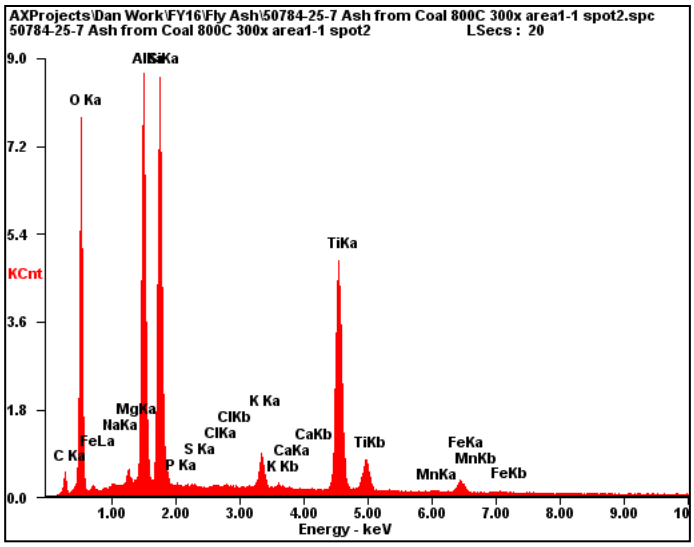

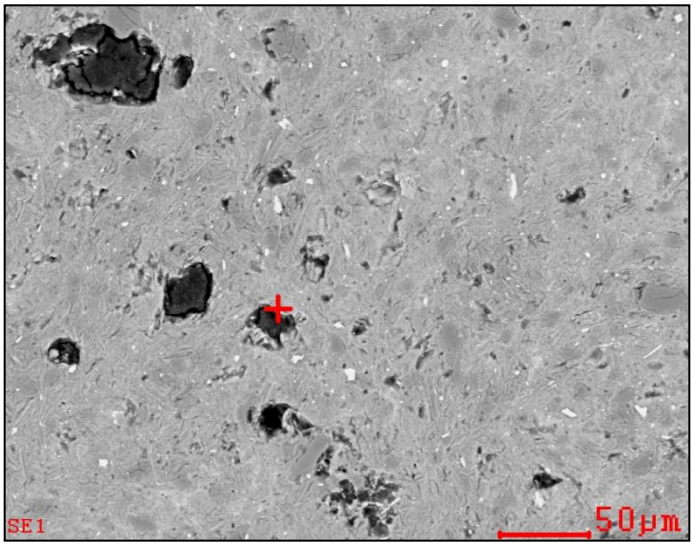

Element	Wt%	At%
OK	38.8	57.14
NaK	00.1	00.12
MgK	00.6	00.59
AlK	15.7	13.74
SiK	18.3	15.35
PK	00.0	00.00
SK	00.0	00.00
ClK	00.1	00.04
KK	01.9	01.13
CaK	00.1	00.05
TiK	22.0	10.82
MnK	00.1	00.04
FeK	02.3	00.98
Matrix	Correction	ZAF

K-AL-SI-OX

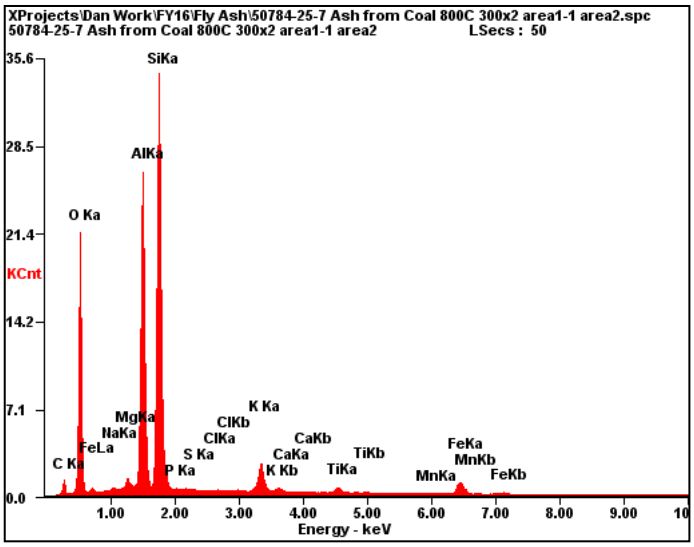

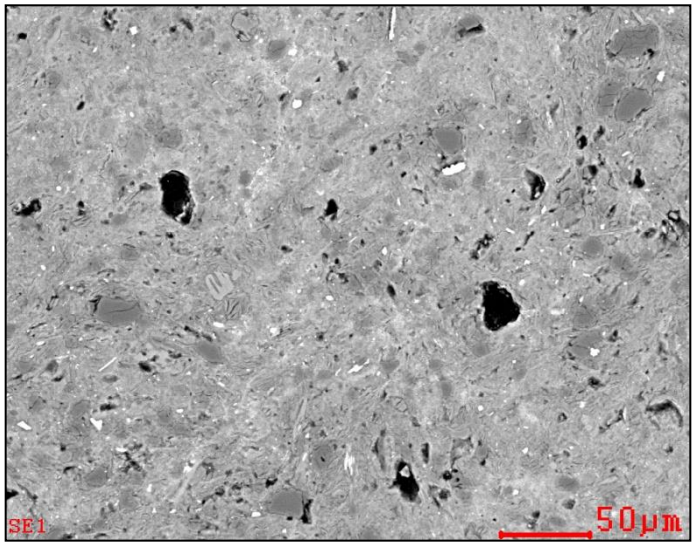

Element	Wt%	At%
CK	06.7	11.79
OK	34.2	45.25
NaK	00.2	00.14
MgK	00.7	00.63
AlK	19.0	14.95
SiK	31.6	23.81
PK	00.0	00.02
SK	00.0	00.00
ClK	00.0	00.00
KK	02.9	01.56
CaK	00.0	00.00
TiK	00.8	00.34
MnK	00.0	00.00
FeK	04.0	01.51
Matrix	Correction	ZAF

TI-OX

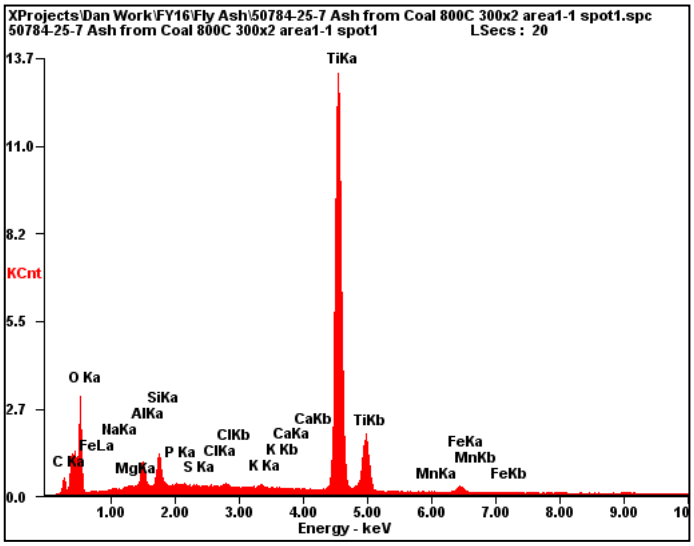

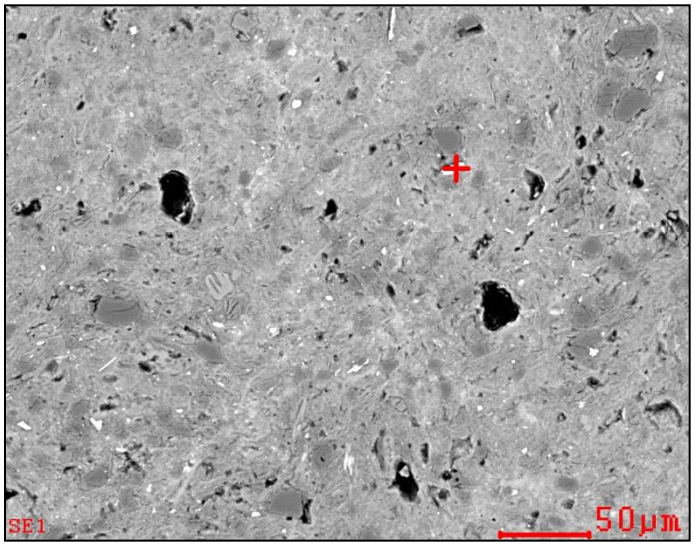

Element	Wt%	At%
OK	28.8	52.98
NaK	00.6	00.72
MgK	00.6	00.76
AlK	02.3	02.55
SiK	02.7	02.82
PK	00.4	00.40
SK	00.3	00.25
ClK	00.2	00.14
KK	00.3	00.25
CaK	00.1	00.07
TiK	61.7	37.96
MnK	00.1	00.06
FeK	02.0	01.03
Matrix	Correction	ZAF

Y-P-OX

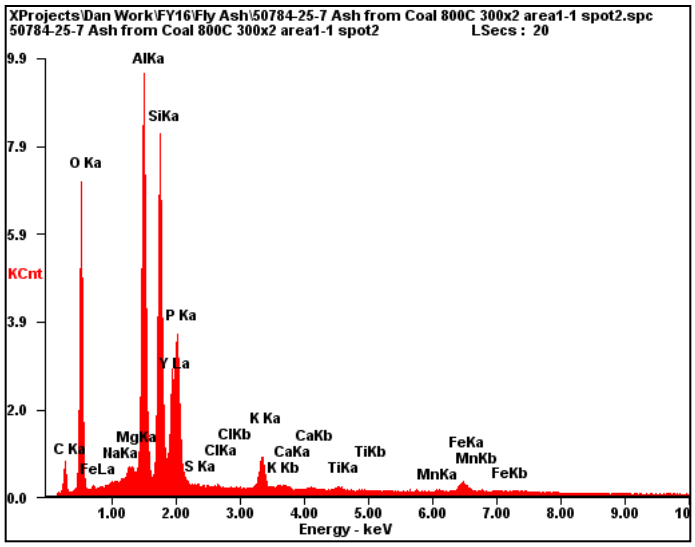

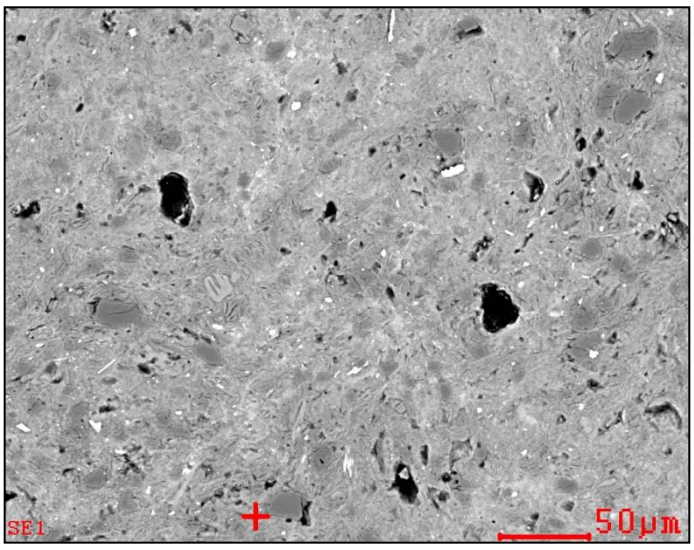

Element	*Wt%*	*At%*
OK	34.3	52.91
NaK	00.0	00.04
MgK	00.7	00.71
AlK	18.4	16.82
SiK	18.8	16.55
YL	14.8	04.12
PK	07.0	05.59
SK	00.0	00.00
ClK	00.0	00.03
KK	02.8	01.74
CaK	00.3	00.18
TiK	00.5	00.25
MnK	00.0	00.00
FeK	02.4	01.07
Matrix	Correction	ZAF

REE-P-OX

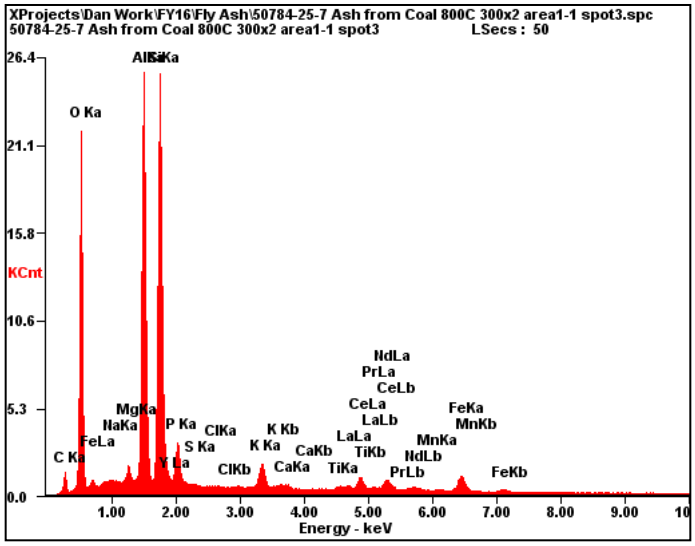

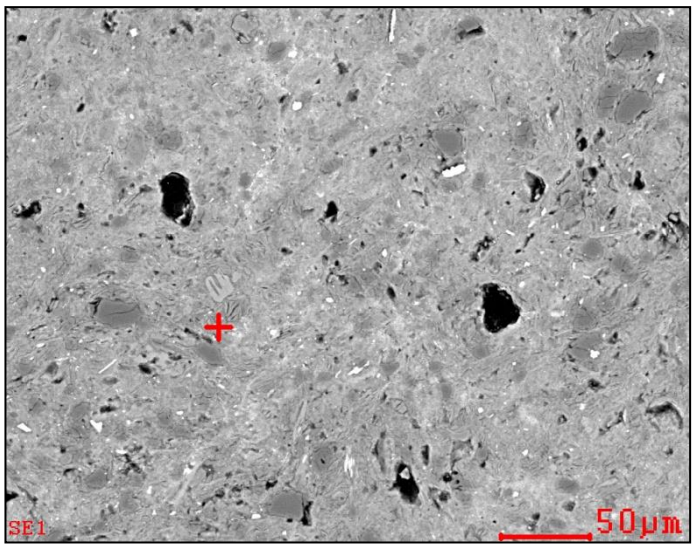

Element	Wt%	At%
OK	32.6	49.17
NaK	00.3	00.26
MgK	00.9	00.90
AlK	21.6	19.34
SiK	27.3	23.51
YL	00.0	00.00
PK	03.1	02.45
SK	00.0	00.00
ClK	00.0	00.00
KK	01.8	01.09
CaK	00.0	00.00
TiK	00.1	00.07
LaL	00.8	00.15
CeL	04.6	00.79
PrL	00.4	00.06
NdL	02.3	00.39
MnK	00.0	00.00
FeK	04.2	01.82
Matrix	Correction	ZAF

FE-OX

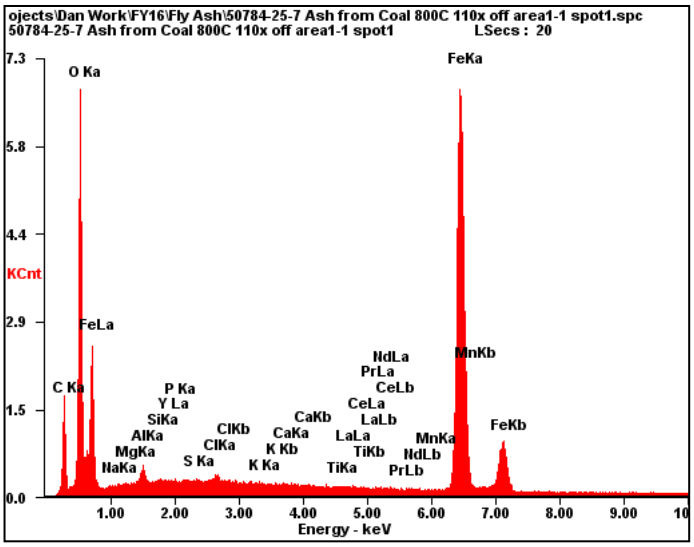

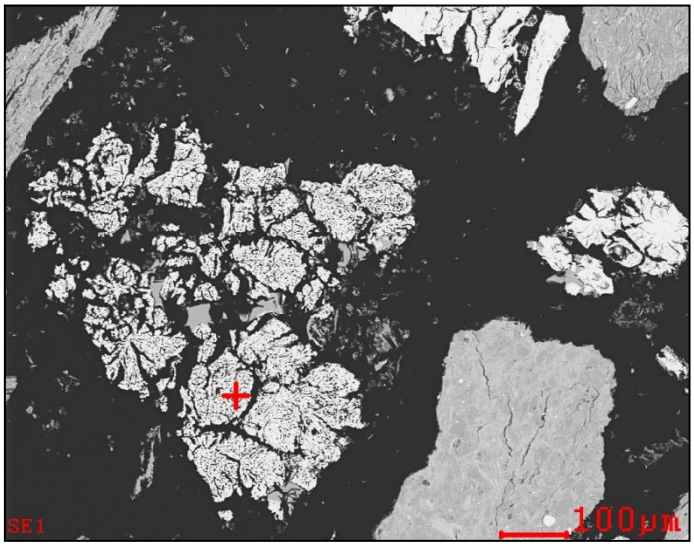

Element	Wt%	At%
OK	18.4	43.54
NaK	00.1	00.13
MgK	00.1	00.11
AlK	01.2	01.64
SiK	00.2	00.23
YL	00.1	00.06
PK	00.0	00.00
SK	00.1	00.15
ClK	00.4	00.45
KK	00.1	00.06
CaK	00.1	00.11
TiK	00.1	00.05
LaL	00.4	00.12
CeL	00.3	00.08
PrL	00.0	00.00
NdL	00.3	00.07
MnK	00.1	00.09
FeK	78.1	53.11
Matrix	Correction	ZAF

AL-SI-OX

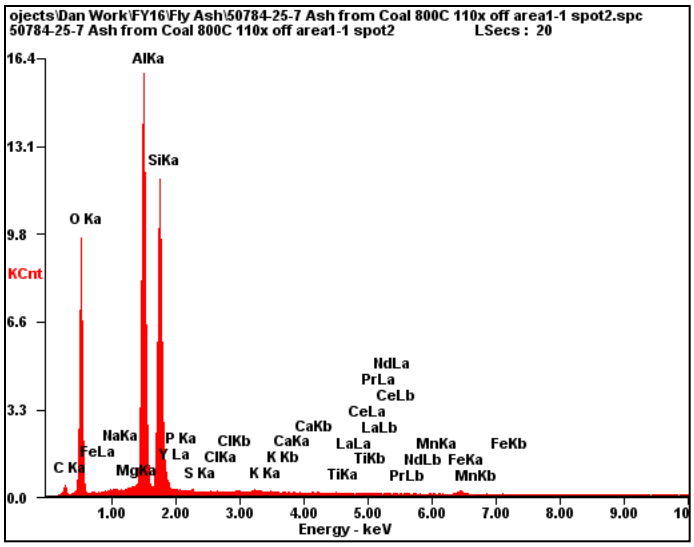

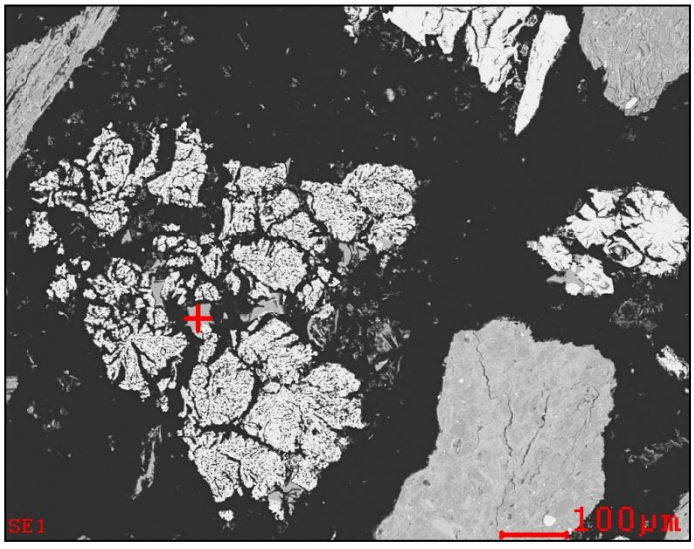

Element	Wt%	At%
OK	36.0	49.56
NaK	00.2	00.18
MgK	00.2	00.18
AlK	29.6	24.13
SiK	32.5	25.25
PK	00.0	00.00
SK	00.0	00.00
ClK	00.0	00.00
KK	00.2	00.10
CaK	00.0	00.02
TiK	00.1	00.02
LaL	00.0	00.02
CeL	00.0	00.01
PrL	00.0	00.02
NdL	00.0	00.00
MnK	00.0	00.01
FeK	01.2	00.49
Matrix	Correction	ZAF

FE-OX

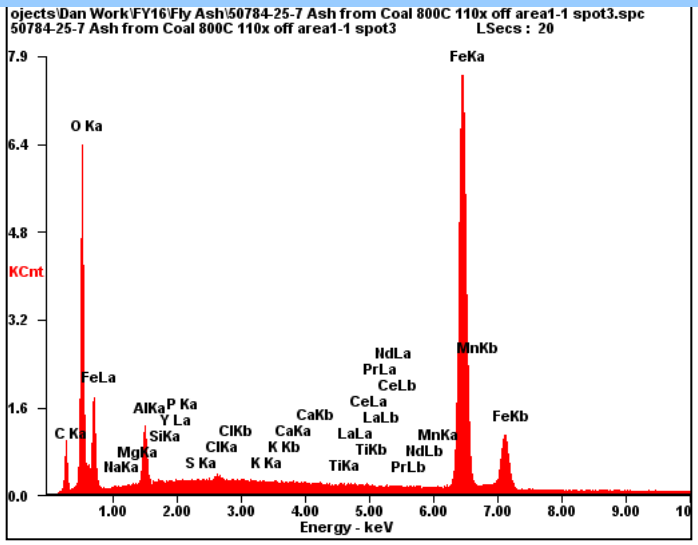

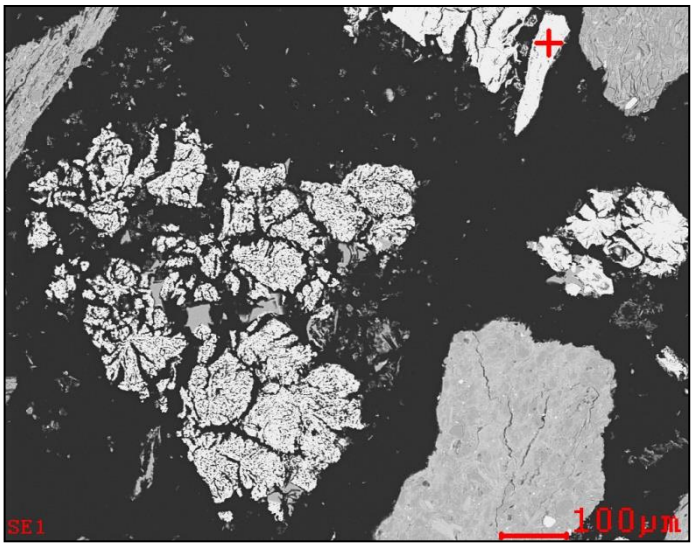

Element	Wt%	At%
OK	15.6	38.26
NaK	00.1	00.17
MgK	00.0	00.00
AlK	03.7	05.32
SiK	00.1	00.11
YL	00.0	00.00
PK	00.1	00.08
SK	00.1	00.16
ClK	00.4	00.44
KK	00.2	00.19
CaK	00.2	00.20
TiK	00.2	00.17
LaL	00.0	00.23
CeL	00.0	00.15
PrL	00.0	00.00
NdL	00.0	00.08
MnK	00.3	00.18
FeK	79.4	54.26
Matrix	Correction	ZAF

AL-SI-OX PROBABLY NO REE

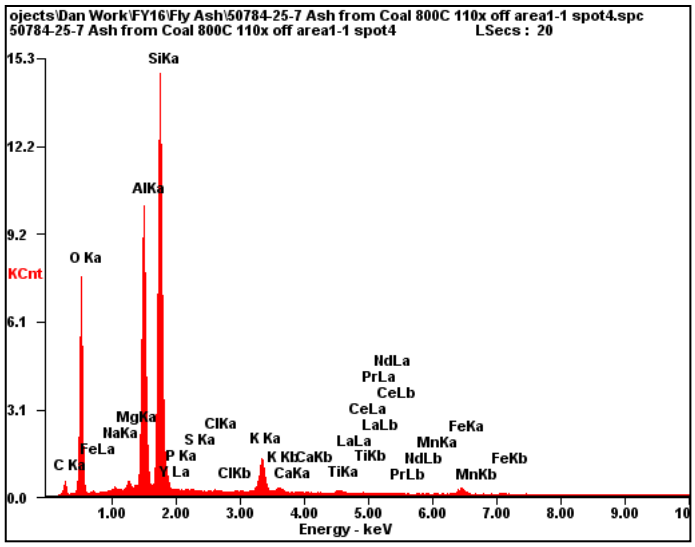

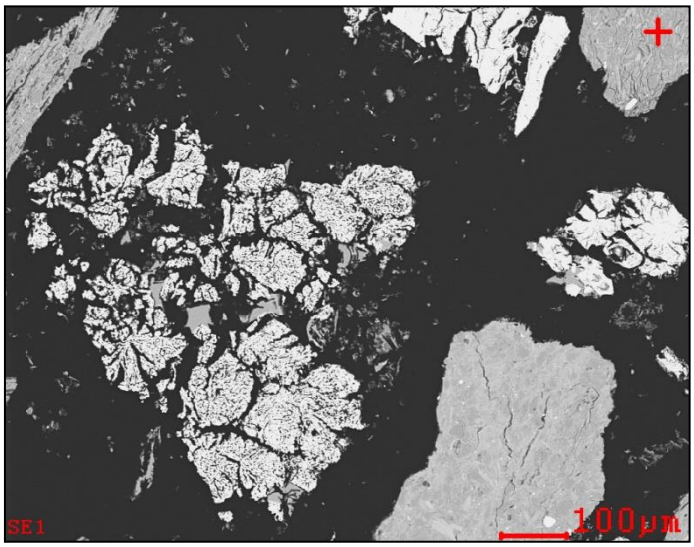

Element	Wt%	At%
OK	33.4	47.78
NaK	00.3	00.29
MgK	00.7	00.66
AlK	19.8	16.80
SiK	37.2	30.30
PK	00.0	00.00
SK	00.0	00.00
ClK	00.2	00.12
KK	04.4	02.57
CaK	00.1	00.07
TiK	00.6	00.28
LaL	00.3	00.04
CeL	00.3	00.04
PrL	00.2	00.03
NdL	00.1	00.02
MnK	00.0	00.01
FeK	02.4	00.99
Matrix	Correction	ZAF

ZR-SI-OX WITH Y

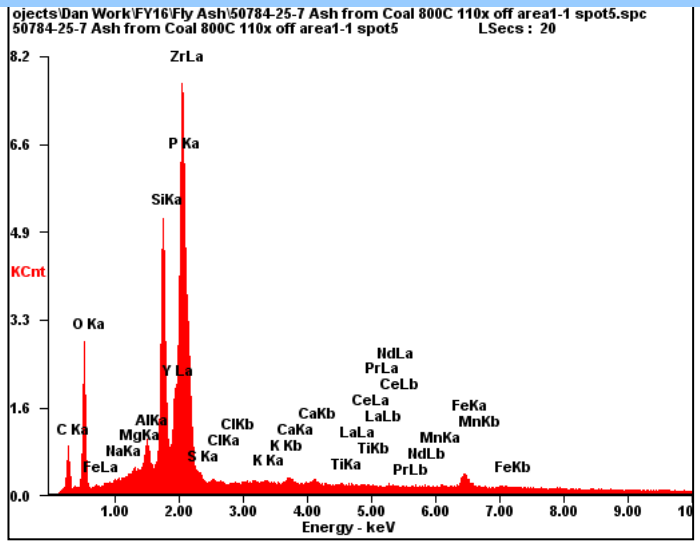

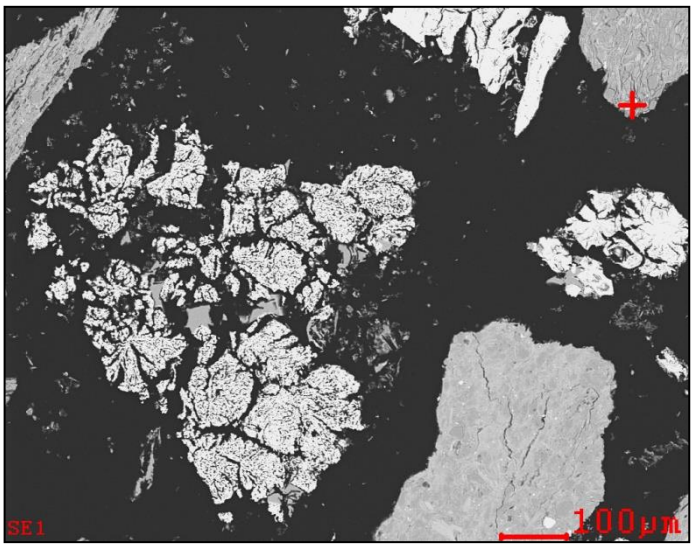

Element	Wt%	At%
OK	23.4	52.47
NaK	00.0	00.00
MgK	00.3	00.38
AlK	01.6	02.07
SiK	12.9	16.57
YL	08.3	03.37
PK	03.5	04.05
ZrL	45.2	17.82
SK	00.1	00.06
ClK	00.0	00.00
KK	00.3	00.26
CaK	00.6	00.57
TiK	00.1	00.06
LaL	00.0	00.00
CeL	00.2	00.06
PrL	00.0	00.00
NdL	00.1	00.04
MnK	00.0	00.00
FeK	03.5	02.22
Matrix	Correction	ZAF

ZR-SI-OX WITH HF

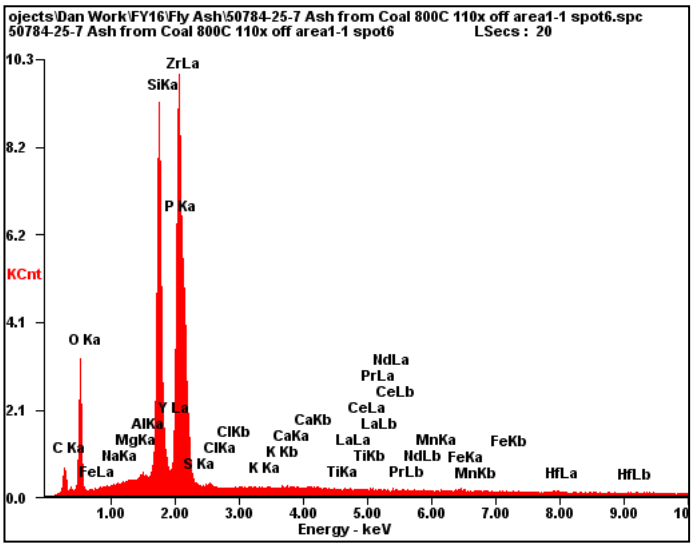

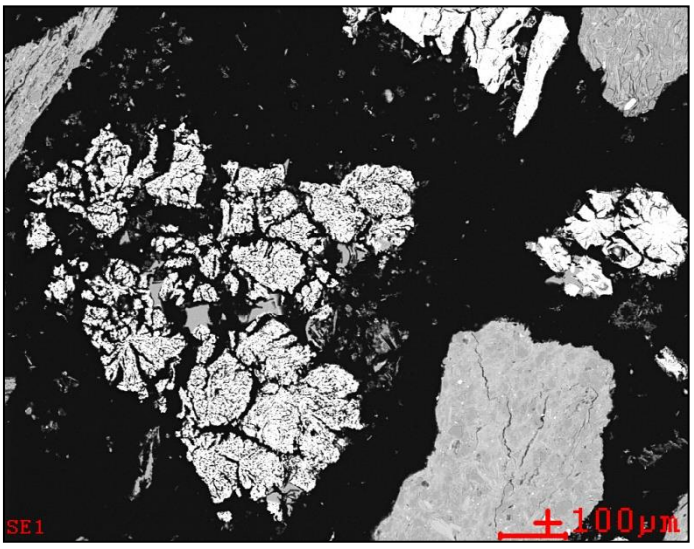

Element	Wt%	At%
OK	22.4	51.40
NaK	00.0	00.04
MgK	00.1	00.14
AlK	00.2	00.33
SiK	19.2	25.01
YL	00.0	00.00
PK	00.0	00.00
ZrL	56.1	22.57
SK	00.0	00.00
ClK	00.0	00.00
KK	00.0	00.00
CaK	00.0	00.00
TiK	00.0	00.00
LaL	00.0	00.00
CeL	00.0	00.00
PrL	00.0	00.00
NdL	00.0	00.00
MnK	00.0	00.00
FeK	00.2	00.14
HfL	01.7	00.35
Matrix	Correction	ZAF

TI-OX

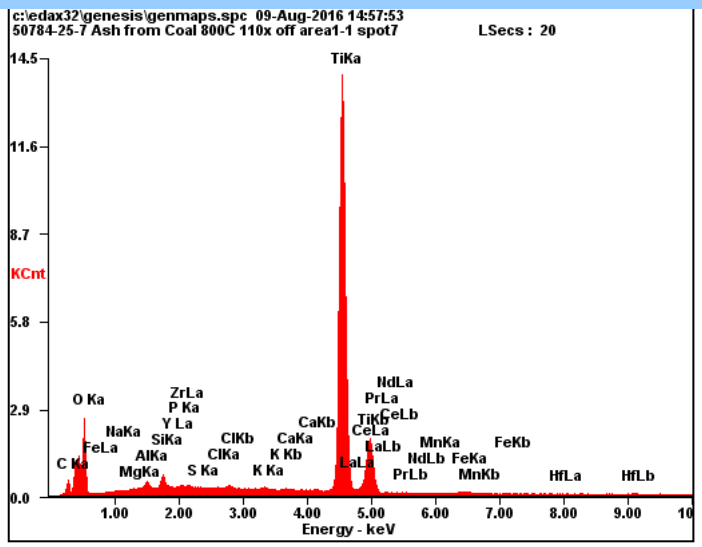

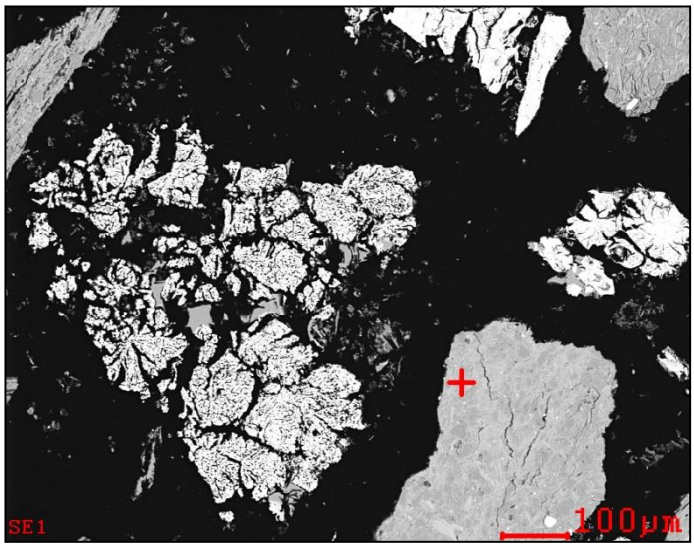

Element	Wt%	At%
OK	27.0	51.96
NaK	00.5	00.62
MgK	00.4	00.54
AlK	00.9	01.04
SiK	01.2	01.35
YL	00.0	00.00
PK	00.0	00.00
ZrL	00.0	00.00
SK	00.2	00.19
ClK	00.2	00.14
KK	00.2	00.17
CaK	00.2	00.12
TiK	68.7	43.96
PrL	00.0	00.00
NdL	00.0	00.00
MnK	00.0	00.00
FeK	00.6	00.34
HfL	00.0	00.00
Matrix	Correction	ZAF

ZR-SI-OX WITH HF

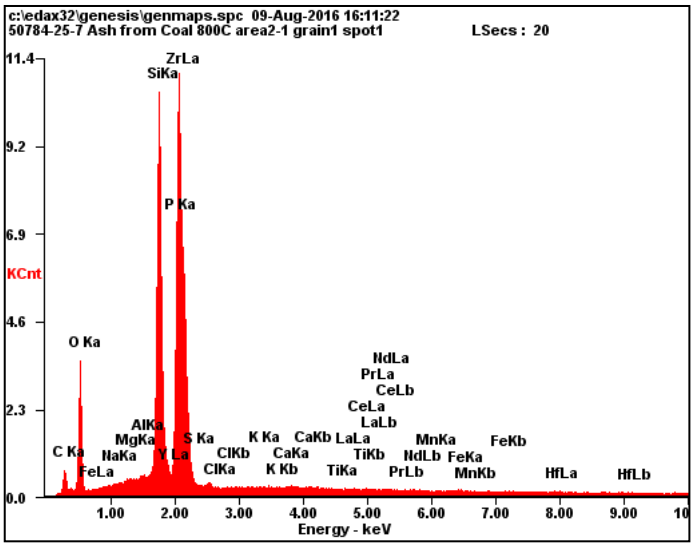

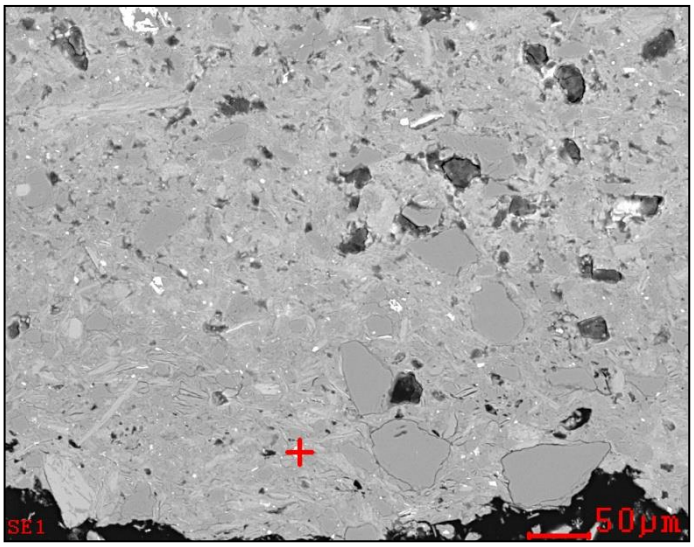

Element	Wt%	At%
OK	21.6	50.26
NaK	00.0	00.00
MgK	00.1	00.10
AlK	00.2	00.22
SiK	19.5	25.81
YL	00.0	00.00
PK	00.0	00.00
ZrL	55.9	22.82
SK	00.0	00.00
ClK	00.0	00.00
KK	00.0	00.00
CaK	00.0	00.00
TiK	00.0	00.00
LaL	00.0	00.00
CeL	00.2	00.04
PrL	00.3	00.07
NdL	00.2	00.06
MnK	00.0	00.00
FeK	00.3	00.23
HfL	01.9	00.40
Matrix	Correction	ZAF

TI-OX

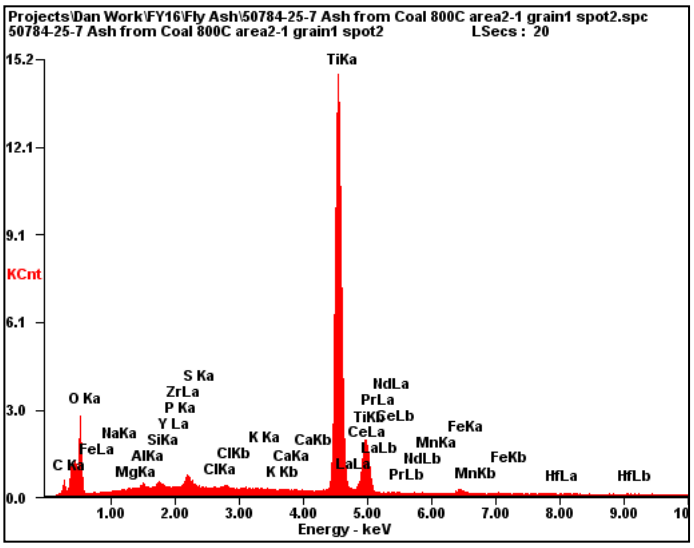

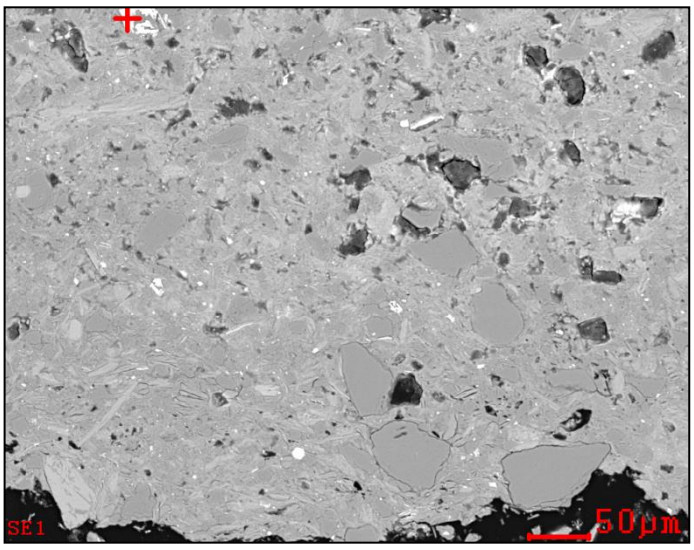

Element	Wt%	At%
OK	27.5	52.38
NaK	00.4	00.54
MgK	00.5	00.61
AlK	00.8	00.92
SiK	00.8	00.90
PK	00.0	00.00
SK	00.5	00.45
ClK	00.2	00.16
KK	00.1	00.07
CaK	00.1	00.09
TiK	67.8	43.13
PrL	00.0	00.00
NdL	00.0	00.00
MnK	00.0	00.00
FeK	01.3	00.73
HfL	00.0	00.00
Matrix	Correction	ZAF

REE-P-OX

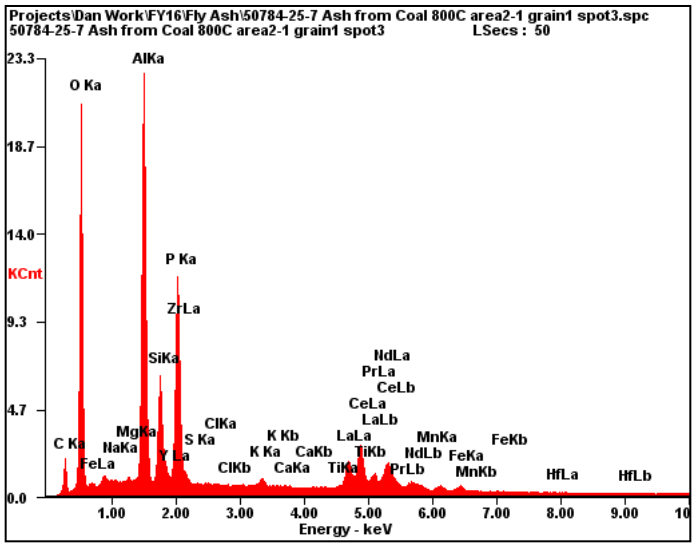

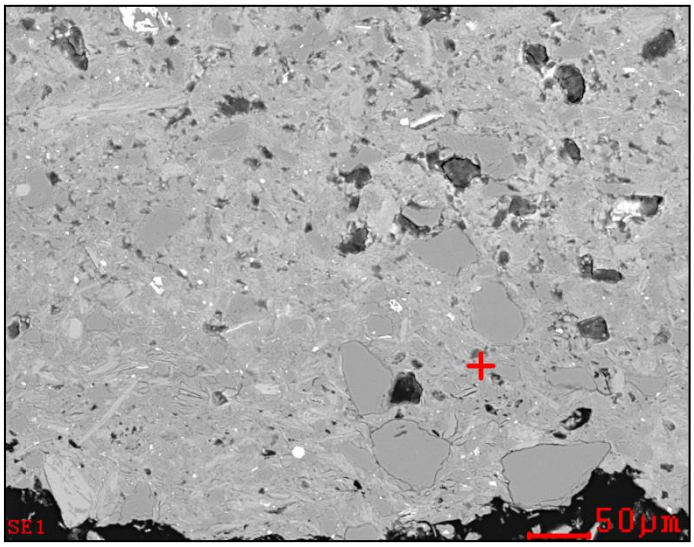

Element	Wt%	At%
OK	27.7	50.12
NaK	00.2	00.28
MgK	00.2	00.23
AlK	22.3	23.92
SiK	06.6	06.83
YL	00.5	00.17
PK	12.4	11.59
ZrL	01.3	00.42
SK	00.0	00.00
ClK	00.0	00.00
KK	00.4	00.28
CaK	00.0	00.00
TiK	00.1	00.04
LaL	08.3	01.74
CeL	14.8	03.06
PrL	01.0	00.21
NdL	03.2	00.63
MnK	00.0	00.00
FeK	00.9	00.48
HfL	00.0	00.00
Matrix	Correction	ZAF

TI-SI-OX

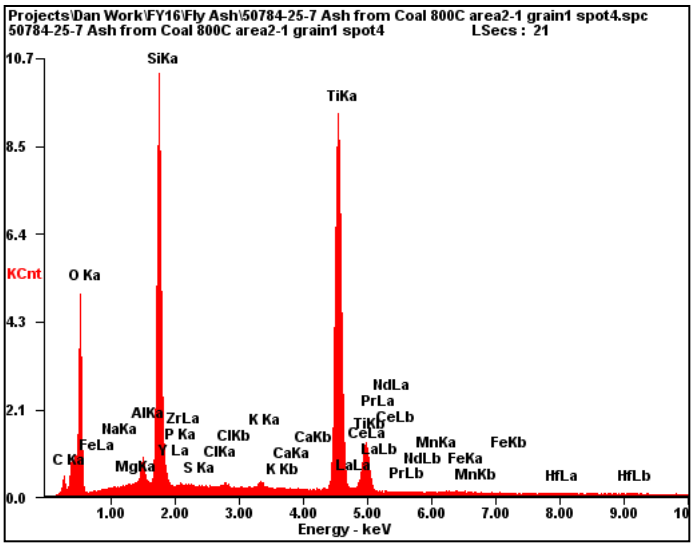

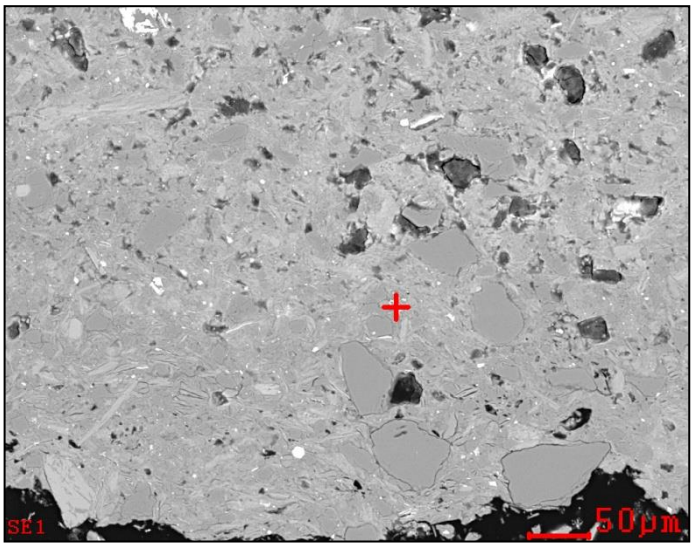

Element	Wt%	At%
OK	35.4	57.24
NaK	00.0	00.05
MgK	00.0	00.03
AlK	01.1	01.09
SiK	19.3	17.75
PK	00.0	00.00
SK	00.1	00.04
ClK	00.1	00.07
KK	00.5	00.33
CaK	00.1	00.07
TiK	42.9	23.14
PrL	00.0	00.00
NdL	00.0	00.00
MnK	00.0	00.00
FeK	00.4	00.19
Matrix	Correction	ZAF

REE-P-OX

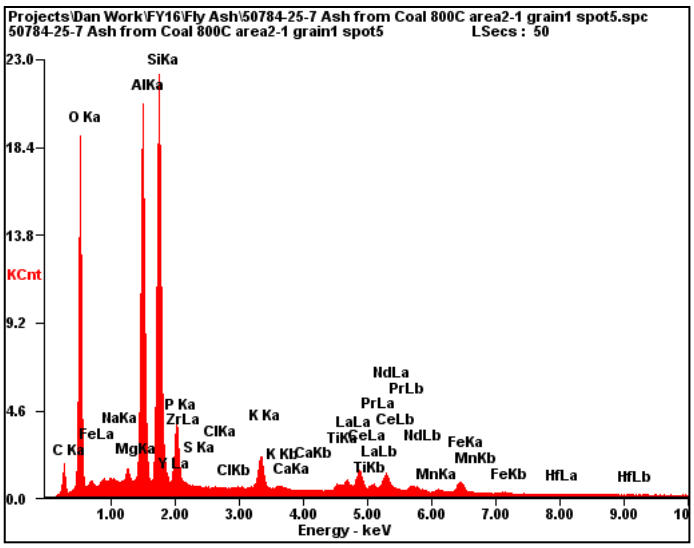

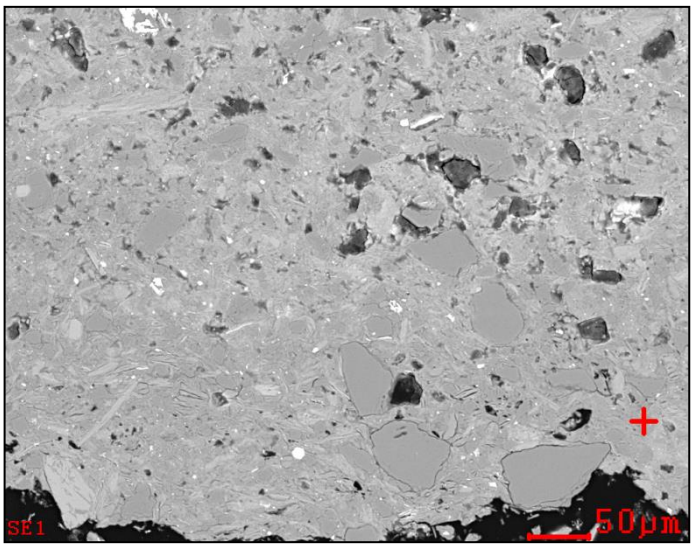

Element	*Wt%*	*At%*
OK	30.5	48.43
NaK	00.4	00.39
MgK	00.8	00.82
AlK	19.6	18.49
SiK	25.5	23.06
YL	00.0	00.00
PK	04.3	03.55
ZrL	00.0	00.00
SK	00.0	00.00
ClK	00.0	00.00
KK	02.2	01.43
CaK	00.0	00.00
TiK	00.4	00.21
LaL	02.7	00.50
CeL	07.4	01.33
PrL	00.6	00.11
NdL	03.3	00.57
MnK	00.0	00.00
FeK	02.4	01.11
Matrix	Correction	ZAF

K-AL-SI-OX

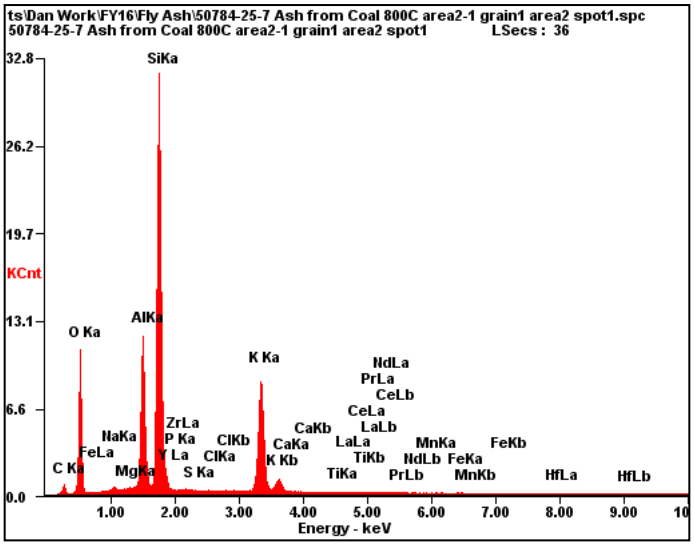

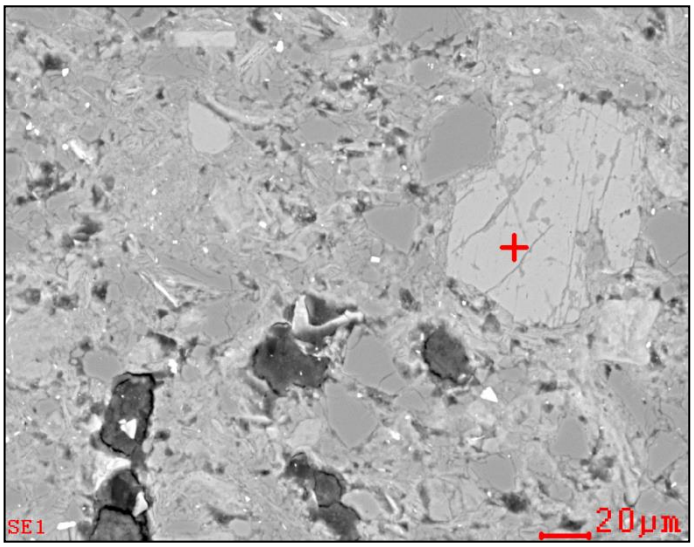

Element	Wt%	At%
OK	31.8	46.60
NaK	00.4	00.40
MgK	00.1	00.10
AlK	12.2	10.58
SiK	38.8	32.43
PK	00.0	00.00
ZrL	00.0	00.00
SK	00.0	00.00
ClK	00.0	00.00
KK	16.4	09.82
CaK	00.0	00.00
TiK	00.0	00.00
LaL	00.0	00.00
CeL	00.1	00.01
PrL	00.0	00.04
NdL	00.0	00.00
MnK	00.0	00.00
FeK	00.0	00.02
HfL	00.0	00.00
Matrix	Correction	ZAF

SI-OX

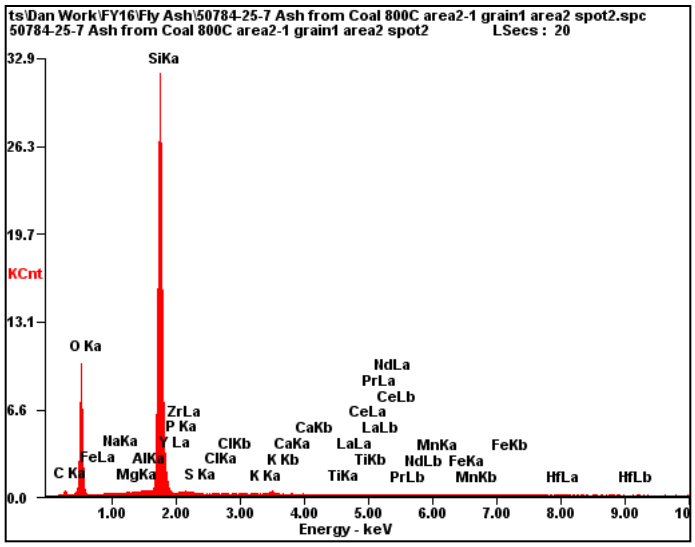

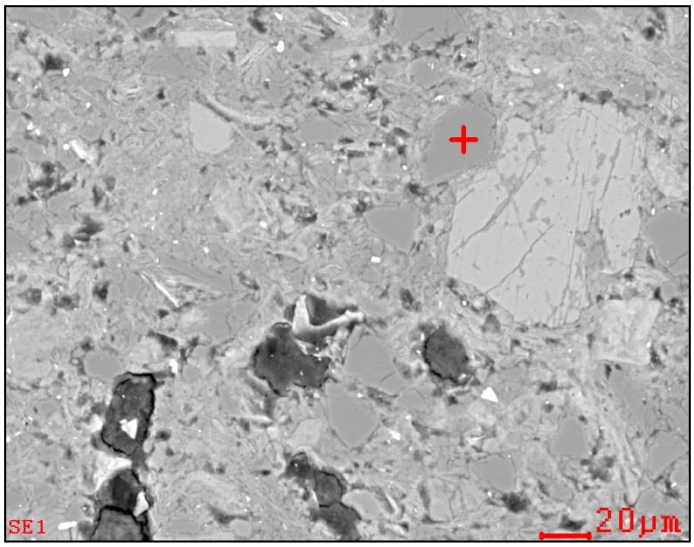

Element	Wt%	At%
OK	38.5	52.46
NaK	00.1	00.05
MgK	00.0	00.03
AlK	00.4	00.29
SiK	60.4	46.83
PK	00.0	00.00
SK	00.1	00.07
ClK	00.0	00.00
KK	00.1	00.05
CaK	00.1	00.05
TiK	00.1	00.05
MnK	00.0	00.00
FeK	00.3	00.12
Matrix	Correction	ZAF

TI-OX

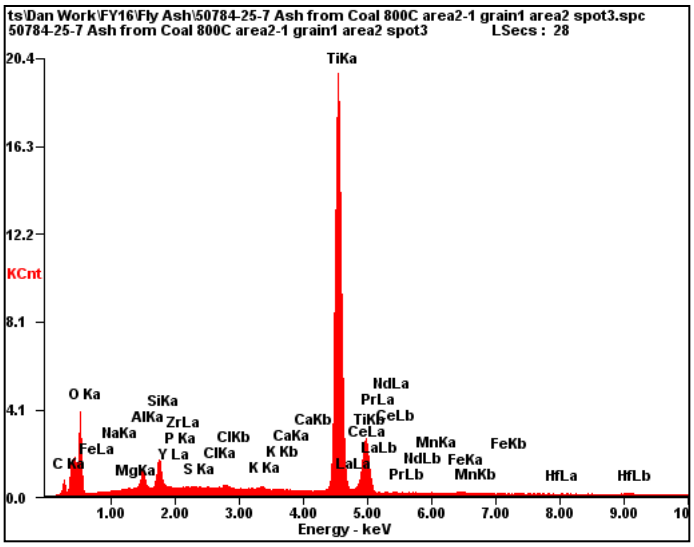

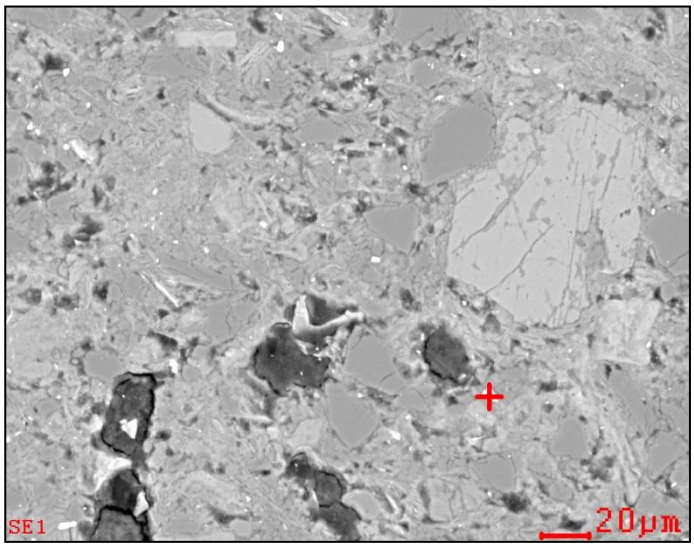

Element	Wt%	At%
OK	27.7	51.90
NaK	00.5	00.59
MgK	00.5	00.67
AlK	02.0	02.24
SiK	02.6	02.74
PK	00.0	00.00
SK	00.3	00.26
ClK	00.2	00.18
KK	00.3	00.25
CaK	00.1	00.05
TiK	65.3	40.85
MnK	00.0	00.00
FeK	00.5	00.27
Matrix	Correction	ZAF

TI-SI-OX

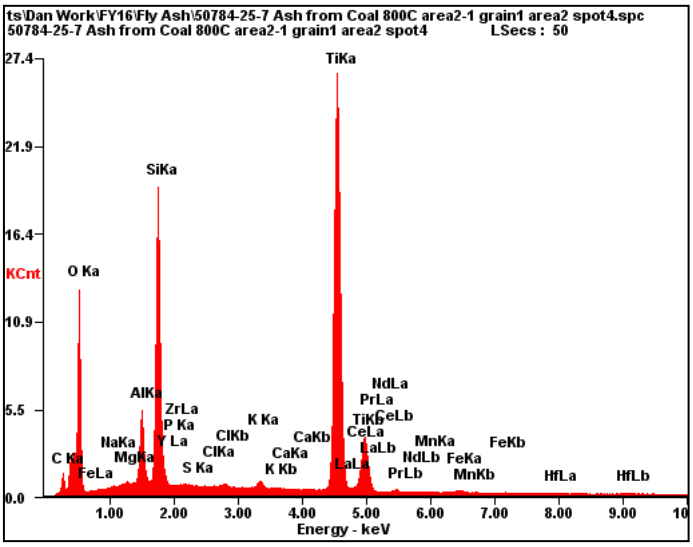

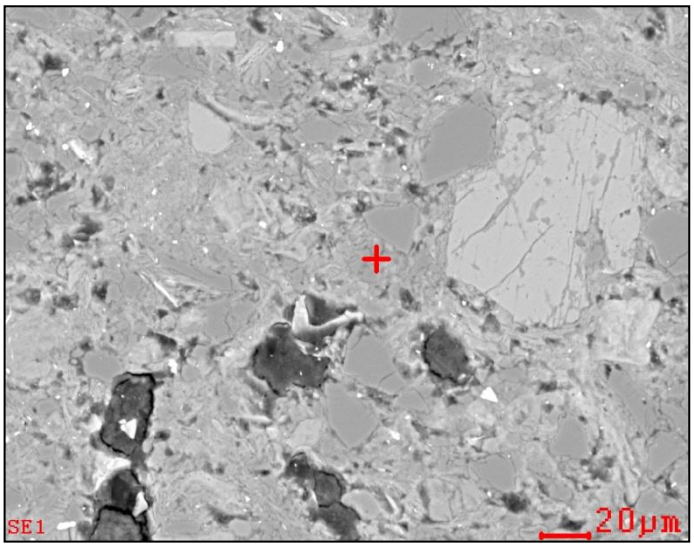

Element	Wt%	At%
OK	35.6	57.84
NaK	00.1	00.10
MgK	00.2	00.26
AlK	03.7	03.57
SiK	14.2	13.16
PK	00.0	00.00
SK	00.0	00.03
ClK	00.1	00.04
KK	00.5	00.32
CaK	00.0	00.02
TiK	44.9	24.34
PrL	00.0	00.00
NdL	00.0	00.00
MnK	00.1	00.05
FeK	00.6	00.26
Matrix	Correction	ZAF

K-AL-SI-OX

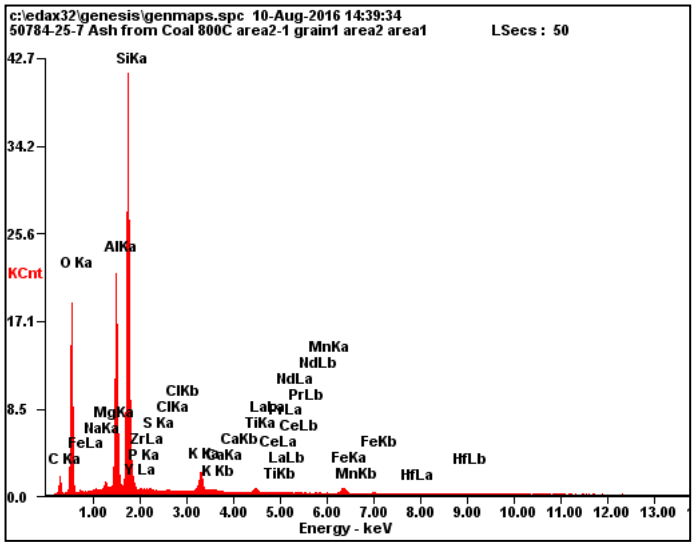

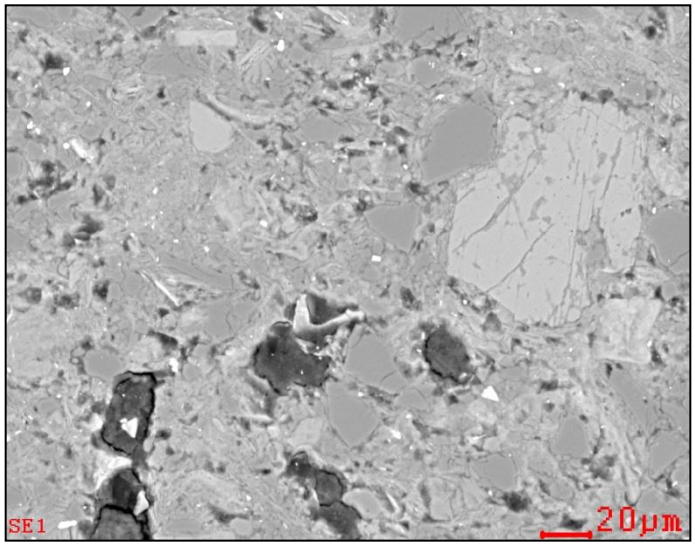

Element	Wt%	At%
CK	09.6	16.33
OK	33.9	43.37
NaK	00.1	00.12
MgK	00.6	00.48
AlK	15.0	11.41
SiK	35.6	25.95
PK	00.0	00.00
SK	00.0	00.00
ClK	00.0	00.01
KK	02.5	01.30
CaK	00.0	00.00
TiK	00.7	00.29
MnK	00.0	00.00
FeK	02.0	00.74
Matrix	Correction	ZAF

K-AL-SI-OX

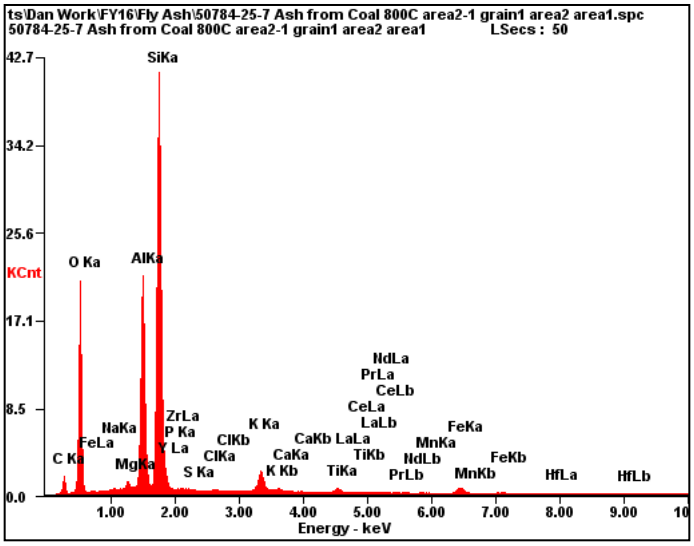

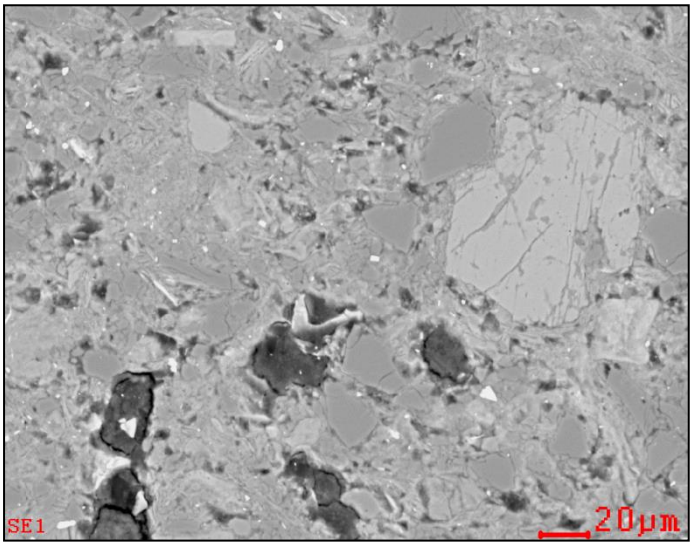

Element	*Wt%*	*At%*
CK	09.6	16.33
OK	33.9	43.37
NaK	00.1	00.12
MgK	00.6	00.48
AlK	15.0	11.41
SiK	35.6	25.95
PK	00.0	00.00
SK	00.0	00.00
ClK	00.0	00.01
KK	02.5	01.30
CaK	00.0	00.00
TiK	00.7	00.29
MnK	00.0	00.00
FeK	02.0	00.74
Matrix	Correction	ZAF

AL-SI-OX

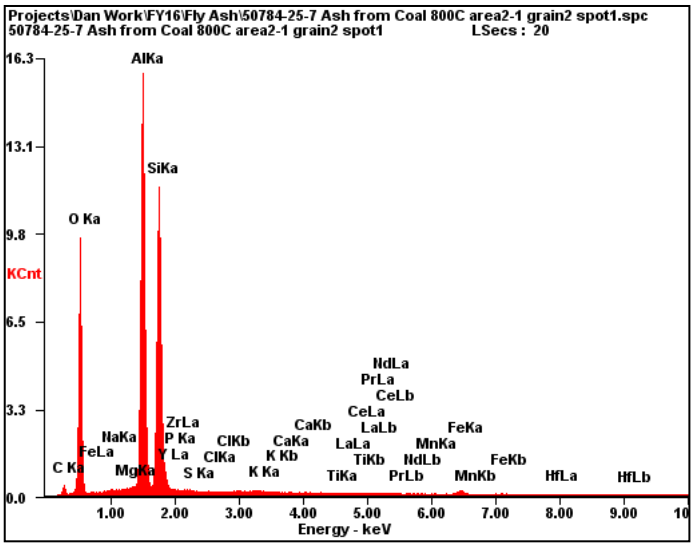

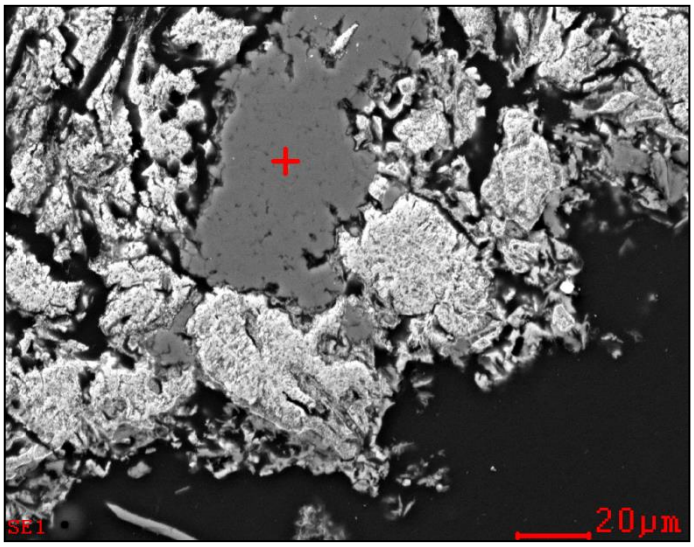

Element	Wt%	At%
OK	36.0	49.50
NaK	00.1	00.09
MgK	00.1	00.10
AlK	29.8	24.26
SiK	32.4	25.41
PK	00.0	00.00
ZrL	00.0	00.00
SK	00.0	00.00
ClK	00.0	00.00
KK	00.1	00.07
CaK	00.0	00.00
TiK	00.0	00.00
LaL	00.0	00.00
CeL	00.0	00.00
PrL	00.0	00.00
NdL	00.0	00.00
MnK	00.0	00.00
FeK	01.5	00.59
Matrix	Correction	ZAF

FE-OX

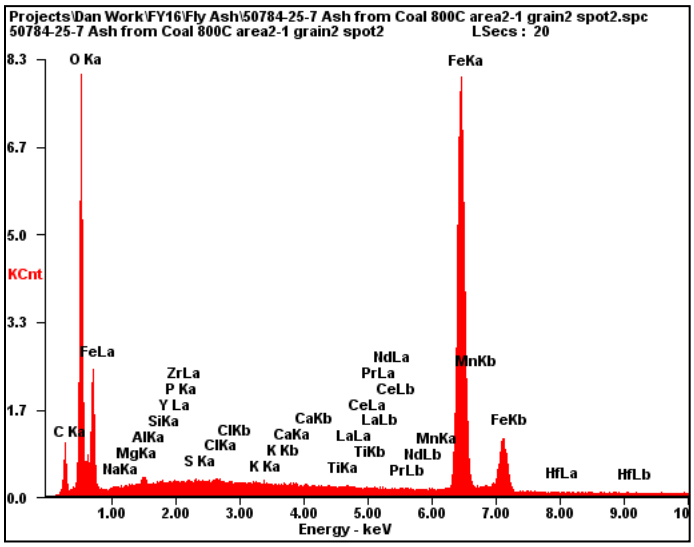

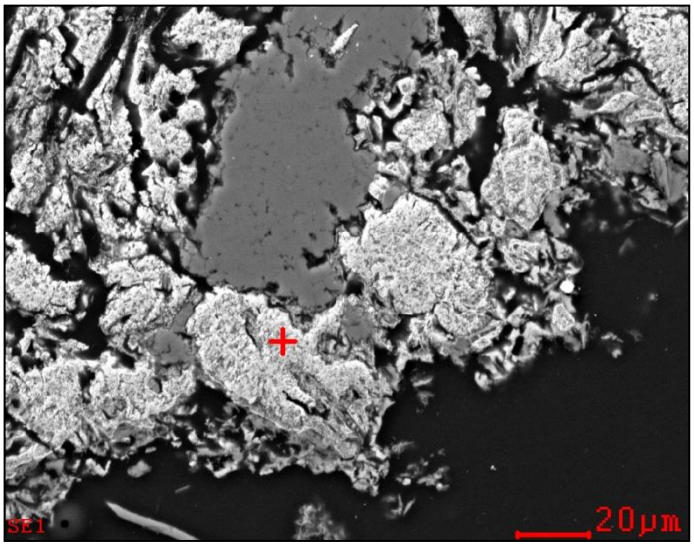

Element	Wt%	At%
OK	18.2	43.48
NaK	00.1	00.21
MgK	00.1	00.12
AlK	00.5	00.73
SiK	00.1	00.16
PK	00.0	00.05
ZrL	00.0	00.00
SK	00.1	00.13
ClK	00.3	00.27
KK	00.1	00.11
CaK	00.1	00.12
TiK	00.1	00.09
LaL	00.6	00.17
CeL	00.2	00.04
PrL	00.0	00.00
NdL	00.2	00.06
MnK	00.2	00.14
FeK	79.0	54.12
Matrix	Correction	ZAF

ZN-FE-OX

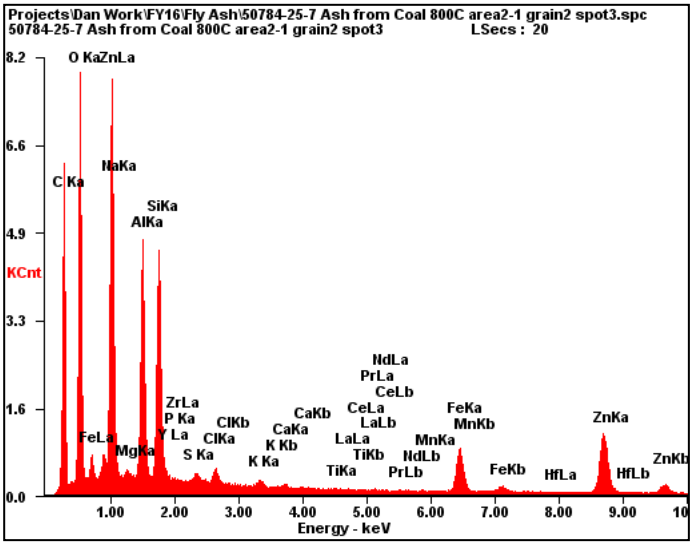

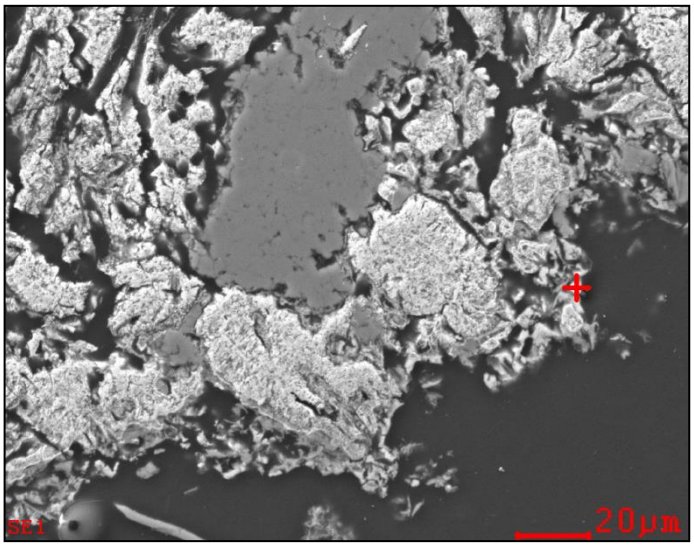

Element	*Wt%*	*At%*
OK	28.8	50.44
NaK	00.0	00.00
MgK	00.5	00.56
AlK	14.5	15.08
SiK	14.8	14.80
PK	00.0	00.00
ZrL	00.0	00.00
SK	00.5	00.47
ClK	01.0	00.76
KK	00.5	00.34
CaK	00.2	00.12
TiK	00.0	00.02
LaL	00.0	00.00
CeL	00.0	00.00
PrL	00.0	00.00
NdL	00.0	00.00
MnK	00.0	00.00
FeK	08.5	04.25
ZnK	30.7	13.15
Matrix	Correction	ZAF

Appendix D: Liquefaction Ash SEM/EDX Results

FE-S

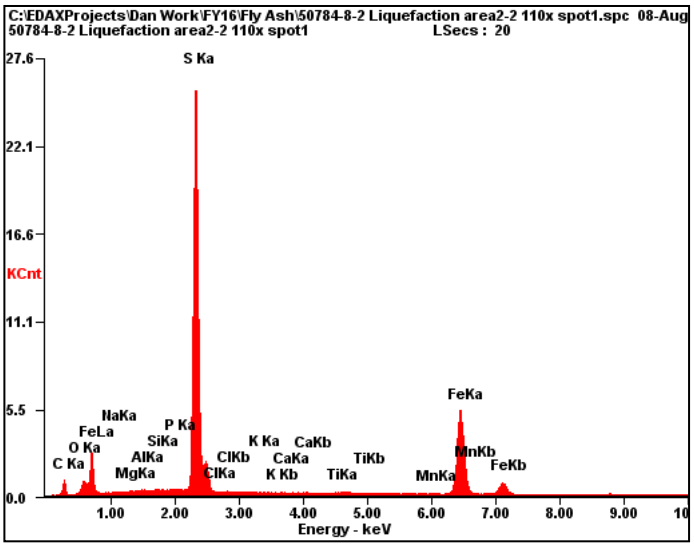

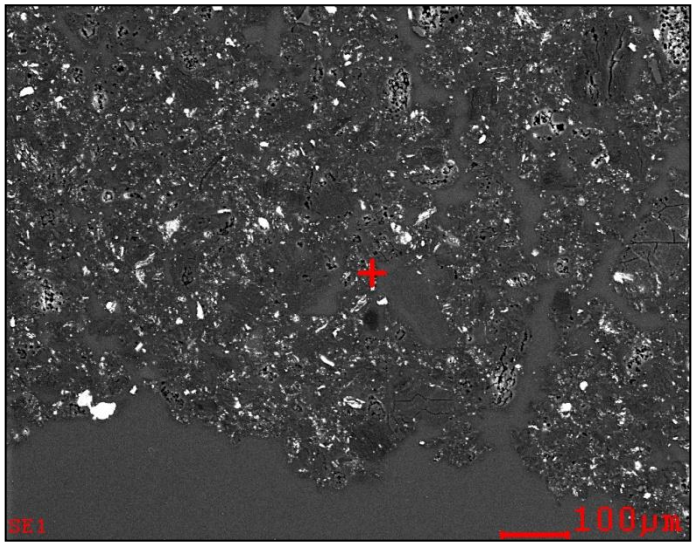

Element	Wt%	At%
OK	01.6	03.88
NaK	00.0	00.00
MgK	00.0	00.06
AlK	00.2	00.22
SiK	00.2	00.23
PK	00.2	00.25
SK	50.4	61.89
ClK	00.0	00.00
KK	00.0	00.00
CaK	00.0	00.00
TiK	00.2	00.12
MnK	00.1	00.04
FeK	47.3	33.31
Matrix	Correction	ZAF

SI-OX

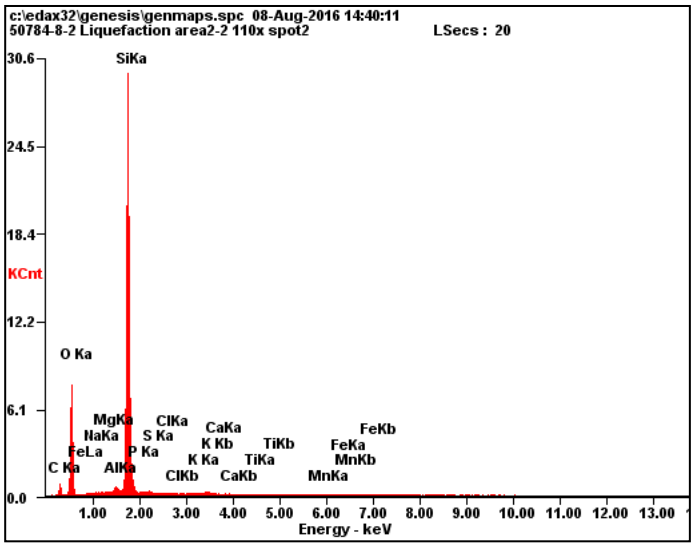

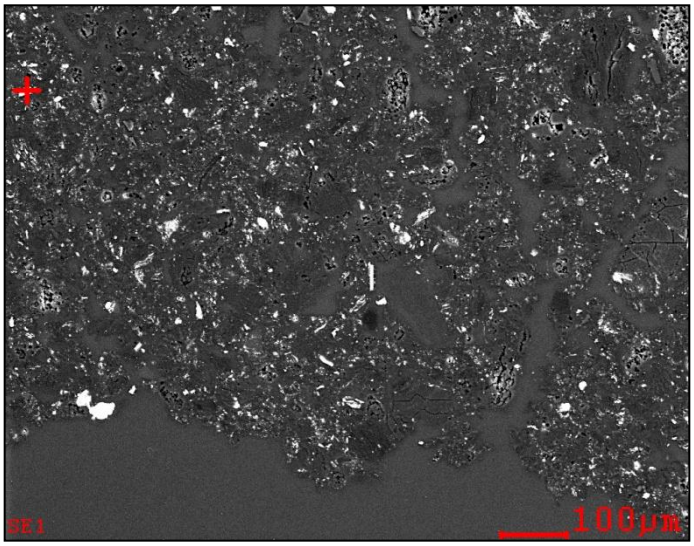

Element	Wt%	At%
OK	36.9	50.65
NaK	00.2	00.15
MgK	00.1	00.06
AlK	00.9	00.72
SiK	61.5	48.10
PK	00.2	00.11
SK	00.1	00.04
ClK	00.0	00.00
KK	00.1	00.06
CaK	00.1	00.06
TiK	00.1	00.03
MnK	00.0	00.00
FeK	00.1	00.02
Matrix	Correction	ZAF

CA-S-OX

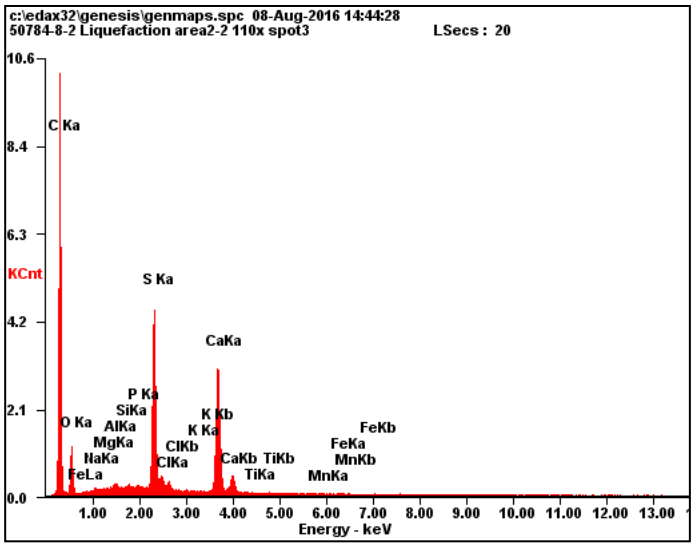

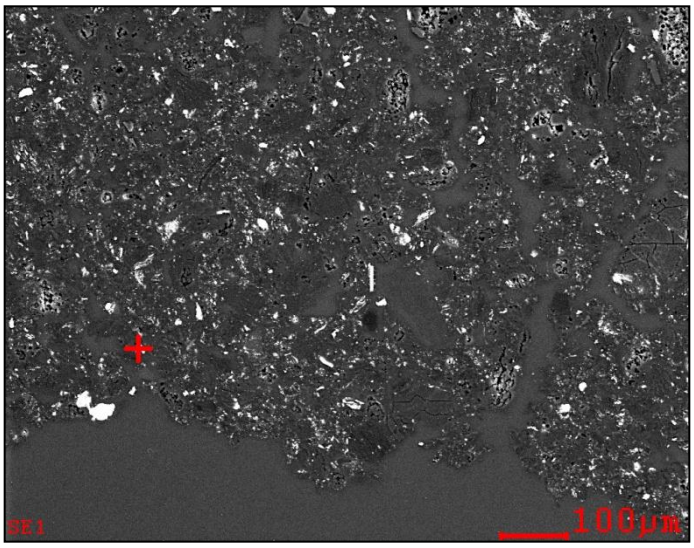

Element	Wt%	At%
OK	31.1	50.21
NaK	00.4	00.45
MgK	00.1	00.10
AlK	00.8	00.75
SiK	00.6	00.52
PK	00.2	00.12
SK	28.4	22.90
ClK	01.9	01.38
KK	00.1	00.09
CaK	35.9	23.17
TiK	00.1	00.04
MnK	00.2	00.09
FeK	00.4	00.17
Matrix	Correction	ZAF

AVERAGE OF GRAIN

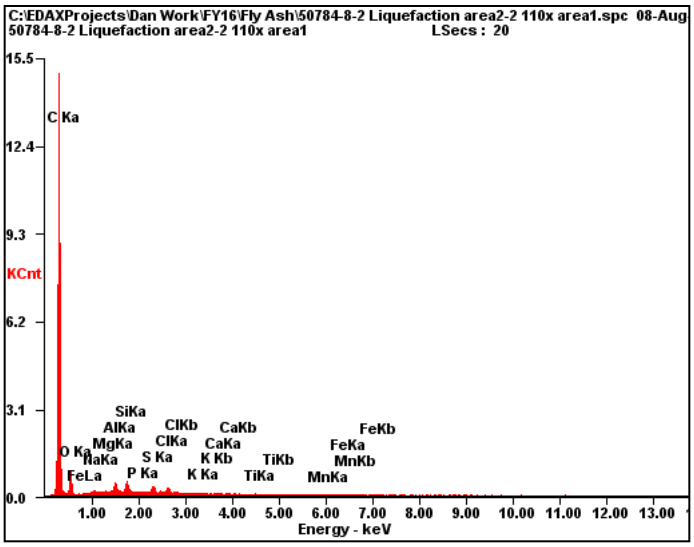

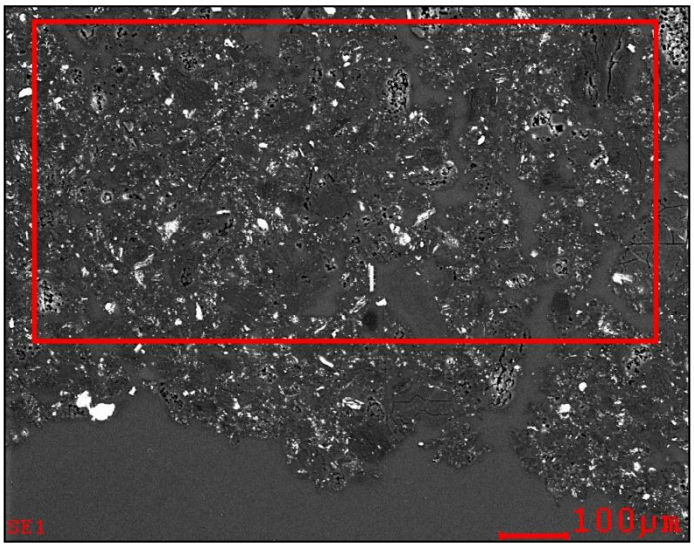

Element	*Wt%*	*At%*
CK	83.7	88.94
OK	11.4	09.05
NaK	00.2	00.13
MgK	00.1	00.03
AlK	00.9	00.45
SiK	01.1	00.50
PK	00.1	00.02
SK	00.9	00.38
ClK	00.9	00.32
KK	00.1	00.02
CaK	00.2	00.06
TiK	00.1	00.01
MnK	00.1	00.01
FeK	00.4	00.09
Matrix	Correction	ZAF

AL-SI-OX

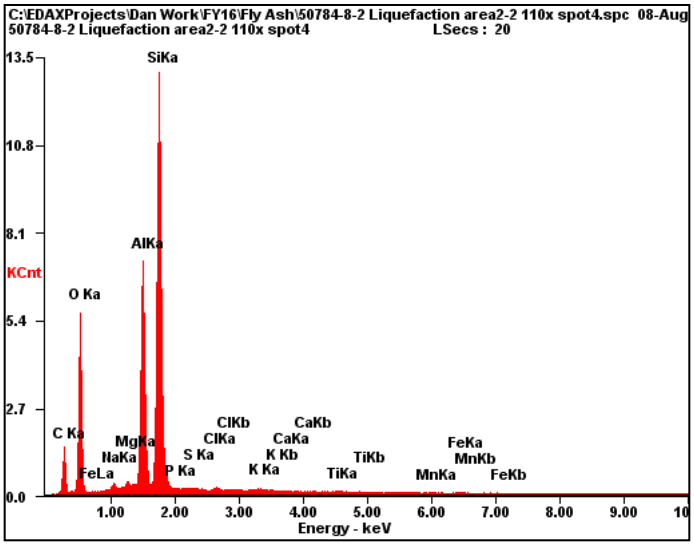

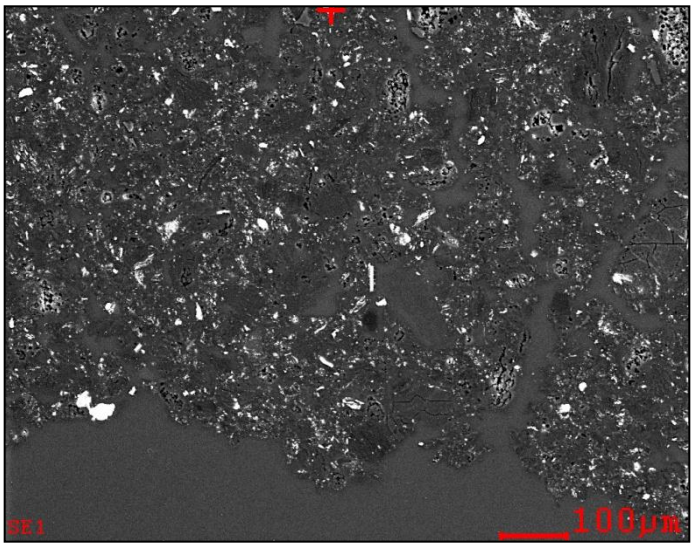

Element	*Wt%*	*At%*
OK	32.9	46.15
NaK	00.6	00.57
MgK	00.5	00.47
AlK	19.0	15.76
SiK	45.4	36.25
PK	00.0	00.00
SK	00.1	00.10
ClK	00.2	00.11
KK	00.3	00.14
CaK	00.1	00.03
TiK	00.3	00.13
MnK	00.2	00.09
FeK	00.6	00.22
Matrix	Correction	ZAF

NA-CL

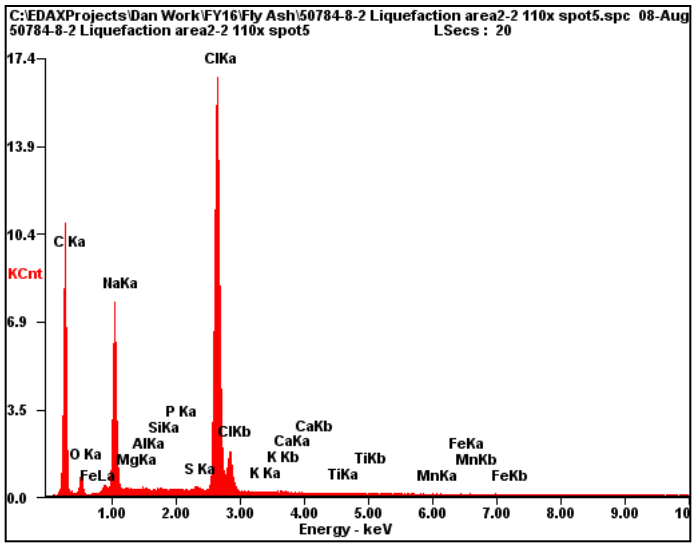

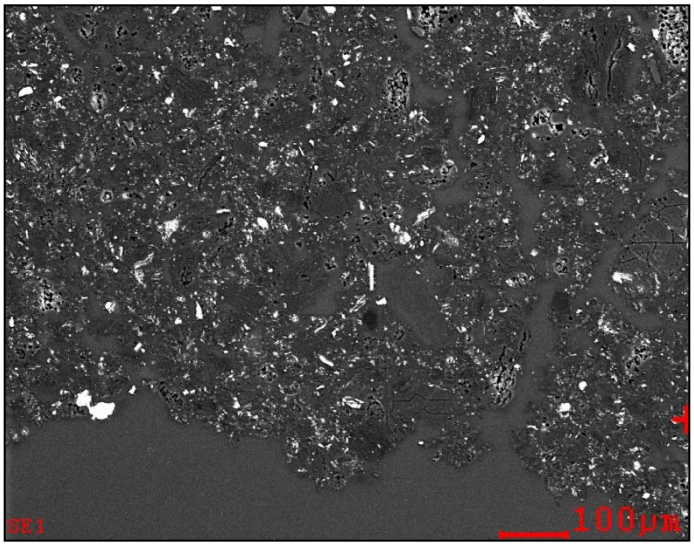

Element	*Wt%*	*At%*
OK	09.4	16.67
NaK	24.9	30.62
MgK	00.5	00.52
AlK	00.2	00.26
SiK	00.3	00.25
PK	00.2	00.14
SK	00.5	00.45
ClK	63.5	50.73
KK	00.1	00.03
CaK	00.3	00.17
TiK	00.1	00.03
MnK	00.1	00.02
FeK	00.2	00.09
Matrix	Correction	ZAF

FE-S

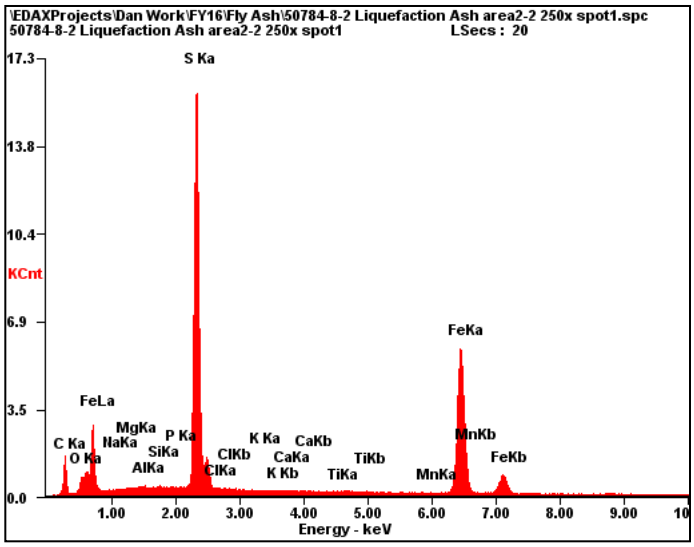

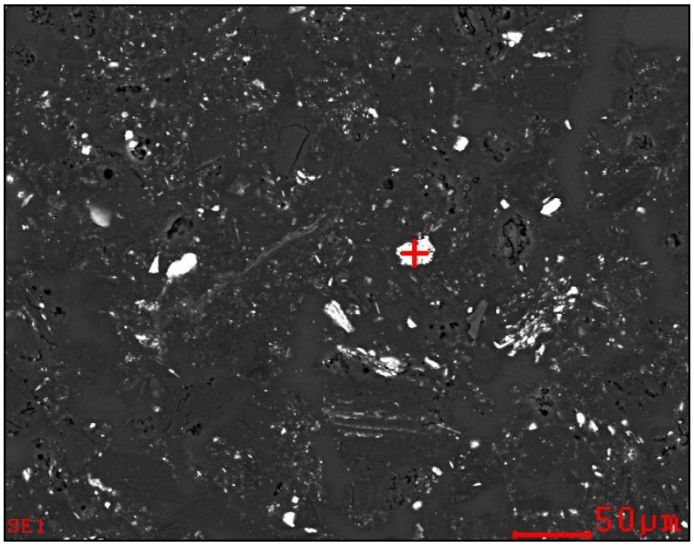

Element	Wt%	At%
OK	02.8	07.12
NaK	00.2	00.27
MgK	00.2	00.26
AlK	00.2	00.34
SiK	00.2	00.23
PK	00.2	00.20
SK	37.4	47.99
ClK	00.2	00.21
KK	00.0	00.00
CaK	00.0	00.03
TiK	00.1	00.08
MnK	00.1	00.10
FeK	58.6	43.16
Matrix	Correction	ZAF

AL-SI-OX

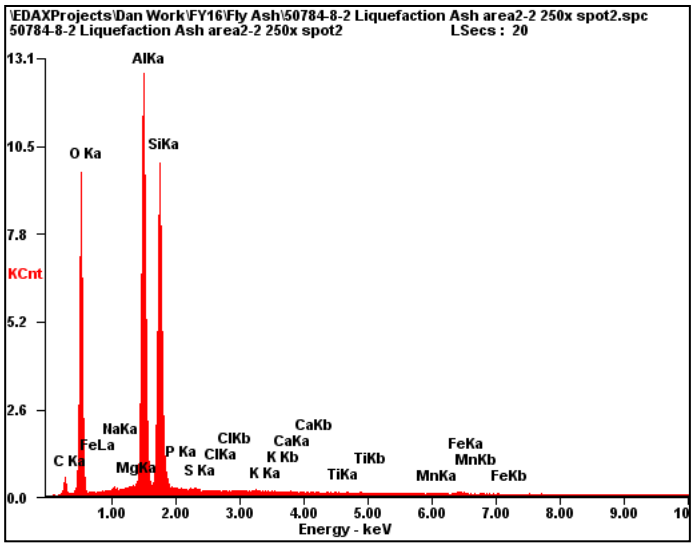

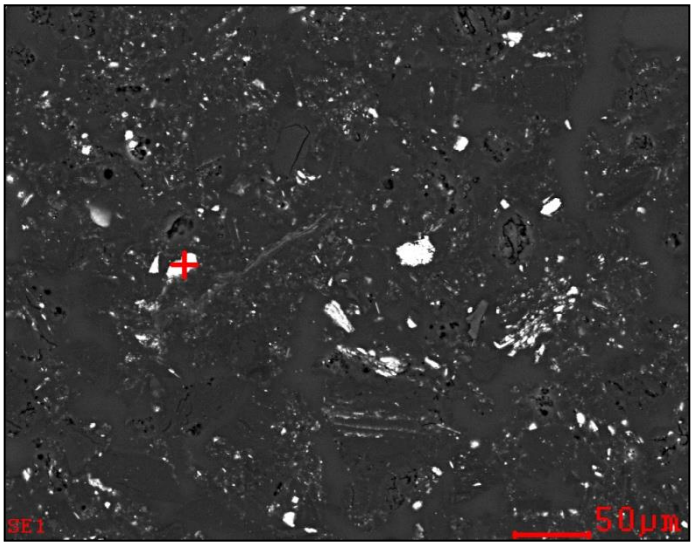

Element	Wt%	At%
OK	39.8	53.45
NaK	00.2	00.20
MgK	00.2	00.19
AlK	27.8	22.09
SiK	30.9	23.59
PK	00.1	00.06
SK	00.1	00.05
ClK	00.0	00.00
KK	00.0	00.00
CaK	00.0	00.00
TiK	00.0	00.00
MnK	00.1	00.04
FeK	00.8	00.32
Matrix	Correction	ZAF

AVERAGE OF GRAIN

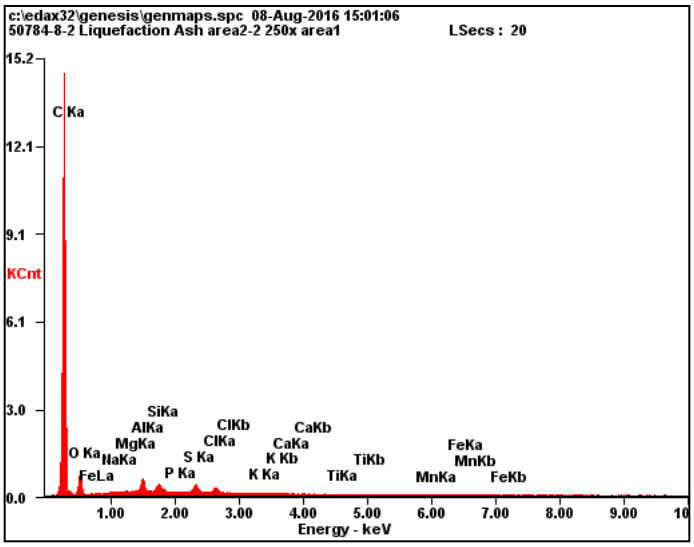

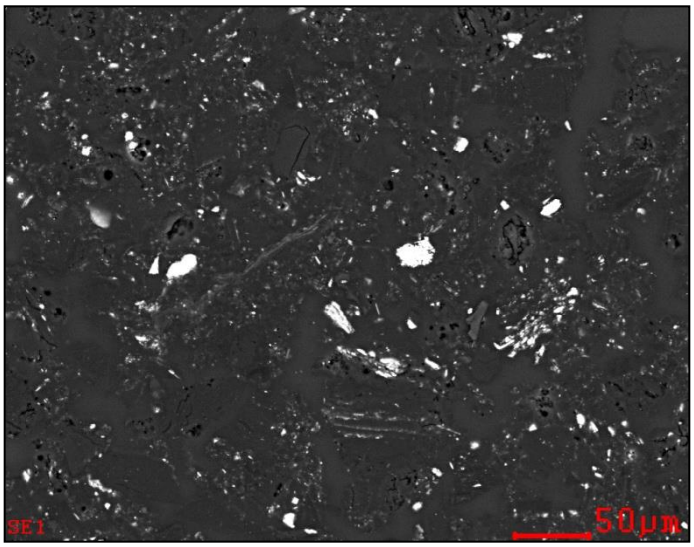

Element	Wt%	At%
CK	84.0	89.24
OK	10.9	08.67
NaK	00.2	00.10
MgK	00.1	00.03
AlK	01.4	00.64
SiK	01.0	00.43
PK	00.1	00.02
SK	01.1	00.42
ClK	00.8	00.27
KK	00.1	00.02
CaK	00.1	00.03
TiK	00.1	00.02
MnK	00.1	00.02
FeK	00.4	00.10
Matrix	Correction	ZAF

AVERAGE OF GRAIN

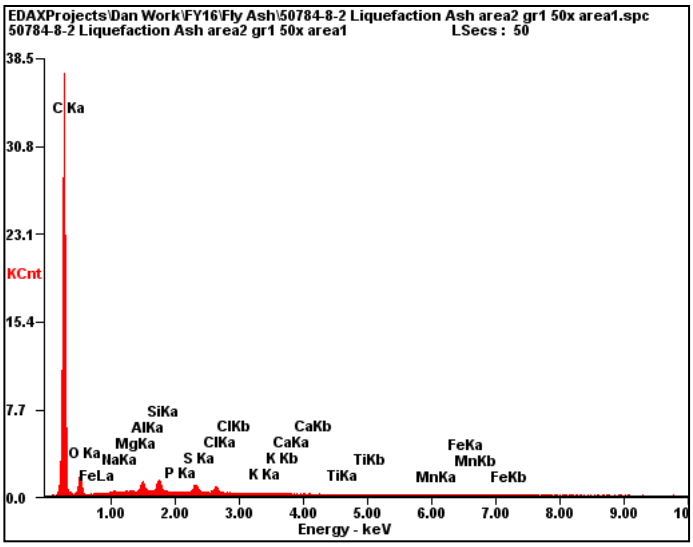

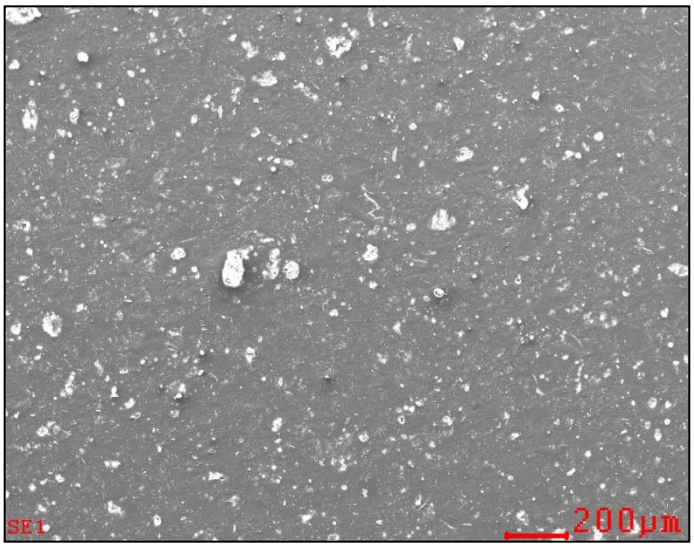

Element	Wt%	At%
CK	84.0	89.31
OK	10.7	08.51
NaK	00.2	00.10
MgK	00.1	00.03
AlK	01.1	00.51
SiK	01.3	00.59
PK	00.0	00.01
SK	01.0	00.39
ClK	01.0	00.34
KK	00.1	00.03
CaK	00.1	00.05
TiK	00.1	00.03
MnK	00.1	00.02
FeK	00.4	00.08
Matrix	Correction	ZAF

AVERAGE OF GRAIN

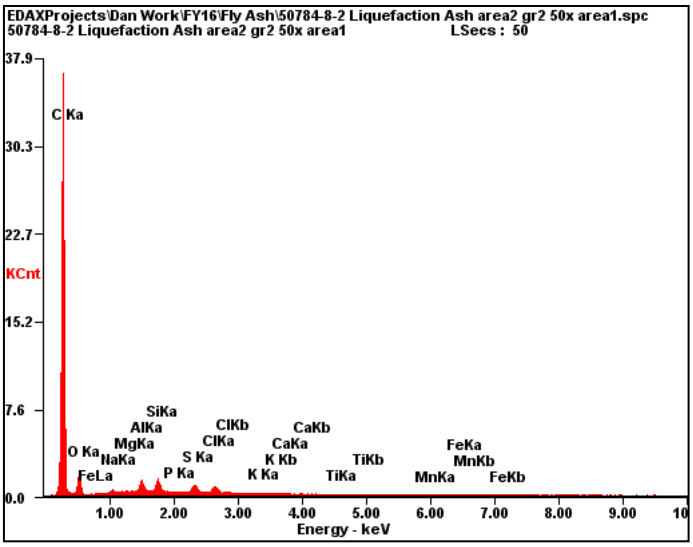

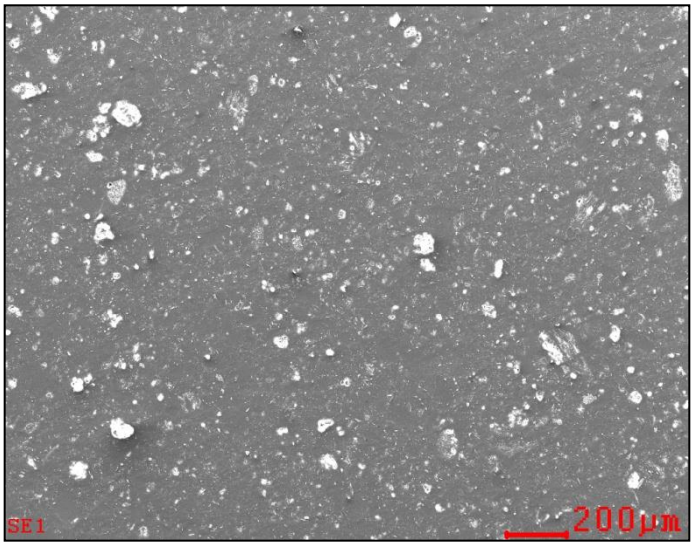

Element	*Wt%*	*At%*
CK	83.5	88.90
OK	11.2	08.92
NaK	00.3	00.15
MgK	00.1	00.02
AlK	01.1	00.51
SiK	01.3	00.59
PK	00.0	00.02
SK	01.0	00.40
ClK	00.9	00.32
KK	00.1	00.02
CaK	00.1	00.03
TiK	00.1	00.01
MnK	00.1	00.02
FeK	00.4	00.10
Matrix	Correction	ZAF

K-AL-SI-OX

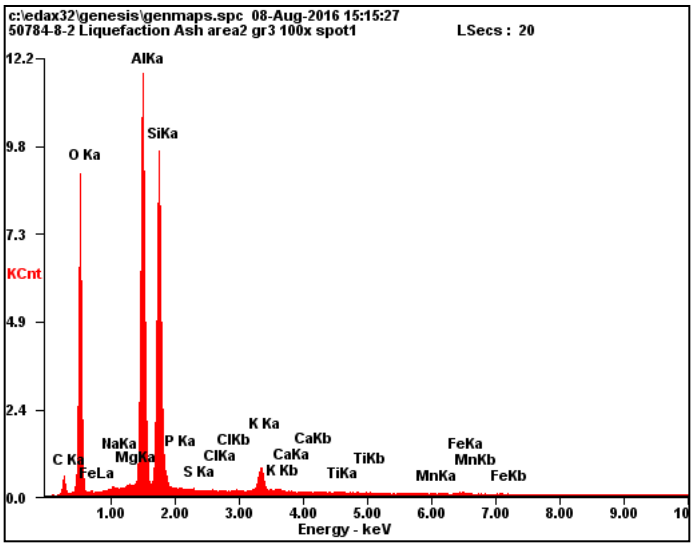

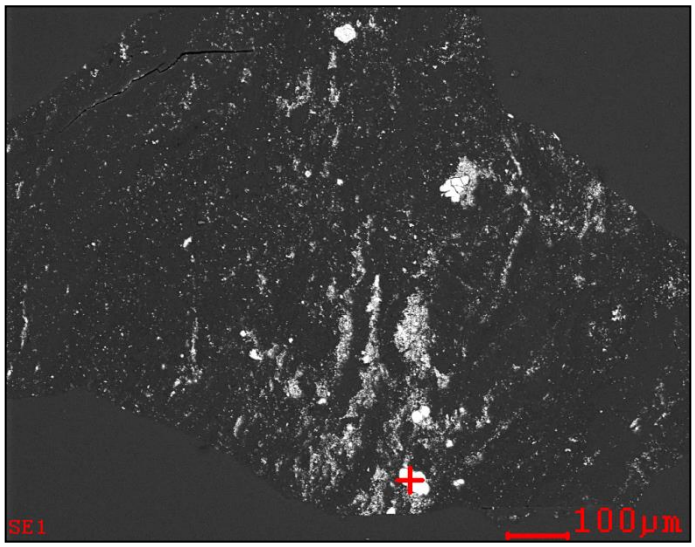

Element	*Wt%*	*At%*
OK	39.4	53.34
NaK	00.2	00.19
MgK	00.3	00.26
AlK	26.3	21.11
SiK	29.9	23.09
PK	00.1	00.04
SK	00.0	00.00
ClK	00.0	00.00
KK	02.9	01.59
CaK	00.0	00.00
TiK	00.2	00.08
MnK	00.1	00.03
FeK	00.7	00.28
Matrix	Correction	ZAF

AVERAGE OF GRAIN

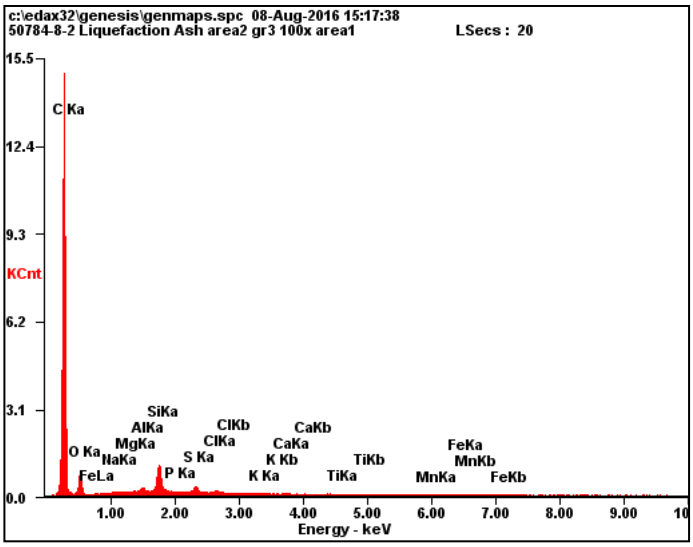

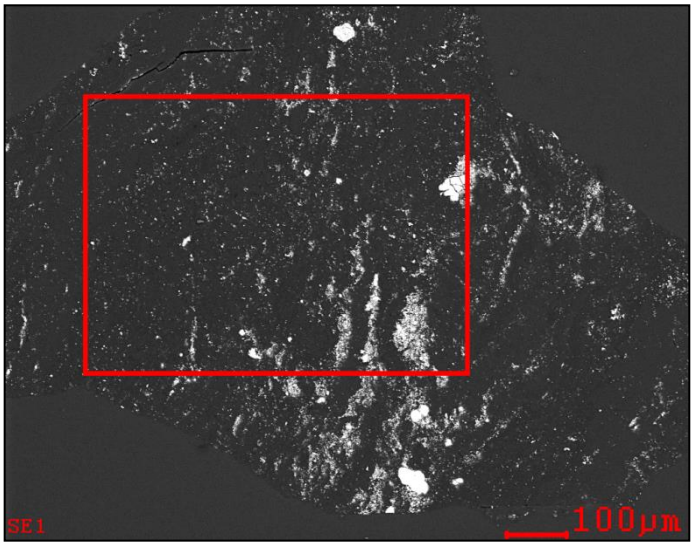

Element	Wt%	At%
CK	83.9	88.75
OK	11.6	09.22
NaK	00.1	00.07
MgK	00.1	00.04
AlK	00.5	00.21
SiK	03.1	01.38
PK	00.0	00.00
SK	00.7	00.26
ClK	00.2	00.07
KK	00.0	00.00
CaK	00.0	00.00
TiK	00.0	00.00
MnK	00.0	00.00
FeK	00.0	00.00
Matrix	Correction	ZAF

AVERAGE OF GRAIN

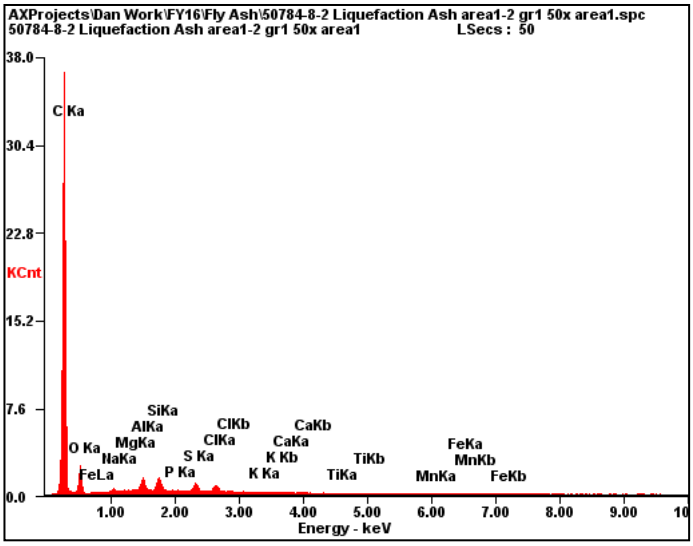

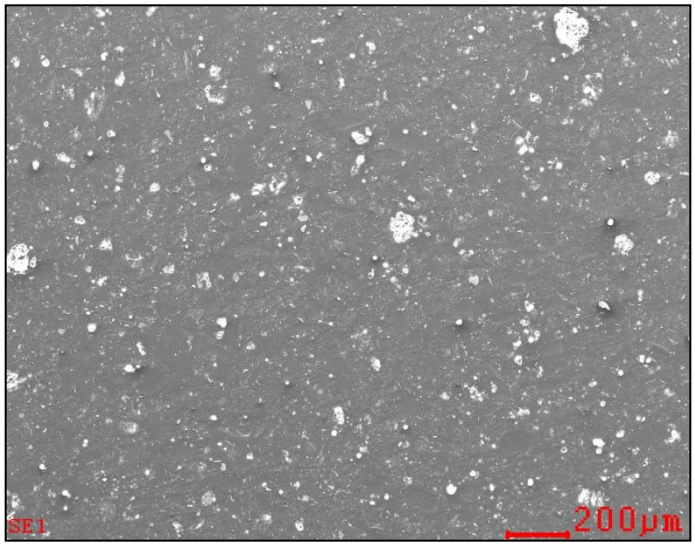

Element	*Wt%*	*At%*
CK	82.8	88.41
OK	11.5	09.22
NaK	00.3	00.16
MgK	00.0	00.02
AlK	01.3	00.60
SiK	01.4	00.65
PK	00.1	00.02
SK	01.0	00.40
ClK	00.9	00.34
KK	00.1	00.03
CaK	00.1	00.04
TiK	00.1	00.02
MnK	00.0	00.00
FeK	00.4	00.09
Matrix	Correction	ZAF

FE-S

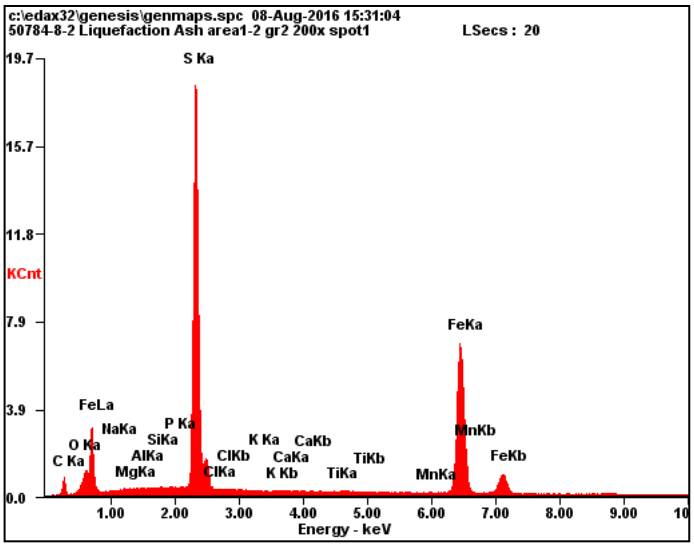

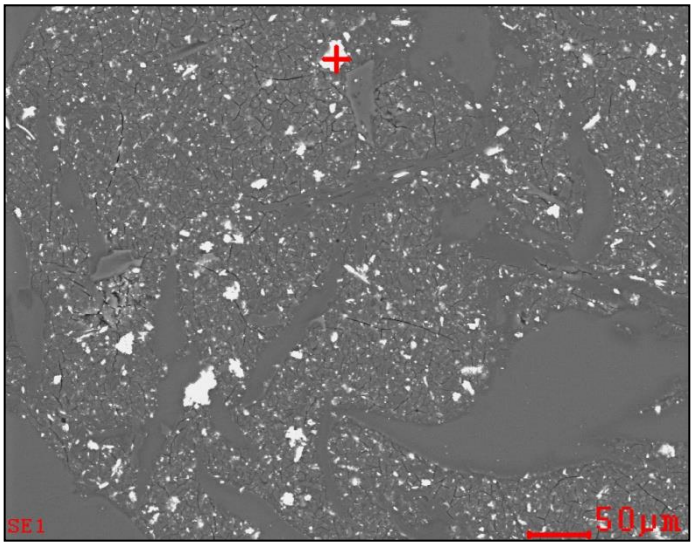

Element	Wt%	At%
OK	01.6	04.15
NaK	00.0	00.00
MgK	00.1	00.18
AlK	00.0	00.05
SiK	00.1	00.11
PK	00.1	00.13
SK	37.4	49.37
ClK	00.0	00.00
KK	00.0	00.00
CaK	00.0	00.00
TiK	00.1	00.04
MnK	00.1	00.07
FeK	60.6	45.89
Matrix	Correction	ZAF

CA-S-OX

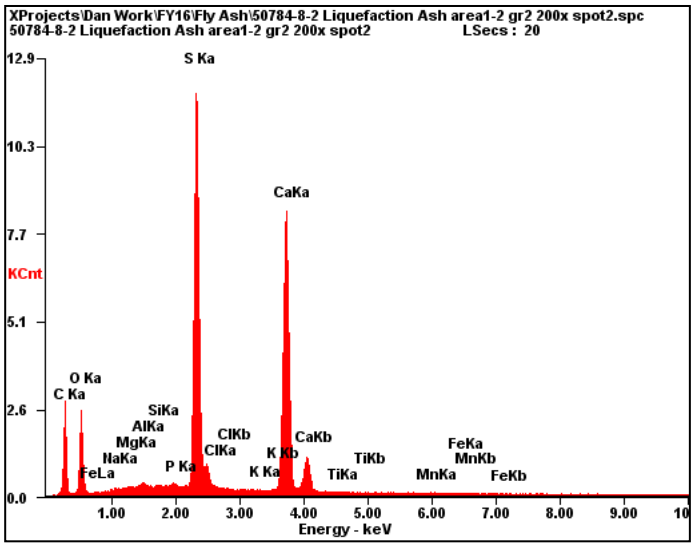

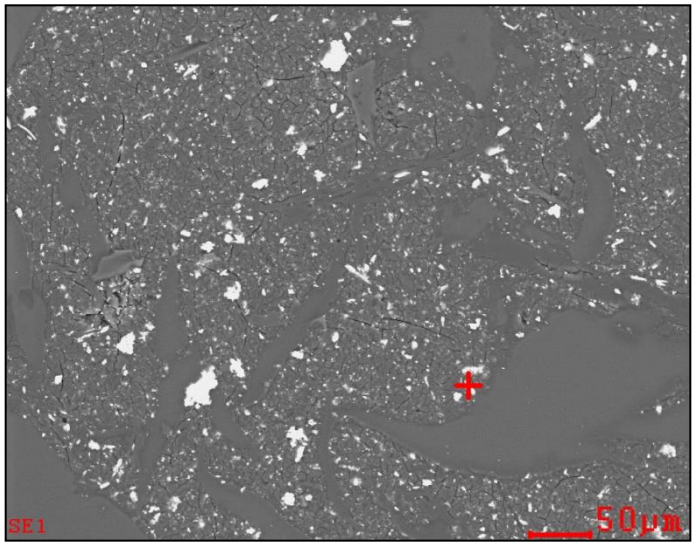

Element	Wt%	At%
OK	27.2	45.64
NaK	00.1	00.06
MgK	00.1	00.13
AlK	00.4	00.39
SiK	00.2	00.16
PK	00.2	00.16
SK	32.0	26.73
ClK	00.2	00.16
KK	00.0	00.00
CaK	39.6	26.50
TiK	00.0	00.00
MnK	00.0	00.00
FeK	00.1	00.07
Matrix	Correction	ZAF

MG-AL-SI-FE WITH S UNKNOWN

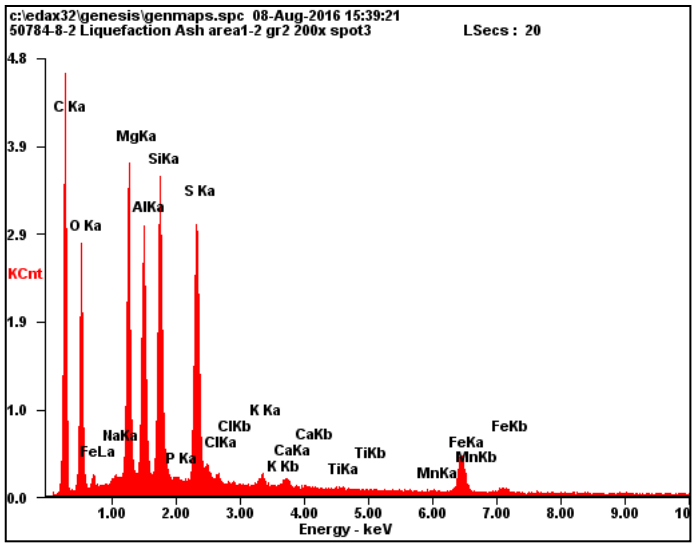

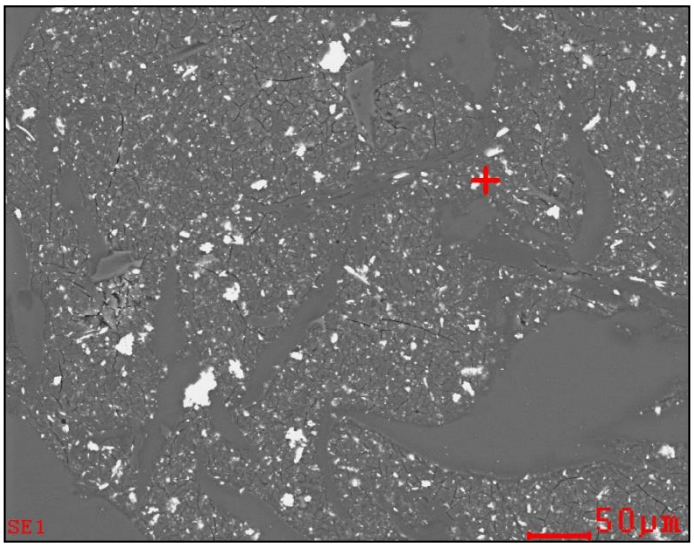

Element	Wt%	At%
CK	47.2	63.42
OK	17.5	17.60
NaK	00.2	00.10
MgK	07.6	05.07
AlK	06.1	03.62
SiK	07.7	04.40
PK	00.1	00.04
SK	07.6	03.80
ClK	00.3	00.14
KK	00.5	00.19
CaK	00.4	00.15
TiK	00.2	00.06
MnK	00.1	00.04
FeK	04.7	01.37
Matrix	Correction	ZAF

CA-CARBONATE

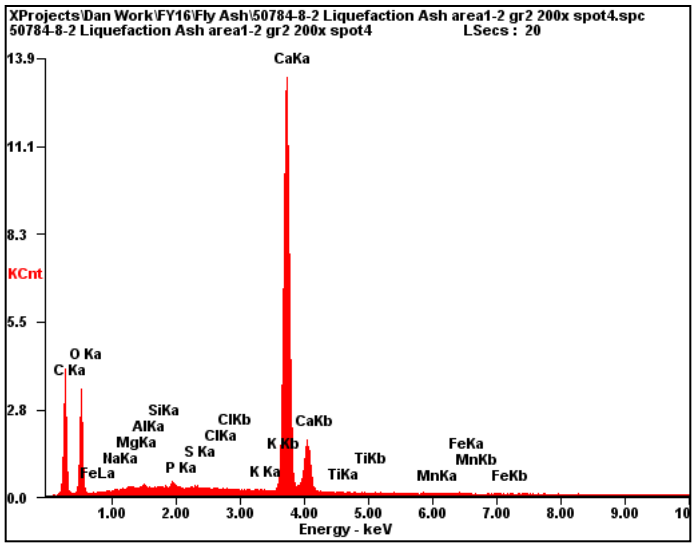

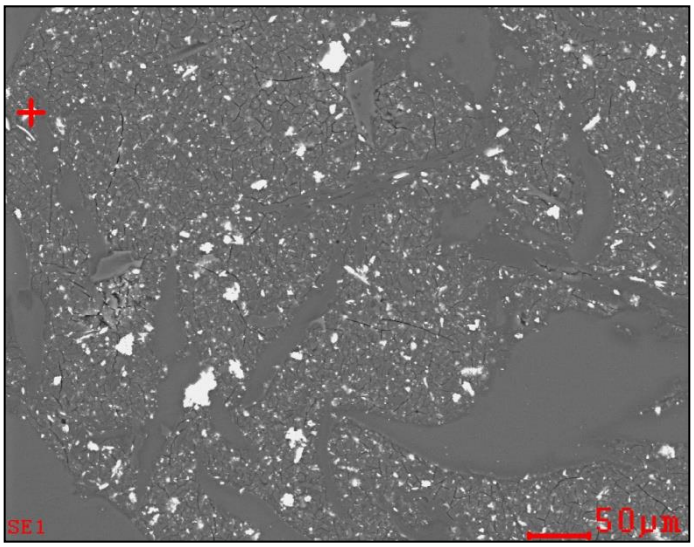

Element	*Wt%*	*At%*
CK	18.9	33.19
OK	29.2	38.57
NaK	00.6	00.57
MgK	00.8	00.69
AlK	00.8	00.61
SiK	00.7	00.50
PK	00.7	00.50
SK	00.6	00.41
ClK	00.6	00.34
KK	00.4	00.24
CaK	45.2	23.78
TiK	00.5	00.20
MnK	00.4	00.15
FeK	00.7	00.24
Matrix	Correction	ZAF

AVERAGE OF GRAIN

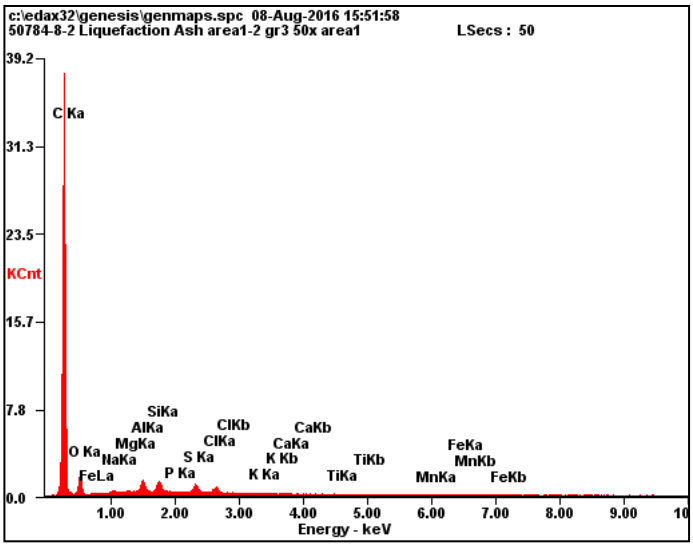

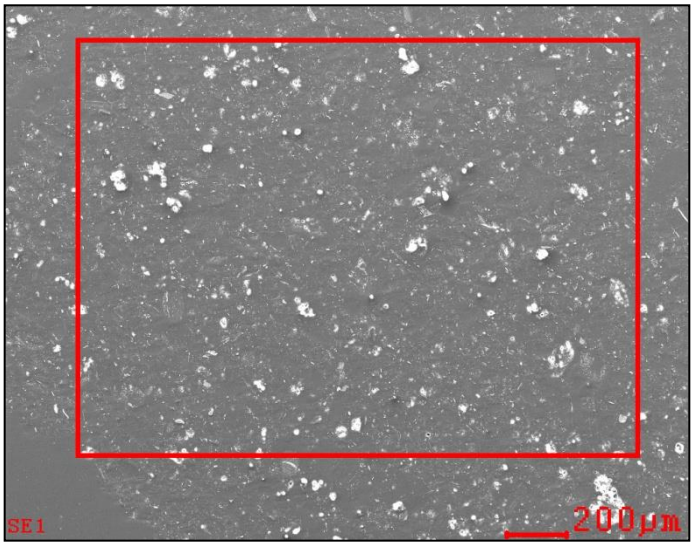

Element	Wt%	At%
CK	83.9	89.17
OK	10.8	08.63
NaK	00.2	00.13
MgK	00.1	00.04
AlK	01.2	00.58
SiK	01.3	00.58
PK	00.0	00.00
SK	01.0	00.40
ClK	00.8	00.30
KK	00.0	00.01
CaK	00.1	00.04
TiK	00.1	00.02
MnK	00.0	00.01
FeK	00.4	00.09
Matrix	Correction	ZAF

FE-S

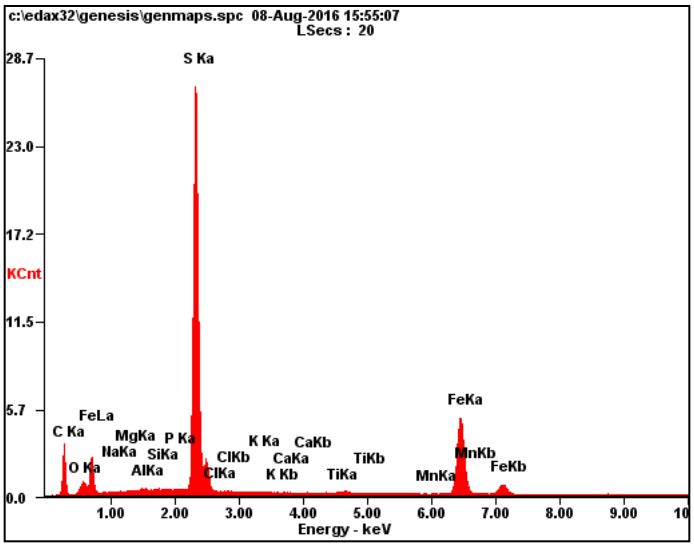

Element	Wt%	At%
OK	02.4	05.77
NaK	00.0	00.00
MgK	00.1	00.14
AlK	00.3	00.42
SiK	00.2	00.25
PK	00.2	00.25
SK	51.6	61.99
ClK	00.1	00.07
KK	00.0	00.00
CaK	00.0	00.00
TiK	00.2	00.13
MnK	00.0	00.00
FeK	45.0	30.99
Matrix	Correction	ZAF

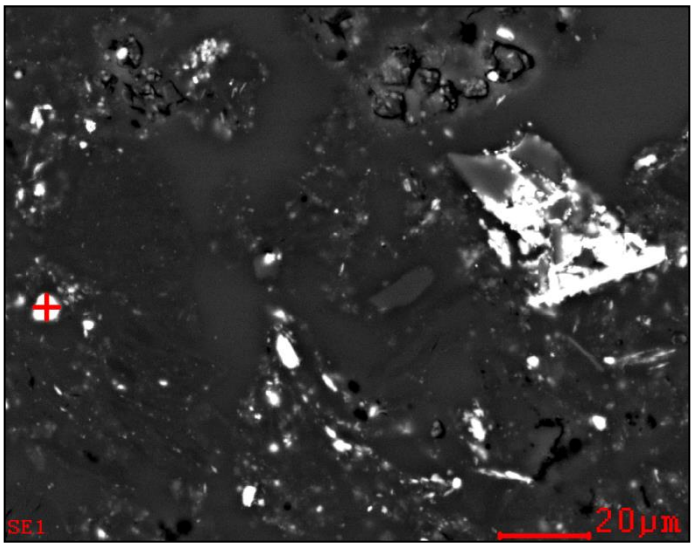

CA-P-OX

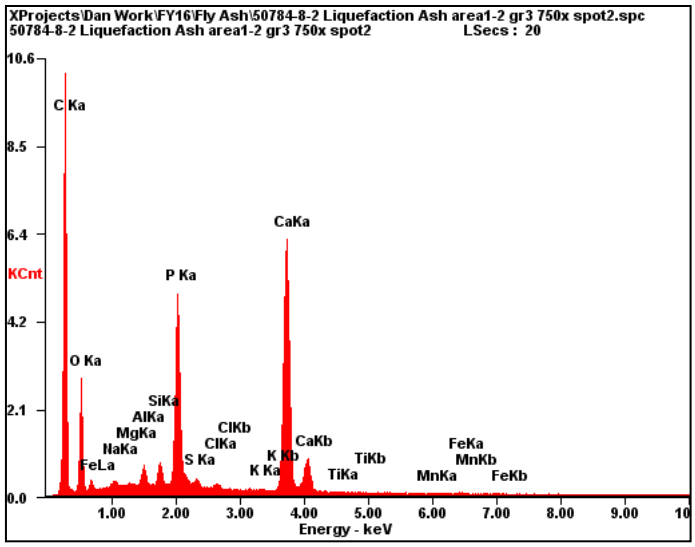

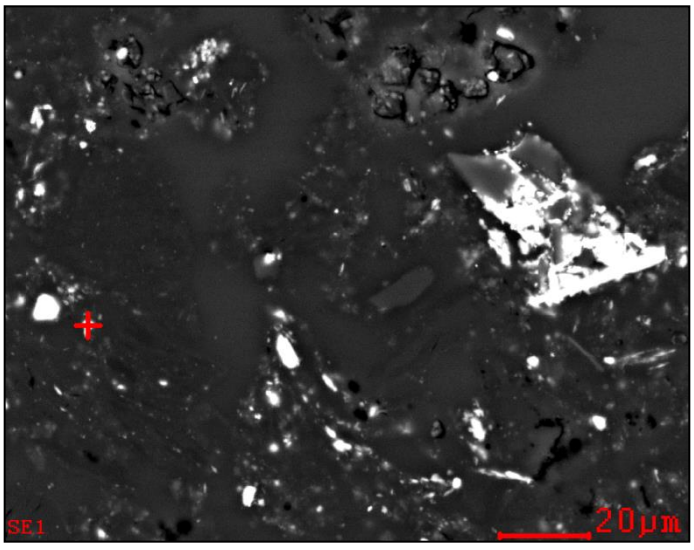

Element	Wt%	At%
OK	36.1	55.71
NaK	01.0	01.02
MgK	00.2	00.16
AlK	01.7	01.59
SiK	01.9	01.71
PK	17.8	14.21
SK	00.9	00.68
ClK	00.6	00.43
KK	00.1	00.09
CaK	39.3	24.24
TiK	00.0	00.00
MnK	00.0	00.00
FeK	00.4	00.17
Matrix	Correction	ZAF

TI-OX

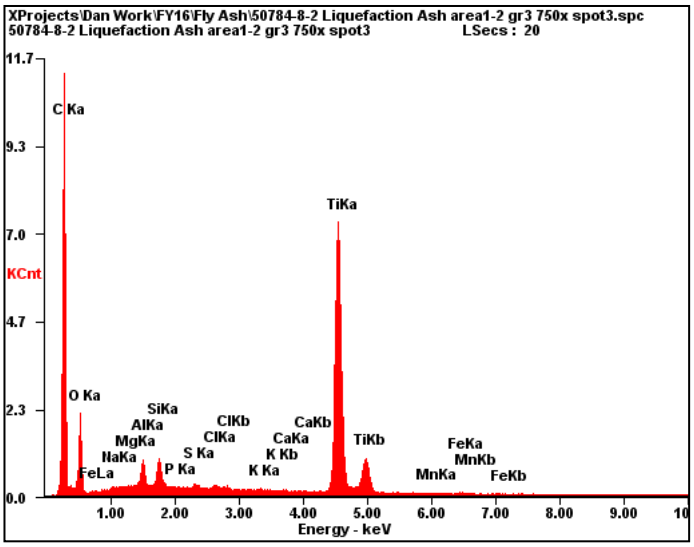

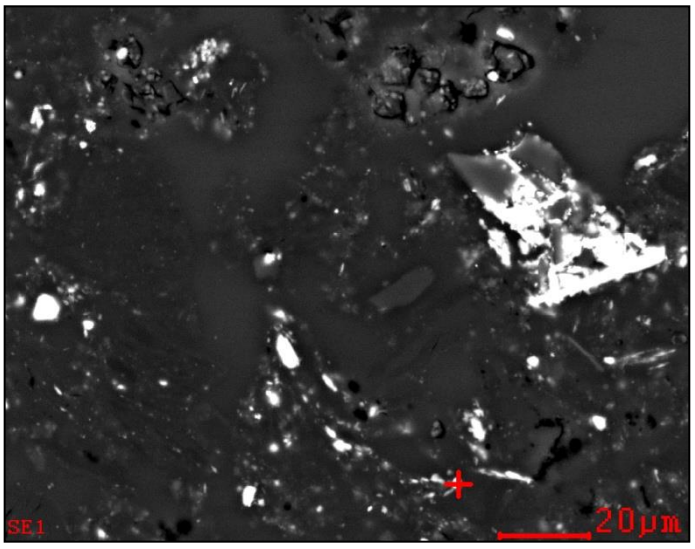

Element	*Wt%*	*At%*
OK	32.4	57.25
NaK	00.2	00.27
MgK	00.2	00.18
AlK	02.7	02.79
SiK	02.8	02.86
PK	00.1	00.05
SK	00.4	00.34
ClK	00.4	00.33
KK	00.2	00.16
CaK	00.1	00.08
TiK	59.7	35.26
MnK	00.2	00.11
FeK	00.6	00.31
Matrix	Correction	ZAF

MG-AL-SI-FE WITH S UNKNOWN

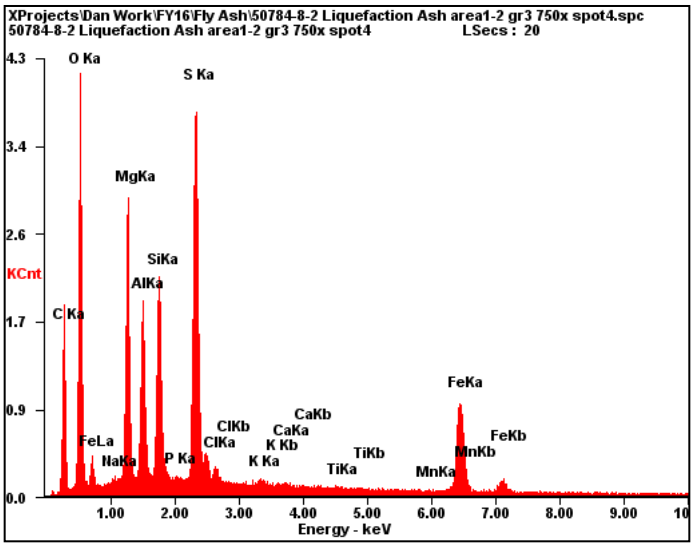

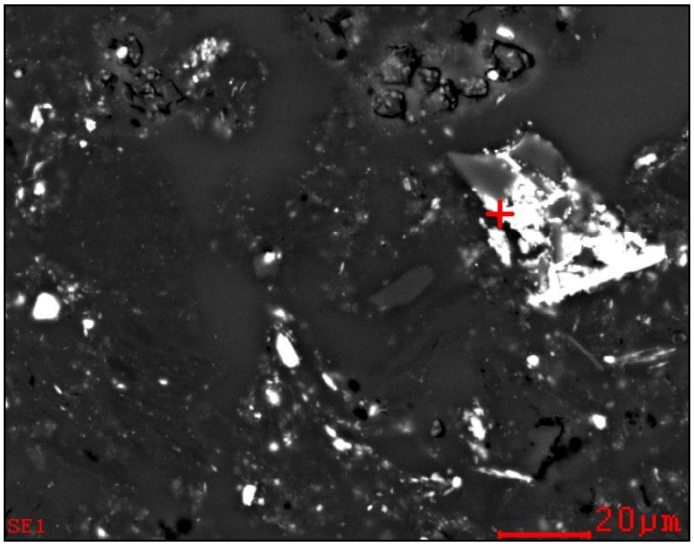

Element	*Wt%*	*At%*
OK	29.1	45.30
NaK	00.4	00.46
MgK	13.5	13.80
AlK	08.5	07.83
SiK	09.9	08.77
PK	00.1	00.07
SK	18.7	14.51
ClK	00.9	00.62
KK	00.4	00.23
CaK	00.3	00.18
TiK	00.2	00.12
MnK	00.2	00.08
FeK	18.0	08.02
Matrix	Correction	ZAF

FE-S

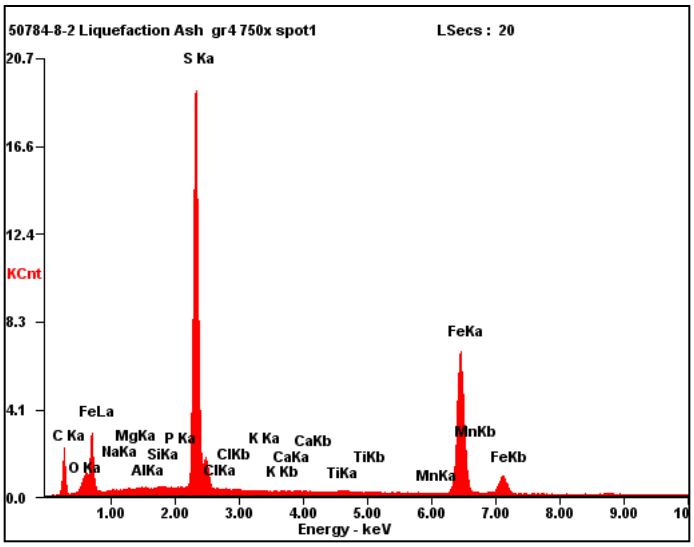

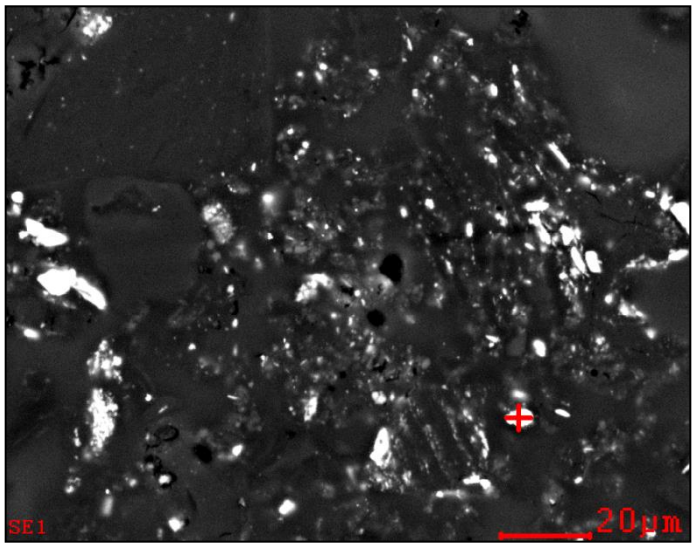

Element	*Wt%*	*At%*
OK	01.4	03.56
NaK	00.1	00.16
MgK	00.2	00.27
AlK	00.2	00.27
SiK	00.2	00.30
PK	00.2	00.22
SK	38.4	50.42
ClK	00.1	00.11
KK	00.0	00.00
CaK	00.0	00.00
TiK	00.1	00.07
MnK	00.0	00.00
FeK	59.3	44.61
Matrix	Correction	ZAF

FE-S

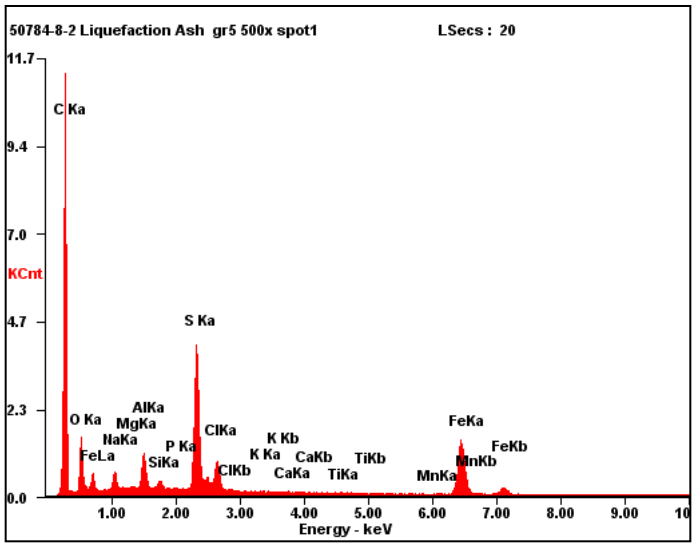

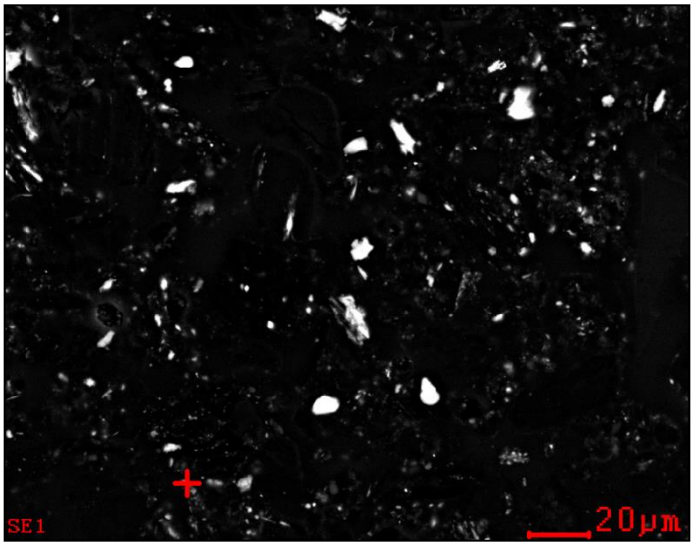

Element	*Wt%*	*At%*
OK	17.0	32.84
NaK	05.3	07.14
MgK	00.1	00.17
AlK	06.5	07.41
SiK	01.3	01.48
PK	00.1	00.11
SK	24.2	23.35
ClK	06.5	05.67
KK	00.2	00.17
CaK	00.3	00.26
TiK	00.3	00.18
MnK	00.0	00.00
FeK	38.3	21.22
Matrix	Correction	ZAF

TI-OX

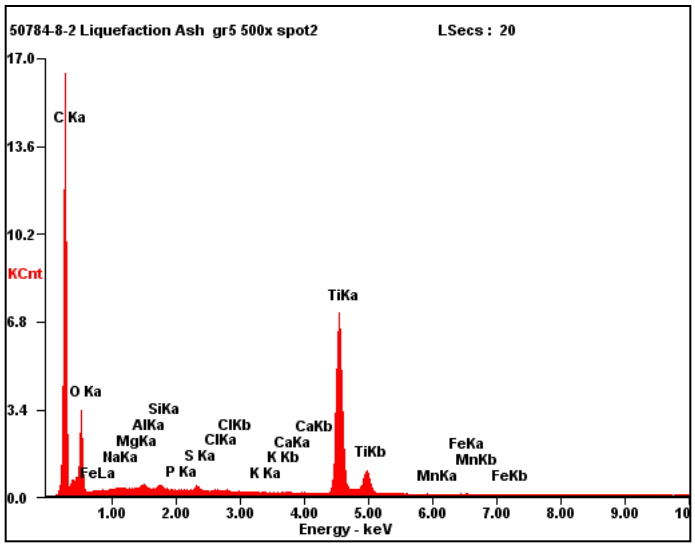

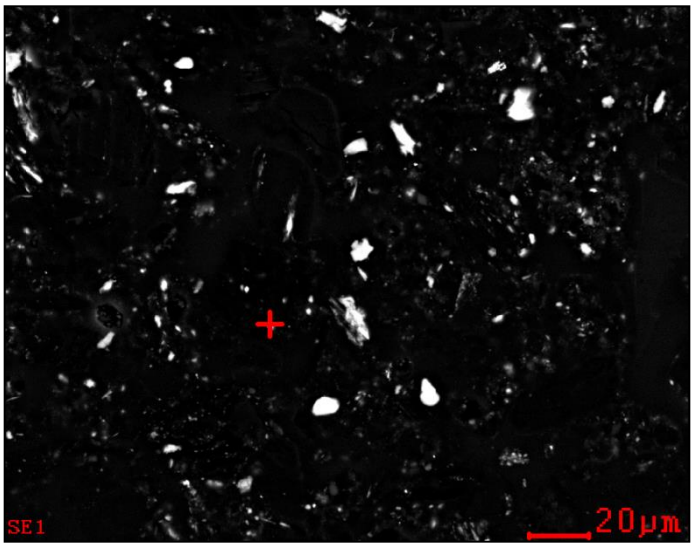

Element	*Wt%*	*At%*
OK	43.3	68.99
NaK	00.3	00.37
MgK	00.1	00.07
AlK	00.6	00.57
SiK	00.5	00.49
PK	00.0	00.00
SK	00.6	00.47
ClK	00.2	00.11
KK	00.0	00.00
CaK	00.1	00.03
TiK	54.0	28.71
MnK	00.0	00.00
FeK	00.4	00.19
Matrix	Correction	ZAF

NA-CL

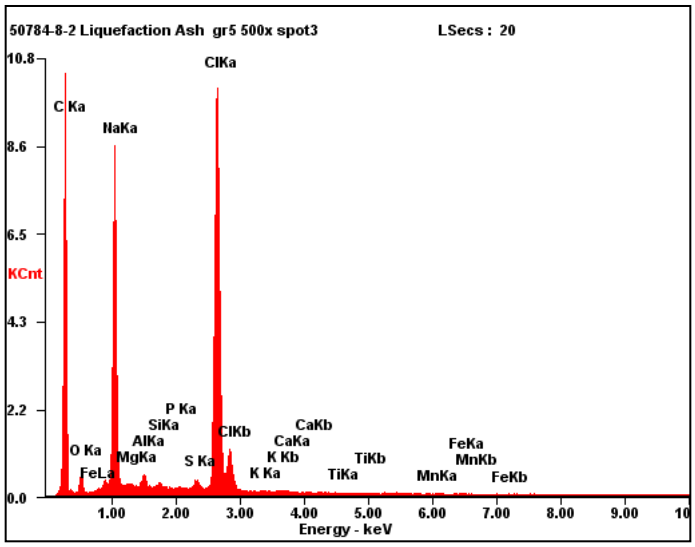

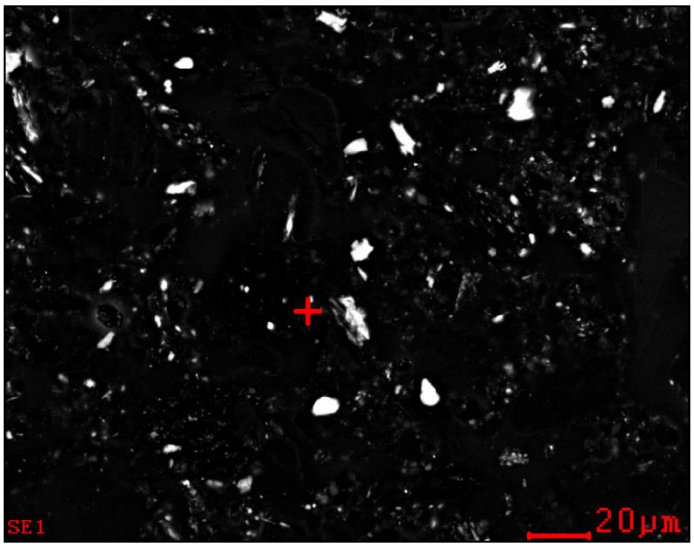

Element	*Wt%*	*At%*
OK	07.3	12.58
NaK	34.1	41.00
MgK	00.6	00.65
AlK	01.7	01.69
SiK	00.6	00.57
PK	00.1	00.10
SK	01.1	00.93
ClK	54.0	42.13
KK	00.0	00.00
CaK	00.2	00.17
TiK	00.0	00.00
MnK	00.1	00.03
FeK	00.3	00.15
Matrix	Correction	ZAF

1.800.201.2011 | solutions@battelle.org | www.battelle.org

Appendix B: Budget Period 1 Feasibility Study Report

Recovery of Rare Earth Elements from Coal and Coal Byproducts via a Closed Loop Leaching Process:

Feasibility Study Report

National Energy Technology Laboratory

3610 Collins Ferry Road

Morgantown, WV 26507-0880

5 January 2017

Recovery of Rare Earth Elements from Coal and Coal Byproducts via a Closed Loop Leaching Process: Feasibility Study Report

Prepared by:

Battelle
505 King Avenue
Columbus, Ohio 43201

Submitted to:

National Energy Technology Laboratory
3610 Collins Ferry Road
Morgantown, WV 26507-0880

5 January 2017

Contents

List of Tables

List of Figures

Executive Summary

Battelle aims to validate the economic viability of recovering rare earth elements (REEs) from coal ash using its patented closed-loop Acid Digestion Process (ADP). This will be accomplished by selecting a source of coal ash that consistently provides concentrations of rare earth elements above 300 parts per million by weight from a power generation station, and is in a form suitable for leaching. Based on the results of the Sampling and Characterization Report, the feasibility study focused on Pulverized Coal Combustion (PCC) Plant A fly ash as a feedstock for Battelle's Recycling Acid Leach Process. The regional availability of REE laden coal ash, the market for rare earth concentrates and coal combustion byproducts, and the system cost for rare earth recovery will be accounted for in a Techno-Economic Analysis (TEA). The assumptions and economic sensitivities in the process that are used in the TEA, and certain required design parameters validated in the laboratory, inform the TEA assumptions and allow design of a bench scale system to demonstrate the process on a continuous basis.

This report examines the feasibility of constructing a rare earth recovery plant sized to process up to 30 tonnes of ash per hour, which is the ash production rate for an approximately 2,000 MW power plant operating a full capacity. Operating costs for both a First-of-a-Kind and an N^{th}-of-a-Kind plant are determined. These costs to recover rare earths from coal ash are then compared to the value of rare earths present in a variety of coal ashes around the country. Values for coal ash were obtained through determination of the concentrations of rare earth elements in coal samples adjusted to account for changes in concentration associated with the combustion process. Current market pricing information for REEs was used to determine the value associated with each of the coal sources.

The results of the feasibility study indicate that when a First-of-a-Kind plant is considered, approximately 5% of U.S. coal sources contain sufficient rare earth material to cover the costs of the recovery plant. When an N^{th}-of-a-Kind plant is considered, over 20% of all coal sources reviewed contain sufficient recoverable rare earths to cover recovery costs at current REE market prices. When historical high REE prices are considered, more than 25% of coal sources can be treated with a First-of-a-Kind plant, and more than 47% of sources with an N^{th}-of-a-Kind plant. These results are based on the standard deterministic case which incorporates the current understanding and developmental status of the recovery process, and it should be noted that further downstream purification costs are not included in this assessment. A probabilistic sensitivity analysis was conducted which examines how the cost to recover rare earth materials may change due to technology developments, uncertainties in capital requirements for the plant, or prices of REEs due to shifting market dynamics. Under certain sensitivity scenarios, the recovery plant can be economically viable processing an even greater range of coal sources.

This report is the basis of the project's "GO/NO GO" decision point as defined in the Statement of Project Objectives. Based on the results of the feasibility study, it has been determined that an economically viable plant capable of recovering REEs from ash generated at power generation facilities is feasible. The plant is capable of producing a REE concentrate stream greater than 2% in concentration of REEs. Battelle's previous Sampling and Characterization[1] report indicates that feedstocks are available for such a plant which contain greater than 300 ppm REEs. With these criteria satisfied, Battelle recommends that a "GO" decision be made, and that this project proceeds into the process design task.

[1] "Recovery of Rare Earth Elements from Coal and Coal Byproducts via a Closed Loop Leaching Process: Sampling and Characterization Report." DE-FE0027012. Battelle. August 18, 2016.

1.0 Background

As directed by Congress, the United States (U.S.) Department of Energy (DOE) is investigating the economic feasibility of recovery of REEs from domestic U.S. coal and coal byproducts. DOE's National Energy Technology Laboratory (NETL) has characterized a number of REE-bearing samples of coal and coal-related materials. REEs have been found in varying concentrations ranging up to 1,000 parts per million by weight in the following materials in the United States: coal mine roof and floor materials, run-of-mine coal, prepared coal, partings, pit cleanings, coal preparation refuse, and tailings. REEs can be found in coal byproducts, including ash, coal-related sludge, and mine drainage. Certain coals can contain a higher ratio of heavy (generally more valuable) REEs than found in other sources of REEs such as natural ores. Given the potentially low REE concentrations in the feed materials, and subsequent potentially low yield of REEs from any separation process, minimizing costs is a key challenge. Physical and chemical separations may be useful in recovering REEs from coal and coal by-products. The forms in which REEs are present in these materials could drive the design of separation processes.

Battelle aims to validate the economic viability of recovering REEs from coal ash using its patented (US6011193) closed-loop Acid Digestion Process (ADP). This will be accomplished by selecting a source of coal ash that consistently provides concentrations of rare earth elements above 300 parts per million by weight and in a form suitable for leaching. This feasibility report focuses on ash sourced from a power generation station rather than liquefication residual or low temperature ash sources evaluated as part of the Sampling and Characterization Report, as ash sourced from power generation facilities is much more readily accessible than other sources of ash. The regional availability of REE laden coal ash, the regional market for rare earth concentrates and coal combustion byproducts, and the system cost for rare earth recovery will be accounted for in the Techno-Economic Analysis (TEA). The assumptions and economic sensitivities in the process that are used in the TEA, and certain required design parameters will direct a small lab testing portion to validate the TEA and allow design of a bench scale system to prove the process on a continuous basis

This report covers the feasibility study portion of the project, in which the economic feasibility of recovering REEs from coal ash is assessed. As part of the feasibility study, the value associated with REEs present in regional coal deposits was assessed to determine which coal ash sources would support the most economical operation of a recovery plant. Up to date market pricing information was collected for each of the REEs through cooperation with a REE market consultant. Next, a TEA was conducted for the proposed recovery process to determine the costs associated with a REE recovery plant. The TEA was informed by limited laboratory testing to determine REE recovery rates, as well as a CHEMCAD model which simulated the proposed recovery process. Scenarios in which economical recovery of REEs are possible are presented, along with a deterministic base case of the TEA, and a sensitivity analysis.

2.0 REE Market Review

Rare Earth Uses and Production

Rare earth elements are widely used in catalysts, glass manufacture, sensors, and magnets. The magnetic rare earths are particularly valuable as their high magnetism reduces the size of motors and generators used in electric vehicles and wind turbines. They additionally find use in defense applications for armoring alloys, weapons guidance systems, night vision goggles, and communication systems[3]. As shown in Figure 1, lanthanum and cerium find the most use by volume, as they are the most common rare earths and commonly used in petroleum upgrading catalyst and glass manufacture. By value, however, the magnetic rare earths, such as neodymium, praseodymium, and dysprosium far outweigh most others.

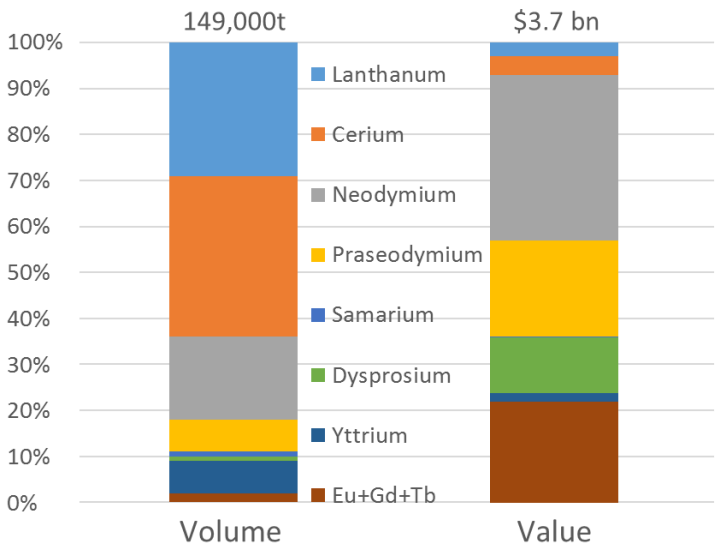

Figure 1: Global rare earth consumption by volume and value in 2015[2].

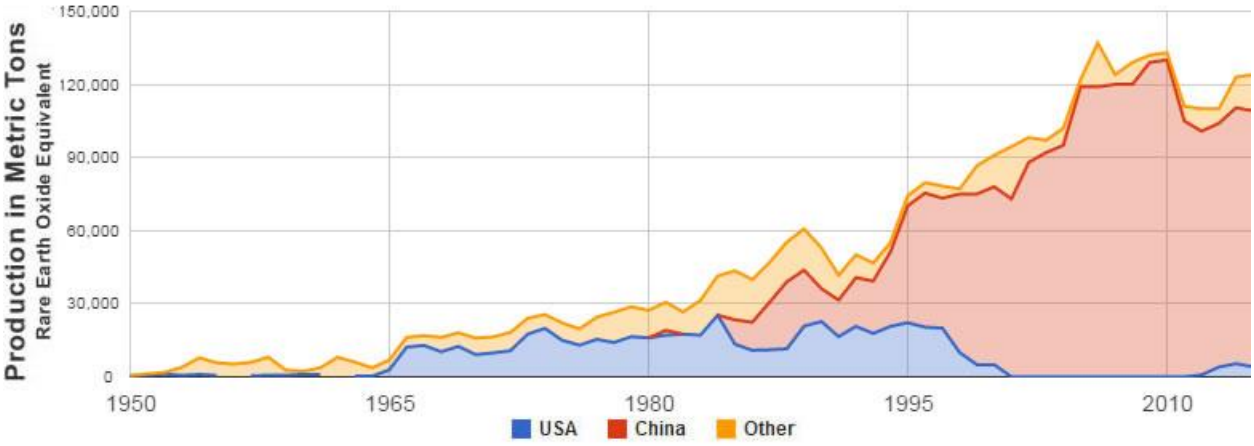

Figure 2: History of rare earth production, in metric tons of rare earth oxide equivalent, between 1950 and 2015. The United States' market share increased in the mid-1960s when color television increased demand. When China began selling rare earths at very low prices in the late-1980s and early-1990s, mines in the United States were forced to close because they could no longer make a profit. When China cut exports in 2010, rare earth prices skyrocketed. That motivated new production in many areas[3].

Application of rare earth elements began in earnest with the advent of color television, which relied heavily on europium. The US controlled most of the REE supply for a few decades before China began to

[2] Argus. (2016). Argus Americas Rare Earths Summit. Argus Americas Rare Earths Summit. Denver, CO.

[3] King, H. (2016). REE - Rare Earth elements and their Uses. United States of America. Retrieved from http://geology.com/articles/rare-earth-elements/

dominate production in the 1990s, as illustrated in Figure 2. US production came back online from the Mountain Pass mine in California briefly around 2013 after Chinese export restrictions caused a spike in REE prices. China has since relaxed these restrictions, lowering prices and causing the shuttering of the Mountain Pass mine.

China has enjoyed decades as the low cost supplier of REE, due to a combination of subsidies to state owned businesses and competitive deposits in the Bayan Obo region, Sichuan region, and South China adsorption clays. There is also production of REE from an Australian deposit, and there are known deposits around the world that have not yet or are not currently being exploited due to economic constraints, including the idled Mountain Pass mine in California. Figure 3 provides a flow chart of the typical REE value chain, with typical concentration ranges at each step. Mining of the ore is typically followed by physical beneficiation, which consists of milling and usually flotation or occasionally magnetic separation steps. The upgraded mineral concentrate is then 'cracked' to leach the rare earths into an acidic solution, which may be cleaned by selective precipitation and then fed to a solvent extraction circuit. Solvent extraction separates and purifies the individual rare earths, and due to the chemical similarity between sequential rare earths this process can take hundreds of mixer settler stages. It is common for the concentrated strip solutions from solvent extraction to be precipitated with oxalate addition, then calcined to oxides for sale in the market.

The South China Clays are notable as a deposit since they are similar in both concentration of REE and distribution of heavy REE to many coal deposits. However, they are ion exchangeable deposits, which are simpler to exploit than phosphate minerals more common to coal deposits, which require chemical cracking. The South China clays are leached with ammonium sulfate solution, precipitated with oxalic acid, then calcined and sent for separation and purification with little need for mineral beneficiation and none for chemical cracking.

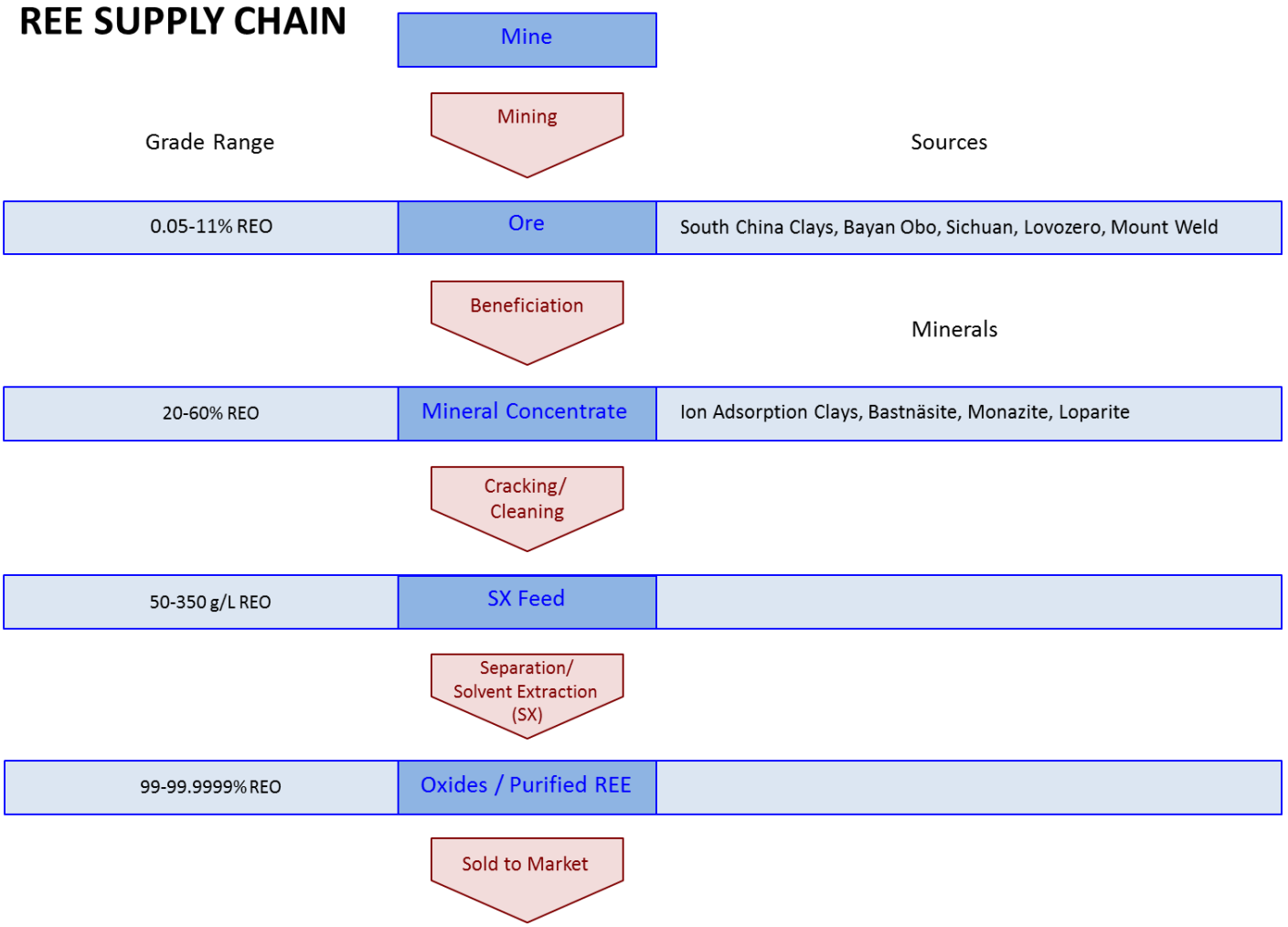

Figure 3: A flow chart of the REE supply chain, as provided by REE market consultants.

Rare earth price history

Recent REE price history has been dominated by Chinese trade policies, notably around 2010 when China installed export restrictions on rare earths, causing a spike in prices. The elevated prices led to the opening of new deposits, including the Mountain Pass mine. Since the relaxing of Chinese export restrictions, prices have dropped, pushing some producers out, although Australia continues to produce. From USGS's Mineral Commodity 2016 Summary[4]:

Through October 2015, China had exported 26,800 tons of rare-earth materials, a 20% increase compared with exports for the same period in 2014. Production of rare-earth oxide equivalent in Malaysia, derived from Australian mine production, was 7,750 tons through September 2015, a 55% increase compared with the same period in 2014. U.S. domestic consumption of rare-earth compounds and metals was estimated to be nearly unchanged compared with that of 2014. In October, the Mountain Pass mining and separation operations were idled indefinitely. Price declines were cited as a key factor in the suspension of operations. The suspension resulted in a decline in mine production and exports of rare-earth compounds.

[4] U.S. Geological Survey. (2016). Mineral Commodities Summaries, Rare Earth Elements. U.S. geological Survey.

Prices for REE have varied considerably based on natural market influence such as product demand, but have also been strongly influenced by geo-political policies, notably Chinese export restrictions as discussed earlier. Table 1 provides indicative global rare earth prices as available for consumption outside of China's domestic market. The highest prices are generally from the 2011 crisis, while current prices are near to an economical bottom. Battelle contracted with an external REE market consultant to obtain more specific current prices and peak prices for the economic analysis, but the data is proprietary and included in a proprietary appendix.

Table 1: Indicative current and peak prices for rare earth oxides.

Element	Indicative Current Price	Indicative Peak Price
Sc	$4200	N/A
Ce	$2	$60
Dy	$230	$2,032
Er	$34	N/A
Eu	$150	$3,800
Gd	$32	N/A
La	$2	$67
Nd	$42	$244
Pr	$52	N/A
Tb	$400	$2,974
Y	$6	$56

Current prices from mineralprices.com. Retrieved 12/12/2016. http://mineralprices.com/
Indicative peak prices from Humphries, M. (2013). Rare Earth Elements: The Global Supply Chain. Washington, D.C.: Congressional Research Service

Previous work performed by TetraTech under DOE contract DE-FE- 0004002 summarized published information concerning geology, geochemistry, and resource estimates of select coal basins in the Unites States, with emphasis on discerning distributions of rare earth elements. The U.S. Geological Survey (USGS) Coal Quality (CoalQual) Database is a collection of coal samples taken across the country to better understand the inherent heterogeneity of coal, and was used extensively in this evaluation. Figure 4 shows the locations of samples from the lower 48 States included in the CoalQual Database.

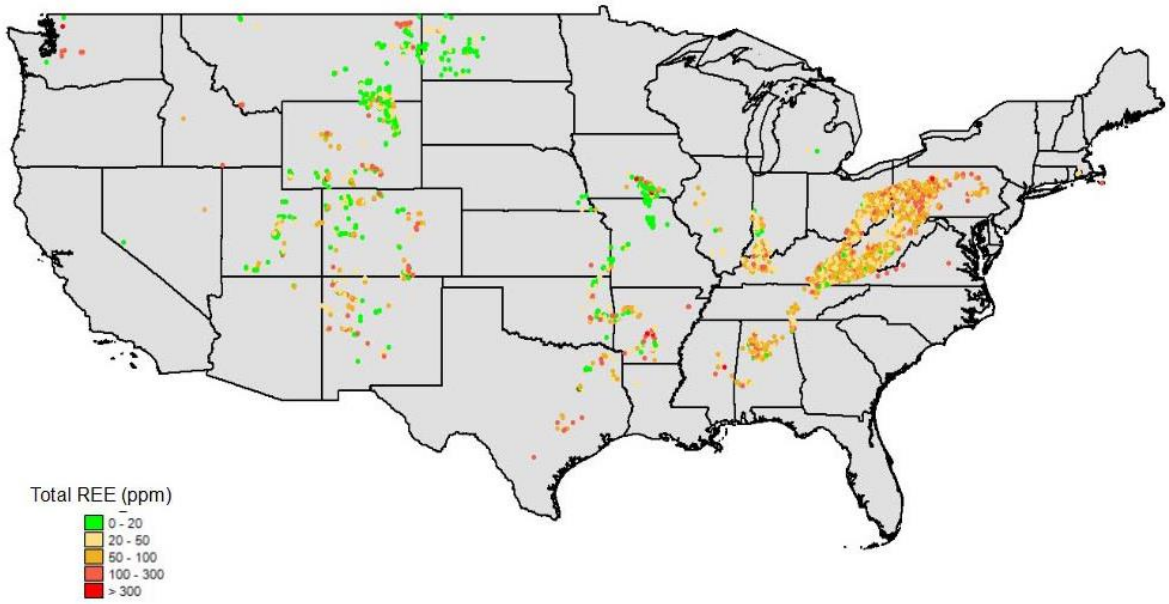

Figure 4: Sample distribution of Analyzed coals in USGS CoalQual Database[5].

TetraTech evaluated these data with respect to criteria that could be useful in defining "sweet spots" of these metals in coals and associated waste rock and/or ash and found the greatest REE content in certain areas of Pennsylvania, Kentucky, and West Virginia. Plants that primarily burn these coals will produce ash with high rare earth content. The grade of REE required for economic recovery is one of the outcomes of the technoeconomic study performed as part of Battelle's work effort and the results are presented later in this report.

To expand our understanding of REE concentration to a nationally relevant level, Battelle used a weighting system when analyzing the REE content of the CoalQual samples. The U.S. Energy Information Administration (EIA) collects and reports coal disposition by state. Using the 2015 data collected by EIA, the percent of total US coal produced by each state was related to the number of samples USGS collected from that state. Dividing the percent of total coal the state produced by the percent of USGS samples from that state a weighted value was calculated. This weighting was used to generate a histogram with weighted counts such that it more closely represented the population of coal deposits in the US. We used current market prices of each REE to establish a baseline price. Next, we took the values in Table 1 and multiplied them by the concentration of each rear earth in the samples. This new value was divided by the percent ash of the sample finally producing a value per tonne of ash for each sample in the database. Using this, we determined the economic viability of REE extraction from coal on a national level to target potential sources capable of supporting an economically viable extraction plant. Following this we complied our data into a histogram (see Section 5) to analyze the bulk number of samples that are financially prudent to pursue for our process of REE extraction.

3.0 Battelle REE Recovery Process Description

3.1 Process Flow Discussion

This process description is written to be used with the PFD shown in Figure 5. The integrated, closed-loop leaching process has three subsystems consisting of the leach, acid regeneration, and NOx

[5] Bryan, R., Richers, D., & Andersen, H. (2015). Assessment of Rare Earth Elemental Contents in Select United States Coal Basins. Tetra Tech.

absorption processes. The proposed production scale plant will process 30,000 kg (30 tonnes) of ash per hour, resulting in a production rate of dry rare earth concentrate of approximately 2,120 kg/hr. The scale of the pilot plant was chosen to be an appropriate size for development of the continuous rare earth recovery process while being reflective of a future full scale plant.

At the start of the process, coal ash, which is optionally washed to remove soluble ionic species, is fed to the process at a rate of 30,000 kg/hr and mixed with a dilute nitric acid stream (approximately 34 wt.%) before being pumped through a heater to an elevated, sub-boiling temperature, and into the leaching reactor. The leaching temperature is expected to be between room temperature and 120°C. Approximately 137,000 kg/hr of acid is charged to the reactor for every 30,000 kg/hr of ash fed. Within the reactor, mixing causes intimate contact of the ash with the nitric acid, allowing the REEs to be dissolved into the nitric acid solution. Selectivity for the rare earths is higher than that for iron, aluminum, and silicon in the ash, causing enrichment of the REE in the leach solution over the ash. The leach reactor is expected to resemble a Plug Flow Reactor (PFR), with a residence time of up to 30 minutes.

After the leach reaction, the ash is filtered out in a vacuum drum filter at a rate of 55,099 kg/hr, and transferred to an ash drying operation. The ash dryer is important for economic recovery of REE since the high temperatures will boil off and convert any entrained nitrates, allowing them to be recovered in the system. Additionally, this prevents the discharge of nitrates from the ash wherever it is used or stored. The ash dryer is expected to be a rotary-type drum dryer, heated to a temperature of 155°C, and is indirectly heated to minimize costs associated with off-gas treatment. When the ash is dried, it is removed from the system at a rate of approximately 28,071/hr. It is expected that the leaching operation will increase the surface area of the ash while removing some surface contaminants, which will improve the pozzolanic activity of the ash and make it ideal for use in cements. The leachate, containing unreacted nitric acid, is recycled to the reactor at a rate of 540,000 kg/hr to ensure complete utilization of the acid fed to the process.

Off gases from the process, made up of nitric acid with NOx components, are swept with an air stream maintained at a minimum flow of 800 kg/hr, and fed along with the REE-loaded leachate into a roasting operation at a flow rate of approximately 380,000 kg/hr. The roaster will operate in two steps, the first to concentrate the slurry, and the second to crystallize the rare-earth salts. The concentration step will likely use a conventional evaporation unit heated to 120°C, while the crystallization step is expected to take place in a custom designed crystallizer, reaching temperatures high enough (approximately 155°C) to convert metal nitrates to oxides. By roasting the metal nitrate salts to dryness and then to a temperature around 155°C, many non-rare earth metal salts are converted to metal oxides, releasing NOx gases, which are swept along with other process off-gases to the absorption column. Rare earth nitrates, however, are not converted to oxides at temperatures less than approximately 400°C, and will therefore remain in their nitrate salt form[6]. This provides a water soluble rare earth concentrate, enriched in rare earth materials, suitable for feed to a hydrometallurgical process to separate and purify the rare earths.

As discussed, all off-gases of the process, consisting of nitric acid vapor and NOx gases, will flow to an absorption column system for recovery at a rate of approximately 600 kg/hr, swept to the column using excess air. Optionally, these vapors may be compressed and fed through a heat exchanger to preheat the acid feed to the roaster, then to a condenser to recover nitric acid for recycle, prior to being fed to the column, although it is anticipated that recovery of low grade heat available at power plants will provide the majority of the heat required for this process. Any NO gas generated in the roaster, leaching, and ash drying processes needs to be oxidized to NO_2 prior to being absorbed back into the acid stream. This oxidation rate is improved at higher temperatures, and can occur in the drying and roasting processes with the presence of air. As the gas passes through the condenser, it is then cooled, which is preferable for the absorption of the NO_2 back into the liquid phase. Gas will be recycled in the absorption column at a rate of 3,010 kg/hr until all NOx gases have been absorbed, at which point the gas will be discharged from the process. The liquid recirculated in the column consists of acid recovered from the roaster. This

[6] Stern, Kurt H. “High Temperature Properties and Decomposition of Inorganic Salts, Part 3. Nitrates and Nitrites.” Journal of Physical and Chemical Reference Data, Volume 1, Number 3. 1972.

acid is recirculated within the column at a rate of 243,000 kg/hr to absorb NOx gases and regenerate the nitric acid to near its original concentration prior to the leaching process.

Nitric acid recovered in the column will be recycled back to the leach reactor to complete the acid recycle process at a rate of 136,000 kg/hr. A small fraction of this stream (approximately 3,000 kg/hr) will be sent to a distillation column, which will distill and separate the water-nitric acid mixture. The concentrated nitric acid recovered in the distillate will be recycled to the acid leaching process, while the water recovered in the bottoms will be treated to a neutral pH and purged from the system at a rate of 1,600 kg/hr. This purge ensures that a buildup of water does not occur in the process. Testing and simulation to date indicates that greater than 95% of acid (calculated as the fraction of makeup acid required verses the total acid feed requirement of the reactor) is able to be recovered through the acid roasting process and the absorption column used to recover the gas-phase nitrates. The process includes a small makeup acid stream, which feeds nitric acid to the process at a rate of 2,500 kg/hr to maintain a constant concentration of nitric acid within the leach reactor.

Table 2: Performance model flow rates in Battelle's REE separation process, as presented in CHEMCAD flowsheet.

Feed/Product Stream	Flow Rate (kg/hr)
Coal Fly Ash Feed (Feed)	28,311
Nitric Acid Makeup (Feed)	997
Process Water (Feed)	1,764
Leached Ash (Product)	28,100
Mixed Rare Earths (Product)	2,122
Process Purge Stream (Product)	25,439

The process is expected to be supported by several ancillary process operations, including material handling, water and wastewater handling facilities, steam facilities, and plant air. The ideal location for a REE processing facility would be co-location with an existing power plant, due to the preexisting coal and ash handling network existing to feed the power plant. Many of these supporting operations, such as wastewater facilities and steam facilities, already exist for most power plants, and may be upgraded to serve both processes.

The estimated heat duty for the overall pilot system is estimated at 73 MW, with an overall cooling duty of 57 MW. This includes partial networking of heat exchangers to minimize overall heating and cooling requirements. Heating for most the plant may be partially supplied by the low-grade heat available at a power plant[7], requiring only minimal additional heat to be supplied to the REE recovery process. Cooling loads are similarly expected to be able to be integrated in with the power plants substantial existing cooling system. The remainder of the pilot plant power requirements are expected to small loads associated with the process pumps, fans, and blowers, and are not expected to be major contributors to the energy requirements. A summary of the major unit operations and their anticipated heat duties is summarized in Table 3. As shown, most the process cooling requirements are associated with the acid recovery condenser (part of the acid roasting system), while much of the heat requirement pertains to the acid roaster.

[7] It is appreciated that the majority of low grade heat available at a power plant is currently utilized in the most efficient manner possible. Initial discussions with plant operators indicate that low grade heat may be available throughout the plant at varying quality for use.

Table 3: Heating and cooling duty of the REE separation process predicted by the CHEMCAD® performance model

Unit Operation	Heat Duty (kW)
Leach Reactor Preheater	17,710
Rotary Drum Ash Dryer	53,463
Roasting Process Evaporator	185,654
Roasting Process Roaster	1,839
Distillation Column Reboiler	5,103
	Cooling Duty (kW)
Absorption Column	<5
Roaster Condenser	<5
Evaporator Condenser	203,843
Distillation Condenser	3,060

The primary product of the process is a REE recovery stream which is greater than 2 percent REEs in concentration. Pertinent process metrics surrounding the process are summarized in Table 4. Note that the average leaching rates for the REEs is presented in the table. Elemental leaching rates, which vary by species, were used in the process model. These are presented in Table 6 under the far-right column, "34% milled." Section 4.4 provides discussion on methods to improve REE concentration to above 50% along with feasibility test results.

Table 4: Pertinent process values

Parameter	
Average REE Yield (% Leached)	44.10%
Final REE Product Concentration	3.55%
Process Acid Recovery	97.88%

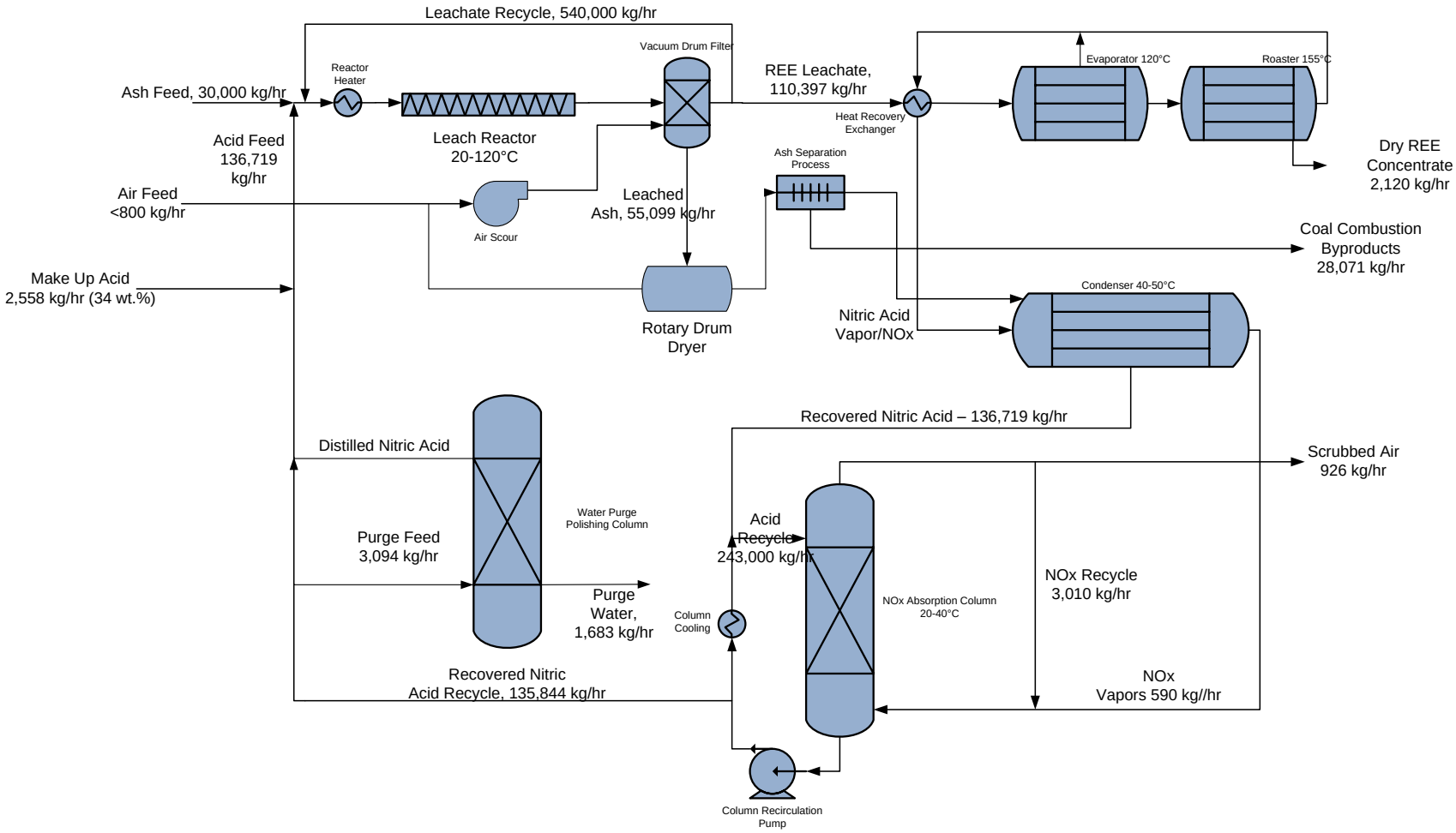

Figure 5: Process Flow Diagram of the proposed continuous, 30 tonne/hr REE plant. Flows as predicted in CHEMCAD flowsheet.

3.2 Environmental Impact

Due to the closed-loop nature of this process, the environmental impacts are low. More than 95% of the nitric acid used in the process is recycled, which minimizes the amount which is produced as waste by the process. The primary process waste, which is a mixture of nitric acid and water, is easily treated to a neutral pH and can be discharged as an industrial process waste stream via the site water treatment plant. Gases produced within the process, primarily NOx gases, are captured in the process absorption column prior to being vented. This not only allows for the plant to comply with any air pollutant permitting requirements, but also captures and converts nitrate-based gases to nitric acid capable of being recycled in the process. No other criteria air pollutants defined in the National Ambient Air Quality Standards (NAAQS) are anticipated to be produced as part of this project.

The primary feed to this process, coal ash, is considered a waste product from coal-fired power plants, and is the subject of ever-evolving regulation. The rare earth recovery process will remove not only rare earths from the coal ash, but will also remove many monovalent, divalent, and transition metals from the ash. Additionally, exposure to the acid leaching process is expected to increase the pozzolanic activity of the ash, which may make the leached ash more desirable for use as a filler compared to typical power plant ash. Therefore, the environmental impacts associated with the leached ash process stream are two-fold. In regions where the ash can be used as a pozzolan, it will be more desirable to place ash from the rare earth recovery process verses standard power plant ash. In regions where placement as a pozzolan is not possible, the leached ash from the rare earth process is expected to be less prone to leaching than traditional power plant ash due to reduced metal content. The leached ash is expected to be neutral in pH after being processed by the process ash dryer, as any remaining nitric acid will have been boiled off and recovered within the plant.

4.0 Laboratory Testing Results Summary

Preliminary laboratory testing was performed to validate some of the assumptions made in the economic modeling portion of the project and understand viable next steps in the REE purification process. The following preliminary tests were run, and will be reported in this section:

1. Leaching tests from pulverized coal combustion (PCC) plant fly ash
2. Leaching tests from Battelle's bio-based direct coal liquefaction residual material
3. Leaching tests from fluidized bed coal combustor plant fly ash
4. Acid loading tests with PCC plant fly ash
5. Roasting tests to understand the conversion of metal nitrates to oxides
6. Thermogravimetric Analysis (TGA) and Differential Scanning Calorimetry (DSC) of the rare earth concentrate material
7. Preliminary selective precipitation tests on re-dissolved rare earth concentrate
8. Preliminary solvent extraction pre-concentration tests on re-dissolved rare earth concentrate
9. Pozzolanic activity tests on the leached ash

Leaching tests were conducted to apply leaching percentages to each element in the CHEMCAD process model. The acid loading tests were used to inform the level of loading the leaching solution could handle before requiring a regeneration, thus dictating the level of acid recycle within the ADP process. DSC and TGA were performed to indicate which temperatures will cause the oxidation of base metals, such as iron and aluminum, without oxidizing rare earth nitrates. The REE concentrate material generated in the ADP process is not saleable as is, and will require additional purification to be place in the market. Preliminary tests on purification steps, such as selective precipitation by pH adjustment and a solvent extraction pre-concentration step were performed to begin assessing the best means for purification of the rare earths going forward. Preliminary pozzolanic activity tests were performed on the leached ash to understand how the leaching affects the opportunity to place the ash as a construction filler material. Analysis was performed for the 59 elements listed in Table 5 on all solutions.

Table 5: Elements analyzed for in solution for the laboratory testing

Element Analyzed in Solution			
Na	Ni	In	Ho
Li	Cu	Sn	Er
Be	Zn	Sb	Tm
Mg	Ga	Te	Yb
Al	Ge	Cs	Lu
Si	As	Ba	Hf
K	Se	La	Hg
Ca	Rb	Ce	Ta
Sc	Sr	Pr	W
Ti	Y	Nd	Tl
V	Zr	Sm	Pb
Cr	Nb	Eu	Bi
Mn	Mo	Gd	Th
Fe	Ag	Tb	U
Co	Cd	Dy	

4.1 Leaching Tests

Leaching tests were performed on PCC plant fly ash, FBC plant fly ash, and coal liquefaction residual material, both ashed and unashed. PCC plant ash typically encounters the highest temperatures of the three during combustion, which causes vitrification of the ash particles. FBC ash usually encounters lower temperatures, but also has high calcium content due to the addition of lime to the coal in the furnace for control of sulfur emissions. Coal liquefaction ash has not been through combustion conditions, but rather liquefaction at moderate temperatures (around 400°C) and pressures around 300-400 psig. As indicated in the sampling and characterization report, the liquefaction ash retains much of the same crystal structure as feed coal, and sees only minor oxidation as indicated by the conversion of pyrite to pyrrhotite. Leaching tests were conducted on all three ashes to understand the differences in leaching efficiency with the three feeds. The percent leached for each element was calculated by mass balances using the concentration of the element in the leach solution and volume of leach solution at each sample.

PCC Ash

Tests on PCC ash were performed at multiple nitric acid concentrations: 17%, 34%, 51%, and 68%. It has been Battelle's experience that some higher nitric acid concentrations can cause passivation of iron materials, reducing leaching efficiency, and this was also the case for PCC sources. Table 6 describes the leaching efficiency for each rare earth according to starting acid concentration, and indicates the reduced leaching efficiency at higher acid concentrations, which is likely due to passivation of the bulk aluminum and iron phases preventing further leaching. Aluminum and iron leach efficiency averaged 11.5% and 6.1%, respectively, in the 17% and 34% acid concentrations, compared to 3.4% and 2.4%, respectively, supporting this hypothesis. The last column indicates the best leaching efficiencies achieved in the preliminary testing, which was after milling of the ash to break up vitrified sections, and which were used in the techno-economic assessment. Milling was done in a ball mill, and caused reduction of particle sizes from 10-100 microns to 1-40 microns as indicated in Figure 6.

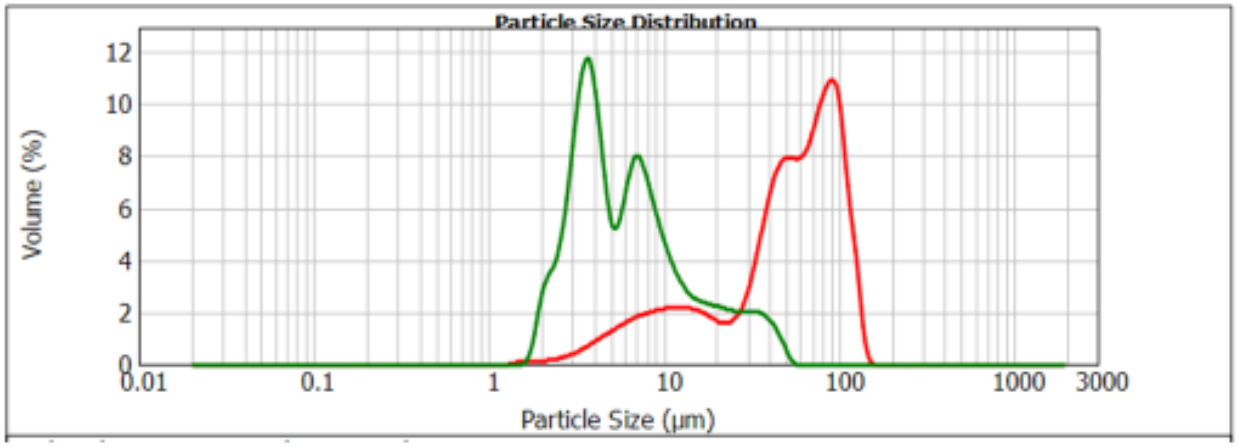

Figure 6: Particle size distributions for PCC ash before (red line) and after (green line) wet ball milling

Table 6: Leaching efficiencies for rare earth elements and starting acid concentrations for the leach.

	Starting Nitric Acid Concentration in PCC Fly Ash Leaches						
Element	17%	17%	17%	34%	51%	68%	34% (milled)
Sc	19.2%	20.8%	21.5%	21.5%	N/A	N/A	55.3%
Y	24.6%	26.7%	28.0%	28.0%	14.9%	13.0%	46.9%
La	19.0%	19.3%	20.0%	19.0%	9.9%	8.2%	35.4%
Ce	21.0%	21.5%	21.7%	27.0%	11.9%	9.9%	34.0%
Pr	20.3%	21.7%	22.4%	22.9%	11.6%	10.0%	36.3%
Nd	20.8%	22.6%	23.4%	23.9%	12.3%	10.5%	39.5%
Sm	22.5%	24.0%	25.0%	25.4%	13.7%	11.8%	40.5%
Eu	22.7%	24.5%	25.4%	26.4%	14.8%	12.7%	42.4%
Gd	25.0%	27.2%	28.5%	28.8%	15.7%	13.7%	45.2%
Tb	23.3%	25.5%	26.9%	28.1%	15.4%	13.4%	44.3%
Dy	24.1%	26.2%	27.6%	28.6%	15.5%	13.0%	41.9%
Ho	24.6%	26.8%	28.0%	28.6%	15.2%	13.3%	41.8%
Er	23.8%	26.2%	27.5%	27.8%	14.8%	12.6%	43.8%
Tm	23.0%	25.2%	26.4%	26.9%	14.4%	12.0%	42.2%
Yb	21.2%	23.1%	24.7%	24.8%	12.9%	10.6%	36.3%
Lu	21.2%	22.6%	23.9%	24.3%	13.0%	10.2%	34.6%

Besides leaching efficiency, selectivity for REE will also affect overall product economics. The percent of REE leached compared to all measured elements (59 elements were analyzed for in the leach solutions) were compared for each test, and results are shown in Table 7. These results suggest that high concentration leaches are more selective, but beyond 34%, seemed to have reduced REE leaching efficiency. There are several strategies for enhancing the purity of the mixed REE concentrate, many of which will be discussed in later sections. It is expected that this number can be improved by selective roasting of the solution, removing bulk iron and aluminum phases, and pre-washing of the material, removing a lot of the calcium and other water soluble salts that would otherwise consume acid in the process. Further testing will focus on use of higher acid concentrations with milling to determine an appropriate balance of leach efficiency and selectivity.

Table 7: Percent of REE in all 59 measured elements by leach concentration, indicating selectivity of the leaches.

Test Concentration	REE+Y+Sc out of total measured
17%	0.24%
17%	0.24%
17%	0.22%
34%	0.33%
51%	0.31%
68%	0.34%
34% (milled)	0.27%

FBC Ash

The fluidized bed combustor ash was run multiple times with 17% nitric acid, and exhibited higher leach efficiencies for REE than PCC ash, as indicated in Table 8. However, the selectivity was significantly lower, as shown in Table 9. The improved efficiency is likely due to the lower furnace temperatures in a fluidized bed combustor, which leads to less vitrification of the ash, providing better access to the REE for the acid leach solution. The reduced selectivity is also likely impacted by reduced vitrification, but also the high calcium concentration in the ash, which is typically acid soluble and 'dilutes' the rare earths that are leached. FBC ash was not pursued further in testing due to its much lower availability than PCC ash and complications with calcium concentrations.

Table 8: Leaching efficiencies by element in the FBC leaching tests, note that cells marked N/A were below detection limits in the analysis.

Element	Starting Nitric Acid Concentration in FBC Leach Tests		
	17%	17%	17%
Sc	N/A	N/A	N/A
Y	37.4%	38.6%	37.9%
La	68.0%	71.7%	70.6%
Ce	62.5%	65.9%	63.7%
Pr	69.2%	73.7%	71.2%
Nd	62.5%	64.6%	62.2%
Sm	65.9%	70.7%	67.9%
Eu	62.8%	66.4%	62.6%
Gd	63.1%	66.2%	63.6%
Tb	56.0%	58.2%	64.4%
Dy	55.2%	59.5%	57.9%
Ho	46.2%	49.8%	46.4%
Er	47.8%	48.9%	46.0%
Tm	38.3%	40.7%	39.5%
Yb	42.3%	42.2%	41.2%
Lu	N/A	N/A	N/A

Table 9: Percent of REE in all 59 measured elements in FBC leach tests, indicating selectivity of the leaches.

Concentration	REE+Y+Sc out of total measured
17%	0.051%
17%	0.051%
17%	0.051%

Coal Liquefaction Residual Material

Residual material from the 1 tpd direct coal liquefaction pilot plant was leached with nitric acid to determine whether the acid digestion process could be applied to it. Results for 2 trials at 17% nitric acid concentration are presented in Table 10. Leaching efficiency was significantly less than either the PCC or FBC ash, and there are a couple possible reasons. The liquefaction residual material contains a large amount of carbon, which is likely blocking access of the leach solution to the mineral portion containing rare earth elements. Additionally, the carbon laden material was less dense than the leach solution, which created difficulties in obtaining good mixing within the round bottom flask where the leaching was performed. To establish whether the carbon residual was impacting the leaching results, a sample was ashed at 500°C and leached with nitric acid. This sample realized an overall REE+Y+Sc leaching efficiency of 66%, which suggests that the carbon must be removed from the liquefaction residual to treat it effectively with the acid digestion process.

Table 10: Leaching efficiencies by element in the liquefaction residual material leaching tests, note that cells marked N/A were below detection limits in the analysis.

Concentration	Starting Nitric Acid Concentration in Liquefaction Residual Leach Tests	
	17%	17%
Sc	N/A	N/A
Y	3.4%	3.0%
La	13.9%	13.5%
Ce	13.2%	10.5%
Pr	10.2%	7.9%
Nd	8.5%	7.7%
Sm	11.0%	8.7%
Eu	N/A	N/A
Gd	8.9%	6.5%
Tb	N/A	N/A
Dy	3.1%	1.9%
Ho	N/A	N/A
Er	3.3%	N/A
Tm	N/A	N/A
Yb	5.0%	3.7%
Lu	N/A	N/A

4.2 Leach Solution Loading Tests

A key parameter in the process economics is the degree to which the nitric acid leach solution can be loaded with metals before it loses leaching efficiency and must be regenerated. To perform these loading tests, PCC fly ash was contacted with 34% nitric acid solution at a ratio of 40g of ash to 257 mL of solution. After leaching at room temperature for 30 minutes, the slurry was filtered to recover the solution. The recovered solution was contacted with ash again, maintaining the same ash to liquid ratio, leached for 30 minutes, and the process repeated four times. Intermediate samples were taken to understand the kinetics with leach solution recycle. Room temperature leaches were selected so that kinetic differences would be easier to detect. There were periodic difficulties during these preliminary tests in keeping the solution stirring in the flask at the high solids loading rates in solution, and this likely explains, for example, the lack of leaching between 1 and 5 minutes in the 3rd contact, as shown in Figure 7. The loading tests suggest that there is a reduction in leach efficiency as the solution is recycled, however, the expectation is that the reduction in efficiency and kinetics will be minimized when run at higher temperatures and more efficient mixing conditions. In the TEA model, it was assumed the leach solution could be recycled four times before requiring regeneration. Future lab testing after the go/no-go decision would derive a kinetic expression for leaching rates of the REE so that the reactor can be designed and performance predicted more accurately.

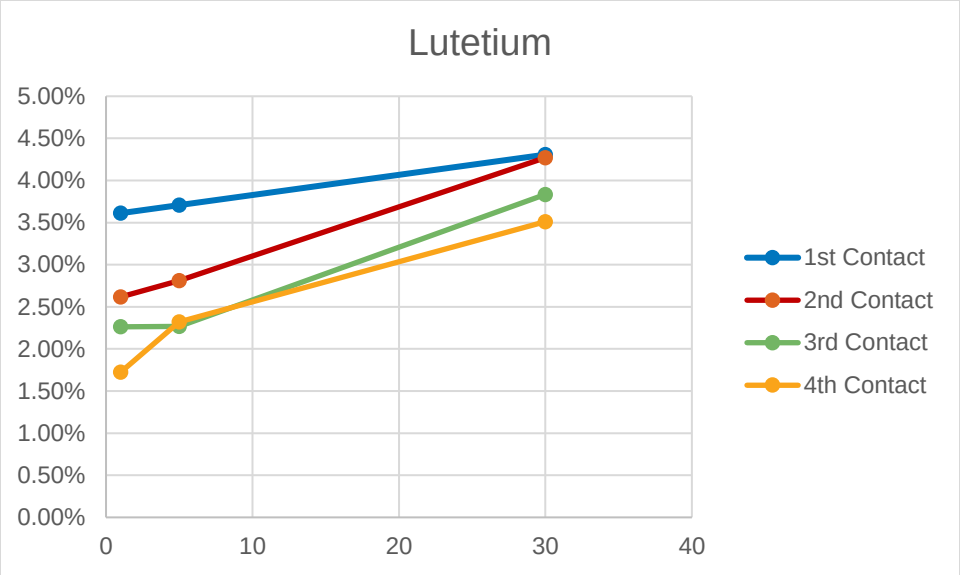

Figure 7: Percent removal of lutetium from PCC ash over time and through contacts at room temperature with leach solution during the loading tests.

4.3 Roasting Tests

Roasting, or drying of the leach solution, is a critical step in the process for both recovery of nitric acid and production of an upgraded REE solution. Literature (refer to footnote 6 on page 8) suggests that rare earth nitrates are thermally converted to oxides at significantly lower temperatures than many base metals, including iron and aluminum, which are key contaminants in the leach solution. The target is for selection of a final roasting temperature that will convert iron and aluminum nitrates to oxides, rendering them insoluble in a following water re-dissolution, so that they will not require selective precipitation. Rare earth nitrates would remain water soluble and leach into the water along with mono and divalent salts, which are easy to separate by solvent extraction and other methods.

Initial tests were run with loaded leach solution in a round bottom flask inside a heating mantle. The heat output of the heating mantle was varied between 50%, 75%, and 100% duty cycle, to determine whether the rate of heat input changed the roasting results. The material was heated to dryness, and collected for leaching tests. Because the round bottom flask was not insulated, there was reflux of acid along the sides of the flask. The dry material from each test was washed with water, to determine whether iron and aluminum were excluded from the water wash, while rare earth elements were dissolved. Results from a single tests are shown in Table 11. The water wash did not liberate any measurable iron or aluminum from the roasted solids, but also did not remove and measurable REE. However, it did show promise in removing mono and divalent metals such as sodium, magnesium, and calcium, which are significant contaminants in the solids. It is projected that complete removal of these wash compounds in the solid material would more than double the purity of the REE concentrate.

Table 11: Preliminary water wash results of the roasted solid material.

Calculated Percent Removal by Water Wash of Dry Solids	
Sodium	104%
Magnesium	90%
Calcium	93%
Potassium	107%
Lithium	59%

Further testing was performed to try and understand the best operation of the roasting step. Temperature control in the flask was not well controlled, as refluxing acid would cool some portions of the solids, but allow other portions to overheat. The hypothesis was that this allowed the rare earth nitrates to oxidize. Loaded leach solution was therefore dried slowly overnight under a 100W light bulb, so that it would not overheat. Figure 8 shows the solids as recovered. These solids were then placed in a Differential Scanning Calorimeter (DSC), which tracks heat flow over a temperature range. Figure 9 shows the spectrum generated from the DSC test, and indicates endothermic peaks between 68°C and 120°C likely due to vaporization of water and nitric acid. Minor variations in exo/endothermic behavior can be seen between 120°C and 290°C, with a large change at 293°C. The experiment was terminated at 400°C, and a picture of solids calcined at 400°C is shown in Figure 8. In future testing, solids will be calcined to a specific temperature, then tested for water leachability to find an operating temperature for the roaster that omits iron and aluminum while maintaining REE as nitrates. X-Ray Diffraction analysis after calcining at temperatures was also done, with results in Table 12. This analysis suggests that there is a transition of sodium nitrate between 200°C and 400°C, which is near the sodium nitrate melting point, and may explain the 300°C peak in the DSC.

Figure 8: Loaded leach solution (L), dried solids (top right), and calcined solids (bottom right)

Table 12: XRD results of dried leach material after set temperature calcinations.

	$Na(NO_3)$	$Ca(SO_4)$	$Mg(NO_3)_2H_2O$	$Ce(PO_4)$
Residual	43.1	50.1	5.1	1.7
120°C	42.6	53.6	3.1	0.7
200°C	41.6	57.4	0.1	0.8
400°C	14.3	85.7	<0.1	<0.1

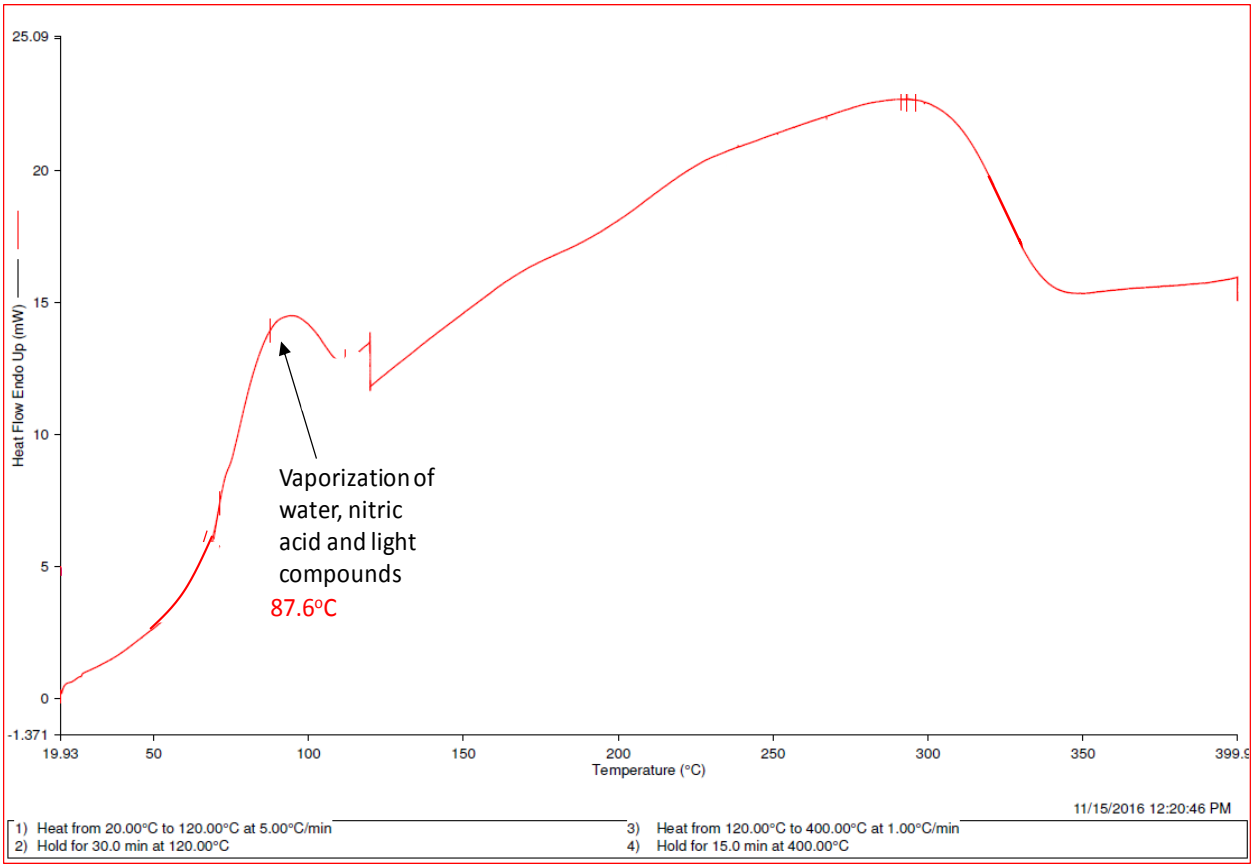

Figure 9: DSC of residual material recovered from leach solutions.

4.4 Preliminary Purification Tests

It is projected that with only thermal processing and water washes to remove iron, aluminum, calcium, magnesium, sodium, and potassium, the purity of the REE solution can be upgraded to 3-5%. However, an additional upgrading of the solution is required even before feeding to a final purification/separation step such as solvent extraction. Preliminary tests were performed to understand what options for pre-purification would be viable for the product.

Initial tests were done for selective extraction of REE using a commercial extractant, Cyanex 572, which is specifically designed for application to rare earth elements. Leach solution was adjusted to between pH 1 and 1.5 with sodium carbonate solution prior to the extraction, which was done with an extractant of 15wt% Cyanex 572 and balance Solvent 467 diluent. Extractant was combined with leach solution at an extractant to aqueous ratio of 1:4, and shaken for 20 minutes to remove REE. Extraction of heavy REE was better than light REE, however recovery of light REE was low, indicating that pH should be elevated for better extraction. Table 13 shows the extraction percent by REE. It is expected that this extraction will omit most mono and divalent metals, and results suggest it omitted aluminum as well. However, the mass balance calculations were inconclusive, with many base metals showing an increase in the extracted solution after contact, and additional replicates are needed. If negative mass balance calculations are assumed to be non-extraction, as expected, then the primary contaminants were iron (91% extracted) and titanium (99.8% extracted).

*Table 13: Percent extraction by 15% Cyanex 572 at a starting pH of 1.0-1.5. *Scandium was below detection limits in the analysis, so removal is at least 47%.*

Element	Percent Extracted
Sc	47.16%*
Y	85.35%
La	None Observed
Ce	None Observed
Pr	None Observed
Nd	None Observed
Sm	None Observed
Eu	None Observed
Gd	None Observed
Tb	25.60%
Dy	55.30%
Ho	74.86%
Er	88.63%
Tm	97.47%
Yb	98.79%
Lu	98.59%

Selective precipitation tests were conducted by pH change, and indicated that titanium could be precipitated with minimal effort. A pH change from 1.5 to 2.5 reduced titanium concentrations from 12,900 µg/L to 1,790 µg/L (86% reduction). With removal of titanium by pH adjustment, recovery of all REE with the higher pH extraction, and prior iron removal by the roasting step, then purity of the extracted REE would be roughly 50%, and indicates this is a promising approach for pre-purification of the REE solution. The approach is outlined conceptually in Figure 10. Additional testing after the go/no-go will investigate this approach further.

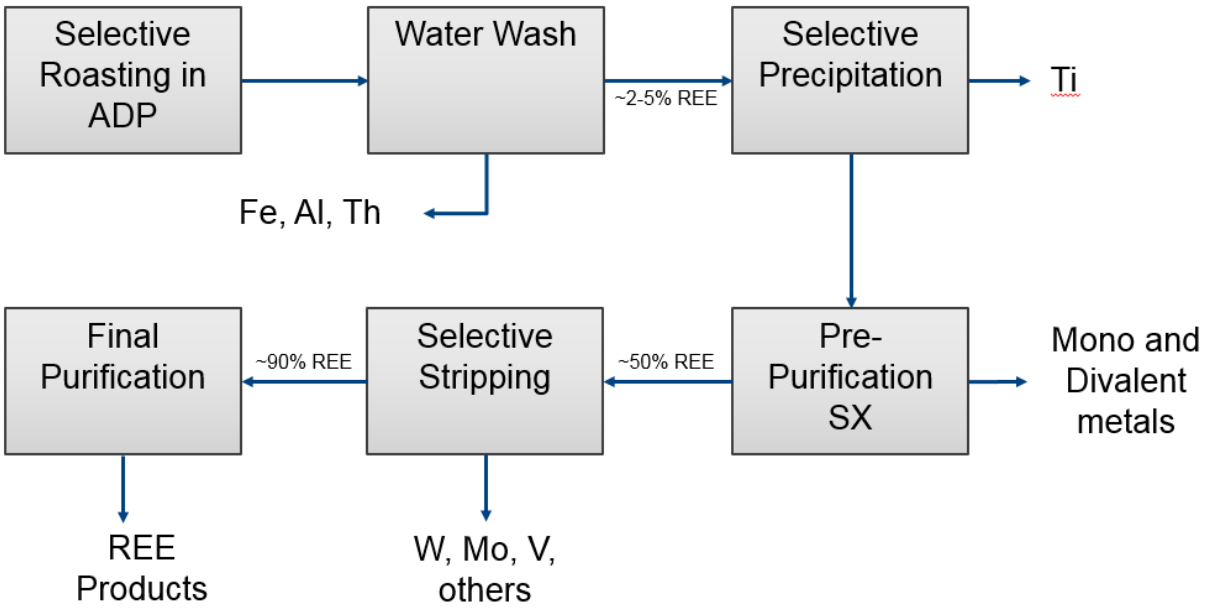

Figure 10: Block flow diagram indicating the conceptual purification scheme for REE out of the ADP process, with projected concentrations at key stages in the process. This schematic will be validated in further testing.

4.5 Pozzolanic Activity Tests

To begin investigating the effect of acid leaching on the utility of the fly ash in concretes, three cylindrical 1.75in x1.75in concrete samples were prepared as described below:

- Sample A: Blend of residual material (fly ash treated with acid to remove REE, heat treated at 200°C to simulate drying in the process), Type 1 Portland cement, sand, and water
- Sample B: Blend of unleached fly ash, Type 1 Portland cement, sand, and water
- Sample C: Type 1 Portland cement, sand, and water

Figure 11 is a photo of the concrete cylinders and Table 14 reports the composition of each concrete sample. Before testing, all samples were dried for 48 hours at room temperature and 28 days in a water bath at 65°C.

Figure 11: Cured concrete samples

Table 14: Composition of the concrete samples

Sample	Description	Cement (wt%)	Ash (wt%)	Sand (wt%)	Water/Cement weight ratio
A	Concrete with post leached fly ash	77	19	4	0.5
B	Concrete with fly ash	77	19	4	0.5
C	Concrete without addition of fly ash	77	0	23	0.5

The compressive strength test was performed at CTL engineering lab following ASTM method C39/C39M. The results were A: 3420 psi, B: 3420psi, and C: 3250psi. This preliminary testing suggests that leaching does not affect the pozzolanic activity of the ash, but more tests are required to reach a final conclusion.

5.0 TEA Discussion

5.1 CHEMCAD Model Narrative

CHEMCAD version 7.0.3 was used to simulate the rare earth recovery plant at scale. Utilization of the process modeling software ensured that closed process mass and energy balances were able to be developed. Several aspects of the CHEMCAD model were informed by laboratory testing or prior engineering efforts conducted by Battelle.

First, an optional water wash step of the ash is simulated using a component separator (Unit Operation 55). This removes the water soluble monovalent species from the ash prior to the acid leach step. The acid leach reactors (Unit Operations 3, 8, and 32) are simulated using stoichiometric reactions for each of the rare earths as leached in nitric acid. Fractional conversion estimates were obtained through laboratory leach testing to ensure that the recovery represented in the model reflected actual conditions. The leachate and the solids are separated using a simulated filter (Unit Operation 6) programmed to yield a moisture fraction of 50% in the solids. From this point, separated solids are dried and roasted to recover residual acid in a stoichiometric reactor (Unit Operations 14 and 33) prior to being discharged as a salable byproduct from the process. Recovered vapors are combined with other vapors collected from the leachate roasting process.

The leachate roasting process converts the depleted nitric acid/rare earth nitrate stream to rare earth nitrate salts, metal oxides, and recovered nitric acid. The first step in this process is to evaporate off and collect water and unused nitric acid from the liquid stream, concentrating the stream in preparation for

crystallization. The evaporator is simulated in Unit Operations 53 and 39. The concentrated stream is sent to the crystallizer (simulated by Unit Operations 7, 38, and 50) where non-rare earth metal nitrates are converted to metal oxides and nitric acid, and the remainder of the liquid is recovered. All vapors are collected and condensed in Unit Operations 10 and 40.

During both the leaching and roasting processes, NOx gases are produced which require treatment prior to being released to the atmosphere. An absorption column is used to capture NOx gases and convert these gases to nitric acid for recycle to the leach reactor. This is simulated by a series of stoichiometric reactors (see Unit Operations 20, 36, 37, 21, and 22). The liquid circulated through the column is the acid which is recovered from the roasting and crystallization process discussed above. Temperature control is maintained in the column (see Unit Operation 24) below 40°C to promote rapid oxidation and absorption of NOx gases. After process gases have been scrubbed of acidic gases, they are discharged in accordance with plant permits. Most the liquid phase of the column is immediately recycled to the leach reactor, and a small portion is discharged as a purge stream to maintain water balance in the system. This stream is first treated in a distillation column (see Unit Operation 16) to recover and concentrate nitric acid present in the purge stream. Recovered nitric acid is recycled to the leach reactor, while the purge water stream is discharged from the process.

Mass and energy balances from the CHEMCAD simulation, as well as a simulation flow sheet, are presented in Appendix A.2. The simulation will continue to be updated throughout the process design phase to reflect the most current iteration of process design.

5.2 TEA Model Narrative

This section describes how the performance model described in the previous sections can be used to estimate the capital and operating costs of Battelle's rare earth elements (REE) process. Cost estimation is important in order to determine whether REE production from coal products is commercially viable under a given set of circumstances.

Process costs describe a First-of-a-Kind (FOAK) plant constructed in 2016 using the current design of the REE separation process. Later sections will discuss potential improvements to the system based on a more thorough understanding of the process resulting in a mature, Nth-of-a-Kind (NOAK) estimate of capital and operating costs. A more thorough understanding of the process is expected to reduce capital and operating costs, thereby reducing the overall capital and operating costs of the system. These improvements and the resulting nth of a kind costs are discussed in later sections.

Summary of TEA Method

The procedure used in this work follows the Electric Power Research Institute's (EPRI) Technical Assessment Guide (TAG™) guidelines for cost estimation of emerging technologies. The total capital requirement (TCR) of a rare earth separation system takes into account the direct costs of purchasing and installing all processing equipment (denoted as the Process Facilities Capital, PFC), plus a number of indirect costs such as the general facilities cost, engineering and home office fees, contingency costs, and several categories of owner's costs. These costs are used to determine the overall cost of Battelle's Acid Digestion Process for recovery of REE. Figure 12 outlines the TAG method developed by EPRI.

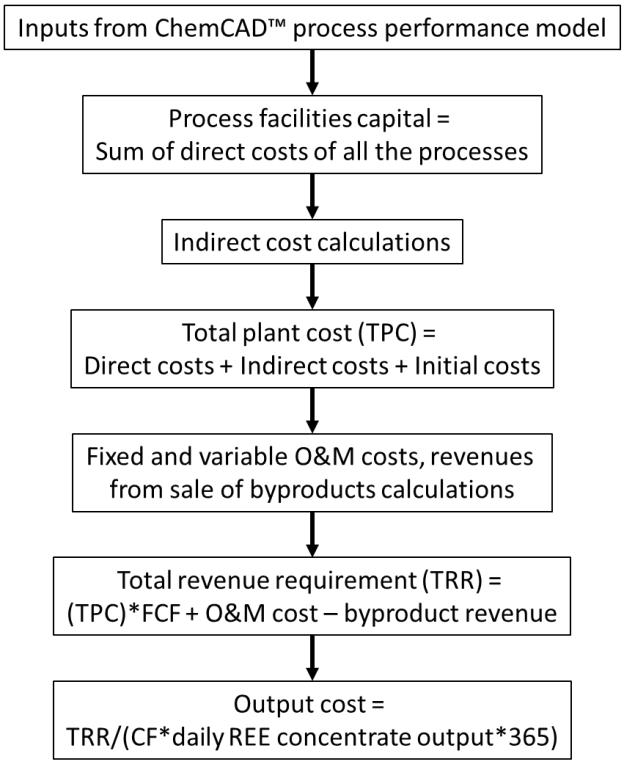

Figure 12: Method of cost assessment (Electric Power Research Institute (EPRI), 1986)

Capital Cost

The process facilities capital (PFC) of a component refers to the capital required to purchase and install a major process at the facility. Ideally, these costs are known and come from prices quoted from an equipment manufacturer. When manufacturer data is not available, installed cost data is derived from references describing costs for installing similar processes. Equipment costs are then scaled using well-documented cost correlations[8]. Table 15 lists the nominal cost values for a FOAK rare earth separation system using Battelle's process.

The total direct capital cost of the rare earth separation system is approximately $30 million. The most capital intensive process area is the evaporator-condenser associated with the acid recovery system, which accounts for approximately half of the total direct capital costs of the system. The evaporator-condenser is used to recover nitric acid from the leaches stream and reduces the annual operating expenses associated with reagent cost. The filter system, electrostatic precipitator, and rotary dryer are also capital intensive processes totaling approximately $10 million.

Table 15: Installed costs for major process areas of the rare earth separation plant.

Direct Costs for All Major Process Areas ($1000, 2015)			
Coal Ash Handling	$350	Evap. Condenser	$15,200
Pre-treatment water wash	$590	Roaster Condenser	$310
Leach Reactor	$230	Reactor Feed pump	$30

[8] Tribe, M. A., & Alpine, R. L. (1986). Scale economies and the "0.6 rule". *Engineering costs and production economies*, 271-278.

Knockout Vessel	$230	Reactor Recirc. Pump	$30
Filter	$4,870	Column Sump Pump	$20
Rotary Dryer	$2,670	Filter Pump	$30
Crystalizer/Custom Rotary Dryer	$1,050	Evaporator Feed Pump	$10
Column	$210	Acid Recycle Pump	$10
ESP	$2,490	Acid Makeup Pump	$10
Reactor Heat Exchanger	$300	Column Blower	$10
Column Heat Exchanger	$210	Distillation Column	$390
Process Facilities Capital			**~$29,900**

In addition to the Process Facilities Capital costs, there are a number of other capital cost items (often referred to as indirect costs) that are applied. Traditionally, these are estimated as percentages of the total PFC. These additional costs are divided into the following categories:

- Engineering and home office fees (EHO)
- General facilities capital (GFC)
- Process contingency
- Process contingency
- Royalty charges

The sum of these costs, called the total plant cost (TPC), is developed on the basis of overnight construction. Overnight cost is the cost of a construction project if no interest was incurred during construction, as if the project was completed "overnight." (Stoft, 2002) These costs are summarized in Table 16.

Table 16: Summary of estimated direct and indirect capital costs for a FOAK rare earth separation process. These costs are the basis for estimating the total plant cost—a major component of the total capital requirement of the plant.

Capital cost elements	**Nominal Value**	**Component Cost ($Million, 2015)**
Process Facilities Capital (PFC)		$29.9
Engineering and Home Office Fees	7% PFC	$2.0
General Facilities	10% PFC	$2.9
Project Contingency	40% PFC	$14.9
Process Contingency	70% PFC	$20.9
Total Plant Cost (TPC) = Sum of the above		**$72.7**

General facilities capital (GFC) is the capital required for the construction of general facilities such as buildings, roads, shops, etc. This cost is usually estimated to be between 5 and 20% of the PFC. Engineering and home office overhead is included if the cost estimates for the general facilities capital do not include these fees as part of the equipment costs. For these fees, 7 and 15% of the PFC is typical. Royalty charges are included as indirect capital costs and typically range from 1 to 10% of PFC.

The EPRI TAG method uses two types of contingencies: the process contingency and the project contingency. The process contingency is a capital cost contingency factor applied to a new technology in an effort to quantify the uncertainty in the technical performance and cost of commercial scale equipment[9]. Therefore, a higher process contingency factor is used for more basic cost estimates. Table 17 shows how the maturity of the technical design influences the process contingency.

Table 17: Process contingency cost guidelines[10].

Technology status	Process contingency cost (%PFC)
New concept with limited data	40+
Concept with bench-scale data	30-70
Small pilot plant data	20-35
Full-sized modules have been operated	5-20
Process is used commercially	0-10

EPRI recommends that separate process contingencies be given for each major process systems. For the REE separation and concentration processes, this work uses a default process contingency of 70% based on the higher value for a technology concept with bench-scale data. As limited laboratory testing has been conducted to date, this contingency factor is used as a conservative estimate of the financial risk associated with process development. Where this work examines the costs of the fully integrated REE supply train, this work uses a default process contingency of 10% for systems outside the bounds of the separation and concentration processes. As process development continues, reductions in the required TPC are expected.

The project contingency is a capital cost contingency factor that is intended to cover the cost of additional equipment or other costs that would result from a more detailed design of a definitive project specific to the actual site[5]. Specifically, the project contingency addresses the need for site preparation, building construction, ancillary process equipment, structural support, and miscellaneous equipment required when the actual plant is built. Table 18 lists the project contingency cost guidelines as suggested by EPRI. This work uses a simplified design intended to be applicable for a range of equipment options.

Table 18: Project contingency costs[6]. The contingency costs are compared to the American Association of Cost Engineers (ACEE) technology Class ranking system.

EPRI cost calculation	Design effort	Project contingency
Class I (~AACE Class 5/4)	Simplified	30-50
Class II (~AACE Class 3)	Preliminary	15-30
Class III (~AACE Class 3/2)	Detailed	10-20

[9] Electric Power Research Institute (EPRI). (1986). *Technical Assessment Guide (TAG) Vol. 1: Electricity supply.* Palo alto: Electric Power Research Institute.

[10] Electric Power Research Institute (EPRI). (1993). *TAG(tm) Technical Assessment Guide Volume 1: Electricity Supply.* Palo Alto: EPRI.

Class IV (~AACE Class 1)	Finalized	5-10

Like the process contingency, EPRI recommends that project contingencies be applied for each plant selection and this work uses finalized design effort values for each supply chain step outside of the separation and concentration process. In regards to Battelle's separation and concentration process, a project contingency factor of 40% is used as the default value. This contingency was selected based on the limited laboratory test data collected to date combined with inherent uncertainty for early stage technology development.

The total capital requirement (TCR) includes all the capital necessary to complete the entire project. These items include:

- Total plant cost (TPC)
- Allowance for funds used during construction (AFUCC)
- Prepaid royalties
- Inventory capital
- Pre-production costs

Table 19 summarizes the steps required to calculate the total capital requirement. The total capital requirement for the rare earth separation process is approximately $70 million. This includes all direct and indirect capital costs associated with the project.

Table 19: Indirect capital costs for a FOAK rare earth element separation plant.

Capital cost elements	Nominal Value	Component Cost ($1000, 2015
Total Plant Cost (TPC)		**$68,500**
AFUDC (interest during construction)	% TPC	$343
Royalty Fees	0.5% PFC	$145
Pre-Production (fixed)	1 month fixed O&M	$390
Pre-production (variable)	1 month variable O&M	$406
Inventory Capital	0.5% TPC	$343
Total Capital Requirement (TCR)		**$70,200**

Operating Costs

The operating and maintenance (O&M) costs are usually estimated for one year of operation. These can be divided into fixed O&M and variable O&M costs. These costs are discussed in this section. Note that all reference costs are adjusted to 2015 dollars from the source year using the SRI Chemical Engineer Handbook Price Index.

The fixed O&M (FOM) costs include the costs of plant maintenance (materials and labor) and labor (operating labor, administrative, and support labor). Operating labor costs are estimated based on correlations between labor hour requirements and the plant's daily capacity[11].

Table 20: Fixed operating and maintenance cost parameters and their deterministic values.

Fixed O&M Costs	Units	Nominal Value
Major processing steps	#	9
Cor'l'n for Op. Labor	Hrs./day-step	14
Operating Labor Rate	$/hr	$34.65
Total Maintenance Cost	%TPC	2.5%
Maint. Cost allocated to labor	% FOM maint.	40%
Admin. & Support labor cost	% total labor	30%

The variable O&M (VOM) costs include the cost of materials consumed (make-up acid, process water, etc.), utilities, and services used (waste transport and disposal). These quantities are determined in the CHEMCAD performance model. The unit cost of each item (e.g. dollars per tonne of coal ash or dollars per tonne of transported REE concentrate) is a parameter specified as a cost input to the model. The total annual cost of each item is then calculated by multiplying the unit cost by the total annual quantity used or consumed. Total annual quantities are dependent upon the facility's annual operating capacity factor. The individual components of variable O&M costs are explained in more detail below. Note that the unit costs for all of the consumables are based on publicly available sources.

Table 21: Variable operating and maintenance cost components and their deterministic values.

Variable O&M Costs	Units	Nominal Value
Coal Ash	$/tonne	$-
Makeup Nitric Acid	$/tonne	$600
Dilution Water	$/tonne	$0.3
Leached Ash Disposal	$/tonne	$10.3
Natural Gas	$/GJ	$1.26
Electricity	$/MWh	$6.36
Avg. Price for Salable Byproduct	$/tonne	$(30.00)

The nominal (default) values of all major operating and maintenance (O&M) costs in the REE separation and concentration process model are summarized in Table 22. Note that the cost of coal ash is zero for the deterministic case.

Table 22: Variable and fixed operating cost component results for a rare earth separation plant.

Variable Cost Component	**Variable O&M Cost ($1000/yr)**	**Fixed Cost Component**	**Fixed O&M Cost ($1000/yr, 2015)**
Coal Ash	$0	Operating Labor	$2,130
Makeup Nitric Acid	$3,820	Maintenance Material	$1,770
Makeup Water	$4	Maintenance Labor	$710
Solid waste disposal	$880	Admin. & Support Labor	$850

[11] Peters, T., Timmerhaus, K., & West, R. (2003). *Plant Design and Economics for Chemical Engineers* (5th ed.). New York: McGraw Hill.

Natural Gas	$60	**REE Process Total Fixed Costs ($1000/yr)**	**$5,470**
Electricity	$440		
REE Process Total Variable Costs ($/yr)	**~$5,210**	**Total O&M Costs ($/yr)**	**~$11,000**

A robust way to evaluate the cost of resource intensive processes such as REE processing systems is to normalize the cost of production on the basis of incoming coal ash ($/tonne feedstock) and outgoing rare earth product ($/kg elemental product). The normalized cost, also known as the Levelized Cost of Production (LCOP), represents the income that the processing facility would need to receive from the sale of products to fully recover all capital and operating costs, while earning a specified rate of return over the plant life. The LCOP is calculated first by quantifying the annual revenue requirement as shown in Equation 1.

Equation 1:

$$Total\ annual\ revenue\ requirement\ \left(\frac{\$}{yr}\right) = TCR * FCF + Fixed\ O\&M + Variable\ O\&M + Byproduct\ credits$$

Financial parameters such as the annual rate of return, plant life, and other plant assumptions are embedded in the fixed charge factor (FCF) to annualize the total capital costs. Thus, the reported value represents the "levelized" annual revenue stream, defined as the uniform yearly revenue stream that a processing facility must realize from the sale of REE concentrate to produce the same net present value as a stream of variable year-to-year costs over the life of the plant.

A summary of the levelized production costs reported on the basis of the ash feedstock and mixed rare earths products (sold as oxides) is shown in Table 23. Note that these results represent the costs if a plant were constructed immediately using the current understanding of the process (i.e. FOAK plant).

Table 23: Cost model results using FOAK plant assumptions. These costs represent the cost of producing rare earths using the current understanding of the rare earth process.

Cost Component	$Million per year (2015)	$/tonne Coal Ash Processed	$/kg REE oxides
Annual Fixed Cost	$5.4	$29	$109
Annual Variable Cost	$5.2	$28	$104
Annualized Capital Cost	10.0	$56	$208
By-Product Credits	$(2.1)	($11)	($40)
Total Annual Revenue Requirement	**$19.1**	**$103**	**$382**

The cost of production will undoubtedly decrease as improvements are made to the process. The cost of production for a mature version of this design may be estimated by lowering the process and project contingency costs to 10% and adjusting the financial assumptions to reflect a low risk, NOAK plant. The cost results using these assumptions are shown in Table 24.

Table 24: Cost model results using n^{th}-of-a-kind plant assumptions. These costs represent the cost of producing rare earths from coal ash given an improved understanding of the separation process.

Cost Component	$Million per year (2015)	$/tonne Coal Ash Processed	$/kg REE oxides

Annual Fixed Cost	$3.6	$20	$92
Annual Variable Cost	$5.2	$28	$133
Annualized Capital Cost	4.7	$26	$122
By-Product Credits	$(2.0)	($11)	($97)
Total Annual Revenue Requirement	**$11.6**	**$62**	**$295**

5.3 Sensitivity Analysis

The deterministic FOAK and NOAK cases presented above reflect specific sets of parameters believed to be representative of the conceptualized process. A sensitivity analysis is able to be conducted through evaluation of a population of parameter values. This was the objective of the deterministic exercise in the previous section. However, if one considers the population of potential parameter values for this process than most of the parameters are better represented as ranges of values (or probability distributions) in lieu of deterministic values. Various combinations of these parameter values then represent a set of possible configurations for the rare earth separation process.

In practice, the values of the cost parameters are not all completely independent of one another. Moreover, some parameters are more uncertain than others. Thus, several analyses are used to characterize the uncertainty regarding the cost of a full-scale system. First, a probabilistic analysis was undertaken to more realistically characterize the range of key system cost parameters relative to the deterministic results presented in the previous section. For the sake of brevity, details regarding the uncertainty parameters, their distributions, and referenced sources are listed in Appendix A3 rather than in this section.

The uncertainty distributions developed for the cost model parameters based on vendor quotes and current literature and reflect both uncertainty and/or variability in the model parameters for indirect costs. The direct cost estimates for each major component of the process (i.e. leach reactor, evaporator condenser, leached ash filter, etc.) contribute to the overall uncertainty of cost estimates for this technology. Data about the variability or uncertainty for direct capital costs are unavailable at this early stage of development and a range of ±10% of the deterministic reference cost is used.

The results represent a range of potentially feasible coal ash-based rare earth separation systems capable of producing a dry rare earth product at a concentration greater than 2%. Figure 13 shows the probabilistic curve obtained by including uncertainty distributions for the cost parameters of the rare earth system for both FOAK and NOAK systems.

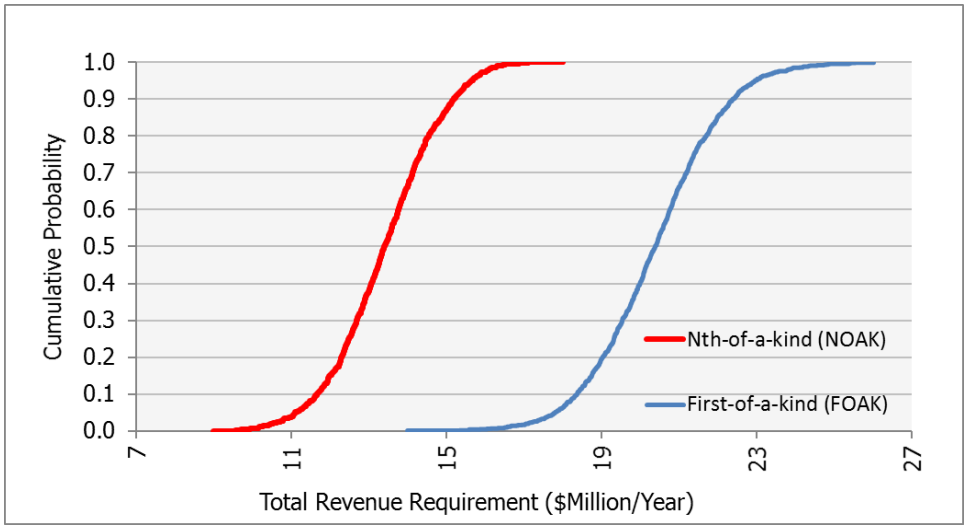

Figure 13: Cumulative distribution functions for a FOAK and NOAK rare earth separation plant. Theses curves represent the probability of the process having less than a given total revenue requirement.

Table 25 summarizes the probabilistic results for both a FOAK and NOAK system by looking at three representative data points for each system representing the 90% confidence interval and median value. The parameters exhibiting the most influence on the distribution mean are the total maintenance cost (expressed as a percentage of the total plant cost), the coal ash cost, and the labor correlation per processing step (hours per day per process step).

Table 25: Summary data for the probabilistic uncertainty cost distributions representing the 90th percential, mean and median. All dollars are expressed in 2015 U.S. dollars.

Total Annual Revenue Requirement Probability Estimates		
Uncertainty Scenario	Median Cost (50th percentile), ($Million)	Cost Range (5th and 95th percentile), ($Million)
First-of-a-kind	$20.4	$18.0 – 22.9
Nth-of-a-kind	$13.4	$11.1 – $15.6

The parameter with the greatest influence on the total annual revenue requirement calculation is the influence of total maintenance cost as a percentage of the total plant cost. This parameter is important because of its influence on the total maintenance material and maintenance labor.

5.4 Deterministic Case Results Discussion

Several scenarios which were evaluated as part of the TEA were found to suggest profitable operation of Battelle's REE recovery process as feasible. Plant revenue requirements presented in Table 23 and Table 24 were compared against the value of coal sources (modified to reflect the combustion process) compiled using data from the CoalQual database and REE market price information (see Section 3.0). These data are presented in the histograms shown in Figure 14 and Figure 15. On the "x" axis of the histograms, the value of REEs in the coal source (on a per tonne of ash basis) is shown. On the "y" axis, the number of coal sources which the given value is displayed. Note that on each histogram, outliers which are exceptionally high in value (up to $630/tonne) exist. It is important to note that these charts and

the analysis only pertain to the costs of the acid digestion process, where there will be other steps to convert the product to a purified, salable commodity.

Figure 14 shows the value of potential coal sources using current market pricing for both a FOAK and a NOAK plant. With a FOAK plant, economical operation scenarios exist with approximately 5% of coal feedstocks, while with a NOAK plant, approximately 20% of coal sources result in economical REE recovery scenarios. Figure 15 shows a similar set of scenarios, but utilizes historical high REE prices. Under this set of conditions, 25% of coal sources are economical with a FOAK plant, while almost half of all coal sources are able of sustaining economical recovery operations when a NOAK plant is considered. These results are also summarized in Table 26.

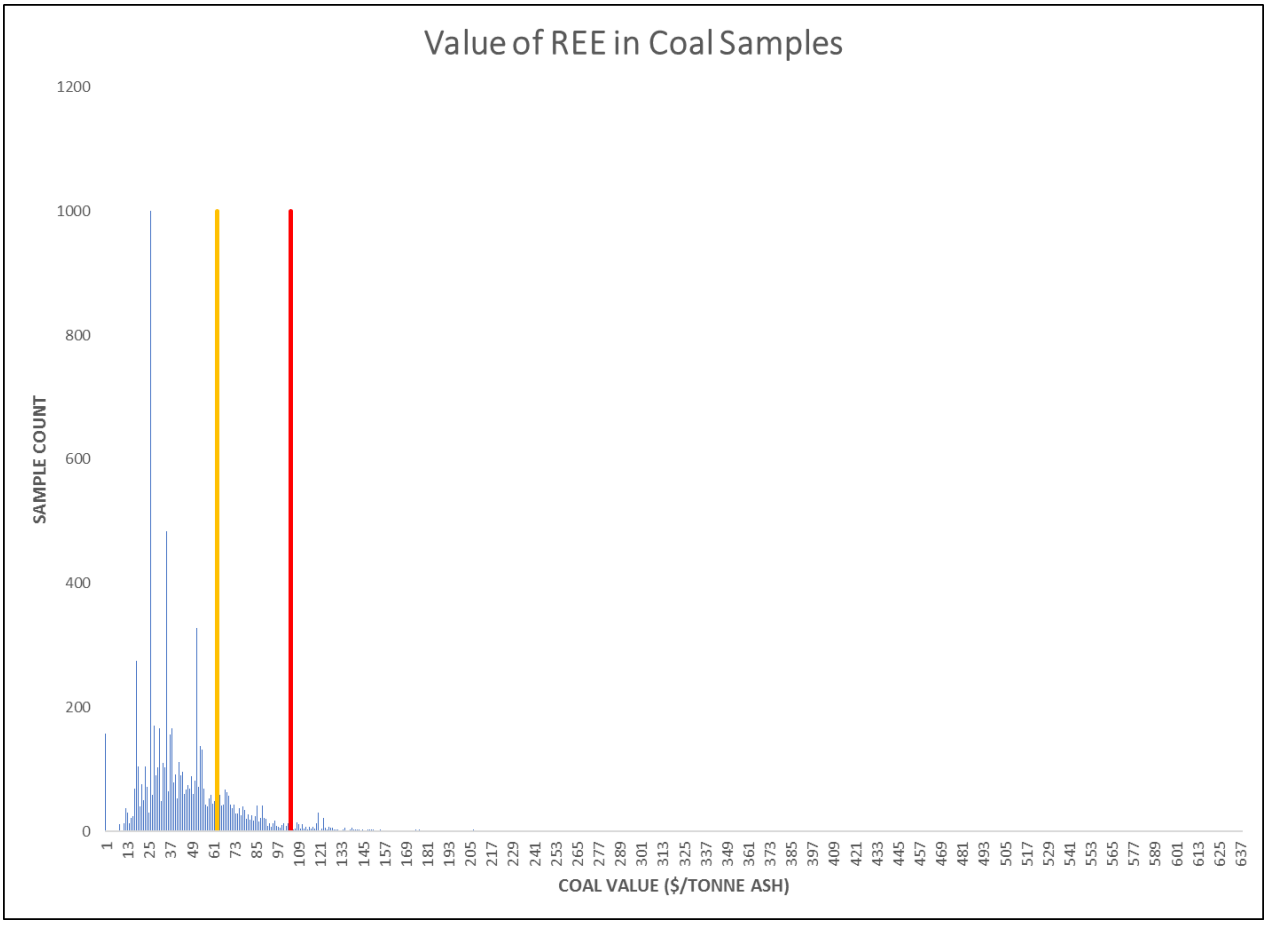

Figure 14: Histogram of REE value in coal sources using current market pricing, obtained from CoalQual database. Coal sources to the right of the red line are considered economical sources for a FOAK plant, while those to the right of the orange line are economical for a NOAK plant.

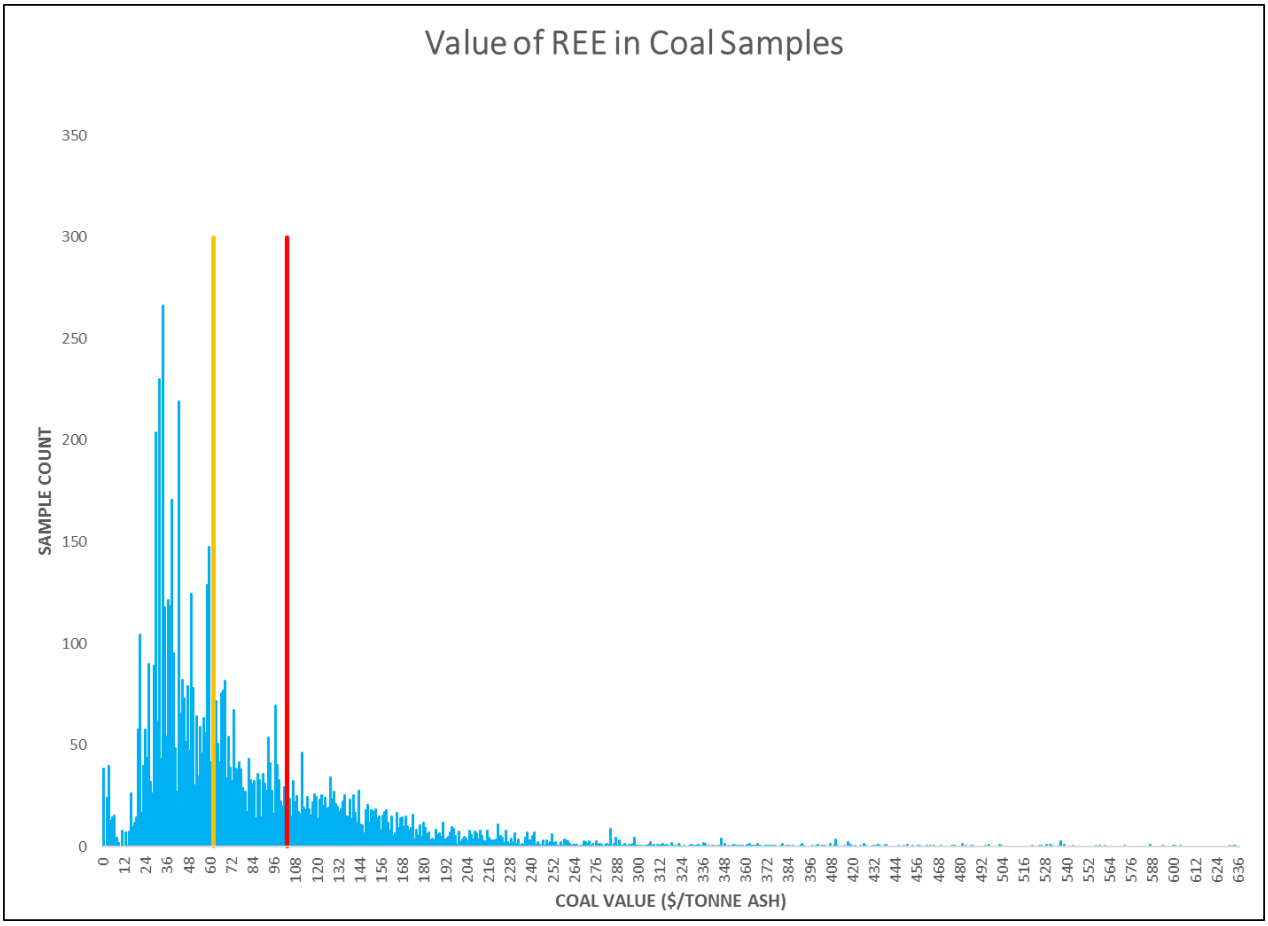

Figure 15: Histogram of REE value in coal sources using high value market pricing, obtained from CoalQual database. Coal sources to the right of the red line are considered economical sources for a FOAK plant, while those to the right of the orange line are economical for a NOAK plant.

Table 26: Summary of viable coal sources for FOAK and NOAK plants under current and high REE pricing environments.

Summary of Viable Coal Sources			
Scenario	Revenue Requirement ($/tonne Coal Ash Processed)	Percentage of Viable Coal Sources, Current Prices	Percentage of Viable Coal Sources, Historical High Prices
First-of-a-kind	103	5	25
Nth-of-a-kind	62	20	47

As with any processing plant, it is expected that additional costs associated with construction of a FOAK process will result in higher operating costs and reduced profitability. This is reflected in our analysis, as NOAK plants show promise as being a more profitable venture than the first plant. It should also be noted that current REE prices used in this analysis represent a near historical low, and that even with these low price conditions, economically feasible scenarios exist for recovery of REEs from coal ash. Should import of REEs from overseas become restricted, it can be reasonably assumed that REE prices would climb

(possibly near their historical high prices, as they did in 2010), which only further supports economical operation of Battelle's REE recovery process.

6.0 Conclusions and Next Steps

The results of the feasibility study indicate that a rare earth recovery process based on Battelle's Acid Digestion Process will be capable of recovering rare earth elements from coal ash generated by power generation facilities under a variety of economic conditions utilizing a variety of feedstock coals. The feasibility study results indicate that when a FOAK plant is considered, approximately 5% of coal sources contain sufficient rare earth material to support an economical recovery plant, while 20% of coal sources may sustain a NOAK plant at current REE market prices. Considering historical high REE prices, which may again be seen if import restrictions occur, more than 25% of coal sources can be treated with a FOAK plant, and more than 47% of sources with an NOAK plant.

Task 4 of this project includes the process design task. As part of this task, laboratory testing will be conducted to inform the process design. It is expected that a large portion of the laboratory testing will be in support of the reactor design. Several process variables which impact leaching efficiency, including type of reactor, pretreatment (crushing, water wash, etc.), and reaction conditions will be optimized to maximize rare earth recovery and will be scaled for a continuous demonstration system. Additional laboratory testing may be conducted to support other areas of process design, such as the roasting and acid recovery process. Testing would be specifically conducted to evaluate means to increase the concentration of REEs in the product stream in anticipation of the downstream need for separation and purification of REE into salable products.

A process design package will be generated which reflects the results of all laboratory testing conducted as part of this phase. The design package will include an updated process flow diagram, updates to mass and energy balances, a process description for the continuous, bench-scale demonstration system, a process and instrumentation diagram, an equipment list, and identification of any environmental, utility, or other process requirements. At this point, the TEA will be updated to reflect any relevant information collected during the process design task.

This report is the basis of the projects "GO/NO GO" decision point as defined in the Statement of Project Objectives. Based on the results of the feasibility study, it has been determined that an economically viable plant capable of recovering REEs from ash generated at power generation facilities is feasible. The plant is capable of producing a REE concentrate stream greater than 2% in concentration of REEs. Battelle's previous Sampling and Characterization report indicates that feedstocks are available for such a plant which contain greater than 300 ppm REEs. With these criteria satisfied, Battelle recommends that a "GO" decision be made, and that this project proceeds into the process design task.

A.1 CHEMCAD Modeling

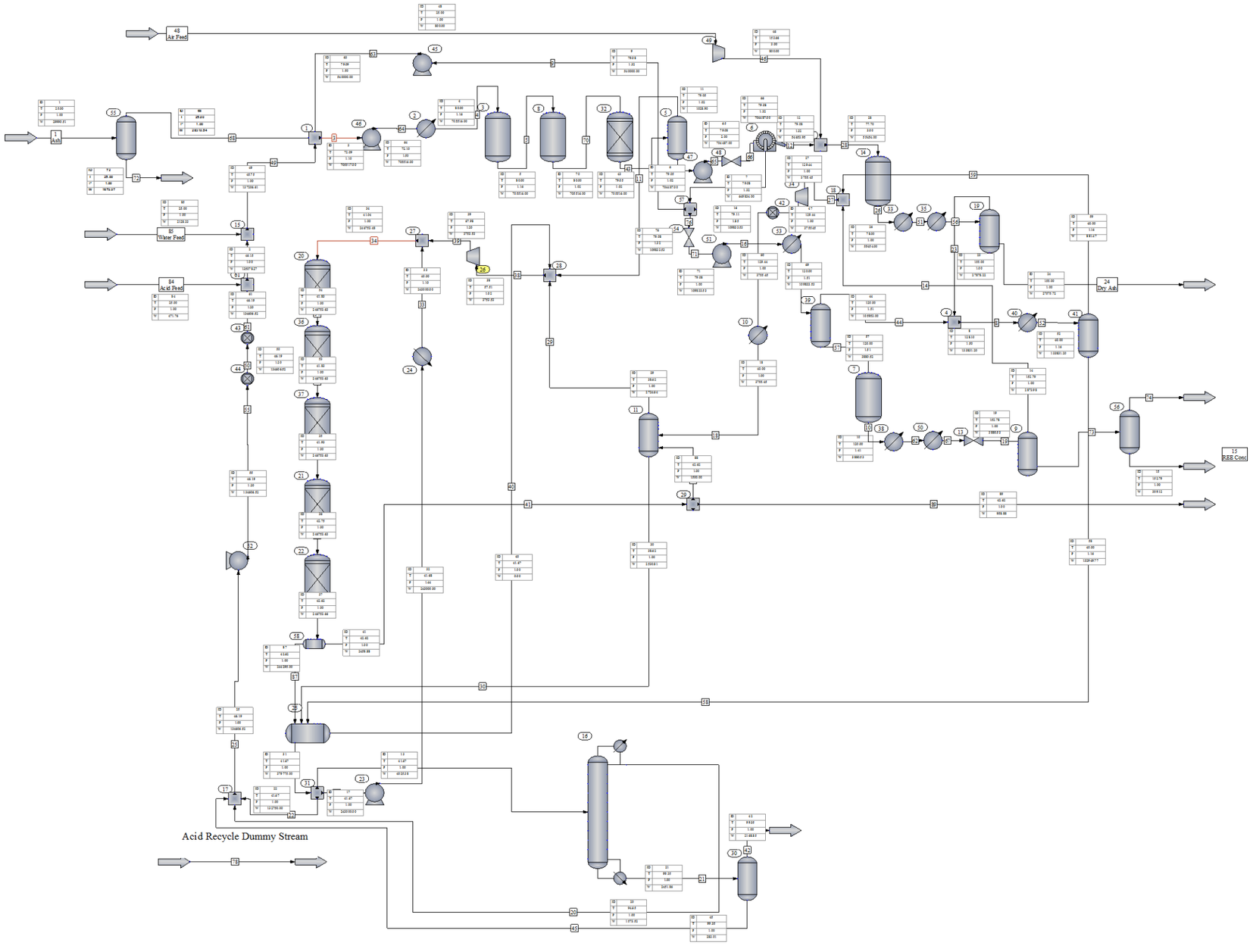

Simulation: REE Base V12

EQUIPMENT SUMMARIES

Mixer Summary

Equip. No.	1	4	12	15	17	18	27	28	61
Name									
Output Pressure atm	1.1	1.5	3				1	1.02	

Heat Exchanger Summary

Equip. No.	2	10	24	33	35	38	40	50	53
Name									
1st Stream dp atm	0.34		0.34				0.34		0.34
1st Stream T Out C	80	40	40		155		40	155	120
Input heat duty kJ/h				-2.80E+06		-270400			
Calc Ht Duty kJ/h	1.88E+07	-2.51E+06	-1.38E+06	-2.80E+06	5.31E+07	-270400	-2.56E+08	936623	1.90E+08
LMTD Corr Factor	1	1	1	1	1	1	1	1	1
1st Stream Pout atm	1.16	1	1.1	1	1	1.41	1.16	1.41	1.51
P1 out specifed atm	1.16	1	1.1	1	1	1.41	1.16	1.41	1.51

Equilibrium Reactor Summary

Equip. No.	3	7	8	14
Name				
Thermal mode	1	2	2	2
Pressure Drop atm		0.1	0.14	2
Temperature C	79.9991	120	80	78
Heat duty kJ/h		-4.60E+08	6.04E+08	-1.14E+08
Reaction phase	2	2	2	2
No of Reactions	16	2	20	2
Calc IG Ht of Rxn (kJ/h)	-13601.53	-4.62E+08	6.03E+08	-1.15E+08
Calc Liq H of Rxn (kJ/h)	8006.0981	-4.62E+08	6.03E+08	-1.15E+08

Reaction Stoichiometrics and Parameters for unit no. 3

Reaction no.	1	2	3	4
Base component	45	60	26	8
Frac.conversion	0.132	0.2158	0.1524	0.1774
Comp	45	60	26	8
Stoic. coeff.	-1	-1	-1	-1
Comp	37	37	37	37
Stoic. coeff.	-6	-6	-6	-4
Comp	44	61	25	7
Stoic. coeff.	2	2	2	1
Comp	57	57	57	57
Stoic. coeff.	3	3	3	2
Reaction no.	5	6	7	8
Base component	40	35	43	17
Frac.conversion	0.1705	0.1776	0.1928	0.1989
Comp	40	35	43	17
Stoic. coeff.	-1	-1	-1	-1
Comp	37	37	37	37
Stoic. coeff.	-6	-6	-6	-6
Comp	39	34	42	16
Stoic. coeff.	2	2	2	2
Comp	57	57	57	57
Stoic. coeff.	3	3	3	3
Reaction no.	9	10	11	12
Base component	19	50	13	23
Frac.conversion	0.2184	0.2087	0.2125	0.2145
Comp	19	50	13	23
Stoic. coeff.	-1	-1	-1	-1
Comp	37	37	37	37
Stoic. coeff.	-6	-6	-6	-6
Comp	18	49	12	22
Stoic. coeff.	2	2	2	2
Comp	57	57	57	57
Stoic. coeff.	3	3	3	3
Reaction no.	13	14	15	16
Base component	15	54	59	30
Frac.conversion	0.2088	0.1999	0.1836	0.1802
Comp	15	54	59	30
Stoic. coeff.	-1	-1	-1	-1
Comp	37	37	37	37
Stoic. coeff.	-6	-6	-6	-6

Comp	14	53	58	29
Stoic. coeff.	2	2	2	2
Comp	57	57	57	57
Stoic. coeff.	3	3	3	3

Reaction Stoichiometrics and Parameters for unit no. 7

Reaction no.	1	2
Base component	74	70
Frac.conversion	0.95	0.95
Comp	74	1
Stoic. coeff.	-2	1
Comp	37	37
Stoic. coeff.	6	6
Comp	24	57
Stoic. coeff.	1	-3
Comp	57	70
Stoic. coeff.	-3	-2

Reaction Stoichiometrics and Parameters for unit no. 8

Reaction no.	1	2	3	4
Base component	1	3	4	6
Frac.conversion	0.0878	1	0.1364	0.438
Comp	1	3	4	6
Stoic. coeff.	-1	-1	-1	-1
Comp	37	37	37	37
Stoic. coeff.	-6	-2	-2	-2
Comp	70	57	64	65
Stoic. coeff.	2	-2	1	1
Comp	57	71	57	57
Stoic. coeff.	3	2	1	1
Comp	0	63	0	0
Stoic. coeff.		1		
Reaction no.	5	6	7	8
Base component	10	11	24	20
Frac.conversion	0.1286	0.2742	0.049	0.2297
Comp	10	11	24	20
Stoic. coeff.	-1	-1	-1	-1

Comp	37	37	37	37
Stoic. coeff.	-2	-2	-6	-6
Comp	72	73	74	75
Stoic. coeff.	1	1	2	2
Comp	57	57	57	57
Stoic. coeff.	1	1	3	3
Reaction no.	9	10	11	12
Base component	38	28	31	32
Frac.conversion	0.0992	0.2251	0.1863	0.1535
Comp	38	28	31	32
Stoic. coeff.	-1	-1	-1	-1
Comp	37	37	37	37
Stoic. coeff.	-2	-2	-2	-2
Comp	66	81	67	76
Stoic. coeff.	2	2	1	1
Comp	57	57	57	57
Stoic. coeff.	1	1	1	1
Reaction no.	13	14	15	16
Base component	36	27	41	2
Frac.conversion	0.1418	0.2453	0.0783	0.3009
Comp	36	27	41	2
Stoic. coeff.	-1	-1	-1	-1
Comp	37	37	37	37
Stoic. coeff.	-2	-2	-2	-4
Comp	77	78	82	83
Stoic. coeff.	1	1	2	1
Comp	57	57	57	68
Stoic. coeff.	1	1	1	4
Comp	0	0	0	57
Stoic. coeff.				2
Reaction no.	17	18	19	20
Base component	47	52	55	62
Frac.conversion	0.2193	0.1178	0.2003	0.2596
Comp	47	52	55	62
Stoic. coeff.	-1	-1	-1	-1
Comp	37	37	37	37
Stoic. coeff.	-2	-4	-4	-2
Comp	84	85	79	80
Stoic. coeff.	1	1	1	1
Comp	57	57	68	57
Stoic. coeff.	1	2	2	1
Comp	0	0	57	0
Stoic. coeff.			2	

Reaction Stoichiometrics and Parameters for unit no. 14

Reaction no.	1	2
Base component	74	70
Frac.conversion	0.95	0.95
Comp	74	1
Stoic. coeff.	-2	1
Comp	37	37
Stoic. coeff.	6	6
Comp	24	70
Stoic. coeff.	1	-2
Comp	57	57
Stoic. coeff.	-3	-3

Flash Summary

Equip. No.	5	9	11	19	25	39	41	58
Name								
Param 1		1	40				1	
Param 2			1					

K values:								
Aluminum Oxide	1.00E-10	1.00E-10	1.00E-10	1.00E-10	1.00E-10	1.00E-10	1.00E-10	1.00E-10
Antimony Trioxi	1.00E-10	1.00E-10	1.00E-10	1.00E-10	1.00E-10	1.00E-10	1.00E-10	1.00E-10
Arsenic Oxide	1.00E-10	1.00E-10	1.00E-10	1.00E-10	1.00E-10	1.00E-10	1.00E-10	1.00E-10
Barium Oxide	1.00E-10	1.00E-10	1.00E-10	1.00E-10	1.00E-10	1.00E-10	1.00E-10	1.00E-10
Boron Trioxide	1.00E-10	1.00E-10	1.00E-10	1.00E-10	1.00E-10	1.00E-10	1.00E-10	1.00E-10
Calcium Oxide	1.00E-10	1.00E-10	1.00E-10	1.00E-10	1.00E-10	1.00E-10	1.00E-10	1.00E-10
Cerium Nitrate	9.68E-08	9.87E-08	9.87E-08	9.87E-08	9.87E-08	6.54E-08	8.51E-08	9.87E-08
Cerium Oxide	1.00E-10	1.00E-10	1.00E-10	1.00E-10	1.00E-10	1.00E-10	1.00E-10	1.00E-10
Chromium(III) O	1.00E-10	1.00E-10	1.00E-10	1.00E-10	1.00E-10	1.00E-10	1.00E-10	1.00E-10
Cobalt(II) Oxid	1.00E-10	1.00E-10	1.00E-10	1.00E-10	1.00E-10	1.00E-10	1.00E-10	1.00E-10
Copper(II) Oxid	1.00E-10	1.00E-10	1.00E-10	1.00E-10	1.00E-10	1.00E-10	1.00E-10	1.00E-10
Dysprosium Nitr	9.68E-08	9.87E-08	9.87E-08	9.87E-08	9.87E-08	6.54E-08	8.51E-08	9.87E-08
Dysprosium Oxid	1.00E-10	1.00E-10	1.00E-10	1.00E-10	1.00E-10	1.00E-10	1.00E-10	1.00E-10
Erbium Nitrate	9.68E-08	9.87E-08	9.87E-08	9.87E-08	9.87E-08	6.54E-08	8.51E-08	9.87E-08
Erbium Oxide	1.00E-10	1.00E-10	1.00E-10	1.00E-10	1.00E-10	1.00E-10	1.00E-10	1.00E-10
Europium Nitrat	9.68E-08	9.87E-08	9.87E-08	9.87E-08	9.87E-08	6.54E-08	8.51E-08	9.87E-08

Europium Oxide	1.00E-10	1.00E-10	1.00E-10	1.00E-10	1.00E-10	1.00E-10	1.00E-10	1.00E-10
Gadolinium Nitr	9.68E-08	9.87E-08	9.87E-08	9.87E-08	9.87E-08	6.54E-08	8.51E-08	9.87E-08
Gadolinium Oxid	1.00E-10	1.00E-10	1.00E-10	1.00E-10	1.00E-10	1.00E-10	1.00E-10	1.00E-10
Gallium(III) Ox	1.00E-10	1.00E-10	1.00E-10	1.00E-10	1.00E-10	1.00E-10	1.00E-10	1.00E-10
Germanium Dioxi	1.00E-10	1.00E-10	1.00E-10	1.00E-10	1.00E-10	1.00E-10	1.00E-10	1.00E-10
Holmium Nitrate	9.68E-08	9.87E-08	9.87E-08	9.87E-08	9.87E-08	6.54E-08	8.51E-08	9.87E-08
Holmium Oxide	1.00E-10	1.00E-10	1.00E-10	1.00E-10	1.00E-10	1.00E-10	1.00E-10	1.00E-10
Iron(iii) oxide	1.00E-10	1.00E-10	1.00E-10	1.00E-10	1.00E-10	1.00E-10	1.00E-10	1.00E-10
Lanthanum Nitra	9.68E-08	9.87E-08	9.87E-08	9.87E-08	9.87E-08	6.54E-08	8.51E-08	9.87E-08
Lanthanum Oxide	1.00E-10	1.00E-10	1.00E-10	1.00E-10	1.00E-10	1.00E-10	1.00E-10	1.00E-10
Lead(II) Oxide	1.00E-10	1.00E-10	1.00E-10	1.00E-10	1.00E-10	1.00E-10	1.00E-10	1.00E-10
Lithium Oxide	1.00E-10	1.00E-10	1.00E-10	1.00E-10	1.00E-10	1.00E-10	1.00E-10	1.00E-10
Lutetium Nitrat	9.68E-08	9.87E-08	9.87E-08	9.87E-08	9.87E-08	6.54E-08	8.51E-08	9.87E-08
Lutetium Oxide	1.00E-10	1.00E-10	1.00E-10	1.00E-10	1.00E-10	1.00E-10	1.00E-10	1.00E-10
Magnesium Oxide	1.00E-10	1.00E-10	1.00E-10	1.00E-10	1.00E-10	1.00E-10	1.00E-10	1.00E-10
Manganese(II)Ox	1.00E-10	1.00E-10	1.00E-10	1.00E-10	1.00E-10	1.00E-10	1.00E-10	1.00E-10
Molybdenum Trio	1.00E-10	1.00E-10	1.00E-10	1.00E-10	1.00E-10	1.00E-10	1.00E-10	1.00E-10
Neodymium Nitra	9.68E-08	9.87E-08	9.87E-08	9.87E-08	9.87E-08	6.54E-08	8.51E-08	9.87E-08
Neodymium Oxide	1.00E-10	1.00E-10	1.00E-10	1.00E-10	1.00E-10	1.00E-10	1.00E-10	1.00E-10
Nickel(II) Oxid	1.00E-10	1.00E-10	1.00E-10	1.00E-10	1.00E-10	1.00E-10	1.00E-10	1.00E-10
Nitric Acid	0.856	7.813	0.165	8.262	0.19	2.141	0.152	0.199
Potassium Oxide	1.00E-10	1.00E-10	1.00E-10	1.00E-10	1.00E-10	1.00E-10	1.00E-10	1.00E-10
Praseodymium Ni	9.68E-08	9.87E-08	9.87E-08	9.87E-08	9.87E-08	6.54E-08	8.51E-08	9.87E-08
Praseodymium Ox	1.00E-10	1.00E-10	1.00E-10	1.00E-10	1.00E-10	1.00E-10	1.00E-10	1.00E-10
Rubidium Oxide	1.00E-10	1.00E-10	1.00E-10	1.00E-10	1.00E-10	1.00E-10	1.00E-10	1.00E-10
Samarium Nitrat	9.68E-08	9.87E-08	9.87E-08	9.87E-08	9.87E-08	6.54E-08	8.51E-08	9.87E-08
Samarium Oxide	1.00E-10	1.00E-10	1.00E-10	1.00E-10	1.00E-10	1.00E-10	1.00E-10	1.00E-10
Scandium Nitrat	9.68E-08	9.87E-08	9.87E-08	9.87E-08	9.87E-08	6.54E-08	8.51E-08	9.87E-08
Scandium(III) O	1.00E-10	1.00E-10	1.00E-10	1.00E-10	1.00E-10	1.00E-10	1.00E-10	1.00E-10
Silicon Dioxide	1.00E-10	1.00E-10	1.00E-10	1.00E-10	1.00E-10	1.00E-10	1.00E-10	1.00E-10
Strontium Oxide	1.00E-10	1.00E-10	1.00E-10	1.00E-10	1.00E-10	1.00E-10	1.00E-10	1.00E-10
Calcium Sulfate	1.00E-20	1.00E-20	1.00E-20	1.00E-20	1.00E-20	1.00E-20	1.00E-20	1.00E-20
Terbium Nitrate	9.68E-08	9.87E-08	9.87E-08	9.87E-08	9.87E-08	6.54E-08	8.51E-08	9.87E-08
Terbium Oxide	1.00E-10	1.00E-10	1.00E-10	1.00E-10	1.00E-10	1.00E-10	1.00E-10	1.00E-10
Titanium Dioxid	1.00E-10	1.00E-10	1.00E-10	1.00E-10	1.00E-10	1.00E-10	1.00E-10	1.00E-10
Thorium(IV) Oxi	1.00E-10	1.00E-10	1.00E-10	1.00E-10	1.00E-10	1.00E-10	1.00E-10	1.00E-10
Thulium Nitrate	9.68E-08	9.87E-08	9.87E-08	9.87E-08	9.87E-08	6.54E-08	8.51E-08	9.87E-08
Thulium Oxide	1.00E-10	1.00E-10	1.00E-10	1.00E-10	1.00E-10	1.00E-10	1.00E-10	1.00E-10
Uranium(IV) Oxi	1.00E-10	1.00E-10	1.00E-10	1.00E-10	1.00E-10	1.00E-10	1.00E-10	1.00E-10
Vanadium(V) Oxi	1.00E-10	1.00E-10	1.00E-10	1.00E-10	1.00E-10	1.00E-10	1.00E-10	1.00E-10
Water	0.441	5.06	0.068	5.363	0.08	1.298	0.063	0.084
Ytterbium Nitra	9.68E-08	9.87E-08	9.87E-08	9.87E-08	9.87E-08	6.54E-08	8.51E-08	9.87E-08
Ytterbium Oxide	1.00E-10	1.00E-10	1.00E-10	1.00E-10	1.00E-10	1.00E-10	1.00E-10	1.00E-10

Yttrium Oxide	1.00E-10	1.00E-10	1.00E-10	1.00E-10	1.00E-10	1.00E-10	1.00E-10	1.00E-10
Yttrium(III) Ni	9.68E-08	9.87E-08	9.87E-08	9.87E-08	9.87E-08	6.54E-08	8.51E-08	9.87E-08
Zinc Oxide	1.00E-10	1.00E-10	1.00E-10	1.00E-10	1.00E-10	1.00E-10	1.00E-10	1.00E-10
Nitrogen Trioxi	14.059	70.321	4.298	73.289	4.768	24.462	3.884	4.922
Barium Nitrate	9.68E-08	9.87E-08	9.87E-08	9.87E-08	9.87E-08	6.54E-08	8.51E-08	9.87E-08
Calcium Nitrate	9.68E-08	9.87E-08	9.87E-08	9.87E-08	9.87E-08	6.54E-08	8.51E-08	9.87E-08
Potassium Nitra	9.68E-08	9.87E-08	9.87E-08	9.87E-08	9.87E-08	6.54E-08	8.51E-08	9.87E-08
Magnesium Nitra	9.68E-08	9.87E-08	9.87E-08	9.87E-08	9.87E-08	6.54E-08	8.51E-08	9.87E-08
Nitrogen Dioxid	9.789	87.101	2.168	92.169	2.462	23.734	1.98	2.56
Sulfuric Acid	1.88E-14	1.05E-03	1.02E-12	2.23E-04	2.15E-18	5.96E-10	9.07E-19	2.97E-18
Aluminum Nitrat	9.68E-08	9.87E-08	9.87E-08	9.87E-08	9.87E-08	6.54E-08	8.51E-08	9.87E-08
Arsenic Acid	0.251	2.313	0.044	2.437	0.051	0.651	0.04	0.053
Cobalt(II) Nitr	9.68E-08	9.87E-08	9.87E-08	9.87E-08	9.87E-08	6.54E-08	8.51E-08	9.87E-08
Copper(II) Nitr	9.68E-08	9.87E-08	9.87E-08	9.87E-08	9.87E-08	6.54E-08	8.51E-08	9.87E-08
Iron(III) Nitra	9.68E-08	9.87E-08	9.87E-08	9.87E-08	9.87E-08	6.54E-08	8.51E-08	9.87E-08
Gallium(III) Ni	9.68E-08	9.87E-08	9.87E-08	9.87E-08	9.87E-08	6.54E-08	8.51E-08	9.87E-08
Mn(II) Nitrate	9.68E-08	9.87E-08	9.87E-08	9.87E-08	9.87E-08	6.54E-08	8.51E-08	9.87E-08
Nickel(II) Nitr	9.68E-08	9.87E-08	9.87E-08	9.87E-08	9.87E-08	6.54E-08	8.51E-08	9.87E-08
Lead(II) Nitrat	9.68E-08	9.87E-08	9.87E-08	9.87E-08	9.87E-08	6.54E-08	8.51E-08	9.87E-08
Uranyl Nitrate	9.68E-08	9.87E-08	9.87E-08	9.87E-08	9.87E-08	6.54E-08	8.51E-08	9.87E-08
Zinc Nitrate	9.68E-08	9.87E-08	9.87E-08	9.87E-08	9.87E-08	6.54E-08	8.51E-08	9.87E-08
Lithium Nitrate	9.68E-08	9.87E-08	9.87E-08	9.87E-08	9.87E-08	6.54E-08	8.51E-08	9.87E-08
Rubidium Nitrat	9.68E-08	9.87E-08	9.87E-08	9.87E-08	9.87E-08	6.54E-08	8.51E-08	9.87E-08
Antimony Pentox	1.00E-10	1.00E-10	1.00E-10	1.00E-10	1.00E-10	1.00E-10	1.00E-10	1.00E-10
Strontium Nitra	9.68E-08	9.87E-08	9.87E-08	9.87E-08	9.87E-08	6.54E-08	8.51E-08	9.87E-08
Thorium(IV) Nit	9.68E-08	9.87E-08	9.87E-08	9.87E-08	9.87E-08	6.54E-08	8.51E-08	9.87E-08
Nitrogen	1.61E+05	1.28E+05	1.16E+05	1.28E+05	1.21E+05	1.05E+05	1.02E+05	1.23E+05
Oxygen	91847.5	1.08E+05	58350.898	1.08E+05	61271.766	73419.172	51440.469	62179.348
Carbon Monoxide	1.11E+05	1.07E+05	79035.93	1.07E+05	82324.695	78902.609	69422.758	83333.25
Methane	65948.156	54226.445	50297.398	54226.449	52262.531	42345.68	44134.938	52855.742
Carbon Dioxide	10279.171	99496.867	2648.972	99496.883	2946.21	26310.916	2396.174	3044.984
N2O4	4.984	21.333	1.699	22.114	1.866	7.969	1.528	1.92
Nitric Oxide	57357.383	52473.832	39537.695	52473.84	41361.949	40024.848	34798.496	41922.055
dinitrogen pent	2.454	12.463	0.715	12.963	0.796	4.381	0.647	0.823
Nitrous Acid	0.065	0.867	8.50E-03	0.921	0.01	0.213	7.94E-03	0.011

Filter Summary

Equip. No.	6
Name	
Filter type	2

Moisture frac.	0.5

Valve Summary

Equip. No.	13	48	54
Name			
Pressure out atm	1		1
Pressure drop atm		0.68	

TOWR Rigorous Distillation Summary

Equip. No.	16
Name	
No. of stages	20
1st feed stage	10
Condenser type	1
Condenser mode	6
Condenser spec.	0.374
Cond comp i	37
Reboiler mode	6
Reboiler spec.	0.957
Reboiler comp i	57
Initial flag	1
Calc cond duty kJ/h	-3.63E+06
Calc rebr duty kJ/h	6.07E+06
Est. Dist. rate (kmol/h)	39.5144
Est. Reflux rate (kmol/h)	139.7848
Est. T top C	33.7304
Est. T bottom C	100.9399
Est. T 2 C	98.3003
Calc Reflux ratio	2.1019
Calc Reflux mole (kmol/h)	94.0289
Calc Reflux mass kg/h	2760.4102
Optimization flag	1

Reactor Summary

Equip. No.	20	21	22	32	36	37
Name						
Thermal mode	0	0	0	1	0	0
Temperature C	41.8278	42.7465	42.6187	79.0508	44.4138	41.9257
Key Component	92	68	91	37	91	93
Frac. Conversion	1	1	1	0.0108	1	1
Calc H of Reac. (kJ/kmol)	-84699	-46495.0039	31199.33	52901.3398	-111261.3	-28020.52
Stoichiometrics:						
Nitric Acid	0.00E+00	4	2	-1.073	0.00E+00	2
Water	0.00E+00	-2	-1	0.522	1	-1
Nitrogen Dioxid	0.00E+00	-4	0.00E+00	0.737	1	0.00E+00
Oxygen	-1	-1	0.00E+00	0.32	0.00E+00	0.00E+00
N2O4	1	0.00E+00	-1.5	0.00E+00	0.00E+00	0.00E+00
Nitric Oxide	-2	0.00E+00	1	0.162	1	0.00E+00
dinitrogen pent	0.00E+00	0.00E+00	0.00E+00	0.073	0.00E+00	-1
Nitrous Acid	0.00E+00	0.00E+00	0.00E+00	0.028	-2	0.00E+00

Pump Summary

Equip. No.	23	45	46	47	51	52
Name						
Output pressure atm	1.44	1.5	1.5	2		1.2
Pressure increase atm					0.85	
Efficiency	0.88	0.88	0.88	0.88	0.88	0.88
Calculated power kJ/h	11115.797	10662.5313	29983.738	74215.6953	10241.216	2800.9045
Calculated Pout atm	1.44	1.5	1.5	2	1.85	1.2
Head m	4.1019	1.7706	3.785	9.3874	8.3612	1.8659
Vol. flow rate m3/h	219.2516	514.0942	646.1183	653.1286	104.5653	121.5411
Mass flow rate kg/h	243000	540000	705516	704487	109833.53	134606.52

Compressor Summary

*** Equip. 26 ***
Warning: Liquid present in compressor inlet.

Equip. No.	26	34	49
Name			
Pressure out atm	1.2	1.4	3
Type of Compressor	1	1	1
Efficiency	0.88	0.75	0.88
Actual power kJ/h	60759.469		100789.31
Cp/Cv	1.3404	1.2076	1.4003
Theoretical power (kJ/h)	53468.332		88694.594
Ideal Cp/Cv	1.3378	1.2026	1.3989
Calc Pout atm	1.2	1	3
Calc. mass flowrate (kg/h)	3754	3755	800
Compressor off	0	1	0

Divider Summary

Equip. No.	29	31	57
Name			
Split based on	3	3	3
Output stream #1	1500		
Output stream #2		243000	540000
Output stream #3		132750	

Component Separator Summary

Equip. No.	30	55	56
Name			
Split Destination	1	1	0
Heat duty kJ/h	138795.25		-33.7619
Component No. 1			1
Component No. 6		1	
Component No. 24			1
Component No. 28		1	
Component No. 37	1		
Component No. 38		1	

Component No. 48		1	

Controller Summary

Equip. No.	42	43	44
Name			
Mode	0	1	1
Output signal		4692.1719	1040.0469
Equip No. adj.	34	0	0
Stream No. adj.	0	85	84
Variable No. adj.	3	6	6
Minimum Value	1		
Maximum Value	1.2		
Unit of Min/Max	4	0	0
Rel Step Size	0.005	0.005	0.005
Tolerance	0.001	0.001	0.001
Iterations	20	20	20

Measured variables:

Independent Type 1	0	0	0
Independent ID 1	16	78	78
Independent Variable 1	1	-257	-237
Independent Operator	0	2	2
Independent Type 2	0	0	0
Independent ID 2	0	50	55
Independent Variable 2	0	-257	-237
Target Units	2	0	0
Target Constant	101		
Measured Comp. A	0	57	37
Measured Comp. B	0	57	37

STREAM PROPERTIES

Stream No.	1	2	3	4
Name	Ash			
- - Overall - -				
Molar flow kmol/h	381.40	5597.14	28510.65	28510.69
Mass flow kg/h	29990.51	135078.27	705517.00	705516.00
Temp C	25.00	46.15	72.09	80.00
Pres atm	1.00	1.00	1.10	1.16
Vapor mole fraction	0.0000	1.672E-006	0.0000	0.0000
Actual dens kg/m3	3273.65	1106.26	1091.93	1084.78
Actual vol m3/h	9.16	122.10	646.12	650.38
Std liq m3/h	9.15	119.76	623.10	623.10
Std vap 0 C m3/h	8548.65	125452.38	639027.75	639028.63
- - Vapor only - -				
Molar flow kmol/h		0.01		
Mass flow kg/h		0.27		
Actual dens kg/m3		1.12		
Actual vol m3/h		0.25		
Std liq m3/h		0.00		
Std vap 0 C m3/h		0.21		
Cp kJ/kg-K		1.04		
- - Liquid only - -				
Molar flow kmol/h	4.98	5597.13	28148.26	28148.30
Mass flow kg/h	677.86	135078.00	677207.00	677206.00
Actual dens kg/m3	5583.29	1108.49	1062.41	1055.37
Actual vol m3/h	0.12	121.86	637.43	641.68
Std liq m3/h	0.12	119.76	614.47	614.46
Std vap 0 C m3/h	111.60	125452.20	630905.19	630906.00
Cp kJ/kg-K	0.06	3.36	3.47	3.48

Stream No.	5	6	7	8
Name				
- - Overall - -				
Molar flow kmol/h	28510.66	28484.12	26995.74	5671.86

Mass flow kg/h	705516.00	704487.00	649834.00	133831.20
Temp C	80.00	79.05	79.08	128.10
Pres atm	1.16	1.02	1.32	1.50
Vapor mole fraction	0.0000	0.0000	0.0000	1.000
Actual dens kg/m3	1084.77	1078.64	1050.39	1.09
Actual vol m3/h	650.39	653.13	618.66	123062.75
Std liq m3/h	623.11	626.09	592.76	120.24
Std vap 0 C m3/h	639027.81	638433.13	605073.00	127127.11
- - Vapor only - -				
Molar flow kmol/h				5671.86
Mass flow kg/h				133831.20
Actual dens kg/m3				1.09
Actual vol m3/h				123062.75
Std liq m3/h				120.24
Std vap 0 C m3/h				127127.11
Cp kJ/kg-K				1.65
- - Liquid only - -				
Molar flow kmol/h	28148.28	28130.97	26995.74	
Mass flow kg/h	677210.00	677160.00	649834.00	
Actual dens kg/m3	1055.36	1050.41	1050.39	
Actual vol m3/h	641.68	644.66	618.66	
Std liq m3/h	614.47	617.69	592.76	
Std vap 0 C m3/h	630905.63	630517.63	605073.00	
Cp kJ/kg-K	3.48	3.50	3.50	

Stream No.	9	10	11	12
Name				
- - Overall - -				
Molar flow kmol/h	22433.00	67.13	33.93	1488.39
Mass flow kg/h	540000.00	3880.53	1028.90	54653.95
Temp C	79.08	120.00	79.05	79.08
Pres atm	1.32	1.41	1.02	1.32
Vapor mole fraction	0.0000	0.9371	1.000	0.0000

Actual dens kg/m3	1050.39	3.02	1.08	1584.97
Actual vol m3/h	514.09	1285.96	957.03	34.48
Std liq m3/h	492.57	2.53	0.92	33.33
Std vap 0 C m3/h	502804.84	1504.62	760.56	33360.17
- - Vapor only - -				
Molar flow kmol/h		57.18	33.93	
Mass flow kg/h		2789.71	1028.90	
Actual dens kg/m3		2.17	1.08	
Actual vol m3/h		1285.35	957.03	
Std liq m3/h		1.97	0.92	
Std vap 0 C m3/h		1281.53	760.56	
Cp kJ/kg-K		1.18	1.16	
- - Liquid only - -				
Molar flow kmol/h	22433.00	3.84		1135.23
Mass flow kg/h	540000.00	393.40		27326.97
Actual dens kg/m3	1050.39	888.83		1050.39
Actual vol m3/h	514.09	0.44		26.02
Std liq m3/h	492.57	0.40		24.93
Std vap 0 C m3/h	502804.84	86.05		25444.69
Cp kJ/kg-K	3.50	32.59		3.50

Stream No.	13	14	15	16
Name			REE Conc	
- - Overall - -				
Molar flow kmol/h	168.00	59.09	1.92	4562.77
Mass flow kg/h	4025.38	2873.98	309.12	109833.53
Temp C	41.67	152.79	152.79	79.11
Pres atm	1.00	1.00	1.00	1.85
Vapor mole fraction	0.0000	1.000	0.0000	0.0000
Actual dens kg/m3	1108.32	1.40	805.04	1050.38
Actual vol m3/h	3.63	2045.63	0.38	104.57
Std liq m3/h	3.58	2.04	0.33	100.19
Std vap 0 C m3/h	3765.55	1324.51	43.07	102268.21

- - Vapor only - -				
Molar flow kmol/h		59.09		
Mass flow kg/h		2873.98		
Actual dens kg/m3		1.40		
Actual vol m3/h		2045.63		
Std liq m3/h		2.04		
Std vap 0 C m3/h		1324.51		
Cp kJ/kg-K		1.25		
- - Liquid only - -				
Molar flow kmol/h	168.00		1.92	4562.77
Mass flow kg/h	4025.38		309.12	109833.53
Actual dens kg/m3	1108.32		805.04	1050.38
Actual vol m3/h	3.63		0.38	104.57
Std liq m3/h	3.58		0.33	100.19
Std vap 0 C m3/h	3765.55		43.07	102268.21
Cp kJ/kg-K	3.38		44.42	3.50

Stream No.	17	18	19	20
Name				
- - Overall - -				
Molar flow kmol/h	10141.80	89.37	67.13	44.74
Mass flow kg/h	243000.00	3755.45	3880.53	1573.52
Temp C	41.67	40.00	152.78	94.65
Pres atm	1.00	1.00	1.00	1.00
Vapor mole fraction	0.0000	0.3622	0.9685	1.000
Actual dens kg/m3	1108.32	4.51	1.90	1.18
Actual vol m3/h	219.25	832.31	2046.17	1334.08
Std liq m3/h	216.11	3.03	2.53	1.21
Std vap 0 C m3/h	227314.83	2003.12	1504.62	1002.68
- - Vapor only - -				
Molar flow kmol/h		32.37	59.09	44.74
Mass flow kg/h		1053.90	2873.98	1573.52
Actual dens kg/m3		1.27	1.40	1.18

Actual vol m3/h		830.33	2045.62	1334.08
Std liq m3/h		1.10	2.04	1.21
Std vap 0 C m3/h		725.44	1324.51	1002.68
Cp kJ/kg-K		1.00	1.25	1.26
- - Liquid only - -				
Molar flow kmol/h	10141.80	57.00	1.92	
Mass flow kg/h	243000.00	2701.55	309.12	
Actual dens kg/m3	1108.32	1363.19	805.05	
Actual vol m3/h	219.25	1.98	0.38	
Std liq m3/h	216.11	1.93	0.33	
Std vap 0 C m3/h	227314.83	1277.69	43.07	
Cp kJ/kg-K	3.38	2.15	44.42	

Stream No.	21	22	23	24
Name				Dry Ash
- - Overall - -				
Molar flow kmol/h	123.27	5540.43	1164.00	355.16
Mass flow kg/h	2451.86	132750.00	27878.22	27575.72
Temp C	99.35	41.67	155.00	155.00
Pres atm	1.00	1.00	1.00	1.00
Vapor mole fraction	0.0000	0.0000	1.000	0.0000
Actual dens kg/m3	983.77	1108.32	0.69	3173.98
Actual vol m3/h	2.49	119.78	40640.79	8.69
Std liq m3/h	2.37	118.06	25.10	8.52
Std vap 0 C m3/h	2762.87	124181.23	26089.46	7960.40
- - Vapor only - -				
Molar flow kmol/h			1164.00	
Mass flow kg/h			27878.22	
Actual dens kg/m3			0.69	
Actual vol m3/h			40640.79	
Std liq m3/h			25.10	
Std vap 0 C m3/h			26089.46	
Cp kJ/kg-K			1.65	
- - Liquid only - -				
Molar flow kmol/h	123.27	5540.43		0.48
Mass flow kg/h	2451.86	132750.00		75.23

Actual dens kg/m3	983.77	1108.32		796.65
Actual vol m3/h	2.49	119.78		0.09
Std liq m3/h	2.37	118.06		0.08
Std vap 0 C m3/h	2762.87	124181.23		10.83
Cp kJ/kg-K	3.97	3.38		45.62

Stream No.	25	26	27	28
Name				
- - Overall - -				
Molar flow kmol/h	5589.66	1519.16	89.37	1516.12
Mass flow kg/h	134606.52	55454.00	3755.45	55454.00
Temp C	46.19	78.00	129.44	77.70
Pres atm	1.00	1.00	1.00	3.00
Vapor mole fraction	1.690E-006	0.04935	1.000	0.02884
Actual dens kg/m3	1105.25	32.97	1.28	156.05
Actual vol m3/h	121.79	1682.01	2934.81	355.36
Std liq m3/h	119.45	33.63	3.03	34.25
Std vap 0 C m3/h	125284.59	34049.86	2003.12	33981.67
- - Vapor only - -				
Molar flow kmol/h	0.01	57.47	89.37	33.54
Mass flow kg/h	0.28	1668.26	3755.45	970.57
Actual dens kg/m3	1.12	1.01	1.28	3.02
Actual vol m3/h	0.25	1648.98	2934.81	321.06
Std liq m3/h	0.00	1.64	3.03	1.06
Std vap 0 C m3/h	0.21	1288.12	2003.12	751.77
Cp kJ/kg-K	1.04	1.20	1.17	1.07
- - Liquid only - -				
Molar flow kmol/h	5589.65	1107.01		1129.42
Mass flow kg/h	134606.25	26285.19		27156.40

Actual dens kg/m3	1107.50	1071.98		1051.10
Actual vol m3/h	121.54	24.52		25.84
Std liq m3/h	119.45	23.54		24.79
Std vap 0 C m3/h	125284.39	24812.16		25314.43
Cp kJ/kg-K	3.36	3.53		3.50

Stream No.	29	30	31	32
Name				
- - Overall - -				
Molar flow kmol/h	84.95	55.92	15850.23	10141.80
Mass flow kg/h	2724.64	2530.81	379775.00	243000.00
Temp C	38.62	38.62	41.67	41.68
Pres atm	1.00	1.00	1.00	1.44
Vapor mole fraction	1.000	0.0000	0.0000	0.0000
Actual dens kg/m3	1.26	1348.18	1108.32	1108.31
Actual vol m3/h	2170.19	1.88	342.66	219.25
Std liq m3/h	2.86	1.84	337.75	216.11
Std vap 0 C m3/h	1904.10	1253.30	355261.56	227314.83
- - Vapor only - -				
Molar flow kmol/h	84.95			
Mass flow kg/h	2724.64			
Actual dens kg/m3	1.26			
Actual vol m3/h	2170.19			
Std liq m3/h	2.86			
Std vap 0 C m3/h	1904.10			
Cp kJ/kg-K	1.00			
- - Liquid only - -				
Molar flow kmol/h		55.92	15850.23	10141.80
Mass flow kg/h		2530.81	379775.00	243000.00
Actual dens kg/m3		1348.18	1108.32	1108.31
Actual vol m3/h		1.88	342.66	219.25
Std liq m3/h		1.84	337.75	216.11
Std vap 0 C m3/h		1253.30	355261.56	227314.83

Cp kJ/kg-K		2.22	3.38	3.38

Stream No.	33	34	35	36
Name				
- - Overall - -				
Molar flow kmol/h	10141.80	10260.69	10253.81	10236.06
Mass flow kg/h	243000.00	246753.48	246753.63	246753.63
Temp C	40.00	41.04	41.93	42.75
Pres atm	1.10	1.00	1.00	1.00
Vapor mole fraction	0.0000	0.009663	0.008660	0.008022
Actual dens kg/m3	1109.42	88.96	98.16	105.14
Actual vol m3/h	219.03	2773.63	2513.76	2346.91
Std liq m3/h	216.11	219.89	219.81	219.66
Std vap 0 C m3/h	227314.83	229979.45	229825.33	229427.48
- - Vapor only - -				
Molar flow kmol/h		99.15	88.80	82.11
Mass flow kg/h		2928.03	2612.01	2392.46
Actual dens kg/m3		1.15	1.14	1.13
Actual vol m3/h		2553.85	2293.59	2126.61
Std liq m3/h		3.17	2.85	2.66
Std vap 0 C m3/h		2222.25	1990.24	1840.48
Cp kJ/kg-K		1.03	1.03	1.04
- - Liquid only - -				
Molar flow kmol/h	10141.80	10161.54	10165.02	10153.95
Mass flow kg/h	243000.00	243825.44	244141.61	244361.00
Actual dens kg/m3	1109.42	1109.37	1108.92	1109.19
Actual vol m3/h	219.03	219.79	220.16	220.31
Std liq m3/h	216.11	216.71	216.96	217.01
Std vap 0 C m3/h	227314.83	227757.17	227835.09	227587.03

Cp kJ/kg-K	3.38	3.37	3.37	3.36
Stream No.	37	38	39	40
Name				
- - Overall - -				
Molar flow kmol/h	10237.15	118.89	118.89	0.00
Mass flow kg/h	246753.66	3753.53	3753.53	0.00
Temp C	42.62	57.51	67.98	41.67
Pres atm	1.00	1.02	1.20	1.00
Vapor mole fraction	0.008246	0.9947	1.000	1.000
Actual dens kg/m3	102.58	1.20	1.36	0.00
Actual vol m3/h	2405.39	3138.88	2767.05	0.00
Std liq m3/h	219.40	3.78	3.78	0.00
Std vap 0 C m3/h	229451.91	2664.66	2664.66	0.00
- - Vapor only - -				
Molar flow kmol/h	84.42	118.25	118.89	0.00
Mass flow kg/h	2458.88	3734.46	3753.53	0.00
Actual dens kg/m3	1.13	1.19	1.36	
Actual vol m3/h	2185.46	3138.87	2767.05	
Std liq m3/h	2.73	3.76	3.78	
Std vap 0 C m3/h	1892.14	2650.41	2664.66	
Cp kJ/kg-K	1.04	1.04	1.05	
- - Liquid only - -				
Molar flow kmol/h	10152.73	0.64		
Mass flow kg/h	244295.00	19.07		
Actual dens kg/m3	1110.77	1184.99		
Actual vol m3/h	219.93	0.02		
Std liq m3/h	216.67	0.02		
Std vap 0 C m3/h	227559.75	14.25		
Cp kJ/kg-K	3.36	2.88		

Stream No.	41	42	43	44
Name				
- - Overall - -				
Molar flow kmol/h	84.42	118.78	28518.06	4507.86
Mass flow kg/h	2458.88	2168.85	705516.00	105953.00
Temp C	42.62	99.35	79.05	120.00

Pres atm	1.00	1.00	1.02	1.51
Vapor mole fraction	1.000	0.0000	0.001205	1.000
Actual dens kg/m3	1.13	948.64	438.16	1.11
Actual vol m3/h	2185.46	2.29	1610.18	95114.84
Std liq m3/h	2.73	2.19	627.01	95.14
Std vap 0 C m3/h	1892.14	2662.20	639193.69	101037.65
- - Vapor only - -				
Molar flow kmol/h	84.42		33.93	4507.86
Mass flow kg/h	2458.88		1028.92	105953.00
Actual dens kg/m3	1.13		1.08	1.11
Actual vol m3/h	2185.46		957.05	95114.84
Std liq m3/h	2.73		0.92	95.14
Std vap 0 C m3/h	1892.14		760.58	101037.65
Cp kJ/kg-K	1.04		1.16	1.65
- - Liquid only - -				
Molar flow kmol/h		118.78	28130.97	
Mass flow kg/h		2168.85	677160.00	
Actual dens kg/m3		948.64	1050.41	
Actual vol m3/h		2.29	644.66	
Std liq m3/h		2.19	617.69	
Std vap 0 C m3/h		2662.20	630517.56	
Cp kJ/kg-K		4.27	3.50	

Stream No.	45	46	47	48
Name				Air Feed
- - Overall - -				
Molar flow kmol/h	4.49	27.73	89.37	27.73
Mass flow kg/h	283.01	800.00	3755.45	800.00
Temp C	99.35	153.66	129.44	25.00
Pres atm	1.00	3.00	1.00	1.00
Vapor mole fraction	1.000	1.000	1.000	1.000
Actual dens kg/m3	2.10	2.47	1.28	1.18

Actual vol m3/h	134.92	324.04	2934.81	678.20
Std liq m3/h	0.19	0.92	3.03	0.92
Std vap 0 C m3/h	100.67	621.50	2003.12	621.50
- - Vapor only - -				
Molar flow kmol/h	4.49	27.73	89.37	27.73
Mass flow kg/h	283.01	800.00	3755.45	800.00
Actual dens kg/m3	2.10	2.47	1.28	1.18
Actual vol m3/h	134.92	324.04	2934.81	678.20
Std liq m3/h	0.19	0.92	3.03	0.92
Std vap 0 C m3/h	100.67	621.50	2003.12	621.50
Cp kJ/kg-K	0.97	1.02	1.17	1.01

Stream No.	49	50	51	52
Name				
- - Overall - -				
Molar flow kmol/h	5715.29	5589.66	1519.16	5671.86
Mass flow kg/h	137206.61	134606.52	55454.00	133831.20
Temp C	45.75	46.19	60.84	40.00
Pres atm	1.00	1.20	1.00	1.16
Vapor mole fraction	1.371E-006	0.0000	0.03213	0.005338
Actual dens kg/m3	1104.88	1107.49	52.49	169.20
Actual vol m3/h	124.18	121.54	1056.45	790.96
Std liq m3/h	121.89	119.45	33.63	120.24
Std vap 0 C m3/h	128100.39	125284.59	34049.86	127127.11
- - Vapor only - -				
Molar flow kmol/h	0.01		37.41	30.28
Mass flow kg/h	0.23		1095.70	881.47
Actual dens kg/m3	1.12		1.07	1.32
Actual vol m3/h	0.20		1023.27	670.10

Std liq m3/h	0.00		1.16	0.99
Std vap 0 C m3/h	0.18		838.48	678.61
Cp kJ/kg-K	1.04		1.09	1.03
- - Liquid only - -				
Molar flow kmol/h	5715.28	5589.66	1127.07	5641.59
Mass flow kg/h	137206.38	134606.52	26857.75	132949.77
Actual dens kg/m3	1106.71	1107.49	1088.01	1100.11
Actual vol m3/h	123.98	121.54	24.69	120.85
Std liq m3/h	121.89	119.45	24.02	119.25
Std vap 0 C m3/h	128100.22	125284.59	25261.81	126448.50
Cp kJ/kg-K	3.37	3.36	3.50	3.43

Stream No.	53	54	55	56
Name				
- - Overall - -				
Molar flow kmol/h	10253.81	10253.81	5589.66	1519.16
Mass flow kg/h	246753.63	246753.63	134606.52	55454.00
Temp C	41.83	41.83	46.19	155.00
Pres atm	1.00	1.00	1.20	1.00
Vapor mole fraction	0.008656	0.008656	0.0000	0.9996
Actual dens kg/m3	98.22	98.22	1107.49	1.36
Actual vol m3/h	2512.30	2512.30	121.54	40649.48
Std liq m3/h	220.05	220.05	119.45	33.63
Std vap 0 C m3/h	229825.33	229825.33	125284.59	34049.86
- - Vapor only - -				
Molar flow kmol/h	88.76	88.76		1164.00
Mass flow kg/h	2611.85	2611.85		27878.22
Actual dens kg/m3	1.14	1.14		0.69
Actual vol m3/h	2291.90	2291.90		40640.79

Std liq m3/h	2.85	2.85		25.10
Std vap 0 C m3/h	1989.39	1989.39		26089.46
Cp kJ/kg-K	1.03	1.03		1.65
- - Liquid only - -				
Molar flow kmol/h	10165.06	10165.06	5589.66	0.48
Mass flow kg/h	244141.73	244141.73	134606.52	75.23
Actual dens kg/m3	1107.71	1107.71	1107.49	796.65
Actual vol m3/h	220.40	220.40	121.54	0.09
Std liq m3/h	217.20	217.20	119.45	0.08
Std vap 0 C m3/h	227835.95	227835.95	125284.59	10.83
Cp kJ/kg-K	3.37	3.37	3.36	45.62

Stream No.	57	58	59	60
Name				
- - Overall - -				
Molar flow kmol/h	54.90	5641.59	30.28	89.37
Mass flow kg/h	3880.52	132949.77	881.47	3755.45
Temp C	120.00	40.00	40.00	129.44
Pres atm	1.51	1.16	1.16	1.00
Vapor mole fraction	0.0000	0.0000	1.000	1.000
Actual dens kg/m3	679.10	1100.11	1.32	1.28
Actual vol m3/h	5.71	120.85	670.10	2934.81
Std liq m3/h	5.05	119.25	0.99	3.03
Std vap 0 C m3/h	1230.55	126448.50	678.61	2003.12
- - Vapor only - -				
Molar flow kmol/h			30.28	89.37
Mass flow kg/h			881.47	3755.45
Actual dens kg/m3			1.32	1.28
Actual vol m3/h			670.10	2934.81

Std liq m3/h				0.99
3.03				
Std vap 0 C m3/h				678.61
2003.12				
Cp kJ/kg-K				1.03
1.17				
- - Liquid only - -				
Molar flow kmol/h	54.90	5641.59		
Mass flow kg/h	3880.52	132949.77		
Actual dens kg/m3	679.10	1100.11		
Actual vol m3/h	5.71	120.85		
Std liq m3/h	5.05	119.25		
Std vap 0 C m3/h	1230.55	126448.50		
Cp kJ/kg-K	5.24	3.43		

Stream No.	61	62	63
64			
Name			
- - Overall - -			
Molar flow kmol/h	5589.66	67.13	22433.00
28510.69			
Mass flow kg/h	134606.52	3880.53	540000.00
705516.00			
Temp C	46.19	110.21	79.09
72.10			
Pres atm	1.20	1.41	1.50
1.50			
Vapor mole fraction	0.0000	0.8858	0.0000
0.0000			
Actual dens kg/m3	1107.49	3.28	1050.39
1091.93			
Actual vol m3/h	121.54	1183.77	514.09
646.12			
Std liq m3/h	119.45	2.53	492.57
623.10			
Std vap 0 C m3/h	125284.59	1504.62	502804.84
639028.63			
- - Vapor only - -			
Molar flow kmol/h		54.05	
Mass flow kg/h		2652.37	
Actual dens kg/m3		2.24	
Actual vol m3/h		1183.05	
Std liq m3/h		1.87	
Std vap 0 C m3/h		1211.36	
Cp kJ/kg-K		1.15	
- - Liquid only - -			
Molar flow kmol/h	5589.66	6.97	22433.00
28148.30			
Mass flow kg/h	134606.52	530.73	540000.00
677206.00			
Actual dens kg/m3	1107.49	955.46	1050.39
1062.41			
Actual vol m3/h	121.54	0.56	514.09
637.43			

Std liq m3/h	119.45	0.50	492.57	614.46
Std vap 0 C m3/h	125284.59	156.22	502804.84	630906.00
Cp kJ/kg-K	3.36	24.20	3.50	3.47

Stream No.	65	66	67	68
Name				
- - Overall - -				
Molar flow kmol/h	28484.12	28484.12	67.13	362.39
Mass flow kg/h	704487.00	704487.00	3880.53	28310.54
Temp C	79.08	79.08	155.00	25.00
Pres atm	2.00	1.32	1.41	1.00
Vapor mole fraction	0.0000	0.0000	0.9663	0.0000
Actual dens kg/m3	1078.63	1078.61	2.68	3275.69
Actual vol m3/h	653.13	653.14	1450.12	8.64
Std liq m3/h	626.09	626.09	2.53	8.63
Std vap 0 C m3/h	638433.13	638433.13	1504.62	8122.59
- - Vapor only - -				
Molar flow kmol/h			58.96	
Mass flow kg/h			2867.84	
Actual dens kg/m3			1.98	
Actual vol m3/h			1449.56	
Std liq m3/h			2.04	
Std vap 0 C m3/h			1321.43	
Cp kJ/kg-K			1.25	
- - Liquid only - -				
Molar flow kmol/h	28130.97	28130.97	2.06	
Mass flow kg/h	677160.00	677160.00	315.26	
Actual dens kg/m3	1050.41	1050.39	806.08	
Actual vol m3/h	644.66	644.67	0.39	
Std liq m3/h	617.69	617.69	0.33	
Std vap 0 C m3/h	630517.63	630517.63	46.15	
Cp kJ/kg-K	3.50	3.50	43.87	

Stream No.	69	70	71	72
Name				
- - Overall - -				
Molar flow kmol/h	4562.77	28493.37	4562.77	19.01
Mass flow kg/h	109833.53	705516.00	109833.53	1679.97

Temp C	120.00	80.00	79.08	25.00	
Pres atm	1.51	1.02	1.00	1.00	
Vapor mole fraction	0.9880	4.178E-006	0.0000	0.0000	
Actual dens kg/m3	1.15	1073.31	1050.38	3239.78	
Actual vol m3/h	95120.55	657.33	104.57	0.52	
Std liq m3/h	100.19	626.46	100.19	0.52	
Std vap 0 C m3/h	102268.21	638640.25	102268.21	426.06	
- - Vapor only - -					
Molar flow kmol/h	4507.86	0.12			
Mass flow kg/h	105953.00	3.50			
Actual dens kg/m3	1.11	1.05			
Actual vol m3/h	95114.84	3.33			
Std liq m3/h	95.14	0.00			
Std vap 0 C m3/h	101037.64	2.64			
Cp kJ/kg-K	1.65	1.18			
- - Liquid only - -					
Molar flow kmol/h	54.90	28140.10	4562.77	4.98	
Mass flow kg/h	3880.55	678186.00	109833.53	677.86	
Actual dens kg/m3	679.10	1050.58	1050.38	5583.29	
Actual vol m3/h	5.71	645.53	104.57	0.12	
Std liq m3/h	5.05	618.06	100.19	0.12	
Std vap 0 C m3/h	1230.56	630722.19	102268.21	111.60	
Cp kJ/kg-K	5.24	3.49	3.50	0.06	

Stream No.	73	74	76	84	
Name					Acid Feed
- - Overall - -					
Molar flow kmol/h	8.04	6.11	4562.77	7.49	
Mass flow kg/h	1006.55	697.43	109833.53	471.76	
Temp C	152.79	152.79	79.08	25.00	
Pres atm	1.00	1.00	1.32	1.00	
Vapor mole fraction	0.0000	0.0000	0.0000	0.0000	

Actual dens kg/m3	1824.93	4161.89	1050.39	1508.52
Actual vol m3/h	0.55	0.17	104.56	0.31
Std liq m3/h	0.49	0.16	100.19	0.31
Std vap 0 C m3/h	180.10	137.03	102268.21	167.80
- - Liquid only - -				
Molar flow kmol/h	1.92		4562.77	7.49
Mass flow kg/h	309.12		109833.53	471.76
Actual dens kg/m3	805.04		1050.39	1508.52
Actual vol m3/h	0.38		104.56	0.31
Std liq m3/h	0.33		100.19	0.31
Std vap 0 C m3/h	43.07		102268.21	167.80
Cp kJ/kg-K	44.42		3.50	1.75

Stream No.	85	87	88	89
Name	Water Feed			
- - Overall - -				
Molar flow kmol/h	118.14	10152.73	51.50	32.92
Mass flow kg/h	2128.33	244295.00	1500.00	958.88
Temp C	25.00	42.62	42.62	42.62
Pres atm	1.00	1.00	1.00	1.00
Vapor mole fraction	0.0000	0.0000	1.000	1.000
Actual dens kg/m3	996.71	1110.77	1.13	1.13
Actual vol m3/h	2.14	219.93	1333.21	852.25
Std liq m3/h	2.13	216.67	1.66	1.06
Std vap 0 C m3/h	2648.00	227559.75	1154.27	737.87
- - Vapor only - -				
Molar flow kmol/h			51.50	32.92
Mass flow kg/h			1500.00	958.88
Actual dens kg/m3			1.13	1.13

Actual vol m3/h			1333.21
852.25			
Std liq m3/h			1.66
1.06			
Std vap 0 C m3/h			1154.27
737.87			
Cp kJ/kg-K			1.04
1.04			
- - Liquid only - -			
Molar flow kmol/h	118.14	10152.73	
Mass flow kg/h	2128.33	244295.00	
Actual dens kg/m3	996.71	1110.77	
Actual vol m3/h	2.14	219.93	
Std liq m3/h	2.13	216.67	
Std vap 0 C m3/h	2648.00	227559.75	
Cp kJ/kg-K	4.19	3.36	

FLOW SUMMARIES:

Stream No.	1	2	3	4
Stream Name	Ash			
Temp C	25.0000	46.1539	72.0888	80.0000
Pres atm	1.0000	1.0000	1.1000	1.1600
Enth kJ/h	-7.7900E+009	-1.4989E+009	-1.4742E+010	-1.4723E+010
Vapor mass frac.	0.00000	2.0283E-006	0.00000	0.00000
Total kmol/h	381.40	5597.14	28510.66	28510.69
Total kg/h	29990.51	135078.27	705517.00	705516.00
Total std L m3/h	9.15	119.76	623.10	623.10
Total std V m3/h	8548.65	125452.41	639027.81	639028.63
Flow rates in kg/h				
Aluminum Oxide	7375.95	0.00	7375.95	7375.95
Antimony Trioxi	0.47	0.00	0.47	0.47
Arsenic Oxide	5.75	0.00	5.75	5.75
Barium Oxide	15.50	0.00	15.50	15.50
Boron Trioxide	61.90	0.00	61.90	61.90
Calcium Oxide	433.10	0.00	0.00	0.00
Cerium Nitrate	0.00	0.00	10.20	10.19
Cerium Oxide	6.48	0.00	6.48	6.48
Chromium(III) Ox	7.62	0.00	7.62	7.62
Cobalt(II) Oxide	1.91	0.00	1.91	1.91
Copper(II) Oxid	5.18	0.00	5.18	5.18
Dysprosium Nitr	0.00	0.00	0.98	0.99
Dysprosium Oxid	0.61	0.00	0.61	0.61
Erbium Nitrate	0.00	0.00	0.56	0.56
Erbium Oxide	0.37	0.00	0.37	0.37
Europium Nitrat	0.00	0.00	0.22	0.21
Europium Oxide	0.14	0.00	0.14	0.14
Gadolinium Nitr	0.00	0.00	1.06	1.06
Gadolinium Oxid	0.65	0.00	0.65	0.65
Gallium(III) Ox	2.72	0.00	2.72	2.72
Germanium Dioxi	4.33	0.00	4.33	4.33
Holmium Nitrate	0.00	0.00	0.21	0.21
Holmium Oxide	0.13	0.00	0.13	0.13
Iron(iii) oxide	5497.09	0.00	5497.09	5497.09
Lanthanum Nitrat	0.00	0.00	3.39	3.39
Lanthanum Oxide	2.83	0.00	2.83	2.83
Lead(II) Oxide	2.85	0.00	2.85	2.85
Lithium Oxide	11.64	0.00	0.00	0.00
Lutetium Nitrat	0.00	0.00	0.03	0.03
Lutetium Oxide	0.03	0.00	0.03	0.03
Magnesium Oxide	216.12	0.00	216.12	216.12
Manganese(II)Ox	0.00	0.00	0.00	0.00
Molybdenum Trio	1.03	0.00	1.03	1.03
Neodymium Nitra	0.00	0.00	3.96	3.97
Neodymium Oxide	2.87	0.00	2.87	2.87
Nickel(II) Oxid	4.98	0.00	4.98	4.98
Nitric Acid	0.00	45900.00	204678.00	204678.50
Potassium Oxide	557.37	0.00	0.00	0.00
Praseodymium Ni	0.00	0.00	0.98	0.98
Praseodymium Ox	0.73	0.00	0.73	0.73
Rubidium Oxide	4.20	0.00	4.20	4.20

Samarium Nitrat	0.00	0.00	0.87	0.87
Samarium Oxide	0.59	0.00	0.59	0.59
Scandium Nitrate	0.00	0.00	3.18	3.18
Scandium(III) Ox	1.83	0.00	1.83	1.83
Silicon Dioxide	14636.83	0.00	14636.83	14636.83
Strontium Oxide	39.24	0.00	39.24	39.24
Calcium Sulfate	677.86	0.00	0.00	0.00
Terbium Nitrate	0.00	0.00	0.17	0.17
Terbium Oxide	0.11	0.00	0.11	0.11
Titanium Dioxide	380.55	0.00	380.55	380.55
Thorium(IV) Oxi	0.83	0.00	0.83	0.83
Thulium Nitrate	0.00	0.00	0.07	0.07
Thulium Oxide	0.05	0.00	0.05	0.05
Uranium(IV) Oxi	0.71	0.00	0.71	0.71
Vanadium(V) Oxi	15.65	0.00	15.65	15.65
Water	0.00	86971.66	441947.00	441949.00
Ytterbium Nitra	0.00	0.00	0.41	0.41
Ytterbium Oxide	0.31	0.00	0.31	0.31
Yttrium Oxide	4.51	0.00	4.51	4.51
Yttrium(III) Nit	0.00	0.00	9.24	9.22
Zinc Oxide	6.89	0.00	6.89	6.89
Nitrogen Trioxid	0.00	70.97	336.50	336.41
Barium Nitrate	0.00	0.00	13.83	13.74
Calcium Nitrate	0.00	0.00	0.00	0.00
Potassium Nitrat	0.00	0.00	0.00	0.00
Magnesium Nitrat	0.00	0.01	583.29	583.29
Nitrogen Dioxide	0.00	554.53	6667.69	6667.81
Sulfuric Acid	0.00	0.00	0.00	0.00
Aluminum Nitrat	0.00	0.02	10650.42	10650.51
Arsenic Acid	0.00	280.29	1415.71	1415.99
Cobalt(II) Nitr	0.00	0.00	2.37	2.37
Copper(II) Nitr	0.00	0.00	13.19	13.19
Iron(III) Nitra	0.00	0.01	3211.60	3211.63
Gallium(III) Ni	0.00	0.00	6.70	6.69
Mn(II) Nitrate	0.00	0.00	0.00	0.00
Nickel(II) Nitr	0.00	0.00	6.78	6.77
Lead(II) Nitrat	0.00	0.00	4.10	4.10
Uranyl Nitrate	0.00	0.00	0.81	0.81
Zinc Nitrate	0.00	0.00	17.05	17.22
Lithium Nitrate	0.00	0.00	0.00	0.00
Rubidium Nitrat	0.00	0.00	2.04	2.04
Antimony Pentox	0.00	0.00	0.00	0.00
Strontium Nitra	0.00	0.00	69.41	69.45
Thorium(IV) Nit	0.00	0.00	0.70	0.70
Nitrogen	0.00	0.96	0.96	0.96
Oxygen	0.00	0.64	3.00	3.00
Carbon Monoxide	0.00	0.00	0.00	0.00
Methane	0.00	0.00	0.00	0.00
Carbon Dioxide	0.00	0.00	0.00	0.00
N2O4	0.00	0.00	0.00	0.00
Nitric Oxide	0.00	0.07	1.86	1.86
dinitrogen pent	0.00	138.67	1659.08	1659.11
Nitrous Acid	0.00	1160.43	5879.18	5875.52

Stream No.	5	6	7	8
Stream Name				
Temp C	79.9991	79.0504	79.0817	128.0979
Pres atm	1.1600	1.0200	1.3200	1.5000
Enth kJ/h	-1.4723E+010	-1.4116E+010	-7.2432E+009	-1.2615E+009
Vapor mass frac.	0.00000	0.00000	0.00000	1.0000
Total kmol/h	28510.66	28484.12	26995.74	5671.86
Total kg/h	705516.00	704487.00	649834.00	133831.20
Total std L m3/h	623.11	626.09	592.76	120.24
Total std V m3/h	639027.81	638433.13	605073.00	127127.11
Flow rates in kg/h				
Aluminum Oxide	7375.95	6728.49	0.00	0.00
Antimony Trioxi	0.47	0.33	0.00	0.00
Arsenic Oxide	5.75	0.00	0.00	0.00
Barium Oxide	15.50	13.38	0.00	0.00
Boron Trioxide	61.90	61.90	0.00	0.00
Calcium Oxide	0.00	0.00	0.00	0.00
Cerium Nitrate	12.79	12.79	12.27	0.00
Cerium Oxide	5.33	5.33	0.00	0.00
Chromium(III) Ox	7.62	7.62	0.00	0.00
Cobalt(II) Oxide	1.91	1.67	0.00	0.00
Copper(II) Oxid	5.18	3.76	0.00	0.00
Dysprosium Nitr	1.23	1.23	1.18	0.00
Dysprosium Oxid	0.48	0.48	0.00	0.00
Erbium Nitrate	0.70	0.70	0.68	0.00
Erbium Oxide	0.29	0.29	0.00	0.00
Europium Nitrat	0.27	0.27	0.26	0.00
Europium Oxide	0.11	0.11	0.00	0.00
Gadolinium Nitr	1.32	1.32	1.27	0.00
Gadolinium Oxid	0.50	0.50	0.00	0.00
Gallium(III) Ox	2.72	2.09	0.00	0.00
Germanium Dioxi	4.33	4.33	0.00	0.00
Holmium Nitrate	0.26	0.26	0.25	0.00
Holmium Oxide	0.10	0.10	0.00	0.00
Iron(iii) oxide	5497.09	5227.80	0.00	0.00
Lanthanum Nitrat	4.25	4.25	4.08	0.00
Lanthanum Oxide	2.40	2.40	0.00	0.00
Lead(II) Oxide	2.85	2.15	0.00	0.00
Lithium Oxide	0.00	0.00	0.00	0.00
Lutetium Nitrat	0.04	0.04	0.04	0.00
Lutetium Oxide	0.02	0.02	0.00	0.00
Magnesium Oxide	216.12	175.87	0.00	0.00
Manganese(II)Ox	0.00	0.00	0.00	0.00
Molybdenum Trio	1.03	1.03	0.00	0.00
Neodymium Nitra	4.97	4.97	4.77	0.00
Neodymium Oxide	2.36	2.36	0.00	0.00
Nickel(II) Oxid	4.98	4.27	0.00	0.00
Nitric Acid	204672.67	199107.58	191072.55	40721.70
Potassium Oxide	0.00	0.00	0.00	0.00
Praseodymium Ni	1.22	1.22	1.17	0.00
Praseodymium Ox	0.61	0.61	0.00	0.00
Rubidium Oxide	4.20	3.88	0.00	0.00
Samarium Nitrat	1.09	1.09	1.04	0.00
Samarium Oxide	0.48	0.48	0.00	0.00

Scandium Nitrate	3.99	3.99	3.83	0.00
Scandium(III) Ox	1.59	1.59	0.00	0.00
Silicon Dioxide	14636.83	14636.83	0.00	0.00
Strontium Oxide	39.24	30.64	0.00	0.00
Calcium Sulfate	0.00	0.00	0.00	0.00
Terbium Nitrate	0.21	0.21	0.20	0.00
Terbium Oxide	0.09	0.09	0.00	0.00
Titanium Dioxide	380.55	380.55	0.00	0.00
Thorium(IV) Oxi	0.83	0.74	0.00	0.00
Thulium Nitrate	0.09	0.09	0.09	0.00
Thulium Oxide	0.04	0.04	0.00	0.00
Uranium(IV) Oxi	0.71	0.57	0.00	0.00
Vanadium(V) Oxi	15.65	15.65	0.00	0.00
Water	441949.53	442470.00	424614.00	88873.00
Ytterbium Nitra	0.51	0.51	0.49	0.00
Ytterbium Oxide	0.25	0.25	0.00	0.00
Yttrium Oxide	3.54	3.54	0.00	0.00
Yttrium(III) Nit	11.59	11.59	11.12	0.00
Zinc Oxide	6.89	5.10	0.00	0.00
Nitrogen Trioxid	336.41	332.97	319.54	67.42
Barium Nitrate	13.74	17.34	16.64	0.00
Calcium Nitrate	0.00	0.00	0.00	0.00
Potassium Nitrat	0.00	0.00	0.00	0.00
Magnesium Nitrat	583.29	731.43	701.91	0.01
Nitrogen Dioxide	6667.81	7665.91	7356.55	1552.11
Sulfuric Acid	0.00	0.00	0.00	0.00
Aluminum Nitrat	10650.51	13355.62	12816.65	0.02
Arsenic Acid	1415.99	1423.81	1366.35	284.15
Cobalt(II) Nitr	2.37	2.97	2.85	0.00
Copper(II) Nitr	13.19	16.54	15.87	0.00
Iron(III) Nitra	3211.63	4027.35	3864.82	0.01
Gallium(III) Ni	6.69	8.40	8.06	0.00
Mn(II) Nitrate	0.00	0.00	0.00	0.00
Nickel(II) Nitr	6.77	8.50	8.16	0.00
Lead(II) Nitrat	4.10	5.14	4.93	0.00
Uranyl Nitrate	0.81	1.02	0.98	0.00
Zinc Nitrate	17.22	21.38	20.52	0.00
Lithium Nitrate	0.00	0.00	0.00	0.00
Rubidium Nitrat	2.04	2.56	2.46	0.00
Antimony Pentox	0.00	0.16	0.00	0.00
Strontium Nitra	69.45	87.03	83.52	0.00
Thorium(IV) Nit	0.70	0.88	0.85	0.00
Nitrogen	0.96	0.00	0.00	613.67
Oxygen	3.00	2.96	2.85	186.93
Carbon Monoxide	0.00	0.00	0.00	0.00
Methane	0.00	0.00	0.00	0.00
Carbon Dioxide	0.00	0.00	0.00	0.00
N2O4	0.00	0.00	0.00	0.00
Nitric Oxide	1.86	2.25	2.16	0.46
dinitrogen pent	1659.11	1906.59	1829.65	385.33
Nitrous Acid	5875.52	5917.31	5678.52	1146.46

Stream No.	9	10	11	12
Stream Name				

Temp C	79.0817	120.0000	79.0504	79.0817
Pres atm	1.3200	1.4100	1.0200	1.3200
Enth kJ/h	-6.0190E+009	-4.8511E+008	-3.0132E+006	-6.8725E+009
Vapor mass frac.	0.00000	0.87641	1.0000	0.00000
Total kmol/h	22433.00	67.13	33.93	1488.39
Total kg/h	540000.00	3880.53	1028.90	54653.95
Total std L m3/h	492.57	2.53	0.92	33.33
Total std V m3/h	502804.84	1504.62	760.56	33360.17
Flow rates in kg/h				
Aluminum Oxide	0.00	492.56	0.00	6728.49
Antimony Trioxi	0.00	0.00	0.00	0.33
Arsenic Oxide	0.00	0.00	0.00	0.00
Barium Oxide	0.00	0.00	0.00	13.38
Boron Trioxide	0.00	0.00	0.00	61.90
Calcium Oxide	0.00	0.00	0.00	0.00
Cerium Nitrate	10.20	2.07	0.00	0.52
Cerium Oxide	0.00	0.00	0.00	5.33
Chromium(III) Ox	0.00	0.00	0.00	7.62
Cobalt(II) Oxide	0.00	0.00	0.00	1.67
Copper(II) Oxid	0.00	0.00	0.00	3.76
Dysprosium Nitr	0.98	0.20	0.00	0.05
Dysprosium Oxid	0.00	0.00	0.00	0.48
Erbium Nitrate	0.56	0.11	0.00	0.03
Erbium Oxide	0.00	0.00	0.00	0.29
Europium Nitrat	0.22	0.04	0.00	0.01
Europium Oxide	0.00	0.00	0.00	0.11
Gadolinium Nitr	1.06	0.21	0.00	0.05
Gadolinium Oxid	0.00	0.00	0.00	0.50
Gallium(III) Ox	0.00	0.00	0.00	2.09
Germanium Dioxi	0.00	0.00	0.00	4.33
Holmium Nitrate	0.21	0.04	0.00	0.01
Holmium Oxide	0.00	0.00	0.00	0.10
Iron(iii) oxide	0.00	204.87	0.00	5227.80
Lanthanum Nitrat	3.39	0.69	0.00	0.17
Lanthanum Oxide	0.00	0.00	0.00	2.40
Lead(II) Oxide	0.00	0.00	0.00	2.15
Lithium Oxide	0.00	0.00	0.00	0.00
Lutetium Nitrat	0.03	0.01	0.00	0.00
Lutetium Oxide	0.00	0.00	0.00	0.02
Magnesium Oxide	0.00	0.00	0.00	175.87
Manganese(II)Ox	0.00	0.00	0.00	0.00
Molybdenum Trio	0.00	0.00	0.00	1.03
Neodymium Nitra	3.96	0.81	0.00	0.20
Neodymium Oxide	0.00	0.00	0.00	2.36
Nickel(II) Oxid	0.00	0.00	0.00	4.27
Nitric Acid	158778.00	2494.17	205.51	8035.03
Potassium Oxide	0.00	0.00	0.00	0.00
Praseodymium Ni	0.98	0.20	0.00	0.05
Praseodymium Ox	0.00	0.00	0.00	0.61
Rubidium Oxide	0.00	0.00	0.00	3.88
Samarium Nitrat	0.87	0.18	0.00	0.04
Samarium Oxide	0.00	0.00	0.00	0.48
Scandium Nitrate	3.18	0.65	0.00	0.16
Scandium(III) Ox	0.00	0.00	0.00	1.59

Silicon Dioxide	0.00	0.00	0.00	14636.83
Strontium Oxide	0.00	0.00	0.00	30.64
Calcium Sulfate	0.00	0.00	0.00	0.00
Terbium Nitrate	0.17	0.03	0.00	0.01
Terbium Oxide	0.00	0.00	0.00	0.09
Titanium Dioxide	0.00	0.00	0.00	380.55
Thorium(IV) Oxi	0.00	0.00	0.00	0.74
Thulium Nitrate	0.07	0.01	0.00	0.00
Thulium Oxide	0.00	0.00	0.00	0.04
Uranium(IV) Oxi	0.00	0.00	0.00	0.57
Vanadium(V) Oxi	0.00	0.00	0.00	15.65
Water	352847.00	336.48	235.59	17856.00
Ytterbium Nitra	0.41	0.08	0.00	0.02
Ytterbium Oxide	0.00	0.00	0.00	0.25
Yttrium Oxide	0.00	0.00	0.00	3.54
Yttrium(III) Nit	9.24	1.88	0.00	0.47
Zinc Oxide	0.00	0.00	0.00	5.10
Nitrogen Trioxid	265.53	0.03	5.65	13.44
Barium Nitrate	13.83	2.81	0.00	0.70
Calcium Nitrate	0.00	0.00	0.00	0.00
Potassium Nitrat	0.00	0.00	0.00	0.00
Magnesium Nitrat	583.28	118.63	0.00	29.52
Nitrogen Dioxide	6113.16	0.64	90.52	309.36
Sulfuric Acid	0.00	0.00	0.00	0.00
Aluminum Nitrat	10650.40	108.31	0.00	538.97
Arsenic Acid	1135.42	4.24	0.43	57.46
Cobalt(II) Nitr	2.37	0.48	0.00	0.12
Copper(II) Nitr	13.19	2.68	0.00	0.67
Iron(III) Nitra	3211.60	32.66	0.00	162.52
Gallium(III) Ni	6.70	1.36	0.00	0.34
Mn(II) Nitrate	0.00	0.00	0.00	0.00
Nickel(II) Nitr	6.78	1.38	0.00	0.34
Lead(II) Nitrat	4.10	0.83	0.00	0.21
Uranyl Nitrate	0.81	0.17	0.00	0.04
Zinc Nitrate	17.05	3.47	0.00	0.86
Lithium Nitrate	0.00	0.00	0.00	0.00
Rubidium Nitrat	2.04	0.42	0.00	0.10
Antimony Pentox	0.00	0.00	0.00	0.16
Strontium Nitra	69.41	14.12	0.00	3.51
Thorium(IV) Nit	0.70	0.14	0.00	0.04
Nitrogen	0.00	0.00	0.96	0.00
Oxygen	2.36	0.00	328.46	0.12
Carbon Monoxide	0.00	0.00	0.00	0.00
Methane	0.00	0.00	0.00	0.00
Carbon Dioxide	0.00	0.00	0.00	0.00
N2O4	0.00	0.00	0.00	0.00
Nitric Oxide	1.79	0.00	155.66	0.09
dinitrogen pent	1520.41	0.86	5.64	76.94
Nitrous Acid	4718.74	52.00	0.47	238.79
Stream No.	13	14	15	16
Stream Name			REE Conc	
Temp C	41.6707	152.7859	152.7859	79.1085
Pres atm	1.0000	1.0000	1.0000	1.8500

Enth kJ/h	-4.5126E+007	-9.5553E+006	-5.5491E+006	-1.2242E+009
Vapor mass frac.	0.00000	1.0000	0.00000	0.00000
Total kmol/h	168.00	59.09	1.92	4562.77
Total kg/h	4025.38	2873.98	309.12	109833.53
Total std L m3/h	3.58	2.04	0.33	100.19
Total std V m3/h	3765.55	1324.51	43.07	102268.21
Flow rates in kg/h				
Aluminum Oxide	0.00	0.00	0.00	0.00
Antimony Trioxi	0.00	0.00	0.00	0.00
Arsenic Oxide	0.00	0.00	0.00	0.00
Barium Oxide	0.00	0.00	0.00	0.00
Boron Trioxide	0.00	0.00	0.00	0.00
Calcium Oxide	0.00	0.00	0.00	0.00
Cerium Nitrate	0.00	0.00	2.07	2.07
Cerium Oxide	0.00	0.00	0.00	0.00
Chromium(III) Ox	0.00	0.00	0.00	0.00
Cobalt(II) Oxide	0.00	0.00	0.00	0.00
Copper(II) Oxid	0.00	0.00	0.00	0.00
Dysprosium Nitr	0.00	0.00	0.20	0.20
Dysprosium Oxid	0.00	0.00	0.00	0.00
Erbium Nitrate	0.00	0.00	0.11	0.11
Erbium Oxide	0.00	0.00	0.00	0.00
Europium Nitrat	0.00	0.00	0.04	0.04
Europium Oxide	0.00	0.00	0.00	0.00
Gadolinium Nitr	0.00	0.00	0.21	0.21
Gadolinium Oxid	0.00	0.00	0.00	0.00
Gallium(III) Ox	0.00	0.00	0.00	0.00
Germanium Dioxi	0.00	0.00	0.00	0.00
Holmium Nitrate	0.00	0.00	0.04	0.04
Holmium Oxide	0.00	0.00	0.00	0.00
Iron(iii) oxide	0.00	0.00	0.00	0.00
Lanthanum Nitrat	0.00	0.00	0.69	0.69
Lanthanum Oxide	0.00	0.00	0.00	0.00
Lead(II) Oxide	0.00	0.00	0.00	0.00
Lithium Oxide	0.00	0.00	0.00	0.00
Lutetium Nitrat	0.00	0.00	0.01	0.01
Lutetium Oxide	0.00	0.00	0.00	0.00
Magnesium Oxide	0.00	0.00	0.00	0.00
Manganese(II)Ox	0.00	0.00	0.00	0.00
Molybdenum Trio	0.00	0.00	0.00	0.00
Neodymium Nitra	0.00	0.00	0.81	0.81
Neodymium Oxide	0.00	0.00	0.00	0.00
Nickel(II) Oxid	0.00	0.00	0.00	0.00
Nitric Acid	1336.98	2483.83	10.34	32294.69
Potassium Oxide	0.00	0.00	0.00	0.00
Praseodymium Ni	0.00	0.00	0.20	0.20
Praseodymium Ox	0.00	0.00	0.00	0.00
Rubidium Oxide	0.00	0.00	0.00	0.00
Samarium Nitrat	0.00	0.00	0.18	0.18
Samarium Oxide	0.00	0.00	0.00	0.00
Scandium Nitrate	0.00	0.00	0.65	0.65
Scandium(III) Ox	0.00	0.00	0.00	0.00
Silicon Dioxide	0.00	0.00	0.00	0.00
Strontium Oxide	0.00	0.00	0.00	0.00

Calcium Sulfate	0.00	0.00	0.00	0.00
Terbium Nitrate	0.00	0.00	0.03	0.03
Terbium Oxide	0.00	0.00	0.00	0.00
Titanium Dioxide	0.00	0.00	0.00	0.00
Thorium(IV) Oxi	0.00	0.00	0.00	0.00
Thulium Nitrate	0.00	0.00	0.01	0.01
Thulium Oxide	0.00	0.00	0.00	0.00
Uranium(IV) Oxi	0.00	0.00	0.00	0.00
Vanadium(V) Oxi	0.00	0.00	0.00	0.00
Water	2622.17	334.34	2.15	71767.45
Ytterbium Nitra	0.00	0.00	0.08	0.08
Ytterbium Oxide	0.00	0.00	0.00	0.00
Yttrium Oxide	0.00	0.00	0.00	0.00
Yttrium(III) Nit	0.00	0.00	1.88	1.88
Zinc Oxide	0.00	0.00	0.00	0.00
Nitrogen Trioxid	2.09	0.03	0.00	54.01
Barium Nitrate	0.00	0.00	2.81	2.81
Calcium Nitrate	0.00	0.00	0.00	0.00
Potassium Nitrat	0.00	0.00	0.00	0.00
Magnesium Nitrat	0.00	0.00	118.63	118.64
Nitrogen Dioxide	16.32	0.64	0.00	1243.39
Sulfuric Acid	0.00	0.00	0.00	0.00
Aluminum Nitrat	0.00	0.00	108.31	2166.24
Arsenic Acid	8.50	4.18	0.06	230.94
Cobalt(II) Nitr	0.00	0.00	0.48	0.48
Copper(II) Nitr	0.00	0.00	2.68	2.68
Iron(III) Nitra	0.00	0.00	32.66	653.22
Gallium(III) Ni	0.00	0.00	1.36	1.36
Mn(II) Nitrate	0.00	0.00	0.00	0.00
Nickel(II) Nitr	0.00	0.00	1.38	1.38
Lead(II) Nitrat	0.00	0.00	0.83	0.83
Uranyl Nitrate	0.00	0.00	0.17	0.17
Zinc Nitrate	0.00	0.00	3.47	3.47
Lithium Nitrate	0.00	0.00	0.00	0.00
Rubidium Nitrat	0.00	0.00	0.42	0.42
Antimony Pentox	0.00	0.00	0.00	0.00
Strontium Nitra	0.00	0.00	14.12	14.12
Thorium(IV) Nit	0.00	0.00	0.14	0.14
Nitrogen	0.03	0.00	0.00	0.00
Oxygen	0.02	0.00	0.00	0.48
Carbon Monoxide	0.00	0.00	0.00	0.00
Methane	0.00	0.00	0.00	0.00
Carbon Dioxide	0.00	0.00	0.00	0.00
N2O4	0.00	0.00	0.00	0.00
Nitric Oxide	0.00	0.00	0.00	0.36
dinitrogen pent	4.08	0.86	0.00	309.24
Nitrous Acid	35.19	50.12	1.88	959.77

Stream No.	17	18	19	20
Stream Name				
Temp C	41.6707	40.0000	152.7841	94.6531
Pres atm	1.0000	1.0000	1.0000	1.0000
Enth kJ/h	-2.7241E+009	-1.2511E+007	-4.8444E+008	-8.8416E+006
Vapor mass frac.	0.00000	0.28063	0.90289	1.0000

Total kmol/h	10141.80	89.37	67.13	44.74
Total kg/h	243000.00	3755.45	3880.53	1573.52
Total std L m3/h	216.11	3.03	2.53	1.21
Total std V m3/h	227314.83	2003.12	1504.62	1002.68
Flow rates in kg/h				
Aluminum Oxide	0.00	0.00	492.56	0.00
Antimony Trioxi	0.00	0.00	0.00	0.00
Arsenic Oxide	0.00	0.00	0.00	0.00
Barium Oxide	0.00	0.00	0.00	0.00
Boron Trioxide	0.00	0.00	0.00	0.00
Calcium Oxide	0.00	0.00	0.00	0.00
Cerium Nitrate	0.00	0.00	2.07	0.00
Cerium Oxide	0.00	0.00	0.00	0.00
Chromium(III) Ox	0.00	0.00	0.00	0.00
Cobalt(II) Oxide	0.00	0.00	0.00	0.00
Copper(II) Oxid	0.00	0.00	0.00	0.00
Dysprosium Nitr	0.00	0.00	0.20	0.00
Dysprosium Oxid	0.00	0.00	0.00	0.00
Erbium Nitrate	0.00	0.00	0.11	0.00
Erbium Oxide	0.00	0.00	0.00	0.00
Europium Nitrat	0.00	0.00	0.04	0.00
Europium Oxide	0.00	0.00	0.00	0.00
Gadolinium Nitr	0.00	0.00	0.21	0.00
Gadolinium Oxid	0.00	0.00	0.00	0.00
Gallium(III) Ox	0.00	0.00	0.00	0.00
Germanium Dioxi	0.00	0.00	0.00	0.00
Holmium Nitrate	0.00	0.00	0.04	0.00
Holmium Oxide	0.00	0.00	0.00	0.00
Iron(iii) oxide	0.00	0.00	204.87	0.00
Lanthanum Nitrat	0.00	0.00	0.69	0.00
Lanthanum Oxide	0.00	0.00	0.00	0.00
Lead(II) Oxide	0.00	0.00	0.00	0.00
Lithium Oxide	0.00	0.00	0.00	0.00
Lutetium Nitrat	0.00	0.00	0.01	0.00
Lutetium Oxide	0.00	0.00	0.00	0.00
Magnesium Oxide	0.00	0.00	0.00	0.00
Manganese(II)Ox	0.00	0.00	0.00	0.00
Molybdenum Trio	0.00	0.00	0.00	0.00
Neodymium Nitra	0.00	0.00	0.81	0.00
Neodymium Oxide	0.00	0.00	0.00	0.00
Nickel(II) Oxid	0.00	0.00	0.00	0.00
Nitric Acid	80709.44	2516.94	2494.17	1053.97
Potassium Oxide	0.00	0.00	0.00	0.00
Praseodymium Ni	0.00	0.00	0.20	0.00
Praseodymium Ox	0.00	0.00	0.00	0.00
Rubidium Oxide	0.00	0.00	0.00	0.00
Samarium Nitrat	0.00	0.00	0.18	0.00
Samarium Oxide	0.00	0.00	0.00	0.00
Scandium Nitrate	0.00	0.00	0.65	0.00
Scandium(III) Ox	0.00	0.00	0.00	0.00
Silicon Dioxide	0.00	0.00	0.00	0.00
Strontium Oxide	0.00	0.00	0.00	0.00
Calcium Sulfate	0.00	0.00	0.00	0.00
Terbium Nitrate	0.00	0.00	0.03	0.00

Terbium Oxide	0.00	0.00	0.00	0.00
Titanium Dioxide	0.00	0.00	0.00	0.00
Thorium(IV) Oxi	0.00	0.00	0.00	0.00
Thulium Nitrate	0.00	0.00	0.01	0.00
Thulium Oxide	0.00	0.00	0.00	0.00
Uranium(IV) Oxi	0.00	0.00	0.00	0.00
Vanadium(V) Oxi	0.00	0.00	0.00	0.00
Water	158292.64	364.29	336.48	496.98
Ytterbium Nitra	0.00	0.00	0.08	0.00
Ytterbium Oxide	0.00	0.00	0.00	0.00
Yttrium Oxide	0.00	0.00	0.00	0.00
Yttrium(III) Nit	0.00	0.00	1.88	0.00
Zinc Oxide	0.00	0.00	0.00	0.00
Nitrogen Trioxid	126.09	1.40	0.03	2.09
Barium Nitrate	0.00	0.00	2.81	0.00
Calcium Nitrate	0.00	0.00	0.00	0.00
Potassium Nitrat	0.00	0.00	0.00	0.00
Magnesium Nitrat	0.01	0.00	118.63	0.00
Nitrogen Dioxide	985.20	16.96	0.64	16.32
Sulfuric Acid	0.00	0.00	0.00	0.00
Aluminum Nitrat	0.03	0.00	108.31	0.00
Arsenic Acid	513.03	4.24	4.24	0.02
Cobalt(II) Nitr	0.00	0.00	0.48	0.00
Copper(II) Nitr	0.00	0.00	2.68	0.00
Iron(III) Nitra	0.01	0.00	32.66	0.00
Gallium(III) Ni	0.00	0.00	1.36	0.00
Mn(II) Nitrate	0.00	0.00	0.00	0.00
Nickel(II) Nitr	0.00	0.00	1.38	0.00
Lead(II) Nitrat	0.00	0.00	0.83	0.00
Uranyl Nitrate	0.00	0.00	0.17	0.00
Zinc Nitrate	0.00	0.00	3.47	0.00
Lithium Nitrate	0.00	0.00	0.00	0.00
Rubidium Nitrat	0.00	0.00	0.42	0.00
Antimony Pentox	0.00	0.00	0.00	0.00
Strontium Nitra	0.00	0.00	14.12	0.00
Thorium(IV) Nit	0.00	0.00	0.14	0.00
Nitrogen	1.71	612.55	0.00	0.03
Oxygen	1.14	186.26	0.00	0.02
Carbon Monoxide	0.00	0.00	0.00	0.00
Methane	0.00	0.00	0.00	0.00
Carbon Dioxide	0.00	0.00	0.00	0.00
N2O4	0.00	0.00	0.00	0.00
Nitric Oxide	0.12	0.45	0.00	0.00
dinitrogen pent	246.37	2.19	0.86	4.08
Nitrous Acid	2124.19	50.17	52.00	0.00

Stream No.	21	22	23	24
Stream Name				Dry Ash
Temp C	99.3457	41.6707	155.0000	155.0000
Pres atm	1.0000	1.0000	1.0000	1.0000
Enth kJ/h	-3.3850E+007	-1.4882E+009	-2.5175E+008	-6.6843E+009
Vapor mass frac.	0.00000	0.00000	1.0000	0.00000
Total kmol/h	123.27	5540.43	1164.00	355.16
Total kg/h	2451.86	132750.00	27878.22	27575.72

Total std L m3/h	2.37	118.06	25.10	8.52
Total std V m3/h	2762.87	124181.23	26089.46	7960.40
Flow rates in kg/h				
Aluminum Oxide	0.00	0.00	0.00	6851.04
Antimony Trioxi	0.00	0.00	0.00	0.33
Arsenic Oxide	0.00	0.00	0.00	0.00
Barium Oxide	0.00	0.00	0.00	13.38
Boron Trioxide	0.00	0.00	0.00	61.90
Calcium Oxide	0.00	0.00	0.00	0.00
Cerium Nitrate	0.00	0.00	0.00	0.52
Cerium Oxide	0.00	0.00	0.00	5.33
Chromium(III) Ox	0.00	0.00	0.00	7.62
Cobalt(II) Oxide	0.00	0.00	0.00	1.67
Copper(II) Oxid	0.00	0.00	0.00	3.76
Dysprosium Nitr	0.00	0.00	0.00	0.05
Dysprosium Oxid	0.00	0.00	0.00	0.48
Erbium Nitrate	0.00	0.00	0.00	0.03
Erbium Oxide	0.00	0.00	0.00	0.29
Europium Nitrat	0.00	0.00	0.00	0.01
Europium Oxide	0.00	0.00	0.00	0.11
Gadolinium Nitr	0.00	0.00	0.00	0.05
Gadolinium Oxid	0.00	0.00	0.00	0.50
Gallium(III) Ox	0.00	0.00	0.00	2.09
Germanium Dioxi	0.00	0.00	0.00	4.33
Holmium Nitrate	0.00	0.00	0.00	0.01
Holmium Oxide	0.00	0.00	0.00	0.10
Iron(iii) oxide	0.00	0.00	0.00	5278.77
Lanthanum Nitrat	0.00	0.00	0.00	0.17
Lanthanum Oxide	0.00	0.00	0.00	2.40
Lead(II) Oxide	0.00	0.00	0.00	2.15
Lithium Oxide	0.00	0.00	0.00	0.00
Lutetium Nitrat	0.00	0.00	0.00	0.00
Lutetium Oxide	0.00	0.00	0.00	0.02
Magnesium Oxide	0.00	0.00	0.00	175.87
Manganese(II)Ox	0.00	0.00	0.00	0.00
Molybdenum Trio	0.00	0.00	0.00	1.03
Neodymium Nitra	0.00	0.00	0.00	0.20
Neodymium Oxide	0.00	0.00	0.00	2.36
Nickel(II) Oxid	0.00	0.00	0.00	4.27
Nitric Acid	283.01	44091.27	8609.71	0.43
Potassium Oxide	0.00	0.00	0.00	0.00
Praseodymium Ni	0.00	0.00	0.00	0.05
Praseodymium Ox	0.00	0.00	0.00	0.61
Rubidium Oxide	0.00	0.00	0.00	3.88
Samarium Nitrat	0.00	0.00	0.00	0.04
Samarium Oxide	0.00	0.00	0.00	0.48
Scandium Nitrate	0.00	0.00	0.00	0.16
Scandium(III) Ox	0.00	0.00	0.00	1.59
Silicon Dioxide	0.00	0.00	0.00	14636.83
Strontium Oxide	0.00	0.00	0.00	30.64
Calcium Sulfate	0.00	0.00	0.00	0.00
Terbium Nitrate	0.00	0.00	0.00	0.01
Terbium Oxide	0.00	0.00	0.00	0.09
Titanium Dioxide	0.00	0.00	0.00	380.55

Thorium(IV) Oxi	0.00	0.00	0.00	0.74
Thulium Nitrate	0.00	0.00	0.00	0.00
Thulium Oxide	0.00	0.00	0.00	0.04
Uranium(IV) Oxi	0.00	0.00	0.00	0.57
Vanadium(V) Oxi	0.00	0.00	0.00	15.65
Water	2125.19	86474.68	17772.41	1.38
Ytterbium Nitra	0.00	0.00	0.00	0.02
Ytterbium Oxide	0.00	0.00	0.00	0.25
Yttrium Oxide	0.00	0.00	0.00	3.54
Yttrium(III) Nit	0.00	0.00	0.00	0.47
Zinc Oxide	0.00	0.00	0.00	5.10
Nitrogen Trioxid	0.00	68.88	13.44	0.00
Barium Nitrate	0.00	0.00	0.00	0.70
Calcium Nitrate	0.00	0.00	0.00	0.00
Potassium Nitrat	0.00	0.00	0.00	0.00
Magnesium Nitrat	0.00	0.01	0.01	29.51
Nitrogen Dioxide	0.00	538.21	309.36	0.00
Sulfuric Acid	0.00	0.00	0.00	0.00
Aluminum Nitrat	0.00	0.02	0.01	26.94
Arsenic Acid	8.47	280.27	57.45	0.01
Cobalt(II) Nitr	0.00	0.00	0.00	0.12
Copper(II) Nitr	0.00	0.00	0.00	0.67
Iron(III) Nitra	0.00	0.01	0.00	8.12
Gallium(III) Ni	0.00	0.00	0.00	0.34
Mn(II) Nitrate	0.00	0.00	0.00	0.00
Nickel(II) Nitr	0.00	0.00	0.00	0.34
Lead(II) Nitrat	0.00	0.00	0.00	0.21
Uranyl Nitrate	0.00	0.00	0.00	0.04
Zinc Nitrate	0.00	0.00	0.00	0.86
Lithium Nitrate	0.00	0.00	0.00	0.00
Rubidium Nitrat	0.00	0.00	0.00	0.10
Antimony Pentox	0.00	0.00	0.00	0.16
Strontium Nitra	0.00	0.00	0.00	3.51
Thorium(IV) Nit	0.00	0.00	0.00	0.04
Nitrogen	0.00	0.93	613.67	0.00
Oxygen	0.00	0.62	186.45	0.00
Carbon Monoxide	0.00	0.00	0.00	0.00
Methane	0.00	0.00	0.00	0.00
Carbon Dioxide	0.00	0.00	0.00	0.00
N2O4	0.00	0.00	0.00	0.00
Nitric Oxide	0.00	0.07	0.09	0.00
dinitrogen pent	0.00	134.59	76.94	0.00
Nitrous Acid	35.19	1160.43	238.69	0.11

Stream No.	25	26	27	28
Stream Name				
Temp C	46.1860	78.0000	129.4426	77.6975
Pres atm	1.0000	1.0000	1.0000	3.0000
Enth kJ/h	-1.4976E+009	-6.9864E+009	-1.0003E+007	-6.8724E+009
Vapor mass frac.	2.0545E-006	0.059680	1.0000	0.034507
Total kmol/h	5589.66	1519.16	89.37	1516.12
Total kg/h	134606.52	55454.00	3755.45	55454.00
Total std L m3/h	119.45	33.63	3.03	34.25
Total std V m3/h	125284.60	34049.86	2003.12	33981.68

Flow rates in kg/h				
Aluminum Oxide	0.00	6851.04	0.00	6728.49
Antimony Trioxi	0.00	0.33	0.00	0.33
Arsenic Oxide	0.00	0.00	0.00	0.00
Barium Oxide	0.00	13.38	0.00	13.38
Boron Trioxide	0.00	61.90	0.00	61.90
Calcium Oxide	0.00	0.00	0.00	0.00
Cerium Nitrate	0.00	0.52	0.00	0.52
Cerium Oxide	0.00	5.33	0.00	5.33
Chromium(III) Ox	0.00	7.62	0.00	7.62
Cobalt(II) Oxide	0.00	1.67	0.00	1.67
Copper(II) Oxid	0.00	3.76	0.00	3.76
Dysprosium Nitr	0.00	0.05	0.00	0.05
Dysprosium Oxid	0.00	0.48	0.00	0.48
Erbium Nitrate	0.00	0.03	0.00	0.03
Erbium Oxide	0.00	0.29	0.00	0.29
Europium Nitrat	0.00	0.01	0.00	0.01
Europium Oxide	0.00	0.11	0.00	0.11
Gadolinium Nitr	0.00	0.05	0.00	0.05
Gadolinium Oxid	0.00	0.50	0.00	0.50
Gallium(III) Ox	0.00	2.09	0.00	2.09
Germanium Dioxi	0.00	4.33	0.00	4.33
Holmium Nitrate	0.00	0.01	0.00	0.01
Holmium Oxide	0.00	0.10	0.00	0.10
Iron(iii) oxide	0.00	5278.77	0.00	5227.80
Lanthanum Nitrat	0.00	0.17	0.00	0.17
Lanthanum Oxide	0.00	2.40	0.00	2.40
Lead(II) Oxide	0.00	2.15	0.00	2.15
Lithium Oxide	0.00	0.00	0.00	0.00
Lutetium Nitrat	0.00	0.00	0.00	0.00
Lutetium Oxide	0.00	0.02	0.00	0.02
Magnesium Oxide	0.00	175.87	0.00	175.87
Manganese(II)Ox	0.00	0.00	0.00	0.00
Molybdenum Trio	0.00	1.03	0.00	1.03
Neodymium Nitra	0.00	0.20	0.00	0.20
Neodymium Oxide	0.00	2.36	0.00	2.36
Nickel(II) Oxid	0.00	4.27	0.00	4.27
Nitric Acid	45428.24	8610.14	2516.94	8035.03
Potassium Oxide	0.00	0.00	0.00	0.00
Praseodymium Ni	0.00	0.05	0.00	0.05
Praseodymium Ox	0.00	0.61	0.00	0.61
Rubidium Oxide	0.00	3.88	0.00	3.88
Samarium Nitrat	0.00	0.04	0.00	0.04
Samarium Oxide	0.00	0.48	0.00	0.48
Scandium Nitrate	0.00	0.16	0.00	0.16
Scandium(III) Ox	0.00	1.59	0.00	1.59
Silicon Dioxide	0.00	14636.83	0.00	14636.83
Strontium Oxide	0.00	30.64	0.00	30.64
Calcium Sulfate	0.00	0.00	0.00	0.00
Terbium Nitrate	0.00	0.01	0.00	0.01
Terbium Oxide	0.00	0.09	0.00	0.09
Titanium Dioxide	0.00	380.55	0.00	380.55
Thorium(IV) Oxi	0.00	0.74	0.00	0.74
Thulium Nitrate	0.00	0.00	0.00	0.00

Thulium Oxide	0.00	0.04	0.00	0.04
Uranium(IV) Oxi	0.00	0.57	0.00	0.57
Vanadium(V) Oxi	0.00	15.65	0.00	15.65
Water	86971.66	17773.79	364.29	17856.00
Ytterbium Nitra	0.00	0.02	0.00	0.02
Ytterbium Oxide	0.00	0.25	0.00	0.25
Yttrium Oxide	0.00	3.54	0.00	3.54
Yttrium(III) Nit	0.00	0.47	0.00	0.47
Zinc Oxide	0.00	5.10	0.00	5.10
Nitrogen Trioxid	70.97	13.44	1.40	13.44
Barium Nitrate	0.00	0.70	0.00	0.70
Calcium Nitrate	0.00	0.00	0.00	0.00
Potassium Nitrat	0.00	0.00	0.00	0.00
Magnesium Nitrat	0.01	29.52	0.00	29.52
Nitrogen Dioxide	554.53	309.36	16.96	309.36
Sulfuric Acid	0.00	0.00	0.00	0.00
Aluminum Nitrat	0.02	26.95	0.00	538.97
Arsenic Acid	280.29	57.46	4.24	57.46
Cobalt(II) Nitr	0.00	0.12	0.00	0.12
Copper(II) Nitr	0.00	0.67	0.00	0.67
Iron(III) Nitra	0.01	8.13	0.00	162.52
Gallium(III) Ni	0.00	0.34	0.00	0.34
Mn(II) Nitrate	0.00	0.00	0.00	0.00
Nickel(II) Nitr	0.00	0.34	0.00	0.34
Lead(II) Nitrat	0.00	0.21	0.00	0.21
Uranyl Nitrate	0.00	0.04	0.00	0.04
Zinc Nitrate	0.00	0.86	0.00	0.86
Lithium Nitrate	0.00	0.00	0.00	0.00
Rubidium Nitrat	0.00	0.10	0.00	0.10
Antimony Pentox	0.00	0.16	0.00	0.16
Strontium Nitra	0.00	3.51	0.00	3.51
Thorium(IV) Nit	0.00	0.04	0.00	0.04
Nitrogen	0.96	613.67	612.55	613.67
Oxygen	0.64	186.45	186.26	186.45
Carbon Monoxide	0.00	0.00	0.00	0.00
Methane	0.00	0.00	0.00	0.00
Carbon Dioxide	0.00	0.00	0.00	0.00
N2O4	0.00	0.00	0.00	0.00
Nitric Oxide	0.07	0.09	0.45	0.09
dinitrogen pent	138.67	76.94	2.19	76.94
Nitrous Acid	1160.43	238.79	50.17	238.79

Stream No.	29	30	31	32
Stream Name				
Temp C	38.6223	38.6223	41.6707	41.6844
Pres atm	1.0000	1.0000	1.0000	1.4400
Enth kJ/h	-1.5158E+006	-1.1931E+007	-4.2574E+009	-2.7241E+009
Vapor mass frac.	1.0000	0.00000	0.00000	0.00000
Total kmol/h	84.95	55.92	15850.23	10141.80
Total kg/h	2724.64	2530.81	379775.00	243000.00
Total std L m3/h	2.86	1.84	337.75	216.11
Total std V m3/h	1904.10	1253.30	355261.56	227314.83
Flow rates in kg/h				
Aluminum Oxide	0.00	0.00	0.00	0.00

Antimony Trioxi	0.00	0.00	0.00	0.00
Arsenic Oxide	0.00	0.00	0.00	0.00
Barium Oxide	0.00	0.00	0.00	0.00
Boron Trioxide	0.00	0.00	0.00	0.00
Calcium Oxide	0.00	0.00	0.00	0.00
Cerium Nitrate	0.00	0.00	0.00	0.00
Cerium Oxide	0.00	0.00	0.00	0.00
Chromium(III) Ox	0.00	0.00	0.00	0.00
Cobalt(II) Oxide	0.00	0.00	0.00	0.00
Copper(II) Oxid	0.00	0.00	0.00	0.00
Dysprosium Nitr	0.00	0.00	0.00	0.00
Dysprosium Oxid	0.00	0.00	0.00	0.00
Erbium Nitrate	0.00	0.00	0.00	0.00
Erbium Oxide	0.00	0.00	0.00	0.00
Europium Nitrat	0.00	0.00	0.00	0.00
Europium Oxide	0.00	0.00	0.00	0.00
Gadolinium Nitr	0.00	0.00	0.00	0.00
Gadolinium Oxid	0.00	0.00	0.00	0.00
Gallium(III) Ox	0.00	0.00	0.00	0.00
Germanium Dioxi	0.00	0.00	0.00	0.00
Holmium Nitrate	0.00	0.00	0.00	0.00
Holmium Oxide	0.00	0.00	0.00	0.00
Iron(iii) oxide	0.00	0.00	0.00	0.00
Lanthanum Nitrat	0.00	0.00	0.00	0.00
Lanthanum Oxide	0.00	0.00	0.00	0.00
Lead(II) Oxide	0.00	0.00	0.00	0.00
Lithium Oxide	0.00	0.00	0.00	0.00
Lutetium Nitrat	0.00	0.00	0.00	0.00
Lutetium Oxide	0.00	0.00	0.00	0.00
Magnesium Oxide	0.00	0.00	0.00	0.00
Manganese(II)Ox	0.00	0.00	0.00	0.00
Molybdenum Trio	0.00	0.00	0.00	0.00
Neodymium Nitra	0.00	0.00	0.00	0.00
Neodymium Oxide	0.00	0.00	0.00	0.00
Nickel(II) Oxid	0.00	0.00	0.00	0.00
Nitric Acid	520.76	2080.24	126137.67	80709.44
Potassium Oxide	0.00	0.00	0.00	0.00
Praseodymium Ni	0.00	0.00	0.00	0.00
Praseodymium Ox	0.00	0.00	0.00	0.00
Rubidium Oxide	0.00	0.00	0.00	0.00
Samarium Nitrat	0.00	0.00	0.00	0.00
Samarium Oxide	0.00	0.00	0.00	0.00
Scandium Nitrate	0.00	0.00	0.00	0.00
Scandium(III) Ox	0.00	0.00	0.00	0.00
Silicon Dioxide	0.00	0.00	0.00	0.00
Strontium Oxide	0.00	0.00	0.00	0.00
Calcium Sulfate	0.00	0.00	0.00	0.00
Terbium Nitrate	0.00	0.00	0.00	0.00
Terbium Oxide	0.00	0.00	0.00	0.00
Titanium Dioxide	0.00	0.00	0.00	0.00
Thorium(IV) Oxi	0.00	0.00	0.00	0.00
Thulium Nitrate	0.00	0.00	0.00	0.00
Thulium Oxide	0.00	0.00	0.00	0.00
Uranium(IV) Oxi	0.00	0.00	0.00	0.00

Vanadium(V) Oxi	0.00	0.00	0.00	0.00
Water	40.23	391.20	247389.48	158292.64
Ytterbium Nitra	0.00	0.00	0.00	0.00
Ytterbium Oxide	0.00	0.00	0.00	0.00
Yttrium Oxide	0.00	0.00	0.00	0.00
Yttrium(III) Nit	0.00	0.00	0.00	0.00
Zinc Oxide	0.00	0.00	0.00	0.00
Nitrogen Trioxid	4.04	0.62	197.06	126.09
Barium Nitrate	0.00	0.00	0.00	0.00
Calcium Nitrate	0.00	0.00	0.00	0.00
Potassium Nitrat	0.00	0.00	0.00	0.00
Magnesium Nitrat	0.00	0.00	0.02	0.01
Nitrogen Dioxide	13.01	3.95	1539.74	985.20
Sulfuric Acid	0.00	0.00	0.00	0.00
Aluminum Nitrat	0.00	0.00	0.05	0.03
Arsenic Acid	0.27	4.11	801.79	513.03
Cobalt(II) Nitr	0.00	0.00	0.00	0.00
Copper(II) Nitr	0.00	0.00	0.00	0.00
Iron(III) Nitra	0.00	0.00	0.02	0.01
Gallium(III) Ni	0.00	0.00	0.00	0.00
Mn(II) Nitrate	0.00	0.00	0.00	0.00
Nickel(II) Nitr	0.00	0.00	0.00	0.00
Lead(II) Nitrat	0.00	0.00	0.00	0.00
Uranyl Nitrate	0.00	0.00	0.00	0.00
Zinc Nitrate	0.00	0.00	0.00	0.00
Lithium Nitrate	0.00	0.00	0.00	0.00
Rubidium Nitrat	0.00	0.00	0.00	0.00
Antimony Pentox	0.00	0.00	0.00	0.00
Strontium Nitra	0.00	0.00	0.00	0.00
Thorium(IV) Nit	0.00	0.00	0.00	0.00
Nitrogen	1572.50	0.01	2.67	1.71
Oxygen	531.85	0.01	1.78	1.14
Carbon Monoxide	0.00	0.00	0.00	0.00
Methane	0.00	0.00	0.00	0.00
Carbon Dioxide	0.00	0.00	0.00	0.00
N2O4	0.00	0.00	0.00	0.00
Nitric Oxide	40.19	0.00	0.19	0.12
dinitrogen pent	1.14	1.05	385.04	246.37
Nitrous Acid	0.64	49.64	3319.81	2124.19

Stream No.	33	34	35	36
Stream Name				
Temp C	40.0000	41.0394	41.9257	42.7465
Pres atm	1.1000	1.0000	1.0000	1.0000
Enth kJ/h	-2.7255E+009	-2.7299E+009	-2.7298E+009	-2.7298E+009
Vapor mass frac.	0.00000	0.011866	0.010585	0.0096957
Total kmol/h	10141.80	10260.69	10253.81	10236.06
Total kg/h	243000.00	246753.48	246753.63	246753.63
Total std L m3/h	216.11	219.89	219.81	219.66
Total std V m3/h	227314.83	229979.42	229825.33	229427.52
Flow rates in kg/h				
Aluminum Oxide	0.00	0.00	0.00	0.00
Antimony Trioxi	0.00	0.00	0.00	0.00
Arsenic Oxide	0.00	0.00	0.00	0.00

Barium Oxide	0.00	0.00	0.00	0.00
Boron Trioxide	0.00	0.00	0.00	0.00
Calcium Oxide	0.00	0.00	0.00	0.00
Cerium Nitrate	0.00	0.00	0.00	0.00
Cerium Oxide	0.00	0.00	0.00	0.00
Chromium(III) Ox	0.00	0.00	0.00	0.00
Cobalt(II) Oxide	0.00	0.00	0.00	0.00
Copper(II) Oxid	0.00	0.00	0.00	0.00
Dysprosium Nitr	0.00	0.00	0.00	0.00
Dysprosium Oxid	0.00	0.00	0.00	0.00
Erbium Nitrate	0.00	0.00	0.00	0.00
Erbium Oxide	0.00	0.00	0.00	0.00
Europium Nitrat	0.00	0.00	0.00	0.00
Europium Oxide	0.00	0.00	0.00	0.00
Gadolinium Nitr	0.00	0.00	0.00	0.00
Gadolinium Oxid	0.00	0.00	0.00	0.00
Gallium(III) Ox	0.00	0.00	0.00	0.00
Germanium Dioxi	0.00	0.00	0.00	0.00
Holmium Nitrate	0.00	0.00	0.00	0.00
Holmium Oxide	0.00	0.00	0.00	0.00
Iron(iii) oxide	0.00	0.00	0.00	0.00
Lanthanum Nitrat	0.00	0.00	0.00	0.00
Lanthanum Oxide	0.00	0.00	0.00	0.00
Lead(II) Oxide	0.00	0.00	0.00	0.00
Lithium Oxide	0.00	0.00	0.00	0.00
Lutetium Nitrat	0.00	0.00	0.00	0.00
Lutetium Oxide	0.00	0.00	0.00	0.00
Magnesium Oxide	0.00	0.00	0.00	0.00
Manganese(II)Ox	0.00	0.00	0.00	0.00
Molybdenum Trio	0.00	0.00	0.00	0.00
Neodymium Nitra	0.00	0.00	0.00	0.00
Neodymium Oxide	0.00	0.00	0.00	0.00
Nickel(II) Oxid	0.00	0.00	0.00	0.00
Nitric Acid	80709.44	81435.70	81741.00	83232.26
Potassium Oxide	0.00	0.00	0.00	0.00
Praseodymium Ni	0.00	0.00	0.00	0.00
Praseodymium Ox	0.00	0.00	0.00	0.00
Rubidium Oxide	0.00	0.00	0.00	0.00
Samarium Nitrat	0.00	0.00	0.00	0.00
Samarium Oxide	0.00	0.00	0.00	0.00
Scandium Nitrate	0.00	0.00	0.00	0.00
Scandium(III) Ox	0.00	0.00	0.00	0.00
Silicon Dioxide	0.00	0.00	0.00	0.00
Strontium Oxide	0.00	0.00	0.00	0.00
Calcium Sulfate	0.00	0.00	0.00	0.00
Terbium Nitrate	0.00	0.00	0.00	0.00
Terbium Oxide	0.00	0.00	0.00	0.00
Titanium Dioxide	0.00	0.00	0.00	0.00
Thorium(IV) Oxi	0.00	0.00	0.00	0.00
Thulium Nitrate	0.00	0.00	0.00	0.00
Thulium Oxide	0.00	0.00	0.00	0.00
Uranium(IV) Oxi	0.00	0.00	0.00	0.00
Vanadium(V) Oxi	0.00	0.00	0.00	0.00
Water	158292.64	158568.45	158517.70	158304.52

Ytterbium Nitra	0.00	0.00	0.00	0.00
Ytterbium Oxide	0.00	0.00	0.00	0.00
Yttrium Oxide	0.00	0.00	0.00	0.00
Yttrium(III) Nit	0.00	0.00	0.00	0.00
Zinc Oxide	0.00	0.00	0.00	0.00
Nitrogen Trioxid	126.09	135.78	135.74	135.74
Barium Nitrate	0.00	0.00	0.00	0.00
Calcium Nitrate	0.00	0.00	0.00	0.00
Potassium Nitrat	0.00	0.00	0.00	0.00
Magnesium Nitrat	0.01	0.01	0.01	0.01
Nitrogen Dioxide	985.20	1088.73	1088.76	0.00
Sulfuric Acid	0.00	0.00	0.00	0.00
Aluminum Nitrat	0.03	0.03	0.03	0.03
Arsenic Acid	513.03	513.73	513.83	513.83
Cobalt(II) Nitr	0.00	0.00	0.00	0.00
Copper(II) Nitr	0.00	0.00	0.00	0.00
Iron(III) Nitra	0.01	0.01	0.01	0.01
Gallium(III) Ni	0.00	0.00	0.00	0.00
Mn(II) Nitrate	0.00	0.00	0.00	0.00
Nickel(II) Nitr	0.00	0.00	0.00	0.00
Lead(II) Nitrat	0.00	0.00	0.00	0.00
Uranyl Nitrate	0.00	0.00	0.00	0.00
Zinc Nitrate	0.00	0.00	0.00	0.00
Lithium Nitrate	0.00	0.00	0.00	0.00
Rubidium Nitrat	0.00	0.00	0.00	0.00
Antimony Pentox	0.00	0.00	0.00	0.00
Strontium Nitra	0.00	0.00	0.00	0.00
Thorium(IV) Nit	0.00	0.00	0.00	0.00
Nitrogen	1.71	1575.17	1575.15	1575.15
Oxygen	1.14	861.45	756.95	567.63
Carbon Monoxide	0.00	0.00	0.00	0.00
Methane	0.00	0.00	0.00	0.00
Carbon Dioxide	0.00	0.00	0.00	0.00
N2O4	0.00	0.00	300.47	300.47
Nitric Oxide	0.12	195.98	0.00	0.00
dinitrogen pent	246.37	253.15	0.00	0.00
Nitrous Acid	2124.19	2125.29	2123.94	2123.94

Stream No.	37	38	39	40
Stream Name				
Temp C	42.6187	57.5088	67.9835	41.6707
Pres atm	1.0000	1.0200	1.2000	1.0000
Enth kJ/h	-2.7298E+009	-4.5290E+006	-4.4682E+006	0.00000
Vapor mass frac.	0.0099649	0.99492	1.0000	1.0000
Total kmol/h	10237.15	118.89	118.89	0.00
Total kg/h	246753.66	3753.53	3753.53	0.00
Total std L m3/h	219.40	3.78	3.78	0.00
Total std V m3/h	229451.91	2664.66	2664.66	0.00
Flow rates in kg/h				
Aluminum Oxide	0.00	0.00	0.00	0.00
Antimony Trioxi	0.00	0.00	0.00	0.00
Arsenic Oxide	0.00	0.00	0.00	0.00
Barium Oxide	0.00	0.00	0.00	0.00
Boron Trioxide	0.00	0.00	0.00	0.00

Calcium Oxide	0.00	0.00	0.00	0.00
Cerium Nitrate	0.00	0.00	0.00	0.00
Cerium Oxide	0.00	0.00	0.00	0.00
Chromium(III) Ox	0.00	0.00	0.00	0.00
Cobalt(II) Oxide	0.00	0.00	0.00	0.00
Copper(II) Oxid	0.00	0.00	0.00	0.00
Dysprosium Nitr	0.00	0.00	0.00	0.00
Dysprosium Oxid	0.00	0.00	0.00	0.00
Erbium Nitrate	0.00	0.00	0.00	0.00
Erbium Oxide	0.00	0.00	0.00	0.00
Europium Nitrat	0.00	0.00	0.00	0.00
Europium Oxide	0.00	0.00	0.00	0.00
Gadolinium Nitr	0.00	0.00	0.00	0.00
Gadolinium Oxid	0.00	0.00	0.00	0.00
Gallium(III) Ox	0.00	0.00	0.00	0.00
Germanium Dioxi	0.00	0.00	0.00	0.00
Holmium Nitrate	0.00	0.00	0.00	0.00
Holmium Oxide	0.00	0.00	0.00	0.00
Iron(iii) oxide	0.00	0.00	0.00	0.00
Lanthanum Nitrat	0.00	0.00	0.00	0.00
Lanthanum Oxide	0.00	0.00	0.00	0.00
Lead(II) Oxide	0.00	0.00	0.00	0.00
Lithium Oxide	0.00	0.00	0.00	0.00
Lutetium Nitrat	0.00	0.00	0.00	0.00
Lutetium Oxide	0.00	0.00	0.00	0.00
Magnesium Oxide	0.00	0.00	0.00	0.00
Manganese(II)Ox	0.00	0.00	0.00	0.00
Molybdenum Trio	0.00	0.00	0.00	0.00
Neodymium Nitra	0.00	0.00	0.00	0.00
Neodymium Oxide	0.00	0.00	0.00	0.00
Nickel(II) Oxid	0.00	0.00	0.00	0.00
Nitric Acid	83506.63	726.27	726.27	0.00
Potassium Oxide	0.00	0.00	0.00	0.00
Praseodymium Ni	0.00	0.00	0.00	0.00
Praseodymium Ox	0.00	0.00	0.00	0.00
Rubidium Oxide	0.00	0.00	0.00	0.00
Samarium Nitrat	0.00	0.00	0.00	0.00
Samarium Oxide	0.00	0.00	0.00	0.00
Scandium Nitrate	0.00	0.00	0.00	0.00
Scandium(III) Ox	0.00	0.00	0.00	0.00
Silicon Dioxide	0.00	0.00	0.00	0.00
Strontium Oxide	0.00	0.00	0.00	0.00
Calcium Sulfate	0.00	0.00	0.00	0.00
Terbium Nitrate	0.00	0.00	0.00	0.00
Terbium Oxide	0.00	0.00	0.00	0.00
Titanium Dioxide	0.00	0.00	0.00	0.00
Thorium(IV) Oxi	0.00	0.00	0.00	0.00
Thulium Nitrate	0.00	0.00	0.00	0.00
Thulium Oxide	0.00	0.00	0.00	0.00
Uranium(IV) Oxi	0.00	0.00	0.00	0.00
Vanadium(V) Oxi	0.00	0.00	0.00	0.00
Water	158265.33	275.83	275.83	0.00
Ytterbium Nitra	0.00	0.00	0.00	0.00
Ytterbium Oxide	0.00	0.00	0.00	0.00

Yttrium Oxide	0.00	0.00	0.00	0.00
Yttrium(III) Nit	0.00	0.00	0.00	0.00
Zinc Oxide	0.00	0.00	0.00	0.00
Nitrogen Trioxid	135.74	9.69	9.69	0.00
Barium Nitrate	0.00	0.00	0.00	0.00
Calcium Nitrate	0.00	0.00	0.00	0.00
Potassium Nitrat	0.00	0.00	0.00	0.00
Magnesium Nitrat	0.01	0.00	0.00	0.00
Nitrogen Dioxide	0.00	103.53	103.53	0.00
Sulfuric Acid	0.00	0.00	0.00	0.00
Aluminum Nitrat	0.03	0.00	0.00	0.00
Arsenic Acid	513.83	0.70	0.70	0.00
Cobalt(II) Nitr	0.00	0.00	0.00	0.00
Copper(II) Nitr	0.00	0.00	0.00	0.00
Iron(III) Nitra	0.01	0.00	0.00	0.00
Gallium(III) Ni	0.00	0.00	0.00	0.00
Mn(II) Nitrate	0.00	0.00	0.00	0.00
Nickel(II) Nitr	0.00	0.00	0.00	0.00
Lead(II) Nitrat	0.00	0.00	0.00	0.00
Uranyl Nitrate	0.00	0.00	0.00	0.00
Zinc Nitrate	0.00	0.00	0.00	0.00
Lithium Nitrate	0.00	0.00	0.00	0.00
Rubidium Nitrat	0.00	0.00	0.00	0.00
Antimony Pentox	0.00	0.00	0.00	0.00
Strontium Nitra	0.00	0.00	0.00	0.00
Thorium(IV) Nit	0.00	0.00	0.00	0.00
Nitrogen	1575.15	1573.46	1573.46	0.00
Oxygen	567.63	860.31	860.31	0.00
Carbon Monoxide	0.00	0.00	0.00	0.00
Methane	0.00	0.00	0.00	0.00
Carbon Dioxide	0.00	0.00	0.00	0.00
N2O4	0.00	0.00	0.00	0.00
Nitric Oxide	65.33	195.85	195.85	0.00
dinitrogen pent	0.00	6.78	6.78	0.00
Nitrous Acid	2123.94	1.11	1.11	0.00
Stream No.	41	42	43	44
Stream Name				
Temp C	42.6187	99.3457	79.0508	120.0000
Pres atm	1.0000	1.0000	1.0200	1.5100
Enth kJ/h	-1.5346E+006	-3.3108E+007	-1.4119E+010	-1.0097E+009
Vapor mass frac.	1.0000	0.00000	0.0015172	1.0000
Total kmol/h	84.42	118.78	28518.06	4507.86
Total kg/h	2458.88	2168.85	705516.00	105953.00
Total std L m3/h	2.73	2.19	627.01	95.14
Total std V m3/h	1892.14	2662.20	639193.69	101037.65
Flow rates in kg/h				
Aluminum Oxide	0.00	0.00	6728.49	0.00
Antimony Trioxi	0.00	0.00	0.33	0.00
Arsenic Oxide	0.00	0.00	0.00	0.00
Barium Oxide	0.00	0.00	13.38	0.00
Boron Trioxide	0.00	0.00	61.90	0.00
Calcium Oxide	0.00	0.00	0.00	0.00
Cerium Nitrate	0.00	0.00	12.79	0.00

Cerium Oxide	0.00	0.00	5.33	0.00
Chromium(III) Ox	0.00	0.00	7.62	0.00
Cobalt(II) Oxide	0.00	0.00	1.67	0.00
Copper(II) Oxid	0.00	0.00	3.76	0.00
Dysprosium Nitr	0.00	0.00	1.23	0.00
Dysprosium Oxid	0.00	0.00	0.48	0.00
Erbium Nitrate	0.00	0.00	0.70	0.00
Erbium Oxide	0.00	0.00	0.29	0.00
Europium Nitrat	0.00	0.00	0.27	0.00
Europium Oxide	0.00	0.00	0.11	0.00
Gadolinium Nitr	0.00	0.00	1.32	0.00
Gadolinium Oxid	0.00	0.00	0.50	0.00
Gallium(III) Ox	0.00	0.00	2.09	0.00
Germanium Dioxi	0.00	0.00	4.33	0.00
Holmium Nitrate	0.00	0.00	0.26	0.00
Holmium Oxide	0.00	0.00	0.10	0.00
Iron(iii) oxide	0.00	0.00	5227.80	0.00
Lanthanum Nitrat	0.00	0.00	4.25	0.00
Lanthanum Oxide	0.00	0.00	2.40	0.00
Lead(II) Oxide	0.00	0.00	2.15	0.00
Lithium Oxide	0.00	0.00	0.00	0.00
Lutetium Nitrat	0.00	0.00	0.04	0.00
Lutetium Oxide	0.00	0.00	0.02	0.00
Magnesium Oxide	0.00	0.00	175.87	0.00
Manganese(II)Ox	0.00	0.00	0.00	0.00
Molybdenum Trio	0.00	0.00	1.03	0.00
Neodymium Nitra	0.00	0.00	4.97	0.00
Neodymium Oxide	0.00	0.00	2.36	0.00
Nickel(II) Oxid	0.00	0.00	4.27	0.00
Nitric Acid	137.79	0.00	199313.00	32112.00
Potassium Oxide	0.00	0.00	0.00	0.00
Praseodymium Ni	0.00	0.00	1.22	0.00
Praseodymium Ox	0.00	0.00	0.61	0.00
Rubidium Oxide	0.00	0.00	3.88	0.00
Samarium Nitrat	0.00	0.00	1.09	0.00
Samarium Oxide	0.00	0.00	0.48	0.00
Scandium Nitrate	0.00	0.00	3.99	0.00
Scandium(III) Ox	0.00	0.00	1.59	0.00
Silicon Dioxide	0.00	0.00	14636.83	0.00
Strontium Oxide	0.00	0.00	30.64	0.00
Calcium Sulfate	0.00	0.00	0.00	0.00
Terbium Nitrate	0.00	0.00	0.21	0.00
Terbium Oxide	0.00	0.00	0.09	0.00
Titanium Dioxide	0.00	0.00	380.55	0.00
Thorium(IV) Oxi	0.00	0.00	0.74	0.00
Thulium Nitrate	0.00	0.00	0.09	0.00
Thulium Oxide	0.00	0.00	0.04	0.00
Uranium(IV) Oxi	0.00	0.00	0.57	0.00
Vanadium(V) Oxi	0.00	0.00	15.65	0.00
Water	110.05	2125.19	442706.00	71100.56
Ytterbium Nitra	0.00	0.00	0.51	0.00
Ytterbium Oxide	0.00	0.00	0.25	0.00
Yttrium Oxide	0.00	0.00	3.54	0.00
Yttrium(III) Nit	0.00	0.00	11.59	0.00

Zinc Oxide	0.00	0.00	5.10	0.00
Nitrogen Trioxid	5.34	0.00	338.62	53.98
Barium Nitrate	0.00	0.00	17.34	0.00
Calcium Nitrate	0.00	0.00	0.00	0.00
Potassium Nitrat	0.00	0.00	0.00	0.00
Magnesium Nitrat	0.00	0.00	731.43	0.00
Nitrogen Dioxide	0.00	0.00	7756.43	1242.75
Sulfuric Acid	0.00	0.00	0.00	0.00
Aluminum Nitrat	0.00	0.00	13355.62	0.01
Arsenic Acid	0.23	8.47	1424.24	226.70
Cobalt(II) Nitr	0.00	0.00	2.97	0.00
Copper(II) Nitr	0.00	0.00	16.54	0.00
Iron(III) Nitra	0.00	0.00	4027.35	0.00
Gallium(III) Ni	0.00	0.00	8.40	0.00
Mn(II) Nitrate	0.00	0.00	0.00	0.00
Nickel(II) Nitr	0.00	0.00	8.50	0.00
Lead(II) Nitrat	0.00	0.00	5.14	0.00
Uranyl Nitrate	0.00	0.00	1.02	0.00
Zinc Nitrate	0.00	0.00	21.38	0.00
Lithium Nitrate	0.00	0.00	0.00	0.00
Rubidium Nitrat	0.00	0.00	2.56	0.00
Antimony Pentox	0.00	0.00	0.16	0.00
Strontium Nitra	0.00	0.00	87.03	0.00
Thorium(IV) Nit	0.00	0.00	0.88	0.00
Nitrogen	1573.61	0.00	0.96	0.00
Oxygen	566.53	0.00	331.42	0.48
Carbon Monoxide	0.00	0.00	0.00	0.00
Methane	0.00	0.00	0.00	0.00
Carbon Dioxide	0.00	0.00	0.00	0.00
N2O4	0.00	0.00	0.00	0.00
Nitric Oxide	65.14	0.00	157.91	0.36
dinitrogen pent	0.00	0.00	1912.24	308.39
Nitrous Acid	0.19	35.19	5917.78	907.77

Stream No.	45	46	47	48
Stream Name				Air Feed
Temp C	99.3457	153.6650	129.4426	25.0000
Pres atm	1.0000	3.0000	1.0000	1.0000
Enth kJ/h	-6.0351E+005	1.0079E+005	-1.0003E+007	0.019465
Vapor mass frac.	1.0000	1.0000	1.0000	1.0000
Total kmol/h	4.49	27.73	89.37	27.73
Total kg/h	283.01	800.00	3755.45	800.00
Total std L m3/h	0.19	0.92	3.03	0.92
Total std V m3/h	100.67	621.50	2003.12	621.50
Flow rates in kg/h				
Aluminum Oxide	0.00	0.00	0.00	0.00
Antimony Trioxi	0.00	0.00	0.00	0.00
Arsenic Oxide	0.00	0.00	0.00	0.00
Barium Oxide	0.00	0.00	0.00	0.00
Boron Trioxide	0.00	0.00	0.00	0.00
Calcium Oxide	0.00	0.00	0.00	0.00
Cerium Nitrate	0.00	0.00	0.00	0.00
Cerium Oxide	0.00	0.00	0.00	0.00
Chromium(III) Ox	0.00	0.00	0.00	0.00

Cobalt(II) Oxide	0.00	0.00	0.00	0.00
Copper(II) Oxid	0.00	0.00	0.00	0.00
Dysprosium Nitr	0.00	0.00	0.00	0.00
Dysprosium Oxid	0.00	0.00	0.00	0.00
Erbium Nitrate	0.00	0.00	0.00	0.00
Erbium Oxide	0.00	0.00	0.00	0.00
Europium Nitrat	0.00	0.00	0.00	0.00
Europium Oxide	0.00	0.00	0.00	0.00
Gadolinium Nitr	0.00	0.00	0.00	0.00
Gadolinium Oxid	0.00	0.00	0.00	0.00
Gallium(III) Ox	0.00	0.00	0.00	0.00
Germanium Dioxi	0.00	0.00	0.00	0.00
Holmium Nitrate	0.00	0.00	0.00	0.00
Holmium Oxide	0.00	0.00	0.00	0.00
Iron(iii) oxide	0.00	0.00	0.00	0.00
Lanthanum Nitrat	0.00	0.00	0.00	0.00
Lanthanum Oxide	0.00	0.00	0.00	0.00
Lead(II) Oxide	0.00	0.00	0.00	0.00
Lithium Oxide	0.00	0.00	0.00	0.00
Lutetium Nitrat	0.00	0.00	0.00	0.00
Lutetium Oxide	0.00	0.00	0.00	0.00
Magnesium Oxide	0.00	0.00	0.00	0.00
Manganese(II)Ox	0.00	0.00	0.00	0.00
Molybdenum Trio	0.00	0.00	0.00	0.00
Neodymium Nitra	0.00	0.00	0.00	0.00
Neodymium Oxide	0.00	0.00	0.00	0.00
Nickel(II) Oxid	0.00	0.00	0.00	0.00
Nitric Acid	283.01	0.00	2516.94	0.00
Potassium Oxide	0.00	0.00	0.00	0.00
Praseodymium Ni	0.00	0.00	0.00	0.00
Praseodymium Ox	0.00	0.00	0.00	0.00
Rubidium Oxide	0.00	0.00	0.00	0.00
Samarium Nitrat	0.00	0.00	0.00	0.00
Samarium Oxide	0.00	0.00	0.00	0.00
Scandium Nitrate	0.00	0.00	0.00	0.00
Scandium(III) Ox	0.00	0.00	0.00	0.00
Silicon Dioxide	0.00	0.00	0.00	0.00
Strontium Oxide	0.00	0.00	0.00	0.00
Calcium Sulfate	0.00	0.00	0.00	0.00
Terbium Nitrate	0.00	0.00	0.00	0.00
Terbium Oxide	0.00	0.00	0.00	0.00
Titanium Dioxide	0.00	0.00	0.00	0.00
Thorium(IV) Oxi	0.00	0.00	0.00	0.00
Thulium Nitrate	0.00	0.00	0.00	0.00
Thulium Oxide	0.00	0.00	0.00	0.00
Uranium(IV) Oxi	0.00	0.00	0.00	0.00
Vanadium(V) Oxi	0.00	0.00	0.00	0.00
Water	0.00	0.00	364.29	0.00
Ytterbium Nitra	0.00	0.00	0.00	0.00
Ytterbium Oxide	0.00	0.00	0.00	0.00
Yttrium Oxide	0.00	0.00	0.00	0.00
Yttrium(III) Nit	0.00	0.00	0.00	0.00
Zinc Oxide	0.00	0.00	0.00	0.00
Nitrogen Trioxid	0.00	0.00	1.40	0.00

Barium Nitrate	0.00	0.00	0.00	0.00
Calcium Nitrate	0.00	0.00	0.00	0.00
Potassium Nitrat	0.00	0.00	0.00	0.00
Magnesium Nitrat	0.00	0.00	0.00	0.00
Nitrogen Dioxide	0.00	0.00	16.96	0.00
Sulfuric Acid	0.00	0.00	0.00	0.00
Aluminum Nitrat	0.00	0.00	0.00	0.00
Arsenic Acid	0.00	0.00	4.24	0.00
Cobalt(II) Nitr	0.00	0.00	0.00	0.00
Copper(II) Nitr	0.00	0.00	0.00	0.00
Iron(III) Nitra	0.00	0.00	0.00	0.00
Gallium(III) Ni	0.00	0.00	0.00	0.00
Mn(II) Nitrate	0.00	0.00	0.00	0.00
Nickel(II) Nitr	0.00	0.00	0.00	0.00
Lead(II) Nitrat	0.00	0.00	0.00	0.00
Uranyl Nitrate	0.00	0.00	0.00	0.00
Zinc Nitrate	0.00	0.00	0.00	0.00
Lithium Nitrate	0.00	0.00	0.00	0.00
Rubidium Nitrat	0.00	0.00	0.00	0.00
Antimony Pentox	0.00	0.00	0.00	0.00
Strontium Nitra	0.00	0.00	0.00	0.00
Thorium(IV) Nit	0.00	0.00	0.00	0.00
Nitrogen	0.00	613.67	612.55	613.67
Oxygen	0.00	186.33	186.26	186.33
Carbon Monoxide	0.00	0.00	0.00	0.00
Methane	0.00	0.00	0.00	0.00
Carbon Dioxide	0.00	0.00	0.00	0.00
N2O4	0.00	0.00	0.00	0.00
Nitric Oxide	0.00	0.00	0.45	0.00
dinitrogen pent	0.00	0.00	2.19	0.00
Nitrous Acid	0.00	0.00	50.17	0.00

Stream No.	49	50	51	52
Stream Name				
Temp C	45.7469	46.1920	60.8397	40.0000
Pres atm	1.0000	1.2000	1.0000	1.1600
Enth kJ/h	-1.5327E+009	-1.4976E+009	-6.9892E+009	-1.5176E+009
Vapor mass frac.	1.6692E-006	0.00000	0.039197	0.0065864
Total kmol/h	5715.29	5589.66	1519.16	5671.86
Total kg/h	137206.61	134606.52	55454.00	133831.20
Total std L m3/h	121.89	119.45	33.63	120.24
Total std V m3/h	128100.39	125284.60	34049.86	127127.11
Flow rates in kg/h				
Aluminum Oxide	0.00	0.00	6851.04	0.00
Antimony Trioxi	0.00	0.00	0.33	0.00
Arsenic Oxide	0.00	0.00	0.00	0.00
Barium Oxide	0.00	0.00	13.38	0.00
Boron Trioxide	0.00	0.00	61.90	0.00
Calcium Oxide	0.00	0.00	0.00	0.00
Cerium Nitrate	0.00	0.00	0.52	0.00
Cerium Oxide	0.00	0.00	5.33	0.00
Chromium(III) Ox	0.00	0.00	7.62	0.00
Cobalt(II) Oxide	0.00	0.00	1.67	0.00
Copper(II) Oxid	0.00	0.00	3.76	0.00

Dysprosium Nitr	0.00	0.00	0.05	0.00
Dysprosium Oxid	0.00	0.00	0.48	0.00
Erbium Nitrate	0.00	0.00	0.03	0.00
Erbium Oxide	0.00	0.00	0.29	0.00
Europium Nitrat	0.00	0.00	0.01	0.00
Europium Oxide	0.00	0.00	0.11	0.00
Gadolinium Nitr	0.00	0.00	0.05	0.00
Gadolinium Oxid	0.00	0.00	0.50	0.00
Gallium(III) Ox	0.00	0.00	2.09	0.00
Germanium Dioxi	0.00	0.00	4.33	0.00
Holmium Nitrate	0.00	0.00	0.01	0.00
Holmium Oxide	0.00	0.00	0.10	0.00
Iron(iii) oxide	0.00	0.00	5278.77	0.00
Lanthanum Nitrat	0.00	0.00	0.17	0.00
Lanthanum Oxide	0.00	0.00	2.40	0.00
Lead(II) Oxide	0.00	0.00	2.15	0.00
Lithium Oxide	0.00	0.00	0.00	0.00
Lutetium Nitrat	0.00	0.00	0.00	0.00
Lutetium Oxide	0.00	0.00	0.02	0.00
Magnesium Oxide	0.00	0.00	175.87	0.00
Manganese(II)Ox	0.00	0.00	0.00	0.00
Molybdenum Trio	0.00	0.00	1.03	0.00
Neodymium Nitra	0.00	0.00	0.20	0.00
Neodymium Oxide	0.00	0.00	2.36	0.00
Nickel(II) Oxid	0.00	0.00	4.27	0.00
Nitric Acid	45900.00	45428.24	8610.14	40721.70
Potassium Oxide	0.00	0.00	0.00	0.00
Praseodymium Ni	0.00	0.00	0.05	0.00
Praseodymium Ox	0.00	0.00	0.61	0.00
Rubidium Oxide	0.00	0.00	3.88	0.00
Samarium Nitrat	0.00	0.00	0.04	0.00
Samarium Oxide	0.00	0.00	0.48	0.00
Scandium Nitrate	0.00	0.00	0.16	0.00
Scandium(III) Ox	0.00	0.00	1.59	0.00
Silicon Dioxide	0.00	0.00	14636.83	0.00
Strontium Oxide	0.00	0.00	30.64	0.00
Calcium Sulfate	0.00	0.00	0.00	0.00
Terbium Nitrate	0.00	0.00	0.01	0.00
Terbium Oxide	0.00	0.00	0.09	0.00
Titanium Dioxide	0.00	0.00	380.55	0.00
Thorium(IV) Oxi	0.00	0.00	0.74	0.00
Thulium Nitrate	0.00	0.00	0.00	0.00
Thulium Oxide	0.00	0.00	0.04	0.00
Uranium(IV) Oxi	0.00	0.00	0.57	0.00
Vanadium(V) Oxi	0.00	0.00	15.65	0.00
Water	89100.00	86971.66	17773.79	88873.00
Ytterbium Nitra	0.00	0.00	0.02	0.00
Ytterbium Oxide	0.00	0.00	0.25	0.00
Yttrium Oxide	0.00	0.00	3.54	0.00
Yttrium(III) Nit	0.00	0.00	0.47	0.00
Zinc Oxide	0.00	0.00	5.10	0.00
Nitrogen Trioxid	70.97	70.97	13.44	67.42
Barium Nitrate	0.00	0.00	0.70	0.00
Calcium Nitrate	0.00	0.00	0.00	0.00

Potassium Nitrat	0.00	0.00	0.00	0.00
Magnesium Nitrat	0.01	0.01	29.52	0.01
Nitrogen Dioxide	554.53	554.53	309.36	1552.11
Sulfuric Acid	0.00	0.00	0.00	0.00
Aluminum Nitrat	0.02	0.02	26.95	0.02
Arsenic Acid	280.29	280.29	57.46	284.15
Cobalt(II) Nitr	0.00	0.00	0.12	0.00
Copper(II) Nitr	0.00	0.00	0.67	0.00
Iron(III) Nitra	0.01	0.01	8.13	0.01
Gallium(III) Ni	0.00	0.00	0.34	0.00
Mn(II) Nitrate	0.00	0.00	0.00	0.00
Nickel(II) Nitr	0.00	0.00	0.34	0.00
Lead(II) Nitrat	0.00	0.00	0.21	0.00
Uranyl Nitrate	0.00	0.00	0.04	0.00
Zinc Nitrate	0.00	0.00	0.86	0.00
Lithium Nitrate	0.00	0.00	0.00	0.00
Rubidium Nitrat	0.00	0.00	0.10	0.00
Antimony Pentox	0.00	0.00	0.16	0.00
Strontium Nitra	0.00	0.00	3.51	0.00
Thorium(IV) Nit	0.00	0.00	0.04	0.00
Nitrogen	0.96	0.96	613.67	613.67
Oxygen	0.64	0.64	186.45	186.93
Carbon Monoxide	0.00	0.00	0.00	0.00
Methane	0.00	0.00	0.00	0.00
Carbon Dioxide	0.00	0.00	0.00	0.00
N2O4	0.00	0.00	0.00	0.00
Nitric Oxide	0.07	0.07	0.09	0.46
dinitrogen pent	138.67	138.67	76.94	385.33
Nitrous Acid	1160.43	1160.43	238.79	1146.46

Stream No.	53	54	55	56
Stream Name				
Temp C	41.8278	41.8278	46.1920	155.0000
Pres atm	1.0000	1.0000	1.2000	1.0000
Enth kJ/h	-2.7298E+009	-2.7298E+009	-1.4976E+009	-6.9360E+009
Vapor mass frac.	0.010585	0.010585	0.00000	0.99731
Total kmol/h	10253.81	10253.81	5589.66	1519.16
Total kg/h	246753.63	246753.63	134606.52	55454.00
Total std L m3/h	220.05	220.05	119.45	33.63
Total std V m3/h	229825.36	229825.36	125284.60	34049.86
Flow rates in kg/h				
Aluminum Oxide	0.00	0.00	0.00	6851.04
Antimony Trioxi	0.00	0.00	0.00	0.33
Arsenic Oxide	0.00	0.00	0.00	0.00
Barium Oxide	0.00	0.00	0.00	13.38
Boron Trioxide	0.00	0.00	0.00	61.90
Calcium Oxide	0.00	0.00	0.00	0.00
Cerium Nitrate	0.00	0.00	0.00	0.52
Cerium Oxide	0.00	0.00	0.00	5.33
Chromium(III) Ox	0.00	0.00	0.00	7.62
Cobalt(II) Oxide	0.00	0.00	0.00	1.67
Copper(II) Oxid	0.00	0.00	0.00	3.76
Dysprosium Nitr	0.00	0.00	0.00	0.05
Dysprosium Oxid	0.00	0.00	0.00	0.48

Erbium Nitrate	0.00	0.00	0.00	0.03
Erbium Oxide	0.00	0.00	0.00	0.29
Europium Nitrat	0.00	0.00	0.00	0.01
Europium Oxide	0.00	0.00	0.00	0.11
Gadolinium Nitr	0.00	0.00	0.00	0.05
Gadolinium Oxid	0.00	0.00	0.00	0.50
Gallium(III) Ox	0.00	0.00	0.00	2.09
Germanium Dioxi	0.00	0.00	0.00	4.33
Holmium Nitrate	0.00	0.00	0.00	0.01
Holmium Oxide	0.00	0.00	0.00	0.10
Iron(iii) oxide	0.00	0.00	0.00	5278.77
Lanthanum Nitrat	0.00	0.00	0.00	0.17
Lanthanum Oxide	0.00	0.00	0.00	2.40
Lead(II) Oxide	0.00	0.00	0.00	2.15
Lithium Oxide	0.00	0.00	0.00	0.00
Lutetium Nitrat	0.00	0.00	0.00	0.00
Lutetium Oxide	0.00	0.00	0.00	0.02
Magnesium Oxide	0.00	0.00	0.00	175.87
Manganese(II)Ox	0.00	0.00	0.00	0.00
Molybdenum Trio	0.00	0.00	0.00	1.03
Neodymium Nitra	0.00	0.00	0.00	0.20
Neodymium Oxide	0.00	0.00	0.00	2.36
Nickel(II) Oxid	0.00	0.00	0.00	4.27
Nitric Acid	81445.62	81445.62	45428.24	8610.14
Potassium Oxide	0.00	0.00	0.00	0.00
Praseodymium Ni	0.00	0.00	0.00	0.05
Praseodymium Ox	0.00	0.00	0.00	0.61
Rubidium Oxide	0.00	0.00	0.00	3.88
Samarium Nitrat	0.00	0.00	0.00	0.04
Samarium Oxide	0.00	0.00	0.00	0.48
Scandium Nitrate	0.00	0.00	0.00	0.16
Scandium(III) Ox	0.00	0.00	0.00	1.59
Silicon Dioxide	0.00	0.00	0.00	14636.83
Strontium Oxide	0.00	0.00	0.00	30.64
Calcium Sulfate	0.00	0.00	0.00	0.00
Terbium Nitrate	0.00	0.00	0.00	0.01
Terbium Oxide	0.00	0.00	0.00	0.09
Titanium Dioxide	0.00	0.00	0.00	380.55
Thorium(IV) Oxi	0.00	0.00	0.00	0.74
Thulium Nitrate	0.00	0.00	0.00	0.00
Thulium Oxide	0.00	0.00	0.00	0.04
Uranium(IV) Oxi	0.00	0.00	0.00	0.57
Vanadium(V) Oxi	0.00	0.00	0.00	15.65
Water	158560.00	158560.00	86971.66	17773.79
Ytterbium Nitra	0.00	0.00	0.00	0.02
Ytterbium Oxide	0.00	0.00	0.00	0.25
Yttrium Oxide	0.00	0.00	0.00	3.54
Yttrium(III) Nit	0.00	0.00	0.00	0.47
Zinc Oxide	0.00	0.00	0.00	5.10
Nitrogen Trioxid	135.74	135.74	70.97	13.44
Barium Nitrate	0.00	0.00	0.00	0.70
Calcium Nitrate	0.00	0.00	0.00	0.00
Potassium Nitrat	0.00	0.00	0.00	0.00
Magnesium Nitrat	0.01	0.01	0.01	29.52

Nitrogen Dioxide	1088.76	1088.76	554.53	309.36
Sulfuric Acid	0.00	0.00	0.00	0.00
Aluminum Nitrat	0.03	0.03	0.02	26.95
Arsenic Acid	513.83	513.83	280.29	57.46
Cobalt(II) Nitr	0.00	0.00	0.00	0.12
Copper(II) Nitr	0.00	0.00	0.00	0.67
Iron(III) Nitra	0.01	0.01	0.01	8.13
Gallium(III) Ni	0.00	0.00	0.00	0.34
Mn(II) Nitrate	0.00	0.00	0.00	0.00
Nickel(II) Nitr	0.00	0.00	0.00	0.34
Lead(II) Nitrat	0.00	0.00	0.00	0.21
Uranyl Nitrate	0.00	0.00	0.00	0.04
Zinc Nitrate	0.00	0.00	0.00	0.86
Lithium Nitrate	0.00	0.00	0.00	0.00
Rubidium Nitrat	0.00	0.00	0.00	0.10
Antimony Pentox	0.00	0.00	0.00	0.16
Strontium Nitra	0.00	0.00	0.00	3.51
Thorium(IV) Nit	0.00	0.00	0.00	0.04
Nitrogen	1575.15	1575.15	0.96	613.67
Oxygen	756.95	756.95	0.64	186.45
Carbon Monoxide	0.00	0.00	0.00	0.00
Methane	0.00	0.00	0.00	0.00
Carbon Dioxide	0.00	0.00	0.00	0.00
N2O4	300.47	300.47	0.00	0.00
Nitric Oxide	0.00	0.00	0.07	0.09
dinitrogen pent	253.16	253.16	138.67	76.94
Nitrous Acid	2123.94	2123.94	1160.43	238.79

Stream No.	57	58	59	60
Stream Name				
Temp C	120.0000	40.0000	40.0000	129.4426
Pres atm	1.5100	1.1600	1.1600	1.0000
Enth kJ/h	-2.4761E+007	-1.5172E+009	-4.4740E+005	-1.0003E+007
Vapor mass frac.	0.00000	0.00000	1.0000	1.0000
Total kmol/h	54.90	5641.59	30.28	89.37
Total kg/h	3880.52	132949.77	881.47	3755.45
Total std L m3/h	5.05	119.25	0.99	3.03
Total std V m3/h	1230.55	126448.50	678.61	2003.12
Flow rates in kg/h				
Aluminum Oxide	0.00	0.00	0.00	0.00
Antimony Trioxi	0.00	0.00	0.00	0.00
Arsenic Oxide	0.00	0.00	0.00	0.00
Barium Oxide	0.00	0.00	0.00	0.00
Boron Trioxide	0.00	0.00	0.00	0.00
Calcium Oxide	0.00	0.00	0.00	0.00
Cerium Nitrate	2.07	0.00	0.00	0.00
Cerium Oxide	0.00	0.00	0.00	0.00
Chromium(III) Ox	0.00	0.00	0.00	0.00
Cobalt(II) Oxide	0.00	0.00	0.00	0.00
Copper(II) Oxid	0.00	0.00	0.00	0.00
Dysprosium Nitr	0.20	0.00	0.00	0.00
Dysprosium Oxid	0.00	0.00	0.00	0.00
Erbium Nitrate	0.11	0.00	0.00	0.00
Erbium Oxide	0.00	0.00	0.00	0.00

Europium Nitrat	0.04	0.00	0.00	0.00
Europium Oxide	0.00	0.00	0.00	0.00
Gadolinium Nitr	0.21	0.00	0.00	0.00
Gadolinium Oxid	0.00	0.00	0.00	0.00
Gallium(III) Ox	0.00	0.00	0.00	0.00
Germanium Dioxi	0.00	0.00	0.00	0.00
Holmium Nitrate	0.04	0.00	0.00	0.00
Holmium Oxide	0.00	0.00	0.00	0.00
Iron(iii) oxide	0.00	0.00	0.00	0.00
Lanthanum Nitrat	0.69	0.00	0.00	0.00
Lanthanum Oxide	0.00	0.00	0.00	0.00
Lead(II) Oxide	0.00	0.00	0.00	0.00
Lithium Oxide	0.00	0.00	0.00	0.00
Lutetium Nitrat	0.01	0.00	0.00	0.00
Lutetium Oxide	0.00	0.00	0.00	0.00
Magnesium Oxide	0.00	0.00	0.00	0.00
Manganese(II)Ox	0.00	0.00	0.00	0.00
Molybdenum Trio	0.00	0.00	0.00	0.00
Neodymium Nitra	0.81	0.00	0.00	0.00
Neodymium Oxide	0.00	0.00	0.00	0.00
Nickel(II) Oxid	0.00	0.00	0.00	0.00
Nitric Acid	182.70	40688.59	33.11	2516.94
Potassium Oxide	0.00	0.00	0.00	0.00
Praseodymium Ni	0.20	0.00	0.00	0.00
Praseodymium Ox	0.00	0.00	0.00	0.00
Rubidium Oxide	0.00	0.00	0.00	0.00
Samarium Nitrat	0.18	0.00	0.00	0.00
Samarium Oxide	0.00	0.00	0.00	0.00
Scandium Nitrate	0.65	0.00	0.00	0.00
Scandium(III) Ox	0.00	0.00	0.00	0.00
Silicon Dioxide	0.00	0.00	0.00	0.00
Strontium Oxide	0.00	0.00	0.00	0.00
Calcium Sulfate	0.00	0.00	0.00	0.00
Terbium Nitrate	0.03	0.00	0.00	0.00
Terbium Oxide	0.00	0.00	0.00	0.00
Titanium Dioxide	0.00	0.00	0.00	0.00
Thorium(IV) Oxi	0.00	0.00	0.00	0.00
Thulium Nitrate	0.01	0.00	0.00	0.00
Thulium Oxide	0.00	0.00	0.00	0.00
Uranium(IV) Oxi	0.00	0.00	0.00	0.00
Vanadium(V) Oxi	0.00	0.00	0.00	0.00
Water	666.90	88843.00	29.96	364.29
Ytterbium Nitra	0.08	0.00	0.00	0.00
Ytterbium Oxide	0.00	0.00	0.00	0.00
Yttrium Oxide	0.00	0.00	0.00	0.00
Yttrium(III) Nit	1.88	0.00	0.00	0.00
Zinc Oxide	0.00	0.00	0.00	0.00
Nitrogen Trioxid	0.03	66.04	1.38	1.40
Barium Nitrate	2.81	0.00	0.00	0.00
Calcium Nitrate	0.00	0.00	0.00	0.00
Potassium Nitrat	0.00	0.00	0.00	0.00
Magnesium Nitrat	118.64	0.01	0.00	0.00
Nitrogen Dioxide	0.64	1535.79	16.32	16.96
Sulfuric Acid	0.00	0.00	0.00	0.00

Aluminum Nitrat	2166.22	0.02	0.00	0.00
Arsenic Acid	4.24	284.09	0.06	4.24
Cobalt(II) Nitr	0.48	0.00	0.00	0.00
Copper(II) Nitr	2.68	0.00	0.00	0.00
Iron(III) Nitra	653.22	0.01	0.00	0.00
Gallium(III) Ni	1.36	0.00	0.00	0.00
Mn(II) Nitrate	0.00	0.00	0.00	0.00
Nickel(II) Nitr	1.38	0.00	0.00	0.00
Lead(II) Nitrat	0.83	0.00	0.00	0.00
Uranyl Nitrate	0.17	0.00	0.00	0.00
Zinc Nitrate	3.47	0.00	0.00	0.00
Lithium Nitrate	0.00	0.00	0.00	0.00
Rubidium Nitrat	0.42	0.00	0.00	0.00
Antimony Pentox	0.00	0.00	0.00	0.00
Strontium Nitra	14.12	0.00	0.00	0.00
Thorium(IV) Nit	0.14	0.00	0.00	0.00
Nitrogen	0.00	1.12	612.55	612.55
Oxygen	0.00	0.67	186.26	186.26
Carbon Monoxide	0.00	0.00	0.00	0.00
Methane	0.00	0.00	0.00	0.00
Carbon Dioxide	0.00	0.00	0.00	0.00
N2O4	0.00	0.00	0.00	0.00
Nitric Oxide	0.00	0.00	0.45	0.45
dinitrogen pent	0.86	383.99	1.33	2.19
Nitrous Acid	52.00	1146.41	0.05	50.17

Stream No.	61	62	63	64
Stream Name				
Temp C	46.1920	110.2100	79.0875	72.1013
Pres atm	1.2000	1.4100	1.5000	1.5000
Enth kJ/h	-1.4976E+009	-4.8538E+008	-6.0190E+009	-1.4742E+010
Vapor mass frac.	0.00000	0.83327	0.00000	0.00000
Total kmol/h	5589.66	67.13	22433.00	28510.69
Total kg/h	134606.52	3880.53	540000.00	705516.00
Total std L m3/h	119.45	2.53	492.57	623.10
Total std V m3/h	125284.60	1504.62	502804.84	639028.63
Flow rates in kg/h				
Aluminum Oxide	0.00	492.56	0.00	7375.95
Antimony Trioxi	0.00	0.00	0.00	0.47
Arsenic Oxide	0.00	0.00	0.00	5.75
Barium Oxide	0.00	0.00	0.00	15.50
Boron Trioxide	0.00	0.00	0.00	61.90
Calcium Oxide	0.00	0.00	0.00	0.00
Cerium Nitrate	0.00	2.07	10.20	10.19
Cerium Oxide	0.00	0.00	0.00	6.48
Chromium(III) Ox	0.00	0.00	0.00	7.62
Cobalt(II) Oxide	0.00	0.00	0.00	1.91
Copper(II) Oxid	0.00	0.00	0.00	5.18
Dysprosium Nitr	0.00	0.20	0.98	0.99
Dysprosium Oxid	0.00	0.00	0.00	0.61
Erbium Nitrate	0.00	0.11	0.56	0.56
Erbium Oxide	0.00	0.00	0.00	0.37
Europium Nitrat	0.00	0.04	0.22	0.21
Europium Oxide	0.00	0.00	0.00	0.14

Gadolinium Nitr	0.00	0.21	1.06	1.06
Gadolinium Oxid	0.00	0.00	0.00	0.65
Gallium(III) Ox	0.00	0.00	0.00	2.72
Germanium Dioxi	0.00	0.00	0.00	4.33
Holmium Nitrate	0.00	0.04	0.21	0.21
Holmium Oxide	0.00	0.00	0.00	0.13
Iron(iii) oxide	0.00	204.87	0.00	5497.09
Lanthanum Nitrat	0.00	0.69	3.39	3.39
Lanthanum Oxide	0.00	0.00	0.00	2.83
Lead(II) Oxide	0.00	0.00	0.00	2.85
Lithium Oxide	0.00	0.00	0.00	0.00
Lutetium Nitrat	0.00	0.01	0.03	0.03
Lutetium Oxide	0.00	0.00	0.00	0.03
Magnesium Oxide	0.00	0.00	0.00	216.12
Manganese(II)Ox	0.00	0.00	0.00	0.00
Molybdenum Trio	0.00	0.00	0.00	1.03
Neodymium Nitra	0.00	0.81	3.96	3.97
Neodymium Oxide	0.00	0.00	0.00	2.87
Nickel(II) Oxid	0.00	0.00	0.00	4.98
Nitric Acid	45428.24	2494.17	158778.00	204678.50
Potassium Oxide	0.00	0.00	0.00	0.00
Praseodymium Ni	0.00	0.20	0.98	0.98
Praseodymium Ox	0.00	0.00	0.00	0.73
Rubidium Oxide	0.00	0.00	0.00	4.20
Samarium Nitrat	0.00	0.18	0.87	0.87
Samarium Oxide	0.00	0.00	0.00	0.59
Scandium Nitrate	0.00	0.65	3.18	3.18
Scandium(III) Ox	0.00	0.00	0.00	1.83
Silicon Dioxide	0.00	0.00	0.00	14636.83
Strontium Oxide	0.00	0.00	0.00	39.24
Calcium Sulfate	0.00	0.00	0.00	0.00
Terbium Nitrate	0.00	0.03	0.17	0.17
Terbium Oxide	0.00	0.00	0.00	0.11
Titanium Dioxide	0.00	0.00	0.00	380.55
Thorium(IV) Oxi	0.00	0.00	0.00	0.83
Thulium Nitrate	0.00	0.01	0.07	0.07
Thulium Oxide	0.00	0.00	0.00	0.05
Uranium(IV) Oxi	0.00	0.00	0.00	0.71
Vanadium(V) Oxi	0.00	0.00	0.00	15.65
Water	86971.66	336.48	352847.00	441949.00
Ytterbium Nitra	0.00	0.08	0.41	0.41
Ytterbium Oxide	0.00	0.00	0.00	0.31
Yttrium Oxide	0.00	0.00	0.00	4.51
Yttrium(III) Nit	0.00	1.88	9.24	9.22
Zinc Oxide	0.00	0.00	0.00	6.89
Nitrogen Trioxid	70.97	0.03	265.53	336.41
Barium Nitrate	0.00	2.81	13.83	13.74
Calcium Nitrate	0.00	0.00	0.00	0.00
Potassium Nitrat	0.00	0.00	0.00	0.00
Magnesium Nitrat	0.01	118.63	583.28	583.29
Nitrogen Dioxide	554.53	0.64	6113.16	6667.81
Sulfuric Acid	0.00	0.00	0.00	0.00
Aluminum Nitrat	0.02	108.31	10650.40	10650.51
Arsenic Acid	280.29	4.24	1135.42	1415.99

Cobalt(II) Nitr	0.00	0.48	2.37	2.37
Copper(II) Nitr	0.00	2.68	13.19	13.19
Iron(III) Nitra	0.01	32.66	3211.60	3211.63
Gallium(III) Ni	0.00	1.36	6.70	6.69
Mn(II) Nitrate	0.00	0.00	0.00	0.00
Nickel(II) Nitr	0.00	1.38	6.78	6.77
Lead(II) Nitrat	0.00	0.83	4.10	4.10
Uranyl Nitrate	0.00	0.17	0.81	0.81
Zinc Nitrate	0.00	3.47	17.05	17.22
Lithium Nitrate	0.00	0.00	0.00	0.00
Rubidium Nitrat	0.00	0.42	2.04	2.04
Antimony Pentox	0.00	0.00	0.00	0.00
Strontium Nitra	0.00	14.12	69.41	69.45
Thorium(IV) Nit	0.00	0.14	0.70	0.70
Nitrogen	0.96	0.00	0.00	0.96
Oxygen	0.64	0.00	2.36	3.00
Carbon Monoxide	0.00	0.00	0.00	0.00
Methane	0.00	0.00	0.00	0.00
Carbon Dioxide	0.00	0.00	0.00	0.00
N2O4	0.00	0.00	0.00	0.00
Nitric Oxide	0.07	0.00	1.79	1.86
dinitrogen pent	138.67	0.86	1520.41	1659.11
Nitrous Acid	1160.43	52.00	4718.74	5875.52

Stream No.	65	66	67	68
Stream Name				
Temp C	79.0817	79.0817	155.0000	25.0000
Pres atm	2.0000	1.3200	1.4100	1.0000
Enth kJ/h	-1.4116E+010	-1.4116E+010	-4.8444E+008	-7.1899E+009
Vapor mass frac.	0.00000	0.00000	0.90096	0.00000
Total kmol/h	28484.12	28484.12	67.13	362.39
Total kg/h	704487.00	704487.00	3880.53	28310.54
Total std L m3/h	626.09	626.09	2.53	8.63
Total std V m3/h	638433.13	638433.13	1504.62	8122.59
Flow rates in kg/h				
Aluminum Oxide	6728.49	6728.49	492.56	7375.95
Antimony Trioxi	0.33	0.33	0.00	0.47
Arsenic Oxide	0.00	0.00	0.00	5.75
Barium Oxide	13.38	13.38	0.00	15.50
Boron Trioxide	61.90	61.90	0.00	61.90
Calcium Oxide	0.00	0.00	0.00	0.00
Cerium Nitrate	12.79	12.79	2.07	0.00
Cerium Oxide	5.33	5.33	0.00	6.48
Chromium(III) Ox	7.62	7.62	0.00	7.62
Cobalt(II) Oxide	1.67	1.67	0.00	1.91
Copper(II) Oxid	3.76	3.76	0.00	5.18
Dysprosium Nitr	1.23	1.23	0.20	0.00
Dysprosium Oxid	0.48	0.48	0.00	0.61
Erbium Nitrate	0.70	0.70	0.11	0.00
Erbium Oxide	0.29	0.29	0.00	0.37
Europium Nitrat	0.27	0.27	0.04	0.00
Europium Oxide	0.11	0.11	0.00	0.14
Gadolinium Nitr	1.32	1.32	0.21	0.00
Gadolinium Oxid	0.50	0.50	0.00	0.65

Gallium(III) Ox	2.09	2.09	0.00	2.72
Germanium Dioxi	4.33	4.33	0.00	4.33
Holmium Nitrate	0.26	0.26	0.04	0.00
Holmium Oxide	0.10	0.10	0.00	0.13
Iron(iii) oxide	5227.80	5227.80	204.87	5497.09
Lanthanum Nitrat	4.25	4.25	0.69	0.00
Lanthanum Oxide	2.40	2.40	0.00	2.83
Lead(II) Oxide	2.15	2.15	0.00	2.85
Lithium Oxide	0.00	0.00	0.00	0.00
Lutetium Nitrat	0.04	0.04	0.01	0.00
Lutetium Oxide	0.02	0.02	0.00	0.03
Magnesium Oxide	175.87	175.87	0.00	216.12
Manganese(II)Ox	0.00	0.00	0.00	0.00
Molybdenum Trio	1.03	1.03	0.00	1.03
Neodymium Nitra	4.97	4.97	0.81	0.00
Neodymium Oxide	2.36	2.36	0.00	2.87
Nickel(II) Oxid	4.27	4.27	0.00	4.98
Nitric Acid	199107.58	199107.58	2494.17	0.00
Potassium Oxide	0.00	0.00	0.00	0.00
Praseodymium Ni	1.22	1.22	0.20	0.00
Praseodymium Ox	0.61	0.61	0.00	0.73
Rubidium Oxide	3.88	3.88	0.00	4.20
Samarium Nitrat	1.09	1.09	0.18	0.00
Samarium Oxide	0.48	0.48	0.00	0.59
Scandium Nitrate	3.99	3.99	0.65	0.00
Scandium(III) Ox	1.59	1.59	0.00	1.83
Silicon Dioxide	14636.83	14636.83	0.00	14636.83
Strontium Oxide	30.64	30.64	0.00	39.24
Calcium Sulfate	0.00	0.00	0.00	0.00
Terbium Nitrate	0.21	0.21	0.03	0.00
Terbium Oxide	0.09	0.09	0.00	0.11
Titanium Dioxide	380.55	380.55	0.00	380.55
Thorium(IV) Oxi	0.74	0.74	0.00	0.83
Thulium Nitrate	0.09	0.09	0.01	0.00
Thulium Oxide	0.04	0.04	0.00	0.05
Uranium(IV) Oxi	0.57	0.57	0.00	0.71
Vanadium(V) Oxi	15.65	15.65	0.00	15.65
Water	442470.00	442470.00	336.48	0.00
Ytterbium Nitra	0.51	0.51	0.08	0.00
Ytterbium Oxide	0.25	0.25	0.00	0.31
Yttrium Oxide	3.54	3.54	0.00	4.51
Yttrium(III) Nit	11.59	11.59	1.88	0.00
Zinc Oxide	5.10	5.10	0.00	6.89
Nitrogen Trioxid	332.97	332.97	0.03	0.00
Barium Nitrate	17.34	17.34	2.81	0.00
Calcium Nitrate	0.00	0.00	0.00	0.00
Potassium Nitrat	0.00	0.00	0.00	0.00
Magnesium Nitrat	731.43	731.43	118.63	0.00
Nitrogen Dioxide	7665.91	7665.91	0.64	0.00
Sulfuric Acid	0.00	0.00	0.00	0.00
Aluminum Nitrat	13355.62	13355.62	108.31	0.00
Arsenic Acid	1423.81	1423.81	4.24	0.00
Cobalt(II) Nitr	2.97	2.97	0.48	0.00
Copper(II) Nitr	16.54	16.54	2.68	0.00

Iron(III) Nitra	4027.35	4027.35	32.66	0.00
Gallium(III) Ni	8.40	8.40	1.36	0.00
Mn(II) Nitrate	0.00	0.00	0.00	0.00
Nickel(II) Nitr	8.50	8.50	1.38	0.00
Lead(II) Nitrat	5.14	5.14	0.83	0.00
Uranyl Nitrate	1.02	1.02	0.17	0.00
Zinc Nitrate	21.38	21.38	3.47	0.00
Lithium Nitrate	0.00	0.00	0.00	0.00
Rubidium Nitrat	2.56	2.56	0.42	0.00
Antimony Pentox	0.16	0.16	0.00	0.00
Strontium Nitra	87.03	87.03	14.12	0.00
Thorium(IV) Nit	0.88	0.88	0.14	0.00
Nitrogen	0.00	0.00	0.00	0.00
Oxygen	2.96	2.96	0.00	0.00
Carbon Monoxide	0.00	0.00	0.00	0.00
Methane	0.00	0.00	0.00	0.00
Carbon Dioxide	0.00	0.00	0.00	0.00
N2O4	0.00	0.00	0.00	0.00
Nitric Oxide	2.25	2.25	0.00	0.00
dinitrogen pent	1906.59	1906.59	0.86	0.00
Nitrous Acid	5917.31	5917.31	52.00	0.00

Stream No.	69	70	71	72
Stream Name				
Temp C	120.0000	80.0000	79.0816	25.0000
Pres atm	1.5100	1.0200	1.0000	1.0000
Enth kJ/h	-1.0345E+009	-1.4119E+010	-1.2242E+009	-6.0010E+008
Vapor mass frac.	0.96467	5.1660E-006	0.00000	0.00000
Total kmol/h	4562.77	28493.37	4562.77	19.01
Total kg/h	109833.53	705516.00	109833.53	1679.97
Total std L m3/h	100.19	626.46	100.19	0.52
Total std V m3/h	102268.21	638640.25	102268.21	426.06
Flow rates in kg/h				
Aluminum Oxide	0.00	6728.49	0.00	0.00
Antimony Trioxi	0.00	0.33	0.00	0.00
Arsenic Oxide	0.00	0.00	0.00	0.00
Barium Oxide	0.00	13.38	0.00	0.00
Boron Trioxide	0.00	61.90	0.00	0.00
Calcium Oxide	0.00	0.00	0.00	433.10
Cerium Nitrate	2.07	12.79	2.07	0.00
Cerium Oxide	0.00	5.33	0.00	0.00
Chromium(III) Ox	0.00	7.62	0.00	0.00
Cobalt(II) Oxide	0.00	1.67	0.00	0.00
Copper(II) Oxid	0.00	3.76	0.00	0.00
Dysprosium Nitr	0.20	1.23	0.20	0.00
Dysprosium Oxid	0.00	0.48	0.00	0.00
Erbium Nitrate	0.11	0.70	0.11	0.00
Erbium Oxide	0.00	0.29	0.00	0.00
Europium Nitrat	0.04	0.27	0.04	0.00
Europium Oxide	0.00	0.11	0.00	0.00
Gadolinium Nitr	0.21	1.32	0.21	0.00
Gadolinium Oxid	0.00	0.50	0.00	0.00
Gallium(III) Ox	0.00	2.09	0.00	0.00
Germanium Dioxi	0.00	4.33	0.00	0.00

Holmium Nitrate	0.04	0.26	0.04	0.00
Holmium Oxide	0.00	0.10	0.00	0.00
Iron(iii) oxide	0.00	5227.80	0.00	0.00
Lanthanum Nitrat	0.69	4.25	0.69	0.00
Lanthanum Oxide	0.00	2.40	0.00	0.00
Lead(II) Oxide	0.00	2.15	0.00	0.00
Lithium Oxide	0.00	0.00	0.00	11.64
Lutetium Nitrat	0.01	0.04	0.01	0.00
Lutetium Oxide	0.00	0.02	0.00	0.00
Magnesium Oxide	0.00	175.87	0.00	0.00
Manganese(II)Ox	0.00	0.00	0.00	0.00
Molybdenum Trio	0.00	1.03	0.00	0.00
Neodymium Nitra	0.81	4.97	0.81	0.00
Neodymium Oxide	0.00	2.36	0.00	0.00
Nickel(II) Oxid	0.00	4.27	0.00	0.00
Nitric Acid	32294.69	201483.66	32294.69	0.00
Potassium Oxide	0.00	0.00	0.00	557.37
Praseodymium Ni	0.20	1.22	0.20	0.00
Praseodymium Ox	0.00	0.61	0.00	0.00
Rubidium Oxide	0.00	3.88	0.00	0.00
Samarium Nitrat	0.18	1.09	0.18	0.00
Samarium Oxide	0.00	0.48	0.00	0.00
Scandium Nitrate	0.65	3.99	0.65	0.00
Scandium(III) Ox	0.00	1.59	0.00	0.00
Silicon Dioxide	0.00	14636.83	0.00	0.00
Strontium Oxide	0.00	30.64	0.00	0.00
Calcium Sulfate	0.00	0.00	0.00	677.86
Terbium Nitrate	0.03	0.21	0.03	0.00
Terbium Oxide	0.00	0.09	0.00	0.00
Titanium Dioxide	0.00	380.55	0.00	0.00
Thorium(IV) Oxi	0.00	0.74	0.00	0.00
Thulium Nitrate	0.01	0.09	0.01	0.00
Thulium Oxide	0.00	0.04	0.00	0.00
Uranium(IV) Oxi	0.00	0.57	0.00	0.00
Vanadium(V) Oxi	0.00	15.65	0.00	0.00
Water	71767.45	442404.00	71767.45	0.00
Ytterbium Nitra	0.08	0.51	0.08	0.00
Ytterbium Oxide	0.00	0.25	0.00	0.00
Yttrium Oxide	0.00	3.54	0.00	0.00
Yttrium(III) Nit	1.88	11.59	1.88	0.00
Zinc Oxide	0.00	5.10	0.00	0.00
Nitrogen Trioxid	54.01	338.62	54.01	0.00
Barium Nitrate	2.81	17.34	2.81	0.00
Calcium Nitrate	0.00	0.00	0.00	0.00
Potassium Nitrat	0.00	0.00	0.00	0.00
Magnesium Nitrat	118.64	731.43	118.64	0.00
Nitrogen Dioxide	1243.39	6667.95	1243.39	0.00
Sulfuric Acid	0.00	0.00	0.00	0.00
Aluminum Nitrat	2166.24	13355.62	2166.24	0.00
Arsenic Acid	230.94	1424.24	230.94	0.00
Cobalt(II) Nitr	0.48	2.97	0.48	0.00
Copper(II) Nitr	2.68	16.54	2.68	0.00
Iron(III) Nitra	653.22	4027.35	653.22	0.00
Gallium(III) Ni	1.36	8.40	1.36	0.00

Mn(II) Nitrate	0.00	0.00	0.00	0.00
Nickel(II) Nitr	1.38	8.50	1.38	0.00
Lead(II) Nitrat	0.83	5.14	0.83	0.00
Uranyl Nitrate	0.17	1.02	0.17	0.00
Zinc Nitrate	3.47	21.38	3.47	0.00
Lithium Nitrate	0.00	0.00	0.00	0.00
Rubidium Nitrat	0.42	2.56	0.42	0.00
Antimony Pentox	0.00	0.16	0.00	0.00
Strontium Nitra	14.12	87.03	14.12	0.00
Thorium(IV) Nit	0.14	0.88	0.14	0.00
Nitrogen	0.00	0.96	0.00	0.00
Oxygen	0.48	3.00	0.48	0.00
Carbon Monoxide	0.00	0.00	0.00	0.00
Methane	0.00	0.00	0.00	0.00
Carbon Dioxide	0.00	0.00	0.00	0.00
N2O4	0.00	0.00	0.00	0.00
Nitric Oxide	0.36	1.86	0.36	0.00
dinitrogen pent	309.24	1659.11	309.24	0.00
Nitrous Acid	959.77	5875.52	959.77	0.00

Stream No.	73	74	76	84
Stream Name				Acid Feed
Temp C	152.7859	152.7859	79.0817	25.0000
Pres atm	1.0000	1.0000	1.3200	1.0000
Enth kJ/h	-4.7489E+008	-4.6934E+008	-1.2242E+009	-1.2984E+006
Vapor mass frac.	0.00000	0.00000	0.00000	0.00000
Total kmol/h	8.04	6.11	4562.77	7.49
Total kg/h	1006.55	697.43	109833.53	471.76
Total std L m3/h	0.49	0.16	100.19	0.31
Total std V m3/h	180.10	137.03	102268.21	167.80
Flow rates in kg/h				
Aluminum Oxide	492.56	492.56	0.00	0.00
Antimony Trioxi	0.00	0.00	0.00	0.00
Arsenic Oxide	0.00	0.00	0.00	0.00
Barium Oxide	0.00	0.00	0.00	0.00
Boron Trioxide	0.00	0.00	0.00	0.00
Calcium Oxide	0.00	0.00	0.00	0.00
Cerium Nitrate	2.07	0.00	2.07	0.00
Cerium Oxide	0.00	0.00	0.00	0.00
Chromium(III) Ox	0.00	0.00	0.00	0.00
Cobalt(II) Oxide	0.00	0.00	0.00	0.00
Copper(II) Oxid	0.00	0.00	0.00	0.00
Dysprosium Nitr	0.20	0.00	0.20	0.00
Dysprosium Oxid	0.00	0.00	0.00	0.00
Erbium Nitrate	0.11	0.00	0.11	0.00
Erbium Oxide	0.00	0.00	0.00	0.00
Europium Nitrat	0.04	0.00	0.04	0.00
Europium Oxide	0.00	0.00	0.00	0.00
Gadolinium Nitr	0.21	0.00	0.21	0.00
Gadolinium Oxid	0.00	0.00	0.00	0.00
Gallium(III) Ox	0.00	0.00	0.00	0.00
Germanium Dioxi	0.00	0.00	0.00	0.00
Holmium Nitrate	0.04	0.00	0.04	0.00
Holmium Oxide	0.00	0.00	0.00	0.00

Iron(iii) oxide	204.87	204.87	0.00	0.00
Lanthanum Nitrat	0.69	0.00	0.69	0.00
Lanthanum Oxide	0.00	0.00	0.00	0.00
Lead(II) Oxide	0.00	0.00	0.00	0.00
Lithium Oxide	0.00	0.00	0.00	0.00
Lutetium Nitrat	0.01	0.00	0.01	0.00
Lutetium Oxide	0.00	0.00	0.00	0.00
Magnesium Oxide	0.00	0.00	0.00	0.00
Manganese(II)Ox	0.00	0.00	0.00	0.00
Molybdenum Trio	0.00	0.00	0.00	0.00
Neodymium Nitra	0.81	0.00	0.81	0.00
Neodymium Oxide	0.00	0.00	0.00	0.00
Nickel(II) Oxid	0.00	0.00	0.00	0.00
Nitric Acid	10.34	0.00	32294.69	471.76
Potassium Oxide	0.00	0.00	0.00	0.00
Praseodymium Ni	0.20	0.00	0.20	0.00
Praseodymium Ox	0.00	0.00	0.00	0.00
Rubidium Oxide	0.00	0.00	0.00	0.00
Samarium Nitrat	0.18	0.00	0.18	0.00
Samarium Oxide	0.00	0.00	0.00	0.00
Scandium Nitrate	0.65	0.00	0.65	0.00
Scandium(III) Ox	0.00	0.00	0.00	0.00
Silicon Dioxide	0.00	0.00	0.00	0.00
Strontium Oxide	0.00	0.00	0.00	0.00
Calcium Sulfate	0.00	0.00	0.00	0.00
Terbium Nitrate	0.03	0.00	0.03	0.00
Terbium Oxide	0.00	0.00	0.00	0.00
Titanium Dioxide	0.00	0.00	0.00	0.00
Thorium(IV) Oxi	0.00	0.00	0.00	0.00
Thulium Nitrate	0.01	0.00	0.01	0.00
Thulium Oxide	0.00	0.00	0.00	0.00
Uranium(IV) Oxi	0.00	0.00	0.00	0.00
Vanadium(V) Oxi	0.00	0.00	0.00	0.00
Water	2.15	0.00	71767.45	0.00
Ytterbium Nitra	0.08	0.00	0.08	0.00
Ytterbium Oxide	0.00	0.00	0.00	0.00
Yttrium Oxide	0.00	0.00	0.00	0.00
Yttrium(III) Nit	1.88	0.00	1.88	0.00
Zinc Oxide	0.00	0.00	0.00	0.00
Nitrogen Trioxid	0.00	0.00	54.01	0.00
Barium Nitrate	2.81	0.00	2.81	0.00
Calcium Nitrate	0.00	0.00	0.00	0.00
Potassium Nitrat	0.00	0.00	0.00	0.00
Magnesium Nitrat	118.63	0.00	118.64	0.00
Nitrogen Dioxide	0.00	0.00	1243.39	0.00
Sulfuric Acid	0.00	0.00	0.00	0.00
Aluminum Nitrat	108.31	0.00	2166.24	0.00
Arsenic Acid	0.06	0.00	230.94	0.00
Cobalt(II) Nitr	0.48	0.00	0.48	0.00
Copper(II) Nitr	2.68	0.00	2.68	0.00
Iron(III) Nitra	32.66	0.00	653.22	0.00
Gallium(III) Ni	1.36	0.00	1.36	0.00
Mn(II) Nitrate	0.00	0.00	0.00	0.00
Nickel(II) Nitr	1.38	0.00	1.38	0.00

Lead(II) Nitrat	0.83	0.00	0.83	0.00
Uranyl Nitrate	0.17	0.00	0.17	0.00
Zinc Nitrate	3.47	0.00	3.47	0.00
Lithium Nitrate	0.00	0.00	0.00	0.00
Rubidium Nitrat	0.42	0.00	0.42	0.00
Antimony Pentox	0.00	0.00	0.00	0.00
Strontium Nitra	14.12	0.00	14.12	0.00
Thorium(IV) Nit	0.14	0.00	0.14	0.00
Nitrogen	0.00	0.00	0.00	0.00
Oxygen	0.00	0.00	0.48	0.00
Carbon Monoxide	0.00	0.00	0.00	0.00
Methane	0.00	0.00	0.00	0.00
Carbon Dioxide	0.00	0.00	0.00	0.00
N2O4	0.00	0.00	0.00	0.00
Nitric Oxide	0.00	0.00	0.36	0.00
dinitrogen pent	0.00	0.00	309.24	0.00
Nitrous Acid	1.88	0.00	959.77	0.00

Stream No.	85	87	88	89
Stream Name	Water Feed			
Temp C	25.0000	42.6187	42.6187	42.6187
Pres atm	1.0000	1.0000	1.0000	1.0000
Enth kJ/h	-3.3753E+007	-2.7283E+009	-9.3618E+005	-5.9845E+005
Vapor mass frac.	0.00000	0.00000	1.0000	1.0000
Total kmol/h	118.14	10152.73	51.50	32.92
Total kg/h	2128.33	244295.00	1500.00	958.88
Total std L m3/h	2.13	216.67	1.66	1.06
Total std V m3/h	2648.00	227559.75	1154.27	737.87
Flow rates in kg/h				
Aluminum Oxide	0.00	0.00	0.00	0.00
Antimony Trioxi	0.00	0.00	0.00	0.00
Arsenic Oxide	0.00	0.00	0.00	0.00
Barium Oxide	0.00	0.00	0.00	0.00
Boron Trioxide	0.00	0.00	0.00	0.00
Calcium Oxide	0.00	0.00	0.00	0.00
Cerium Nitrate	0.00	0.00	0.00	0.00
Cerium Oxide	0.00	0.00	0.00	0.00
Chromium(III) Ox	0.00	0.00	0.00	0.00
Cobalt(II) Oxide	0.00	0.00	0.00	0.00
Copper(II) Oxid	0.00	0.00	0.00	0.00
Dysprosium Nitr	0.00	0.00	0.00	0.00
Dysprosium Oxid	0.00	0.00	0.00	0.00
Erbium Nitrate	0.00	0.00	0.00	0.00
Erbium Oxide	0.00	0.00	0.00	0.00
Europium Nitrat	0.00	0.00	0.00	0.00
Europium Oxide	0.00	0.00	0.00	0.00
Gadolinium Nitr	0.00	0.00	0.00	0.00
Gadolinium Oxid	0.00	0.00	0.00	0.00
Gallium(III) Ox	0.00	0.00	0.00	0.00
Germanium Dioxi	0.00	0.00	0.00	0.00
Holmium Nitrate	0.00	0.00	0.00	0.00
Holmium Oxide	0.00	0.00	0.00	0.00
Iron(iii) oxide	0.00	0.00	0.00	0.00
Lanthanum Nitrat	0.00	0.00	0.00	0.00

Lanthanum Oxide	0.00	0.00	0.00	0.00
Lead(II) Oxide	0.00	0.00	0.00	0.00
Lithium Oxide	0.00	0.00	0.00	0.00
Lutetium Nitrat	0.00	0.00	0.00	0.00
Lutetium Oxide	0.00	0.00	0.00	0.00
Magnesium Oxide	0.00	0.00	0.00	0.00
Manganese(II)Ox	0.00	0.00	0.00	0.00
Molybdenum Trio	0.00	0.00	0.00	0.00
Neodymium Nitra	0.00	0.00	0.00	0.00
Neodymium Oxide	0.00	0.00	0.00	0.00
Nickel(II) Oxid	0.00	0.00	0.00	0.00
Nitric Acid	0.00	83368.84	84.06	53.73
Potassium Oxide	0.00	0.00	0.00	0.00
Praseodymium Ni	0.00	0.00	0.00	0.00
Praseodymium Ox	0.00	0.00	0.00	0.00
Rubidium Oxide	0.00	0.00	0.00	0.00
Samarium Nitrat	0.00	0.00	0.00	0.00
Samarium Oxide	0.00	0.00	0.00	0.00
Scandium Nitrate	0.00	0.00	0.00	0.00
Scandium(III) Ox	0.00	0.00	0.00	0.00
Silicon Dioxide	0.00	0.00	0.00	0.00
Strontium Oxide	0.00	0.00	0.00	0.00
Calcium Sulfate	0.00	0.00	0.00	0.00
Terbium Nitrate	0.00	0.00	0.00	0.00
Terbium Oxide	0.00	0.00	0.00	0.00
Titanium Dioxide	0.00	0.00	0.00	0.00
Thorium(IV) Oxi	0.00	0.00	0.00	0.00
Thulium Nitrate	0.00	0.00	0.00	0.00
Thulium Oxide	0.00	0.00	0.00	0.00
Uranium(IV) Oxi	0.00	0.00	0.00	0.00
Vanadium(V) Oxi	0.00	0.00	0.00	0.00
Water	2128.33	158155.27	67.14	42.92
Ytterbium Nitra	0.00	0.00	0.00	0.00
Ytterbium Oxide	0.00	0.00	0.00	0.00
Yttrium Oxide	0.00	0.00	0.00	0.00
Yttrium(III) Nit	0.00	0.00	0.00	0.00
Zinc Oxide	0.00	0.00	0.00	0.00
Nitrogen Trioxid	0.00	130.40	3.26	2.08
Barium Nitrate	0.00	0.00	0.00	0.00
Calcium Nitrate	0.00	0.00	0.00	0.00
Potassium Nitrat	0.00	0.00	0.00	0.00
Magnesium Nitrat	0.00	0.01	0.00	0.00
Nitrogen Dioxide	0.00	0.00	0.00	0.00
Sulfuric Acid	0.00	0.00	0.00	0.00
Aluminum Nitrat	0.00	0.03	0.00	0.00
Arsenic Acid	0.00	513.60	0.14	0.09
Cobalt(II) Nitr	0.00	0.00	0.00	0.00
Copper(II) Nitr	0.00	0.00	0.00	0.00
Iron(III) Nitra	0.00	0.01	0.00	0.00
Gallium(III) Ni	0.00	0.00	0.00	0.00
Mn(II) Nitrate	0.00	0.00	0.00	0.00
Nickel(II) Nitr	0.00	0.00	0.00	0.00
Lead(II) Nitrat	0.00	0.00	0.00	0.00
Uranyl Nitrate	0.00	0.00	0.00	0.00

Zinc Nitrate	0.00	0.00	0.00	0.00
Lithium Nitrate	0.00	0.00	0.00	0.00
Rubidium Nitrat	0.00	0.00	0.00	0.00
Antimony Pentox	0.00	0.00	0.00	0.00
Strontium Nitra	0.00	0.00	0.00	0.00
Thorium(IV) Nit	0.00	0.00	0.00	0.00
Nitrogen	0.00	1.54	959.96	613.65
Oxygen	0.00	1.10	345.61	220.93
Carbon Monoxide	0.00	0.00	0.00	0.00
Methane	0.00	0.00	0.00	0.00
Carbon Dioxide	0.00	0.00	0.00	0.00
N2O4	0.00	0.00	0.00	0.00
Nitric Oxide	0.00	0.19	39.74	25.40
dinitrogen pent	0.00	0.00	0.00	0.00
Nitrous Acid	0.00	2123.75	0.12	0.07

A.2 Additional TEA Information

Table 27: Rare earth separation system cost model parameters and uncertainties for a system that would be built using today's state-of-the-art system. These values are used in the FOAK and NOAK scenarios.

Parameter	Units*	Nominal Value	Unc. Representation (Distribution Function)
Capital Costs			
Direct capital costs	% of reference cost	Variable	Triangular (-10%, reference cost, +10%)
General Facilities Capital[12]	%PFC	10	Triangular (5,10,15)
Engineering and Home Office Fees[8]	%PFC	7	Triangular (5,7,10)
Project Contingency Cost[13]	%PFC	50	Triangular (40,50,50)
Process Contingency Cost[9]	%PFC	70	Uniform (60,80)
Royalty Fees[8]	%PFC	0.5	Triangular (0,0.5,0.5)
Pre-Production Months FOM[8]	Months	1	Triangular (0,1,2)
Pre-Production Months VOM[8]	Months	1	Triangular (0,1,2)
AFUDC[8]	%TPC	0.5%	Uniform (0.4,0.6)
Coal Ash	$/tonne	$0	Uniform (0.0,12.9)
Makeup Nitric Acid	$/tonne	$600	Triangular (300,600,842)
Water[14]	$/tonne	$0.3	Uniform (0.23,0.38)

[12] Versteeg, P. (2012). Ph.D. Thesis. Advanced amines and ammonia systems for greenhouse gas control at fossil fuel power plants. . Pittsburgh, PA: Carnegie Mellon University.

[13] EPRI. (2011). Advanced Coal Power Systems with CO2 Capture: EPRI CoalFleet for Tomorrow(R) Vision-- 2011 Update. Palo Alto, CA: EPRI.

[14] Versteeg, P., & Rubin, P. (2012). IECM Technical Documentation: Ammonia-Based Post-Combustion CO2 Capture. Pittsburgh, PA: Carnegie Mellon University.

Leached ash disposal[10]	$/tonne	10.3	Uniform (7.7,12.9)
Natural gas price[15]	$/GJ	1.26	Uniform (0.95,1.6)
Electricity[16]	$/MWh	6.4	Uniform (5.7,8.0)
Avg. price for salable byproduct[17]	$/tonne	30	Uniform (20,40)
Correlation for operating labor[11]	Hours/day-step	14	Uniform (10,18)
Operating labor rate[18]	$/hr	46.43	Uniform (41,51)
Total maintenance cost[10]	%TPC	2.5	Triangular (1,5)
Maint. cost allocated to labor[19]	$\%FOM_{maint.}$	40	Triangular (30,40,50)
Admin. and support labor cost[8]	%Total labor	30	Triangular (25,30,35)

[15] Peters, T., Timmerhaus, K., & West, R. (2003). Plant Design and Economics for Chemical Engineers (5th ed.). New York: McGraw Hill.

[16] EIA 2007 Average Annual Price (wholesale)

[17] American Coal Ash Association. (2015). 2015 Coal Combustion Product (CPP) Production and Use Survey Report. Farmington Hills, MI: ACAA. Retrieved from https://www.acaa-usa.org/Portals/9/Files/PDFs/ACAA-Brochure-Web.pdf

[18] Engineering News-Record Indexes, December 2001

[19] EPRI. (1993). Technical assessment guide (TAG) Vol. 1: Electricity supply. Palo Alto, CA: EPRI.

20

Appendix C: Laboratory Testing Plan

Battelle Project 100075292

Budget Period 2 Experimental Test Plan for Laboratory Scale Feasibility Assessment of Rare Earths Elements (REE) Recovery from Coal and Coal By-Products

National Energy Technology Laboratory

3610 Collins Ferry Road

Morgantown, WV 26507-0880

26 February 2017

Goal

The goal of this testing is to provide leaching kinetics, capacity data, and roasting parameters needed for a design of rare earth elements (REE) recovery process using coal fly ash. The tests are needed to enable a design of the 100 lb/8hr pilot-scale REE recovery unit as well as larger commercial systems.

Objectives

The proposed approach for the testing planned in Budget Period 2 to inform the Bench Scale Process Design tasks is shown in Figure 1.

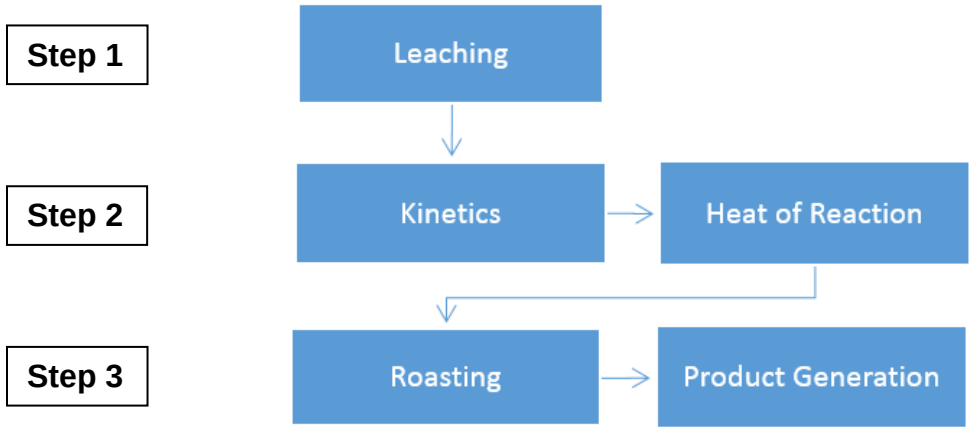

Figure 1: Proposed approach of laboratory feasibility testing.

Each step above addresses a specific objective of the design testing work. One of the first objectives is to determine the optimum conditions at which the REE can be leached from the coal by-product. This will be addressed in **Step 1** of testing (detailed below), and will drive process economic factors associated with the purchase and recycle of acid. **Step 2** of testing includes the collection of kinetic and heat of reaction data. These data will be used in the process design phase to fine tune reactor sizing and process utility costs. **Step 3** will determine the ability to recover REE and regenerate the reacted nitric acid through a roasting process. This will be used to inform the design of the product and acid recovery operations.

Test Approach

Leaching and Kinetics Tests

Battelle is experimenting with the possibility of combining milling and leaching steps to improve leaching efficiency. The expectation is that milling will remove passivation of the ash particles, allowing for better access of the acid to the REE containing components. The experiments will be divided into two sets as shown in Figure 2. The first set of experiments will test feasibility of the combined milling-leaching approach and evaluate advantages of elevated temperature leaching (up to 90°C). Results of these tests will be used to select one of two processes: (1) the combined milling-leaching approach, or (2) separate milling-leaching method. The second set of experiments will focus on the selected version of the process and will quantify leaching rate and REE recovery efficiency in terms of relevant reaction parameters. The second group of tests will constitute most of the testing effort and will follow the design of experiments (DoE) methodology, which ensures statistical validity at minimum experimental cost.

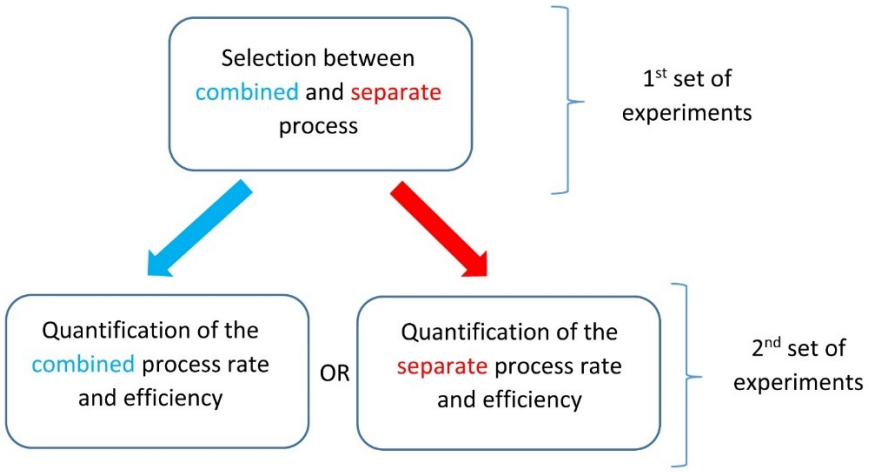

Figure 2: The testing approach proposed for selection and development of the REE recovery process.

Sections below present specific experiments in more details.

1st Set of Experiments – Selection Between Combined and Separate Processes

Baseline combined milling-leaching test

Based on previous laboratory work conducted under Task 3 of this project, milling the ash prior to leaching has the potential to reduce particle size and enhance REE recovery rates by up to 10%.[1] Feasibility of the combined process will be tested experimentally by carrying out the following experiments:

- Two combined milling-leaching experiments will be carried out using a ball mill that has been previously used for size reduction of ash.
- Instead of water, the milling will be done in nitric acid at 34% and 68% concentrations
- The ash and liquid amounts used will be the same as previously employed for milling.
- The same type and number of milling balls will be used as used in previous milling tests.
- Both experiments will be carried out at room temperature.
- Liquid acid bath samples will be collected for analysis after 30 min of milling and after overnight milling. The 30-min sample should be filtered. Two overnight samples will be collected, one to be filtered, another without filtering. The sample without filtering will be collected at a well-defined time after stop of the milling operation (1 or 2 minutes is preferred).

Feasibility of the combined milling-leaching approach will be demonstrated if at least one of the experiments will achieve a statistically significant REE recovery efficiency increase above the current highest efficiency of around 40% for milled ash.

Flask leaching tests at 90°C

Effectiveness of the leaching reaction at elevated temperatures will be evaluated by carrying out the following experiments:

Temperature Range Finding Tests

- Two extraction experiments will be done, using the 250-mL capacity leaching setup used in previous leaching tests and acid concentrations of 68% and 34%.
- 1 g of ash treated with 250 mL of acid solution will be used.

[1] "Recovery of Rare Earth Elements from Coal and Coal Byproducts via a Closed Loop Leaching Process: Feasibility Study Report." Battelle. February 2017.

- Ash will be milled following the procedure used in previous tests.
- Acid bath temperature will be 90°C
- Liquid acid bath samples will be collected for analysis after 1 min, 5 mins, and 30 mins of leaching, as in previous tests.

Temperature Dependence Tests

If milling in acid is found to be favorable to the process, reaction dependence on temperature will need to be determined. As temperature control in the laboratory mill will be difficult to achieve, separate milling and elevated temperature leaching tests will be conducted. Should milling be found to not be beneficial to the process, , the temperature dependence will be found in the later experiments.

- Extraction experiments will be done using the 250-mL capacity leaching setup used in previous leaching tests and acid concentration of 34%
- 1 g of ash treated with 250 mL of acid solution
- Ash will be milled following the procedure used in previous tests.
- Acid bath temperature will be 90°C
- Liquid acid bath samples will be collected for analysis after 1 min, 5 mins, and 30 mins of leaching, as in previous tests.
- Liquid samples will be filtered through a syringe microfilter
- Repeat twice so that there are 9 samples at 90°C
- Repeat at 60°C and 30°C in triplicate, for a total of 27 samples.

An advantage of leaching at elevated temperatures will be demonstrated if at least one of the experiments will achieve a REE recovery efficiency significantly above 40% or if the reaction. Additionally, the data collected may be used for the evaluation of the temperature effect on the reaction rate.

2nd Set of Experiments – Quantification of the Separate Process Rate and Efficiency

Results of the leaching test, carried out to date as analysis of similar leaching processes, indicate that the rate and efficiency of REE recovery is likely to be affected by five factors: (1) reaction temperature, (2) available surface area of ash particles (equivalent to initial particle size), (3) nitric acid concentration, (4) acid freshness (function of number of times acid was used and concentration of dissolved reaction products), and (5) total time of leaching. Table 1 lists these factors together with expected values of lower and upper limits that may be used in the process.

Table 1: Factors expected to influence outcome of the separate version of the process

Factor	*Low level (-1)*	*Intermediate level (0)*	*High level (1)*
Temperature	30°C	60°C	90°C
Ash particle size	Smallest particles	Medium particles	Largest particles
Acid concentration	34%	51%	68%
Acid "freshness"	Fresh acid	Acid used once	Acid used twice
Time	10 min	20 min	30 min

Influence of these factors will be evaluated by the Box-Behnken surface response design of experiment (DoE) with 46 flask leaching experiments as listed in Table 2. This DoE will generate a complete

quadratic model of the process and will include all linear, quadratic, and cross-term contributions. Table 2 lists all 46 experiments required by this DoE scheme.

Table 2: 46 experiments required by the 5-factor Box-Behnken Design of Experiment

Trial	*Time, min*	*Acid Concentration, wt%*	*Temperature, °C*	*Particle Size*	*Acid Freshness*
1	5	68	60	Small	1x
2	5	51	90	Small	1x
3	5	68	60	Med	Fresh
4	30	51	60	Med	Fresh
5	30	34	60	Med	1x
6	5	51	60	Med	1x
7	5	68	30	Med	1x
8	5	51	60	Med	1x
9	5	51	60	Small	2x
10	5	51	30	Small	1x
11	5	34	60	Large	1x
12	5	34	60	Small	1x
13	5	34	60	Med	Fresh
14	1	51	60	Med	Fresh
15	5	34	30	Med	1x
16	5	34	60	Med	2x
17	5	51	60	Med	1x
18	5	51	30	Large	1x
19	1	51	60	Large	1x
20	5	51	60	Large	Fresh
21	5	68	60	Med	2x
22	5	51	60	Small	Fresh
23	5	68	90	Med	1x
24	5	51	60	Med	1x
25	30	51	60	Large	1x
26	1	34	60	Med	1x
27	5	51	60	Med	1x
28	30	51	30	Med	1x
29	5	51	30	Med	Fresh
30	5	51	90	Med	2x
31	30	51	90	Med	1x
32	5	34	90	Med	1x
33	1	51	60	Med	2x
34	5	68	60	Large	1x
35	1	51	90	Med	1x
36	30	51	60	Med	2x

37	1	51	30	Med	1x
38	5	51	60	Large	2x
39	5	51	90	Large	1x
40	1	51	60	Small	1x
41	5	51	30	Med	2x
42	5	51	60	Med	1x
43	1	68	60	Med	1x
44	30	68	60	Med	1x
45	30	51	60	Small	1x
46	5	51	90	Med	Fresh

2nd Set of Experiments – Quantification of the Combined Process Rate and Efficiency

In case the combined milling-leaching process is selected, it will undergo a similar quantification procedure based on the DoE methodology. This version of the process is also expected to be influenced by five factors. An ash loading into the milling-leaching vessel is expected to significantly influence an overall reaction outcome. Table 3 lists the factors affecting this version of the process together with their limits.

Table 3: Factors expected to influence outcome of the combined version of the process

Factor	*Low level (-1)*	*Intermediate level (0)*	*High level (1)*
Temperature	30°C	60°C	90°C
Ash particle loading	160 g/l	320 g/l	480 g/l
Acid concentration	34%	51%	68%
Acid "freshness"	Fresh acid	Acid used once	Acid used twice
Time	20 min	40 min	60 min

Again, the combined version of the process will be evaluated by the Box-Behnken surface response DoE with 27 combined milling-leaching experiments listed in Table 4, noting that temperature effects will be evaluated from previous tests.

Table 4: 27 experiments required by the Box-Behnken 4 factor design of experiment

Trial	Time, minutes	*Acid Concentration, wt%*	*Media to Ash Ratio*	*Acid Freshness*
1	1	51	Small	1x
2	1	51	Med	Fresh
3	5	68	Large	1x
4	30	51	Med	2x
5	5	51	Small	2x
6	1	68	Med	1x
7	5	68	Small	1x
8	5	34	Large	1x
9	30	68	Med	1x
10	30	51	Med	Fresh
11	30	34	Med	1x
12	1	51	Large	1x
13	30	51	Small	1x
14	30	51	Large	1x
15	5	51	Med	1x
16	5	34	Small	1x
17	5	34	Med	2x
18	1	51	Med	2x
19	5	51	Large	2x
20	5	68	Med	Fresh
21	5	51	Med	1x
22	5	34	Med	Fresh
23	5	68	Med	2x
24	5	51	Large	Fresh
25	5	51	Med	1x
26	1	34	Med	1x
27	5	51	Small	Fresh

Detailed Testing Procedures

Flask leaching tests

The reaction will be performed in a round bottom flask in a heating mantle with forced air in the headspace that exhausts through a caustic bath. This will neutralize any NOx fumes that may be generated in the reaction. The tests will also be run inside a fume hood. See Figure 3 for a diagram of the test apparatus.

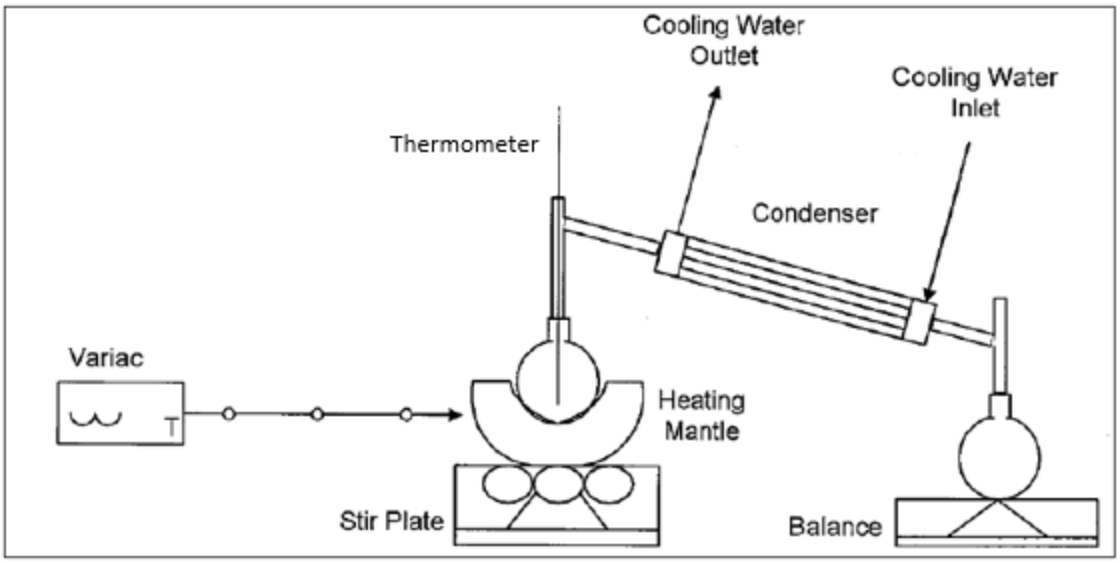

Figure 3: Test apparatus used for acid roasting tests

The procedure for the elevated temperature leaching experiments is as follows:

1. Determine the desired acid concentration, ash loading, reaction temperature, sampling times, and total reaction time using the test descriptions outlined above. Confirm these values with Project Manager prior to each experiment. Note that the DoE procedure calls for changing these parameters from one reaction to another. It is critical that the correct parameters are applied during each reaction.
2. In a fume hood, add 250 mL of nitric acid solution with desired concentration to a round bottom flask, with a running air purge, to a caustic bath and a thermometer in the top stem. Add a stir bar and begin mixing the solution.
3. Set the temperature controller to the desired temperature. Wait for the acid to reach this temperature.
4. Add desired amount of milled ash to the solution and begin a timer.
5. Take a 10 mL sample(s) of the solution after desired sampling times. Use a polyethylene sample container. Filter the samples using a new microfilter within 5 minutes after collection.
6. Terminate the reaction after the desired reaction time by turning off the heater. Wait for the solution to cool down.
7. When the reaction is complete, retain a 50 mL sample of the solution, and discard the remaining ash and solution in a waste container appropriate for low pH oxidizing waste. Ensure that all samples are fully cooled prior to transfer to plastic storage containers, as the heat generated may melt the plastic.
8. Send samples for analysis by ICP-MS.

Activation Laboratories, Ltd. (Act Labs) is the laboratory of choice for the U.S. Geological Survey (USGS) for analysis of coal sources. Therefore, it will be used for this project to ensure that data collected from this analysis is directly comparable to characterization data evaluated as part of the sampling and characterization study Battelle is conducting. Act Labs will conduct characterization via ICP-MS to determine the concentration of REEs which have been leached into the acid.

Combined milling-leaching tests

The reaction will be performed in the ball milling apparatus used in the previous tests with an acid solution used instead of water. The milling procedure needs to be performed under the 1/3-1/3-1/3 rule, meaning about 1/3 of vessel's volume needs to be filled with liquid, 1/3 with ash, and 1/3 with the zirconia oxide cylinder milling media. Volumes of ash and zirconia cylinders need to be measured as bulk volumes

without forced compaction. Two milling vessels with 1.0 and 0.5 liter volumes are available. The 0.5-liter vessel should be used for all combined milling-leaching experiments. The procedure for the combined milling-leaching tests is as follows:

1. Determine the desired acid concentration, reaction temperature, sampling times, and total reaction time using the test descriptions outlined above. Confirm these values with Project Leads prior to each experiment. Note that the DoE procedure calls for changing these parameters from one reaction to another. It is critical that the correct parameters are applied during each reaction.
2. Load the vessel with 167 mL of acid. Record the mass of added acid.
3. Add 166 mL of dry zirconia cylinders. Record the mass of added cylinders.
4. Add 166 mL of ash. Record the mass of added ash.
5. Place the milling vessel inside of the secondary confinement vessel.
6. Place both vessels on the rotation device for 1 minute.
7. Take a 10 mL sample(s) of the solution after desired sampling times. Use a polyethylene sample container. Filter the samples using a new microfilter within 5 minutes after collection.
8. When the reaction is complete, retain a 50 mL sample of the solution, and discard the remaining ash and solution in a waste container appropriate for low pH oxidizing waste. Ensure that all samples are fully cooled prior to transfer to plastic storage containers, as the heat generated may melt the plastic.
9. Send samples to Activation Laboratories (Act Labs) for analysis by ICP-MS.

Dilution of nitric acid

Nitric acid used during testing will be prepared using common laboratory dilution procedures. The required solutions of 51%, 34% and 17% nitric acid to be prepared are shown in the table below. Note: the intent of these percentages is to dilute the stock nitric acid solution to three-quarters, half, and one quarter concentration, respectively. Stock solutions of nitric acid typically range from 66–70 wt%, so 68 wt% nitric acid is the example used in this test plan. Actual concentrations will be adjusted as needed.

Table 5 Nitric acid dilution instructions

Desired Acid Concentration	This Mass of 68% Nitric Acid	To This Mass of Water	Yields This Final Volume
51 wt%	250 g	83.33 g	253 mL
34 wt%	155 g	155 g	257 mL
17 wt%	70 g	210 g	255 mL

Calorimetry Tests

The goal of this testing is to provide heat of reaction data for use in the process design phase of the larger program, which focuses on the recovery of rare earth elements (REE) from coal and coal by-products. Specifically, the calorimetry data will be used to fine tune reactor sizing and process utility costs.

A Parr Instruments model 6755 Solution Calorimeter (Figure 4) will be used to gather calorimetric data.

Figure 4: Parr 6755 Solution Calorimeter with 6772 Precision Thermometer

The instrument makes use of a high precision thermometer to track the temperature change resulting from the mixture of two reactants in an adiabatic chamber. The calorimeter itself is standardized prior to each analysis by measuring the temperature change of a thermodynamically well-characterized reaction. By carefully tracking the temperature change from the mixture of a small amount of coal ash with a fixed volume of 17% nitric acid, and knowing the heat capacity of the instrument, the enthalpy of reaction of the ash-nitric acid reaction can be calculated.

Step 1: Standardization of the Calorimeter Apparatus

For standardizing the 6755 Solution Calorimeter, solid TRIS (tris(hydroxymethyl) aminomethane) can be dissolved in dilute hydrochloric acid in a controlled reaction for which the amount of heat evolved is well established. In the manufacturer recommended standardization procedure described below, 0.5 gram of TRIS is dissolved in 100 mL of 0.1 N HCl to evolve 58.738 calories per gram of TRIS at 25 °C.

1. Place the instrument into Standardization mode and allow at least 20 minutes for the calorimeter to warm up.
2. Tare the Dewar on a solution or trip balance and add exactly 100.00 ± .05 grams of 0.100 N HCl.
3. Weigh 0.50 ±.01 gram of TRIS into the 126C Teflon Dish on an analytical balance to an accuracy of ± 0.0001 g.
4. Assemble the rotating cell; place it in the calorimeter and start the motor.
5. Let the calorimeter come to equilibrium; then initiate the reaction by depressing the push rod.
6. At the conclusion of the test, the instrument will report an energy equivalent for the empty calorimeter. The value will be electronically stored for use in the determination of enthalpy change in test reactions.
7. Repeat the standardization using a minimum of three replicates.

Step 2: Determination of the Change of Enthalpy for the Ash-Nitric Acid Reaction

1. Place the instrument into Determination mode and allow at least 20 minutes for the calorimeter to warm up.
2. Tare the Dewar on a solution or trip balance and add exactly 100.00 ± .05 grams of 17% HNO_3.
3. Weigh 1.00 ± 0.01 gram of coal by-product ash into the 126C Teflon Dish on an analytical balance to an accuracy of ± 0.0001 g.
4. Assemble the rotating cell; place it in the calorimeter and start the motor.

5. Let the calorimeter come to equilibrium; then initiate the reaction by depressing the push rod.
6. At the conclusion of the test, the instrument will report an enthalpy change for the reaction in calories/gram of the coal by-product ash.
7. Sample the leachate from this reaction through a microfilter, and send the leachate for elemental analysis
8. Repeat the determination using a minimum of three replicates.

Additional information regarding standardization, determination, and overall operation can be found in the Parr 6755 Operating Instruction Manual, 593M, dated 3/15/2011. Using analysis of the leachate solution, a heat of reaction per equivalence of metals dissolved will be calculated and used in design of the process.

Roasting/Product Recovery Tests

It was demonstrated in Budget Period 1 that it is possible to extract Rare Earth Elements (REE) from fly ash, but this acid treatment leads to extraction of others compounds such as Fe, Na, Si, Al and Mg. The objective of this plan is to develop a roasting process that allows separation of REE from other compounds. This will be achieved by accomplishing three subtasks (Figure 5):

Subtask 1: Identify and prepare a synthetic solution with similar composition to the solution to that produced from acid digestion of fly ash.

Subtask 2: Roasting of model solution. We will conduct this process under different conditions (temperature and oxygen concentration) and characterize the residual material after each treatment with various techniques (EDS, XRD, ICP and TGA). In this task, best roasting condition, which allows efficient separation of rare earth from other elements, will be selected.

Subtask 3: Apply the developed method in subtask 2 to solution obtained from acid digested of fly ash

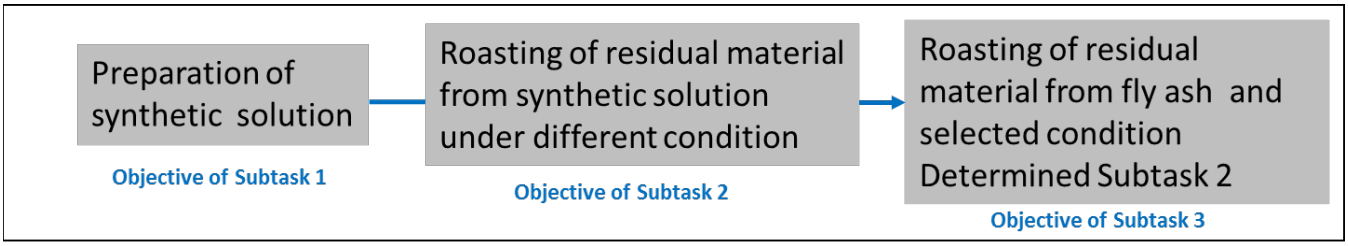

Figure 5: Objectives for roasting subtasks

Testing Approach

As mention in the objective, three subtasks will be performed. Below is the description of the approach used to accomplish each.

Subtask 1:

The digestion of fly ash in nitric acid leads to a solution that has mixed salts including rear earth nitrates, sodium nitrate, calcium nitrate, aluminum nitrate and iron nitrate. Based on the Energy Dispersive X-ray Spectroscopy (EDS) analysis of the residual material (obtained by vaporization of water under a heat lamp) and Inductively Coupled Plasma Mass Spectrometry (ICP-MS) analysis of acid solution we will prepare a synthetic blend solution that has a known concentration of the relevant compounds. The solution will be characterized by ICP to confirm the starting composition and use it in subtask 2.

Subtask 2:

The model solution prepared in subtask 1 will be evaporated under inert conditions at a temperature of 70°C to prevent oxidation of residual salts. After that, the material will be heat treated under inert conditions (Nitrogen or Argon) at 100°C. It will then be re-dissolved in DI water and filtered via 0.2 microns to separate undissolved material. The filtered solution will again be evaporated in a vacuum oven at 70°C, followed by heat treatment at 200°C. This process will be repeated for a temperature of 300°C and 400°C as described in Figure 6. If the reaction does not proceed in an inert atmosphere, the same tests will be performed in an oxidative environment using 2-5% oxygen. The residual material will be characterized after each treatment (evaporation and temperature treatment) to determine the amount and nature of elements that we can separate under each condition. Based on the outcome of above tests, the best condition(s) will be selected to separate rare earth from other components and conduct a final test with the model compound to confirm the separation.

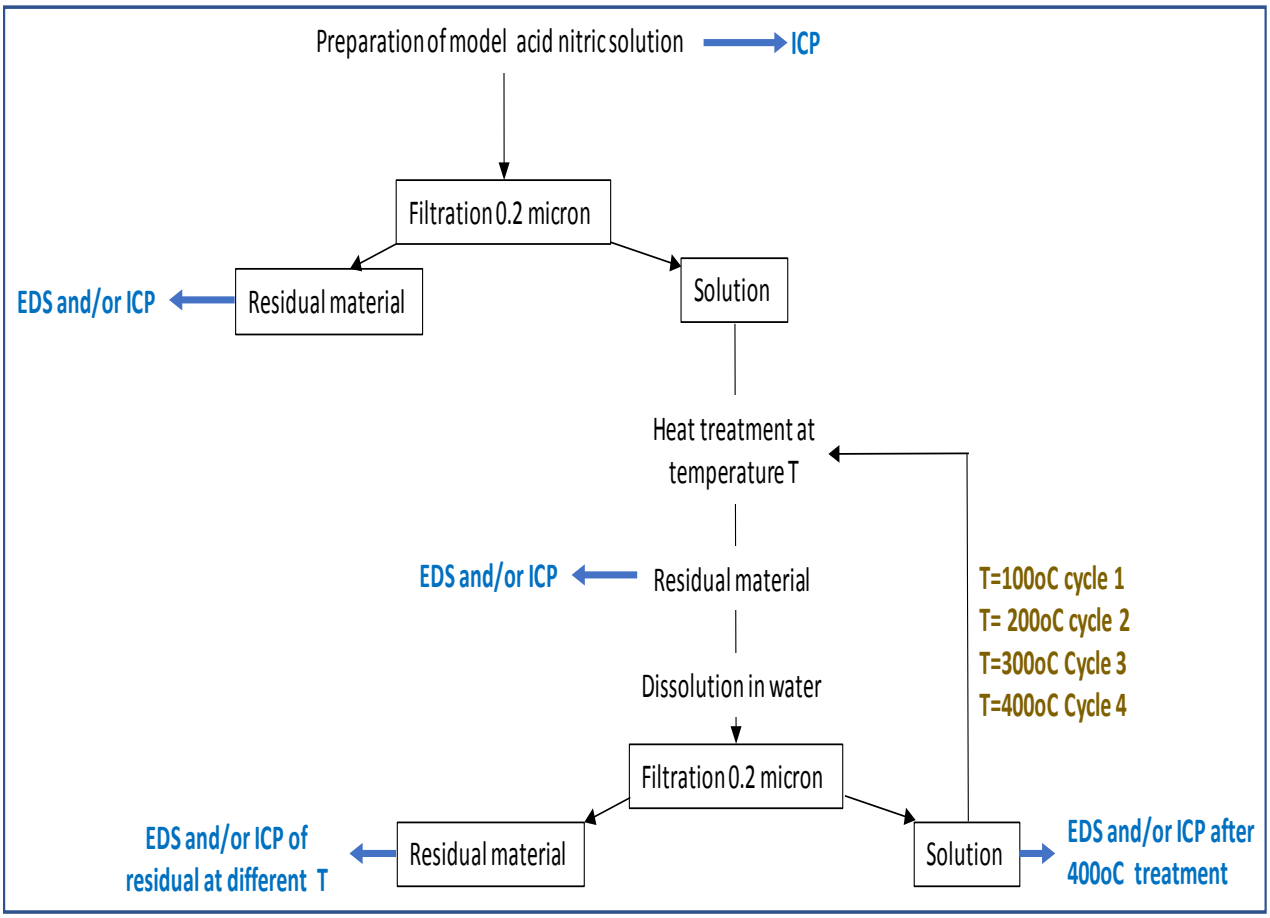

Figure 6: Diagram of roasting (under inert and oxidation condition) of residual material from model synthetic solution

Subtask 3:

In this subtask, we will subject fly ash to the treatment described in Figure 7 under the conditions determined in subtask 2. This test will be repeated multiple times to confirm results.

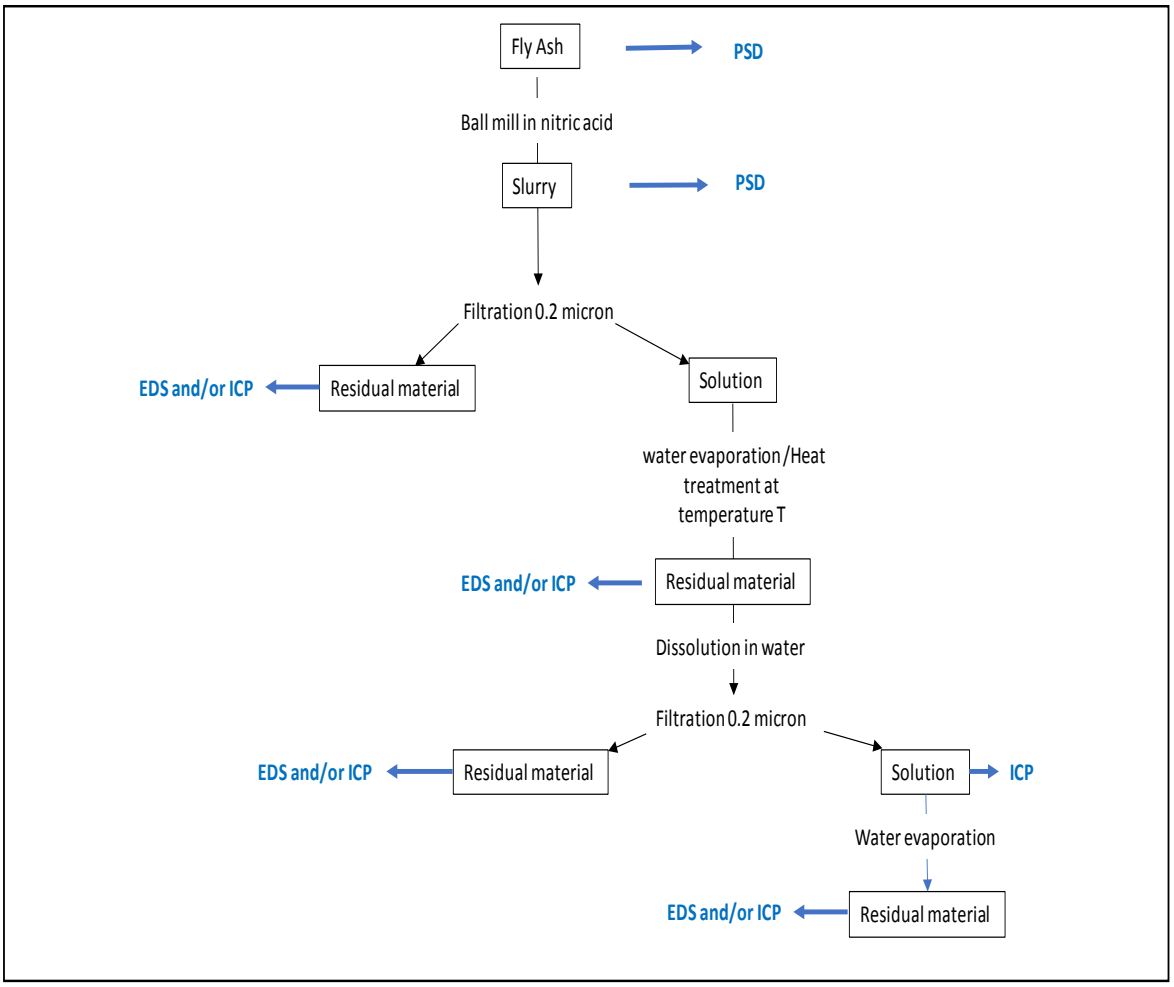

Figure 7: Separation of rare earth from fly ash

Safety Considerations

The safety considerations below are specific to these experiments conducted in Battelle laboratories 5-2-20, 5-2-30, and 5-2-36. If other lab spaces are used for testing, the safety considerations may need to be updated.

Special Concerns

1. The leaching tests will generate a small amount of NOx gas, which may cause pressurization of the milling vessel. The initial milling test will be conducted in secondary containment, and will be frequently vented inside the fume hood to ensure the mill vessel is not broken by pressure. When venting the mill vessel, wear a splash shield (available in the lab) and keep the hood sash as low as possible. Surround the lid with paper towels to prevent splashes while venting. Based on past reaction efficiencies with safety factors, the reaction should not generate more than 2-3 psi of pressure in a sealed milling vessel.
2. Nitric acid (HNO_3) is a strong acid and oxidizer, which is hazardous if contacting the skin (corrosive, irritant, permeator), eyes (irritant, corrosive), or inhaled into the lungs (lung sensitizer). Exposure to skin is characterized by burning, itching, or redness. Exposure to eyes is characterized by redness, watering, or itching. Exposure to lungs is characterized by coughing, choking, or shortness of breath.
3. Nitrogen monoxide (NO) is a colorless, nonflammable, poisonous and oxidizing gas with an irritating odor. Exposure to skins, eyes, and lungs produces a burning sensation. The gas is known to support and enhance combustion. The OSHA permissible exposure limit for NO is 25 ppm.
4. Nitrogen dioxide (NO_2) is yellow or brown gas and is a known irritant. Exposure to skins, eyes, and lungs produces a burning feeling in quantities as low as 5 PPM (OSHA ceiling).
5. Dinitrogen tetroxide (N_2O_4) is a corrosive, toxic, and oxidizing gas, or liquefied gas at temperatures below 20.9 °C, known to strongly support combustion. It is toxic if inhaled and may have delayed adverse effects. Skin and eye contact results in reddening and burning sensations.

Specific Safeguards

1. Prior to testing, the SDS for nitric acid and oxides of nitrogen as well as this SOP should be reviewed by personnel conducting the test. In addition, spill kits are on hand in laboratory 5-2-036 to mitigate any acid spills during testing. An eye wash station is in the laboratory with a body wash station in the hallway near where testing will be conducted. Laboratory personnel have been advised to call Battelle Emergency Services at 4-4444 in the event of any accidents.
2. Prior to testing, a fume hood has been used to house all hardware exposed to acid and corrosive gases with a secondary containment unit at the bottom of the hood lined with spill pads.
3. All process vent gas will be sent to a caustic soda bath to neutralize acidic materials.
4. Personal protective equipment has been identified and sent to the laboratory for testing along with instructions for don/doffing the equipment.
5. Laboratory personnel have been advised for the initial testing not to test without having oversight from a secondary test operator in the event an accident occurs. This two-deep operation will be observed until it is proven that no adverse chemical reactions posing undue risk occur, at which point it is permissible to operate with a single staff member.

Emergency and First Aid Procedures

Management of Leaks - If a person experiences any of the symptoms described in the SDS (located in 5-2-36) or significant amounts of brown-yellow gases are observed outside of the hood of the hood, execute the following:

1. Evacuate the laboratory as quickly as possible.

2. Notify staff working in the laboratory and adjacent laboratories to evacuate. Post staff or signs at laboratory doors to prevent re-entry into the laboratory until the Health and Safety Representative gives permission.
3. Notify the Control Center by calling 4-4444. Give them your name, location and nature of emergency. The Control Center will notify ESH&Q.
4.]Notify Energy Management
5. Test team members will not re-enter the laboratory until permission is obtained from the Safety and Health representative.

First aid

1. If a sudden stimulation of breathing or a pungent odor is noticed during activities with NOx gases, evacuate the laboratory. Immediately call 4-4444 and ask for medical attention.
2. If liquid from the process and associated subsystems contacts skin, immediately flush affected areas with copious amounts of water.
3. If liquid from the ADP system and associated subsystems contacts eyes, immediately head to the eye wash station to thoroughly wash affected areas with copious amounts of water.

Emergency shutdown procedure

In the event of an emergency situation, the test stand can be shut down by shutting off any heat supplied to the reaction and fully closing the fume hood door (if open). Cooling water and purge air should remain on. When these conditions have been met, the system can be abandoned in the event of an emergency.

Preliminary Hazards Assessment (PHA)

Preliminary Hazards Assessment (PHA)						
Item No.	**Hazard Description**	**Location**	**Form / Quantity / Type**	**Postulated Accident Events Associated with the Identified Hazard**	**Initial Hazard "Risk" Level (score calculated in cell H-J)**	**Controls**
HA1	Corrosive substance - sodium hydroxide or calcium carbonate	20% Sodium hydroxide or calcium carbonate (w/w) is used to neutralize acid overflow in the caustic bath	Caustic bath with 3.5 liters 20% (w/w) solution	Potential for spill of alkaline solution	Low	**Administrative** - protocol established with appropriate personal protective equipment to prevent skin/eye contact during a spill event; **Engineered -** Spill cleanup kit added to laboratory to contain spill; **Engineered** - Test stand built within fume hood with sash to contain spills. **Administrative** - Hood sash remains in the lowered position during operation to contain splashes.
HA2	Oxidizing agent-nitric acid	68% nitric acid (w/w) is used to throughout process	Several different formulations at several different volumes	Potential for spill of acidic solution	Low	**Administrative** - protocol established with appropriate personal protective equipment to prevent skin/eye contact during a spill event; **Engineered -** Spill cleanup kit added to laboratory to contain spill; **Engineered** - Test stand built within fume hood with sash to contain spills. **Administrative** - Hood sash remains in the lowered position during operation to contain splashes. ***Always add acid to water.***

Preliminary Hazards Assessment (PHA)						
Item No.	**Hazard Description**	**Location**	**Form / Quantity / Type**	**Postulated Accident Events Associated with the Identified Hazard**	**Initial Hazard "Risk" Level (score calculated in cell H-J)**	**Controls**
HA3	Overheating - risk with system heaters	Heaters exist for: (1) acid digestion unit and (2) acid roasting unit.	Heaters within ARP and ADP subsystems	Pressure can build within system or thermal decomposition of components can occur from runaway heater.	Low	**Engineered –** System designed to operate at low pressure; **Engineered -** Test stand built within fume hood to capture any unintended reaction products vented during operation; **Administrative** - Hood sash remains in the lowered position during operation to assist in drawing errant vapors to exhaust.
HA4	Distillation Systems - ARP components act as *ad hoc* distillation system	The ARP and downstream condenser function as a pot still system	Acid roaster and condenser (HE05) exist within system	Potential for gas heating and expansion; a runaway heater could lead to thermal decomposition, causing the system to over-pressurize.	Low	See HA4. **Administrative -** Hood sash remains in the lowered position during operation to assist in drawing errant vapors to exhaust. **Engineered –** System designed to operate at low pressure

Preliminary Hazards Assessment (PHA)						
Item No.	**Hazard Description**	**Location**	**Form / Quantity / Type**	**Postulated Accident Events Associated with the Identified Hazard**	**Initial Hazard "Risk" Level (score calculated in cell H-J)**	**Controls**
HA5	Chemical Reactions - Conversion of metals to metal nitrates with NOx evolution for ADP subsystem	ADP reaction	Location for ADP reactions in ADP reactor; Involves liquids and solids: M (metal), MNO_3, HNO_3; Gases evolved: NO, NO_2, N_2O_4	(1) Potential for rapid gas evolution and pressurization; (2) Potential irritant and asphyxiant release (NOx gases).	Low	**Engineered –** System headspace vented to caustic bath; **Engineered -** Test stand built within fume hood to capture any released asphyxiants or irritants; **Engineered** – System designed to operate at low pressure; **Administrative** - Hood sash remains in the lowered position during operation to assist in drawing errant vapors to exhaust.
HA6	Chemical Reactions - ARP converts metal nitrates to metal oxides with evolution of NOx gases	ARP roaster	Location in the ARP roaster; nitrates are converted to oxides, generating NO, NO_2, and N_2O_4 gases	(1) Potential for rapid gas evolution and pressurization; (2) Potential irritant and asphyxiant release (NOx gases)	Low	**Engineered –** System designed to operate at low pressure; **Engineered -** Test stand built within fume hood to capture any released asphyxiants or irritants; **Administrative** - Hood sash remains in the lowered position during operation to assist in drawing errant vapors to exhaust.

Preliminary Hazards Assessment (PHA)						
Item No.	**Hazard Description**	**Location**	**Form / Quantity / Type**	**Postulated Accident Events Associated with the Identified Hazard**	**Initial Hazard "Risk" Level (score calculated in cell H-J)**	**Controls**
HA7	Increased pressure caused by heating - ADP relies on heat to increase reaction kinetics	ADP reaction	Location for ADP reactions in ADP reactor	Potential for rapid pressure increase and burst of system plumbing releasing energy and toxic components.	Low	**Engineered -** Test stand built within fume hood to capture any gas released during operation. **Engineered** – system designed to operate at low pressure.
HA8	Increased pressure caused by heating - ARP relies on heat to increase reaction kinetics	ARP roaster	Location in the ARP roaster	Potential for rapid pressure increase and burst of system plumbing releasing energy and toxic components.	Low	**Engineered –** system designed to operate at low pressure; **Engineered -** Test stand built within fume hood to capture any gas released during operation; **Administrative** - Hood sash remains in the lowered position during operation to assist in drawing errant vapors to exhaust.
HA9	Increased volatility caused by heating - ADP relies on heat to increase reaction kinetics	ADP reaction	Location for ADP reactions in ADP reactor	Potential for release of irritants and asphyxiants	Low	**Engineered -** Test stand built within fume hood to capture any gas released during operation; **Administrative** - Hood sash remains in the lowered position during operation to assist in drawing errant vapors to exhaust.

Preliminary Hazards Assessment (PHA)						
Item No.	**Hazard Description**	**Location**	**Form / Quantity / Type**	**Postulated Accident Events Associated with the Identified Hazard**	**Initial Hazard "Risk" Level (score calculated in cell H-J)**	**Controls**
HA10	Increased volatility caused by heating - ARP relies on heat to increase reaction kinetics	ARP roaster	Location in the ARP roaster	Potential for release of irritants and asphyxiants	Low	**Engineered -** Test stand built within fume hood to capture any gas released during operation; **Administrative** - Hood sash remains in the lowered position during operation to assist in drawing errant vapors to exhaust.
HA11	Pressurization of the ceramic mill vessel	Fume hood	Over pressurization, broken ceramic, acid spillage.	Breakage of the vessel, leading to acid leakage or sharp ceramic pieces.	Low	Will vent the mill periodically, keep it in secondary containment, lower fume hood sash as low as possible, wear splash shield when venting, and keep lid surrounded with paper towels. Calculations predict a pressure rise of only 2-3 psi under liberal assumptions. Worst possible case was calculated to be 18 psi. Lid will not detatch from vessel while venting due to vessels locking mechanism at calculated pressures. Mill vessel will be handled with absorbent and work gloves to avoid cuts if it breaks, and mill roller will be covered to prevent splashes if the mill vessel breaks. Regular inspections will be done of the lid deal to be sure metal portions are not corroded and in good repair. Plastic and spill pads will be placed under the

	Preliminary Hazards Assessment (PHA)					
Item No.	**Hazard Description**	**Location**	**Form / Quantity / Type**	**Postulated Accident Events Associated with the Identified Hazard**	**Initial Hazard "Risk" Level (score calculated in cell H-J)**	**Controls**
						rollers in the machine to prevent leakage of acid into the drive.

Appendix D: Laboratory Testing Report

Recovery of Rare Earth Elements from Coal and Coal Byproducts via a Closed Loop Leaching Process:

Lab Testing Report

National Energy Technology Laboratory

3610 Collins Ferry Road

Morgantown, WV 26507-0880

7 June 2017

BATTELLE

DE-FE0027012
DUNS: 007901598

Recovery of Rare Earth Elements from Coal and Coal Byproducts via a Closed Loop Leaching Process:

Lab Testing Report

Prepared by:

Battelle
505 King Avenue
Columbus, Ohio 43201

Principal Investigator: Rick Peterson, P.E.

Submitted to:

U.S. Department of Energy
National Energy Technology Laboratory
3610 Collins Ferry Road
Morgantown, WV 26507-0880

7 June 2017

BATTELLE

Table of Contents

List of Tables

List of Figures

Executive Summary

This report documents and summarizes the additional lab work performed in Phase 1 after the original feasibility study (Battelle, 2017) to inform the design of a continuous bench scale pilot unit for the recovery of rare earth elements. The lab testing focused on means to improve leaching efficiency for REEs, improve purity of the REE concentrate produced by the process, and generate additional high value byproducts from the process.

Based on the laboratory testing, ball milling and caustic pretreatment of the ash allows for high recovery of REE, with leaching efficiencies for scandium as high as 86% and near complete recovery of total REE as a weighted average. Milling of the ash to approximately 4-5 µm allows these recoveries to be realized with only a 60 minute contact with 10% sodium hydroxide solution at 90 °C, and leaching in 34% nitric acid for 30 minutes at 90 °C. Traditional aluminosilicate recovery from fly ash requires a caustic leach of 6 hours or more (Hollman, Steenbruggen, & Janssen-Jurkovicova, 1999), so this method represents a significant decrease in reaction time. The acid leaching reaction is slightly exothermic, at approximately 102 calories per gram of ash leached, which will reduce energy costs to heat the leach reactor.

Additionally, the caustic pretreatment leach should allow for production of a zeolite byproduct that can be used as an adsorbent or catalyst support material. A zeolite material was made in the lab with the milled fly ash, but additional work would be done in Phase 2 to make a higher value zeolite with the use of seed material or zeolite scaffolds.

A first recovery of the rare earth elements by thermal roasting of the loaded acid can oxidize the iron and aluminum between 100 °C and 200 °C, generating an insoluble oxide material. In testing with actual leach solutions, 90% of the REE could be recovered from the roasted solids with a water leach, while omitting over 90% of the iron and aluminum, and over 60% of the uranium and thorium. The water leach had a concentration of 1.2% REE, effectively leading to over a 20x increase in purity of the REE over the fly ash feed.

Solvent extraction testing suggested that extraction for REE is satisfactory at pH of 3.4, where 61% of REEs are extracted at over 7% purity (over 120x concentration over the feed fly ash). The primary contaminants were sodium (due to a high starting concentration), aluminum, silica, calcium, and iron, but sodium, potassium, magnesium, and calcium were largely excluded from the extract. At pH 5, near quantitative REE can be achieved (over 99%), including less valuable lanthanum and cerium, but purity drops to about 1.0% in the extract. In selective stripping tests, the REE were stripped in hydrochloric acid at around one molar. The scandium is expected to be recoverable by precipitating in sodium carbonate solution. These REE solutions could then be separated with commercial operations such as further solvent extraction or ion exchange, or an emerging technology could be used such as electrowinning or electrophoresis.

The results of the laboratory testing were used in the updated technoeconomic assessment model to predict the economics of the process, and they were used in the design of a continuous bench scale unit that integrates all of the operations. The key parameters that were used are a one-hour leach in 10% sodium hydroxide at 90 °C, with fly ash milled to ~4.5 µm, then acid leaching in 34% nitric acid at 90 °C. The loaded acid will be roasted at 150 °C to calcine iron and aluminum, separating them from REE in a water wash. This loaded water will be extracted at pH 3.5-4.0, scrubbed around pH 3.5 to remove base metals, stripped with 1 molar hydrochloric acid to recover REE, scrubbed with 2 M HCl to remove iron, then scandium recovered by precipitation with 10% sodium carbonate solution. Additional work to improve the stripping process will be done in pending Phase 2 testing.

1.0 Introduction

As directed by Congress, the United States (U.S.) Department of Energy (DOE) is investigating the economic feasibility of recovery of rare earth elements (REEs) from domestic U.S. coal and coal byproducts. DOE's National Energy Technology Laboratory (NETL) has characterized a number of REE-bearing samples of coal and coal-related materials. Rare earth elements have been found in varying concentrations ranging up to 1,000 parts per million by weight in the following materials in the United States: coal mine roof and floor materials, run-of-mine coal, prepared coal, partings, pit cleanings, coal preparation refuse, and tailings. REEs can be found in coal byproducts, including ash, coal-related sludge, and mine drainage. Certain coals can contain a higher ratio of heavy (generally more valuable) REEs than found in other sources of REEs such as natural ores, and DOE is particularly interested in sources that have higher than 300 ppm REE. Since most coal materials start at REE concentrations well below 1,000 ppm, the yield of REEs from any separation process is likely to be low, and minimizing costs is a key challenge. DOE therefore funded groups with novel processes able to recover REE from coal sources while minimizing the processing costs.

The rare earth elements are the 14 naturally occurring elements between lanthanum and lutetium on the periodic table, along with yttrium and scandium which have similar chemical properties. Their symbols and atomic numbers are listed in Table 1 for reference. They have become critical in renewable energy and defense applications, where they are used to make magnets for motors and generators, metal alloys, and in various sensor components. Occasionally, yttrium and scandium are considered separately, and so the group of rare earth elements is sometimes referred to as REE+Y+Sc for clarity in this report. Element 61, promethium, is not naturally occurring and not included in the analyses for this report.

Table 1. List of rare earth elements, their symbols, and their atomic numbers.

Rare Earth Elements, Symbols, and Atomic Numbers											
Sc	Scandium	21	**Pr**	Praseodymium	59	**Gd**	Gadolinium	64	**Er**	Erbium	68
Y	Yttrium	39	**Nd**	Neodymium	60	**Tb**	Terbium	65	**Tm**	Thulium	69
La	Lanthanum	57	**Sm**	Samarium	62	**Dy**	Dysprosium	66	**Yb**	Ytterbium	70
Ce	Cerium	58	**Eu**	Europium	63	**Ho**	Holmium	67	**Lu**	Lutetium	71

Battelle is validating the economic viability of recovering REEs from coal ash using its patented (US6011193) closed-loop Acid Digestion Process (ADP). Based on results from the sampling and characterization work (Battelle, 2016), a Pulverized Coal Combustion (PCC) plant fly ash was selected as the target feedstock for the process. This plant is operating in Ohio on primarily Appalachian Basin coals, and had a high total REE+Y+Sc concentration at 545 ppm +/- 13 ppm. A preliminary Technoeconomic analysis (TEA) done on Battelle's ADP process suggested that it could be economically applied to between 5% and 47% of U.S. coal sources, and based on this finding, additional lab testing and design work was started.

This report documents and summarizes the additional lab work performed to inform the design of a continuous bench scale pilot unit. The lab testing focused on means to improve leaching

efficiency for REEs, improve purity of the REE concentrate produced by the process, and generate additional valuable byproducts from the process. A separate, final report final report for this project will include a summary of the results in this report, along with updated process economic based on the lab findings, and a summary of the process design package.

2.0 Laboratory Testing

2.1 Test Planning and Progression

Prior to the commencement of testing, a plan was developed to ensure that key results for leaching parameters, calorimetry, and product recovery would be statistically valid and defensible. This test plan is available as Appendix A. Beyond this test plan, some preliminary tests were performed to investigate options to improve process performance. In particular, tests were performed to improve the REE leaching efficiency, generate a catalyst and adsorbent support product from the caustic pretreatment step, and enhance product quality with solvent extraction.

The leaching efficiency tests included grinding, ball milling, thermal shock to the ash, and pre-treatment with caustic solution. The solvent extraction tests investigated selectivity for metals extraction with pH, and selectivity for metals stripping with pH, acid concentration, and acid type. The catalyst support product testing investigated how a zeolite type product may be generated from the ash pretreatment solution.

2.2 Leaching Efficiency Improvement Testing

Preliminary laboratory testing was performed to improve leaching efficiency, validate some of the assumptions made in the economic modeling portion of the project, and understand viable next steps in the REE purification process. The following preliminary tests were run to investigate which method was the most efficient. These tests will be reported in this section; Pulverized Coal Combustion (PCC) plant fly ash was used for all the tests:

1. **High Temperature Leaching**: testing of temperature effects on total leach efficiency of PCC fly ash at different concentrations of nitric acid
2. **Comminution**: grinding and ball milling of PCC fly ash, along with combined milling and leaching
3. **Thermal Shock**: leaching of PCC fly ash after thermal shock at different conditions
4. **Caustic Pretreatment**: leaching of PCC fly ash after pretreatment with different concentrations of sodium hydroxide solution

The same set up and test apparatus was used for all the leaching tests (See Figure 1). Reactions were performed in a round-bottom flask in a heating mantle with forced air in the headspace that exhausts through a caustic bath. This set up neutralizes any noxious fumes that may be generated in the reaction. The tests were also run inside a fume hood.

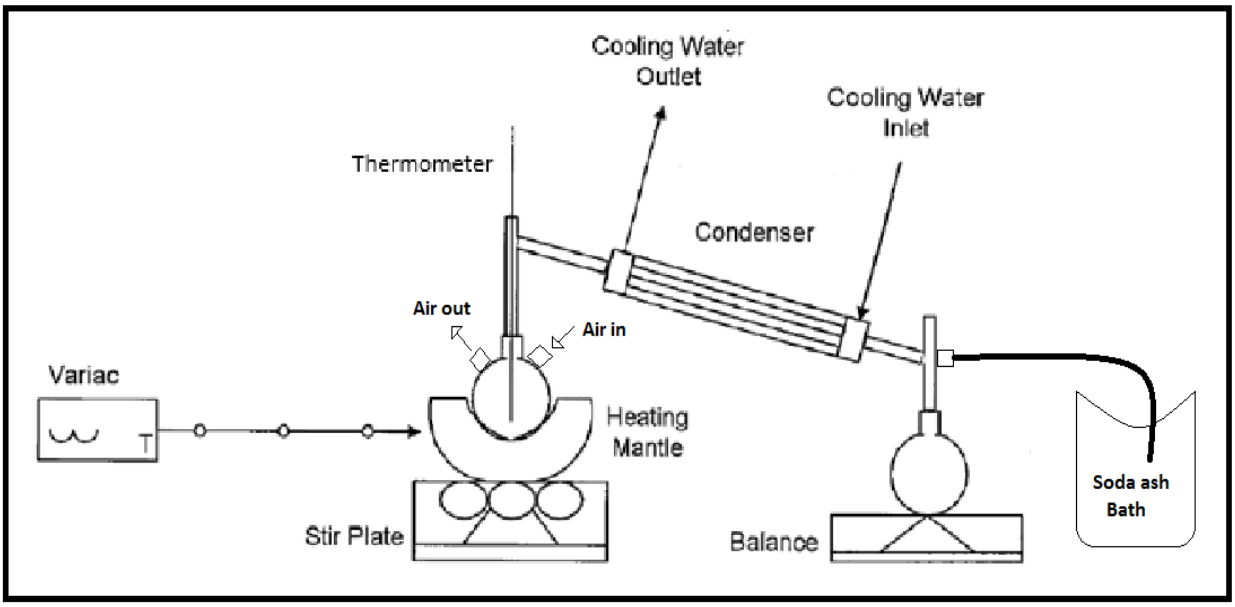

Figure 1 - Test apparatus and set up used for every leaching experiment.

All leaching tests with nitric acid followed the same procedure:

a) In a fume hood, add 250 mL of nitric acid solution with desired concentration to a round-bottom flask with a running air purge to a caustic bath, and a thermometer in the top stem. Add a stir bar and begin mixing the solution.
b) Set the temperature controller to the desired temperature. Wait for the acid to reach this temperature.
c) Add desired amount of PCC fly ash (pretreated or not pretreated) to the solution and begin a timer.
d) Aliquot 10-mL sample(s) of the solution after desired sampling times, into a polyethylene sample container. Filter the samples using either syringe filters or EMD Millipore 142mm Hazardous Waste Pressure Filter System (See Figure 2, Figure 3, Figure 4).
e) End the experiment after the desired reaction time by turning off the heater. Wait for the solution to cool down, and discard the remaining ash and solution in a waste container appropriate for low pH oxidizing waste.
f) Send samples to Activation Laboratories (Act Labs) for analysis by Inductively Coupled Plasma Mass Spectrometry (ICP-MS).

Figure 2 - EMD Millipore 142mm Hazardous Waste Pressure Filter System used.

Figure 4 - Syringe filters used

Figure 3 - Filters used for Pressure Filter System

The samples taken in each leaching were sent to Act Labs for analysis by ICP-MS to quantify the concentration of target elements in the coal ash to a level of 500 parts per billion or less (See Figure 5). Act Labs was the laboratory of choice for the U.S. Geological Survey (USGS) for analysis of coal sources. Therefore, it was used for this project to ensure that data collected from this analysis is comparable to characterization data evaluated as part of the sampling and characterization study Battelle conducted. Figure 5 illustrates which elements were part of the ICP-MS analysis of the leach solutions; the 59 analytes cover the vast majority of naturally occurring metals that could be in solution. Omitted metals included noble metals such as gold, platinum, and palladium which are unreactive and not expected to be in solution at measurable quantities. It should be noted that purities for REE elements in leach solutions were calculated from this analysis as a fraction of the concentration of all analyzed elements. This is not a perfect representation of purity, since it assumes that the analysis is comprehensive. Additionally, it omits most anions, so the purity is REE out of all analyzed cations. Purity is calculated in this manner due to the difficulty of obtaining enough material for solids analysis by ICP-MS in our existing lab equipment.

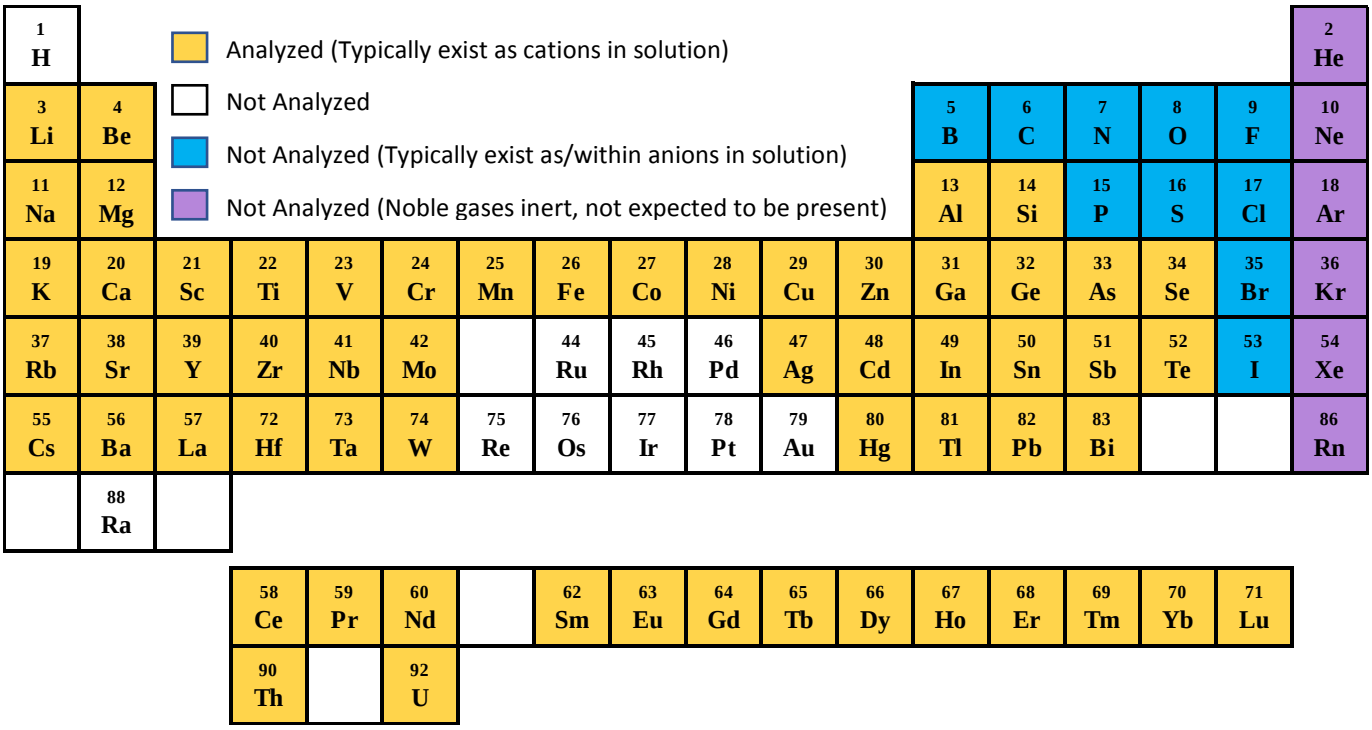

Figure 5: Analyzed elements by ICP-MS

The highest leaching efficiency for scandium, which is the rare earth element of highest value (approximately $4,000 per kg as an oxide, (mineralprices.com, 2016)), obtained from Battelle's previous Phase 1 work was about 55.3% of the scandium available (See Table 2). This result was obtained by leaching 1 gram of milled PCC Fly Ash with 250 mL of 34% nitric acid at room temperature for 30 minutes.

Table 2 - Leaching efficiencies for rare earth elements with 34% nitric acid at room temperature, and using milled PCC Fly Ash (Battelle, 2017)**.**

Element	% Leached from milled PCC Fly Ash
Sc	55.3%
Y	46.9%
La	35.4%
Ce	34.0%
Pr	36.3%
Nd	39.5%
Sm	40.5%
Eu	42.4%
Gd	45.2%
Tb	44.3%
Dy	41.9%
Ho	41.8%
Er	43.8%
Tm	42.2%
Yb	36.3%
Lu	34.6%

2.2.1 High Temperature Leaching

It was expected that high temperatures will improve leaching efficiency for REE from coal ash. For high temperature tests, 34% and 68% nitric acid were used. The experimental setup for these tests is shown in Figure 1, and the target temperature for the tests was 90 °C. For these tests, the soda ash bath was important for safety because the NO_x gas created is neutralized in the bath.

For each test, 250 mL of nitric acid was added to a 1,000 mL round-bottom flask, and heated to 90 °C. After the acid reached the desired temperature, 1 gram of unmilled PCC fly ash was added, and the solution was stirred at 300 rotations per minute (rpm) for 30 minutes. Samples were taken after 1, 5, and 30 minutes of leaching. Samples were filtered using a 0.45 µm polyethersulfone syringe filter and sent for ICP-MS analysis. Table 3 shows the percent of rare earth elements leached in these tests.

Table 3 – Leaching efficiency for rare earth elements at two different nitric acid concentration and different leaching times and 90 ºC.

Element	% Leached					
	34% HNO_3, 1 min	34% HNO_3, 5 min	34% HNO_3, 30 min	68% HNO_3, 1 min	68% HNO_3, 5 min	68% HNO_3, 30 min
Sc	11.5%	19.9%	26.0%	12.9%	12.9%	19.4%
Y	21.6%	27.1%	39.6%	11.6%	19.9%	25.3%
La	12.7%	18.3%	25.3%	6.3%	11.7%	17.1%
Ce	12.5%	17.4%	25.8%	6.2%	11.9%	15.9%
Pr	14.7%	17.5%	30.7%	7.3%	14.3%	16.0%
Nd	16.3%	19.2%	32.6%	8.2%	15.8%	17.2%
Sm	18.4%	21.1%	35.9%	9.5%	18.2%	19.0%
Eu	19.4%	22.7%	36.5%	10.8%	18.5%	20.6%
Gd	18.6%	24.7%	34.5%	11.4%	17.9%	22.1%
Tb	21.1%	22.9%	39.5%	10.1%	19.9%	20.4%
Dy	20.7%	24.4%	39.2%	10.8%	19.7%	21.6%
Ho	19.8%	24.6%	38.0%	10.4%	19.3%	21.6%
Er	19.6%	23.7%	38.1%	9.9%	18.8%	21.2%
Tm	19.0%	23.1%	36.8%	9.5%	17.9%	20.6%
Yb	17.2%	21.2%	35.0%	8.5%	16.2%	18.9%
Lu	24.8%	23.3%	49.4%	9.2%	25.0%	19.9%

These results were compared to data obtained for experiments performed at room temperature (20 °C), 34% and 68% nitric acid, and leaching time of 30 minutes. Table 4 shows that the percent of rare earth elements leached with a reaction temperature of 90 °C is higher than the percent leached at room temperature (20 °C). This supported our expectation for higher leaching efficiencies at higher temperatures.

Table 4 - Leaching efficiency for rare earth elements at 90 °C and 20 °C, and two different nitric acid concentration.

Element	%Leached			
	34% HNO_3, 30 min, 90 °C	34% HNO_3, 30 min, 20 °C	68% HNO_3, 30 min, 90 °C	68% HNO_3, 30 min, 20 °C
Sc	26.0%	4.5%	19.4%	3.6%
Y	39.6%	7.1%	25.3%	5.4%
La	25.3%	5.9%	17.1%	8.2%
Ce	25.8%	4.9%	15.9%	3.5%
Pr	30.7%	5.9%	16.0%	4.2%
Nd	32.6%	5.6%	17.2%	4.6%
Sm	35.9%	6.5%	19.0%	5.2%
Eu	36.5%	7.8%	20.6%	5.5%
Gd	34.5%	8.3%	22.1%	6.0%
Tb	39.5%	9.2%	20.4%	6.5%
Dy	39.2%	6.6%	21.6%	5.4%
Ho	38.0%	8.1%	21.6%	5.7%
Er	38.1%	8.0%	21.2%	5.4%
Tm	36.8%	7.3%	20.6%	5.1%
Yb	35.0%	6.5%	18.9%	4.4%
Lu	49.4%	6.5%	19.9%	4.3%

2.2.2 Comminution

The efficiency and rate of leaching depends on surface are area of fly ash exposed to the leaching media. Fly ash with small particles will have high exposed surface area; therefore, the leaching will be more pronounced than on large particles. The particle size was reduced by grinding and ball milling, and measured by a Malvern Mastersizer instrument. This technique measures the angular variation in intensity of light scattered as a laser beam passes through a dispersed wet particulate sample. Large particles scatter light at small angles relative to the laser beam and small particles scatter light at large angles. The angular scattering intensity data is then analyzed to calculate the size of the particles responsible for creating the scattering pattern, using the Mie theory of light scattering. The particle size is reported as a volume equivalent sphere diameter.

We reduced the particle size with two techniques: grinding and ball milling. Table 5 reports the 10^{th} (D10), 50^{th} (D50), and 90^{th} (D90) percentile particle sizes for fly ash before and after grinding in an IKA universal mill for 5 minutes, 10 minutes and 20 minutes. The mill was water cooled, but was run in a cycle of 5 seconds on and 5 seconds off for the time specified to prevent overheating and enhance mixing. Figure 6 shows a particle size distribution for the unground ash and the three grinding time steps. Much of the particle size reduction took place in the first five minutes of grinding. Figure 7 is a cross section Scanning Electron Microscope (SEM) image of unground and ground fly ash. It suggests the grinding reduced the particle size without affecting their shape as the particles still appear spherical after grinding. The inductively coupled plasma mass spectrometry (ICP-MS) analysis of 34% nitric acid leach solution from unground and ground fly ash is reported in Figure 8. It appears that grinding has an inhibitory effect on the leaching. However, in testing prior to the GO/NO GO decision regarding initial

feasibility it was demonstrated that ball milling improves the leaching. Future testing focused on ball milling rather than grinding of the ash.

Table 5: Particle size (in µm) of fly ash before and after grinding

Particle Sizes (µm) of Ash Milled at Indicated Time Intervals				
Time	0	5 min	10 min	20 min
d10	7.3	6.5	7	6.0
d50	31.1	24.8	24	20
d90	124	107	92	70

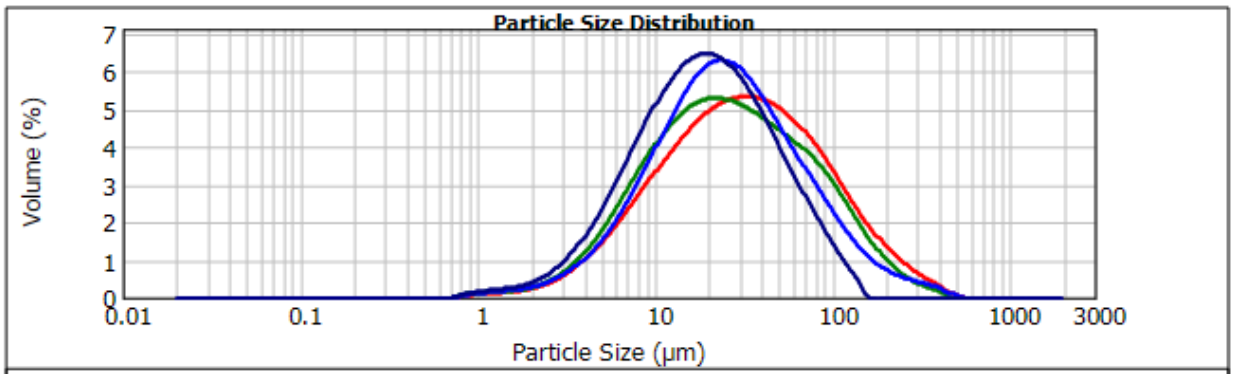

Figure 6: Particle size distribution for unground ash (red), 5 minutes of grinding (green), 10 minutes of grinding (light blue), and 20 minutes of grinding (navy blue).

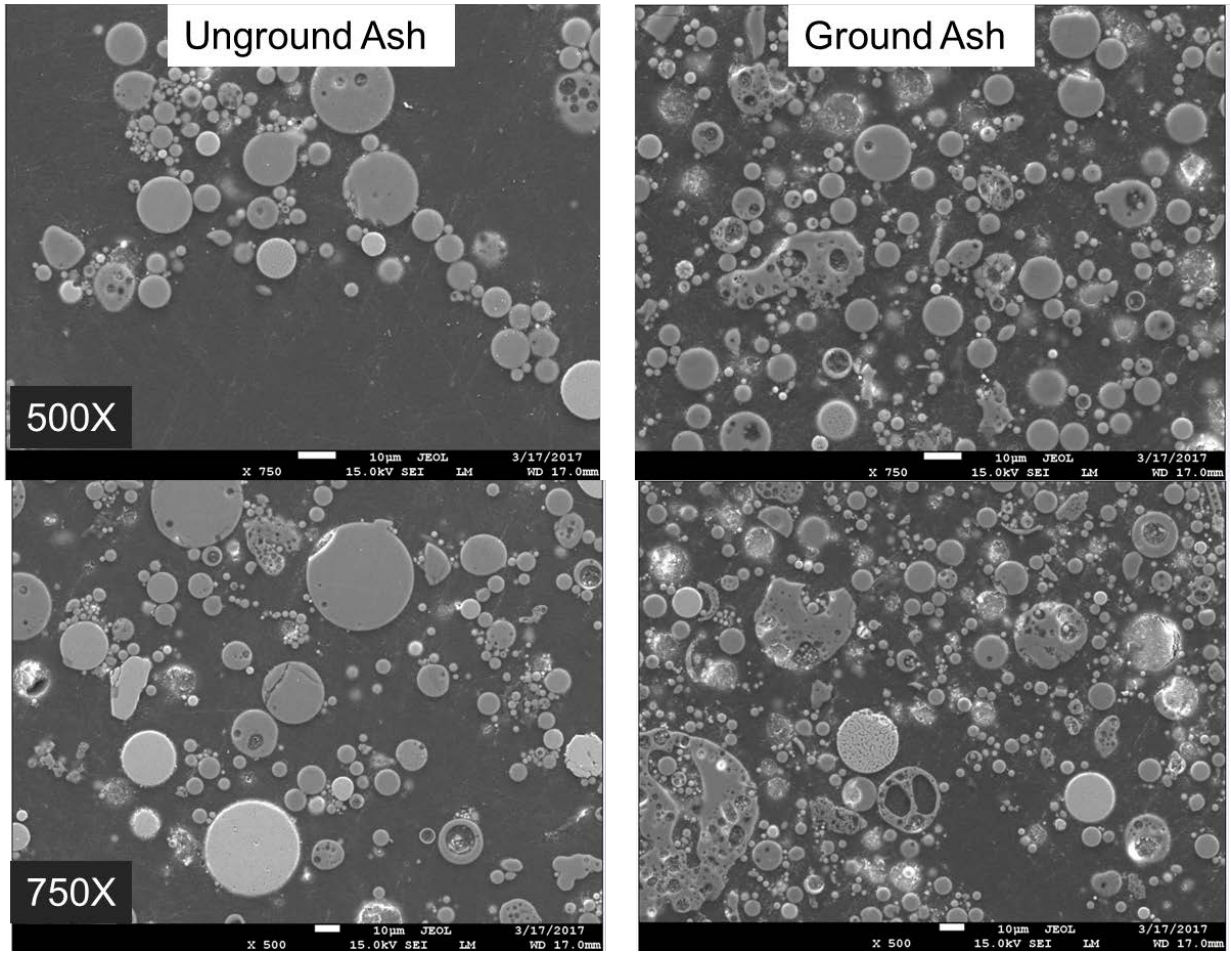

Figure 7: SEM image of unground and ground fly ash

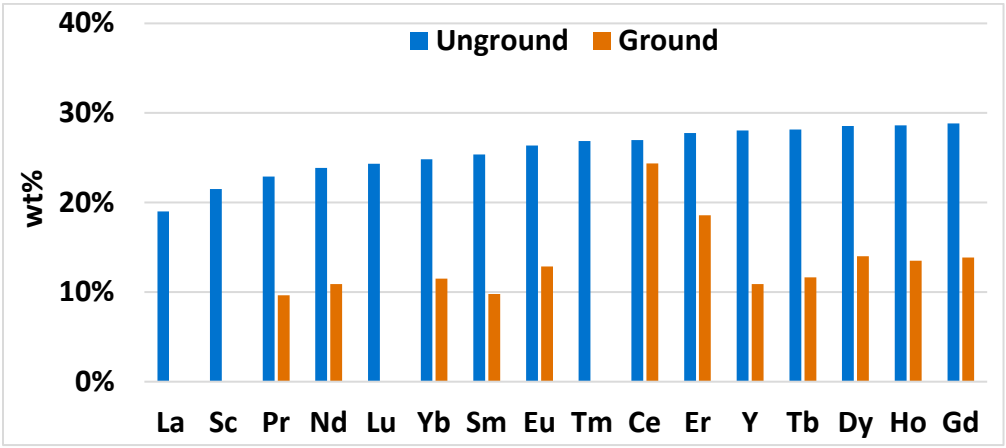

Figure 8: ICP analysis of 34% nitric acid leach solution from ground and unground fly ash.

Fly ash was ball milled for period of 30 minutes and 24 hours (Table 6). In a 300-mL ceramic jar, 40 grams of fly ash, 400 grams of grinding media (zirconium oxide ¼ inch pellets) and 100 grams of deionized (DI) water were mixed and ball milled at a speed of 100 rotations per minute. Figure 9, Figure 10, and Figure 11 show significant particle size reduction. The optimum ball milling time and condition will depend on grinding media and volume ratio between milling

media and fly ash. At a commercial scale, there are several technologies that can be used for particle size reduction to single digit µm scales, including jet mills and stirred media mills.

Table 6: Particle size (in µm) of fly ash after 5 minutes of grinding and after ball milling intervals

Particle Sizes (µm) of Ash Milled at Indicated Time Intervals			
	5 min grinding	Ball milling 0.5 hrs	Ball milling 24 hrs
d10	6.5	4.6	2.1
d50	24.8	10.5	4.1
d90	107	23.1	7.9

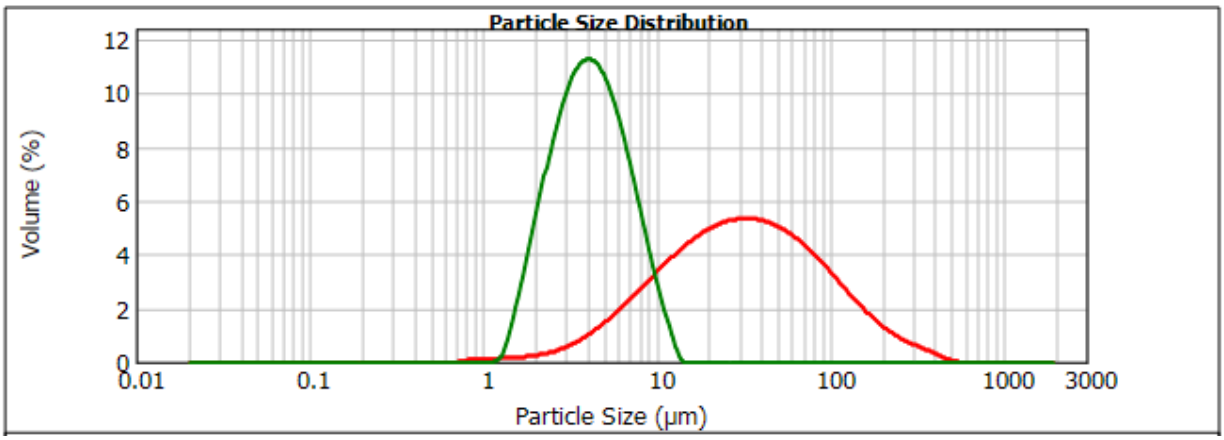

Figure 9: Particle size distribution for unmilled (red) and ball milled for 24 hours (green) fly ash.

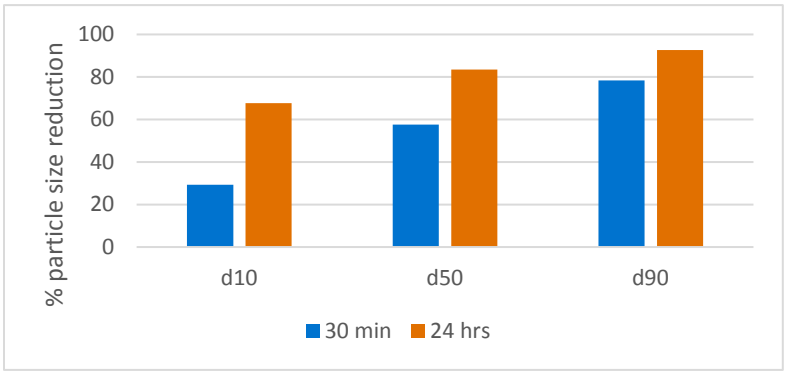

Figure 10: Percent particle size reduction compared to 5 minutes of grinding. The blue bars are ball milling for 30 minutes and the orange bars are ball milling for 24 hours.

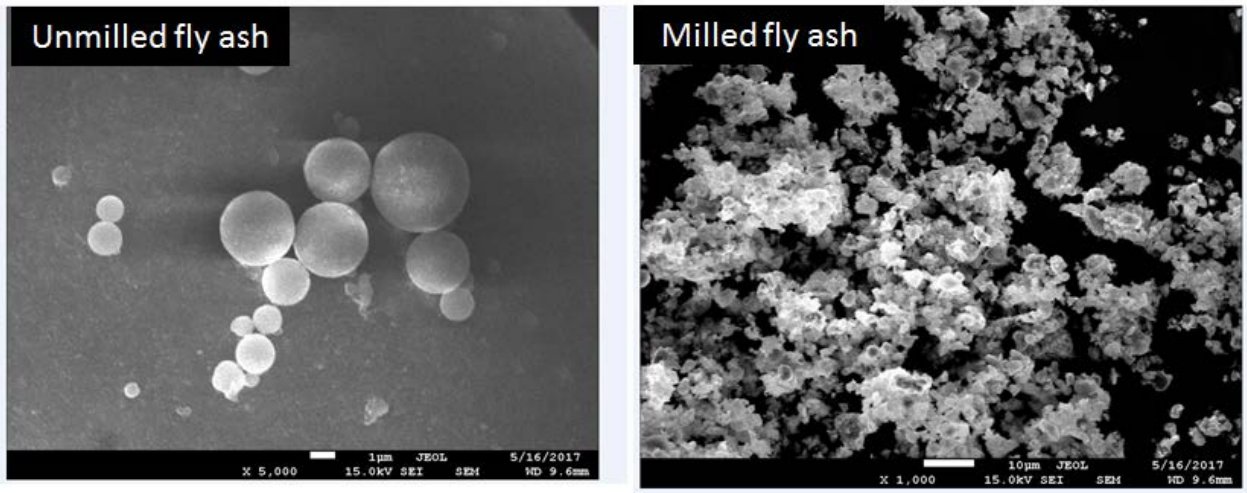

Figure 11: SEM of unmilled and milled fly ash.

Figure 12 reports the leaching efficiency of scandium, yttrium, and REE on unmilled and milled fly ash. The leaching was in nitric acid at concentration 34% and 68% for periods of 30 minutes and 24 hours. As expected the leaching of small particles is more efficient than the large particles. The 34% acid leads to better leaching than the 68%, which is possibly related to passivation of ash surface at high acid concentration. The leaching is more complete in 24 hours than in 30 minutes. These same observations were made for the leaching of other compounds (Figure 13).

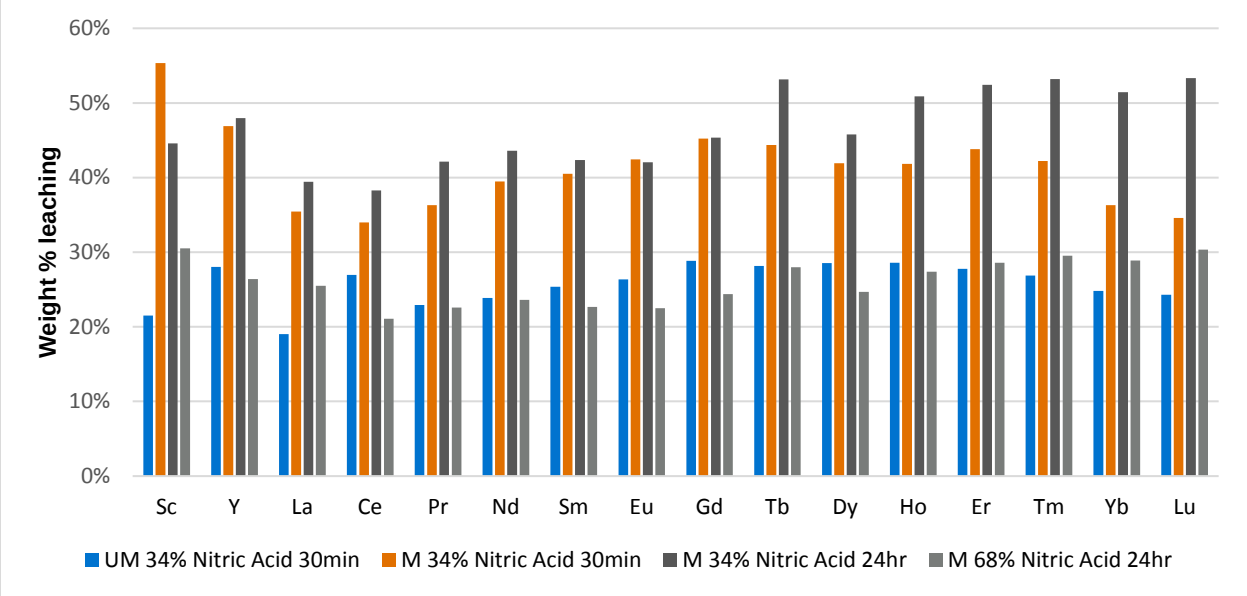

Figure 12: Leaching efficiency results by ICP-MS for unmilled (UM) and milled (M) fly ash.

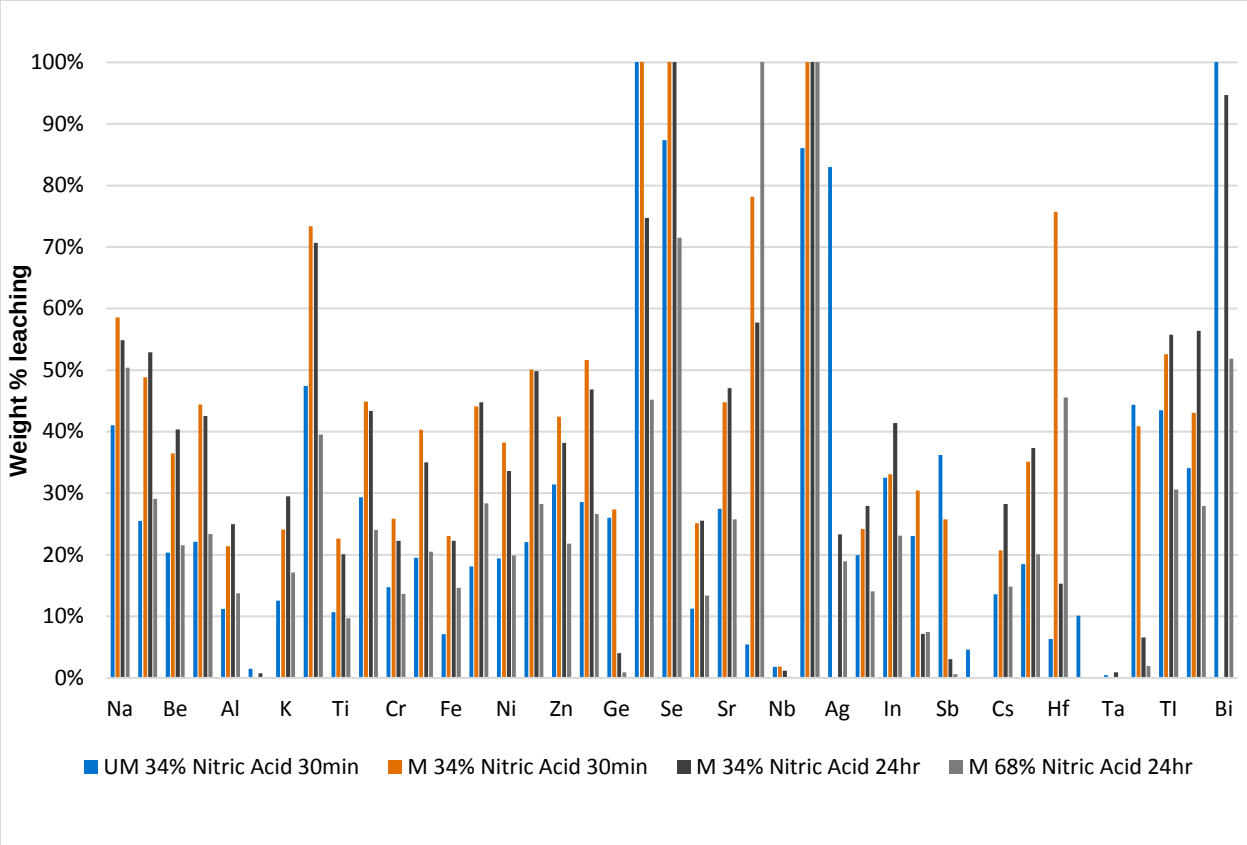

Figure 13: Leaching efficiency results by ICP-MS for unmilled (UM) and milled (M) fly ash.

2.2.3 Thermal Shock

It was demonstrated that the acid leaching of ball milled fly ash is more efficient than for larger particles. We also explored the possibility to improve leaching by subjecting ash particles to thermal shock, which should provide better access to the ash particle for leaching solutions. Around 1 to 2 grams of fly ash was heat treated for a period of 2 hours at 300 °C and immediately immersed in 250 mL of DI water (10 °C), 34% HNO_3 (10 °C), dry ice (-78 °C), or liquid nitrogen (-176 °C). The thermal shock is intended to cause cracking of the particles. The cracking was more pronounced in the test performed with liquid nitrogen, however, only a fraction of the particles appeared to crack. This is probably due to poor transfer of heat between particles. Figure 14 is an SEM cross section of the sample before and after thermal shock in liquid nitrogen. The cracks are more pronounced in large particles than small ones. Leaching was performed on unground and thermally shocked fly ash in 34% nitric acid. The ICP-MS analysis (Figure 15) suggests that there is little effect of thermal shock on the leaching.

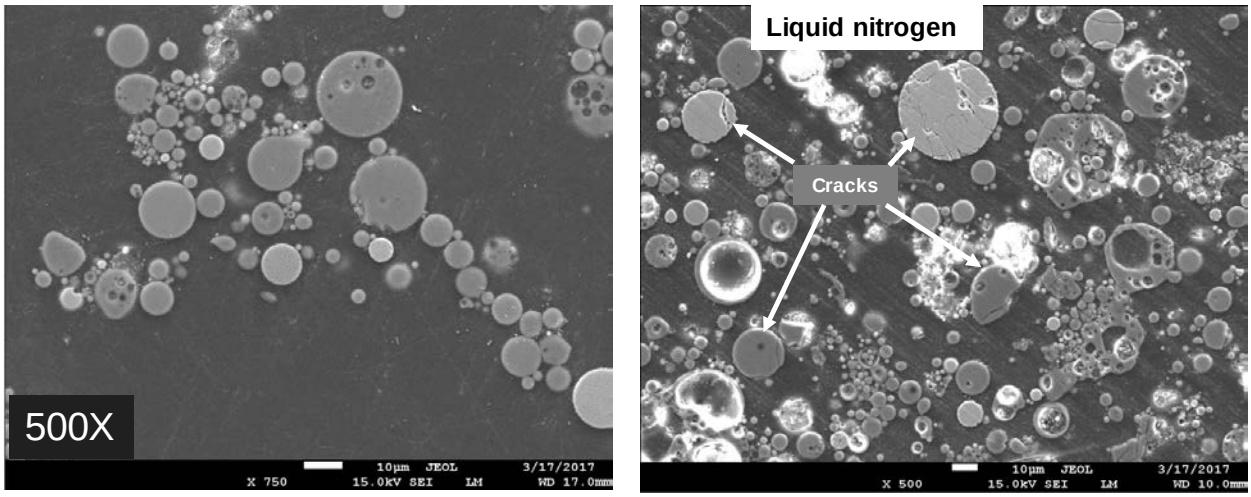

Figure 14: SEM cross section of unmilled (left) and thermally shocked (from 300 °C to -176 °C) fly ash

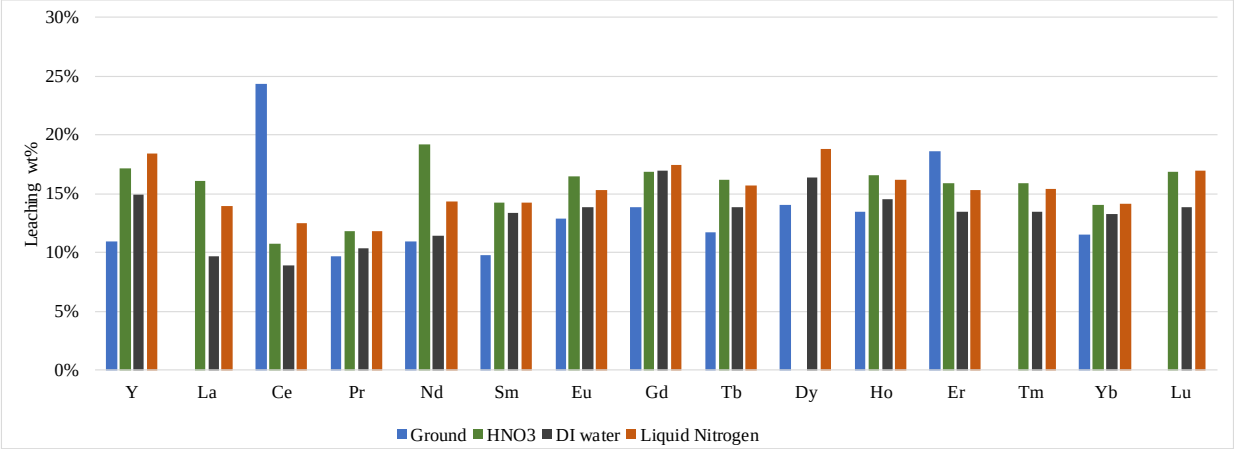

Figure 15: Leaching efficiency of thermally shocked samples in 34% nitric acid. Ground material was not thermally shocked, while the other legend labels indicate the quenching liquid used for the thermal shock.

2.2.4 Caustic Pretreatment

One of the ways to improve leaching efficiency of rare earth elements is by pretreatment of the fly ash with caustic solution. The caustic pretreatment will leach silica and alumina from ash particles giving better access to the rare earth elements in the acid leaching step. There were six caustic pretreatment tests performed using sodium hydroxide at three different concentrations (10%, 5%, and 1%) and at two different temperatures (20 °C and 90 °C). Each pretreatment was done with a residence time of one hour and using unmilled PCC Fly Ash as starting material. After pretreatment, leaching with 34% nitric acid was performed at 90 °C with a residence time of 30 minutes. After leaching, a sample was taken for analysis of scandium via Inductively Coupled Plasma Optical Emission Spectrometry (ICP-OES) through a Battelle method. After the first round of testing, an extra test was done using milled PCC Fly Ash as starting material with 10% sodium hydroxide solution at 90 °C for one hour. See Table 7 for conditions and results for each test. Based on the results of these tests (% of scandium leached), a decision was made to proceed with 10% sodium hydroxide solution at 90 °C for one hour on milled fly ash as the pretreatment method.

Table 7 - Test conditions and results for caustic pretreatment followed by acid leaching

Results of Caustic Pretreatment Followed by Acid Leaching					
Test	Concentration of sodium hydroxide (w/w)	Caustic Temperature/Reaction time	Concentration of nitric acid	Acid Leach Temperature/Reaction time	Scandium % leached
1	10%	20 °C / 1 hour	34%	90 °C / 30 min	23.17%
2	10%	90 °C / 1 hour	34%	90 °C / 30 min	54.27%
3	5%	20 °C / 1 hour	34%	90 °C / 30 min	23.05%
4	5%	90 °C / 1 hour	34%	90 °C / 30 min	38.08%
5	1%	20 °C / 1 hour	34%	90 °C / 30 min	23.40%
6	1%	90 °C / 1 hour	34%	90 °C / 30 min	21.77%
Extra	10% (milled ash)	90 °C / 1 hour	34%	90 °C / 30 min	88.21%

All the tests were done following the same procedure and using the apparatus shown in Figure 1. The parameters that changed during these tests are concentration of sodium hydroxide solution and temperature of caustic reaction. Test 1 will be taken as an example to describe the procedure of all the tests. Each test consists of two steps, caustic pretreatment and acid leaching. Specific procedures for this test are as follows:

Step 1 – Caustic pretreatment:

First, 250 mL of 10% sodium hydroxide solution was added to a 1000-mL round-bottom flask. After the solution reached the desired temperature, in this case 20 °C, 11 grams of unmilled PCC fly ash was added. The reaction was run for 1 hour using a stirring bar at a speed of 300 rpm. At the end of the reaction period, caustic solution was filtered using an EMD Millipore 142-mm Hazardous Waste Pressure Filter System with a 0.45-µm polypropylene filter. The ash remaining was washed further with DI water to get rid of any caustic solution absorbed by the ash. Then, the filter was dried for 15 minutes at 80 °C. The ash was then recovered for the acid leaching step. The ash recovered after filtration was about 10 g (about 1 g of ash was lost for each test).

Step 2 – Acid leaching:

Second, 250 mL of 34% nitric acid solution was added to a 1,000- mL round-bottom flask. After the solution reached the desired temperature, in this case 90 °C, the 10 g of ash remaining after the caustic pretreatment step was added. The reaction was run for 30 minutes using a stirring bar at a speed of 300 rpm. At the end of the reaction period, 10 mL of nitric acid solution was filtered using a polytetrafluoroethylene (PTFE) syringe filter. The 10 mL sample was sent for ICP-OES testing.

2.3 Product Roasting Testing

After pretreatment of fly ash, the REE was extracted with nitric acid solution. The acid digestion leads to formation of nitrate salts with the general molecule formula $M(NO_3)_x$, where $M(Al^{3+}$, Si^{2+}, Sc^{3+}, Eu^{3+}…) is the cation extracted from fly ash and X is the valence: +1 (for Na, K,..), +2 (Ca, Mg, Sr,..) and +3 (Ce, La, Cu, Fe, Al, Si,..). Figure 16 presents the structure of different possible extracted solutes.

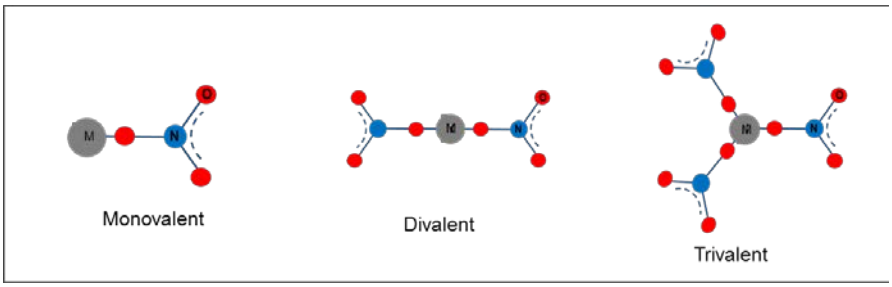

Figure 16: Structure of precursors extracted from fly ash by nitric acid leaching

The thermal decomposition of nitrate salts $M(NO_3)_x$ will lead to formation of metal oxides following the general reaction "1". Reactions 2 and 3 are respectively examples of decomposition for divalent and trivalent precursors.

$$2M(NO_3)_x \overset{Heat}{\Longrightarrow} M_2O_x + 2NO_2 + \frac{3x}{2}O_2 \qquad \text{Reaction 1}$$

$$2Ca(NO_3)_2 \overset{Heat}{\Longrightarrow} 2CaO + 4NO_2 + O_2 \qquad \text{Reaction 2}$$

$$4La(NO_3)_3 \overset{Heat}{\Longrightarrow} 2La_2O_3 + 12NO_2 + 3O_2 \qquad \text{Reaction 3}$$

The Thermal Decomposition (TD) of a nitrate can be initiated through cleavage of the N-O bond therefore, the TD temperature is proportional to the strength of the N-O bond. The nitrate anion has 24 valence electrons with a bond order of 4/3 (Yuvaraj, Fan-Yuan, Tsong-Huei, & Chuin-Tih, 2003). The bond energy can be decreased mainly through polarization of the electronic cloud of the nitrate ion by the high charge density of a metal ion. The polarization is initiated through the charge density (CD) of a metal ion, while the CD of a M ion is the ratio of its electronic charge (e) to its volume (v). Generally, the metal ion is assumed to be a sphere and its CD is given by the ratio $e/(v = (4/3)\pi r^3)$ where "r" is the radius (in nm) of a metal ion. Radius can be taken from Inorganic Chemistry: Principles of Structure and Reactivity (Huheey, 1978). Figure 17 presents the calculated charge density for selected elements. Based on charge density the decomposition temperature of nitrate precursors can be estimated in increasing order:

Al<Fe< Ce<Ca<Na

Shanmugam Yuvaraj, et al established the correlation between charge density and decomposition temperature of nitrate precursors. Their results confirm the above decomposition order, with iron and aluminum nitrate decomposing at 167°C follow by cerium at 300°C, calcium at 600°C and sodium at 750°C. Therefore, it should be possible to separate the REE from other metals by thermal decomposition. The goal of this testing is to evaluate this method.

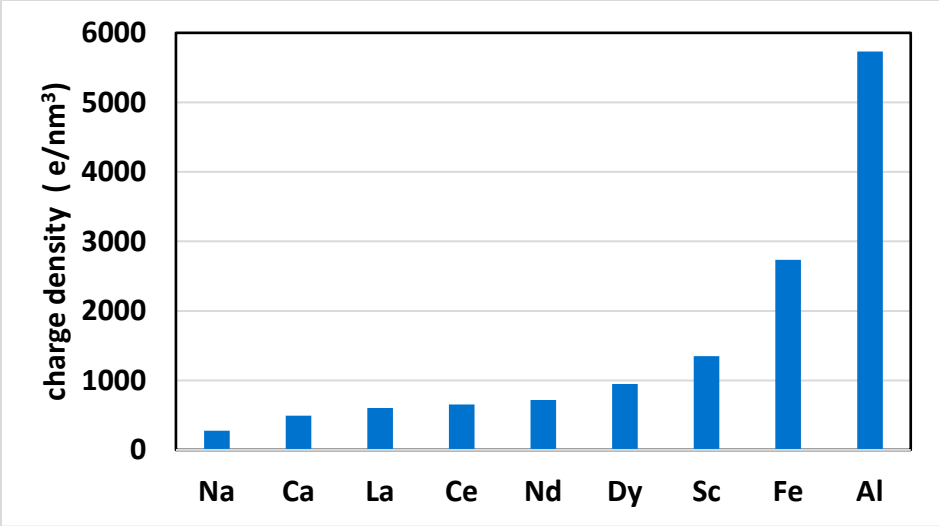

Figure 17: Calculated charge density for selected metal cations

In the first step, we performed analysis of fly ash by inductively couple plasma mass spectrometry (ICP-MS), with a lithium metaborate sinter digestion, to determine the most relevant elements and study the individual thermal decomposition of each nitrate salt independent of the other ones.

Table 8 reports the ICP-MS composition of a Pulverized Coal Combustion plant fly ash. Figure 17 presents the composition of the fly ash by groupings. Silicon and aluminum have a total concentration of ~68%, transition metals ~21% and alkaline and alkaline earths ~8%. The concentration of columns 13 through 15 in the periodic table is estimated to be 2%. REE+Y+Sc is around 0.13% and radioactive elements are less than 0.01%. The fly ash will be leached in nitric acid, therefore, we assumed that the dissolved elements are as nitrate salts.

Table 8: ICP-MS composition of fly ash

REE+Y+Sc	ppm	Transition metal	ppm	Column 13-17	ppm	Column 1 and 2	ppm	Al/Si	ppm	Radioactive	ppm
Lu	0.7	Co	41.3	As	156	Ba	1170	Al	130000	Th	22.5
Sc	36.9	Cr	210	B	90	Be	17	Si	209000	U	9.7
Ce	192	Cu	183	Ga	56.7	Cs	10				
Dy	18.5	Fe	106000	Ge	39.1	Li	170				
Er	10.3	Mn	258	Pb	96.7	Rb	116				
Eu	4.8	Mo	27	S	2500	Sr	878				
Gd	21.4	Nb	24	Sb	9	Mg	4700				
Ho	3.7	Ni	140	Se	10.6	Ca	13200				
La	85.5	Tl	6.3	Sn	5.5	K	17000				
Nd	92.6	V	247	Ta	1.8						
Pr	23.6	W	7	Ti	6700						
Sm	20.4	Zn	220								
Tb	3.5										
Tm	1.4										
Y	116										
Yb	8.6										

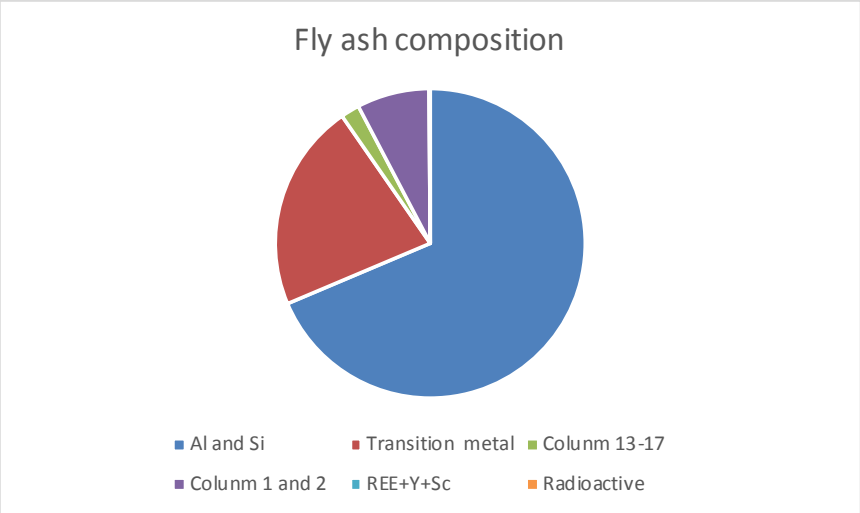

Figure 18: PCC fly ash elemental composition by groups

Based on the ICP-MS analysis of fly ash, we selected representative nitrate elements to briefly study independently their decomposition at different temperatures. Each selected element was dissolved in DI water, dried at temperature below 90 °C (to remove the water) then calcined in a box furnace. The calcined material is leached in DI water and inspected visually for solubility. Presence of residual solids indicated the decomposition of the selected element at the designated temperature. Table 9 reports the list of selected element precursors, their amount, corresponding element amount, and the quantity of water used for dissolution. All precursors are soluble in DI water and the concentration of each precursor is kept at 30%. Table 10 reports the decomposition temperature of each element. The experiment results are in good correlation with theoretical prediction (Figure 17).

Table 9: Selected nitrate compounds for thermal decomposition testing

Surrogate Compounds for Thermal Decomposition Testing			
Compound	Salt (g)	Metal (g)	DI water (g)
$NaNO_3$	1.00	0.271	3.3
$Al(NO_3)_3 \cdot 9H_2O$	1.00	0.072	3.3
$Ca(NO_3)_2 \cdot 4H_2O$	1.00	0.169	3.3
$Fe(NO_3)_3 \cdot 9H_2O$	1.00	0.138	3.3
$La(NO_3)_3 \cdot 6H_2O$	0.20	0.064	0.7
$Nd(NO_3)_3 \cdot 6H_2O$	0.20	0.066	0.7
$Dy(NO_3)_3 \cdot xH_2O$	0.20	0.093	0.7
$Sc(NO_3)_3 \cdot xH_2O$	0.10	0.019	0.3
$Ce(NO_3)_3 \cdot 6H_2O$	0.20	0.065	0.7

Table 10: Approximate thermal decomposition temperatures for selected nitrates

Compound	Approximate decomposition temperature range (°C)
$Fe(NO_3)_3$	100-150
$Al(NO_3)_3$	100-150
$Ce(NO_3)_3$	200-300
$Dy(NO_3)_3$	200-300
$Sc(NO_3)_3$	200-300
$Nd(NO_3)_3$	200-300
$La(NO_3)_3$	200-300
$Ca(NO_3)_2$	>450
$NaNO_3$	>450

Thermal decomposition was then performed on blended nitrate streams. Table 11 reports the selected precursors, the amount of each precursor, calculated amount of each element and the concentration of each element. The resulting mixture was dissolved in DI water under strong stirring to promote dissolution, then a heating lamp was used to evaporate water gently. During drying the temperature at solution surface was between 70 °C and 90 °C. After this step, the solid material was subject to cyclical treatments that consist of:

- dissolution in water,
- filtration dry under heating lamp, and,
- heat treatment in a box furnace at different temperatures.

Figure 19 illustrates the process used. Five samples were produced:

1. Blend of nitrates (Na, Al, Ca, Fe, Cs, and Nd) after drying the solution at 100 °C without filtration
2. Residual material from re-dissolved sample 1
3. Undissolved material after heat treatment at 300 °C
4. Undissolved material after heat treatment at 400 °C
5. Material that is soluble after heat treatment at 400 °C

Table 11: Model blended nitrate solution composition

Surrogate Nitrate Solution Composition			
Compound	Salt (g)	Metal (g)	Element (wt%)
$NaNO_3$	5.76	1.558	20
$Al(NO_3)_3 \cdot 9H_2O$	16.24	1.169	15
$Ca(NO_3)_2 \cdot 4H_2O$	11.50	1.948	25
$Fe(NO_3)_3 \cdot 9H_2O$	11.27	1.558	20
$La(NO_3)_3 \cdot 6H_2O$	1.21	0.390	5
$Nd(NO_3)_3 \cdot 6H_2O$	1.18	0.390	5
$Dy(NO_3)_3 \cdot xH_2O$	0.84	0.390	5
$Sc(NO_3)_3 \cdot xH_2O$	2.00	0.390	5
Total	50.00	7.791	100

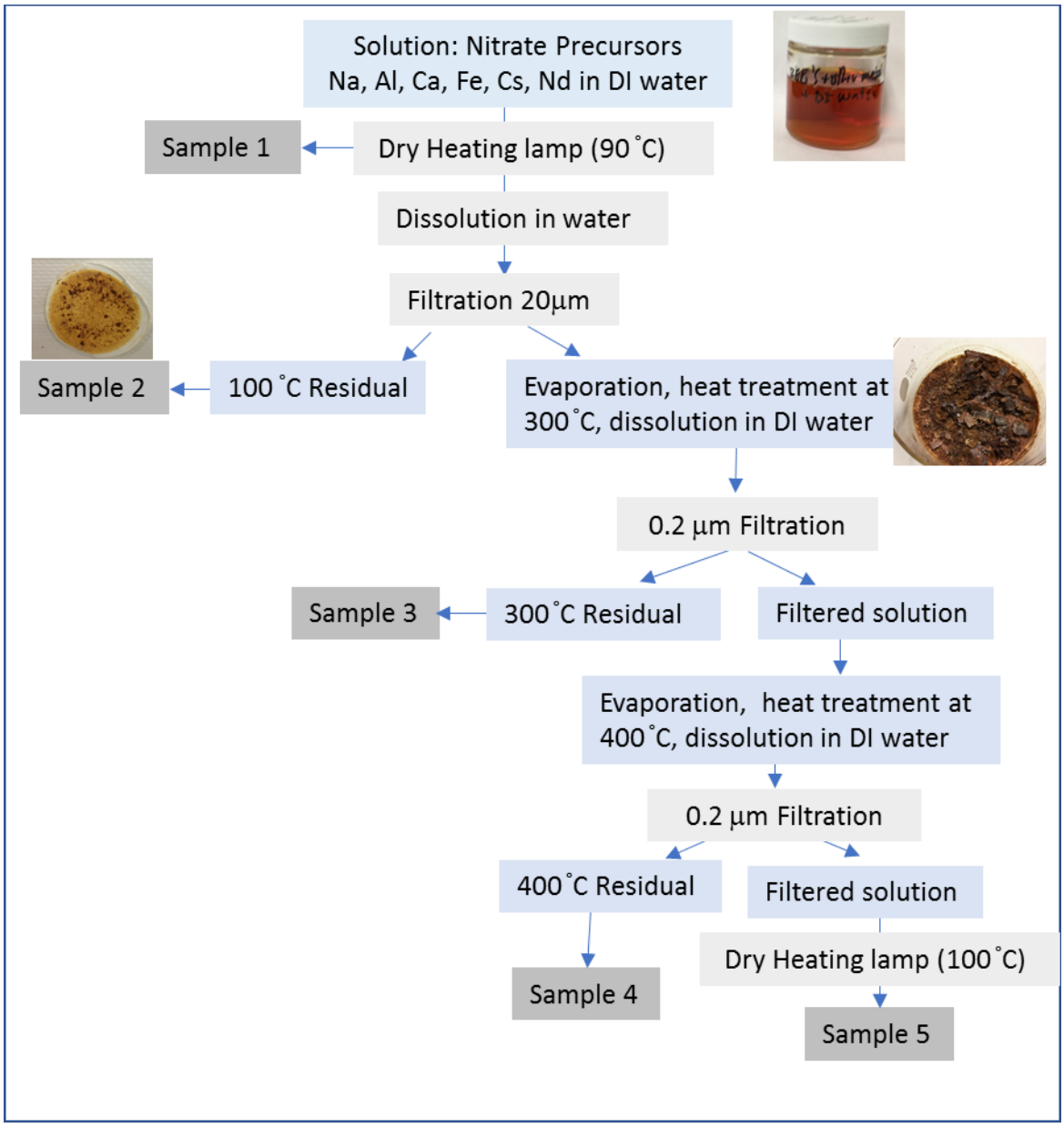

Figure 19: Process for thermal decomposition testing of the blended nitrate solution

Figure 20 displays the Differential Scanning Calorimetry (DSC) profile of the blend dried at 100 °C. For the test, 10 mg of sample was heated in air to 500 °C at 10°C/min. The profile shows at least three endothermic peaks at 136 °C, 160 °C and 220 °C. Figure 21 is DSC performed under nitrogen rather than in air. It also shows three endothermic peaks at 100 °C, 256 °C and 410 °C. These peaks may correspond to thermal decomposition of different salts and it suggests that roasting can be used to separates different elements, however DSC is not sensitive enough to allow distinction between separate decomposing compounds.

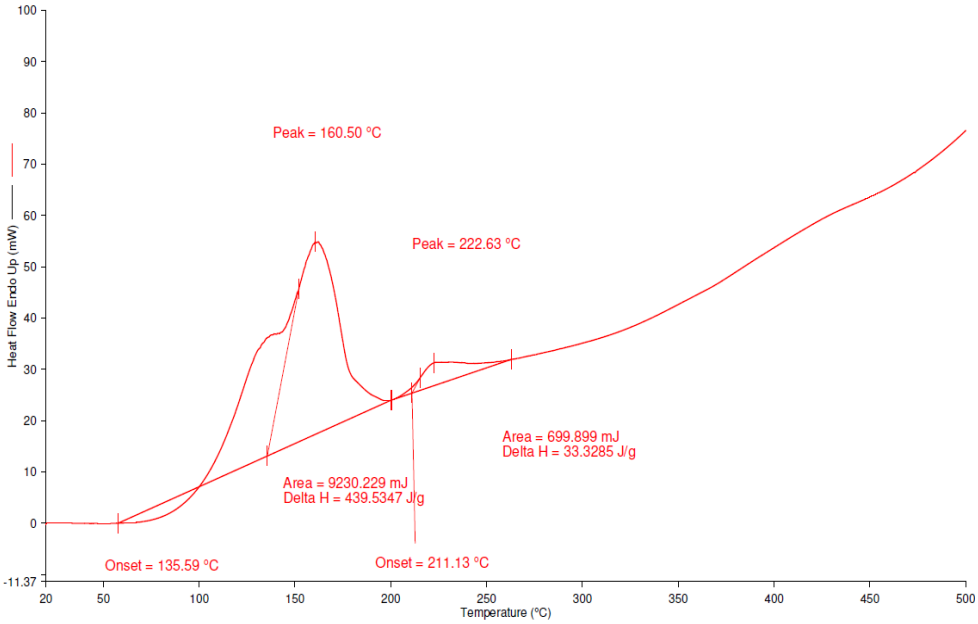

Figure 20: Differential Scanning Calorimetry results for the blended nitrate mixture in air

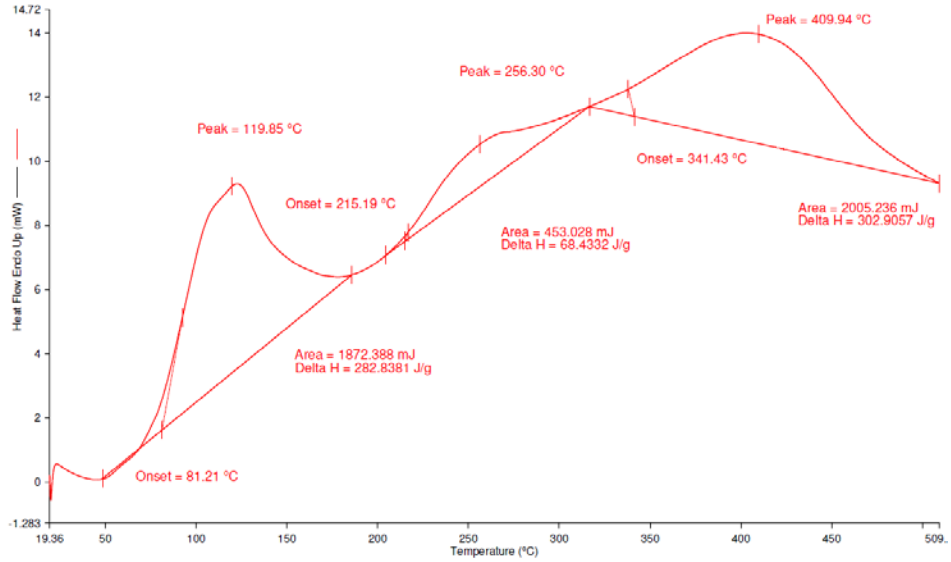

Figure 21: Differential Scanning Calorimetry results for the blended nitrate solution in nitrogen

Table 12 reports the Energy Dispersive Spectroscopy (EDS) analysis of the sample produced from the roasting process described in Figure 19. Iron and aluminum nitrates can decompose at temperature between 100 °C to 200 °C, REE nitrates decomposed at temperature between 300 °C and 400 °C and sodium and calcium nitrates require temperature above 400 °C to decompose. The order of decomposition is in good correlation with electronic charge density theory discussed earlier, and suggest that separation between iron, aluminum, and REE can be achieved by controlling the temperature of calcination of the dried nitrate solution.

Table 12: Energy Dispersive Spectroscopy analytical results for residues of blended nitrates after calcining at selected temperatures. Results are in molar percent, and highlighted cells indicate key components of each fraction.

EDS Analysis of Calcined Surrogate Solution					
Element	100 °C (no filtration)	100°C - 200°C	300°C	400°C (insoluble)	400°C (soluble)
Dy	1.5%	0.0%	10.1%	9.9%	0.1%
Al	7.0%	20.2%	24.2%	4.7%	0.1%
Sc	2.3%	4.6%	10.2%	0.2%	1.0%
La	2.1%	0.0%	2.0%	16.7%	1.1%
Nd	2.4%	0.0%	6.9%	39.7%	0.0%
Fe	10.6%	39.7%	8.1%	2.9%	0.0%
O	46.1%	32.5%	35.5%	21.0%	50.5%
N	11.2%	2.5%	1.9%	2.5%	15.9%
Na	7.4%	0.4%	0.6%	1.1%	3.6%
Ca	9.2%	0.0%	0.6%	1.3%	27.7%
Si	0.0%	0.1%	0.0%	0.0%	0.0%

Based on testing results from the model compounds, tests were performed on leachate from fly ash. One hundred (100) grams of fly ash was leached in nitric acid for 24 hours, then the slurry was filtered via 0.22-µm nylon filter. The fraction of dissolved material was 11.5% without any pretreatment of ash. This residual material was subject to several cycles of dissolution in DI water, filtration, drying and heat treatment at different temperatures. The goal is to collect the material that decomposed to an insoluble oxide following each heat treatment; however, the amount of material recovered on the filter was small and difficult to evaluate gravimetrically or by SEM analysis. Ultimately, the dissolved material obtained from acid leaching was treated at a single temperature of 200 °C.

Table 13 reports EDS results of material dissolved by acid leaching of fly ash. After acid leaching, the slurry was filtered through a 0.22-µm nylon filter, then the filtrate was dried at 100 °C. This last residual material was heat treated at 200 °C, re-leached in DI water and filtered through a 0.22-µm nylon filter. The residual material analysis is reported in the 200 °C column. The filtered solution was dried at 100 °C and the analysis is in column 200+ °C. This result shows that aluminum and iron can be separated from dissolved material by calcination at temperature between 100 °C and 200 °C. The other elements detectable by EDS remained water soluble. Energy Dispersive Spectroscopy was not sensitive enough to reliably detect the REE elements.

Table 13: EDS analysis of extracted material from fly ash digested in nitric acid, dried and calcined at the indicated temperatures. Values are in molar percent.

EDS of Calcined Fly Ash Leachate			
Element	100°C	200°C	200+ °C
Dy	0.0%	0.0%	0.0%
Al	7.9%	25.5%	1.9%
Sc	0.0%	0.0%	0.3%
Mg	0.2%	0.1%	2.4%
Fe	43.3%	25.1%	0.0%
Si	0.9%	0.1%	0.1%
S	4.2%	2.7%	0.1%
K	0.4%	0.3%	8.0%
Ca	1.0%	0.1%	19.8%
Na	1.6%	0.9%	3.6%
Ti	2.2%	0.9%	0.0%
La	0.0%	0.2%	0.0%
Nd	0.0%	0.0%	0.0%
N	3.8%	2.1%	13.4%
O	34.6%	41.9%	50.5%

Due to low resolution of EDS for trace elements, the solids and water leach solutions were also analyzed by ICP-MS after treatment at 200 °C. Figure 22 and Figure 23 report the % distribution of each element in the two fractions. The distribution of element “E” is calculated as follow:

- % (E) in residual material = $\frac{mass(E) in\ residual}{mass\ (E)\ in\ reisual + mass\ of\ (E)\ in\ solution} * 100$
- % (E) in solution = 100-%(E) in residual

Figure 22 suggests that most of the REE nitrates produced by leaching of fly ash in nitric acid solution are not decomposed to oxides after 200 °C heat treatment. However, most of the aluminum and iron decomposed to oxides therefore they can be separated from the REE. This result is in good correlation with charge density theory. Around 70% of scandium is converted to oxide at 200 °C, and it is anticipated that additional scandium can be recovered at a lower roasting temperature.

Figure 23 shows the % distribution for the other elements between the water leach and residual solids. It illustrates that most of the titanium, vanadium, chromium, niobium, molybdenum, indium, tin, tungsten, and antimony nitrates decompose to insoluble oxide therefore can separated from REE. Other elements such as manganese, gallium, lead, and decomposed partially to insoluble oxides. These preliminary results show that roasting can be used to separate REE from other elements. More work is required to optimize the process temperature and recover additional scandium.

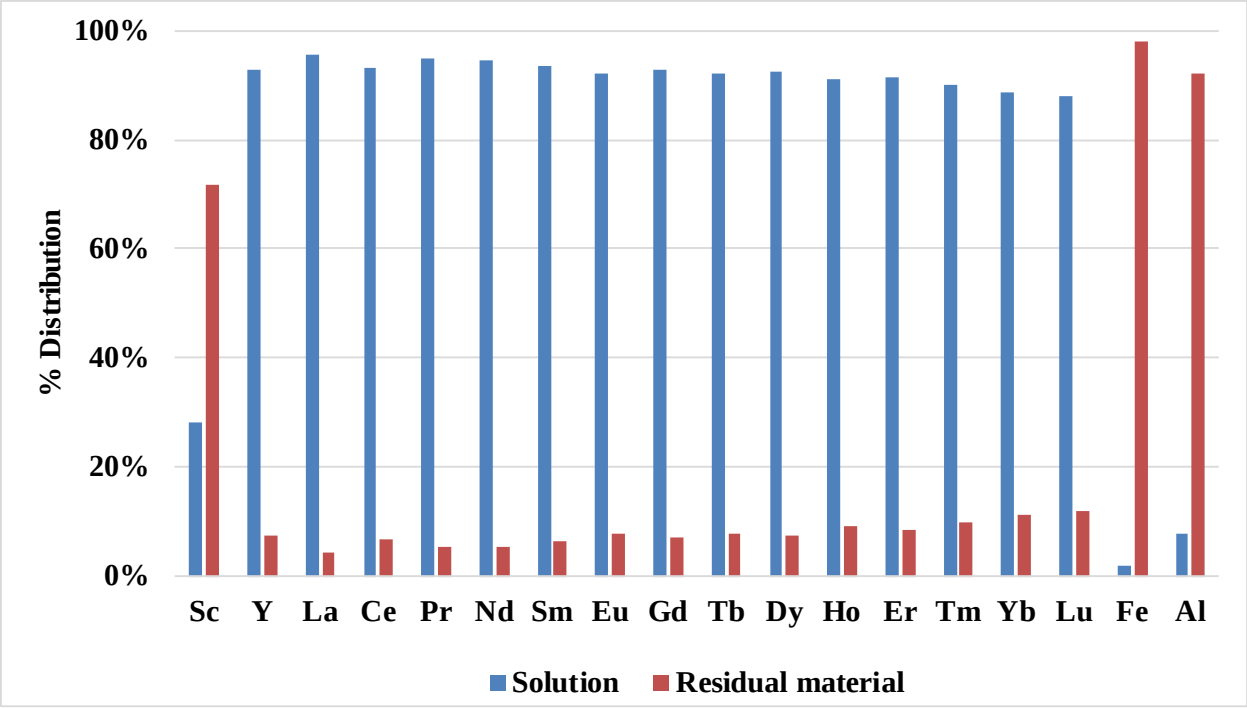

Figure 22: Distribution of REE+Y+Sc in solution and in residual material after treatment at 200 °C and then leaching with DI water. Recovery of REE+Y was high in the water wash, while iron, aluminum, and scandium were preferentially found in the solid residual material.

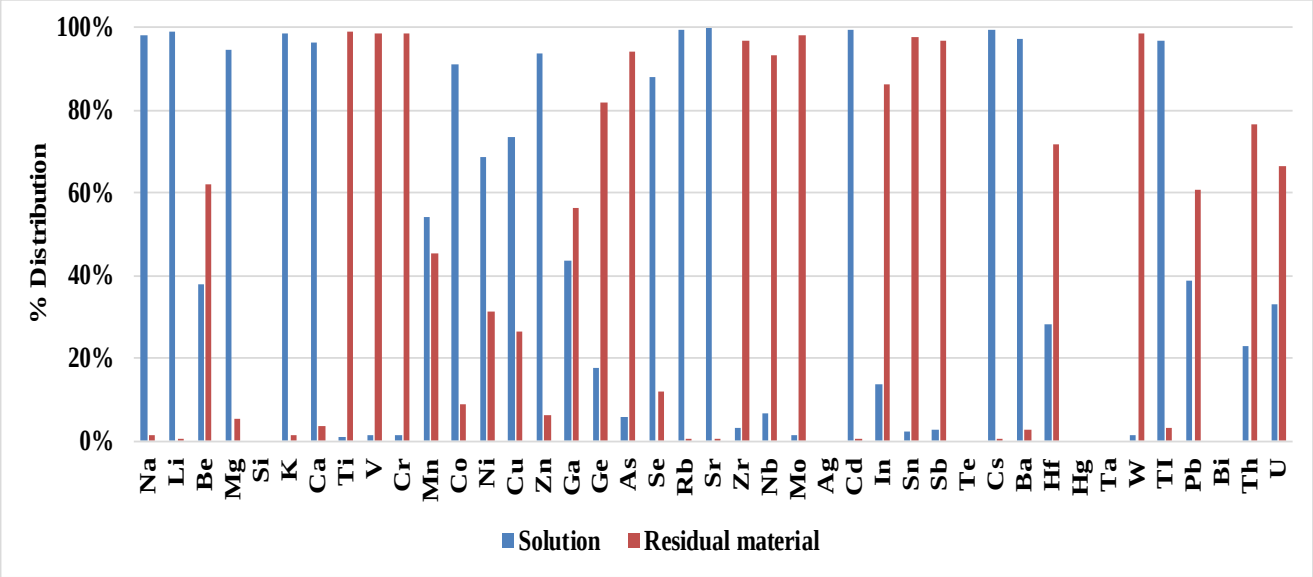

Figure 23: Distribution of other elements in solution and in residual material after treatment at 200 °C and then leaching with DI water.

Table 14 summarizes the total REE distribution in the solution and the residual solid material. Total REE represents 1.2 wt% of the elements detected by ICP-MS analysis in the aqueous solution, suggesting nearly a 1.2 wt% purity on a solid basis. This is over a 20x increase in REE purity over the fly ash starting material with a concentration of approximately 545 ppm REE. Recovery of total REE was 90% across the roasting process.

Table 14: Weight percent total REE in solution and remaining in the residual solids, indicating good separation by thermal roasting of the leach solution.

REE Recovery in DI Leaching Fractions		
	Solution	Residual material
Total REE + Sc + Y	90.0%	10.0%
REE+Y+Sc out of total measured	1.20%	0.10%

2.4 Solvent Extraction Testing

In order to upgrade the rare earth element concentration after leaching, solvent extraction will be used for removal of monovalent and divalent cations along with select transition metals. The preliminary laboratory tests were run to investigate the concentration of rare earth elements that can be achieved. Two sets of tests were run:

1. Extraction of rare earth elements from rare earth loaded leach solution at different pHs.
2. Stripping of rare earth elements using different acids and concentrations for the stripping solution.

CYANEX 572 was used for extraction experiments. CYANEX 572 is a phosphorus-based chelating extractant formulated for the extraction and purification of rare earth elements. It has an extraction strength profile which allows efficient extraction of the heavy rare earth elements while allowing the back extraction / stripping operation to utilize lower strip acid concentrations (Cytec, 2017). The concentration used for the extraction testing was 15% CYANEX 572 in Solvent 467 diluent.

2.4.1 Rare Earth Extraction

Before starting the extraction testing, a solution loaded with rare earth elements was made by leaching 98 grams of PCC Fly Ash with 500 mL of 34% nitric acid at room temperature for 24 hours. For this leaching experiment, a 1 liter beaker with a stirring bar was used. Mixing speed was 450 rpm. After 24 hours, the reaction was stopped, and the solution was filtered using pressure filter system with a 0.45 µm polypropylene filter. The ash was disposed in a low pH waste container, and acid solution was dried using a heating lap (about 150 °C). Dry material was leached in DI water (250 mL). Not all the recovered solids are soluble, as iron in particular is converted to an oxide; therefore, the solution was filtered using a 0.22-µm Magna Nylon filter. The residual material and solution were sent for ICP-MS analysis.

From roasting experiments explained earlier in this report, iron nitrate would calcine at 100 °C-200 °C. Therefore, the material recovered should be rich in iron, which is an undesirable species for extraction processes. It is ideal to remove all the iron before extraction testing. The pH of the solution recovered after filtration was 3.34. This was the solution loaded with rare earth elements used for the first portion of extraction experiments.

Nitric acid at 20% and sodium carbonate at 15% were used to adjust the pH of the starting loaded solution. Table 15 contains the descriptions of the tests performed:

Table 15 - Solvent extraction at different pH testing conditions

Solvent Extraction Test Conditions and Observations			
Test	Adjusted pH	pH Adjusting Solution used	Precipitate formed
1	1	20% nitric acid	No
2	2	20% nitric acid	No
3	2.5	20% nitric acid	No
4 (starting solution)	3.34	NA	NA
5	4	15% sodium carbonate	Yes
6	4.5	15% sodium carbonate	Yes
7	5	15% sodium carbonate	Yes

For each test the following procedure was executed:

1. After pH adjustment in tests 5, 6, and 7, a precipitate was formed. Therefore, the solutions were filtered prior to starting extraction testing. A 0.22-µm Magna Nylon filter was used for filtration. Part of the solution recovered was sent for ICP-MS analysis, and 15 mL was used for extraction testing.
2. 25 mL (15 mL for test 5, 6, and 7) of starting solution was adjusted to the desired pH using the appropriate solution.
3. 6 g (2.5 g for test 5, 6 and 7) of 15% CYNEX 572 was added to the adjusted solution.
4. Two phases were present (organic and aqueous). They were well mixed for 30 minutes at 2400 rpm with an overhead mixer.
5. Using a 60-mL separatory funnel, the aqueous phase was separated from the organic phase. The aqueous solution was sent for ICP-MS analysis.

2.4.2 Extraction Results

As described above, leaching and roasting tests were performed to make a solution loaded with rare earth elements for extraction testing. After acid leaching, acid solution was dried using a heating lap (about 150 °C). Then, dry material was leached in DI water (250 mL). Table 16 shows the percent recovery after DI water leaching. Residual material is the solid material that didn't dissolve after DI water leaching. Loaded solution is the solution used for extraction testing. From these results, it can be concluded that the residual material is rich in iron as was predicted and observed in the roasting experiments.

Table 16 – Percent recoveries of rare earth elements, iron, alumina, and silica after DI water leaching of dry material at 150 °C. Also, purity or selectivity of rare earth elements calculated as a percent of measured solutes as stated.

Species	% Recovery	
	Loaded Solution	Residual material
Sc	43.4%	56.63%
Y	86.7%	13.32%
La	84.7%	15.31%
Ce	77.8%	22.17%
Pr	87.2%	12.78%
Nd	88.3%	11.69%
Sm	87.4%	12.62%
Eu	87.9%	12.11%
Gd	88.0%	11.99%
Tb	86.2%	13.79%
Dy	86.7%	13.28%
Ho	87.2%	12.78%
Er	87.5%	12.50%
Tm	85.6%	14.40%
Yb	83.9%	16.08%
Lu	82.0%	18.02%
Fe	1.9%	98.09%
Al	28.4%	71.61%
Si	25.3%	74.69%
REE+Y+Sc out of total REE+Y+Sc Available	80.5%	19.46%
REE+Y+Sc out of total measured species (purity or selectivity)[1]	0.49%	0.08%

[1]*See Appendix B for additional calculations and other species analyses*

For extraction testing, the loaded solution was adjusted to different pHs (See Table 15). Then, extraction tests were performed following the procedure described in Section 2.4.1. Some key points should be explained regarding the analysis of these results. For the calculation of percent recovery in the extractant (organic phase), a mass balance was performed using the results from ICP-MS analysis done on the aqueous phase after extraction and the solution loaded from leaching and roasting runs. Also, a negative mass in extractant was calculated for some species due to analytical error, so any negative mass calculated was assumed to be zero. Furthermore, some results obtained from ICP-MS analysis were below detection limits. Consequently, calculations were performed using the given detection limit (See Appendix B). Table 17 shows the percent recoveries of rare earth elements and other species in the extractant after extraction of the solution at different pH. Also, this table shows the purity or selectivity at different pH.

Table 17 - Percent recoveries of rare earth elements, iron, alumina, and silica after extraction at different pH. Also, purity or selectivity of rare earth calculated as a percent of measured solutes.

Species	% Recovery						
	pH 1.03	pH 2.04	pH 2.51	pH 3.34	pH 4.01	pH 4.48	pH 4.99
Sc	60.0%	90.00%	90.00%	50.00%	98.00%	60.00%	98.00%
Y	68.4%	99.79%	99.78%	99.78%	99.88%	99.98%	100.00%
La	0.0%	0.00%	0.00%	0.00%	72.02%	86.86%	98.28%
Ce	0.0%	11.75%	7.43%	23.74%	95.23%	98.62%	99.90%
Pr	0.0%	2.39%	5.41%	44.90%	97.20%	99.25%	99.95%
Nd	0.0%	14.09%	18.21%	61.51%	98.12%	99.47%	99.97%
Sm	0.0%	79.28%	82.87%	95.43%	99.70%	99.89%	100.00%
Eu	0.0%	91.43%	92.91%	98.15%	99.81%	99.80%	99.99%
Gd	0.0%	92.40%	94.07%	97.68%	99.77%	99.93%	100.00%
Tb	0.0%	98.09%	98.27%	99.08%	99.83%	99.69%	99.98%
Dy	31.2%	99.49%	99.57%	99.67%	99.89%	99.95%	100.00%
Ho	51.4%	99.73%	99.74%	99.70%	99.90%	99.76%	99.99%
Er	74.4%	99.58%	99.60%	99.67%	99.90%	99.91%	100.00%
Tm	91.5%	99.83%	99.83%	99.15%	99.90%	99.32%	99.97%
Yb	97.2%	99.95%	99.95%	99.85%	99.91%	99.88%	99.99%
Lu	97.4%	99.77%	99.77%	98.84%	99.88%	99.07%	99.95%
Fe	89.6%	97.39%	97.39%	86.95%	99.48%	89.56%	99.48%
Al	7.1%	0.00%	0.00%	0.80%	98.80%	99.47%	99.97%
Si	60.0%	90.00%	90.00%	50.00%	98.00%	60.00%	98.00%
REE+Y+Sc out of total REE+Y+Sc Available	24.4%	50.88%	50.90%	60.98%	95.14%	95.93%	99.66%
REE+Y+Sc out of total measured species (purity or selectivity)[1]	1.37%	4.18%	4.19%	7.15%	0.88%	1.04%	1.04%
REE+Y+Sc out of total measured species excluding Silica (purity or selectivity)[1]	2.11%	18.45%	18.76%	18.51%	0.97%	1.12%	1.17%

[1]*See Appendix B for additional calculations and other species analyses*

The highest purity or selectivity of rare earth elements was achieved when extraction was performed at pH of 3.34. Purity at this pH was 7.15%, and recovery was 60.98% as shown in Table 17. The recovery was lower compared to the recovery at higher pH (4.01, 4.48, and 4.99). Even though at higher pH the recovery was better, selectivity was lower because at higher pH, other species would extract stronger as well. Also, a selectivity calculation excluding silica was done since detection limits for silica were very high (between 4,000 and 200,000 µg/L), and solubility of silica in the nitric acid leach solution is expected to be very low.

2.4.3 Stripping Tests

To generated the REE-loaded solution, 400 grams of PCC fly ash were pretreated with 4 liters of 10% sodium hydroxide solution at 90 °C and for one hour. A 5-liter round-bottom flask and overhead mixer at 700 rpm were used for the reaction. After the reaction was finished, the solution was filtered through a 0.45-µm polyvinylidene fluoride (PVDF) filter. Ash was recovered and washed in a 5-liter round-bottom flask with 4 liters of DI water for 5 minutes. This process was repeated until the pH of the solution dropped to pH 10 (three washes were performed). Ash was recovered after the washing step, and it was dried in an oven at 110 °C for 24 hours. The ash recovered was 356.9 grams.

Using the pretreated ash, three leaching runs with 34% nitric acid were performed. In the first run, 120 grams of pretreated ash was used in 800 mL of 34% nitric acid. Since there were mixing problems with this run, 80 grams of pretreated ash was used instead for the following two runs. The set up and apparatus from Figure 1 were used for these acid leaching runs. The procedure for each run was the following:

- 800 mL of 34% nitric acid was added to a 1 liter round bottom flask.
- The acid was heated to 90 °C, and 120 g (or 80 g) of ash was added.
- Using a stirring bar, the reaction was run for 30 minutes at a stirring speed of 800 rpm.
- After reaction, the solution was filtered through a 0.45 µm PVDF filter. All the solution recovered from the three runs was combined, and three samples of the combined solution were sent for ICP-MS analysis. About 1.5 liters of the acid solution was recovered.

The solution recovered was neutralized using 10% sodium carbonate in the following manner:

- After adding 1.7 liters of 10% sodium carbonate pH test strips showed a pH of 0.
- Due to slow neutralization progress, 15% sodium carbonate was made. 500 mL was added, but pH test strip still showed a pH 0. Three samples were sent for ICP-MS analysis.
- To reduce the volume needed of 15% sodium carbonate to reached the targeted pH, 1,000 mL of solution after Step b was used for neutralization. 300 mL of 15% sodium carbonate was added. pH test strips showed a pH of 1.
- 400 mL of solution at pH 1 was taken and 145 mL of 15% sodium carbonate was added. pH 2.5 was shown using pH test strips. The solution was red (Figure 25) likely due to high iron concentrations. Three samples were sent for ICP-MS analysis.
- 400 mL of solution at pH 1 was taken and 130 mL of 15% sodium carbonate was added. pH 1.5 was shown using pH test strips. This solution was light yellow (Figure 24). Three samples were sent for ICP-MS analysis.

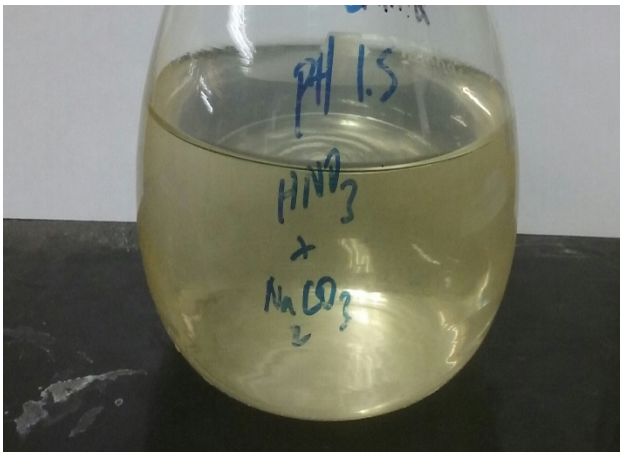

Figure 25 - Solution after neutralization pH 1.5

Figure 24 - Solution after neutralization pH 2.5

There were two sets of stripping experiments. For set one, the solution at pH 2.5 was used (See Table 18), and for set two, the solution of pH 1.5 was used (See Table 19).

Set 1:

- Starting with the solution of pH 2.5 (2.28 by pH probe), 300 mL of solution and 150 mL of 15% CYANEX 572 (2:1 organic : aqueous ratio) was added to a 600 mL beaker. It was mixed at 1,600 to 1,800 rpm for 30 minutes.
- Organic phase was separated from aqueous phase using a 1 liter separatory funnel.
- The pH of the aqueous solution after extraction was 1.9 using pH test strips (1.6 by pH probe). Three samples from the aqueous phase were sent for ICP-MS analysis, and the organic phase was recovered for stripping tests.

Table 18 - Stripping tests conditions for Set 1

Stripping Test Conditions for Set 1		
Test	Stripping solution used	After stripping aqueous phase pH (pH strip / pH probe)
1	pH 3	2.2 / 2.41
2	pH 2.5	1.9 / 2.14
3	pH 2	1.6 / 2.05
4	pH 1.5	1.6 / 1.76
5	pH 1	1.3 / 1.45
6	pH 0	0.5 / 0.94

Each of the tests in Set 1 followed this procedure:

- 20 mL of organic recovered after extraction and 60 mL of stripping solution were added to a 200 mL flask.
- The solution was mixed at 1,600 – 1,800 rpm for 30 minutes.
- The organic and aqueous phases were separated using a 100 mL separatory funnel.
- pH of aqueous solution was measured using pH test strips and a pH probe (Table 18).
- An 11-mLmL sample of the stripping solution was sent for ICP-MS analysis.

Set 2:

- Starting with the pH 1.5 solution (1.27 by pH probe), 360 mL of solution and 180 mL of 15% CYANEX 572 (2:1 organic : aqueous ratio) was added to a 600 mL beaker. It was mixed at 1,600 to 1,800 rpm for 30 minutes.
- After mixing, a white rag layer was formed at the interface. It was therefore left for a day so the layer would settle.
- The organic phase was separated from the aqueous phase using a 1 liter separatory funnel, retaining the rag layer with the organic phase.
- The pH of the aqueous solution after extraction was 1.0 using pH test strips (0.9 by pH probe). Three samples from the aqueous phase were sent for ICP-MS analysis, and the organic phase was well mixed with the white rag layer and recovered for stripping tests.

Table 19 - Stripping tests conditions for Set 2

Stripping Test Conditions for Set 2			
Test	Stripping solution used	Stripping solution preparation	
1	3 M hydrochloric acid (HCl)	37.2% HCl = 29.4 g DI water = 75.1 g	~100 mL of solution
2	5%:5% HCl:Oxalic acid	37.2% HCl = 13.4 g 99.5% oxalic acid = 5.1g DI water = 81.6 g	~100 mL of solution
3	5%:5% Nitric acid (HNO_3):Phosphoric acid (H_3PO_4)	68% HNO3 = 7.4 g 85% H2PO4 = 5 g DI water = 86.8 g	~100 mL of solution
4	10% Sulfuric acid (H_2SO_4)	96.3% H2SO4 = 10.4 g DI water = 89.6 g	~100 mL of solution
5	1 M HCl	37.2% HCl = 12.3 g DI water = 114.4 g	~125 mL of solution
6	1 M HCl (1 mL of 40 % of sodium metabisulfite added)	37.2% HCl = 12.3 g DI water = 114.4 g	~125 mL of solution
7	2 M HCl	37.2% HCl = 49.0 g DI water = 203.0 g	~250 mL of solution
8	10% sodium hydroxide (NaOH) (using organic after 2 M HCl stripping)	NaOH = 10.0 g DI water = 90.0 g	~100 mL of solution
9	10% sodium carbonate (Na_2CO_3) (using organic after 2M HCl stripping)	Na_2CO_3 = 10.0 g DI water = 90.0 g	~100 mL of solution

The procedure for Set 2, Test 1 through Test 4 was as follows:

1. 20 mL of organic recovered after extraction and 60 mL of stripping solution were added to a 200 mL flask
2. The solution was mixed at 1,600 – 1,800 rpm for 30 minutes
3. Organic and aqueous phases were separated using a 100 mL separatory funnel
4. An 11 mL sample of aqueous was sent for ICP-MS analysis.

The procedure for Test 5 and 6 was as follows:

1. 20 mL of organic recovered after extraction and 60 mL of stripping solution were added to two 200 mL flasks
2. The solutions were mixed at 1,600 – 1,800 rpm for 30 minutes
3. For one of the two solutions, 1 mL of 40 % of sodium metabisulfite was added
4. Both solutions were mixed again at 1,600 – 1,800 rpm for 30 minutes
5. Organic and aqueous phases were separated using a 100 mL separatory funnel
6. Two 11 mL samples (one for each test) were sent for ICP-MS analysis.

The procedure for Test 7 was as follows:

1. 20 mL of organic recovered after extraction and 60 mL of stripping solution were added to two 200 mL flasks
2. The solutions were mixed at 1,600 to 1,800 rpm for 30 minutes
3. After mixing, both solutions were combined. Then, organic and aqueous phases were separated using a 500 mL separation funnel. The organic layer was saved for Test 8 and 9
4. An 11 mL sample of aqueous was sent for ICP-MS analysis

The procedure for Tests 8 and 9 was as follows:

1. Two separate solutions were prepared; one with 20 mL of organic recovered from Test 7 and 60 mL of 10% sodium hydroxide (NaOH), and another one with 20 mL of organic recovered from test 7 and 60 mL of 10% sodium carbonate (Na_2CO_3)
2. Before mixing, a precipitate was formed in both solution. The precipitate is orange in solution containing 10% NaOH and white in the solution containing 10% Na_2CO_3 (See Figure 26).

Figure 26 - Before mixing A) solution containing 10% NaOH. B) solution containing 10% Na_2CO_3

3. After mixing for 30 minutes at 1,600 to 1,800 rpm, it appeared that both solutions have three phases (2 organic, 1 aqueous). Also, at the interface of the organic layer with the aqueous phase, a precipitate can still be seen (See Figure 27).
4. Organic and aqueous phase were separated from each solution, and a 11 mL sample of aqueous from each solution was sent for ICP-MS analysis.

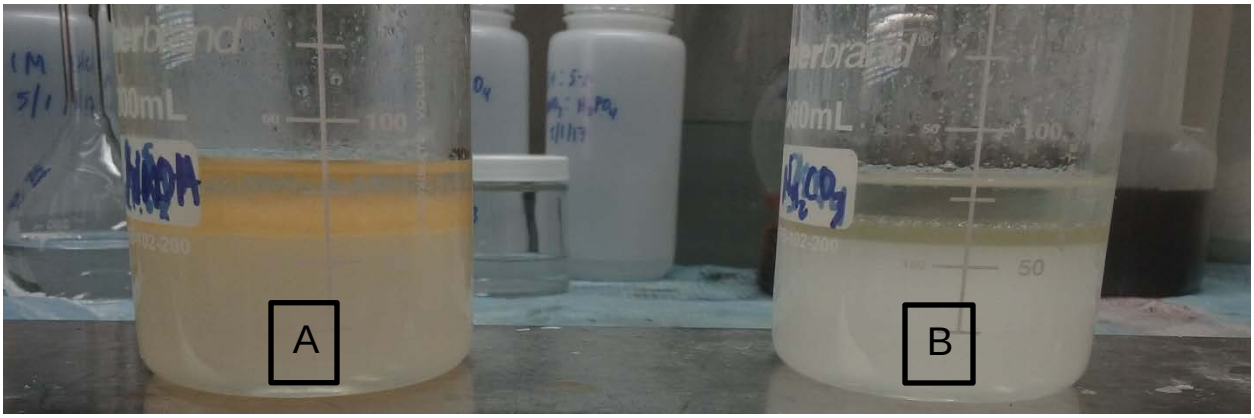

Figure 27 - After mixing A) solution containing 10% NaOH. B) solution containing 10% Na_2CO_3

5. After the organic was recovered, two organic phases could be seen in each sample (See Figure 28).

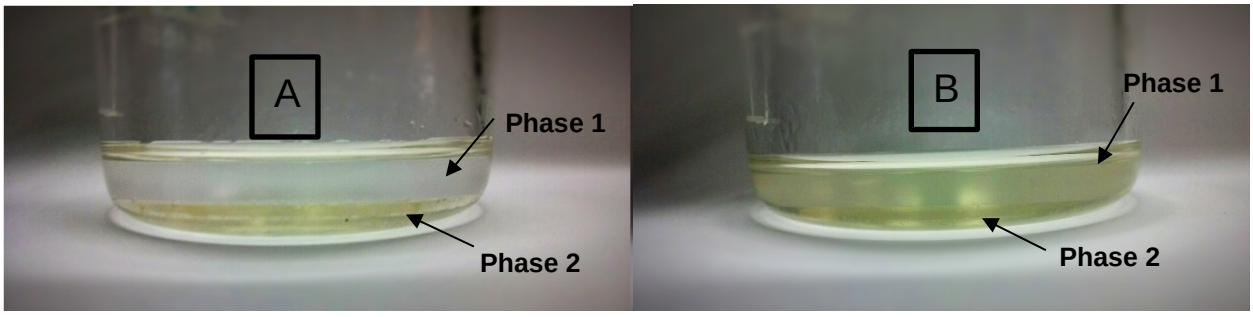

Figure 28 – Two organic phases recovered A) solution containing 10% NaOH. B) solution containing 10% Na_2CO_3

6. 40 mL of 1 M HCl were mixed at 1,600 – 1,800 rpm with the two organic phases recovered from each sample. Acid was added with the intent of recombining the two

organic phases (See Figure 29), and it appears that acidification restores miscibility of the extractant phase, as seen in Figure 29.

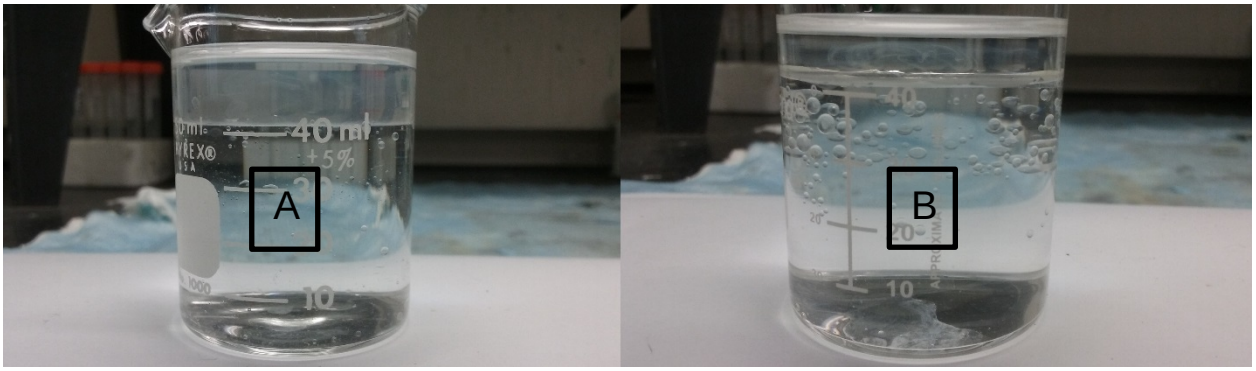

Figure 29 – After addition (HCl) and mixing A) solution containing 10% NaOH. B) solution containing 10% Na_2CO_3

2.4.4 Stripping Results

The percent of each element stripped from the loaded extractant was calculated by mass balance for each of the conditions tested. In the first batch of tests where the extractant was loaded at pH 2.5, stripping was done with hydrochloric acid adjusted to pH levels measured by pH strips. The results are shown in Table 20. Results for scandium were below detection limits and could not be accurately calculated. The results suggest that most of the REE can be stripped at pH 1.0, and at high recoveries at pH 0.5. However, at pH 0.5 there will likely be contamination from iron and aluminum that are not removed in the roasting step. Thorium and Uranium can be excluded from the REE strip solution at pH 0.5. Strippability appears to decrease as the atomic number of the REE increases, with exception of yttrium, which behaves more similarly to the heavier rare earth elements.

Table 21 contains results for stripping done in various high strength acid mixtures. These tests were intended to remove challenging elements such as iron, scandium, uranium, and thorium. Scandium analytical results were generally below detection limits, and the mass balance could not be completed accurately. Sodium metabisulfite addition did not appear to help in stripping. Stripping for many metals appears to decrease from two to three molar hydrochloric acid solution, suggesting a change in the form of the ions. Uranium was not strongly stripped in any of the solutions, but thorium was in the hydrochloric/oxalic acid solution. Stripping in a basic solution of 10% sodium hydroxide or sodium carbonate removed 57% and 50% of the uranium, respectively, and may be used to scrub uranium from the extractant.

Table 20: Percent stripped results of key elements in hydrochloric acid solutions at different starting pH.

Percent Stripped for Key Elements at Different pH Levels						
Species	**pH 3.0**	**pH 2.5**	**pH 2.0**	**pH 1.6**	**pH 1.0**	**pH 0.5**
Sc	N/A	N/A	N/A	N/A	N/A	N/A
Y	0.0%	0.3%	0.1%	0.9%	23.0%	81.6%
La	19.4%	52.9%	81.0%	41.3%	38.0%	39.7%
Ce	5.0%	38.5%	83.9%	79.9%	82.1%	85.0%
Pr	2.8%	25.5%	80.0%	83.0%	86.8%	88.9%
Nd	1.7%	18.3%	72.6%	84.4%	89.0%	91.5%
Sm	0.1%	1.0%	18.7%	68.7%	93.0%	95.6%
Eu	0.2%	0.4%	8.7%	52.7%	88.7%	97.9%
Gd	0.1%	0.4%	6.5%	42.9%	89.2%	97.1%
Tb	0.2%	0.2%	1.3%	11.8%	72.0%	96.4%
Dy	0.0%	0.2%	0.4%	4.5%	50.6%	94.8%
Ho	0.2%	0.3%	0.2%	2.1%	35.8%	92.8%
Er	0.1%	0.4%	0.2%	0.6%	18.5%	88.9%
Tm	0.5%	0.6%	0.5%	0.5%	6.8%	77.0%
Yb	0.1%	0.7%	0.1%	0.2%	2.5%	58.5%
Lu	0.6%	0.7%	0.6%	0.6%	1.8%	41.3%
Fe	0.8%	2.5%	0.8%	0.8%	0.9%	71.4%
Al	0.4%	5.9%	17.6%	4.1%	6.8%	10.5%
Th	1.2%	1.6%	0.4%	0.7%	0.0%	0.0%
U	0.1%	0.1%	0.1%	0.1%	0.0%	0.0%

Table 21: Percent stripped results of key elements in various high strength acid solutions.

Percent Stripped for Key Elements in Different Stripping Solutions							
Species	**1 M HCl**	**1 M HCl + Sodium metabisulfite**	**2 M HCl**	**3 M HCl**	**5%:5% HCl:Oxalic acid**	**5%:5% HNO_3:H_3PO_4**	**10% H_2SO_4**
Sc	N/A	N/A	N/A	N/A	N/A	N/A	N/A
Y	84.7%	77.0%	88.2%	84.4%	88.9%	88.8%	85.2%
La **Ce** **Pr** **Nd** **Sm**	Were not Extracted into the Organic Phase						
Eu	100.0%	100.0%	100.0%	100.0%	100.0%	100.0%	100.0%
Gd	100.0%	100.0%	100.0%	100.0%	100.0%	100.0%	100.0%
Tb	100.0%	93.3%	100.0%	100.0%	100.0%	100.0%	100.0%
Dy	98.7%	88.9%	100.0%	97.4%	100.0%	100.0%	99.9%
Ho	93.6%	83.7%	97.8%	92.4%	100.0%	99.1%	93.6%
Er	91.3%	81.2%	94.8%	92.0%	96.8%	95.6%	89.5%
Tm	91.0%	81.4%	96.2%	93.9%	95.6%	93.3%	88.1%
Yb	89.2%	78.3%	97.0%	94.4%	98.8%	87.5%	90.1%
Lu	83.1%	71.7%	93.1%	90.3%	93.6%	76.5%	85.4%
Fe	69.6%	59.4%	93.6%	93.9%	90.7%	93.2%	84.4%
Al	81.5%	74.7%	85.0%	47.3%	100.0%	100.0%	100.0%
Th	0.2%	0.2%	0.7%	5.1%	84.3%	17.8%	47.7%
U	0.5%	0.4%	1.8%	4.6%	2.9%	3.8%	4.2%

2.5 Aluminosilicate Byproduct Testing

Based on extractability testing, the process for REE extraction from fly ash will include milling, caustic leaching, then acid leaching. To offset the cost of caustic pretreatment, we investigated the possibility of generating an aluminosilicate byproduct from the loaded caustic leach solution. In this testing, we demonstrated that it is possible to recover silicon and aluminum from caustic solution. Three hundred (300) grams of fly ash were ball milled, dried under a heating lamp, then digested in 3.8 L of 10% NaOH solution (2.5 M). The slurry was filtered through a 0.22-µm nylon filter. Two hundred and twenty (220) grams of filtrate was titrated with 34% nitric acid (8.1 M) to drop the pH from greater than 14 to 10. The titration was done slowly and it took more than 4 hours. After titration, the slurry was filtered through a 0.22-µm nylon filter. The residual material washed with DI water until the pH of water dropped to 7. Figure 30 is a photo of the residual material, which is a white powder. The EDS analysis is reported in Figure 30: Photo of residual material obtained from titration of the caustic leach solution

Table 22. The material is composed mainly of alumina, silica, sodium and oxygen. It is our expectation that the sodium cation balanced the charge of the anionic Al_2O_3 that was precipitated. Figure 31 shows an XRD spectrum of the material, and indicates that it is amorphous, which is normal, since no crystallization was performed. In literature, the process of preparing zeolite from fly ash is well documented (see (Jha & Singh, 2016), (Bartholomew & Farrauto, 2006), (Rayalu, Meshram, & Hasan, 2000), (Kumar, Mal, Oumi, Yamanaa, & Sanoc, 2001), (Murayama, Yamamoto, & Shibata, 2002), (Kolay & Singh, 2002), (Fukui, Katoh, Yamamoto, & Yoshida, 2009)). The caustic solution needs to be incubated at 90 °C for period of 48 hours to promote crystallization, although solid seeding or use of a template may be used to initiate it.

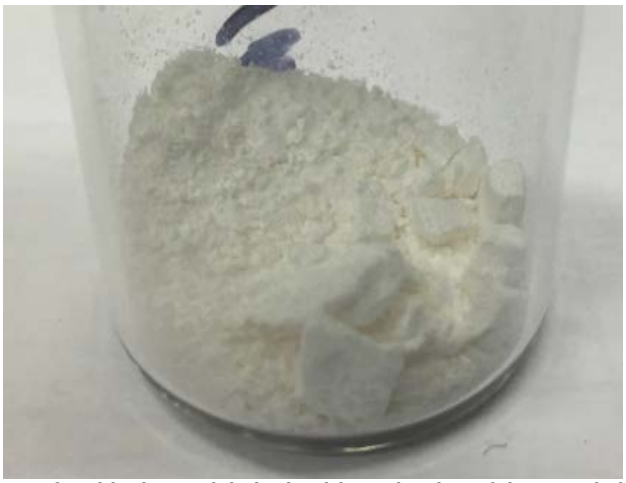

Figure 30: Photo of residual material obtained from titration of the caustic leach solution

Table 22: EDS analysis of the precipitate from the caustic leach solution.

EDS Results for Caustic Leach Precipitate		
Element	Wt%	Mole %
O	**39**	**52**
Na	**10**	**9**
Al	**11**	**9**
Si	**39**	**30**
K	**1**	**1**
Total	**100**	**100**

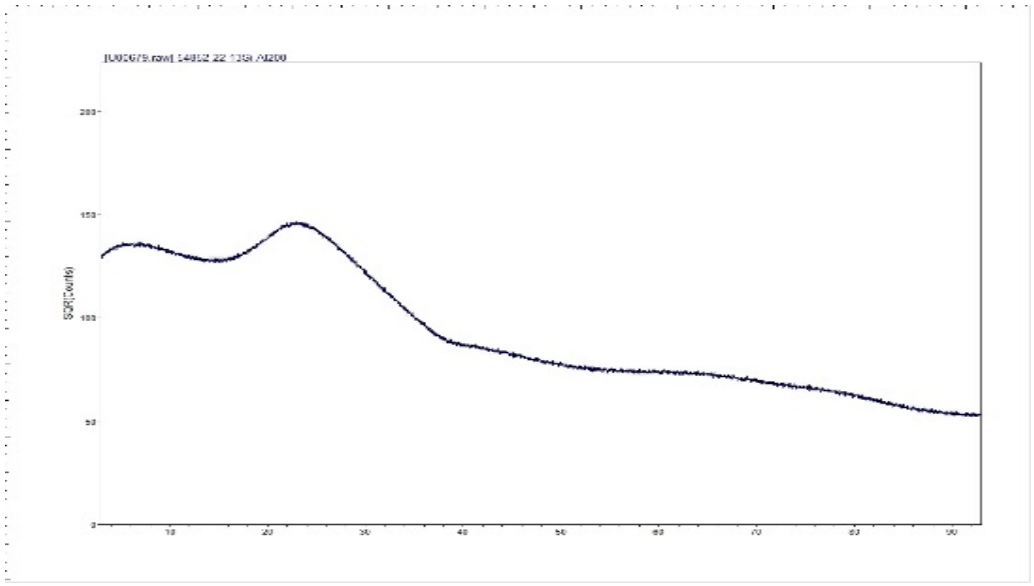

Figure 31: XRD of material precipitated from the caustic leach solution, indicating the lack of crystallinity in the solids.

Hollman, et al proposed two processes to produce zeolite from coal fly ash (Hollman, Steenbruggen, & Janssen-Jurkovicova, 1999).

Step one of synthesis consists of incubation of fly ash in NaOH at 90 ˚C for an extended period (96 hrs). They suggest that there is an induction period prior to the zeolite crystallization. During this initiation period, a part of fly ash dissolves and zeolite nuclei start forming on the surface of residual fly ash particles. Crystallization starts once the size of these nuclei reach a certain minimum from which point further growth is advantageous to minimize the surface energy. In this study, we performed incubation of fly ash (milled and unmilled) in NaOH solution at 90 ˚C, followed by filtration. The residual material was characterized by SEM and/or XRD.

Figure 32 is an SEM micrograph of fly ash without any treatment. The SEM micrograph reveals that fly ash particles are mainly spherical in shape with a relatively smooth surface and different particle size range. During combustion of coal in the electricity generating unit, the temperature can reach 1800 ˚C which causes liquefaction of residual material particles (fly ash) and generating the spherical shape. The surface smooths by rapid drop of temperature as they exit the hot zone.

Figure 33 is an SEM of unmilled fly ash treated with 2.5 M NaOH for 6 hours, at 90 ºC in an autoclave and milled fly ash treated with 2.5 M NaOH for 1 hour at 90 ºC at atmospheric pressure. Caustic soda causes the creation of pore structures on the fly ash. The pores are larger on the milled fly ash, which confirms that milling improves the interaction of NaOH with silica and alumina present in the fly ash. Figure 34 is an SEM micrograph of unmilled fly ash before and after incubation in 2 M NaOH for 24hr at 90 ºC.

Figure 35 is an X-ray Powder Diffraction of fly ash. The major crystalline phases are quartz (SiO_2), Mullite ($Al_{2.26}Si_{0.74}O_{4.87}$), and magnetite ($Fe_3O_4$). Quartz has the most intense peak at 26.8 degrees 2θ while the less intense peaks on the XRD patterns were identified as mullite and magnetite. The fly ash contained an amorphous glassy phase giving rise to a broad hump in the region between 16 and 36 degrees 2θ as indicated in the XRD spectra.

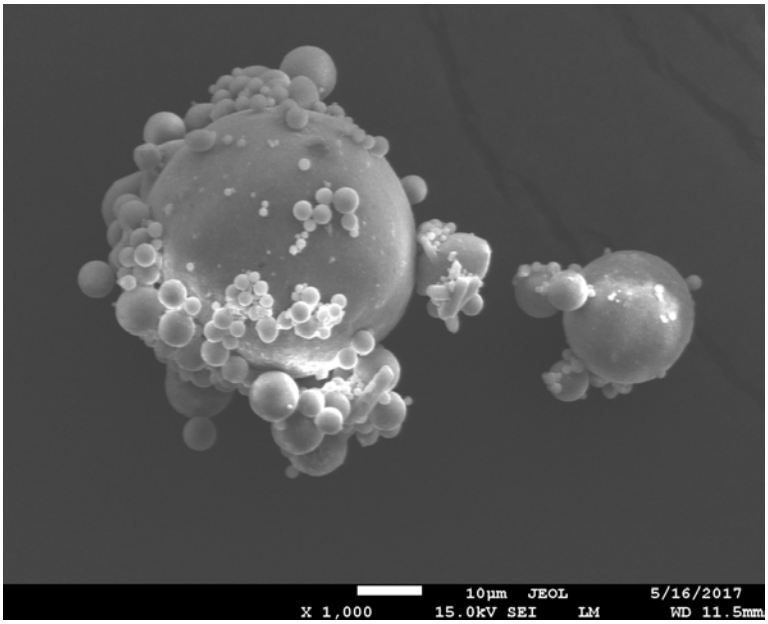

Figure 32: SEM of fly ash prior to any treatment

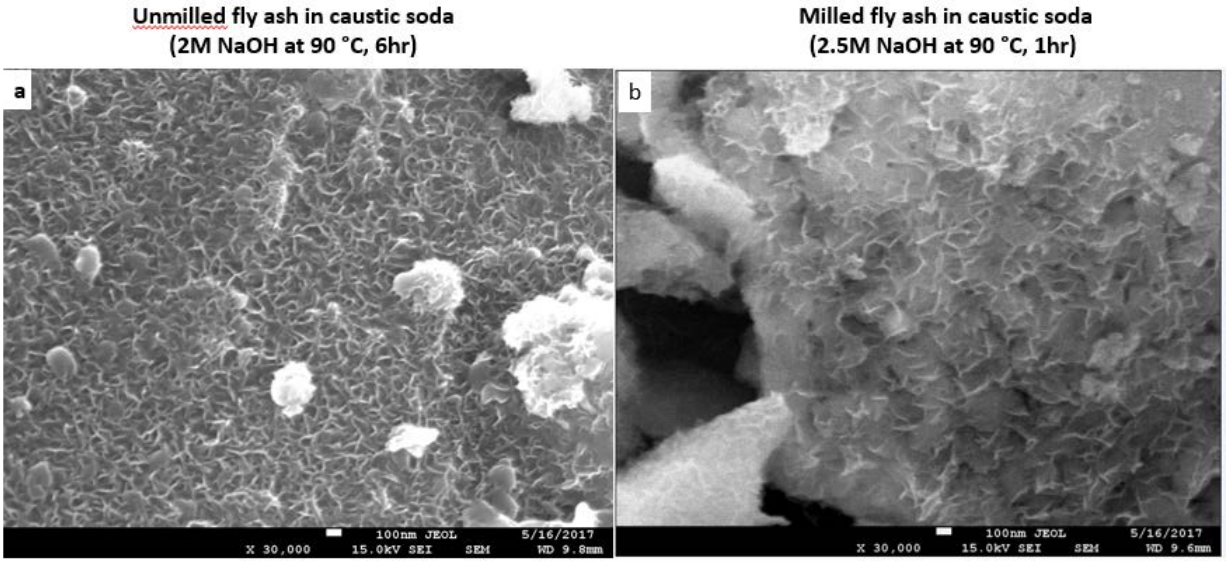

Figure 33: SEM of milled and unmilled fly ash treated with caustic solution.

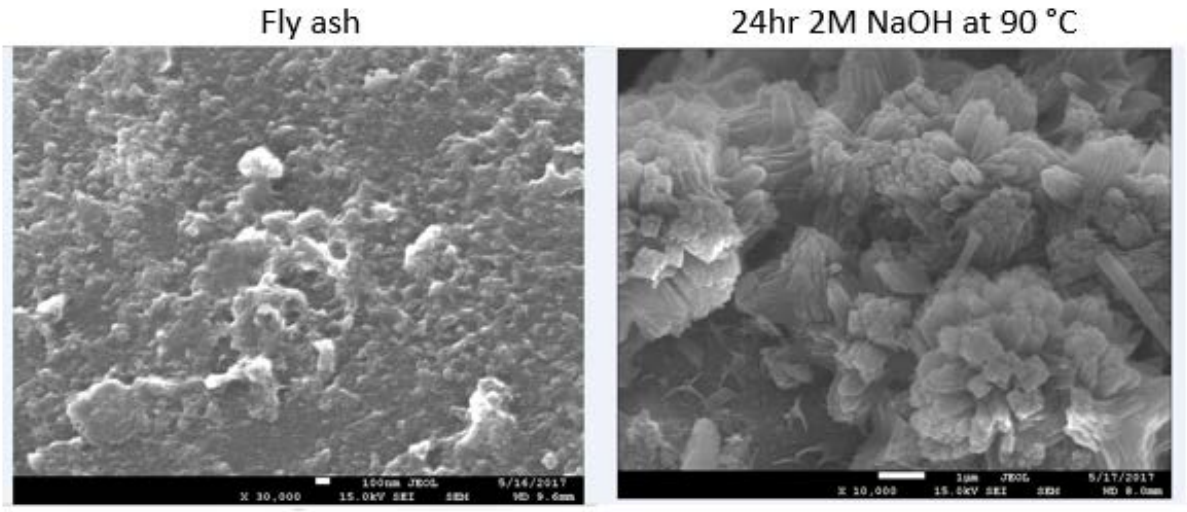

Figure 34: SEM of fly ash before and after caustic solution pretreatment and aging.

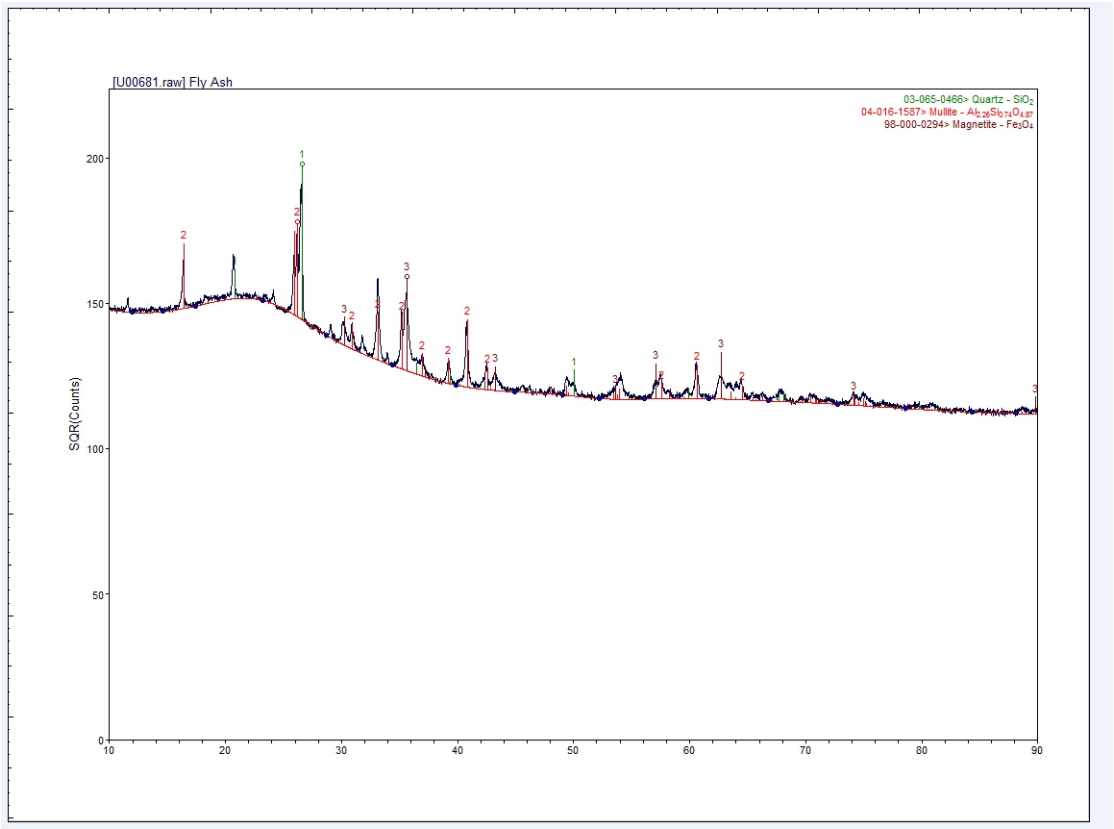

Figure 35: XRD spectra of fly ash before pretreatment (1-Quartz, 2-Mullite, 3-Magnetite)

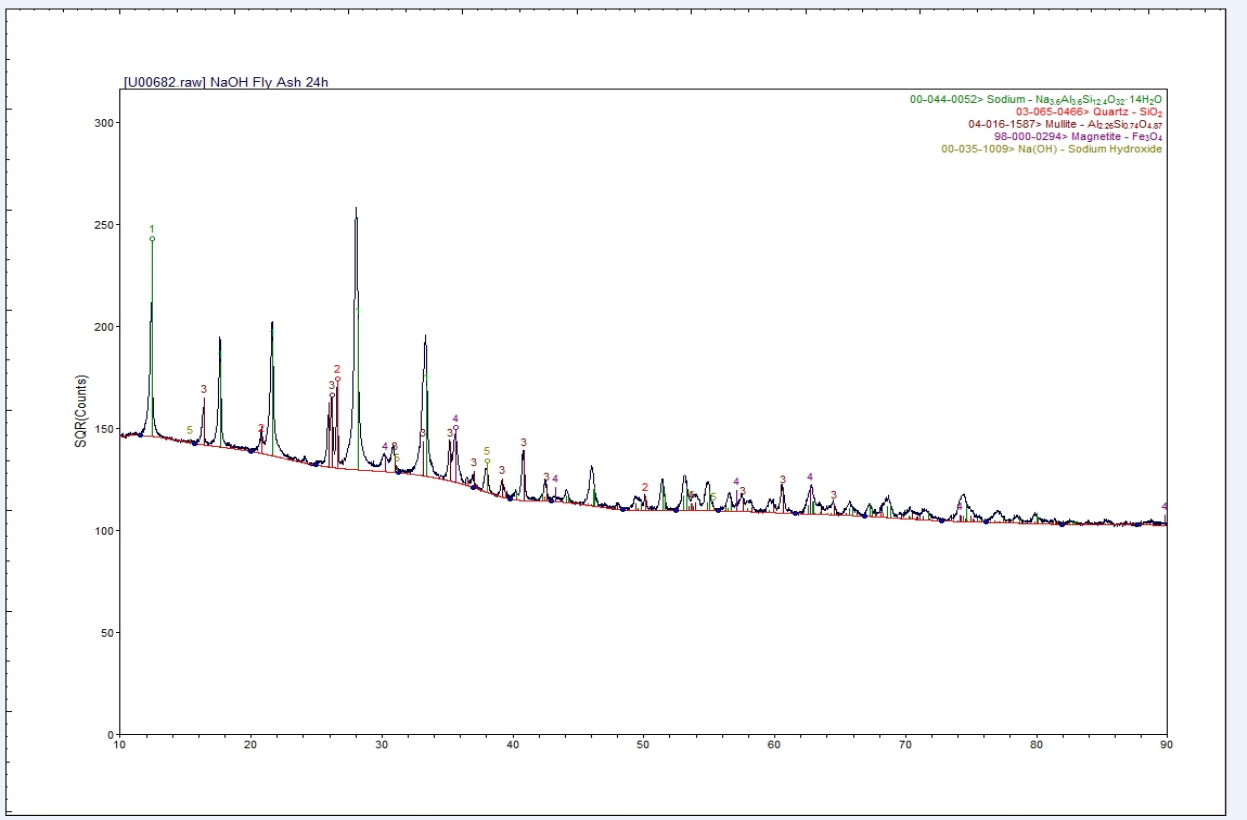

Figure 36: XRD results of zeolite synthesis from treatment of coal fly ash with 2 M sodium hydroxide solution.

Figure 36 shows the XRD profile of the product produced by treatment of fly ash in 2 M NaOH solution for 24 hours at temperature of 110 °C. It shows the loss of the broad hump between 16 ° and 36° 2θ (observed in the raw fly ash XRD profile). This suggests conversion of amorphous phase during the hydrothermal treatment. The zeolitic phase produced has the formulation ($Na_{3.6}Al_{3.6}Si_{12.4}O_{32}$*$14H_2O$). A portion of quartz and mullite remained undissolved from the matrix even after 24 hours.

A two-step process was also investigated to generate a zeolite of higher value since the fly ash impurities would be excluded. Additionally, the conditions were selected to more closely mirror the pretreatments used in Battelle's process. 100 grams of fly ash were leached in 500 mL of 2.5 M NaOH solution at 90 ºC for 1 hour. After filtration, trace amounts of HZSM5 powder (<0.1 mg) were dropped in 20 mL of the filtrate and placed in a 25 mL Teflon coated autoclave at 110 ºC for 48 hours. After cooling the reactor, the solution was filtered and residual material (around 10 mg) was analyzed by XRD and SEM. Table 23 reports the silica and alumina ratios in fly ash and the dissolved amount in caustic solution. The SiO_2/Al_2O_3 ratio is around 6.5. The XRD profile indicates that the deposited material is composed of vishnevite zeolite; $KNa_{6.8}Al_6(SiO_2)6(SO_4)$ $(H_2O)_2$ with a mole ratio of Si/Al = 6.0. The XRD/SEM data (Figure 37 and Figure 38) show the needed crystal structure of the fly ash derived zeolite.

Table 23: Silica and alumina ratios present in the fly ash and in the caustic leachate solution as measured during zeolite experimentation.

Silica and Alumina Ratios in the Caustic Leach Solution				
Material	Element	wt%	Molar Ratio Si/Al	Molar Ratio SiO_2/Al_2O_3
Fly Ash	Al	13	2.1	3.3
	Si	22		
Caustic Leach Solution	Al	3.1	3.3	6.5
	Si	10.6		

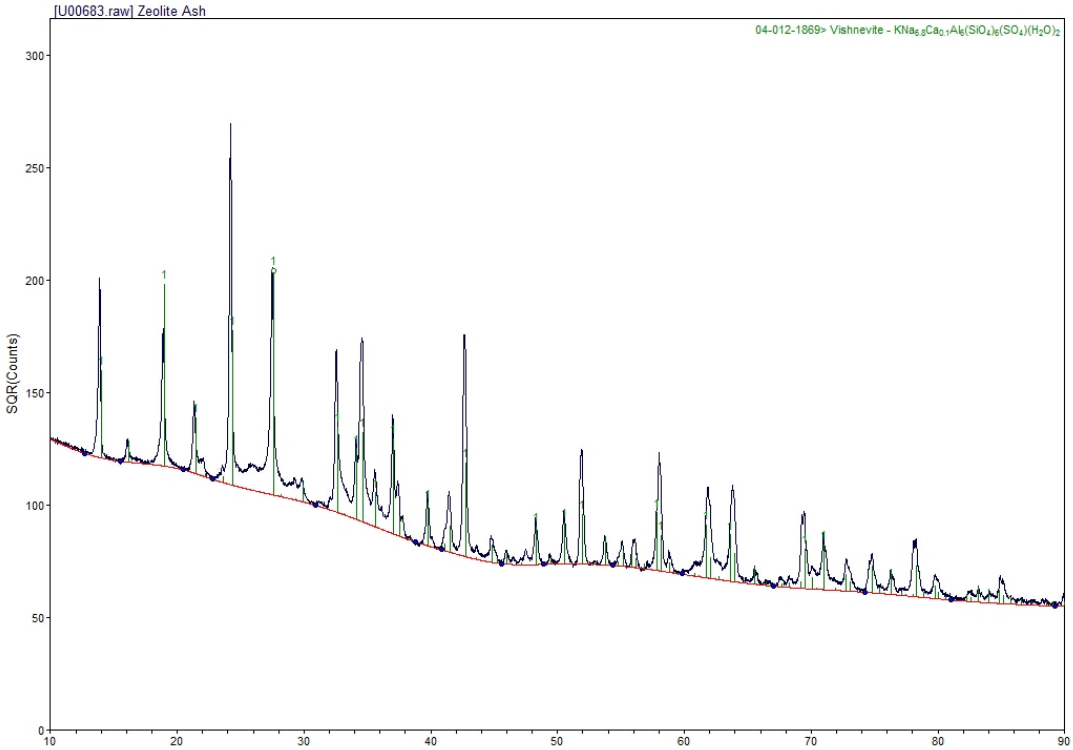

Figure 37: XRD of fly ash zeolite produced from hydrothermal treatment of filtered caustic solution that was contacted with fly ash for one hours at 90 °C.

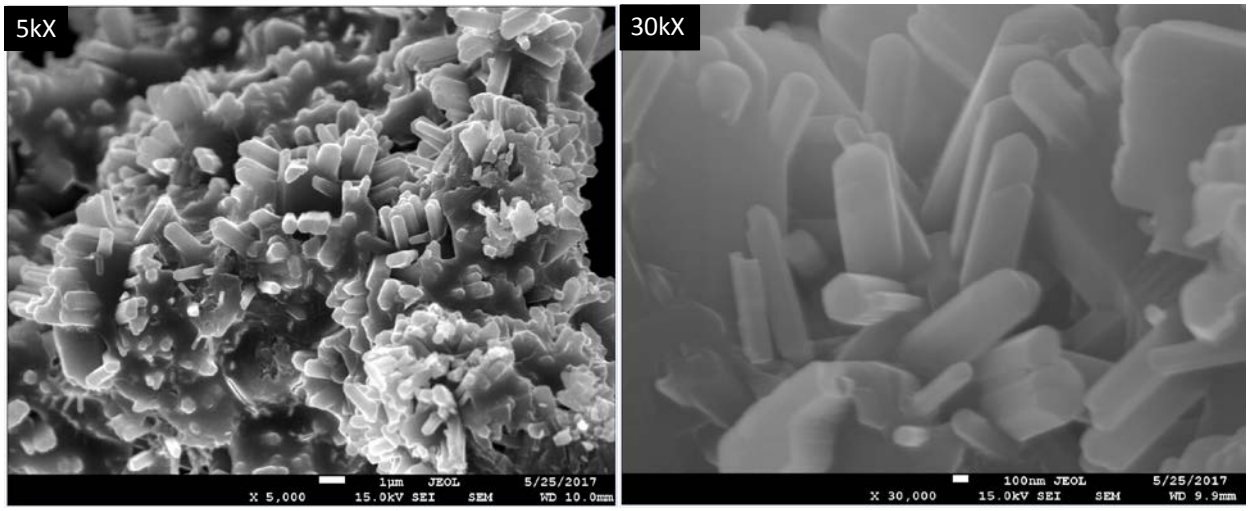

Figure 38: SEM of fly ash zeolite produced from hydrothermal treatment of filtered caustic solution that was contacted with fly ash for one hours at 90 °C.

This preliminary investigation shows that it is possible to prepare zeolite from caustic solution while residual material can be used for extraction of REE. However, more work is required to optimize the zeolite synthesis process and ensure good market outlets for the product. This work would be performed in part during Phase 2.

2.6 Calorimetry Testing

2.6.1 Results

Calorimetry was run on milled ash and milled and caustic pretreated ash to understand how much heat the acid leaching reaction will generate. Variability in the milled ash sample was high, as shown in Table 24, likely because the temperature changes were near the detection limits of the instrument (0.02 °C).

Table 24: Calorimetry results for milled fly ash in nitric acid.

Calorimetry Results for Milled Ash				
Sample ID	Δ T (°C)	T (°C)	Q (cal)	ΔH (cal/g)
Milled Ash #1	0.0290	19.268	3.38	6.76
Milled Ash #2	0.0352	19.292	4.10	8.21

The milled and caustic leached samples were run in triplicate, with results shown in Table 25. The average heat of reaction was 101.85 calories per gram of ash feed, with a standard of deviation of 0.69 calories per gram.

Table 25: Calorimetry results for milled and caustic leached fly ash in nitric acid.

Calorimetry Results for Milled and Caustic Leached Ash				
Sample ID	Δ T (°C)	T (°C)	Q (cal)	ΔH (cal/g)
Caustic Ash #1	0.4333	24.456	50.57	101.14
Caustic Ash #2	0.4365	19.567	50.95	101.89
Caustic Ash #3	0.4392	19.755	51.26	102.52

The heat of reaction for milled and caustic leached ash is much higher than for ash that is only milled. Past testing with the milled ash demonstrated a leaching efficiency for REE around 5-10%, while the caustic pretreated ash was near quantitative for most of the REE. Iron and aluminum leaching efficiency between milled and caustic pretreated ash was between 1-2% and 20-40%, respectively. This level of leaching improvements suggest that the increased heat of reaction for the caustic pretreated ash is likely attributable to greater leaching efficiency.

Other contributors to the increased heat of reaction could be heat of neutralization from entrained caustic or functionalized aluminosilicates. The caustic pretreated ash was rinsed with water until the pH was 10.5, which leaves behind some base that will react with nitric acid, generating heat. However, even if it is liberally assumed that the full mass of ash was entrained basic solution at pH 10.5, the energy contribution would only be 0.004 calories per gram. Neutralization of hydroxyl groups developed on the aluminosilicate could also contribute to the heat of neutralization, and this contribution cannot be ruled out at this time.

2.6.2 Procedure

Calorimetry was performed with a Parr Instruments model 6755 Solution Calorimeter, which was standardized with solid TRIS (tris(hydroxymethyl) aminomethane) dissolved in dilute hydrochloric acid. The heat evolution for this reaction is well established, and this standardization was performed three times to ensure good consistency. More specific steps are included in Appendix A.

Initial calorimetry tests added 1.00 ± 0.01 grams of ash to 100.00 ± 0.05 grams of 17% nitric acid (nominal concentration; actual 1:3 mass dilution of concentrated nitric acid). However, the temperature change in this reaction was too small to detect with the instrument, which has detection limits of 0.02 degrees Celsius. Additional tests were run with a higher amount of ash in 34% nitric acid; 0.50 grams of ash to 100 grams of acid to attempt to accelerate the reaction. Two sets of tests were run, one with a milled ash, and one with a milled and caustic leached ash. These were both expected to be more reactive and provide measurable results. Two replicates were run with milled ash (d_{50} of 4.5 µm), but variability was still high as it approached detection limits of the equipment. The milled and caustic leached ash (leached for 1 hour in 10% sodium hydroxide solution at 90°C) was run in triplicate. Each run had a reaction period of approximately 10 minutes, which is the time taken for temperature to stabilize after mixing of the ash and acid.

2.7 Acid Leaching Parameter Testing

2.7.1 Results

Results of the leaching tests carried out to date and analysis of similar leaching processes indicate that for a given ash particle size and porosity, the efficiency of REE recovery is likely to be affected by four factors: (1) leaching time, (2) leaching temperature, (3) nitric acid concentration, and (4) acid freshness (function of number of times acid was used and concentration of dissolved reaction products). The influence of these factors was evaluated using a design of experiments approach, specifically the Box-Behnken surface response method (Box & Behnken, 1960). Table 26 lists the four experimental factors, together with their ranges, as used in the study.

Table 26: Experimental factors expected to influence the outcome of the ash leaching process, along with the ranges that were tested.

Factors Expected to be Meaningful for Ash Leaching				
Factor	Symbol used in models	*Low level (-1)*	*Intermediate level (0)*	*High level (1)*
Time of leaching	t	1 min	15 min	30 min
Temperature	T	20 °C	55 °C	90 °C
Acid concentration	C	34%	51%	68%
Acid "freshness"	u	0 (fresh acid)	1 (acid used once)	2 (acid used twice)

The design of experiment was used to maximize two types of process outcomes (objective functions): (1) leaching efficiency, and (2) value of the extracted REE material. The leaching efficiency was defined as the fraction of REE element(s) that was extracted from the feed ash. The value of extracted REE material was defined as a total value of REE metal oxides extracted per unit mass of ash. Both quantities are appropriate measures of the REE recovery process and its economics.

The Box-Behnken surface response model with four factors requires 27 experiments. This design of experiment will generate a complete quadratic model of the process and will include all linear, quadratic, and cross-term contributions:

$$\boldsymbol{Efficiency} = \beta_0 + \beta_1 t + \beta_2 T + \beta_3 C + \beta_4 u + \beta_5 tT + \beta_6 tC + \beta_7 TC + \beta_8 tu + \beta_9 Tu + \beta_{10} Cu + \beta_{11} t^2 + \beta_{12} T^2 + \beta_{13} C^2 + \beta_{14} u^2 \quad \text{Equation 1}$$

where t, T, C, and u are time, temperature, acid concentration, and number of times the acid was used, respectively. This model equation represents the most complex form of the leaching reaction efficiency function, with a total of 15 terms, which is not expected to be required in most real leaching situations. Instead, a simpler model equation, with only several terms, is expected. A combination of terms present and magnitude of these terms provide a reliable insight into the mechanism of the leaching reaction and into its scaled-up implementation. The Box-Behnken method provides a well-defined and statistically-sound procedure to estimate values and

standard errors of all coefficients (β's) used in the model, as well their statistical significance. All design of experiment analyses presented in this report were performed using MATLAB, specifically the functions included in the MATLAB Statistical Toolbox extension.

Table 27 lists the leaching results obtained from the 27 experiments. The leaching efficiency was determined using concentrations of specific elements (Sc, Y, REE) detected in the acid solutions after leaching, compared to the total amounts of these elements in the ash. The concentration of scandium was determined by two methods: (1) the ICP-MS method carried out by Activation Laboratories, and (2) an ICP-OES method at Battelle. Concentration of all other elements was determined by the ICP-MS method. The average REE+Y+Sc leaching efficiencies were calculated as a weighted average; weighted by the elemental concentrations of REE+Y+Sc in the feed ash. Some of the leaching efficiencies, reported in Table 27, are larger than the theoretical efficiency limit of 100%. This effect is caused by errors in measurements of both the leached element concentrations and the amounts of elements available in ash. The efficiencies exceeding 100 % were detected using the ICP-MS method, suggesting that this method carries an inherent error. The efficiency measurements based on the ICP-OES method were all below 100%. The total value of oxides extracted was calculated using the concentrations of leached elements and market prices of their oxides from mineralprices.com, accessed in December of 2016.

It is not expected that the errors in REE leaching efficiency measurements have substantial effect on trends and models developed by the design of experiment method. Information about the leaching process mechanism and experimental conditions affecting its outcome are still valid; however, the predicted values of leaching efficiencies and total values will be affected. These effects need to be considered during analysis of these results.

Note that the results presented in Table 27, as well as most tables presenting the analysis, include values with both significant and insignificant digits. Identification and elimination of insignificant digits was not done since it does not affect the outcome and conclusions of the analysis.

Table 27: Results obtained during the 27 leaching experiments. Note that the experiments were carried out in random order which was different from the order presented here.

Test number	Experimental Results			
	Scandium leaching efficiency ICP-MS (%)	Scandium leaching efficiency ICP-OES (%)	REE+Y+Sc average weighted leaching efficiency (%)	Total value of oxides extracted ($/metric ton)
1	68.00	46.62	58.13	187.15
2	89.27	65.27	81.08	245.30
3	117.25	71.01	91.05	321.34
4	152.35	83.35	111.26	416.02
5	110.62	77.93	91.25	303.37
6	117.40	82.09	103.21	323.52
7	88.64	72.82	77.49	244.38
8	87.22	76.44	77.18	240.89
9	72.86	59.52	68.10	201.45
10	104.45	68.78	92.04	287.84
11	134.02	77.01	105.40	366.65
12	90.09	79.84	86.84	249.96
13	81.54	78.50	73.15	225.26
14	116.15	65.29	88.76	317.76
15	135.44	86.58	112.56	372.18
16	99.70	79.56	82.46	274.32
17	78.71	74.24	79.04	219.04
18	67.93	56.96	59.75	187.60
19	108.49	81.47	99.45	299.86
20	71.90	74.60	72.19	198.51
21	104.6	68.94	89.41	287.72
22	94.88	68.43	85.63	261.99
23	107.43	76.23	88.02	294.55
24	139.55	78.07	109.09	382.26
25	98.63	75.98	100.45	271.80
26	79.70	70.80	77.48	221.05
27	87.36	69.24	79.46	241.52

Analysis 1 - Leaching Efficiency for Scandium Measured by the ICP-MS method

The leaching efficiency for scandium, determined by the ICP-MS method, (Table 27, 2nd column from left) were fitted to the full quadratic equation (Equation 1). The estimated values of fitting coefficients are shown in Figure 39. Table 28 lists these values together with their standard errors (SE), and p-values that determine their statistical significance. Coefficients with p-values below 0.05 are considered statistically significant, p-values in the 0.05-0.10 range are considered marginal, while higher p-values indicate coefficients that are not statistically

significant. The p-values listed in Table 28 indicate that the only significant coefficients are: intercept, t, T, C, T×C, t×u, and T^2. The only marginal coefficient is u^2.

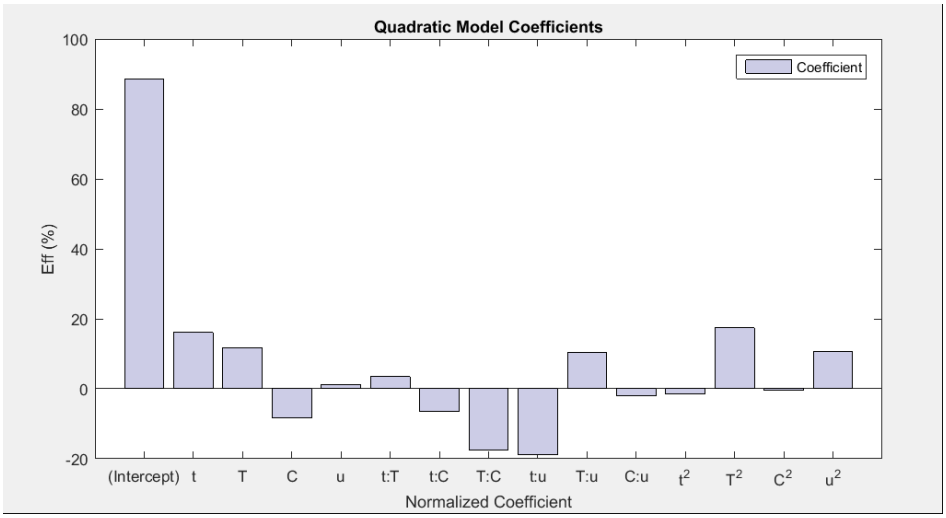

Figure 39: Normalized coefficients estimated for scandium leaching efficiency, measured by the ICP-MS method

Table 28: Values, standard errors, and p-values for coefficients estimated for scandium leaching efficiency and model Equation 1.

Analysis for Significant Coefficients				
Coefficient	Estimate	SE	pValue	Comment
β_0 Intercept	88.563	7.3609	4.696e-08	significant
β_1 (t)	16.073	3.6804	0.00091661	significant
β_2 (T)	11.772	3.6804	0.0076545	significant
β_3 (C)	-8.3883	3.6804	0.041741	significant
β_4 (u)	1.28	3.6804	0.73403	not significant
β_5 (t×T)	3.4575	6.3747	0.59749	not significant
β_6 (t×C)	-6.4525	6.3747	0.33141	not significant
β_7 (T×C)	-17.587	6.3747	0.017313	significant
β_8 (t×u)	-18.88	6.3747	0.011883	significant
β_9 (T×u)	10.475	6.3747	0.12626	not significant
β_{10} (C×u)	-2.05	6.3747	0.7533	not significant
β_{11} (t^2)	-1.4729	5.5206	0.79415	not significant
β_{12} (T^2)	17.39	5.5206	0.0083761	significant
β_{13} (C^2)	-0.42042	5.5206	0.94055	not significant
β_{14} (U^2)	10.59	5.5206	0.07919	marginal

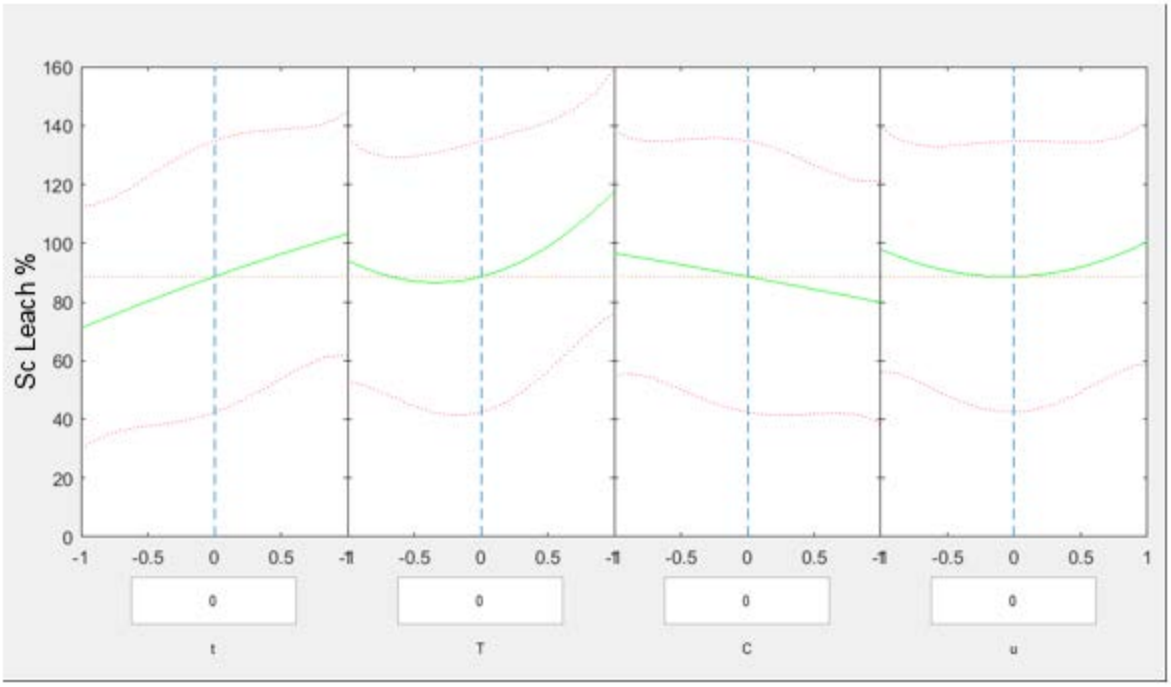

Figure 40: Trends detected in the scandium leaching efficiency. Red dotted lines indicate 95% confidence bounds.

Figure 40 shows trends detected in the scandium leaching efficiency associated with the four factors. The green lines are slices through the regression surface, predicted by the model, obtained with other factors held constant. The red curves are lower and upper bounds calculated at a 95% confidence level. There is a clear increase of efficiency with increased leaching time and with increased temperature. There is a slight increase of leaching efficiency at lower acid concentration. The number of times the acid was used has almost no influence on the leaching efficiency. These trends are consistent with values of coefficients listed in Table 28.

The non-significant coefficients listed in Table 28 were eliminated from the full quadratic model (Equation 1) yielding a simplified model:

$$Efficiency = \beta_0 + \beta_1 t + \beta_2 T + \beta_3 C + \beta_7 TC + \beta_8 tu + \beta_{11} T^2 + \beta_{14} u^2 \quad \text{Equation 2}$$

The analysis was repeated with Equation 2 and the results are given in Figure 41, Table 29, and Figure 42. The predictions of both full (Equation 1) and simplified (Equation 2) models are very similar, however standard error and p-values are smaller for the simplified model (Equation 2).

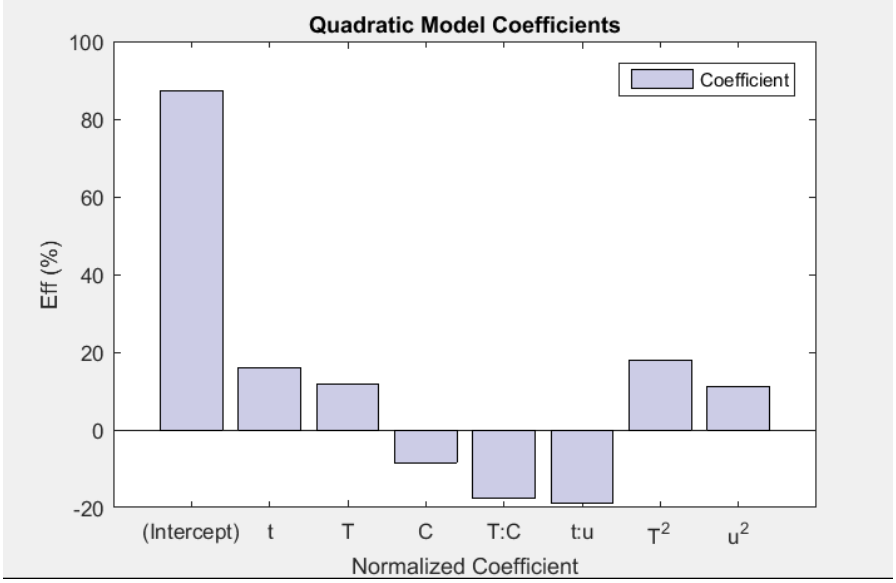

Figure 41: Normalized coefficients estimated for scandium leaching efficiency, measured by the ICP-MS method, using model Equation 2.

Table 29: Values, standard errors, and p-values for coefficients estimated for scandium leaching efficiency and model Equation 2.

Analysis for Significant Coefficients				
Coefficient	Estimate	SE	p-Value	Comment
β_0 Intercept	87.301	3.938	4.8628e-15	significant
β_1 (t)	16.073	3.4104	0.00015142	significant
β_2 (T)	11.772	3.4104	0.0026729	significant
β_3 (C)	-8.3883	3.4104	0.023668	significant
β_7 (T×C)	-17.587	5.9071	0.0077396	significant
β_8 (t×u)	-18.88	5.9071	0.0047547	significant
β_{12} (T^2)	17.863	4.6699	0.0011424	significant
β_{14} (U^2)	11.063	4.6699	0.028588	significant

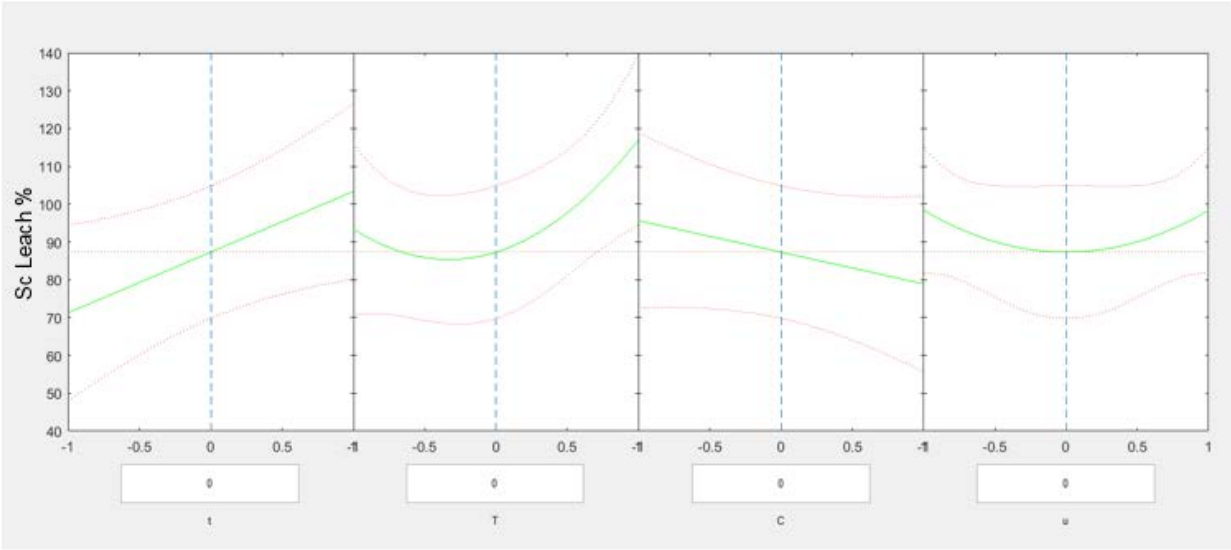

Figure 42: Trends detected in the scandium leaching efficiency based on model Equation 2. Red lines indicate 95% confidence bounds.

The model Equation 2, together with the values of coefficients listed in Table 29, were used to determine optimal conditions that produce maximum value of scandium leaching efficiency. These optimal leaching conditions are listed in Table 30. Note that the predicted optimal value of efficiency is 176% is above the theoretical limit of 100% due to measurement errors. This effect does not influence the significance of the optimal factor values listed.

Table 30: Optimal leaching parameters (factors) that maximize the value of scandium leaching efficiency, based on model Equation 2.

Estimated Optimal Leaching Parameters		
Optimal factor values	Optimal scandium leaching efficiency	Assumptions used in calculations
t=30 min T=90 °C C=34% u=0-2 (not a critical factor)	scandium Eff=176%*	Equation 2 with coefficients listed in Table 29
***Note that efficiency above 100% is predicted due to error in the ICP-MS analysis method affecting the measured leaching efficiency values**		

Analysis 2 - Leaching Efficiency for Scandium measured by ICP-OES

In the 27 test in the design of experiment, three tests were performed at the same conditions: Leaching time of 15 minutes, reaction temperature of 90 °C, acid concentration of 55% nitric acid, and acid used once for acid freshness. Using these results, a comparison between ICP-OES and ICP-MS analysis was performed to understand which method had less variability (See

Table 31). Battelle's internal ICP-OES method for scandium showed less variability than ICP-MS method, with a lower absolute and relative standard deviation. Additionally, the generally lower results were more consistent with other analyses, as the recovery efficiency for scandium was less than 100% in all cases. For economic and design calculations, the ICP-OES results were used to track scandium leaching efficiency.

Table 31: Comparison of Scandium concentration results from ICP-OES and ICP-MS analysis.

Comparison of Scandium Results by ICP-OES and ICP-MS		
Test	ICP-OES: Scandium concentration (µg/mL)	(ICP- MS) Scandium concentration (µg/mL)
1	1086	1260
2	1173	995
3	1097	1160
Average	1118.67	1138.33
Standard Deviation	38.68	109.27
Relative Standard Deviation	3.46%	9.60%

The design of experiment analysis for scandium was repeated using the leaching efficiencies determined by the ICP-OES method (Table 27, 3rd column from left). Initially, the full quadratic model (Equation 1) was used to determine which coefficients are significant. This analysis showed that the only significant coefficients are: intercept, t, T, C, t^2, C^2, and that the following simplified model applies:

$$Efficiency = \beta_0 + \beta_1 t + \beta_2 T + \beta_3 C + \beta_{11} t^2 + \beta_{13} C^2 \quad \text{Equation 3}$$

The estimated values of normalized fitting coefficients are shown in Figure 43 and Table 32. Figure 44 presents effects of leaching time and temperature, as well as acid concentration on the scandium leaching efficiency. These trends are the same as trends observed for the scandium leaching efficiency determined by the ICP-MS method. Increase of both temperature

and leaching time increases scandium leaching efficiency. Increase of acid concentration lowers the efficiency.

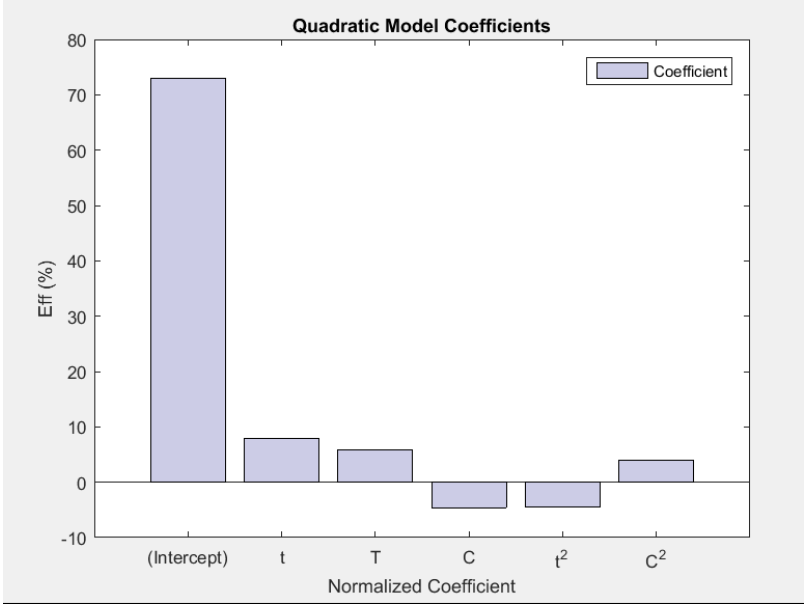

Figure 43: Normalized coefficients estimated for scandium leaching efficiency, measured by the ICP-OES method, and using model Equation 3

Table 32: Values, standard errors, and p-values for coefficients estimated for scandium leaching efficiency, measured by the ICP-OES method, and model Equation 3

Analysis for Significant Coefficients				
Coefficient	Estimate	SE	p-value	Comment
β_0 Intercept	72.968	1.2163	5.6689e-25	significant
β_1 (t)	7.9908	1.0533	1.9085e-07	significant
β_2 (T)	5.8558	1.0533	1.6204e-05	significant
β_3 (C)	-4.595	1.0533	0.00027315	significant
β_{11} (t^2)	-4.4278	1.4423	0.0058116	significant
β_{13} (C^2)	4.0484	1.4423	0.010565	significant

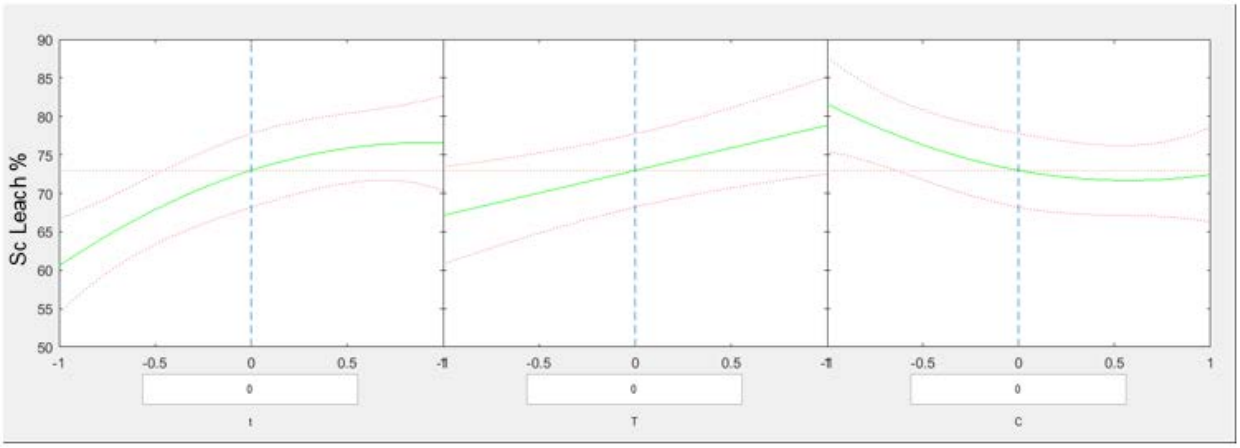

Figure 44: Trends detected in the scandium leaching efficiency based on Equation 3. Red dotted lines indicate 95% confidence bounds.

Model Equation 3 together with the values of coefficients listed in Table 32 was used to determine optimal conditions that produce maximum value of scandium leaching efficiency. These optimal leaching conditions are listed in Table 33. The optimal values of optimal experimental factors listed in Table 30 and Table 33 are in excellent agreement.

Table 33: Optimal leaching parameters (factors) that maximize value of scandium leaching efficiency, based on model Equation 3.

Estimated Optimal Leaching Parameters		
Optimal factor values	Optimal scandium leaching efficiency	**Assumptions used in calculations**
t=25 min T=90 °C C=34%	scandium Eff=94%	Model Equation 3 with coefficients listed in Table 32

Analysis 3 - Weighted Average Leaching Efficiency for REE+Y+Sc

The design of experiment analysis was carried out for an average weighted leaching efficiency calculated for REE+Y+Sc (Table 27, 4th column from left). Initially, the full quadratic model (Equation 1) was used to determine which coefficients are significant. This analysis showed that the only significant coefficients are: intercept, t, T, C, T×C, t×u, and that the following simplified model applies:

$$\boldsymbol{Eff = \beta_0 + \beta_1 t + \beta_2 T + \beta_3 C + \beta_7 TC + \beta_8 tu} \qquad \text{Equation 4}$$

The estimated values of normalized fitting coefficients are shown in Figure 45 and Table 34. Figure 46 presents effects of experimental factors. The trends observed for REE+Y+Sc

weighted average leaching efficiency are identical to trends observed for the scandium leaching efficiency.

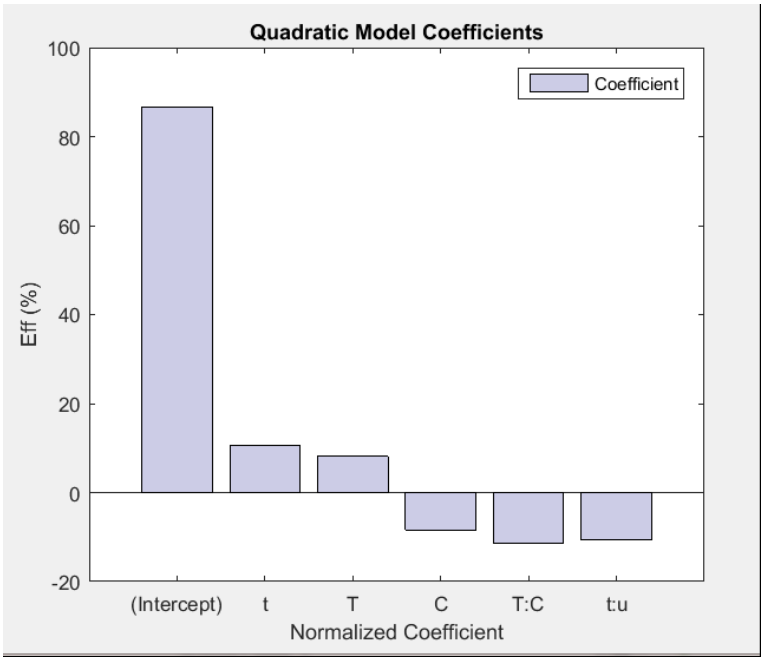

Figure 45: Normalized coefficients estimated for weighted average REE+Y+Sc leaching efficiency using model Equation 4.

Table 34: Values, standard errors, and p-values for coefficients estimated for weighted average REE+Y+Sc leaching efficiency and model Equation 4.

Analysis for Significant Coefficients				
Coefficient	Estimate	SE	p-value	Comment
(Intercept)	86.664	1.6481	8.8697e-24	significant
t	10.671	2.4721	0.00030485	significant
T	8.195	2.4721	0.0032927	significant
C	-8.4025	2.4721	0.0027051	significant
T×C	-11.428	4.2818	0.014368	significant
t×u	-10.625	4.2818	0.021629	significant

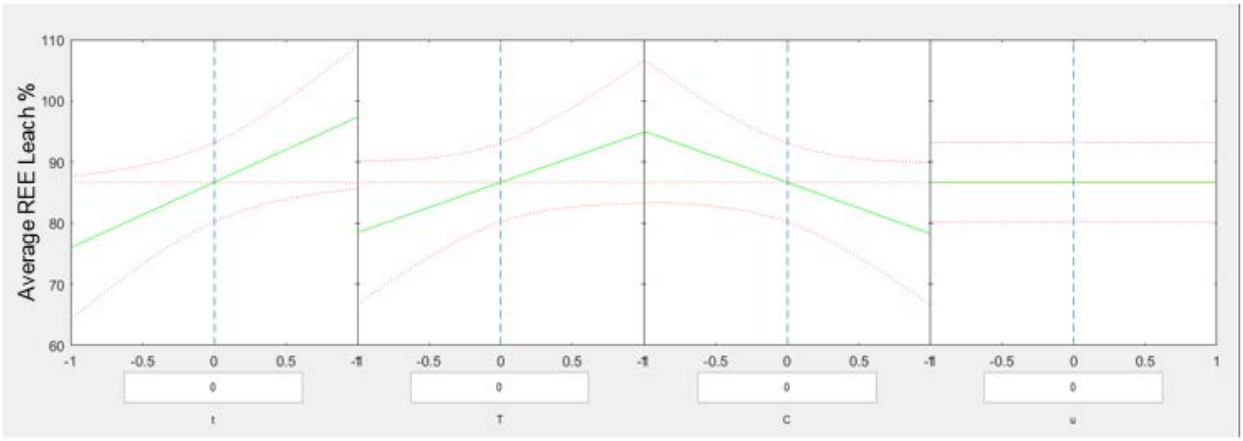

Figure 46: Trends detected in the weighted average REE+Y+Sc leaching efficiency based on model Equation 4. Red dotted lines indicate 95% confidence bounds

Model Equation 4 together with the values of coefficients listed in Table 34 were used to determine optimal conditions that produce maximum value of REE+Y+Sc leaching efficiency. These optimal leaching conditions are listed in Table 35. Again, the predicted optimal leaching efficiency is larger than the 100% limit. This is due to the systematic effort in the ICP-MS solution analysis method that was used for all elements (REEs, Y, and Sc).

Table 35: Optimal leaching parameters (factors) that maximize value of weighted average REE+Y+Sc leaching efficiency, based on model Equation 4.

Estimated Optimal Leaching Parameters		
Optimal factor values	Optimal REE+Y+Sc leaching efficiency	**Assumptions used in calculations**
t=17 min T=90 °C C=34% u=0-2 (not a critical factor)	REE+Y+Sc Eff=128%*	Model Equation 4 with coefficients listed in Table 34
***Note that efficiency above 100% is predicted due to error in the ICP-MS analysis method affecting the measured leaching efficiency values**		

Analysis 4 – Total Value of Oxides Extracted

In the final design of experiment analysis, the total value of REE, yttrium, and scandium oxides was fitted into a full quadratic model (Equation 1). The calculations used scandium leaching efficiencies determined by the ICP-OES method. This analysis indicated that the only significant factors are: intercept, t, T, C, u, t^2, and C^2. The simplified model equation including the significant coefficients is as follows:

$$\$/ton = \beta_0 + \beta_1 t + \beta_2 T + \beta_3 C + \beta_4 u + \beta_{11} t^2 + \beta_{13} C^2 \quad \text{Equation 5}$$

The estimated values of normalized fitting coefficients are shown in Figure 47 and Table 36. Figure 48 presents effects of experimental factors. The trends observed for value of extracted oxides are similar to trends observed for leaching efficiencies.

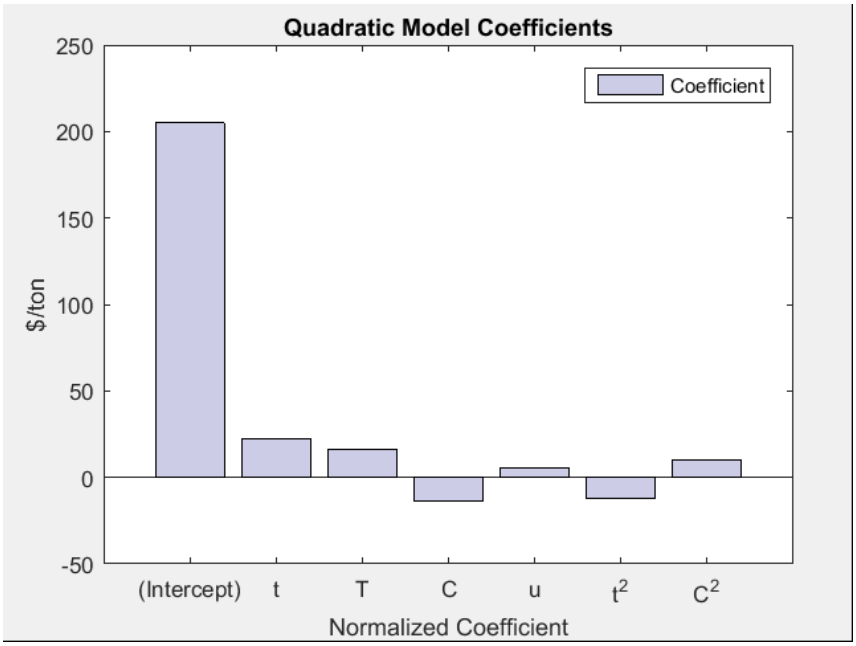

Figure 47: Normalized coefficients estimated for total value of extracted oxides according to model Equation 5.

Table 36: Values, standard errors, and p-values for coefficients estimated for total value of extracted oxides and model Equation 5.

Analysis for Significant Coefficients				
Coefficient	Estimate	SE	p-value	Comment
β_0 Intercept	205.03	3.2408	1.6301e-24	significant
β_1 (t)	22.493	2.8066	1.1338e-07	significant
β_2 (T)	16.458	2.8066	9.7718e-06	significant
β_3 (C)	-13.378	2.8066	0.00011782	significant
β_4 (u)	5.3042	2.8066	0.073358	marginal
β_{11} (t^2)	-12.489	3.8431	0.0040128	significant
β_{13} (C^2)	10.197	3.8431	0.015256	significant

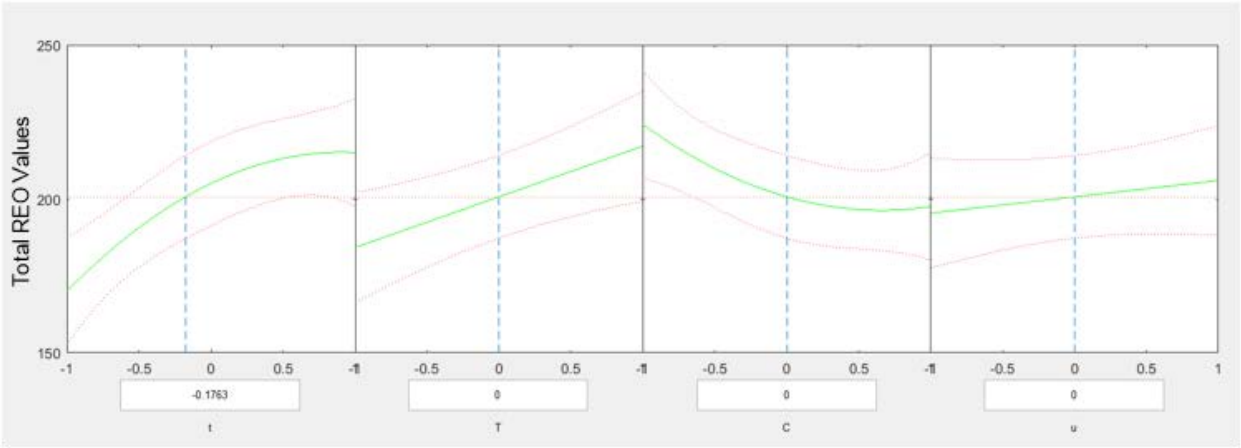

Figure 48: Trends detected for the total value of extracted oxides based on model Equation 5. Red dotted lines indicated 95% confidence bounds.

Model Equation 5, together with the values of coefficients listed in Table 36, were used to determine optimal conditions that produce maximum value of metal. These optimal leaching conditions are listed in Table 37.

Table 37: Optimal leaching parameters (factors) that maximize total value of extracted oxides, based on model Equation 5

Estimated Optimal Leaching Parameters		
Optimal factor values	Optimal total value of extracted oxides	**Assumptions used in calculations**
t=26 min T=90 °C C=34% u=0-2 (not a critical factor)	$267/tonne	Model Equation 5 with coefficients listed in Table 36

Analysis 5 – Selectivity for REE and Scandium

The design of experiment method was used to probe leaching selectivity for REE+Y element group and for scandium. The selectivity for scandium was defined as a concentration of scandium detected in the leachate solution divided by a sum of concentration of all metallic elements, including all common components like Al, Si, Fe and others. The selectivity towards REE+Y was defined by using a sum of concentrations of these elements normalized to the sum of all concentrations. The values selectivity obtained in all 27 experiments are presented in Table 41.

Table 38: Selectivity results obtained during the 27 leaching experiments.

Test number	Experimental results	
	Scandium selectivity ($\times 10^4$)	REE+Y selectivity ($\times 10^4$)
1	1.4348	24.013
2	1.5647	25.786
3	1.3898	24.192
4	1.9578	24.588
5	1.4263	24.067
6	1.2699	19.607
7	1.0601	18.454
8	1.1101	19.594
9	1.0387	17.571
10	1.4459	22.655
11	1.2900	21.619
12	1.3257	22.616
13	1.2353	22.309
14	1.0998	20.459
15	1.2851	23.142
16	1.1885	21.671
17	1.3592	24.458
18	1.7373	25.788
19	1.7582	25.449
20	1.6062	24.869
21	1.8781	24.712
22	1.5397	23.820
23	1.5149	21.015
24	1.7358	24.839
25	1.7020	23.136
26	1.7081	24.430
27	1.6347	24.100

The main goal of the design of experiment analysis was to identify any trends associated with the four main experimental factors listed in Table 26. If such trends are detected they can be used to tailor the leaching process to increase relative concentration of the desired REE, yttrium, or scandium products.

Both selectivity values were initially fitted to the full quadratic model previously used for the leaching efficiency analysis. In a subsequent analysis, simplified models containing only statistically significant terms was used.

The full quadratic model analysis carried out for the REE+Y selectivity produced trends presented in Figure 49. It appears that only leaching temperature and, to a lesser extent, acid freshness have any effect on the REE+Y selectivity. This observation is confirmed by the p-values which indicated that the only significant model coefficients are: intercept, T, and T^2, while

the term associated with u^2 is marginally significant. The coefficient values, their standard errors, and the associated p-values are listed in Table 39.

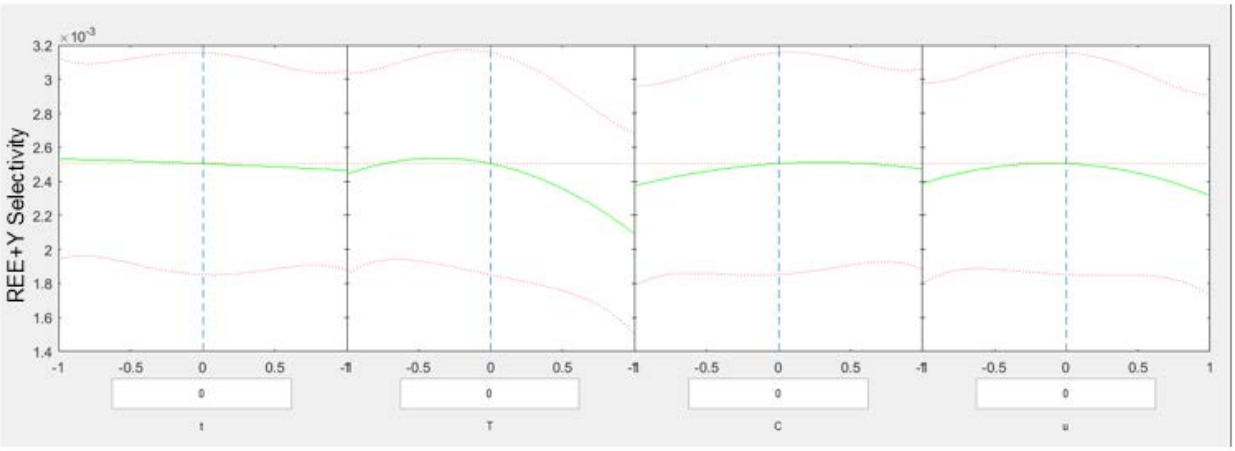

Figure 49: Trends detected for REE+Y selectivity. Red dotted lines indicate 95% confidence bounds

Table 39: Values, standard errors, and p-values for coefficients estimated for REE+Y leaching selectivity.

Analysis for Significant Coefficients				
Coefficient	Estimate	SE	pValue	Comment
β_0 Intercept	0.0024457	5.3854e-05	5.0995e-24	significant
β_2 (T)	-0.00017532	4.6639e-05	0.0010214	significant
β_{12} (T^2)	-0.00021447	6.3863e-05	0.0027194	significant
β_{14} (U^2)	-0.0001304	6.3863e-05	0.0528	marginal

As it can be seen from Figure 49, the REE+Y selectivity is enhanced at lower temperatures (20-50 °C) as compared to selectivity at higher temperature (90 °C). Although this is not a strong improvement of selectivity, it should not be overlooked during REE extraction which is very challenging. It will be balanced with decreased leaching efficiency observed at the lower temperatures to find a target operating point in Phase 2.

The design of experiment analysis for scandium selectivity, shown in Figure 50, indicated selectivity almost independent of all four experimental factors. Out of all possible factors

included in the full quadratic model, only the intercept and the cross T:C term were found statistically significant. In addition, the value of the T:C is very small as shown in Table 40.

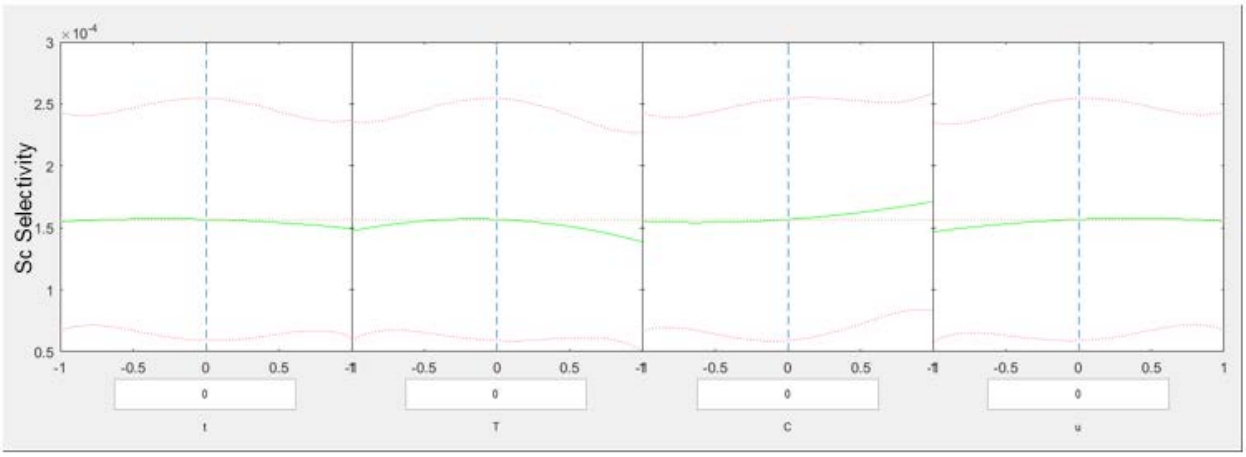

Figure 50: Trends detected for Scandium selectivity. Red dotted lines indicate 95% confidence bounds.

Table 40: Values, standard errors, and p-values for coefficients estimated for Scandium leaching selectivity.

Analysis for Significant Coefficients				
Coefficient	0.00014896	SE	pValue	Comment
β_0 Intercept	0.00014896	4.719e-06	1.1559e-21	significant
β_7 (T:C)	2.9431e-05	1.226e-05	0.02414	significant

There is a small effect of leaching temperature on the REE+Y selectivity. Low temperature leaching (20-50 °C) results in about 20% larger selectivity as compared to selectivity at higher temperature (90 °C). There is no such effect for scandium leaching selectivity.

2.7.2 Procedure

Before starting the 27 experiments for the leaching reactor design two steps were performed. The first step was the preparation of acid used once and twice since acid freshness is one of the factors in the 27 experiment design. The second step was the pretreatment of milled PCC fly ash with 10% sodium hydroxide at 90 °C and 1 hour reaction time. These conditions of caustic pretreatment were selected based on the results from previous testing (See Table 7).

Step 1 – Acid preparation:

Table 41 describes the amount of acid used once and twice that was needed for the 27 experiment design.

Table 41 - Amount of acid solution used once and twice needed for 27 experiment design.

Acid Preparation Requirements		
Acid concentration	Acid freshness	Volume of solution needed
34 wt %	Used once (1x)	1 liter
	Used twice (2x)	0.25 liters
51 wt %	Used once (1x)	1.75 liters
	Used twice (2x)	1 liter
68 wt %	Used once (1x)	1 liter
	Used twice (2x)	0.25 liters

Generation of 34% nitric acid solutions:

Nitric acid used once:

One and a half liters of fresh 34% nitric acid solution and 60 g of PCC fly ash was added to a 5 liter round bottom flask. Using an overhead mixer, the solution was mixed for 30 minutes at 300 rpm and room temperature. After the run was finished, the ash was allowed to settle for 10 minutes. Then, acid was filtered using a pressure filter system with 0.45-µm PVDF filter, and acid was collected. Three samples were taken to send for analysis by ICP-MS.

Nitric acid used twice:

Three hundred mL of used once 34% nitric acid solution and 12 grams of PCC fly ash was added to a 1-liter round-bottom flask. Using a stirring bar, the solution was mixed for 30 minutes at 300 rpm and room temperature. After run was finished, the ash was let to settled for 10 minutes. Then, acid was filtered using a pressure filter system with a 0.45-µm PVDF membrane, and acid was collected. Three samples were taken for analysis by ICP-MS.

Generation of 51% nitric acid solutions:

Nitric acid used once:

Three liters of fresh 51% nitric acid solution and 120 g of PCC fly ash were added to a 5-liter round-bottom flask. Using an overhead mixer, the solution was mixed for 30 minutes at 300 rpm and room temperature. After the run was finished, the ash was allowed to settle for 10 minutes. Then, acid was filtered using a pressure filter system with a 0.45-µm PVDF filter, and acid was collected. Three samples were taken to send for analysis by ICP-MS.

Nitric acid used twice:

One and one-tenth liters of used once 51% nitric acid solution and 44 g of PCC fly ash were added to a 5-liter round-bottom flask. Using an overhead mixer, the solution was mixed for 30 minutes at 300 rpm and room temperature. After the run was finished, the ash was allowed to settle for 10 minutes. Then, acid was filtered using a pressure filter system with a 0.45-µm PVDF filter, and acid was collected. Three samples were taken to send for analysis by ICP-MS.

Note: All 51% samples were diluted to ~34% nitric acid for shipping regulatory reasons. The dilution was done by volume: 8 mL of nitric acid solution and 4 mL of DI water.

Generation of 68% nitric acid solutions:

Nitric acid used once:

One and a half liters of fresh 68% nitric acid solution and 60 g of PCC fly ash were added to a 5-liter round-bottom flask. Using an overhead mixer, the solution was mixed for 30 minutes at 300 rpm and room temperature. After the run was finished, the ash was allowed to settle for 10 minutes. Then, acid was filtered using a pressure filter system with a 0.45-µm PVDF filter, and acid was collected. Three samples were taken to send for analysis by ICP-MS.

Nitric acid used twice:

Three hundred mL of used once 68% nitric acid solution and 12 g of PCC fly ash were added to a 1-liter round-bottom flask. Using a stirring bar, the solution was mixed for 30 minutes at 300 rpm and room temperature. After the run was finished, the ash was allowed to settle for 10 minutes. Then, acid was filtered using a pressure filter system with a 0.45-µm PVDF filter, and acid was collected. Three samples were taken to send for analysis by ICP-MS.

Note: All 68% samples were diluted to 34% nitric acid for shipping regulatory reasons. The dilution was done by volume: 6 mL of nitric acid solution and 6 mL of DI water.

Step 2 – Pretreatment of ash with 10% sodium hydroxide:

Four liters of 10% sodium hydroxide were prepared and added to a 5-liter round-bottom flask. After the solution reached the desired temperature (90 °C), 170 grams of milled PCC fly ash (4.1 µm average particle size) was added and mixed for 1 hour at 700 rpm using an overhead mixer. At the end of the reaction period, the caustic solution was filtered using a pressure filter system with a 0.45-µm PVDF filter. This procedure was done twice to generate the ash needed for testing. Then, the ash was collected and washed with 4 liters of DI water in a round bottom flask using an overhead mixer. The solution was mixed for 5 minutes and then filtered using a pressure filter system with a 0.45-µm PVDF filter. The washing procedure was repeated until solution reached a pH lower than eleven (pH 10.5 was reached after three washes). The amount of ash before caustic pretreatment was 340.0 grams. After caustic pretreatment, washing, and drying for two days at 110 °C, the final amount of ash pretreated with 10% sodium hydroxide was 270.2 grams.

After the acid preparation step and ash pretreatment step, the 27 experiments were done in a random order, and each test followed the same set up and procedure described previously (See Section 2.2 and Figure 1). Table 42 shows the condition of each run for the 27 experiment design:

Table 42 - Conditions for the 27 experiment design

Experimental Design Conditions				
Run	Leaching time (min)	Temperature (°C)	Acid concentration (wt%)	Number of Acid Contacts with Ash
1	1	20	51	1
2	30	55	34	1
3	15	20	51	0
4	15	20	34	1
5	15	20	51	2
6	15	90	51	0
7	15	90	34	1
8	30	90	51	1
9	15	55	34	2
10	15	55	34	0
11	1	90	51	1
12	30	20	51	1
13	15	20	68	1
14	15	90	51	2
15	1	55	51	2
16	30	55	51	0
17	15	55	51	1
18	15	55	51	1
19	1	55	34	1
20	15	55	51	1
21	30	55	68	1
22	1	55	51	0
23	15	90	68	1
24	15	55	68	0
25	15	55	68	2
26	1	55	68	1
27	30	55	51	2

Run 1 will be taken as an example for detailed description of the experiment. 250 mL of 51% nitric acid solution used once was added to a 1-liter round-bottom flask. After the solution reached the desired temperature, in this case 20 °C, 9 grams of pretreated ash was added. The reaction was run for 1 minute using a stirring bar at a speed of 450 rpm. The nitric acid solution was filtered using a pressure filter system with a 0.45-µm PVDF filter. A 10 mL sample was sent for ICP-MS analysis at Activation Laboratories.

Note: Samples of 51% and 68% were diluted to 34% nitric acid solution for shipping restriction purpose. The dilution was done by volume: 8 mL of nitric acid solution and 4 mL of DI water (51% nitric acid samples), 6 mL of nitric acid solution and 6 mL of DI water (68% nitric acid samples).

3.0 Conclusions and Next Steps

Based on the laboratory testing, ball milling and caustic pretreatment of the ash allows for high recovery of REE, with leaching efficiencies for scandium as high as 86% and near complete recovery of total REE as a weighted average. Milling of the ash to approximately 4-5 µm allows these recoveries to be realized with only a 60 minute contact with 10% sodium hydroxide solution at 90 °C, and leaching in 34% nitric acid for 30 minutes at 90°C. Traditional aluminosilicate recovery from fly ash requires a caustic leach of 6 hours or more (Hollman, Steenbruggen, & Janssen-Jurkovicova, 1999), so this method represents a significant decrease in reaction time. The acid leaching reaction is slightly exothermic, at approximately 102 calories per gram of ash leached, which will reduce energy costs to heat the leach reactor.

Additionally, the caustic pretreatment leach should allow for production of a zeolite byproduct that can be used as an adsorbent or catalyst support material, reducing waste streams and increasing the revenue. A zeolite material was made in the lab with the milled fly ash, but additional work needs to be done in Phase 2 to make a higher value zeolite with the use of seed material or zeolite scaffolds.

A first recovery of the rare earth elements by thermal roasting of the loaded acid can oxidize the iron and aluminum between 100 °C and 200 °C, generating an insoluble oxide material. In testing with actual leach solutions, 90% of the REE could be recovered from the roasted solids with a water leach, while omitting over 90% of the iron and aluminum, and over 60% of the uranium and thorium. The water leach had a concentration of 1.2% REE, effectively leading to over a 20x increase in purity of the REE over the fly ash feed.

Solvent extraction testing suggested that extraction for REE is satisfactory at pH of 3.4, where 61% of REEs are extracted at over 7% purity (over 120x concentration over the feed fly ash). The primary contaminants were sodium (due to a high starting concentration), aluminum, silica, calcium, and iron, but sodium, potassium, magnesium, and calcium were largely excluded from the extract. At pH 5, near quantitative REE can be achieved (over 99%), including less valuable lanthanum and cerium, but purity drops to about 1.0% in the extract. In selective stripping tests, the REE were stripped in hydrochloric acid at around one molar. The scandium is expected to be recoverable by precipitating in sodium carbonate solution. These REE solutions could then be separated with commercial operations such as further solvent extraction or ion exchange, or an emerging technology could be used such as electrowinning or electrophoresis.

The results of the laboratory testing were used in the updated technoeconomic assessment model to predict the economics of the process, and they were used in the design of a continuous bench scale unit that integrates all of the operations. The key parameters that were used are a one-hour leach in 10% sodium hydroxide at 90 °C, with fly ash milled to ~4.5 µm, then acid leaching in 34% nitric acid at 90 °C. The loaded acid will be roasted at 150 °C to calcine iron and aluminum, separating them from REE in a water wash. This loaded water will be extracted at pH 3.5-4.0, scrubbed around pH 3.5 to remove base metals, stripped with 1 molar hydrochloric acid to recover REE, scrubbed with 2 M HCl to remove iron, then scandium recovered by precipitation with 10% sodium carbonate solution. Additional work to improve the stripping process will be done in pending Phase 2 testing.

The integrated continuous testing will investigate the impact of recycle streams on the process, which will introduce concentration cycles of contaminants and reduced acid and caustic strengths. Finally, the next phase will include optimization of zeolite production to generate a saleable, high value zeolite product.

4.0 References

Bartholomew, C. H., & Farrauto, R. J. (2006). *Fundamentals of Industrial Catalytic Processes, Second Edition.* Hoboken: John Wiley and Sons.

Battelle. (2016). *Recovery of Rare Earth Elements from Coal and Coal Byproducts via a Closed Loop Leaching Process: Sampling and Characterization Report.* Morgantown: National Energy Technology Laboratory.

Battelle. (2017). *Recovery of Rare Earth Elements from Coal and Coal Byproducts via a Closed Loop Leaching Process: Feasibility Study Report.* Morgantown: National Energy Technology Laboratory.

Box, G., & Behnken, D. (1960). Some New Three Level Designs for the Study of Quantitative Variables. *Technometrics*, 455-475.

Cytec. (2017, April 15). *CYANEX 572 Solvent Extraction Reagent.* Retrieved from Cytec: https://www.cytec.com/sites/default/files/files/CYTEC_CYANEX_572_FINAL.pdf

Fukui, K., Katoh, M., Yamamoto, T., & Yoshida, H. (2009). Utilization of NaCl for Phillipsite Synthesis from Fly Ash by Hydrothermal Treatment with Microwave Heating. *Adv. Powder Technol.*, 35-40.

Hollman, G., Steenbruggen, G., & Janssen-Jurkovicova, M. (1999). A Two-Step Process for the Synthesis of Zeolites from Coal Ash. *Fuel*, 1225-1230.

Huheey, J. E. (1978). *Inorganic Chemistry: Principles of Structure and Reactivity.* New York: Harper International.

Jha, B., & Singh, D. (2016). *Fly Ash Zeolites: Innovations, Applications, and Directions.* Singapore: Springer Science.

Kolay, P., & Singh, D. (2002). Characterization of Alkali Activated Lagoon Ash and its Application for Heavy Metal Retention. *Fuel*, 483-489.

Kumar, P., Mal, N., Oumi, Y., Yamanaa, K., & Sanoc, T. (2001). Mesoporous Materials Prepared Using Coal Fly Ash as the Silicon and Aluminum Source. *J. Mater. Chem.*, 3285-3290.

mineralprices.com. (2016, December). Retrieved April 14, 2016, from http://mineralprices.com/

Murayama, N., Yamamoto, H., & Shibata, J. (2002). Mechanism of Zeolite Synthesis from Coal Fly Ash by Alkali Hydrothermal Reaction. *Inter. J. Miner. Process.*, 1-17.

Park, M., Choi, C. L., Lim, W. T., Kim, M. C., Choi, J., & Heo, N. H. (2000). Molten-Salt Method for the Synthesis of Zeolitic Materials: I. Zeolite Formation in Alkaline Molten-Salt System. *Microporous and Mesoporous Materials*, 81-89.

Rayalu, S., Meshram, S., & Hasan, M. (2000). Highly Crystalline Faujasitic Zeolites from Fly Ash. *J. Hazardous Material*, 123-131.

Yuvaraj, S., Fan-Yuan, L., Tsong-Huei, C., & Chuin-Tih, Y. (2003). Thermal Decomposition of Metal Nitrates in Air and Hydrogen Environments. *J. Phys. Chem. B*, 1044-1047.

Appendices

Appendix A: Laboratory Test Plan

Appendix B: Rare Earth Extraction Results and Calculations

The results from ICP-MS solution analysis are given in micrograms per liter. Solid results are given in ppm. Some results were below detection limit. Consequently, detection limits were used for the analysis of the data obtained (highlighted in green). Also, mass calculated for some of the species were negative. Therefore, any negative calculation was assumed to be zero (highlighted in red).

The first calculations made were for the roasting part of the experiment. First, the mass in residual and solution loaded for each specie were calculated using Equation 2 and Equation 3 respectively. Second, total mass of each specie before roasting was calculated using Equation 1, and percent recovery in solution loaded and residual were calculated using Equation 4 and Equation 5 respectively.

$$\boldsymbol{Total\ mass\ of\ specie\ before\ roasting, \mu g = mass\ of\ specie\ in\ residual, \mu g + mass\ of\ specie\ in\ solution, \mu g}$$

Equation 1

$$\boldsymbol{mass\ of\ specie\ in\ residual, \mu g = mass\ of\ residual\ material, g \times specie\ concentration, ppm}$$

Equation 2

$$\boldsymbol{mass\ of\ specie\ in\ solution\ loaded, \mu g = \frac{Solution\ loaded\ volume, ml}{1000} \times specie\ concentration, \frac{\mu g}{L}}$$

Equation 3

$$\boldsymbol{\%Recovery\ in\ solution\ loaded = \frac{mass\ of\ specie\ in\ solution\ loaded, \mu g}{Total\ mass\ of\ specie\ before\ roasting, \mu g} \times 100}$$

Equation 4

$$\boldsymbol{\%Recovery\ in\ residual = \frac{mass\ of\ specie\ in\ residual, \mu g}{Total\ mass\ of\ specie\ before\ roasting, \mu g} \times 100}$$

Equation 5

For extraction calculations, the mass of each specie in the aqueous and the extractant were calculated using Equation 6 and Equation 7 respectively. Then, Equation 8 and Equation 9 were used to calculate the percent recoveries of each specie in the aqueous and extractant. Lastly, the selectivity and recovery of rear earths plus scandium and Yttrium were calculated using Equation 10 and Equation 11

$$\boldsymbol{mass\ of\ specie\ in\ aqueous, \mu g = \frac{Solution\ volume, ml}{1000} \times specie\ concentration, \frac{\mu g}{L}}$$

Equation 6

$$\boldsymbol{mass\ of\ specie\ in\ extractant, \mu g = \left(mass\ of\ specie\ in\ solution\ loaded, \mu g \times \frac{Solution\ volume, ml}{Solution\ loaded\ volume, ml}\right) - mass\ of\ specie\ in\ aqueous, \mu g}$$

Equation 7

$$\%\boldsymbol{Recovery\ in\ aqueous} = \frac{\boldsymbol{mass\ of\ specie\ in\ aqueous, \mu g}}{\boldsymbol{mass\ of\ specie\ in\ solution\ loaded, \mu g} \times \frac{\boldsymbol{Solution\ volume, ml}}{\boldsymbol{Solution\ loaded\ volume, ml}}} \times \mathbf{100}$$

Equation 8

$$\%\boldsymbol{Recovery\ in\ extractant} = \frac{\boldsymbol{mass\ of\ specie\ in\ extractant, \mu g}}{\boldsymbol{mass\ of\ specie\ in\ solution\ loaded, \mu g} \times \frac{\boldsymbol{Solution\ volume, ml}}{\boldsymbol{Solution\ loaded\ volume, ml}}} \times \mathbf{100}$$

Equation 9

$$\boldsymbol{REE + Sc + Y\ selectivity} = \frac{\sum \boldsymbol{mass\ of\ REE + Sc + Y, \mu g}}{\sum \boldsymbol{mass\ of\ all\ species, \mu g}} \times \mathbf{100}$$

Equation 10

$$\%\boldsymbol{Recovery\ of\ REE + Sc + Y} = \frac{\sum \boldsymbol{mass\ of\ REE + Sc + Y, \mu g}}{\sum \boldsymbol{mass\ of\ specie\ in\ solution\ loaded, \mu g}} \times \mathbf{100}$$

Equation 11

Table 43 – Results and calculations for species analyzed in extraction experiment. Note that green highlighted cells are the reported detection limits, while cells in red were adjusted to zero because the mass balance left a negative mass in the extractant phase due to analytical errors.

			Na				Li			
Description	**Mass of solid, g**	**Solution volume, mL**	**µg/L**	**Mass, µg**	**% Recovery**	**% of measured Solutes**	**µg/L**	**Mass, µg**	**% Recovery**	**% of measured Solutes**
Residual material + Solution loaded (Start)				194780				2065		
Residual material after roasting at 200C	3.2			33280	17.09%	2.34%			0.00%	0.00%
Solution loaded after roasting at 200C (REEs)		250	646000	161500	82.91%	16.48%	8260	2065	100.00%	0.21%
pH 1.03 (Aqueous)		25	595000	14875	92.11%	16.60%	7710	192.75	93.34%	0.22%
Mass in Extractant				1275	7.89%	14.93%		13.75	6.66%	0.16%
pH 2.04 (Aqueous)		25	900000	22500	139.32%	18.59%	9990	249.75	120.94%	0.21%
Mass in Extractant				0	0.00%	0.00%		0	0.00%	0.00%
pH 2.51 (Aqueous)		25	1190000	29750	184.21%	24.66%	9680	242	117.19%	0.20%
Mass in Extractant				0	0.00%	0.00%		0	0.00%	0.00%
pH 3.34 (Aqueous)		25	727000	18175	112.54%	17.37%	9300	232.5	112.59%	0.22%
Mass in Extractant				0	0.00%	0.00%		0	0.00%	0.00%
pH 4.01 (Aqueous)		15	1370000	20550	212.07%	53.26%	4370	65.55	52.91%	0.17%
Mass in Extractant				0	0.00%	0.00%		58.35	47.09%	0.19%
pH 4.48 (Aqueous)		15	1780000	26700	275.54%	53.93%	5030	75.45	60.90%	0.15%
Mass in Extractant				0	0.00%	0.00%		48.45	39.10%	0.18%
pH 4.99 (Aqueous)		15	1950000	29250	301.86%	57.37%	4990	74.85	60.41%	0.15%
Mass in Extractant				0	0.00%	0.00%		49.05	39.59%	0.18%

Table 44 – Results and calculations for species analyzed in extraction experiment continued

			Be				Mg			
Description	**Mass of solid, g**	**Solution volume, mL**	**µg/L**	**Mass, µg**	**% Recovery**	**% of measured Solutes**	**µg/L**	**Mass, µg**	**% Recovery**	**% of measured Solutes**
Residual material + Solution loaded (Start)				239.35				51040		
Residual material after roasting at 200C	3.2			105.6	44.12%	0.01%		7040	13.79%	0.49%
Solution loaded after roasting at 200C (REEs)		250	535	133.75	55.88%	0.01%	176000	44000	86.21%	4.49%
pH 1.03 (Aqueous)		25	443	11.075	82.80%	0.01%	172000	4300	97.73%	4.80%
Mass in Extractant				2.3	17.20%	0.03%		100	2.27%	1.17%
pH 2.04 (Aqueous)		25	296	7.4	55.33%	0.01%	240000	6000	136.36%	4.96%
Mass in Extractant				5.975	44.67%	0.10%		0	0.00%	0.00%
pH 2.51 (Aqueous)		25	277	6.925	51.78%	0.01%	230000	5750	130.68%	4.77%
Mass in Extractant				6.45	48.22%	0.11%		0	0.00%	0.00%
pH 3.34 (Aqueous)		25	363	9.075	67.85%	0.01%	208000	5200	118.18%	4.97%
Mass in Extractant				4.3	32.15%	0.11%		0	0.00%	0.00%
pH 4.01 (Aqueous)		15	2	0.03	0.37%	0.00%	94200	1413	53.52%	3.66%
Mass in Extractant				7.995	99.63%	0.03%		1227	46.48%	3.95%
pH 4.48 (Aqueous)		15	40	0.6	7.48%	0.00%	120000	1800	68.18%	3.64%
Mass in Extractant				7.425	92.52%	0.03%		840	31.82%	3.19%
pH 4.99 (Aqueous)		15	2	0.03	0.37%	0.00%	116000	1740	65.91%	3.41%
Mass in Extractant				7.995	99.63%	0.03%		900	34.09%	3.29%

Table 45 – Results and calculations for species analyzed in extraction experiment continued

			Al				Si			
Description	**Mass of solid, g**	**Solution volume, mL**	**µg/L**	**Mass, µg**	**% Recovery**	**% of measured Solutes**	**µg/L**	**Mass, µg**	**% Recovery**	**% of measured Solutes**
Residual material + Solution loaded (Start)				876270				197520		
Residual material after roasting at 200C	3.2			627520	71.61%	44.11%		147520	74.69%	10.37%
Solution loaded after roasting at 200C (REEs)		250	995000	248750	28.39%	25.38%	200000	50000	25.31%	5.10%
pH 1.03 (Aqueous)		25	924000	23100	92.86%	25.77%	80000	2000	40.00%	2.23%
Mass in Extractant				1775	7.14%	20.79%		3000	60.00%	35.14%
pH 2.04 (Aqueous)		25	1170000	29250	117.59%	24.17%	20000	500	10.00%	0.41%
Mass in Extractant				0	0.00%	0.00%		4500	90.00%	77.37%
pH 2.51 (Aqueous)		25	1040000	26000	104.52%	21.56%	20000	500	10.00%	0.41%
Mass in Extractant				0	0.00%	0.00%		4500	90.00%	77.65%
pH 3.34 (Aqueous)		25	987000	24675	99.20%	23.58%	100000	2500	50.00%	2.39%
Mass in Extractant				200	0.80%	4.91%		2500	50.00%	61.38%
pH 4.01 (Aqueous)		15	11900	178.5	1.20%	0.46%	4000	60	2.00%	0.16%
Mass in Extractant				14746.5	98.80%	47.42%		2940	98.00%	9.45%
pH 4.48 (Aqueous)		15	5310	79.65	0.53%	0.16%	80000	1200	40.00%	2.42%
Mass in Extractant				14845.35	99.47%	56.39%		1800	60.00%	6.84%
pH 4.99 (Aqueous)		15	260	3.9	0.03%	0.01%	4000	60	2.00%	0.12%
Mass in Extractant				14921.1	99.97%	54.46%		2940	98.00%	10.73%

Table 46 – Results and calculations for species analyzed in extraction experiment continued

			K				Ca			
Description	**Mass of solid, g**	**Solution volume, mL**	**µg/L**	**Mass, µg**	**% Recovery**	**% of measured Solutes**	**µg/L**	**Mass, µg**	**% Recovery**	**% of measured Solutes**
Residual material + Solution loaded (Start)				73190				409840		
Residual material after roasting at 200C	3.2			21440	29.29%	1.51%		19840	4.84%	1.39%
Solution loaded after roasting at 200C (REEs)		250	207000	51750	70.71%	5.28%	1560000	390000	95.16%	39.79%
pH 1.03 (Aqueous)		25	210000	5250	101.45%	5.86%	1510000	37750	96.79%	42.12%
Mass in Extractant				0	0.00%	0.00%		1250	3.21%	14.64%
pH 2.04 (Aqueous)		25	279000	6975	134.78%	5.76%	2130000	53250	136.54%	43.99%
Mass in Extractant				0	0.00%	0.00%		0	0.00%	0.00%
pH 2.51 (Aqueous)		25	257000	6425	124.15%	5.33%	1990000	49750	127.56%	41.25%
Mass in Extractant				0	0.00%	0.00%		0	0.00%	0.00%
pH 3.34 (Aqueous)		25	254000	6350	122.71%	6.07%	1820000	45500	116.67%	43.48%
Mass in Extractant				0	0.00%	0.00%		0	0.00%	0.00%
pH 4.01 (Aqueous)		15	125000	1875	60.39%	4.86%	935000	14025	59.94%	36.35%
Mass in Extractant				1230	39.61%	3.96%		9375	40.06%	30.15%
pH 4.48 (Aqueous)		15	152000	2280	73.43%	4.61%	1120000	16800	71.79%	33.94%
Mass in Extractant				825	26.57%	3.13%		6600	28.21%	25.07%
pH 4.99 (Aqueous)		15	152000	2280	73.43%	4.47%	1140000	17100	73.08%	33.54%
Mass in Extractant				825	26.57%	3.01%		6300	26.92%	23.00%

Table 47 – Results and calculations for species analyzed in extraction experiment continued

			Sc				Ti			
Description	**Mass of solid, g**	**Solution volume, mL**	**µg/L**	**Mass, µg**	**% Recovery**	**% of measured Solutes**	**µg/L**	**Mass, µg**	**% Recovery**	**% of measured Solutes**
Residual material + Solution loaded (Start)				576.4				48402		
Residual material after roasting at 200C	3.2			326.4	56.63%	0.02%		47872	98.91%	3.37%
Solution loaded after roasting at 200C (REEs)		250	1000	250	43.37%	0.03%	2120	530	1.09%	0.05%
pH 1.03 (Aqueous)		25	400	10	40.00%	0.01%	40	1	1.89%	0.00%
Mass in Extractant				15	60.00%	0.18%		52	98.11%	0.61%
pH 2.04 (Aqueous)		25	100	2.5	10.00%	0.00%	10	0.25	0.47%	0.00%
Mass in Extractant				22.5	90.00%	0.39%		52.75	99.53%	0.91%
pH 2.51 (Aqueous)		25	100	2.5	10.00%	0.00%	10	0.25	0.47%	0.00%
Mass in Extractant				22.5	90.00%	0.39%		52.75	99.53%	0.91%
pH 3.34 (Aqueous)		25	500	12.5	50.00%	0.01%	50	1.25	2.36%	0.00%
Mass in Extractant				12.5	50.00%	0.31%		51.75	97.64%	1.27%
pH 4.01 (Aqueous)		15	20	0.3	2.00%	0.00%	2	0.03	0.09%	0.00%
Mass in Extractant				14.7	98.00%	0.05%		31.77	99.91%	0.10%
pH 4.48 (Aqueous)		15	400	6	40.00%	0.01%	40	0.6	1.89%	0.00%
Mass in Extractant				9	60.00%	0.03%		31.2	98.11%	0.12%
pH 4.99 (Aqueous)		15	20	0.3	2.00%	0.00%	2	0.03	0.09%	0.00%
Mass in Extractant				14.7	98.00%	0.05%		31.77	99.91%	0.12%

Table 48 – Results and calculations for species analyzed in extraction experiment continued

			V				Cr			
Description	**Mass of solid, g**	**Solution volume, mL**	**µg/L**	**Mass, µg**	**% Recovery**	**% of measured Solutes**	**µg/L**	**Mass, µg**	**% Recovery**	**% of measured Solutes**
Residual material + Solution loaded (Start)				4771				1655		
Residual material after roasting at 200C	3.2			4688	98.26%	0.33%		1440	87.01%	0.10%
Solution loaded after roasting at 200C (REEs)		250	332	83	1.74%	0.01%	860	215	12.99%	0.02%
pH 1.03 (Aqueous)		25	270	6.75	81.33%	0.01%	759	18.975	88.26%	0.02%
Mass in Extractant				1.55	18.67%	0.02%		2.525	11.74%	0.03%
pH 2.04 (Aqueous)		25	132	3.3	39.76%	0.00%	985	24.625	114.53%	0.02%
Mass in Extractant				5	60.24%	0.09%		0	0.00%	0.00%
pH 2.51 (Aqueous)		25	110	2.75	33.13%	0.00%	818	20.45	95.12%	0.02%
Mass in Extractant				5.55	66.87%	0.10%		1.05	4.88%	0.02%
pH 3.34 (Aqueous)		25	63.3	1.5825	19.07%	0.00%	882	22.05	102.56%	0.02%
Mass in Extractant				6.7175	80.93%	0.16%		0	0.00%	0.00%
pH 4.01 (Aqueous)		15	2	0.03	0.60%	0.00%	183	2.745	12.77%	0.01%
Mass in Extractant				4.95	99.40%	0.02%		18.755	87.23%	0.06%
pH 4.48 (Aqueous)		15	40	0.6	12.05%	0.00%	241	3.615	16.81%	0.01%
Mass in Extractant				4.38	87.95%	0.02%		17.885	83.19%	0.07%
pH 4.99 (Aqueous)		15	2	0.03	0.60%	0.00%	190	2.85	13.26%	0.01%
Mass in Extractant				4.95	99.40%	0.02%		18.65	86.74%	0.07%

Table 49 – Results and calculations for species analyzed in extraction experiment continued

			Mn				Fe			
Description	**Mass of solid, g**	**Solution volume, mL**	**µg/L**	**Mass, µg**	**% Recovery**	**% of measured Solutes**	**µg/L**	**Mass, µg**	**% Recovery**	**% of measured Solutes**
Residual material + Solution loaded (Start)				2420.5				500775		
Residual material after roasting at 200C	3.2			928	38.34%	0.07%		491200	98.09%	34.53%
Solution loaded after roasting at 200C (REEs)		250	5970	1492.5	61.66%	0.15%	38300	9575	1.91%	0.98%
pH 1.03 (Aqueous)		25	5480	137	91.79%	0.15%	4000	100	10.44%	0.11%
Mass in Extractant				12.25	8.21%	0.14%		857.5	89.56%	10.04%
pH 2.04 (Aqueous)		25	7900	197.5	132.33%	0.16%	1000	25	2.61%	0.02%
Mass in Extractant				0	0.00%	0.00%		932.5	97.39%	16.03%
pH 2.51 (Aqueous)		25	7510	187.75	125.80%	0.16%	1000	25	2.61%	0.02%
Mass in Extractant				-38.5	-25.80%	-0.66%		932.5	97.39%	16.09%
pH 3.34 (Aqueous)		25	6360	159	106.53%	0.15%	5000	125	13.05%	0.12%
Mass in Extractant				0	0.00%	0.00%		832.5	86.95%	20.44%
pH 4.01 (Aqueous)		15	3100	46.5	51.93%	0.12%	200	3	0.52%	0.01%
Mass in Extractant				43.05	48.07%	0.14%		571.5	99.48%	1.84%
pH 4.48 (Aqueous)		15	3790	56.85	63.48%	0.11%	4000	60	10.44%	0.12%
Mass in Extractant				32.7	36.52%	0.12%		514.5	89.56%	1.95%
pH 4.99 (Aqueous)		15	3660	54.9	61.31%	0.11%	200	3	0.52%	0.01%
Mass in Extractant				34.65	38.69%	0.13%		571.5	99.48%	2.09%

Table 50 – Results and calculations for species analyzed in extraction experiment continued

			Co				Ni			
Description	**Mass of solid, g**	**Solution volume, mL**	**µg/L**	**Mass, µg**	**% Recovery**	**% of measured Solutes**	**µg/L**	**Mass, µg**	**% Recovery**	**% of measured Solutes**
Residual material + Solution loaded (Start)				232.7				633		
Residual material after roasting at 200C	3.2			35.2	15.13%	0.00%		128	20.22%	0.01%
Solution loaded after roasting at 200C (REEs)		250	790	197.5	84.87%	0.02%	2020	505	79.78%	0.05%
pH 1.03 (Aqueous)		25	776	19.4	98.23%	0.02%	2010	50.25	99.50%	0.06%
Mass in Extractant				0.35	1.77%	0.00%		0.25	0.50%	0.00%
pH 2.04 (Aqueous)		25	1010	25.25	127.85%	0.02%	2340	58.5	115.84%	0.05%
Mass in Extractant				0	0.00%	0.00%		0	0.00%	0.00%
pH 2.51 (Aqueous)		25	978	24.45	123.80%	0.02%	2230	55.75	110.40%	0.05%
Mass in Extractant				0	0.00%	0.00%		0	0.00%	0.00%
pH 3.34 (Aqueous)		25	895	22.375	113.29%	0.02%	2160	54	106.93%	0.05%
Mass in Extractant				0	0.00%	0.00%		0	0.00%	0.00%
pH 4.01 (Aqueous)		15	401	6.015	50.76%	0.02%	940	14.1	46.53%	0.04%
Mass in Extractant				5.835	49.24%	0.02%		16.2	53.47%	0.05%
pH 4.48 (Aqueous)		15	482	7.23	61.01%	0.01%	1240	18.6	61.39%	0.04%
Mass in Extractant				4.62	38.99%	0.02%		11.7	38.61%	0.04%
pH 4.99 (Aqueous)		15	460	6.9	58.23%	0.01%	1110	16.65	54.95%	0.03%
Mass in Extractant				4.95	41.77%	0.02%		13.65	45.05%	0.05%

Table 51 – Results and calculations for species analyzed in extraction experiment continued

			Cu				Zn			
Description	**Mass of solid, g**	**Solution volume, mL**	**µg/L**	**Mass, µg**	**% Recovery**	**% of measured Solutes**	**µg/L**	**Mass, µg**	**% Recovery**	**% of measured Solutes**
Residual material + Solution loaded (Start)				1614				1700		
Residual material after roasting at 200C	3.2			704	43.62%	0.05%		160	9.41%	0.01%
Solution loaded after roasting at 200C (REEs)		250	3640	910	56.38%	0.09%	6160	1540	90.59%	0.16%
pH 1.03 (Aqueous)		25	3580	89.5	98.35%	0.10%	5820	145.5	94.48%	0.16%
Mass in Extractant				1.5	1.65%	0.02%		8.5	5.52%	0.10%
pH 2.04 (Aqueous)		25	4740	118.5	130.22%	0.10%	4460	111.5	72.40%	0.09%
Mass in Extractant				0	0.00%	0.00%		42.5	27.60%	0.73%
pH 2.51 (Aqueous)		25	4590	114.75	126.10%	0.10%	3900	97.5	63.31%	0.08%
Mass in Extractant				0	0.00%	0.00%		56.5	36.69%	0.97%
pH 3.34 (Aqueous)		25	4040	101	110.99%	0.10%	1790	44.75	29.06%	0.04%
Mass in Extractant				0	0.00%	0.00%		109.25	70.94%	2.68%
pH 4.01 (Aqueous)		15	1350	20.25	37.09%	0.05%	213	3.195	3.46%	0.01%
Mass in Extractant				34.35	62.91%	0.11%		89.205	96.54%	0.29%
pH 4.48 (Aqueous)		15	1340	20.1	36.81%	0.04%	236	3.54	3.83%	0.01%
Mass in Extractant				34.5	63.19%	0.13%		88.86	96.17%	0.34%
pH 4.99 (Aqueous)		15	304	4.56	8.35%	0.01%	56.1	0.8415	0.91%	0.00%
Mass in Extractant				50.04	91.65%	0.18%		91.5585	99.09%	0.33%

Table 52 – Results and calculations for species analyzed in extraction experiment continued

			Ga				Ge			
Description	**Mass of solid, g**	**Solution volume, mL**	**µg/L**	**Mass, µg**	**% Recovery**	**% of measured Solutes**	**µg/L**	**Mass, µg**	**% Recovery**	**% of measured Solutes**
Residual material + Solution loaded (Start)				824.9				632.55		
Residual material after roasting at 200C	3.2			502.4	60.90%	0.04%		524.8	82.97%	0.04%
Solution loaded after roasting at 200C (REEs)		250	1290	322.5	39.10%	0.03%	431	107.75	17.03%	0.01%
pH 1.03 (Aqueous)		25	921	23.025	71.40%	0.03%	354	8.85	82.13%	0.01%
Mass in Extractant				9.225	28.60%	0.11%		1.925	17.87%	0.02%
pH 2.04 (Aqueous)		25	1500	37.5	116.28%	0.03%	518	12.95	120.19%	0.01%
Mass in Extractant				0	0.00%	0.00%		0	0.00%	0.00%
pH 2.51 (Aqueous)		25	1410	35.25	109.30%	0.03%	474	11.85	109.98%	0.01%
Mass in Extractant				0	0.00%	0.00%		0	0.00%	0.00%
pH 3.34 (Aqueous)		25	491	12.275	38.06%	0.01%	291	7.275	67.52%	0.01%
Mass in Extractant				19.975	61.94%	0.49%		3.5	32.48%	0.09%
pH 4.01 (Aqueous)		15	25.6	0.384	1.98%	0.00%	68.1	1.0215	15.80%	0.00%
Mass in Extractant				18.966	98.02%	0.06%		5.4435	84.20%	0.02%
pH 4.48 (Aqueous)		15	14.2	0.213	1.10%	0.00%	39.5	0.5925	9.16%	0.00%
Mass in Extractant				19.137	98.90%	0.07%		5.8725	90.84%	0.02%
pH 4.99 (Aqueous)		15	0.78	0.0117	0.06%	0.00%	3.29	0.04935	0.76%	0.00%
Mass in Extractant				19.3383	99.94%	0.07%		6.41565	99.24%	0.02%

Table 53 – Results and calculations for species analyzed in extraction experiment continued

			As				Se			
Description	**Mass of solid, g**	**Solution volume, mL**	**µg/L**	**Mass, µg**	**% Recovery**	**% of measured Solutes**	**µg/L**	**Mass, µg**	**% Recovery**	**% of measured Solutes**
Residual material + Solution loaded (Start)				8845				270		
Residual material after roasting at 200C	3.2			8160	92.26%	0.57%			0.00%	0.00%
Solution loaded after roasting at 200C (REEs)		250	2740	685	7.74%	0.07%	1080	270	100.00%	0.03%
pH 1.03 (Aqueous)		25	2600	65	94.89%	0.07%	860	21.5	79.63%	0.02%
Mass in Extractant				3.5	5.11%	0.04%		5.5	20.37%	0.06%
pH 2.04 (Aqueous)		25	3380	84.5	123.36%	0.07%	265	6.625	24.54%	0.01%
Mass in Extractant				0	0.00%	0.00%		20.375	75.46%	0.35%
pH 2.51 (Aqueous)		25	3110	77.75	113.50%	0.06%	231	5.775	21.39%	0.00%
Mass in Extractant				0	0.00%	0.00%		21.225	78.61%	0.37%
pH 3.34 (Aqueous)		25	2170	54.25	79.20%	0.05%	100	2.5	9.26%	0.00%
Mass in Extractant				14.25	20.80%	0.35%		24.5	90.74%	0.60%
pH 4.01 (Aqueous)		15	16.4	0.246	0.60%	0.00%	20.9	0.3135	1.94%	0.00%
Mass in Extractant				40.854	99.40%	0.13%		15.8865	98.06%	0.05%
pH 4.48 (Aqueous)		15	32.4	0.486	1.18%	0.00%	80	1.2	7.41%	0.00%
Mass in Extractant				40.614	98.82%	0.15%		15	92.59%	0.06%
pH 4.99 (Aqueous)		15	12.8	0.192	0.47%	0.00%	14.8	0.222	1.37%	0.00%
Mass in Extractant				40.908	99.53%	0.15%		15.978	98.63%	0.06%

Table 54 – Results and calculations for species analyzed in extraction experiment continued

			Rb				Sr			
Description	**Mass of solid, g**	**Solution volume, mL**	**µg/L**	**Mass, µg**	**% Recovery**	**% of measured Solutes**	**µg/L**	**Mass, µg**	**% Recovery**	**% of measured Solutes**
Residual material + Solution loaded (Start)				373				10396.2		
Residual material after roasting at 200C	3.2			48	12.87%	0.00%		771.2	7.42%	0.05%
Solution loaded after roasting at 200C (REEs)		250	1300	325	87.13%	0.03%	38500	9625	92.58%	0.98%
pH 1.03 (Aqueous)		25	1120	28	86.15%	0.03%	37800	945	98.18%	1.05%
Mass in Extractant				4.5	13.85%	0.05%		17.5	1.82%	0.20%
pH 2.04 (Aqueous)		25	1450	36.25	111.54%	0.03%	49500	1237.5	128.57%	1.02%
Mass in Extractant				0	0.00%	0.00%		0	0.00%	0.00%
pH 2.51 (Aqueous)		25	1430	35.75	110.00%	0.03%	46500	1162.5	120.78%	0.96%
Mass in Extractant				0	0.00%	0.00%		0	0.00%	0.00%
pH 3.34 (Aqueous)		25	1260	31.5	96.92%	0.03%	42700	1067.5	110.91%	1.02%
Mass in Extractant				1	3.08%	0.02%		0	0.00%	0.00%
pH 4.01 (Aqueous)		15	597	8.955	45.92%	0.02%	18300	274.5	47.53%	0.71%
Mass in Extractant				10.545	54.08%	0.03%		303	52.47%	0.97%
pH 4.48 (Aqueous)		15	789	11.835	60.69%	0.02%	23100	346.5	60.00%	0.70%
Mass in Extractant				7.665	39.31%	0.03%		231	40.00%	0.88%
pH 4.99 (Aqueous)		15	798	11.97	61.38%	0.02%	23500	352.5	61.04%	0.69%
Mass in Extractant				7.53	38.62%	0.03%		225	38.96%	0.82%

Table 55 – Results and calculations for species analyzed in extraction experiment continued

			Y				Zr			
Description	**Mass of solid, g**	**Solution volume, mL**	**µg/L**	**Mass, µg**	**% Recovery**	**% of measured Solutes**	**µg/L**	**Mass, µg**	**% Recovery**	**% of measured Solutes**
Residual material + Solution loaded (Start)				1248.9				219.2		
Residual material after roasting at 200C	3.2			166.4	13.32%	0.01%		208	94.89%	0.01%
Solution loaded after roasting at 200C (REEs)		250	4330	1082.5	86.68%	0.11%	44.8	11.2	5.11%	0.00%
pH 1.03 (Aqueous)		25	1370	34.25	31.64%	0.04%	25.9	0.6475	57.81%	0.00%
Mass in Extractant				74	68.36%	0.87%		0.4725	42.19%	0.01%
pH 2.04 (Aqueous)		25	8.93	0.22325	0.21%	0.00%	3.65	0.09125	8.15%	0.00%
Mass in Extractant				108.02675	99.79%	1.86%		1.02875	91.85%	0.02%
pH 2.51 (Aqueous)		25	9.34	0.2335	0.22%	0.00%	3.29	0.08225	7.34%	0.00%
Mass in Extractant				108.0165	99.78%	1.86%		1.03775	92.66%	0.02%
pH 3.34 (Aqueous)		25	9.54	0.2385	0.22%	0.00%	21.5	0.5375	47.99%	0.00%
Mass in Extractant				108.0115	99.78%	2.65%		0.5825	52.01%	0.01%
pH 4.01 (Aqueous)		15	5.11	0.07665	0.12%	0.00%	0.2	0.003	0.45%	0.00%
Mass in Extractant				64.87335	99.88%	0.21%		0.669	99.55%	0.00%
pH 4.48 (Aqueous)		15	1	0.015	0.02%	0.00%	4	0.06	8.93%	0.00%
Mass in Extractant				64.935	99.98%	0.25%		0.612	91.07%	0.00%
pH 4.99 (Aqueous)		15	0.06	0.0009	0.00%	0.00%	0.2	0.003	0.45%	0.00%
Mass in Extractant				64.9491	100.00%	0.24%		0.669	99.55%	0.00%

Table 56 – Results and calculations for species analyzed in extraction experiment continued

			Nb				Mo			
Description	**Mass of solid, g**	**Solution volume, mL**	**µg/L**	**Mass, µg**	**% Recovery**	**% of measured Solutes**	**µg/L**	**Mass, µg**	**% Recovery**	**% of measured Solutes**
Residual material + Solution loaded (Start)				14.05				1532.6		
Residual material after roasting at 200C	3.2			12.8	91.10%	0.00%		1497.6	97.72%	0.11%
Solution loaded after roasting at 200C (REEs)		250	5	1.25	8.90%	0.00%	140	35	2.28%	0.00%
pH 1.03 (Aqueous)		25	2	0.05	40.00%	0.00%	40	1	28.57%	0.00%
Mass in Extractant				0.075	60.00%	0.00%		2.5	71.43%	0.03%
pH 2.04 (Aqueous)		25	37.9	0.9475	758.00%	0.00%	10	0.25	7.14%	0.00%
Mass in Extractant				0	0.00%	0.00%		3.25	92.86%	0.06%
pH 2.51 (Aqueous)		25	35.1	0.8775	702.00%	0.00%	10	0.25	7.14%	0.00%
Mass in Extractant				0	0.00%	0.00%		3.25	92.86%	0.06%
pH 3.34 (Aqueous)		25	3	0.075	60.00%	0.00%	50	1.25	35.71%	0.00%
Mass in Extractant				0.05	40.00%	0.00%		2.25	64.29%	0.06%
pH 4.01 (Aqueous)		15	0.1	0.0015	2.00%	0.00%	2	0.03	1.43%	0.00%
Mass in Extractant				0.0735	98.00%	0.00%		2.07	98.57%	0.01%
pH 4.48 (Aqueous)		15	2	0.03	40.00%	0.00%	40	0.6	28.57%	0.00%
Mass in Extractant				0.045	60.00%	0.00%		1.5	71.43%	0.01%
pH 4.99 (Aqueous)		15	0.1	0.0015	2.00%	0.00%	2	0.03	1.43%	0.00%
Mass in Extractant				0.0735	98.00%	0.00%		2.07	98.57%	0.01%

Table 57 – Results and calculations for species analyzed in extraction experiment continued

			Ag				Cd			
Description	**Mass of solid, g**	**Solution volume, mL**	**µg/L**	**Mass, µg**	**% Recovery**	**% of measured Solutes**	**µg/L**	**Mass, µg**	**% Recovery**	**% of measured Solutes**
Residual material + Solution loaded (Start)				51.6				24.15		
Residual material after roasting at 200C	3.2			1.6	3.10%	0.00%			0.00%	0.00%
Solution loaded after roasting at 200C (REEs)		250	200	50	96.90%	0.01%	96.6	24.15	100.00%	0.00%
pH 1.03 (Aqueous)		25	80	2	40.00%	0.00%	86.2	2.155	89.23%	0.00%
Mass in Extractant				3	60.00%	0.04%		0.26	10.77%	0.00%
pH 2.04 (Aqueous)		25	20	0.5	10.00%	0.00%	142	3.55	147.00%	0.00%
Mass in Extractant				4.5	90.00%	0.08%		0	0.00%	0.00%
pH 2.51 (Aqueous)		25	20	0.5	10.00%	0.00%	135	3.375	139.75%	0.00%
Mass in Extractant				4.5	90.00%	0.08%		0	0.00%	0.00%
pH 3.34 (Aqueous)		25	100	2.5	50.00%	0.00%	93.9	2.3475	97.20%	0.00%
Mass in Extractant				2.5	50.00%	0.06%		0.0675	2.80%	0.00%
pH 4.01 (Aqueous)		15	4	0.06	2.00%	0.00%	39.6	0.594	40.99%	0.00%
Mass in Extractant				2.94	98.00%	0.01%		0.855	59.01%	0.00%
pH 4.48 (Aqueous)		15	80	1.2	40.00%	0.00%	52	0.78	53.83%	0.00%
Mass in Extractant				1.8	60.00%	0.01%		0.669	46.17%	0.00%
pH 4.99 (Aqueous)		15	4	0.06	2.00%	0.00%	43.1	0.6465	44.62%	0.00%
Mass in Extractant				2.94	98.00%	0.01%		0.8025	55.38%	0.00%

Table 58 – Results and calculations for species analyzed in extraction experiment continued

			In				Sn			
Description	**Mass of solid, g**	**Solution volume, mL**	**µg/L**	**Mass, µg**	**% Recovery**	**% of measured Solutes**	**µg/L**	**Mass, µg**	**% Recovery**	**% of measured Solutes**
Residual material + Solution loaded (Start)				2.7				89		
Residual material after roasting at 200C	3.2			2.24	82.96%	0.00%		64	71.91%	0.00%
Solution loaded after roasting at 200C (REEs)		250	1.84	0.46	17.04%	0.00%	100	25	28.09%	0.00%
pH 1.03 (Aqueous)		25	0.4	0.01	21.74%	0.00%	40	1	40.00%	0.00%
Mass in Extractant				0.036	78.26%	0.00%		1.5	60.00%	0.02%
pH 2.04 (Aqueous)		25	0.1	0.0025	5.43%	0.00%	106	2.65	106.00%	0.00%
Mass in Extractant				0.0435	94.57%	0.00%		0	0.00%	0.00%
pH 2.51 (Aqueous)		25	0.1	0.0025	5.43%	0.00%	87.1	2.1775	87.10%	0.00%
Mass in Extractant				0.0435	94.57%	0.00%		0.3225	12.90%	0.01%
pH 3.34 (Aqueous)		25	0.5	0.0125	27.17%	0.00%	50	1.25	50.00%	0.00%
Mass in Extractant				0.0335	72.83%	0.00%		1.25	50.00%	0.03%
pH 4.01 (Aqueous)		15	0.02	0.0003	1.09%	0.00%	2	0.03	2.00%	0.00%
Mass in Extractant				0.0273	98.91%	0.00%		1.47	98.00%	0.00%
pH 4.48 (Aqueous)		15	0.784	0.01176	42.61%	0.00%	40	0.6	40.00%	0.00%
Mass in Extractant				0.01584	57.39%	0.00%		0.9	60.00%	0.00%
pH 4.99 (Aqueous)		15	0.02	0.0003	1.09%	0.00%	2	0.03	2.00%	0.00%
Mass in Extractant				0.0273	98.91%	0.00%		1.47	98.00%	0.01%

Table 59 – Results and calculations for species analyzed in extraction experiment continued

			Sb				Cs			
Description	**Mass of solid, g**	**Solution volume, mL**	**µg/L**	**Mass, µg**	**% Recovery**	**% of measured Solutes**	**µg/L**	**Mass, µg**	**% Recovery**	**% of measured Solutes**
Residual material + Solution loaded (Start)				57.22				34.44		
Residual material after roasting at 200C	3.2			54.72	95.63%	0.00%		5.44	15.80%	0.00%
Solution loaded after roasting at 200C (REEs)		250	10	2.5	4.37%	0.00%	116	29	84.20%	0.00%
pH 1.03 (Aqueous)		25	4	0.1	40.00%	0.00%	117	2.925	100.86%	0.00%
Mass in Extractant				0.15	60.00%	0.00%		0	0.00%	0.00%
pH 2.04 (Aqueous)		25	3.64	0.091	36.40%	0.00%	155	3.875	133.62%	0.00%
Mass in Extractant				0.159	63.60%	0.00%		0	0.00%	0.00%
pH 2.51 (Aqueous)		25	3.67	0.09175	36.70%	0.00%	153	3.825	131.90%	0.00%
Mass in Extractant				0.15825	63.30%	0.00%		0	0.00%	0.00%
pH 3.34 (Aqueous)		25	5	0.125	50.00%	0.00%	126	3.15	108.62%	0.00%
Mass in Extractant				0.125	50.00%	0.00%		0	0.00%	0.00%
pH 4.01 (Aqueous)		15	0.46	0.0069	4.60%	0.00%	63.4	0.951	54.66%	0.00%
Mass in Extractant				0.1431	95.40%	0.00%		0.789	45.34%	0.00%
pH 4.48 (Aqueous)		15	4	0.06	40.00%	0.00%	66.5	0.9975	57.33%	0.00%
Mass in Extractant				0.09	60.00%	0.00%		0.7425	42.67%	0.00%
pH 4.99 (Aqueous)		15	0.5	0.0075	5.00%	0.00%	66.2	0.993	57.07%	0.00%
Mass in Extractant				0.1425	95.00%	0.00%		0.747	42.93%	0.00%

Table 60 – Results and calculations for species analyzed in extraction experiment continued

			Ba				La			
Description	**Mass of solid, g**	**Solution volume, mL**	**µg/L**	**Mass, µg**	**% Recovery**	**% of measured Solutes**	**µg/L**	**Mass, µg**	**% Recovery**	**% of measured Solutes**
Residual material + Solution loaded (Start)				4537.9				658.3		
Residual material after roasting at 200C	3.2			4230.4	93.22%	0.30%		100.8	15.31%	0.01%
Solution loaded after roasting at 200C (REEs)		250	1230	307.5	6.78%	0.03%	2230	557.5	84.69%	0.06%
pH 1.03 (Aqueous)		25	706	17.65	57.40%	0.02%	2890	72.25	129.60%	0.08%
Mass in Extractant				13.1	42.60%	0.15%		0	0.00%	0.00%
pH 2.04 (Aqueous)		25	1200	30	97.56%	0.02%	2870	71.75	128.70%	0.06%
Mass in Extractant				0.75	2.44%	0.01%		0	0.00%	0.00%
pH 2.51 (Aqueous)		25	1450	36.25	117.89%	0.03%	2790	69.75	125.11%	0.06%
Mass in Extractant				0	0.00%	0.00%		0	0.00%	0.00%
pH 3.34 (Aqueous)		25	1150	28.75	93.50%	0.03%	3020	75.5	135.43%	0.07%
Mass in Extractant				2	6.50%	0.05%		0	0.00%	0.00%
pH 4.01 (Aqueous)		15	659	9.885	53.58%	0.03%	624	9.36	27.98%	0.02%
Mass in Extractant				8.565	46.42%	0.03%		24.09	72.02%	0.08%
pH 4.48 (Aqueous)		15	751	11.265	61.06%	0.02%	293	4.395	13.14%	0.01%
Mass in Extractant				7.185	38.94%	0.03%		29.055	86.86%	0.11%
pH 4.99 (Aqueous)		15	715	10.725	58.13%	0.02%	38.4	0.576	1.72%	0.00%
Mass in Extractant				7.725	41.87%	0.03%		32.874	98.28%	0.12%

Table 61 – Results and calculations for species analyzed in extraction experiment continued

			Ce				Pr			
Description	**Mass of solid, g**	**Solution volume, mL**	**µg/L**	**Mass, µg**	**% Recovery**	**% of measured Solutes**	**µg/L**	**Mass, µg**	**% Recovery**	**% of measured Solutes**
Residual material + Solution loaded (Start)				1339.46				180.008		
Residual material after roasting at 200C	3.2			296.96	22.17%	0.02%		23.008	12.78%	0.00%
Solution loaded after roasting at 200C (REEs)		250	4170	1042.5	77.83%	0.11%	628	157	87.22%	0.02%
pH 1.03 (Aqueous)		25	5100	127.5	122.30%	0.14%	753	18.825	119.90%	0.02%
Mass in Extractant				0	0.00%	0.00%		0	0.00%	0.00%
pH 2.04 (Aqueous)		25	3680	92	88.25%	0.08%	613	15.325	97.61%	0.01%
Mass in Extractant				12.25	11.75%	0.21%		0.375	2.39%	0.01%
pH 2.51 (Aqueous)		25	3860	96.5	92.57%	0.08%	594	14.85	94.59%	0.01%
Mass in Extractant				7.75	7.43%	0.13%		0.85	5.41%	0.01%
pH 3.34 (Aqueous)		25	3180	79.5	76.26%	0.08%	346	8.65	55.10%	0.01%
Mass in Extractant				24.75	23.74%	0.61%		7.05	44.90%	0.17%
pH 4.01 (Aqueous)		15	199	2.985	4.77%	0.01%	17.6	0.264	2.80%	0.00%
Mass in Extractant				59.565	95.23%	0.19%		9.156	97.20%	0.03%
pH 4.48 (Aqueous)		15	57.6	0.864	1.38%	0.00%	4.72	0.0708	0.75%	0.00%
Mass in Extractant				61.686	98.62%	0.23%		9.3492	99.25%	0.04%
pH 4.99 (Aqueous)		15	4.25	0.06375	0.10%	0.00%	0.305	0.004575	0.05%	0.00%
Mass in Extractant				62.48625	99.90%	0.23%		9.415425	99.95%	0.03%

Table 62 – Results and calculations for species analyzed in extraction experiment continued

			Nd				Sm			
Description	**Mass of solid, g**	**Solution volume, mL**	**µg/L**	**Mass, µg**	**% Recovery**	**% of measured Solutes**	**µg/L**	**Mass, µg**	**% Recovery**	**% of measured Solutes**
Residual material + Solution loaded (Start)				823.82				215.45		
Residual material after roasting at 200C	3.2			96.32	11.69%	0.01%		27.2	12.62%	0.00%
Solution loaded after roasting at 200C (REEs)		250	2910	727.5	88.31%	0.07%	753	188.25	87.38%	0.02%
pH 1.03 (Aqueous)		25	3330	83.25	114.43%	0.09%	818	20.45	108.63%	0.02%
Mass in Extractant				0	0.00%	0.00%		0	0.00%	0.00%
pH 2.04 (Aqueous)		25	2500	62.5	85.91%	0.05%	156	3.9	20.72%	0.00%
Mass in Extractant				10.25	14.09%	0.18%		14.925	79.28%	0.26%
pH 2.51 (Aqueous)		25	2380	59.5	81.79%	0.05%	129	3.225	17.13%	0.00%
Mass in Extractant				13.25	18.21%	0.23%		15.6	82.87%	0.27%
pH 3.34 (Aqueous)		25	1120	28	38.49%	0.03%	34.4	0.86	4.57%	0.00%
Mass in Extractant				44.75	61.51%	1.10%		17.965	95.43%	0.44%
pH 4.01 (Aqueous)		15	54.8	0.822	1.88%	0.00%	2.24	0.0336	0.30%	0.00%
Mass in Extractant				42.828	98.12%	0.14%		11.2614	99.70%	0.04%
pH 4.48 (Aqueous)		15	15.4	0.231	0.53%	0.00%	0.813	0.012195	0.11%	0.00%
Mass in Extractant				43.419	99.47%	0.16%		11.282805	99.89%	0.04%
pH 4.99 (Aqueous)		15	0.857	0.012855	0.03%	0.00%	0.029	0.000435	0.00%	0.00%
Mass in Extractant				43.637145	99.97%	0.16%		11.294565	100.00%	0.04%

Table 63 – Results and calculations for species analyzed in extraction experiment continued

			Eu				Gd			
Description	**Mass of solid, g**	**Solution volume, mL**	**µg/L**	**Mass, µg**	**% Recovery**	**% of measured Solutes**	**µg/L**	**Mass, µg**	**% Recovery**	**% of measured Solutes**
Residual material + Solution loaded (Start)				55.752				240.3		
Residual material after roasting at 200C	3.2			6.752	12.11%	0.00%		28.8	11.99%	0.00%
Solution loaded after roasting at 200C (REEs)		250	196	49	87.89%	0.00%	846	211.5	88.01%	0.02%
pH 1.03 (Aqueous)		25	199	4.975	101.53%	0.01%	914	22.85	108.04%	0.03%
Mass in Extractant				0	0.00%	0.00%		0	0.00%	0.00%
pH 2.04 (Aqueous)		25	16.8	0.42	8.57%	0.00%	64.3	1.6075	7.60%	0.00%
Mass in Extractant				4.48	91.43%	0.08%		19.5425	92.40%	0.34%
pH 2.51 (Aqueous)		25	13.9	0.3475	7.09%	0.00%	50.2	1.255	5.93%	0.00%
Mass in Extractant				4.5525	92.91%	0.08%		19.895	94.07%	0.34%
pH 3.34 (Aqueous)		25	3.62	0.0905	1.85%	0.00%	19.6	0.49	2.32%	0.00%
Mass in Extractant				4.8095	98.15%	0.12%		20.66	97.68%	0.51%
pH 4.01 (Aqueous)		15	0.379	0.005685	0.19%	0.00%	1.98	0.0297	0.23%	0.00%
Mass in Extractant				2.934315	99.81%	0.01%		12.6603	99.77%	0.04%
pH 4.48 (Aqueous)		15	0.4	0.006	0.20%	0.00%	0.579	0.008685	0.07%	0.00%
Mass in Extractant				2.934	99.80%	0.01%		12.681315	99.93%	0.05%
pH 4.99 (Aqueous)		15	0.02	0.0003	0.01%	0.00%	0.02	0.0003	0.00%	0.00%
Mass in Extractant				2.9397	99.99%	0.01%		12.6897	100.00%	0.05%

Table 64 – Results and calculations for species analyzed in extraction experiment continued

			Tb				Dy			
Description	**Mass of solid, g**	**Solution volume, mL**	**µg/L**	**Mass, µg**	**% Recovery**	**% of measured Solutes**	**µg/L**	**Mass, µg**	**% Recovery**	**% of measured Solutes**
Residual material + Solution loaded (Start)				37.12				243.32		
Residual material after roasting at 200C	3.2			5.12	13.79%	0.00%		32.32	13.28%	0.00%
Solution loaded after roasting at 200C (REEs)		250	128	32	86.21%	0.00%	844	211	86.72%	0.02%
pH 1.03 (Aqueous)		25	135	3.375	105.47%	0.00%	581	14.525	68.84%	0.02%
Mass in Extractant				0	0.00%	0.00%		6.575	31.16%	0.08%
pH 2.04 (Aqueous)		25	2.44	0.061	1.91%	0.00%	4.27	0.10675	0.51%	0.00%
Mass in Extractant				3.139	98.09%	0.05%		20.99325	99.49%	0.36%
pH 2.51 (Aqueous)		25	2.21	0.05525	1.73%	0.00%	3.67	0.09175	0.43%	0.00%
Mass in Extractant				3.14475	98.27%	0.05%		21.00825	99.57%	0.36%
pH 3.34 (Aqueous)		25	1.18	0.0295	0.92%	0.00%	2.78	0.0695	0.33%	0.00%
Mass in Extractant				3.1705	99.08%	0.08%		21.0305	99.67%	0.52%
pH 4.01 (Aqueous)		15	0.214	0.00321	0.17%	0.00%	0.894	0.01341	0.11%	0.00%
Mass in Extractant				1.91679	99.83%	0.01%		12.64659	99.89%	0.04%
pH 4.48 (Aqueous)		15	0.4	0.006	0.31%	0.00%	0.4	0.006	0.05%	0.00%
Mass in Extractant				1.914	99.69%	0.01%		12.654	99.95%	0.05%
pH 4.99 (Aqueous)		15	0.02	0.0003	0.02%	0.00%	0.02	0.0003	0.00%	0.00%
Mass in Extractant				1.9197	99.98%	0.01%		12.6597	100.00%	0.05%

Table 65 – Results and calculations for species analyzed in extraction experiment continued

			Ho				Er			
Description	**Mass of solid, g**	**Solution volume, mL**	**µg/L**	**Mass, µg**	**% Recovery**	**% of measured Solutes**	**µg/L**	**Mass, µg**	**% Recovery**	**% of measured Solutes**
Residual material + Solution loaded (Start)				47.58				130.57		
Residual material after roasting at 200C	3.2			6.08	12.78%	0.00%		16.32	12.50%	0.00%
Solution loaded after roasting at 200C (REEs)		250	166	41.5	87.22%	0.00%	457	114.25	87.50%	0.01%
pH 1.03 (Aqueous)		25	80.7	2.0175	48.61%	0.00%	117	2.925	25.60%	0.00%
Mass in Extractant				2.1325	51.39%	0.02%		8.5	74.40%	0.10%
pH 2.04 (Aqueous)		25	0.451	0.011275	0.27%	0.00%	1.93	0.04825	0.42%	0.00%
Mass in Extractant				4.138725	99.73%	0.07%		11.37675	99.58%	0.20%
pH 2.51 (Aqueous)		25	0.431	0.010775	0.26%	0.00%	1.85	0.04625	0.40%	0.00%
Mass in Extractant				4.139225	99.74%	0.07%		11.37875	99.60%	0.20%
pH 3.34 (Aqueous)		25	0.5	0.0125	0.30%	0.00%	1.53	0.03825	0.33%	0.00%
Mass in Extractant				4.1375	99.70%	0.10%		11.38675	99.67%	0.28%
pH 4.01 (Aqueous)		15	0.169	0.002535	0.10%	0.00%	0.465	0.006975	0.10%	0.00%
Mass in Extractant				2.487465	99.90%	0.01%		6.848025	99.90%	0.02%
pH 4.48 (Aqueous)		15	0.4	0.006	0.24%	0.00%	0.4	0.006	0.09%	0.00%
Mass in Extractant				2.484	99.76%	0.01%		6.849	99.91%	0.03%
pH 4.99 (Aqueous)		15	0.02	0.0003	0.01%	0.00%	0.02	0.0003	0.00%	0.00%
Mass in Extractant				2.4897	99.99%	0.01%		6.8547	100.00%	0.03%

Table 66 – Results and calculations for species analyzed in extraction experiment continued

			Tm				Yb			
Description	**Mass of solid, g**	**Solution volume, mL**	**µg/L**	**Mass, µg**	**% Recovery**	**% of measured Solutes**	**µg/L**	**Mass, µg**	**% Recovery**	**% of measured Solutes**
Residual material + Solution loaded (Start)				17.114				99.5		
Residual material after roasting at 200C	3.2			2.464	14.40%	0.00%		16	16.08%	0.00%
Solution loaded after roasting at 200C (REEs)		250	58.6	14.65	85.60%	0.00%	334	83.5	83.92%	0.01%
pH 1.03 (Aqueous)		25	4.96	0.124	8.46%	0.00%	9.51	0.23775	2.85%	0.00%
Mass in Extractant				1.341	91.54%	0.02%		8.11225	97.15%	0.10%
pH 2.04 (Aqueous)		25	0.1	0.0025	0.17%	0.00%	0.158	0.00395	0.05%	0.00%
Mass in Extractant				1.4625	99.83%	0.03%		8.34605	99.95%	0.14%
pH 2.51 (Aqueous)		25	0.1	0.0025	0.17%	0.00%	0.159	0.003975	0.05%	0.00%
Mass in Extractant				1.4625	99.83%	0.03%		8.346025	99.95%	0.14%
pH 3.34 (Aqueous)		25	0.5	0.0125	0.85%	0.00%	0.5	0.0125	0.15%	0.00%
Mass in Extractant				1.4525	99.15%	0.04%		8.3375	99.85%	0.20%
pH 4.01 (Aqueous)		15	0.058	0.00087	0.10%	0.00%	0.292	0.00438	0.09%	0.00%
Mass in Extractant				0.87813	99.90%	0.00%		5.00562	99.91%	0.02%
pH 4.48 (Aqueous)		15	0.4	0.006	0.68%	0.00%	0.4	0.006	0.12%	0.00%
Mass in Extractant				0.873	99.32%	0.00%		5.004	99.88%	0.02%
pH 4.99 (Aqueous)		15	0.02	0.0003	0.03%	0.00%	0.02	0.0003	0.01%	0.00%
Mass in Extractant				0.8787	99.97%	0.00%		5.0097	99.99%	0.02%

Table 67 – Results and calculations for species analyzed in extraction experiment continued

			Lu				Hf			
Description	**Mass of solid, g**	**Solution volume, mL**	**µg/L**	**Mass, µg**	**% Recovery**	**% of measured Solutes**	**µg/L**	**Mass, µg**	**% Recovery**	**% of measured Solutes**
Residual material + Solution loaded (Start)				13.143				6.32		
Residual material after roasting at 200C	3.2			2.368	18.02%	0.00%		5.44	86.08%	0.00%
Solution loaded after roasting at 200C (REEs)		250	43.1	10.775	81.98%	0.00%	3.52	0.88	13.92%	0.00%
pH 1.03 (Aqueous)		25	1.13	0.02825	2.62%	0.00%	2.19	0.05475	62.22%	0.00%
Mass in Extractant				1.04925	97.38%	0.01%		0.03325	37.78%	0.00%
pH 2.04 (Aqueous)		25	0.1	0.0025	0.23%	0.00%	0.696	0.0174	19.77%	0.00%
Mass in Extractant				1.075	99.77%	0.02%		0.0706	80.23%	0.00%
pH 2.51 (Aqueous)		25	0.1	0.0025	0.23%	0.00%	0.453	0.011325	12.87%	0.00%
Mass in Extractant				1.075	99.77%	0.02%		0.076675	87.13%	0.00%
pH 3.34 (Aqueous)		25	0.5	0.0125	1.16%	0.00%	0.5	0.0125	14.20%	0.00%
Mass in Extractant				1.065	98.84%	0.03%		0.0755	85.80%	0.00%
pH 4.01 (Aqueous)		15	0.051	0.000765	0.12%	0.00%	0.02	0.0003	0.57%	0.00%
Mass in Extractant				0.645735	99.88%	0.00%		0.0525	99.43%	0.00%
pH 4.48 (Aqueous)		15	0.4	0.006	0.93%	0.00%	0.4	0.006	11.36%	0.00%
Mass in Extractant				0.6405	99.07%	0.00%		0.0468	88.64%	0.00%
pH 4.99 (Aqueous)		15	0.02	0.0003	0.05%	0.00%	0.02	0.0003	0.57%	0.00%
Mass in Extractant				0.6462	99.95%	0.00%		0.0525	99.43%	0.00%

Table 68 – Results and calculations for species analyzed in extraction experiment continued

			Ta				W			
Description	**Mass of solid, g**	**Solution volume, mL**	**µg/L**	**Mass, µg**	**% Recovery**	**% of measured Solutes**	**µg/L**	**Mass, µg**	**% Recovery**	**% of measured Solutes**
Residual material + Solution loaded (Start)				1.53				168.2		
Residual material after roasting at 200C	3.2			1.28	83.66%	0.00%		163.2	97.03%	0.01%
Solution loaded after roasting at 200C (REEs)		250	1	0.25	16.34%	0.00%	20	5	2.97%	0.00%
pH 1.03 (Aqueous)		25	0.4	0.01	40.00%	0.00%	8	0.2	40.00%	0.00%
Mass in Extractant				0.015	60.00%	0.00%		0.3	60.00%	0.00%
pH 2.04 (Aqueous)		25	2.8	0.07	280.00%	0.00%	45.4	1.135	227.00%	0.00%
Mass in Extractant				0	0.00%	0.00%		0	0.00%	0.00%
pH 2.51 (Aqueous)		25	2.48	0.062	248.00%	0.00%	32.3	0.8075	161.50%	0.00%
Mass in Extractant				0	0.00%	0.00%		0	0.00%	0.00%
pH 3.34 (Aqueous)		25	0.5	0.0125	50.00%	0.00%	10	0.25	50.00%	0.00%
Mass in Extractant				0.0125	50.00%	0.00%		0.25	50.00%	0.01%
pH 4.01 (Aqueous)		15	0.02	0.0003	2.00%	0.00%	0.4	0.006	2.00%	0.00%
Mass in Extractant				0.0147	98.00%	0.00%		0.294	98.00%	0.00%
pH 4.48 (Aqueous)		15	0.4	0.006	40.00%	0.00%	8	0.12	40.00%	0.00%
Mass in Extractant				0.009	60.00%	0.00%		0.18	60.00%	0.00%
pH 4.99 (Aqueous)		15	0.02	0.0003	2.00%	0.00%	0.4	0.006	2.00%	0.00%
Mass in Extractant				0.0147	98.00%	0.00%		0.294	98.00%	0.00%

Table 69 – Results and calculations for species analyzed in extraction experiment continued

			Tl				Pb			
Description	**Mass of solid, g**	**Solution volume, mL**	**µg/L**	**Mass, µg**	**% Recovery**	**% of measured Solutes**	**µg/L**	**Mass, µg**	**% Recovery**	**% of measured Solutes**
Residual material + Solution loaded (Start)				388.1				832.85		
Residual material after roasting at 200C	3.2			105.6	27.21%	0.01%		777.6	93.37%	0.05%
Solution loaded after roasting at 200C (REEs)		250	1130	282.5	72.79%	0.03%	221	55.25	6.63%	0.01%
pH 1.03 (Aqueous)		25	1350	33.75	119.47%	0.04%	221	5.525	100.00%	0.01%
Mass in Extractant				0	0.00%	0.00%		0	0.00%	0.00%
pH 2.04 (Aqueous)		25	1270	31.75	112.39%	0.03%	219	5.475	99.10%	0.00%
Mass in Extractant				0	0.00%	0.00%		0.05	0.90%	0.00%
pH 2.51 (Aqueous)		25	1340	33.5	118.58%	0.03%	197	4.925	89.14%	0.00%
Mass in Extractant				0	0.00%	0.00%		0.6	10.86%	0.01%
pH 3.34 (Aqueous)		25	1410	35.25	124.78%	0.03%	223	5.575	100.90%	0.01%
Mass in Extractant				0	0.00%	0.00%		0	0.00%	0.00%
pH 4.01 (Aqueous)		15	607	9.105	53.72%	0.02%	45.8	0.687	20.72%	0.00%
Mass in Extractant				7.845	46.28%	0.03%		2.628	79.28%	0.01%
pH 4.48 (Aqueous)		15	586	8.79	51.86%	0.02%	28.9	0.4335	13.08%	0.00%
Mass in Extractant				8.16	48.14%	0.03%		2.8815	86.92%	0.01%
pH 4.99 (Aqueous)		15	576	8.64	50.97%	0.02%	5.54	0.0831	2.51%	0.00%
Mass in Extractant				8.31	49.03%	0.03%		3.2319	97.49%	0.01%

Table 70 – Results and calculations for species analyzed in extraction experiment continued

			Th				U			
Description	**Mass of solid, g**	**Solution volume, mL**	**µg/L**	**Mass, µg**	**% Recovery**	**% of measured Solutes**	**µg/L**	**Mass, µg**	**% Recovery**	**% of measured Solutes**
Residual material + Solution loaded (Start)				179.71				149.31		
Residual material after roasting at 200C	3.2			175.36	97.58%	0.01%		106.56	71.37%	0.01%
Solution loaded after roasting at 200C (REEs)		250	17.4	4.35	2.42%	0.00%	171	42.75	28.63%	0.00%
pH 1.03 (Aqueous)		25	2.04	0.051	11.72%	0.00%	0.4	0.01	0.23%	0.00%
Mass in Extractant				0.384	88.28%	0.00%		4.265	99.77%	0.05%
pH 2.04 (Aqueous)		25	0.1	0.0025	0.57%	0.00%	0.1	0.0025	0.06%	0.00%
Mass in Extractant				0.4325	99.43%	0.01%		4.2725	99.94%	0.07%
pH 2.51 (Aqueous)		25	0.1	0.0025	0.57%	0.00%	0.1	0.0025	0.06%	0.00%
Mass in Extractant				0.4325	99.43%	0.01%		4.2725	99.94%	0.07%
pH 3.34 (Aqueous)		25	0.5	0.0125	2.87%	0.00%	0.5	0.0125	0.29%	0.00%
Mass in Extractant				0.4225	97.13%	0.01%		4.2625	99.71%	0.10%
pH 4.01 (Aqueous)		15	0.02	0.0003	0.11%	0.00%	0.02	0.0003	0.01%	0.00%
Mass in Extractant				0.2607	99.89%	0.00%		2.5647	99.99%	0.01%
pH 4.48 (Aqueous)		15	0.4	0.006	2.30%	0.00%	0.4	0.006	0.23%	0.00%
Mass in Extractant				0.255	97.70%	0.00%		2.559	99.77%	0.01%
pH 4.99 (Aqueous)		15	0.02	0.0003	0.11%	0.00%	0.02	0.0003	0.01%	0.00%
Mass in Extractant				0.2607	99.89%	0.00%		2.5647	99.99%	0.01%

Table 71 – Results and calculations for species analyzed in extraction experiment continued

Description	Mass of solid, g	Solution volume, mL	Mass of Measured Species, µg	Total REE +Y+Sc, µg	REE+Y+Sc out of total measured species %	REE+Y+Sc out of total measured species (Excluding Silica) %	REE+Y+Sc out of total REE+Y+Sc Available %
Residual material + Solution loaded (Start)							
Residual material after roasting at 200C	3.2		1422472.352	1153.312	0.08%		19.46%
Solution loaded after roasting at 200C (REEs)		250	980232.465	4773.425	0.49%		80.54%
pH 1.03 (Aqueous)		25	89623.29575	417.5825	0.47%	0.48%	87.48%
Mass in Extractant			8537.42575	116.71	1.37%	2.11%	24.45%
pH 2.04 (Aqueous)		25	121042.7716	250.461975	0.21%	0.21%	52.47%
Mass in Extractant			5816.537375	242.880525	4.18%	18.45%	50.88%
pH 2.51 (Aqueous)		25	120616.5663	248.374	0.21%	0.21%	52.03%
Mass in Extractant			5795.187175	242.9685	4.19%	18.76%	50.90%
pH 3.34 (Aqueous)		25	104635.0213	206.01625	0.20%	0.20%	43.16%
Mass in Extractant			4072.70025	291.07625	7.15%	18.51%	60.98%
pH 4.01 (Aqueous)		15	38583.63468	13.90878	0.04%	0.04%	4.86%
Mass in Extractant			31098.91322	272.49672	0.88%	0.97%	95.14%
pH 4.48 (Aqueous)		15	49504.27794	11.64468	0.02%	0.02%	4.07%
Mass in Extractant			26328.26996	274.76082	1.04%	1.12%	95.93%
pH 4.99 (Aqueous)		15	50985.67487	0.961215	0.00%	0.00%	0.34%
Mass in Extractant			27396.87304	285.444285	1.04%	1.17%	99.66%

BATTELLE

It can be done

Appendix E: Process Flow Diagram

DWG NO	100075292-001	SH	1	REV	A

REVISION HISTORY

ZONE	REV	DESCRIPTION	DATE	APPROVED
	A	INITIAL RELEASE	2017/##/##	XXX

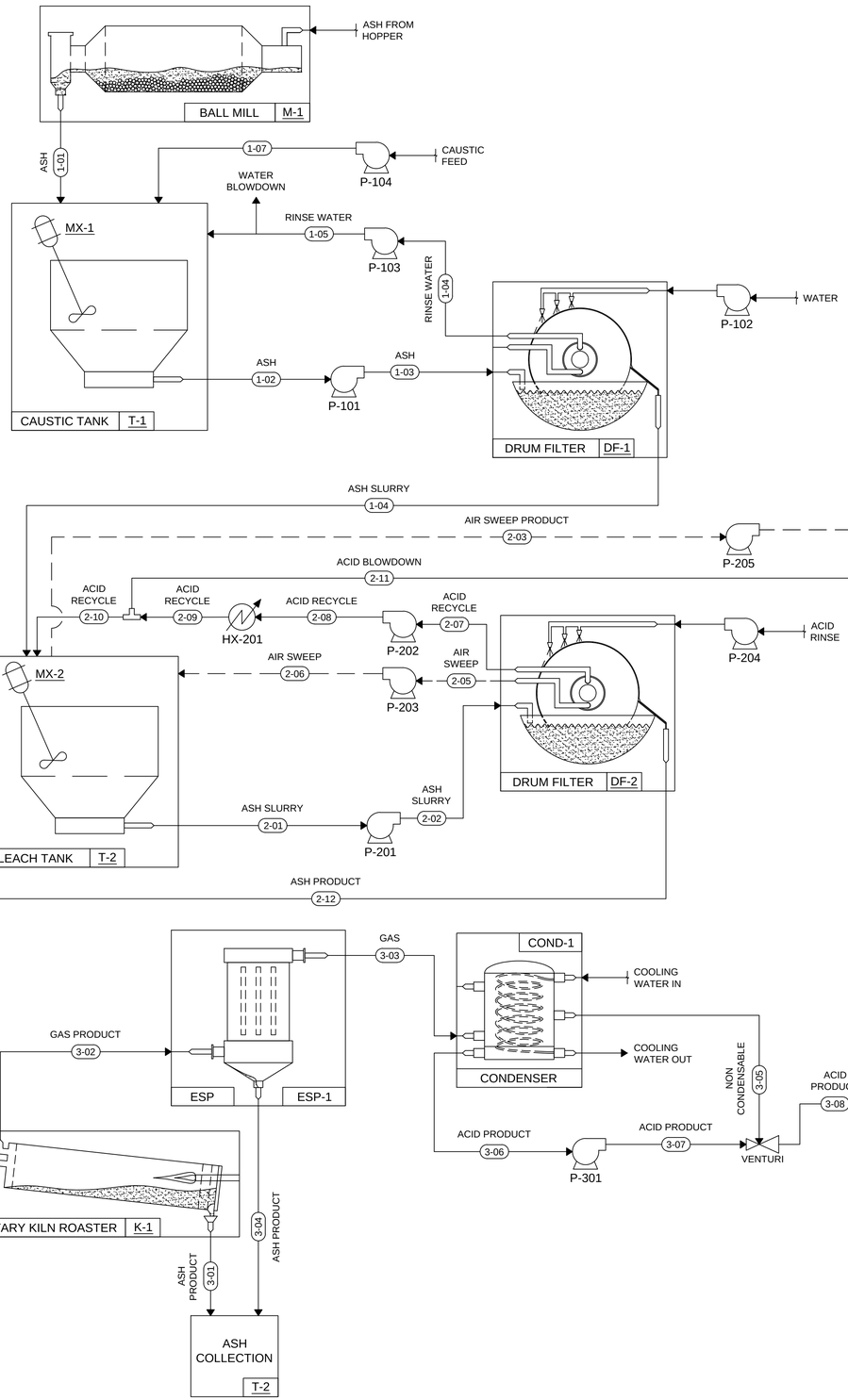

		UNLESS OTHERWISE SPECIFIED DIMENSIONS ARE IN INCHES TOLERANCES ARE: DECIMAL: .XX±.01 .XXX±.005 FRACTIONAL: ±1/32 ANGULAR: ±.5°	CONTRACT NO ###-#-#-####
		THIRD ANGLE PROJECTION	APPROVALS / DATE
			DRAWN CEB 2017/##/##
			CHECKED XXX 2017/##/##
	XXXX		ENGINEER XXX 2017/##/##
NEXT ASSY	USED ON		
APPLICATION			

Battelle
The Business of Innovation
505 KING AVENUE
COLUMBUS, OHIO 43201-2693
TELEPHONE (614) 424-6424

TITLE
PROCESS FLOW DIAGRAM

SIZE	CAGE CODE	DWG NO	REV
D	79986	100075292-001	A

SCALE 1:1 DO NOT SCALE DRAWING SHEET 1 OF 1

PDM
COMPUTER FILE NAME 100075292-001A.DWG
DRAWING

Appendix F: Piping and Instrumentation Diagram

DWG NO	100075292-101	SH	1	REV	A

REVISION HISTORY

ZONE	REV	DESCRIPTION	DATE	APPROVED
	A	INITIAL RELEASE	2017/04/04	XXX

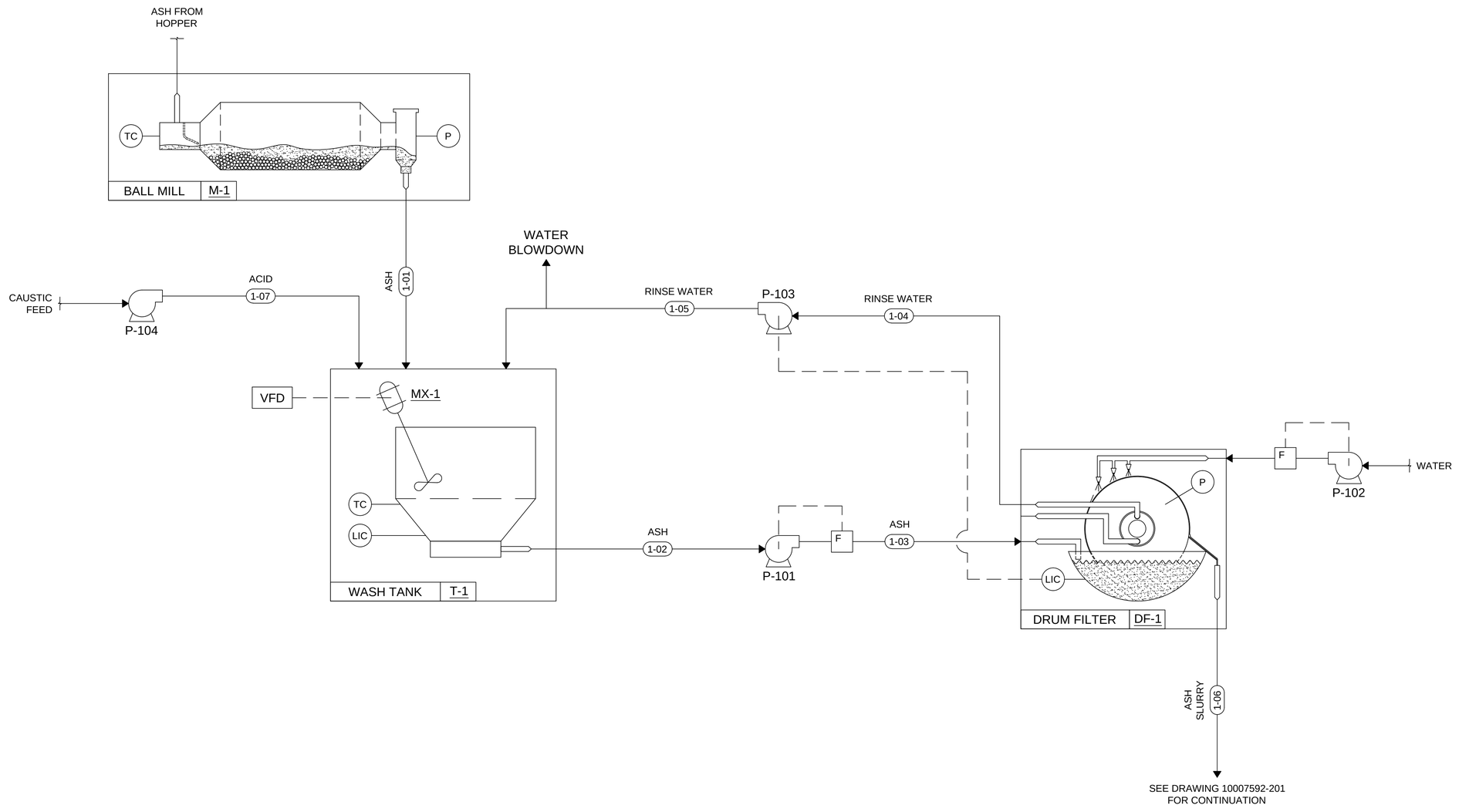

		UNLESS OTHERWISE SPECIFIED DIMENSIONS ARE IN INCHES TOLERANCES ARE: DECIMAL: .XX±.01 .XXX±.005 FRACTIONAL: ±1/32 ANGULAR: ±.5°	CONTRACT NO ###-#-#-###
		THIRD ANGLE PROJECTION	APPROVALS / DATE
			DRAWN CEB 2017/04/04
			CHECKED XXX 2017/04/04
	XXXX		ENGINEER XXX 2017/04/04
NEXT ASSY	USED ON		
APPLICATION			

Battelle
The Business of Innovation
505 KING AVENUE
COLUMBUS, OHIO 43201-2693
TELEPHONE (614) 424-6424

TITLE
PIPING AND INSTRUMENTAITON DIAGRAM, SUBSYSTEM 1

SIZE	CAGE CODE	DWG NO	REV
D	79986	100075292-101	A

SCALE N/A DO NOT SCALE DRAWING SHEET 1 OF 1

PDM
COMPUTER FILE NAME 100075292-101A.DWG
DRAWING

DWG NO	100075292-201	SH	1	REV	A

REVISION HISTORY

ZONE	REV	DESCRIPTION	DATE	APPROVED
	A	INITIAL RELEASE	2017/04/06	XXX

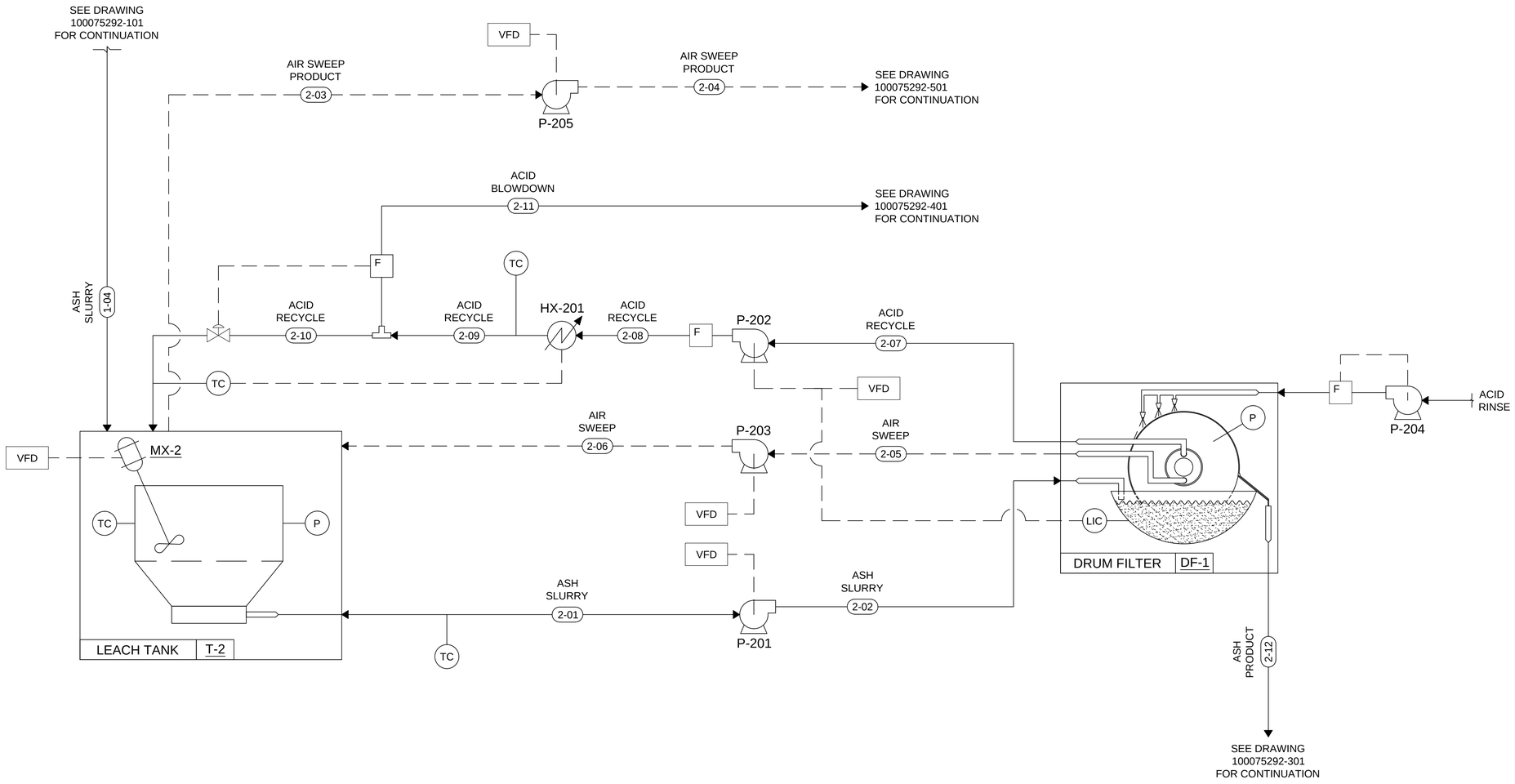

		XXXX	
NEXT ASSY	USED ON		
APPLICATION			

UNLESS OTHERWISE SPECIFIED
DIMENSIONS ARE IN INCHES
TOLERANCES ARE:
DECIMAL: .XX±.01 .XXX±.005
FRACTIONAL: ±1/32 ANGULAR: ±.5°

THIRD ANGLE PROJECTION

CONTRACT NO ###-#-#-###

APPROVALS	DATE
DRAWN CEB	2017/04/06
CHECKED XXX	2017/04/06
ENGINEER XXX	2017/04/06

Battelle
The Business of Innovation
505 KING AVENUE
COLUMBUS, OHIO 43201-2693
TELEPHONE (614) 424-6424

TITLE

PIPING AND INTSTRUMENTATION DIAGRAM, SUBSYSTEM 02

SIZE	CAGE CODE	DWG NO	REV
D	79986	100075292-201	A

SCALE N/A | DO NOT SCALE DRAWING | SHEET 1 OF 1

PDM

COMPUTER FILE NAME 100075292-201A.DWG

DRAWING

DWG NO	100075292-301	SH	1	REV	A

REVISION HISTORY

ZONE	REV	DESCRIPTION	DATE	APPROVED
	A	INITIAL RELEASE	2017/04/07	XXX

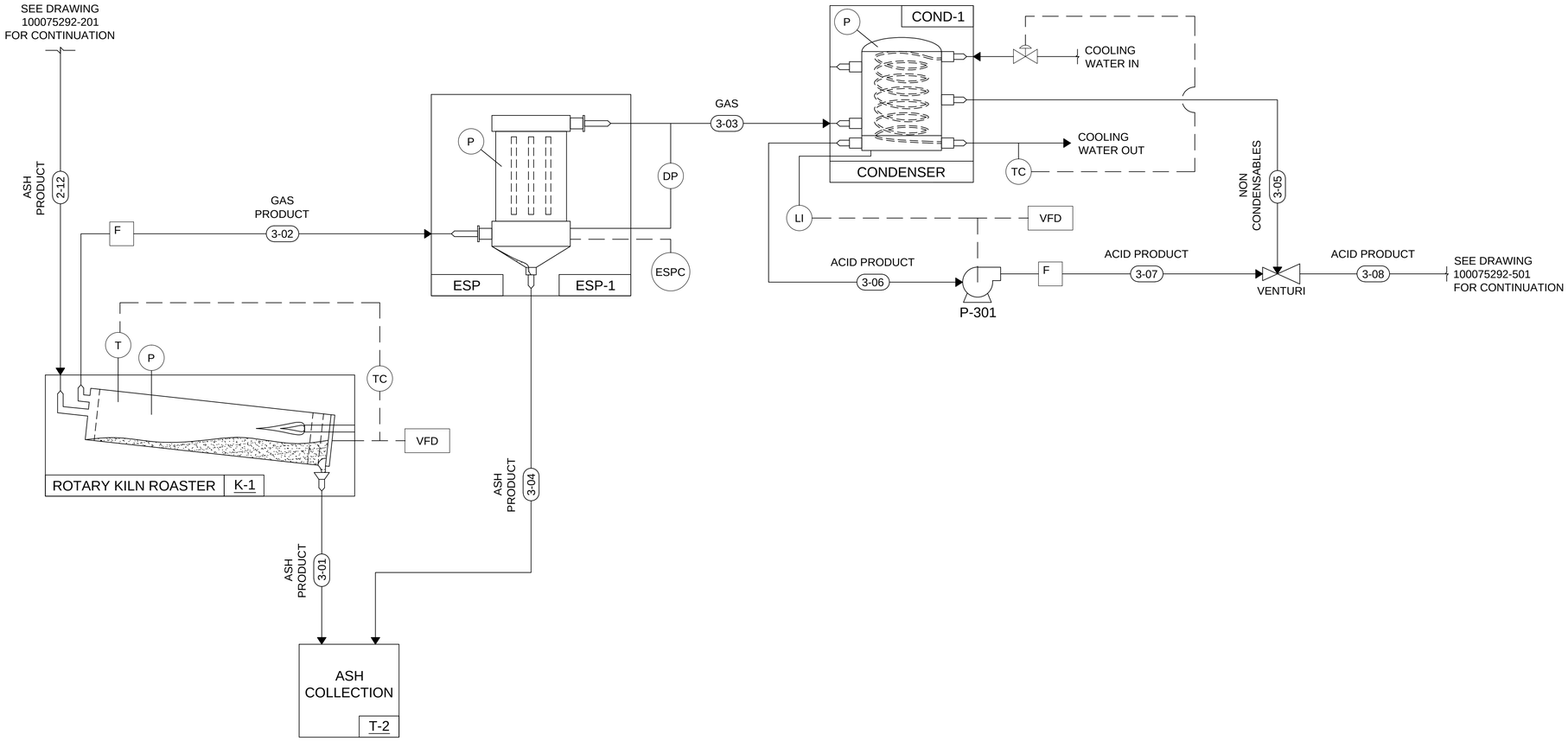

		UNLESS OTHERWISE SPECIFIED DIMENSIONS ARE IN INCHES TOLERANCES ARE: DECIMAL: .XX±.01 .XXX±.005 FRACTIONAL: ±1/32 ANGULAR: ±.5°	CONTRACT NO ###-#-#-###	Battelle *The Business of Innovation*	505 KING AVENUE COLUMBUS, OHIO 43201-2693 TELEPHONE (614) 424-6424
		THIRD ANGLE PROJECTION	APPROVALS / DATE	TITLE	PDM
			DRAWN CEB 2017/##/##	PIPING AND INSTRUMENTATION DIAGRAM, SUBSYSTEM 03	COMPUTER FILE NAME 100075292-301A.DWG
	XXXX		CHECKED XXX 2017/##/##		
NEXT ASSY	USED ON		ENGINEER XXX 2017/##/##	SIZE D / CAGE CODE 79986 / DWG NO 100075292-301 / REV A	DRAWING
APPLICATION				SCALE 1:1 DO NOT SCALE DRAWING SHEET 1 OF 1	

DWG NO	100075292-401	SH	1	REV	A

REVISION HISTORY

ZONE	REV	DESCRIPTION	DATE	APPROVED
	A	INITIAL RELEASE	2017/04/07	XXX

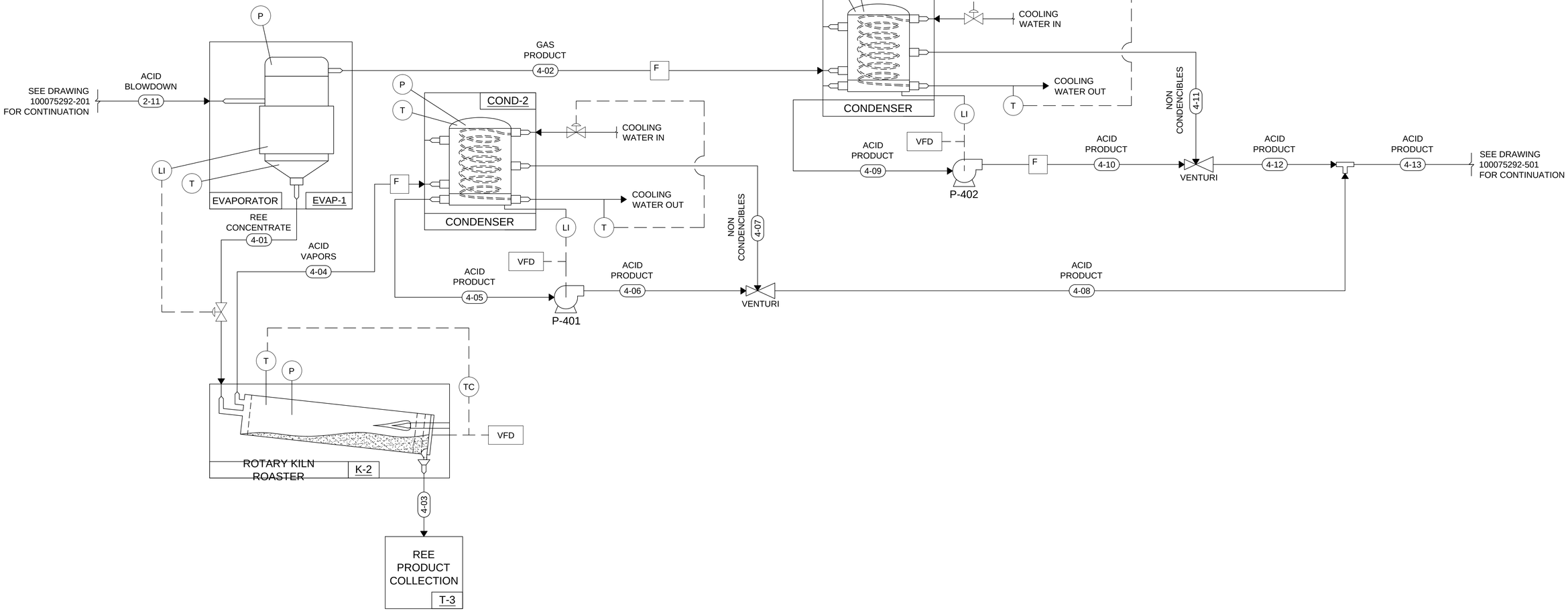

		UNLESS OTHERWISE SPECIFIED DIMENSIONS ARE IN INCHES TOLERANCES ARE: DECIMAL: .XX±.01 .XXX±.005 FRACTIONAL: ±1/32 ANGULAR: ±.5°	CONTRACT NO ###-#-#-###	Battelle *The Business of Innovation*	505 KING AVENUE COLUMBUS, OHIO 43201-2693 TELEPHONE (614) 424-6424
		THIRD ANGLE PROJECTION	APPROVALS / DATE	TITLE	
			DRAWN CEB 2017/##/##	PIPING AND INSTRUMENTATION DIAGRAM, SUBSYSTEM 04	
			CHECKED XXX 2017/##/##		
	XXXX		ENGINEER XXX 2017/##/##	SIZE D / CAGE CODE 79986 / DWG NO 100075292-401 / REV A	
NEXT ASSY	USED ON			SCALE 1:1 DO NOT SCALE DRAWING SHEET 1 OF 1	
APPLICATION					

PDM
COMPUTER FILE NAME 100075292-401A.DWG
DRAWING

DWG NO	100075292-501	SH	1	REV	A

REVISION HISTORY

ZONE	REV	DESCRIPTION	DATE	APPROVED
	A	INITIAL RELEASE	2017/04/07	XXX

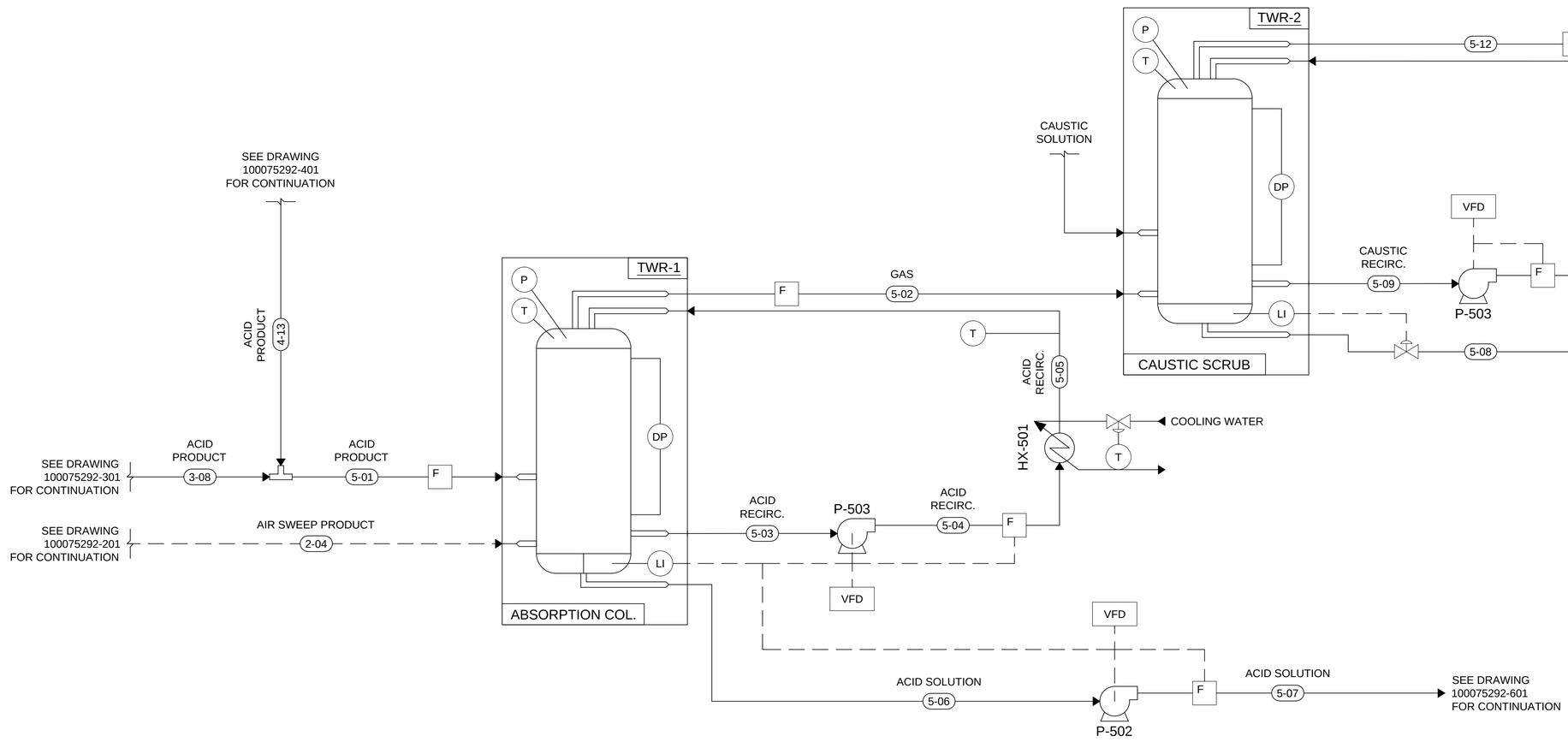

		UNLESS OTHERWISE SPECIFIED DIMENSIONS ARE IN INCHES TOLERANCES ARE: DECIMAL: .XX±.01 .XXX±.005 FRACTIONAL: ±1/32 ANGULAR: ±.5°	CONTRACT NO ###-#-#-###
		THIRD ANGLE PROJECTION	APPROVALS / DATE
			DRAWN CEB 2017/##/##
			CHECKED XXX 2017/##/##
	XXXX		ENGINEER XXX 2017/##/##
NEXT ASSY	USED ON		
APPLICATION			

Battelle
The Business of Innovation
505 KING AVENUE
COLUMBUS, OHIO 43201-2693
TELEPHONE (614) 424-6424

TITLE

PIPING AND INSTRUMENTATION DIAGRAM, SUBSYSTEM 05

SIZE	CAGE CODE	DWG NO	REV
D	79986	100075292-501	A

SCALE 1:1 | DO NOT SCALE DRAWING | SHEET 1 OF 1

PDM

COMPUTER FILE NAME 100075292-501A.DWG

DRAWING

DWG NO	100075292-601	SH 1	REV A

REVISION HISTORY

ZONE	REV	DESCRIPTION	DATE	APPROVED
	A	INITIAL RELEASE	2017/04/07	XXX

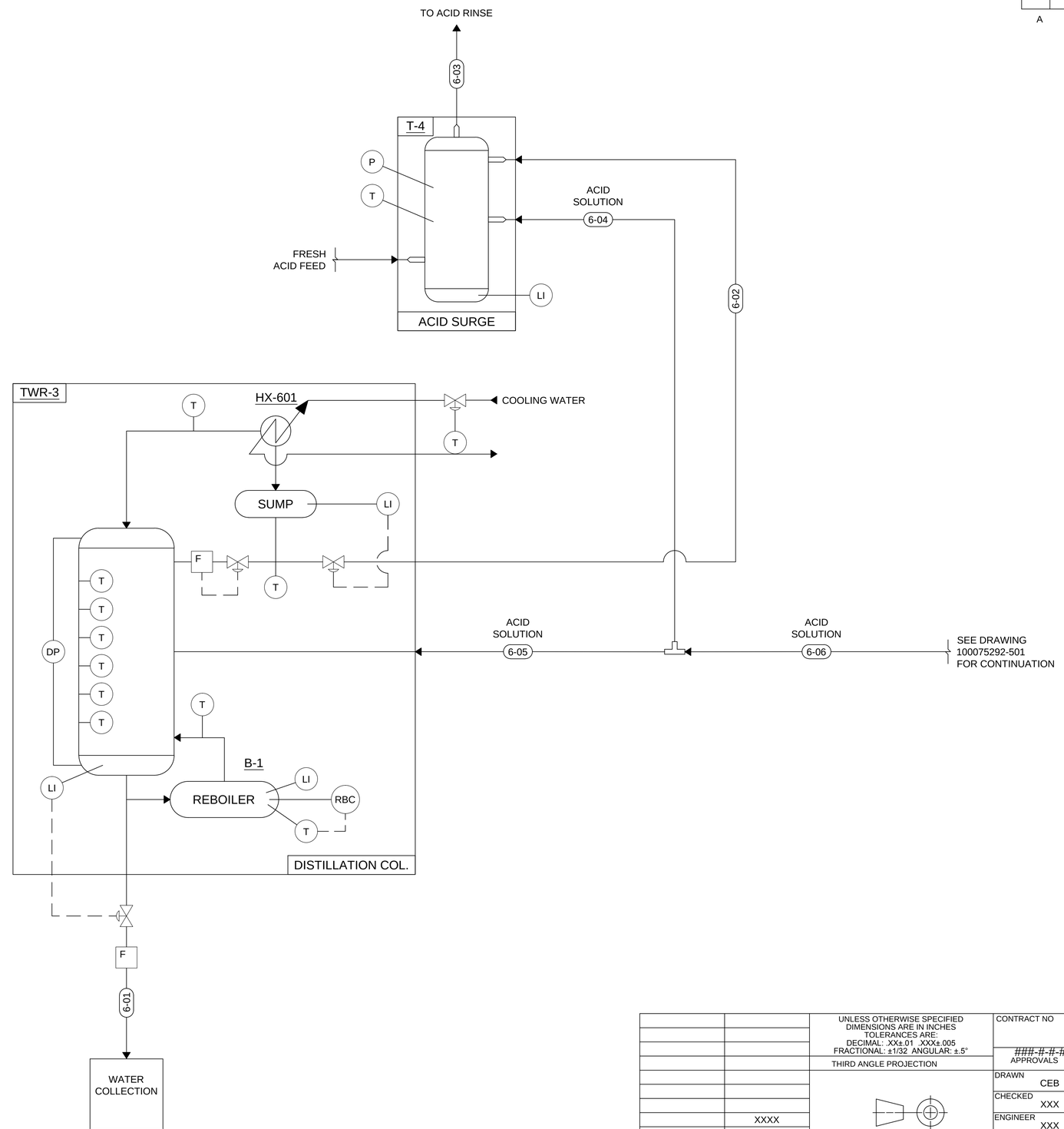

	XXXX
NEXT ASSY	USED ON
APPLICATION	

UNLESS OTHERWISE SPECIFIED
DIMENSIONS ARE IN INCHES
TOLERANCES ARE:
DECIMAL: .XX±.01 .XXX±.005
FRACTIONAL: ±1/32 ANGULAR: ±.5°
THIRD ANGLE PROJECTION

CONTRACT NO

	APPROVALS	DATE
	###-#-#-###	
DRAWN	CEB	2017/##/##
CHECKED	XXX	2017/##/##
ENGINEER	XXX	2017/##/##

Battelle
The Business of Innovation
505 KING AVENUE
COLUMBUS, OHIO 43201-2693
TELEPHONE (614) 424-6424

TITLE

PIPING AND INSTRUMENTATION DIAGRAM, SUBSYSTEM 06

SIZE	CAGE CODE	DWG NO	REV
D	79986	100075292-601	A

SCALE 1:1 | DO NOT SCALE DRAWING | SHEET 1 OF 1

PDM
COMPUTER FILE NAME 100075292-601A.DWG
DRAWING

Appendix G: General Arrangement Drawing

DWG NO	SH	REV
	1	-

REVISION HISTORY

ZONE	REV	DESCRIPTION	DATE	APPROVED

NOTES:

1. APPLICABLE STANDARDS/SPECIFICATIONS:
   ASME Y14.100-2004, ENGINEERING DRAWING PRACTICES
   ASME Y14.5-2009, DIMENSIONS AND TOLERANCES
   ASME Y14.38-2007, ABBREVIATIONS AND ACRONYMS
   ASME Y14.36M-1996, SURFACE TEXTURE SYMBOLS
   ASME Y14.6-2001, SCREW THREAD REPRESENTATION
2. REMOVE ALL BURRS AND SHARP EDGES R.02 OR .02 X 45° CHAMFER.
3. UNLESS OTHERWISE SPECIFIED SURFACE ROUGHNESS IS 125 MICROINCHES OR FINER.
4. MATERIAL:

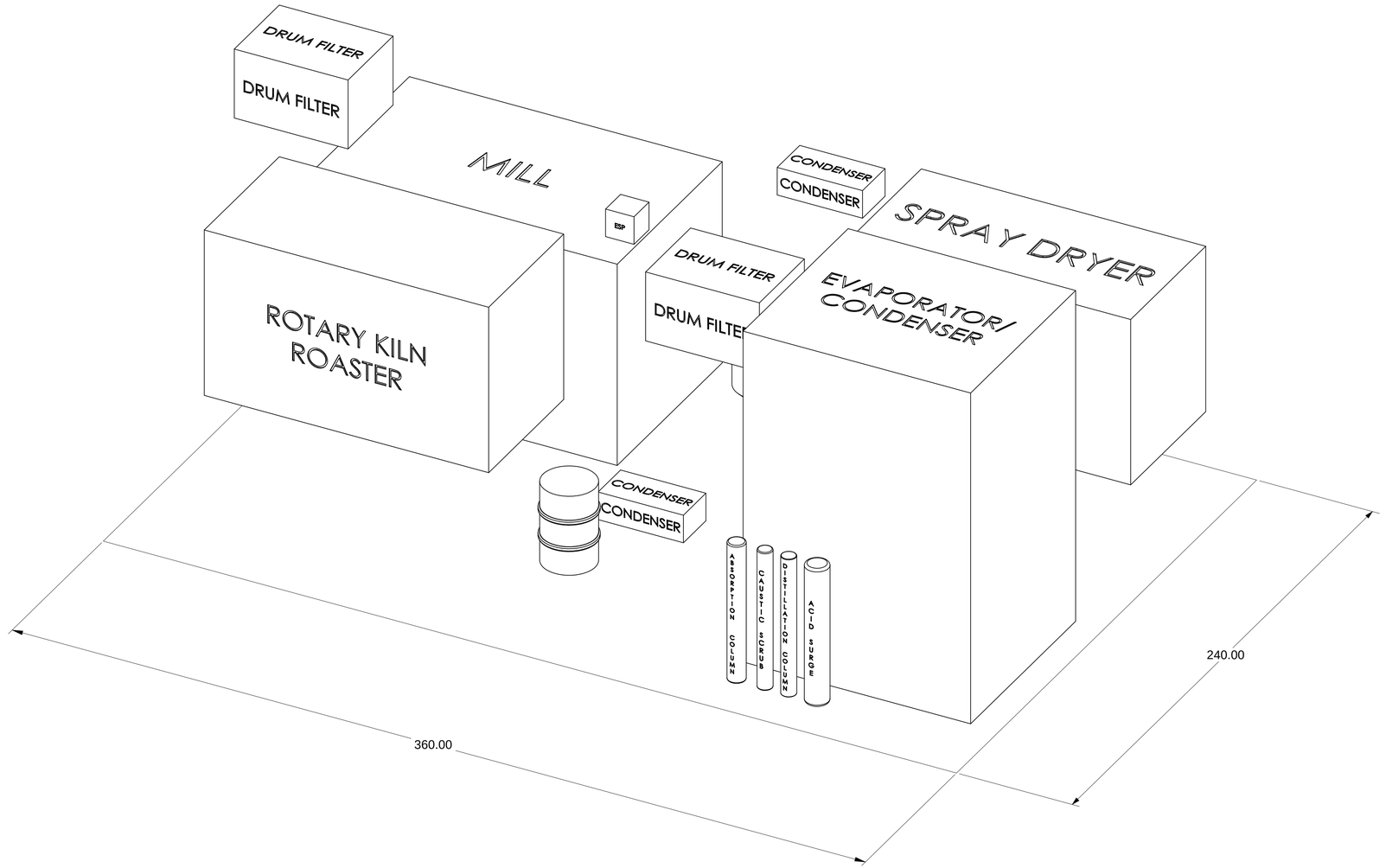

NEXT ASSY	USED ON
APPLICATION	

UNLESS OTHERWISE SPECIFIED
DIMENSIONS ARE IN INCHES
TOLERANCES ARE:
DECIMAL: .XX ±.01 .XXX ±.005
FRACTIONAL: ±1/32 ANGULAR: ±0.5°

THIRD ANGLE PROJECTION

CONTRACT NO

APPROVALS	DATE
DRAWN	X.X.X. YYYY-MM-DD
CHECKED	X.X.X. YYYY-MM-DD
ENGINEER	X.X.X. YYYY-MM-DD

Battelle
The Business of Innovation
505 KING AVENUE
COLUMBUS, OHIO 43201-2693
TELEPHONE (614) 424-6424

TITLE

SIZE	CAGE CODE	DWG NO	REV
D	79986		-

SCALE 1:1 | DO NOT SCALE DRAWING | SHEET 1 OF 1

	PDM
COMPUTER FILE NAME	- -
DRAWING	Equipment Layout
MODEL	Equipment Layout

Appendix H: Process Design Report

100075292

Recovery of Rare Earth Elements from Coal and Coal Byproducts via a Closed Loop Leaching Process: System Design Report

National Energy Technology Laboratory

3610 Collins Ferry Road

Morgantown, WV 26507-0880

7 June 2017

BATTELLE

Table of Contents

List of Tables

Page

List of Figures

Page

Executive Summary

Battelle is validating the economic viability of recovering rare earth elements (REEs) from coal ash using its patented (US6011193) closed-loop Acid Digestion Process (ADP). Based on results from the sampling and characterization work, a pulverized coal combustion (PCC) plant fly ash was selected as the target feedstock for the process. The ash is provided by a plant which is operating in Ohio on primarily Appalachian Basin coals, and was determined to have a high total REE+Y+Sc concentration at 545 ppm +/- 13 ppm as of the results of this study. A preliminary technoeconomic analysis (TEA) done for Battelle's ADP process suggested that it could be economically applied to between 5% and 47% of U.S. coal sources, and based on this finding, additional lab testing and design work was started.

This report documents and summarizes the design of a 12.5 pound per hour integrated bench-scale pilot system for recovery of REE from coal fly ash. It includes the design basis, equipment list, mass and energy balances, and drawings for an integrated process testing system that will validate the process operation in a potential second phase of work. Based upon the design package, it is estimated that a continuous bench-scale unit to process 12.5 lb./hr. (5.7 kg/hr.) of fly ash would require $1,102,206 in capital equipment. Battelle is able to make use of a large amount of existing process equipment on hand for three of the process unit operations, minimizing additional capital costs. Battelle's Columbus laboratories are ideally suited for this bench-scale pilot unit, possessing laboratories of the required size, appropriate utilities, and waste management services to handle the fly ash and chemical products/byproducts produced by the system.

The updated process technoeconomic analysis (TEA) indicates that the proposed technology provides an economical solution for the recovery of REEs from PCC ash. This TEA built upon the analysis conducted as part of the Task 3.0 effort, and included modifications to incorporate updated pretreatment requirements, REE recovery data, and process byproduct economics. The cost to process REEs within the current system configuration was determined to be $140/tonne of coal ash fed. At this processing cost, approximately 42% of US coal sources, if ashed, could be pursued with Battelle's process.

This continuous bench-scale pilot system is a critical step in the scale up and commercialization of the ADP REE recovery technology, as it will provide critical operational data estimated to progress the technology to a technical readiness level (TRL) level 5 from an existing TRL level of 4. Process integration will be similar to the final application, and it would operate on fly ash and process solutions derived from an operating pulverized coal combustion powerplant.

The integrated continuous testing in the prospective Phase 2 work will investigate the impact of recycle streams on the process, which will introduce concentration cycles of contaminants and reduced acid and caustic strengths. Phase 2 efforts will include optimization of zeolite production to generate a saleable, high value zeolite product. Successful validation of the integrated unit will progress the technology to a technology readiness level of 5, which is ready for scaling to an industrial scale pilot. This industrial scale demonstration would likely happen in the 2019-2020 timeframe.

When commercial, this process will reduce the environmental impact and cost of handling coal fly ash by converting it from an environmental liability that requires storage and monitoring into saleable REE and zeolite products. This will in turn elevate the demand for coal in power generation applications. Battelle recommends proceeding with the Phase 2 project to build and

demonstrate the integrated bench-scale pilot unit, such that additional data may be obtained for the design and operation of a future, large scale pilot demonstration facility.

1.0 Introduction

As directed by Congress, the United States (U.S.) Department of Energy (DOE) is investigating the economic feasibility of recovery of rare earth elements (REEs) from domestic U.S. coal and coal byproducts. DOE's National Energy Technology Laboratory (NETL) has characterized a number of REE-bearing samples of coal and coal-related materials. Rare earth elements have been found in varying concentrations ranging up to 1,000 parts per million by weight in the following materials in the United States: coal mine roof and floor materials, run-of-mine coal, prepared coal, partings, pit cleanings, coal preparation refuse, and tailings. Rare earth elements can be found in coal byproducts, including ash, coal-related sludge, and mine drainage. Certain coals can contain a higher ratio of heavy (generally more valuable) REEs than found in other sources of REEs such as natural ores. Given the potentially low REE concentrations in the feed materials, and subsequent potentially low yield of REEs from any separation process, minimizing costs is a key challenge. Physical and chemical separations may be useful in recovering REEs from coal and coal by-products. The forms in which REEs are present in these materials could drive the design of separation processes.

Battelle is doing work to validate the economic viability of recovering REEs from coal ash using its patented (US6011193) closed-loop Acid Digestion Process (ADP). Based on results from the sampling and characterization work (Battelle, 2016a), a pulverized coal combustion (PCC) plant fly ash was selected as the target feedstock for the process. This plant is operating in Ohio on primarily Appalachian Basin coals, and had a high total REE+Y+Sc concentration at 545 ppm +/- 13 ppm. A preliminary technoeconomic analysis (TEA) done on Battelle's ADP process suggested that it could be economically applied to between 5% and 47% of U.S. coal sources, and based on this finding, additional lab testing and design work was started.

This report documents and summarizes the design of a 12.5 pound per hour integrated bench scale pilot system for recovery of REE from coal fly ash. It includes the design basis, equipment list, mass and energy balances, and drawings for an integrated process testing system that will validate the process operation in a potential second phase of work. The final report for this project will include a summary of these designs, along with a summary of the lab testing and updated process economics based on the lab findings.

2.0 Process Design

2.1 Process Description

2.1.1 Pretreatment and Aluminosilicate Byproduct Generation

It was discovered that very high recoveries of REE could be obtained from fly ash by milling and leaching in caustic solution. This process also allows for generation of a potentially valuable byproduct in aluminosilicate zeolite material, which has been synthesized from coal ash before (Hollman, Steenbruggen, & Janssen-Jurkovicova, 1999). Zeolites are commonly used as sorbents for heavy metals, and as catalyst support materials. This provides for a market outlet for sale and reuse of what otherwise would be a waste stream for the process, and contributes favorably to the operating economics of the process.

The pretreatment begins with a milling step, which breaks down the ash particulates from a median particle size of 55 microns to 4.5 microns. This size reduction is intended to provide better access to the particle for leaching. For the bench scale pilot unit, a jet mill has been

preliminarily selected for the comminution operation, though stirred media mill could also be an option.

Once the ash has been milled, it is treated with a sodium hydroxide solution to remove some of the silica and alumina present in the ash. This process provides better access to REE in the acid leaching step. Lab testing suggested that one hour of leaching in 10% sodium hydroxide solution at 90 °C is sufficient to liberate REE in the acid step, and these parameters will be refined in the next phase of testing. The ash is filtered out of the caustic solution, and rinsed with water to remove entrained caustic before proceeding to the acid leaching section.

The caustic solution is loaded with silicate and aluminate, which can be precipitated into zeolite material. The exact conditions for zeolite precipitation are still being developed, but after the leach solution has been recycled several times, it will be taken for zeolite recovery. For this case, it is assumed that neutralization of the solution will be required. Neutralization is done with nitric acid, which will produce a neutral pH sodium nitrate solution that could be used in agriculture for fertilizer. There are other means of zeolite production which may require temperature and aging of the solution, or use of a zeolite scaffold to generate the most useful form. The water rinse solution may also be used for precipitation of aluminosilicates.

2.1.2 Acid Leaching

After the pretreatment and zeolite production step, the ash is fed to the process and mixed with a dilute nitric acid stream (approximately 34 wt.%) before being pumped through a heater to an elevated, sub-boiling temperature, and into the leaching reactor. The leaching temperature is expected to be 90 °C. Within the reactor, mixing causes intimate contact of the ash with the nitric acid, allowing the REEs to be dissolved into the nitric acid solution. Selectivity for the REEs is higher than that for iron, aluminum, and silicon in the ash, causing enrichment of the REE in the leach solution over the ash. The leach reactor is expected to be a continuously stirred tank reactor, with an average residence time of 25 to 30 minutes.

2.1.3 Acid Recovery and Product Generation

After the leach reaction, the ash is filtered out in a vacuum drum filter and transferred to an ash drying operation. The ash dryer is important for economic recovery of REE since the high temperatures will boil off and convert any entrained nitrates, allowing them to be recovered in the system. Additionally, this dryer prevents the discharge of nitrates from the ash wherever it is used or stored. The ash dryer is expected to be a rotary-type drum dryer, heated to a temperature of 155 °C, and is indirectly heated to minimize costs associated with off-gas treatment. It is expected that the leaching operation will increase the surface area of the ash while removing some surface contaminants, which will improve the pozzolanic activity of the ash, making it ideal for use in cements. The leachate, containing unreacted nitric acid, is recycled to the reactor to ensure complete utilization of the acid fed to the process.

Off gases from the process, made up of nitric acid with NOx components, are swept with an air stream, and fed along with the REE-loaded leachate into a roasting operation. The roaster will operate in two steps, the first to concentrate the slurry, and the second to crystallize the rare-earth salts. The concentration step will use a conventional evaporation unit heated to 120 °C, while the crystallization step will be done in a spray dryer, reaching temperatures high enough (approximately 155 °C) to convert metal nitrates to oxides. By roasting the metal nitrate salts to dryness and then to a temperature around 155 °C, many non-rare earth metal salts are converted to metal oxides, releasing NOx gases, which are swept along with other process off-gases to the absorption column. Rare earth nitrates, however, are not converted to oxides at

temperatures less than approximately 400 °C, and will therefore remain in their nitrate salt form (Stern, 1972). The result of the roasting provides a water soluble rare earth concentrate, enriched in rare earth materials, suitable for feed to a hydrometallurgical process to separate and purify the rare earths.

As discussed, all off-gases of the process, consisting of nitric acid vapor and NOx gases, will flow to an absorption column system for recovery, swept to the column using excess air. Optionally, these vapors may be compressed and fed through a heat exchanger to preheat the acid feed to the roaster, then to a condenser to recover nitric acid for recycle, prior to being fed to the column. Any NO gas generated in the roaster, leaching, and ash drying processes needs to be oxidized to NO_2 prior to being absorbed back into the acid stream. This oxidation rate is improved at higher temperatures, and can occur in the drying and roasting processes with the presence of air. As the gas passes through the condenser, it is then cooled, which is preferable for the absorption of the NO_2 back into the liquid phase. Gas will flow through the absorption column in a single pass, where it is contacted with recycled nitric acid as an absorbent. The liquid recirculated in the column consists of acid recovered from the roaster. For the bench-scale unit, the gases from the NOx absorption column will flow through a caustic scrubber tower to ensure no release of NOx gases. This tower will use sodium hydroxide solution to neutralize acidic gases prior to discharge. A small blowdown stream from this column is expected and will become a waste stream.

Nitric acid recovered in the column will be recycled back to the leach reactor to complete the acid recycle process. A small fraction of this stream will be sent to a distillation column, which will distill and separate the water-nitric acid mixture. The concentrated nitric acid recovered in the column will be recycled to the acid leaching process, while the water recovered in the distillate will be treated to a neutral pH and purged from the system. This purge ensures that a buildup of water does not occur in the process. Testing and simulation to date indicates that greater than 95% of acid (calculated as the fraction of makeup acid required verses the total acid feed requirement of the reactor) is able to be recovered through the acid roasting process and the absorption column used to recover the gas-phase nitrates. The process includes a small makeup acid stream, which feeds nitric acid to the process to maintain a constant concentration of nitric acid within the leach reactor.

2.1.4 Solvent Extraction Upgrading

In order to upgrade the REE concentrate, solvent extraction will be used for removal of monovalent and divalent cations along with select transition metals. The target is to provide a mixture of REE in solution that is of sufficient purity to enter a final separation process; it is Battelle's estimate that this purity level needs to be 90% as cations in solution. Schematically, this separation will be performed in six sections after the dried REE concentrate is re-leached to liberate the nitrate salts:

1. **Extraction of the rare earth elements**: The re-leached solution of rare earth nitrates will be contacted with organic extractant to recover the rare earth elements. This step may also include a reducing agent, such as sodium metabisulfite, to reduce ferric iron to ferrous iron, which will then exclude iron from extraction. The pH of this section is carefully controlled to affect which elements are extracted and achieve good selectivity, and monovalent and divalent ions should be nearly completely excluded. However, there will be undesirable multivalent ions extracted. The aqueous phase from this section will be depleted in rare earth elements and a waste stream.

2. **Metal pre-strip**: The organic phase from extraction will be exposed to a low concentration acid stream to remove metals that strip before the rare earth elements. This strip will include most divalent metals that may have been extracted in the first section. It will also likely remove some of the lighter, less valuable REE such as lanthanum and cerium. The aqueous from this section will also be a waste stream.
3. **REE strip**: The organic phase will then be exposed to moderately high concentration acid (near pH 0) in order to strip the REE from the extractant. This will produce a relatively pure REE stream. This section may include a number of cross-flow stages to ensure a high purity REE concentrate for further processing.
4. **Scrub**: The organic phase will be contacted with high molarity acid solution, around 3.5 molar, to remove high valent metals from the extractant. This scrub includes metals such as iron, thorium, titanium, uranium, and others. This aqueous stream will be a waste stream, but could also be used to recover potentially valuable materials.
5. **Scandium strip**: A slip stream of the organic effluent from the scrub section will be sent to scandium stripping. Scandium is expected to remain on the extractant after the scrub section, so it will be removed with a high pH precipitative strip. This strip will cause precipitation of scandium hydroxide or potentially scandium carbonate. This precipitate will be recovered by filtration from the aqueous phase, and the aqueous phase will be recycled within the section.
6. **Water wash**: The organic stream after the scandium strip will be washed with a low ionic strength aqueous stream to remove any entrained base solution. The organic stream will then be mixed with the scrub organic effluent and recycled to the beginning of the process. Aqueous from this section will be a waste stream, and can be used to neutralize acidic waste streams from elsewhere in the process.

2.2 Design Drawings

2.2.1 Process Flow Diagram

Based on the conceptual process design, Battelle developed a Process Flow Diagram (PFD) of the proposed REE recovery process. Figure 1 shows the proposed PFD with pertinent stream flows, temperatures, and pressures. The PFD will be updated to reflect any design changes made to the process during the finalization of process design task at the start of the Phase 2 effort. The overall process mass balance for the 12.5 lb./hr. bench-scale demonstration system is shown in Table 1, while Table 2 and Table 3 show the overall energy balance (heating and cooling requirements) for the proposed system design.

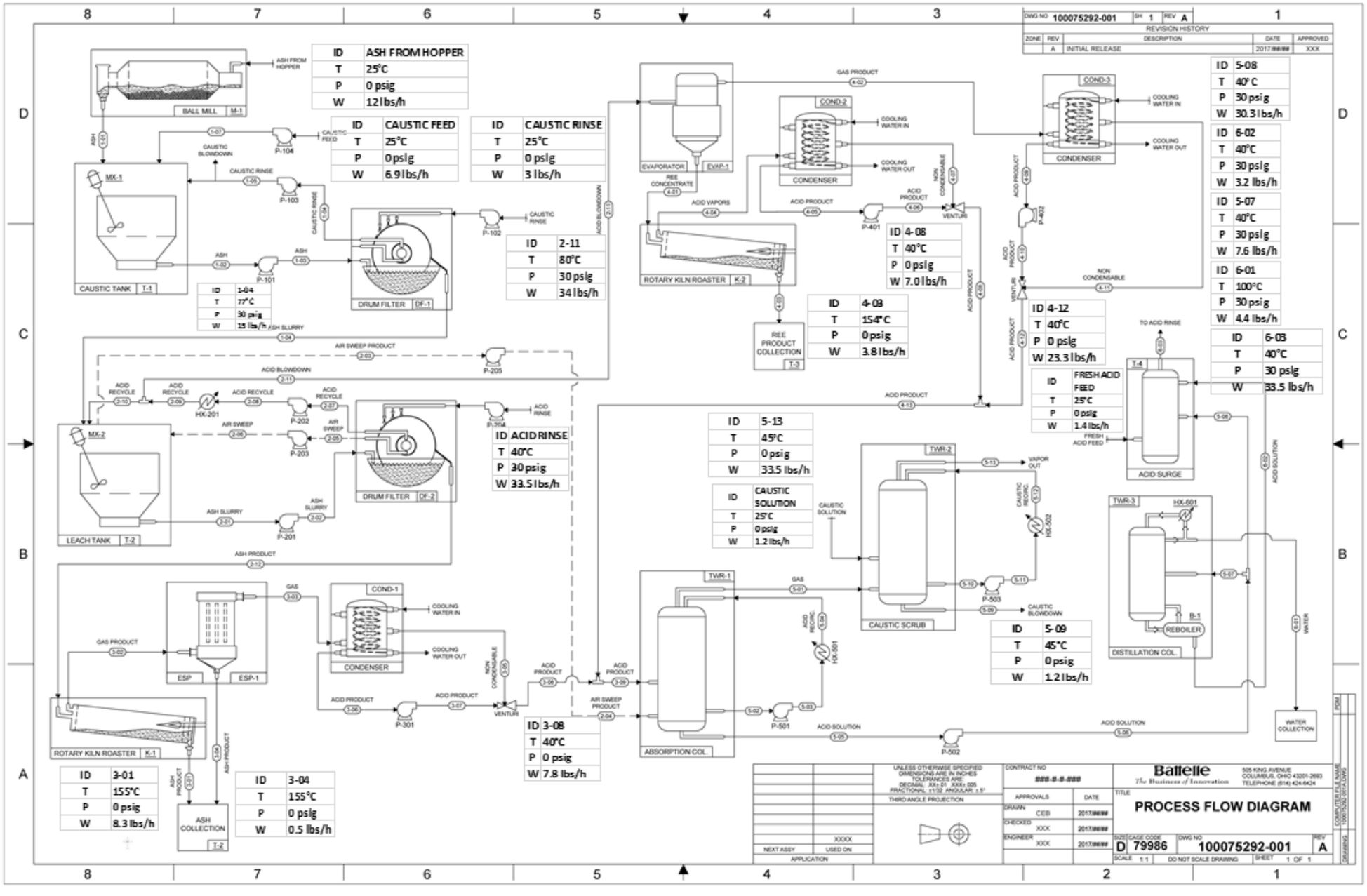

Figure 1: Preliminary PFD with pertinent stream composition.

Table 1: Mass balance for 12.5 lb./hr. bench-scale process.

Feed/Product Stream	Flow Rate (lbs./hr.)
Coal Fly Ash Feed (Feed)	12.09
Caustic Feed (Feed)	6.88
Caustic Rinse (Feed)	2.99
Air Sweep (Feed)	0.34
Caustic Scrubber Make-Up Solution (Feed)	1.17
Nitric Acid Feed (Feed)	2.65
"Water Blowdown" (Product)	7.03
Leached Ash from Roaster (Product)	8.90
Leached Ash from ESP (Product)	0.47
REE Product Stream (Product)	3.83
Caustic Scrubber Vapor Purge (Product)	0.37
Caustic Scrubber Blowdown (Product)	1.17
Distillation Column Water Purge (Product)	4.35

Table 2: Preliminary heat duty required for 12.5 lb./hr. bench-scale process.

Unit Operation	Heat Duty (kW)
Leach Reactor Preheater	0.63
Rotary Drum Ash Dryer	2.18
Roasting Process Evaporator	6.66
Roasting Process Roaster	0.51

Table 3: Preliminary cooling duty required for 12.5 lb./hr. bench-scale process.

Unit Operation	Cooling Duty (kW)
ESP Condenser	1.94
Evaporator Condenser	1.94
Roasting Process Condenser	6.63
Distillation Column Water Product HTXR	1.28
Distillation Column Acid Product HTXR	0.50

2.2.2 Piping and Instrumentation Diagram

Piping and Instrumentation Diagrams (P&IDs) were generated for the proposed process based on the PFD. The overall process is divided into six subsystems, designated by a unique series of identification numbers:

100. Pretreatment (Figure 2)

200. Acid leach (Figure 3)

300. Acid recovery (Figure 4)

400. REE production (Figure 5)

500. NO_x absorption (Figure 6)

600. Acid conditioning (Figure 7)

The P&IDs developed indicate the proposed stream connections, as well as a preliminary indication of required instrumentation for process control and monitoring. As the process design is finalized prior to construction, the P&IDs will be updated to reflect the most recent configuration.

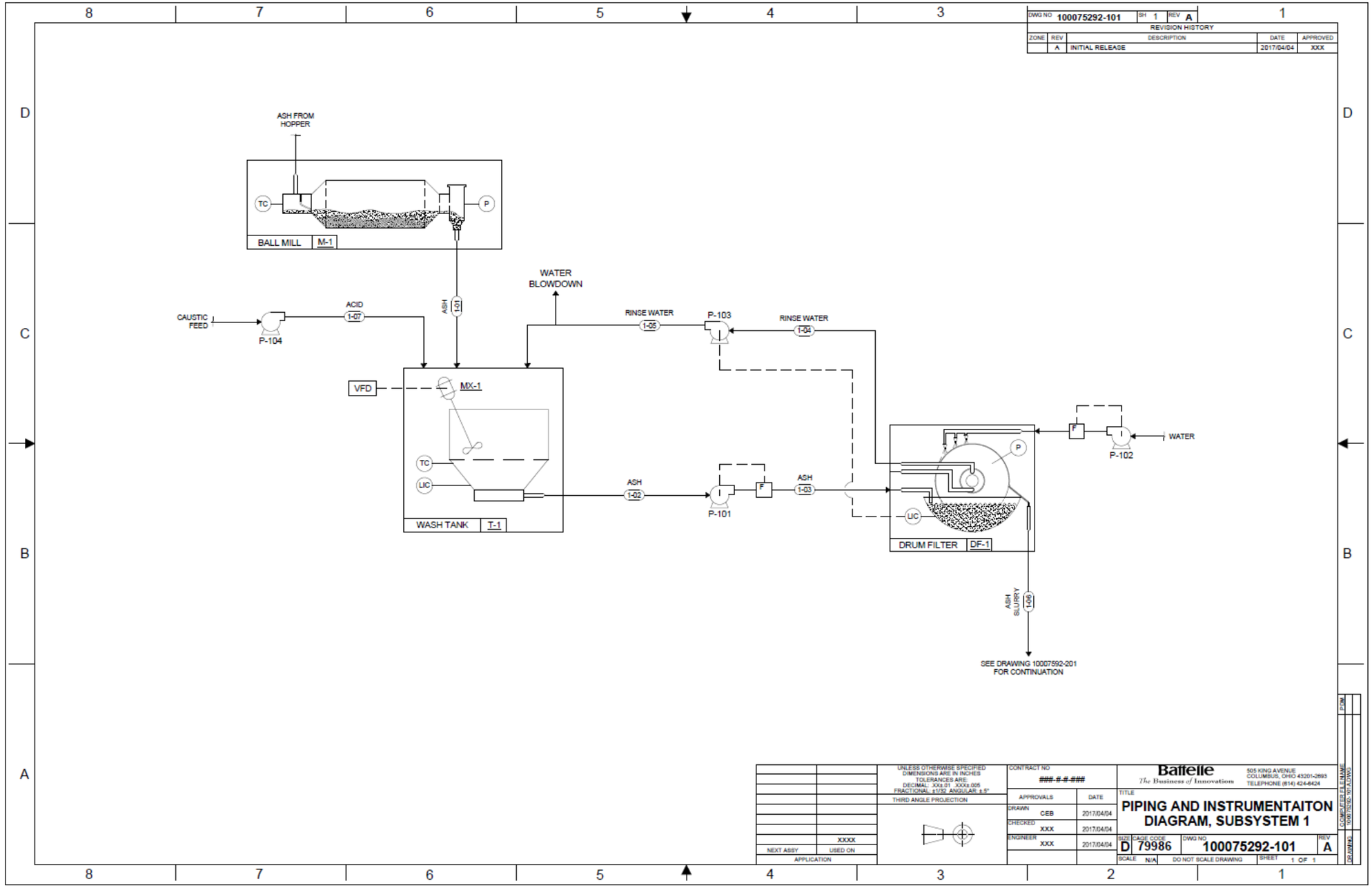

Figure 2: Pretreatment subsystem P&ID.

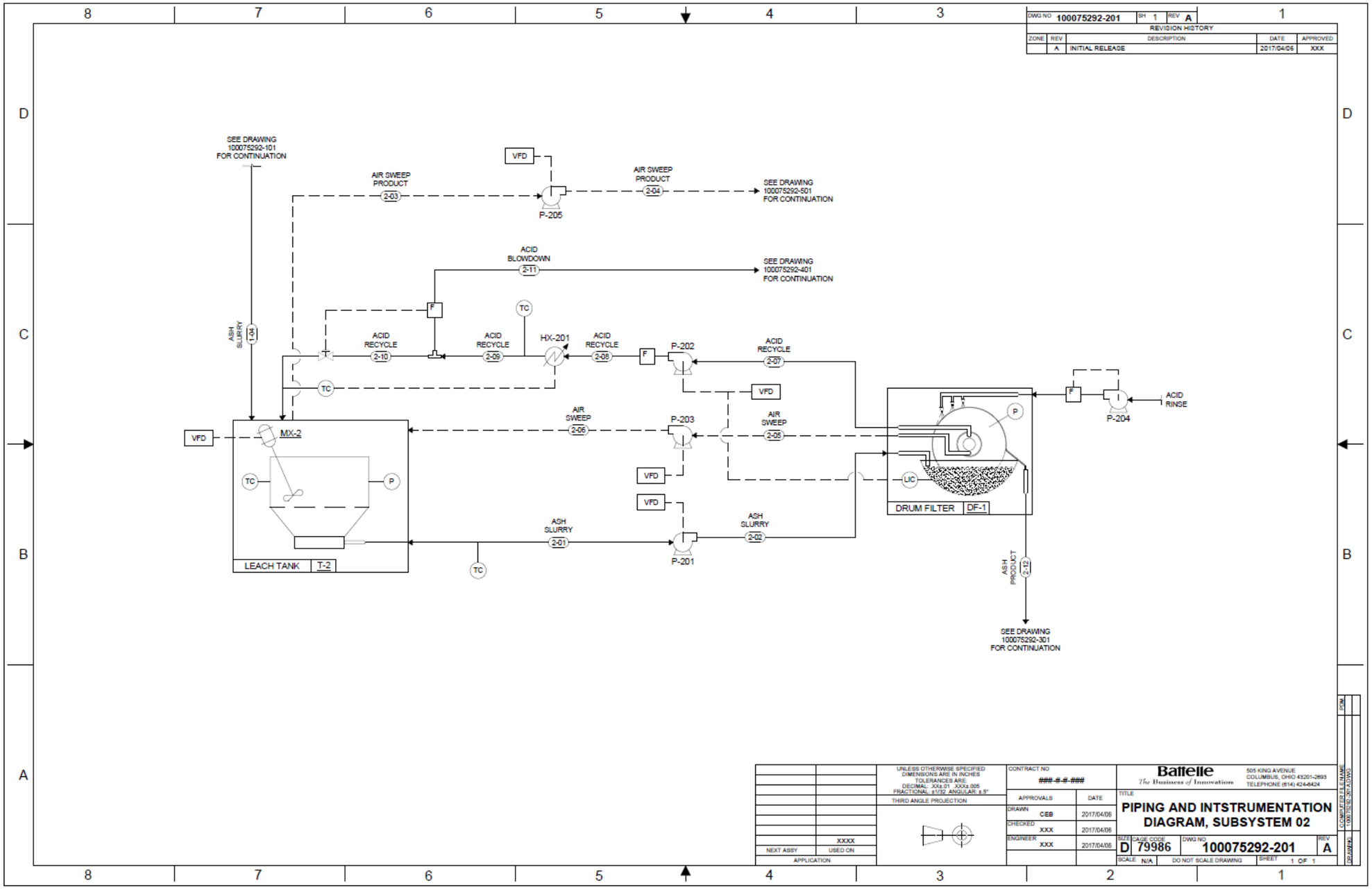

Figure 3: Acid leach subsystem P&ID.

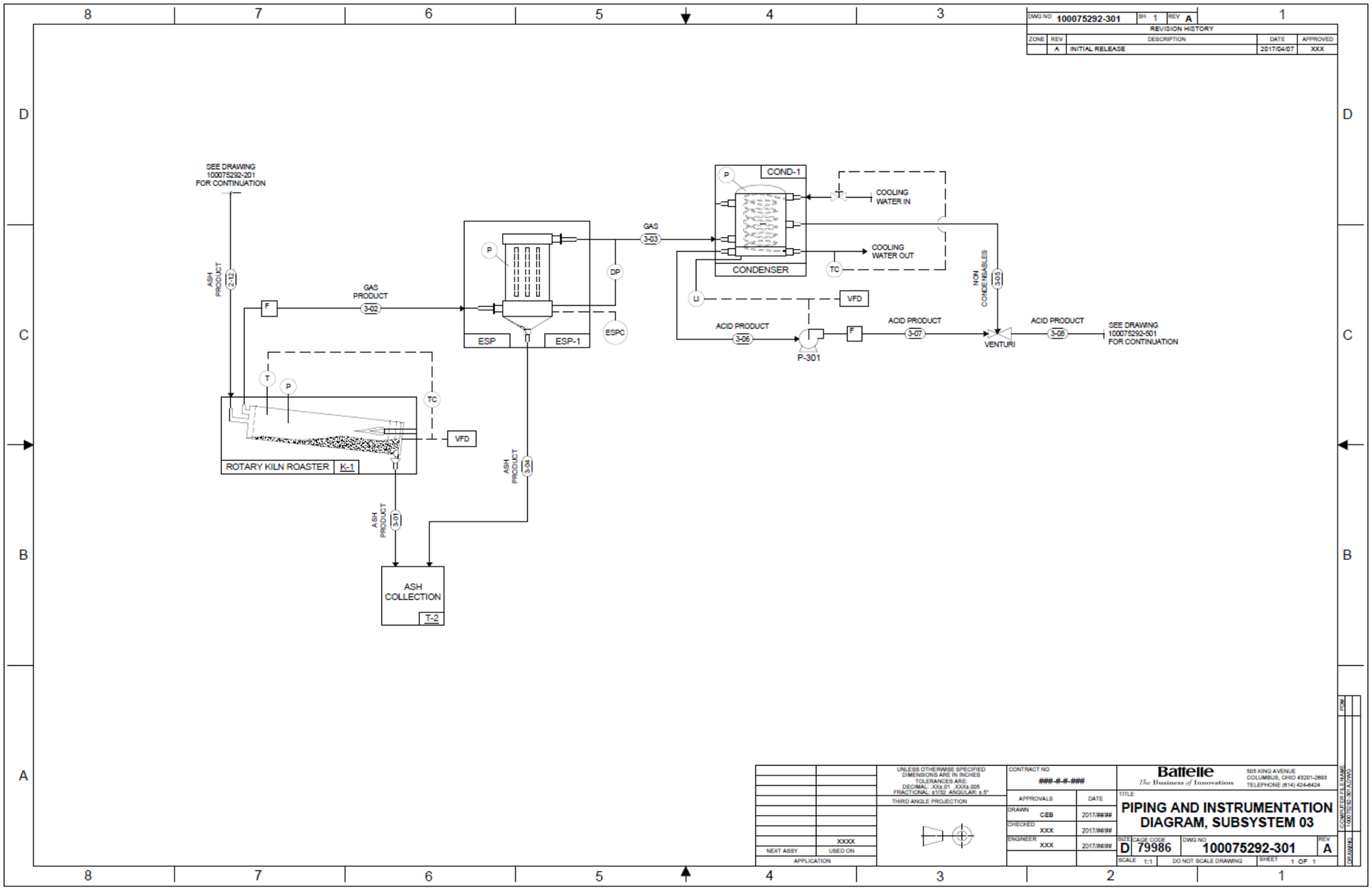

Figure 4: Acid recovery subsystem P&ID.

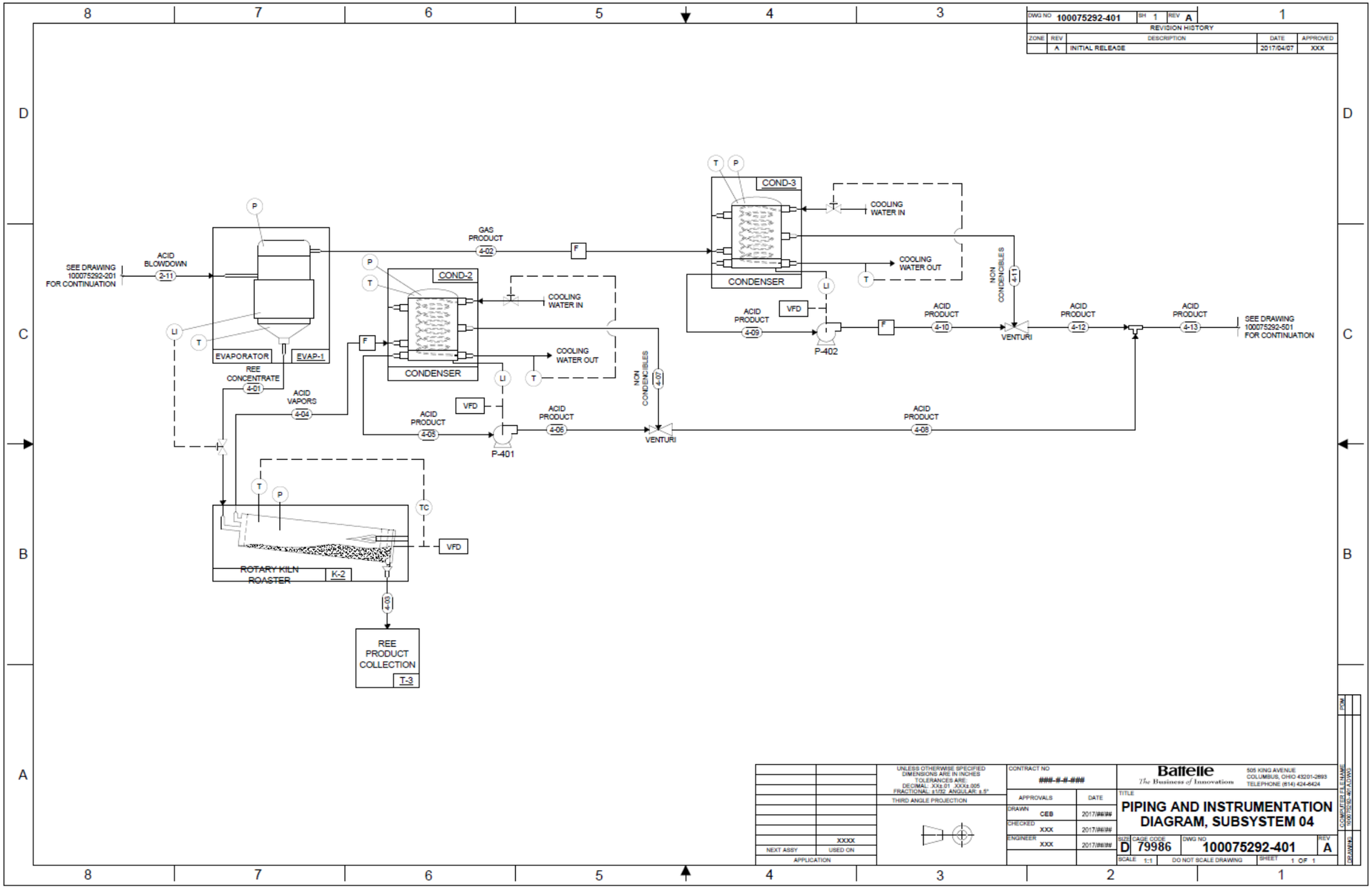

Figure 5: REE production subsystem P&ID.

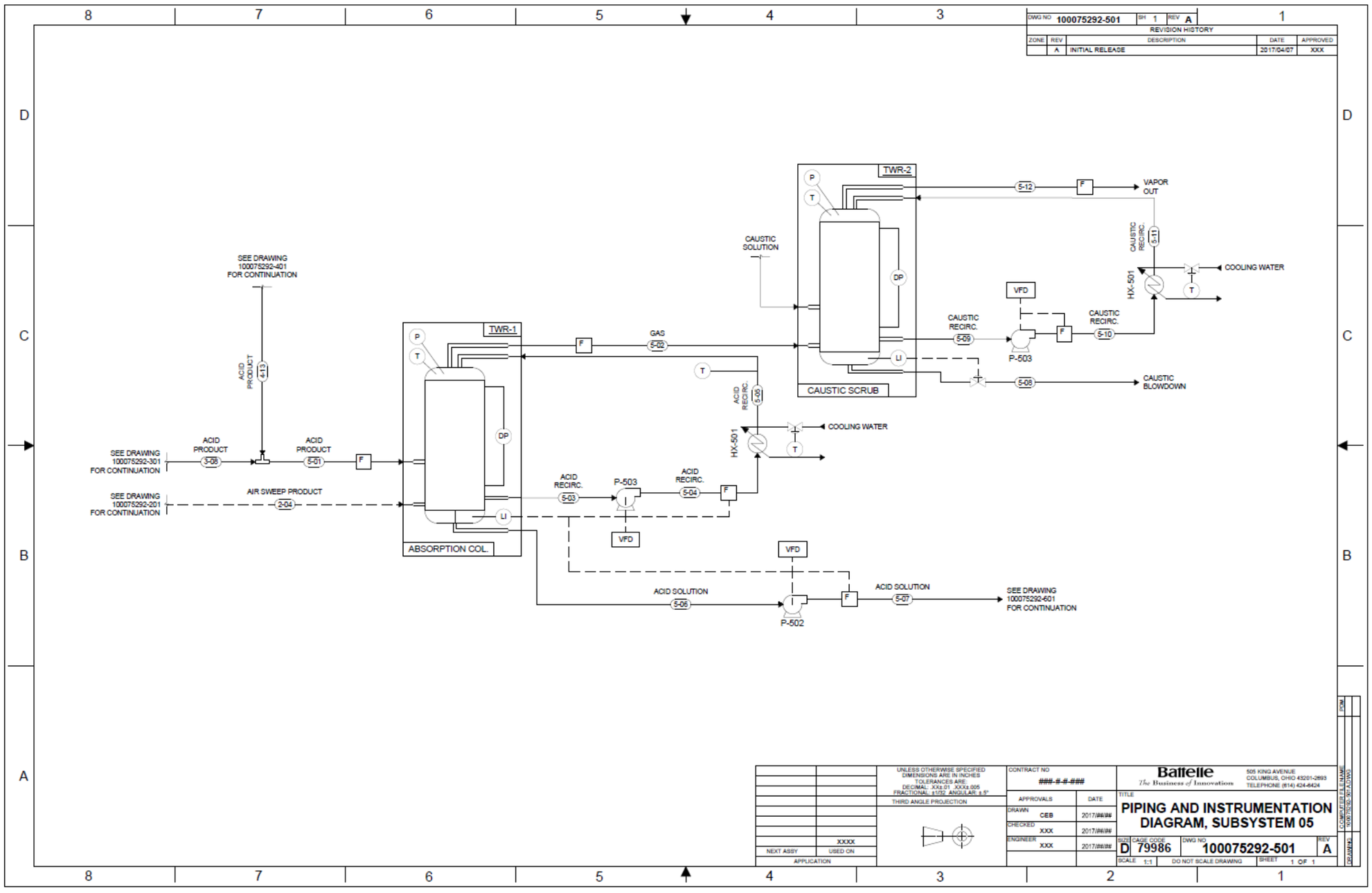

Figure 6: NO_x absorption subsystem P&ID.

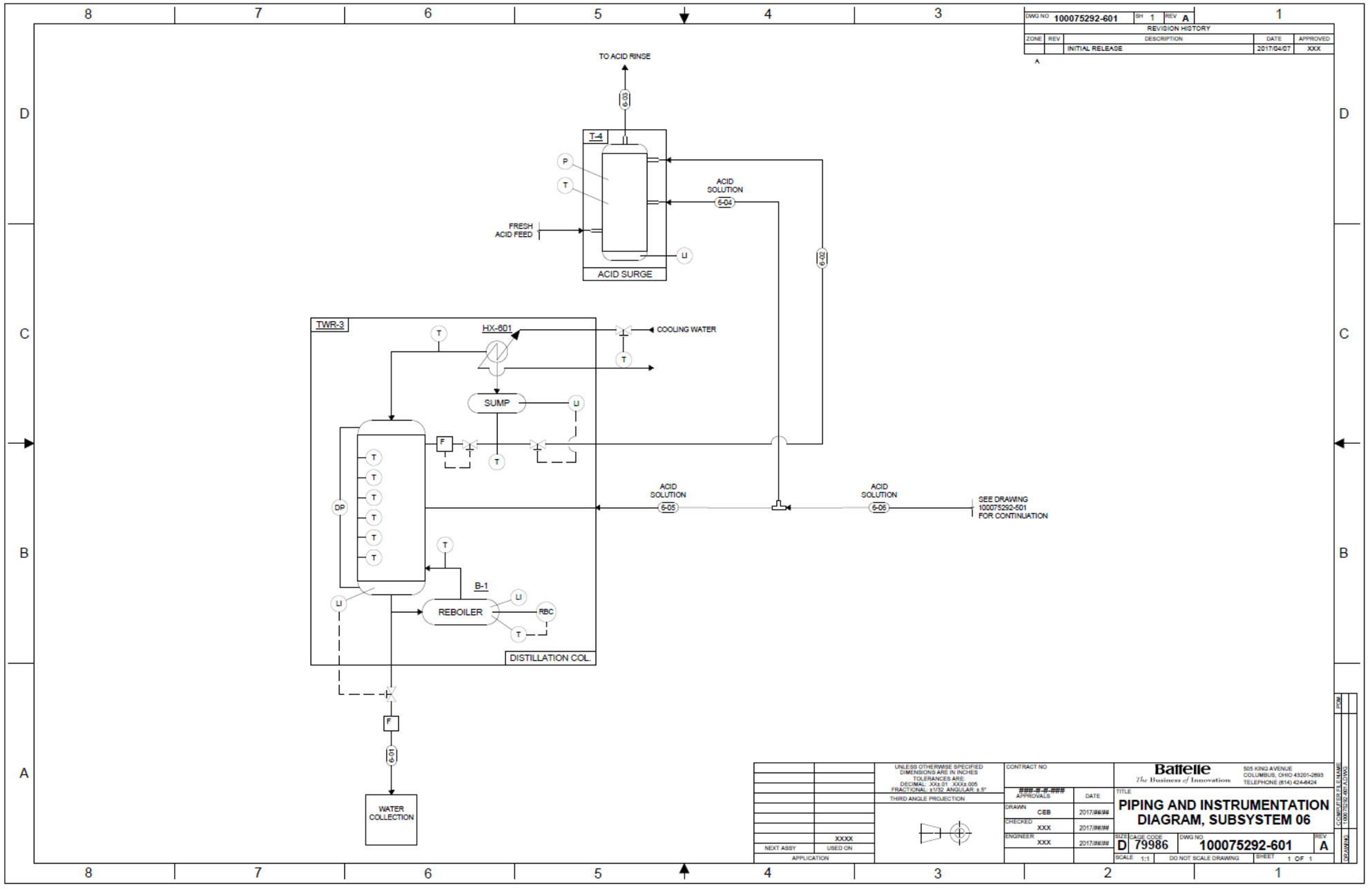

Figure 7: Acid conditioning subsystem P&ID.

2.2.3 Space Claims/General Arrangement Drawings

Battelle obtained dimensional estimates for each major piece of equipment selected for the bench-scale system. Equipment was arranged in 3-D space to determine the optimal arrangement of equipment components not only in relation to one another on the floor space, but also in relation of the heights of the components relative to one another. Figure 8 shows the proposed general arrangement of the equipment specified to date for the bench-scale process. For clarity, component support structures and mounting hardware, process piping, and instrumentation have been eliminated from the drawing.

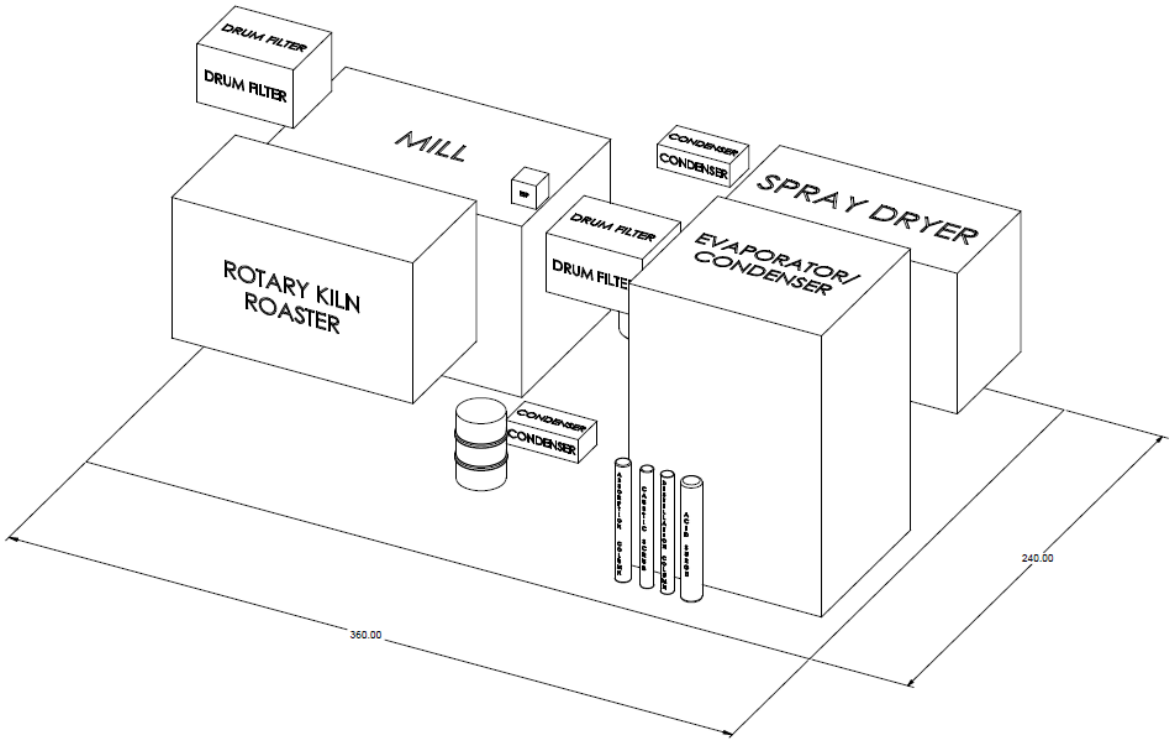

Figure 8: General arrangement drawing showing general space claim estimates for each major piece of equipment (units are in inches).

2.3 Equipment List

Battelle compiled a list of required equipment for the bench-scale demonstration unit based on the PFD and PIDs. For each piece of process equipment, the team reached out to vendors to obtain cost estimates for system components which met the requirements of the bench scale system. Table 4 shows a summary of required process equipment and instrumentation for the proposed bench-scale demonstration system. Equipment indicated with an (*) is process equipment which Battelle already has on had capable of being utilized for the demonstration project. Incorporating readily available equipment into the demonstration system will accelerate the procurement timeline and reduce system costs.

Table 4: Summary of required process equipment and associated purchase cost.

Equipment/Instrumentation	Quantity	Unit Price	Total Price
Mixing tank	1	$25,000	$25,000
Rotary drum filter	2	$64,485	$128,970
Electrostatic precipitator (ESP)*	1	N/A	N/A
Rotary kiln	1	$94,300	$94,300
Fluidized bed mill	1	$300,000	$300,000
Acid recovery system	1	$162,900	$162,900
Spray dryer	1	$190,000	$190,000
Condenser	2	$5,401	$10,802
Absorption column*	1	N/A	N/A
Distillation column*	1	N/A	N/A
Acid surge*	1	N/A	N/A
Caustic scrubber*	1	N/A	N/A
Thermocouples	12	$46	$560
Pressure Sensors (low temp.)	8	$161	$1,288
Pressure Sensors (high temp.)	6	$1,945	$11,670
Differential pressure sensors	4	$745	$2,981
Flowmeters (low temp.)	6	$985	$5,910
Flowmeters (high temp.)	12	$5,498	$65,974
Level Indicator/Controller	4	$540	$2,160
Pumps	14	$3,904	$54,656
Heat Exchanger - Nitric acid	1	$1,280	$1,280
Heat Exchanger - Caustic	1	$1,210	$1,210
Double gate valve - ash feed	1	$701	$701
Control valves	11	$3,302	$36,321
Eductors	3	$276	$827
Solenoid valves	2	$98	$196
Piping and Fittings	N/A	N/A	$4,500
		Total	**$1,102,206**

2.3.1 Primary Equipment Sizing Discussion

Mixing tank

Based on current scale of application, mixing tank volume required is about 2 barrels (84 gallons). Cost of the tank was approximately $25,000 for a 2-barrel tank built using 304 stainless steel (SS) as the material of construction.

Rotary drum filter

The rotary drum filters take in a feed containing 15% wt. of fly ash solids and 85% wt. of nitric acid (34% w/w aqueous solution) at flow rate of 15 lb./hr. and temperature of 70-80 °C. The system has 2.5 ft^2 of nominal filtration area and uses two vacuum receivers to separate mother liquor filtrate and cake wash filtrate. The system includes filtrate pumps for each of the receivers and a direct drive vacuum pump. The price of this system is estimated to be $64,485 with 304L SS as material of construction, two are required for a total price of $128,970

Electrostatic precipitator (ESP)

Battelle maintains an electrostatic precipitator (ESP) for bench and pilot scale processes which can handle flowrates up to 50 lb./hr. of biofuel (cyclohexane), and is shown in Figure 9. This ESP meets the bench-scale requirements, which are:

- Ash mass throughput of 8.8 lb./hr.
- Vapor mass throughput of 9.2 lb./hr.

Use of the existing ESP is expected to save the project approximately $35,000 in equipment costs.

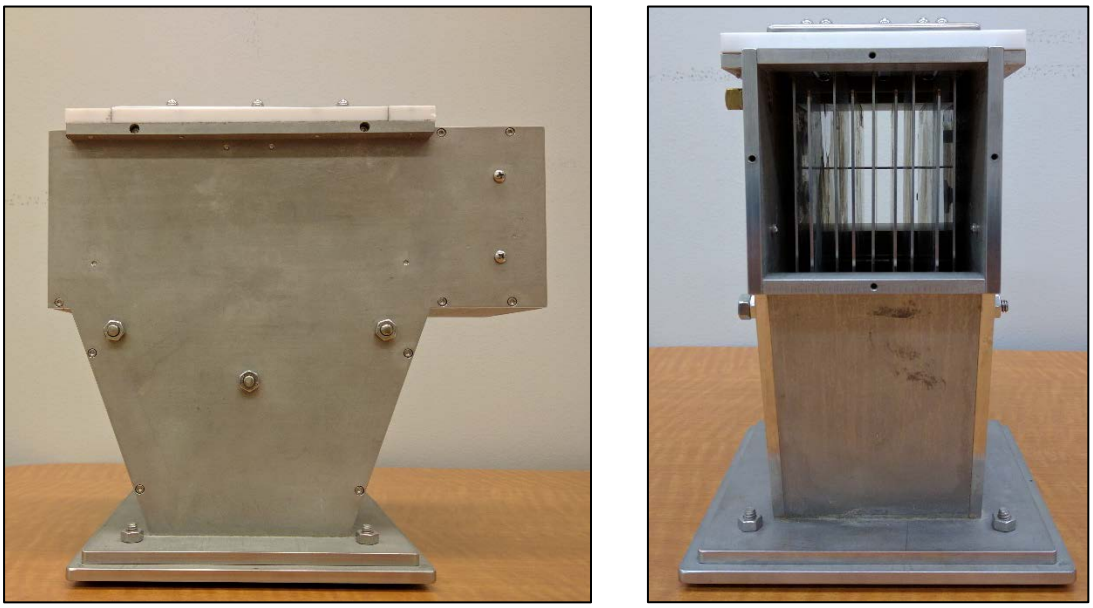

Figure 9. ESP to be utilized for the current application.

Rotary kiln

The rotary kiln feed is the effluent from the rotary drum filter and is in the form of a slurry of finely milled solids and nitric acid. The inlet flowrate is approximately 24 lb./hr. at a temperature of 77 °C. The moisture content of the feed may range was assumed to be 30-40% for design purposes. The final product from the kiln consists of two streams: a bone dry solid stream containing ash which is collected for storage and further analyses, and a vapor stream primarily composed of nitric acid and suspended fly ash particles that flows to an electrostatic precipitator (ESP). Temperatures inside the kiln can reach up to 160 °C. The unit is flexible in terms of design and process requirements and provides breadth for modifying system temperature, rotational speed, slope and the gas environment in the kiln. A price of $ 94,300 is estimated for a research and development scale kiln that is built using 304 SS.

Fluidized bed mill

The fluidized bed mill will be used for size reduction of the fly ash particles fed to the process at a rate of 12.5 lb./hr. under ambient conditions. Feed will have a mean expected particle size of

55 µm while the product is desired to have a mean particle size of 4.5 µm. The mill identified includes a feed system, a base unit for milling and a collection system. Material of construction is 304 SS and requires a supply of 23 standard cubic feet per minute (scfm) of air and 460 VAC electricity for operation. The cost is estimated at $300,000.

Acid recovery system

The acid recovery system includes an evaporator to separate out the solids stream from nitric acid by flashing the vapors and collecting the solids that drop out. The flashed vapor stream is then condensed and nitric acid is recovered for reuse. The expected feed stream flowrate may range between 45-50 lb./hr. of acid and suspended solids with a stream temperature of 120 °C. Outputs from the system include concentrated REEs for feed to the spray dryer and nitric acid at 40 °C. The price of the system is estimated to be $162,900 which includes flash vessel, condenser, and auxiliary equipment such as pumps, valves, level indicators, pressure gauges, temperature sensors, and PLC control.

Spray dryer

The spray dryer will be designed to remove fluid at the rate of 25 lb./hr. and comes with a heater that can release up to 50,000 BTU/hr. of heat. The purpose of the dryer would be to separate the concentrated REE feed stream from the remaining nitric acid, fed to the process at a rate of 2-3 lb./hr. The dryer atomizes and dries a liquid feed using a hot, high-velocity gas stream from either an electric heater and blower, or a gas-fired pulse combustor. The gas stream is introduced into the top center of a tall-form drying chamber, and the liquid feed is delivered to the center of the gas stream at its point of highest velocity, resulting in a co-current dryer configuration. The extreme turbulence caused by the high-velocity gas stream causes rapid and complete mixing of the hot gas with the atomized liquid, resulting in high heat transfer rates, near-instantaneous drying, and low product degradation. The feed material is dried and cooled to dryer exit temperature within five seconds of entering the drying chamber, and there are no “hot spots” in the dryer. The dry powder, drying air, and water vapor are removed from the drying chamber by an exhaust fan, and the powder is separated from the air and water vapor in a cyclone or baghouse. The spray dryer chosen selected is estimated to cost $190,000.

Condenser

The condensers selected for this process are reflux condensers with a surface area of 1 m^2 and a spiral tube volume of 2 liters. This arrangement can handle the vapor flow rates encountered in the system that flow into the condensers which do not exceed 0.36 L/min. This system is characterized by high heat transfer capacity, low coolant consumption and is particularly useful when room heights are limited. The total cost for the two condensers is estimated to be $10,802.

Absorption column

An absorption column is specified to convert NO_x vapors into nitric acid which is recycled back into the system. Battelle selected to construct the absorption in house given the small size of the absorption column and the difficulty sourcing such small units commercially. Calculations determined the volume of the column required based on input flow rates and reaction kinetics of multiple reactions involved in the conversion of NO_x to nitric acid. The five reactions which occur in the absorption column to convert NO_x to nitric acid are:

Gas phase reactions:

(1) $2NO + O_2 \rightarrow 2NO_2$ [NO oxidation]
(2) $2NO_2 \leftrightarrow N_2O_4$ [NO_2 dimerization]

Absorption:

(3) N_2O_4 (g) $\leftrightarrow$ N_2O_4 (l) [N_2O_4 absorption]

Liquid phase reactions:

(4) N_2O_4 (l) + $H_2O \rightarrow HNO_3 + HNO_2$ [HNO_3 formation]
(5) $3HNO_2 \rightarrow HNO_3 + H_2O + 2NO$ [HNO_2 decomposition]

Table 5 describes the resulting volume requirements of each reaction in the absorption column based on the calculations. The column is sized based on the largest volume requirement, which in this case is slightly larger than eight liters.

Table 5. Volume requirements for individual reactions in the absorption column.

Reaction	Volume (L)
NO oxidation	0.606
NO_2 dimerization	6.15E-07
N_2O_4 absorption	0.483
HNO_3 formation	5.35E-05
HNO_2 decomposition	8.023
Sizing volume	**8.023**

Assuming the height of the column is 3-4 times its radius, the dimensions for the calculated volume are a diameter of 7.2 inches and a height of 1 foot. A pipe made from 304 SS shall be used to build the vessel for the column while Cannon Instrument Company's 0.16-inch Pro-Pak suitable for atmospheric operation shall be used as the packing material. This material includes protruding metal cylinders fabricated from a metal ribbon 0.25 inches wide and 0.003 inches thick. 800,000 pieces weighing 27.6 lbs. can fit in a cubic foot of column capacity thereby providing 576 ft^2 of surface area. Packing factor (F_p) is equal to 693. Reflux stream shall be built using instrumentation and piping that shall be acquired in bulk for the overall process. Battelle has used this packing material with success on previous efforts. Reuse of this existing column is expected to save $7,500 in equipment costs.

Distillation column

Similar to the absorption column, Battelle decided to construct the distillation column in house as the size required for the bench-scale demonstration is much smaller than typically provided by vendors. Parameters required for sizing the column are shown in Table 6. Cannon Instrument Company's 0.16 inch Pro-Pak suitable for atmospheric operation shall be used as the packing material.

Table 6. Input parameters for distillation column sizing.

Parameter	Value
Vapor mass flow rate (V)	0.49 lb./hr.
Column diameter (D)	2 in.
Vapor density (ρ_v)	0.15 lb./ft^3
Flood design parameter (f)	0.6

The vapor velocity in the column was then calculated using the following equation:

$$\text{Vapor velocity} = \frac{4V}{\pi D^2 \rho_V f} \quad \text{(Eq. 1)}$$

The resulting vapor velocity value was used in conjunction with design curves, published by Cannon Instrument Company for its Pro-Pak products (Figure 1), to obtain a height equivalent of theoretical plate (HETP) value. This number, multiplied by the number of plates, gives the total height of the column which in this case was around 10 inches as shown in Table 7. Reuse of this existing column is expected to save $7,500 in equipment costs.

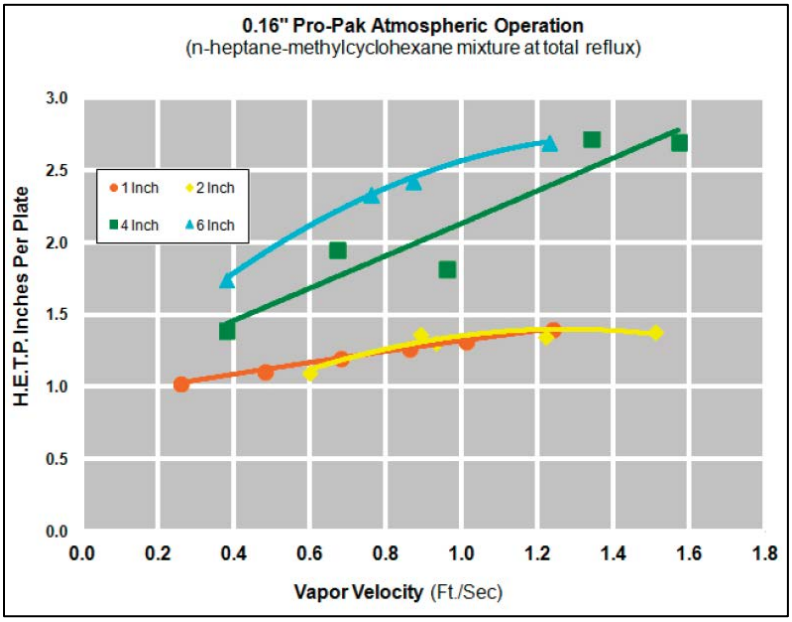

Figure 10. Pro-Pak Atmospheric Operation curves for a n-heptane-methylcyclohexane mixture (Cannon Instrument Company, Revision 3).

Table 7. Distillation column sizing results.

Parameter	Value
Vapor velocity	0.07 ft./s
Diameter of the column	2 in.
HETP (from curve)	0.5 in.
Number of plates	20
Total height of the column	10 in.

Acid surge

The acid surge tank contains the recovered acid from the distillation, absorption, and roasting processes, as well as any fresh nitric acid required as makeup feed to the process. The acid surge vessel feeds acid to the leach reactor. Battelle designed the vessel based on a residence time of 30 minutes and a feed stream of 35-40 lb./hr. when the tank is half full. This design resulted in a tank diameter of 9.6 inches and height of 1 foot. Battelle maintains a selection of tanks available to use for this vessel, which typically cost several hundred dollars for new SS tanks.

Caustic scrubber

The purpose of the caustic scrubber is to remove any NO_x vapors from the outlet stream of the absorption column which have not been converted to nitric acid. The caustic scrubber column is sized similarly as the absorption column, as the flow volumes and rates are similar. Again, this equipment item will be constructed in house by Battelle to similar dimensions as the absorption column discussed above. Reuse of this existing column is expected to save $7,500 in equipment costs.

2.3.2 Auxiliary Equipment Sizing Discussion

Pumps

Pumps used to transport mixtures of finely ground coal ash and nitric acid at moderate to high temperatures are required to be corrosion resistant. The 304 SS is the preferred material of construction. The required head for the pumps selected is no greater than 15 feet, although most flows would require a modest head of about 3 to 5 feet. Fluid viscosity is typically between 1-1.25 centipoise (cP) and flowrate is less than 0.5 gallons per minute. The pumps selected are estimated to cost $3,904 for a single pump assembly and variable frequency drive.

Heat exchangers

Two types of shell and tube heat exchangers, one for 34% nitric acid and another for sodium hydroxide, are required for the process. The preferred material of construction is 304 SS and maximum allowable pressure drop for design calculations was 5 psi. Water is available at 30 °C and will be used as the cooling medium. The heat exchangers selected are estimated to cost $1,280 per unit for nitric acid service and $1,210 per unit for sodium hydroxide service.

Thermocouples

Standard K-type thermocouples with armored cables for increased corrosion resistance to liquids and gases are estimated to cost $46 each, and it is estimated that 12 will be needed.

Pressure Sensors

Two types of pressure sensors are required for the process: low temperature and high temperature compatible sensors. Sensors for low temperature application are estimated to cost $161 apiece, with an estimated eight required. These sensors provide an analog output of 0-10 V and are fabricated using 316 SS. Sensors for higher temperature applications, compatible with process temperatures up to 232 °C, are estimated to cost $1,945 per unit, with an estimated six required.

Flowmeters

Similar to the pressure sensors selected, both a low temperature and a high temperature flow meter were selected depending on the stream to be monitored. Low temperature flow meters are estimated to cost $985 per unit (six are estimated to be required), while high temperature units are estimated to cost $5,498 per unit (12 are estimated to be required). The flow meters are rated for corrosive service.

Level Indicator Controllers

Battelle selected level indicators monitor fluid level in process tanks with a maximum process temperature of 60 °C and relay an analog signal of 4-20 mA. The price of one unit is $540, and it is estimated that four are required.

Valves

Four types of values are needed for this bench scale application:

Double gate ash feed valve: A dual gate valve assembly will be constructed using standard 1.5 inch, national pipe taper (NPT) ball valves with 316 SS as the material of construction to control the flow of ash between process tanks. The valve assembly will include a rack and pinion actuator that is pneumatically controlled. The price of this system is estimated to be $701.

Control valves: Control valves were sized to control the flow of liquid acid and ash slurry throughout the process. The valves were sized for a flow of nitric acid and coal ash assuming a fluid density of 1.2 g/cc and a pipe diameter of 0.5 inches. The pressure drop across the valve was assumed to be 2-3 psi and flow rates ranged between 0.5-60 L/hr. The valves selected include a fail closed actuator, positioner, filter regulator and gauge, and are estimated to cost $3,302 per unit, with an estimated 11 required.

Eductors: Eductors are to be used in conjunction with condensers where the pressure drop is expected to be high and the resultant output flow is at much lower pressure than input, requiring suction to facilitate flow. Eductors constructed of PVC are estimated to cost $276 apiece, with an estimated three required.

Solenoid valves: Corrosion resistant solenoid valves built from 303 SS with a heat resistance of up to 100 °C are estimated to cost $98 per unit, and will be used to provide on/off control of liquid streams, with an estimated two required.

2.4 Environmental, Utility, and Site Requirements

The proposed environmental, utility, and other site requirements for the proposed 12.5 lb./hr. process were evaluated. Due to the closed-loop nature of this bench-scale process, the environmental impacts are expected to be minimal. More than 95% of the nitric acid used in the process is recycled, which minimizes the amount which reduces acid waste. The primary process waste, which is a mixture of nitric acid and water, as well as spent caustic reagent from the pretreatment process is easily treated to a neutral pH and discharged as a process waste stream per Battelle site discharge permits. Similarly, for a larger pilot- or full-scale process, this stream would be treated via an on-site industrial water treatment plant. In certain scenarios, caustic reagent can be neutralized with nitric acid, creating a fertilizer which can be used in agriculture processes.

Gases produced within the process, primarily NOx gases, are captured in the process absorption column prior to being vented. This not only allows for the bench-scale to comply with any air pollutant permitting requirements, but also captures and converts nitrate-based gases to nitric acid capable of being recycled in the process. No other criteria air pollutants defined in the National Ambient Air Quality Standards (NAAQS) are anticipated to be produced as part of this project. A caustic scrubbing system will be used as a backup to the NOx regeneration system specified in the process design.

Leached ash, depleted in metal content, will be the primary solid effluent stream for the process. In a full-scale process, this leached ash may be used as a pozzolan, and it may be more desirable to place ash from Battelle's ADP verses standard power plant ash due to the expected increase in pozzolanic activity of the ash after the leach process. In regions where placement as a pozzolan is not possible, the leached ash from the ADP is expected to be less prone to leaching than traditional power plant ash due to reduced metal content. The leached ash is expected to be neutral in pH after being processed by the process ash dryer, as any remaining nitric acid will have been boiled off and recovered within the plant. For the proposed bench-scale system, the leached ash will be disposed of via a certified waste hauler, due to the relatively small (less than 7 tonnes) of ash expected to be used during testing.

Utility requirements for the proposed bench-scale process are of standard practice for bench- and pilot-scale systems. Due to the bench-scale nature, the majority of utility needs will ultimately be provided by local electrical service. Pumps, immersion heaters, heat trace, mixers, blowers, valves, and other instrumentation will be powered by standard 120 VAC, 240 VAC, or 480 VAC sources. Process cooling will be supplied through existing laboratory cooling water systems at a total rate of 3 gallons per minute (gpm) for the bench-scale process.

Additional site requirements include sufficient floor space and ceiling height for the process equipment specified for the bench-scale system. Battelle's existing facilities and laboratory spaces will be sufficient for the purposes. Finally, fly ash storage and handling capabilities will be required to support this bench-scale demonstration. As mentioned previously, approximately 7 tonnes of ash is expected to be required throughout the demonstration. Battelle will maintain a storage facility, such that a single batch of fly ash can be obtained and used throughout the bench-scale demonstration.

3.0 Technical and Economic Success Criteria

For the proposed bench-scale system, technical success criteria for the Phase 2 effort include:

1. Operation of the system on a semi-continuous basis (up to 8 hours per day) without significant process upsets.
2. Removal of REEs and production of an REE concentrate stream approaching 2 percent by weight.
3. Collection of critical data required for scale up to a pilot scale facility (TRL 6), including critical flow rates, system residence times, and key system control requirements.

Throughout the bench-scale test process, operating economic data will be collected. Economic success criteria for the Phase 2 effort include:

1. Collection of consumable rates, utility requirements, and other process operating cost parameters.
2. Updating of the Phase 1 TEA to include data collected during Phase 2 operation.
3. Indication from the Phase 2 TEA that economic operation of the process is possible.

4.0 Updates to TEA

4.1 TEA Introduction

The technoeconomic assessment developed as part of Battelle's Feasibility Study (Battelle, 2016) was updated based on additional laboratory results and process updates, and followed the same methodology as in the feasibility study report. The CHEMCAD model was updated to include pretreatment steps such as caustic leaching and zeolite production, and a caustic scrubber to prevent NO_x emissions. Solvent extraction and final separation/purification costs were also added in. The levelized cost of Battelle's recovery, from coal ash to salable product, is estimated to be $140 per tonne of ash fed. At this value, approximately 42% of US coal sources, if ashed, could be economically used as a feedstock to the Battelle process.

4.2 CHEMCAD Model Updates

Based upon the laboratory testing results conducted, the CHEMCAD process model developed with the original TEA (Battelle, 2016) was updated to reflect changes. Notably, the pretreatment step was added, a caustic scrubber operation was incorporated, and leaching efficiencies were updated.

The pretreatment involves addition of sodium hydroxide solution to a recycle solution stream, mixing with milled ash, and heating to 90 °C. A stoichiometric reactor converts silica and alumina to sodium silicates and aluminates, according to a user inputted conversion factor (10% in this case). The ash and caustic, aluminate, and silicate solution are separated in a filter, with most of the solution recycled to the reactor. A small blowdown stream maintains mass in the recycle, and fresh caustic is fed to keep 10% sodium hydroxide solution in the system. The ash is washed in three stages on the filter, and the caustic blowdown solution and wash water are combined for aluminosilicate recovery. The ash continues to the leaching reactor. The model assumes, conservatively, that nitric acid will be needed to neutralize the aluminate/silicate solution to generate zeolite products. In this case, the neutralized solution will primarily contain sodium nitrate, which could be used as a nitrogen source at local farmlands. The aluminosilicate precipitate is a zeolite byproduct.

The caustic scrubber is included after the absorption column to neutralize trace amounts of NO_x vapors that may be remaining. It uses a 2% sodium hydroxide solution, which is recycled with a blowdown stream to maintain mass in the recycle loop, and a recirculation pump with a heat exchanger to remove the heat of neutralization in the column.

A final modification to the model is adjustment of the leaching efficiencies based upon the lab testing results with ash pretreatment. Leaching efficiencies affect product yield as well as acid consumption. The updated leach efficiencies used in the model are shown in Table 8.

Table 8: Elemental leach efficiencies, based on laboratory testing, that were used in the updated CHEMCAD model of the process.

Element	Average %	Element	Average %	Element	Average %	Element	Average %
Na	99.00%	Ni	66.81%	In	93.39%	Ho	90.67%
Li	48.84%	Cu	99.00%	Sn	0.00%	Er	96.13%
Be	83.11%	Zn	99.00%	Sb	0.00%	Tm	87.34%
Mg	99.00%	Ga	99.00%	Te	0.00%	Yb	83.32%
Al	52.22%	Ge	0.00%	Cs	72.54%	Lu	74.55%
Si	0.00%	As	99.00%	Ba	99.21%	Hf	1.23%
K	66.33%	Se	99.00%	La	95.24%	Hg	0.00%
Ca	99.00%	Rb	56.46%	Ce	95.07%	Ta	0.00%
Sc	86.58%	Sr	99.00%	Pr	96.47%	W	0.00%
Ti	79.19%	Y	99.00%	Nd	98.41%	Tl	52.59%
V	41.72%	Zr	4.24%	Sm	97.68%	Pb	69.53%
Cr	49.21%	Nb	0.00%	Eu	97.35%	Bi	0.00%
Mn	80.36%	Mo	0.00%	Gd	99.74%	Th	99.99%
Fe	29.21%	Ag	0.00%	Tb	99.99%	U	62.48%
Co	80.45%	Cd	55.12%	Dy	94.59%		

4.3 Technoeconomic Assessment Assumptions

This section describes the key economic assumptions used to estimate the capital and operating costs of Battelle's ADP. These assumptions are important for understanding the context for the reported costs.

The baseline plant configurations, performance, and financial assumptions used for the REE process throughout this report are based on a widely-used set of "baseline" process characteristics specified by the U.S. Department of Energy as shown in Table 9.

Table 9: Key REE process performance and cost assumptions

REE Process Specification	Value
Performance Specifications	
Coal Ash Throughput	30 tonnes/hr.
Coal Ash Source	PCC
Capacity Factor	75%
Financial Assumptions	
Cost Year and Type	2015 Constant Dollars
Annual Inflation Rate	0%
Real Escalation Rate	0%
Fixed Charge Factor	0.113
Years of Construction	3 years
Plant Book Life	30 years
Federal Tax Rate	36%
State Tax Rate	50%
Property Tax rate	0%
Project Contingency	10%
Process Contingency	10%

Process costs describe a mature, Nth-of-a-kind (NOAK) estimate of capital and operating costs. This assumption was selected as the basis for cost estimation. A more thorough understanding of the process is expected to reduce capital and operating costs, thereby reducing the overall capital and operating costs of the system.

The fixed charge factor is calculated based on year-by-year carrying charges and a present worth factor according to Equation 1:

$$FCF = \frac{CC_i * (1+i)^{-1} + CC_2 * (1+i)^{-2} + \cdots + CC_n * (1+i)^{-n}}{a_n}$$

where n is the book life of the plant, i is the interest rate, CC is the year by year carrying charges of the plant, and a_n is the present value worth factor for a uniform series. The year-by-year carrying charges are the sum of: (the return on debt, the return on equity, the payable income taxes, book depreciation, property taxes, and insurance)/the total plant cost (TPC). The value of a_n is calculated according to Equation 2 from (Electronic Power Research Institute (EPRI), 1993)

$$a_n = \frac{(1+i)^n - 1}{i * (1+i)^n}$$

Changes in the assumptions in Table 9 can significantly change the overall results. Due to the large impact that assumptions can have on the final costs, the cost of production shown in this report is most usefully compared to other processes with comparable assumptions and are not to be compared directly with costs that use alternative assumptions.

Additional assumptions regarding specific capital and operating cost parameters, such as direct and indirect cost elements, reagent costs, and labor requirements are specified in the earlier Feasibility Study Report included in Appendix B.

4.3.1 Pretreatment and Byproduct Generation

Pretreatment assumed that zeolite precipitation would require nitric acid addition, which is conservative with regards to operating cost as many zeolite operations use thermal means to generate zeolite rather than chemical addition. The price for the zeolite was back-calculated to cover the cost of the pretreatment operation, which amounts to $45 per tonne.

4.3.2 Purification and Separation

Purification and separation consists of solvent extraction to generate a mixed REE solution, followed by separation and production of salable REE products (99%+ purity oxides) via an emerging separation technology.

Solvent extraction sizes and reagent usage were calculated based on Battelle's past solvent extraction experience. Costs were scaled from a quote for a 300 gpm, 12 stage solvent extraction system obtained by a vendor who built the 100 gpm pilot system for treatment of acid mine drainage water. Figure 11 shows a schematic of the solvent extraction process.

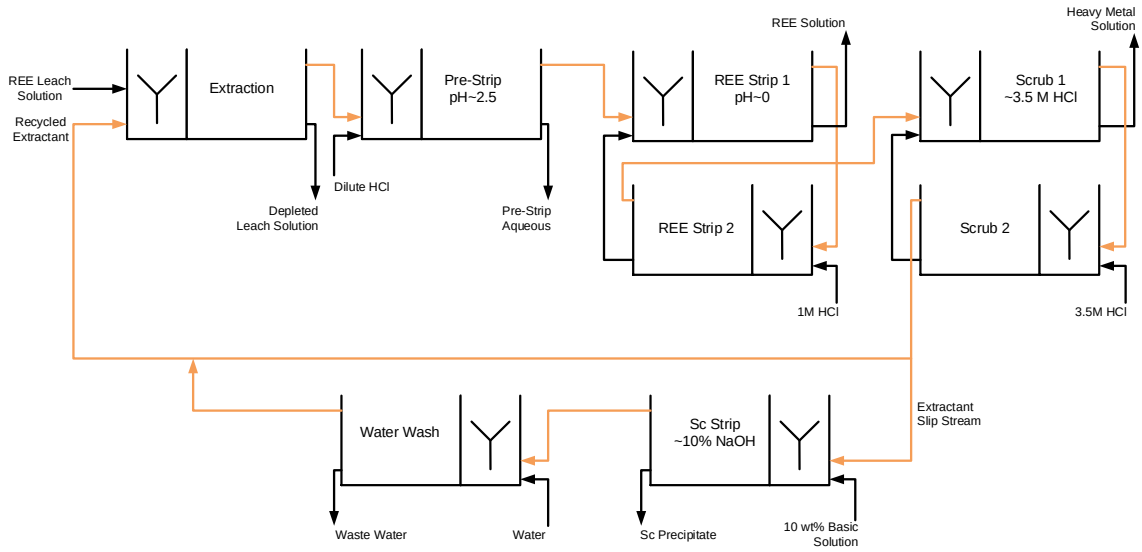

Figure 11: Flow schematic for the solvent extraction circuit to upgrade REE concentrate for feed to the final purification/separation step.

The solvent extraction balance assumed that the feed solution composition is the same as the leach solution, but with 50% of the iron removed by roasting. Organic losses in the aqueous phases were assumed to be 50 ppm, and mixing times and settling times were 5 minutes and 10 minutes, respectively. The extraction stage organic to aqueous ratio was

about 1:2, but the stripping stage organic ratios were assumed to be maintained at 1:4 through internal recycles. Concentration factors were assumed to be 50x in each stripping section, but 100x in the scrubbing section. To be conservative, the extraction was assumed to require two stages, pre-strip two stages, REE strip four stages, scrub four stages, scandium recovery two stages, and one stage for the water wash. Due to the generally low concentration of scandium, only 5% of the extractant is diverted to scandium recovery in each pass of the extractant.

Chemical consumption was calculated for each stage based on stoichiometric consumption of acid (or base) to the respective stripped compound(s), plus the amount of chemical required to achieve the pH or concentration listed for the stage in Figure 11. Feed rates were calculated from the concentration factors.

4.4 Technoeconomic Assessment Results

The procedure used in the technoeconomic assessment follows the Electric Power Research Institute's (EPRI) Technical Assessment Guide (TAG™) guidelines for cost estimation of emerging technologies. The total capital requirement (TCR) of a full scale rare earth separation and purification system includes the direct costs of purchasing and installing all processing equipment (denoted as the process facilities capital, PFC), plus a number of indirect costs such as the general facilities cost, engineering and home office fees, contingency costs, and several categories of owner's costs. These costs are used to determine the overall cost of extracting and purifying rare earth elements from coal ash. Figure 12 outlines the TAG method developed by EPRI.

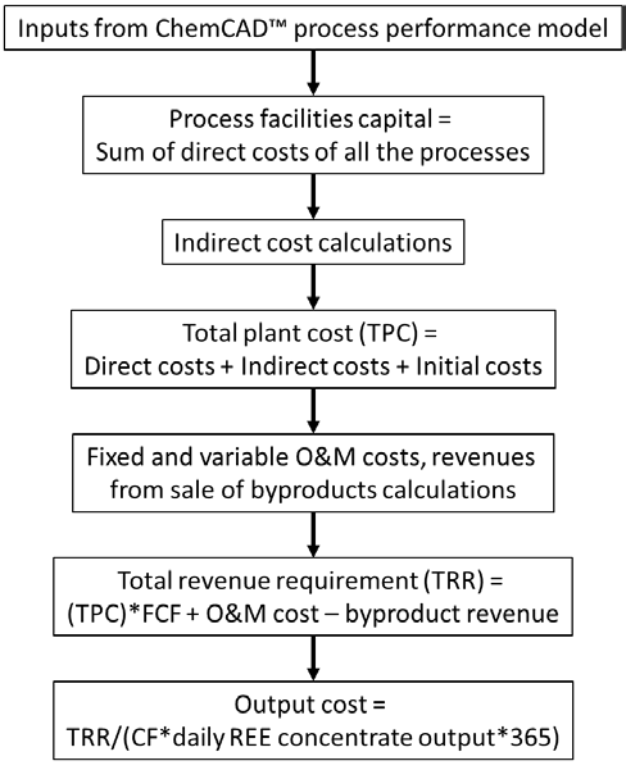

Figure 12: Method of cost assessment (Electronic Power Research Institute (EPRI), 1986).

4.4.1 Capital Cost

The process facilities capital (PFC) of a component refers to the capital required to purchase and install a major process at the facility. Ideally, these costs are known and come from prices quoted from an equipment manufacturer. When manufacturer data is not available, installed cost data is derived from references describing costs for installing similar processes. Equipment costs are then scaled using well-documented cost correlations (Tribe & Alpine, 1986). Table 10 lists the nominal cost values for a NOAK rare earth separation and purification system.

The total direct capital cost of the rare earth separation and purification system is approximately $42 million. The most capital intensive process area is the evaporator-condenser associated with the acid recovery system which accounts for approximately half of the total direct capital costs of the system. The evaporator-condenser is used to recover nitric acid from the leachate stream. Despite the high capital cost, the process is necessary to reduce annual operating expenses associated with reagent cost.

Table 10: Installed costs for major process areas of the ADP.

Direct Costs for All Major Process Areas ($1000, 2015)			
Coal Ash Handling	$361	Evaporator Feed Pump	$7
Pre-treatment water wash	$224	Acid Recycle Pump	$7
Leach Reactor	$271	Acid Makeup Pump	$7
Knockout Vessel	$179	Sweep Blower	$3
Filter	$4,040	Column Blower	$9
Rotary Dryer	$2,277	Distillation Column	$333
Crystallizer/Custom Rotary Dryer	$3,350	Oxide and Nitrate separation	$64
Column	$217	REO SX and Purification	$15,770
ESP	$1,328		
Reactor Heat Exchanger	$199		
Column Heat exchanger	$218		
Evap Condenser	$12,698		
Roaster Condenser	$786		
Reactor Feed pump	$24		
Reactor Recirculation Pump	$19		
Column Sump Pump	$16		
Filter Pump	$24		
Process Facilities Capital*			**$42,400**
***Total Process Facility Capital (PFC) may not equal the some of the components due to rounding error**			

The Process Facilities Capital costs, also known as the direct capital costs, are used to calculate the indirect capital costs associated with the REE separation and purification process. The total of the direct and indirect capital costs make up the elements of the total plant costs. The indirect costs include engineering and home office fees, general facilities capital, project and process contingencies, and royalty charges.

The sum of these costs, called the total plant cost (TPC), is developed on the basis of overnight construction. Overnight cost is the cost of a construction project if no interest was incurred during construction, as if the project was completed "overnight." These costs are summarized in Table 11.

Table 11: Summary of estimated direct and indirect capital costs for a NOAK ADP. These costs are the basis for estimating the total plant cost-- a major component of the total capital requirement of the plant.

Capital Cost Elements	Nominal Value	Component Cost ($Million, 2015)
Process Facilities Capital (PFC)		$42.4
Engineering and Home Office Fees	7% PFC	$2.9
General Facilities	10% PFC	$4.2
Project Contingency	10% PFC	$4.2
Process Contingency	10% PFC	$4.2
Total Plant Cost (TPC) = Sum of the above		$58.1

The total capital requirement (TCR) includes all the capital necessary to complete the entire project. These items include the total plant cost (TPC), allowance for funds used during construction (AFUDC), prepaid royalties, inventory capital, and pre-production costs.

Table 12 summarizes the steps required to calculate the total capital requirement. The TCR for the rare earth separation is approximately $61 million. This includes all direct and indirect capital costs associated with the project.

Table 12: Indirect capital costs for a NOAK rare earth separation and purification facility.

Capital Cost Elements	Nominal Value	Component Cost ($1000, 2015)
Total Plant Cost (TPC)		$58,100
AFUDC (interest during construction)	0.5% TPC	$291
Royalty Fees	0.5% PFC	$212
Pre-Production (fixed)	1 month fixed O&M	$415
Pre-Production Costs (Variable)	1 month variable O&M	$1,494
Inventory Capital	0.5% TPC	$291
Total Capital Requirement (TCR)		**$60,803**

4.4.2 Operating Costs

The operating and maintenance (O&M) costs are usually estimated for one year of operation. These can be divided into fixed O&M and variable O&M costs. These costs are discussed in this section. Note that all reference costs are adjusted to 2015 dollars from the source year using the SDRI Chemical Engineer Handbook Price Index.

The fixed O&M (FOM) costs include the costs of plant maintenance (materials and labor) and labor (operating, administrative, and support labor). Operating labor costs are estimated based on correlations between labor hour requirements and the plant's daily capacity (Peters, Timmerhaus, & West, 2003; Peters, Timmerhaus, & West, 2003).

Table 13: Fixed operating and maintenance cost parameters and their nominal values.

Fixed O&M Costs	Units	Nominal Value
Major Processing Steps	#	12
Cor'l'n for Op. Labor	Hrs./day-step	14
Operating Labor Rate	$/hr.	$46.43
Total Maintenance Cost	%TPC	2.5%
Maint. Cost Allocated to Labor	% FOM Maint.	40%
Admin. & Support Labor Cost	% Total Labor	30%

The variable O&M (VOM) costs include the cost of materials consumed (make-up acid, process water, etc.), utilities, and services used (waste transport and disposal). These quantities are determined in the CHEMCAD performance model. The unit cost of each item (e.g. dollars per tonne of coal ash or dollars per tonne of transported REE concentrate) is a parameter specified as a cost input to the model. The total annual cost of each item is then calculated by multiplying the unit cost by the total annual quantity used or consumed. Total annual quantities are dependent upon the facility's annual operating capacity factor. The individual components of variable O&M costs are explained in more detail below. Note that the unit costs for all of the consumables are based on publicly available sources where available.

Table 14: Variable operating and maintenance cost components and their nominal values. Note that prices in parenthesis indicate a negative cost (or revenue) for marketable by-products. Note that the cost of zeolites was calculated to roughly offset the cost of the pre-treatment process equipment.

Variable O&M Costs	Units	Nominal Value
Coal Ash	$/tonne	$-
Makeup Nitric Acid	$/tonne	$600
Dilution Water	$/tonne	$0.30
Leached Ash Disposal	$/tonne	$10.3
Natural Gas	$/GJ	$1.26
Electricity	$/MWh	$6.73
SMBS inlet rate	$/tonne	$280
Hydrochloric acid	$/tonne	$115
Sodium Hydroxide	$/tonne	$320
Solvent (Extractant)	$/kg	$8.30
Wastewater	$/kliter	$0.30
Hazardous wastewater	$/kliter	$18.79
REO Purification Cost	$/kg	$2.00
Price for Fertilizer	$/tonne	$-
Price for Zeolites	$/tonne	$(45.03)
Price for Salable Ash Byproduct	$/tonne	$(30.00)

The nominal (default) values of all major operating and maintenance (O&M) costs in the REE separation and purification process model are summarized in Table 15.

Table 15: Variable and fixed operating cost component results for a rare earth separation and purification facility.

Variable Cost Component	Variable O&M Cost ($1000/yr., 2015)	Fixed Cost Component	Fixed O&M Cost ($1000/yr. 2015)
Coal Ash	$-	Operating Labor	$2,847
Makeup Nitric Acid	$14,029	Maintenance Material	$1,453
Makeup Water	$339	Maintenance Labor	$581
Solid and hazardous waste disposal	$788	Admin. & Support Labor	$1,029
Natural Gas	$53	**Total Fixed Costs**	**$5,910**
Electricity	$771		
Organic Solvent	$328	**Salable By-Products**	
Caustic	$392	Upgraded Coal Ash	$(2,290)
Hydrochloric Acid	$127	Zeolite	$(948)
Extractant	$407	Fertilizer	$-
Hazardous Disposal Costs	$462	**Total By-product Credits (Salable Products)**	**$(3,237)**
REO Purification O&M	$233		
Total Variable Costs	**$17,929**		

A robust way to evaluate the cost of resource intensive processes such as REE processing systems is to normalize the cost of production on the basis of incoming coal ash ($/tonne feedstock) and outgoing rare earth product ($/kg rare earth oxide). The normalized cost, also known as the levelized cost of production (LCOP), represents the income that the processing facility would need to receive from the sale of products to fully recovery all capital and operating costs while earning a specified rate of return over the plant life. The LCOP is calculated first by quantifying the annual revenue requirement as shown in Equation 3.

$$Total\ Annual\ Revenue\ Requirement\ \left(\frac{\$}{yr}\right) = TCR * FCF + Fixed\ O\&M + Variable\ O\&M + ByProduct\ Credits$$

Financial parameters such as the annual rate of return, plant life, and other plant assumptions are embedded in the fixed charge factor (FCF) in order to annualize the total capital costs. Thus, the reported value represents the "levelized" annual revenue stream that a processing facility must realize from the sale of REE oxides to produce the same net present value as a stream of variable year-to-year costs over the life of the plant.

A summary of the levelized production costs reported based on the ash feedstock and mixed rare earth oxide products is shown in Table 16. Note that these results represent the cost if a plant were constructed using a mature (NOAK) iteration of the rare earth separation and purification process.

Table 16: Cost model results using Nth-of-a-kind (NOAK) plant assumptions. These costs represent the cost of producing rare earth oxides from coal ash given a mature iteration of the separation and purification process.

Cost Component	$Million per year (2015)	$/Tonne Coal Ash Processed	$/kg REE Oxides
Annual Fixed Cost	$5.9	30	50.6
Annual Variable Cost	$17.9	91	153.6
Annualized Capital Cost	$6.9	135	59.0
By-Product Credits	(3.2)	(16)	(27.8)
Total Annual Revenue Requirement	27.5	140	235.4

For context to the levelized cost per tonne of coal ash fed, a histogram of recoverable REE value in US coal sources was generated. This histogram uses USGS CoalQual data (U.S. Geological Survey, 2015) to obtain REE concentrations in coal sources by state. This was converted to a value in coal, on an ash basis, using the ash measurement from the database and the REE prices listed in Table 17.

Table 17: REE prices used in evaluation of coal source values.

Element	Oxide Basis Value, $/kg
Sc	$4,200.00
Ce	$2.00
Dy	$230.00
Er	$34.00
Gd	$32.00
La	$2.00
Nd	$42.00
Pr	$52.00
Tb	$400.00
Y	$6.00

To make the histograms representative of US sources, the sample counts from each state were weighted based on the respective state's coal production from the EIA Coal Data Browser (Energy Information Administration, 2015). This histogram is shown in Figure, and indicates the distribution of recoverable REE values in US coals on a tonne of ash basis. The red line indicates the levelized process cost per tonne of coal ash ($140), from Table 16, of Battelle's recovery process. At this process cost, approximately 42% of US coal sources, if ashed, could be pursued with Battelle's process.

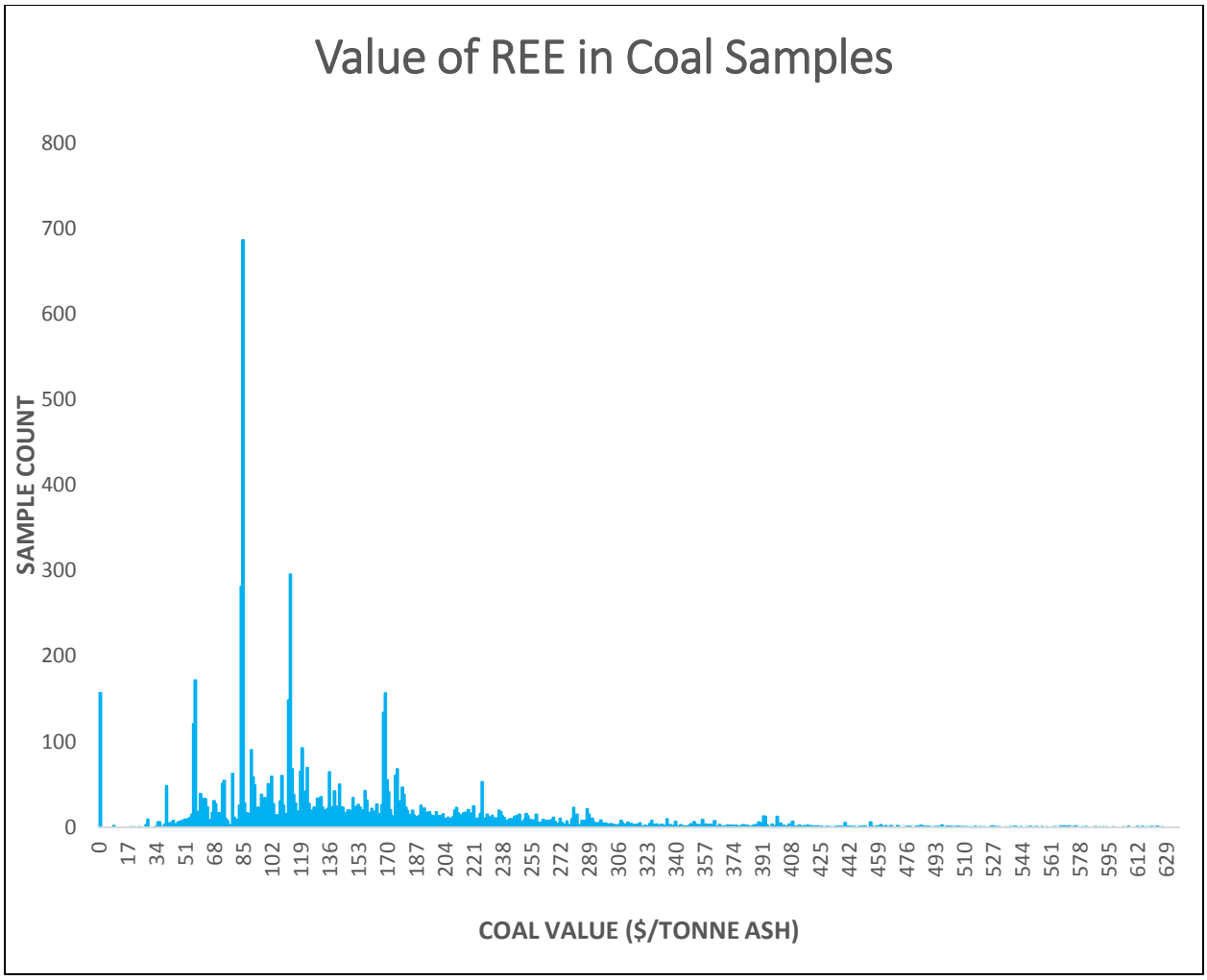

Figure 13: Histogram of REE values in US coal sources on an ash basis.

5.0 Conclusions and Next Steps

Based upon the design package described in this report and budgetary quotes from vendors, it is estimated that a continuous bench-scale unit to process 12.5 lb./hr. (5.7 kg/hr.) of fly ash would require $1,102,206 in capital equipment. This cost includes a rough estimate for piping and plumbing costs, and excludes the solvent extraction equipment, which is pre-existing in Battelle laboratories. The process footprint is estimated to be 300 ft^2, which will fit in a high bay area at Battelle's Columbus laboratories. This high bay area has sufficient electrical service, ventilation, and cooling water to sustain the plant. Additionally, Battelle's Columbus operations have waste management services to handle the fly ash and chemical products/byproducts produced by the continuous system.

This continuous bench scale pilot system is a critical step in scale up and commercialization of the ADP REE recovery technology, as it will provide operational data on the integrated recycling process if Battelle is awarded a Phase 2 project. This operational data obtained from Phase 2, would be used to update the process economics, and understand options to integrate the

process with existing powerplant operations. It would also advance the technology to a TRL 5, as the process integration would be similar to the final application, and it would operate on fly ash and process solutions derived from an operating pulverized coal combustion powerplant.

If commercialized, this technology will reduce the costs associated with handling and disposal of coal combustion residuals, generate new salable products from coal, and create additional jobs that require skillsets similar to those attained in the coal industry. Battelle recommends proceeding with the Phase 2 project to build and demonstrate the integrated bench-scale pilot unit, such that additional data may be obtained for the design and operation of a future, large-scale pilot demonstration facility.

6.0 References

Battelle. (2016). *Recovery of Rare Earth Elements from Coal and Coal Byproducts via a Closed Loop Leaching Process: Feasibility Study Report.*

Battelle. (2016a). *Recovery of Rare Earth Elements from Coal and Coal Byproducts via a Closed Loop Leacing Process: Sampling and Characterization Report.*

Cannon Instrument Company. (Revision 3). *Protruded Metal Distillation Packing.*

Electronic Power Research Institute (EPRI). (1986). *Technical Assessment Guide (TAG) Volume 1: Electricity Supply.* Palo Alto: EPRI.

Electronic Power Research Institute (EPRI). (1993). *TAG(tm) Technical Assessment Guide Volume 1: Electricity Supply. .* Palo Alto: EPRI.

Energy Information Administration. (2015, August). *Coal Data Browser*. Retrieved from www.eia.gov: http://www.eia.gov/beta/coal/data/browser/#/topic/20?agg=0,1&geo=vvvvvvvvvvvvo&sec=vs&freq=A&start=2001&end=2013&ctype=map&ltype=pin&rtype=s&maptype=0&rse=0&pin=

Hollman, G. G., Steenbruggen, G., & Janssen-Jurkovicova, M. (1999). A Two-Step Process for the Synthesis of Zeolites from Coal Fly Ash. *Fuel*, 1225-1230.

Peters, T., Timmerhaus, K., & West, R. (2003). *Plant Design and Economics for Chemical Engineers (5th Ed).* New York: McGraw Hill.

Stern, K. H. (1972). High Temperature Properties and Decomposition of Inorganic Salts, Part 3: Nitrates and Nitrites. *Journal of Physical and Chemical Reference Data, 1*(3).

Tribe, M. A., & Alpine, R. L. (1986). Scale Economies adn the "0.6 Rule". *Engineering Costs and Production Economies*, 271-278.

U.S. Geological Survey. (2015). Coal Quality Database Version 3.0. Reston: USGS.

BATTELLE

It can be done

BATTELLE

It can be done